INTERNATIONAL LAND RECLAMATION AND MINE DRAINAGE CONFERENCE

AND

THIRD INTERNATIONAL CONFERENCE ON THE ABATEMENT OF ACIDIC DRAINAGE

Volume 2 of 4: Mine Drainage

Proceedings of a conference held in Pittsburgh, PA on April 24-29, 1994.
This conference served as the annual meeting for both the American Society for Surface Mining and Reclamation and the Canadian Land Reclamation Association.

These conference proceedings were made possible through contributions provided by:

- United States Department of the Interior
  - *Bureau of Mines
  - *Office of Surface Mining Reclamation and Enforcement
  - *Bureau of Land Management
  - *Geological Survey
- United States Environmental Protection Agency
- Pennsylvania Department of Environmental Resources
- Tennessee Valley Authority
- USDA Soil Conservation Service
- Canada's MEND Program

UNITED STATES DEPARTMENT OF THE INTERIOR
Bureau of Mines Special Publication SP 06B-94

UNITED STATES DEPARTMENT OF THE INTERIOR
Bureau of Mines Special Publication SP 06B-94

INTERNATIONAL LAND RECLAMATION AND MINE DRAINAGE CONFERENCE

AND

THIRD INTERNATIONAL CONFERENCE ON THE ABATEMENT OF ACIDIC DRAINAGE

Volume 2 of 4: Mine Drainage

Proceedings of a conference held in Pittsburgh, PA on April 24-29, 1994.
This conference served as the annual meeting for both the American Society for Surface Mining and Reclamation and the Canadian Land Reclamation Association.

Copies of this and the three companion volumes can be obtained by through NTIS.
Volume 1: Mine Drainage - SP 06A-94
Volume 2: Mine Drainage - SP 06B-94
Volume 3: Reclamation and Revegetation - SP 06C-94
Volume 4: Abandoned Mine Lands and Topical Issues - SP 06D-94

TABLE OF CONTENTS

MINE DRAINAGE - CASE STUDIES

HARD-ROCK MINE CLOSURE CASE STUDY - CYPRUS COPPERSTONE MINE
Miller, S. H., Van Zyl, D., Burns, G. R., and Markkola, K. 2

THE GIBRALTAR NORTH PROJECT ASSESSING ACID ROCK DRAINAGE
Patterson, R. J. L. and Ferguson, K. D. 12

REGULATORY CONTROLLED DESIGN - LOUVICOURT PROJECT - A CASE STUDY
Filion, M. P., Firlotte, F. W., Julien, M. R., and Lacombe, P. F. 22

DECOMMISSIONING OF TAILINGS AND WASTE ROCK AREAS AT STEKENJOKK, SWEDEN
Broman, P. G. and Göransson, T. 32

EVALUATION OF ACID PREVENTION TECHNIQUES USED IN SURFACE MINING
Meek, Jr., F. A. 41

CONTROL OF MINE DRAINAGE - GENERAL

LONG TERM BEHAVIOR OF ACID FORMING ROCK: RESULTS OF 11-YEAR FIELD STUDIES
Ziemkiewicz, P. F. and Meek, Jr., F. A. 49

SURFACE CHEMICAL METHODS OF FORMING HARDPAN IN PYRRHOTITE TAILINGS AND PREVENTION OF THE ACID MINE DRAINAGE
Ahmed, S. M. 57

INTERNATIONAL PERSPECTIVE ON THE ROLE OF ACID GENERATION IN SELECTING DECOMMISSIONING TECHNIQUES FOR URANIUM MINING SITES IN EASTERN GERMANY
Feasby, D. G., Chambers, D. B., Scharer, J. M., Pettit, C. M., Dakers, R. G., and Goldsworthy, M. H. 67

EVALUATION OF ACID GENERATING ROCK AND ACID CONSUMING ROCK MIXING TO PREVENT ACID ROCK DRAINAGE
Day, S. J. 77

MITIGATION OF ACID MINE DRAINAGE BY THE POROUS ENVELOPE EFFECT
St-Arnaud, L. C., Aubé, B. C., Wiseman, M. E., and Aiken, S. R. 87

POTENTIAL MICROENCAPSULATION OF PYRITE BY ARTIFICIAL INDUCEMENT OF $FePO_4$ COATINGS
Evangelou, V. P. 96

CONTROL OF ACID MINE DRAINAGE - DRY COVERS

SHOTCRETE AS A CEMENTITIOUS COVER FOR ACID GENERATING WASTE ROCK PILES
Jones, C. E. and Wong, J. Y. 104

EVALUATION OF A COMPOSITE SOIL COVER TO CONTROL ACID WASTE ROCK PILE DRAINAGE
Bell, A. V., Riley, M. D., and Yanful, E. K. 113

CONTROLLING ACID MINE DRAINAGE USING AN ORGANIC COVER: THE CASE OF THE EAST SULLIVAN MINE, ABITIBI, QUÉBEC
Tremblay, R. L. 122

COLUMN TESTS INVESTIGATION OF MILLING WASTES PROPERTIES USED TO BUILD COVER SYSTEMS
Aachib, M., Aubertin, M., and Chapuis, R. P. 128

FIELD AND LABORATORY PERFORMANCE OF ENGINEERED COVERS ON THE WAITE AMULET TAILINGS
Yanful, E. K., Aubé, B. C., Woyshner, M., and St-Arnaud, L. C. 138

COMPOSTED ORGANIC WASTES AS ANAEROBIC REDUCING COVERS FOR LONG TERM ABANDONMENT OF ACID-GENERATING TAILING
Pierce, W. G., Belzile, N., Wiseman, M. E., and Winterhalder, K. 148

MINE HYDROLOGY

COMPACTION BEHAVIOUR OF LIGHTLY CEMENTED SANDSTONE AS A RESULT OF DEWATERING
Nikraz, H. R., Press, M. E., and Evans, A. W. 158

ASSESSMENT OF ACID MINE DRAINAGE REMEDIATION SCHEMES ON GROUND WATER FLOW REGIMES AT A RECLAIMED MINE SITE
Gabr, M. A., Bowders, J. J., Runner, M. S. 168

HYDROLOGIC AND WATER QUALITY CHARACTERISTICS OF A PARTIALLY-FLOODED, ABANDONED UNDERGROUND COAL MINE
Aljoe, W. W. 178

THE HYDROGEOLOGY AND HYDROGEOCHEMISTRY OF THE STAR FIRE SITE, EASTERN KENTUCKY
Wunsch, D. R. and Dinger, J. S. 188

HYDROGEOLOGIC EVALUATION AND WATER BALANCE OF A THICKENED TAILINGS DEPOSIT NEAR TIMMINS, ON, CANADA
Woyshner, M. R. and St-Arnaud, L. 198

THE PORE-WATER GEOCHEMISTRY OF THE CU-ZN MINE TAILINGS AT KIDD CREEK, NEAR TIMMINS, ONTARIO, CANADA
Al, T. A., Blowes, D. W., and Jambor, J. L. 208

POSTER SESSION

MANUSCRIPTS

LABORATORY TESTING OF COATINGS FOR PREVENTION OF ACID DRAINAGE IN UNDERGROUND COAL MINES
Adams, R. L., Ninesteel, J. J., and Rauch, H. W. 218

ENGINEERING EVALUATION OF AMENDED FLY ASH FOR HYDRAULIC BARRIERS
Bowders, Jr., J. J., Gabr, M. A., Boury, E. M., and Baker, R. C. 226

MOBILIZATION OF MERCURY FROM A GOSSAN TAILINGS PILE, MURRAY BROOK PRECIOUS METAL VAT LEACHING OPERATION, NEW BRUNSWICK, CANADA
Boyle, D. R. and Smith, C. N. 234

GEOCHEMICAL AND GEOHYDROLOGICAL CHARACTERISTICS OF BEDROCK AND SPOIL FROM TWO METHODS OF MINING AT A RECLAIMED SURFACE COAL MINE, CLARION COUNTY, PA, USA
Cravotta III, C. A., Brady, K. B. C., Gustafson-Minnich, L. C., and DiMatteo, M. R. 242

TREATMENT OF ACID MINE DRAINAGE BY PASSIVE TREATMENT SYSTEMS
Faulkner, B. B. and Skousen, J. G. 250

THE RELEVANCE OF THE INTRINSIC OXIDATION RATE TO THE EVOLUTION OF POLLUTED DRAINAGE FROM A PYRITIC WASTE ROCK DUMP
Gibson, D. K., Pantelis, G., and Ritchie, A. I. M. 258

MODELING OF A RECLAIMED SURFACE COAL MINE SPOIL AQUIFER USING MODFLOW
Hawkins, J. W. 265

NEW FUNCTIONAL POLYMERS AS SORBENTS FOR THE SELECTIVE RECOVERY OF TOXIC HEAVY METALS FROM ACID MINE DRAINAGE
Hubbard, K. L., Darling, G. D., Rao, S. R., and Finch, J. A. 273

HYDROLOGIC ASSESSMENT OF WELLHEAD PROTECTION IN THE VICINITY OF A ROOM-AND-PILLAR COAL MINE
Jones, P. M. and Ellenberger, J. L. 281

THE ROLE OF SULFATE AND IONIC STRENGTH ON THE SHIFT FROM ACID TO ALKALINE MINE DRAINAGE IN SOUTHWEST PENNSYLVANIA
Jones, P. M., Mulvay, S. M., and Fish, D. 289

THE APPLICATION OF ECOLOGICAL ENGINEERING TO ACID COAL SEEPAGES IN EASTERN CANADA
Kalin, M., Smith, M. P., and Landry, G. 296

IN SITU TREATMENT OF ACID MINE DRAINAGE BY SULPHATE REDUCING BACTERIA IN OPEN PITS: SCALE-UP EXPERIENCES
Kuyucak, N. and St-Germain, P. 303

POSSIBLE OPTIONS FOR IN SITU TREATMENT OF ACID MINE DRAINAGE SEEPAGES
Kuyucak, N. and St-Germain, P. 311

USE OF BACTERICIDES TO CONTROL ACID MINE DRAINAGE FROM SURFACE OPERATIONS
Parisi, D., Horneman, J., and Rastogi, V. 319

EVALUATION OF HUMIDITY CELL PARAMETERS THEIR EFFECT ON PRECISION AND REPEATABILITY
Pool, D. L. and Balderrama, R. M. 326

SIMULATED WEATHERING OF PYRITIC SHALE WITH ADDED LIMESTONE AND LIME
Rose, A. W. and Daub, G. A. 334

AMD CLEANUP USING NATURAL ZEOLITES
Schultze, L. E., Zamzow, M. J., and Bremner, P. R. 341

A DEMONSTRATION OF THE FEASIBILITY OF TREATING ACID MINE DRAINAGE BY AN IN SITU ELECTROCHEMICAL METHOD
Shelp, G., Chesworth, W., Spiers, G., and Liu, L. 348

AN EVALUATION OF A PEAT-WOOD CHIP-MICROFLORA ADMIXTURE TO ACT AS AN AMELIORANT FOR ACID MINE DRAINAGE
Shelp, G., Southam, G., Spiers, G., Liu, L., and Chesworth, W. 356

MASS BALANCE ASSESSMENT OF INITIAL WEATHERING PROCESSES DERIVED FROM OXYGEN CONSUMPTION RATES IN WASTE SULFIDE ORE
Strömberg, B., Banwart, S., Bennett, J. W., and Ritchie, A. I. M. 363

IRON AND MANGANESE DYNAMICS IN LABORATORY WETLAND MESOCOSMS: IMPLICATIONS FOR COAL MINE DRAINAGE TREATMENT
Tarutis Jr., W. J. and Unz, R. F. 371

LABORATORY AND PILOT-SCALE STUDIES ON THE TREATMENT OF ACID ROCK DRAINAGE AT A CLOSED GOLD-MINING OPERATION IN CALIFORNIA
Wildeman, T., Cevaal, J., Whiting, K., Gusek, J., and Scheuering, J. 379

PROOF-OF-PRINCIPLE STUDIES FOR PASSIVE TREATMENT OF ACID ROCK DRAINAGE AND MILL TAILING SOLUTIONS FROM A GOLD OPERATION IN NEVADA
Wildeman, T. R., Filipek, L. H., and Gusek, J. 387

AMD/TIME: A SIMPLE SPREADSHEET FOR PREDICTING ACID MINE DRAINAGE
Ziemkiewicz, P. F. 395

ABSTRACTS 401-430

Mine Drainage abstracts, listed alphabetically by last name of first author. Page numbers are listed in Author Index at the back of this volume.

AUTHOR INDEX 431-433

UNIT OF MEASURE ABBREVIATIONS USED IN THESE PROCEEDINGS

Å	angstrom
ac	acre
Bq	becquerel
bu	bushel
cal	calorie
cm	centimeter
cmol	centimole
cps	count per second
°C	degree Celsius
d	day
dS	decisiemen
ft	foot
g	gram
gal	gallon
gpd	gallon per day
gpm	gallon per minute
h	hour
ha	hectare
hL	hectoliter
hp	horse power
Hz	hertz
in	inch
J	joule
K	kelvin
kcal	kilocalorie
kg	kilogram
kHz	kilohertz
km	kilometer
kmt	kilo metric ton
kN	kilonewton
kPa	kilopascal
kV	kilovolt
L	liter
lb	pound
m	meter
M	molar
mA	milliampere
meq	milliequivalent
mg	milligram
Mg	megagram
min	minute
mL	milliliter
mm	millimeter
mmho	millimho
mol	mole
mmol	millimole
MPa	megapascal
mS	millisiemen
mt	metric ton
mV	millivolt
MW	megawatt
μg	microgram
μL	microliter
μm	micrometer
μmho	micromho
μmol	micromole
N	normal
N	newton
nm	nanometer
Pa	pascal
pCi	picocurie
ppb	part per billion
ppm	part per million
ppt	part per thousand
psi	pound per square inch
psig	pound per square inch gauge
r	revolution
rad	radian
rpm	revolutions per minute
s	second
st	short ton
vol %	volume percent
wt %	weight percent
yd	yard
yr	year

INTERNATIONAL LAND RECLAMATION AND MINE DRAINAGE CONFERENCE AND THIRD INTERNATIONAL CONFERENCE ON THE ABATEMENT OF ACIDIC DRAINAGE

Proceedings of a conference serving as the annual meetings of the American Society for Surface Mining and Reclamation, the Canadian Land Reclamation Association, and the West Virginia Surface Mine Drainage Task Force, in conjunction with the Third International Conference on the Abatement of Acidic Drainage.

ABSTRACT

Mine drainage and mine reclamation are topics of major interest to the mining industry, federal and local governments, and the general public. This publication and its companion three volumes are the proceedings of a conference held in Pittsburgh, Pennsylvania, April 24-29, 1994. There were twelve sessions (69 papers) that dealt with mine drainage, including modeling, geochemistry, prediction, treatment, control strategies, characterization, hydrology, and case studies. These sessions comprise volumes 1 and 2. The six sessions (34 papers) that dealt with reclamation and revegetation of disturbed lands are included in volume 3. Volume 4 includes the six sessions (34 papers) that dealt with such topical issues as fires at abandoned mine sites, subsidence, hydrology, mine wastes, and policy. Poster session presentations are represented by 49 papers and 92 abstracts that have been placed in the back of volumes 2, 3, and 4, consistent with the subject of that volume.

Reference to companies and specific products in these papers does not imply endorsement by the Bureau of Mines.

HARD-ROCK MINE CLOSURE CASE STUDY - CYPRUS COPPERSTONE MINE[1]

Scott H. Miller, Dirk Van Zyl, P.E., Ph.D.[2]
George R. Burns, Kurt Markkola[3]

Abstract: This paper presents a case study of permitting and issues associated with hard rock gold mine closure. A mine closure design for the Cyprus Copperstone Mine in Arizona was prepared and submitted to State and Federal agencies for review and comment. Issues addressed as part of the mine closure design included: open pit stability; heap leach pad detoxification; tailings impoundment closure; and, waste rock disposal area closure. The mine closure was designed to minimize long-term environmental impacts, reduce physical hazards, and return the area to the pre-mining land uses.

Introduction

This paper presents a case study of recent planning and ongoing activities for hard-rock precious metals mine closure at the Cyprus Copperstone Mine (Copperstone) in Arizona. This paper discusses the general environmental and permitting issues involved in hard rock mine closure, as well as the site-specific operational and physical conditions at Copperstone. Successful mine closure and permitting require the following elements--

Accurate prediction of site water balance, including capacity for stormwater retention and/or discharge, evaporation, and process requirements.
Accurate prediction of geochemical behavior of waste rock, tailings, ore heaps, open pit, or underground workings when exposed to an oxidizing environment.
Adequate physical and geochemical stabilization of mine waste materials through operational or reclamation activities.
Adequate environmental and operational monitoring to identify changes in initial design assumptions.

It is further very beneficial if the mine has a clean operating history and complete monitoring history.

This paper reviews the issues addressed during the ongoing Copperstone closure and is organized into the following sections:

Copperstone site and project description.
Open pit stability and waste rock disposal area closure.
Mine contractor's compound closure.
Heap leach pad detoxification and regrading.
Plant closure
Tailings impoundment closure.
Compliance point monitoring and postclosure activities.

---

[1]Paper presented at the International Land Reclamation and Mine Drainage Conference and the Third International Conference on the Abatement of Acidic Drainage, Pittsburgh, PA, April 24-29, 1994.

[2]Scott H. Miller, Senior Project Manager, Environmental Permitting, Dirk Van Zyl, P.E., Ph.D., Director, Mining, Golder Associates Inc., Lakewood, Colorado, USA.

[3]George Burns, Resident Manager, Kurt Markkola, Chief Metallurgist, Cyprus Copperstone Gold Corporation, Parker, Arizona, USA.

The objectives of successful mine closure are to provide long-term environmental protection to surface and ground water resources, establish a stable physical setting, return the site to premining or other land uses, and develop a low-maintenance or "walk-away" situation for the mining company. A period of postclosure monitoring is typically required by the existing permits, and is recommended for the mining company to verify successful closure.

Cyprus Copperstone Site and Project Description

The Copperstone Mine is located approximately 18 miles south of Parker, AZ, on unpatented mining claims administered by the U.S. Department of the Interior's Bureau of Land Management (BLM). The Copperstone Mine operated under the following Federal and State approvals and permits: Plan of Operations (Federal, administered by BLM); Groundwater Quality Protection Permit (State, administered by Arizona Department of Environmental Quality, ADEQ); and, Air Quality Operating Permit (State, administered by ADEQ).

The Copperstone Mine is situated on the northern portion of the La Posa Plain, a desert basin located between the Plomosa Mountains to the east and the Dome Rock Mountains to the southwest. The project site is on a relatively flat desert surface water drainage divide with local northeast trending stabilized sand dunes. Surface elevations range from 725 to 899 ft above mean sea level (msl).

The surficial materials are Quaternary eolian and alluvial sands which overlie the Pliocene-aged Bouse Formation. The Bouse Formation is comprised of lenticular deposits of clay, sand, and gravel, which are generally moderately to highly cemented with calcium carbonate.

The mine consists of an elliptical-shaped open pit excavation. The mine pit walls expose alluvial materials 0 to 170 ft thick, which are underlain by faulted and altered quartz latite and basalt. Below the quartz latite, Paleozoic-aged limestones and clastic rocks are exposed locally in the northern portion of the open pit. Mining was completed to an elevation of 350 ft above msl with an ultimate mine pit depth of approximately 540 ft below the original ground surface.

Mining was performed by drilling, blasting, loading, and hauling. Unmineralized rock and overburden were hauled and deposited in waste rock disposal areas. Ore was hauled to the processing area, which consisted of rock crushing and milling equipment and a carbon-in-leach (CIL) processing plant. Ore was crushed using a two stage crushing system, ground with ball mills, and then cyanide-leached. Spent ore was piped, in slurry form, to two separate lined tailings facilities for final deposition. The first area, cell A, was constructed and used for the ore processed beginning in 1987. Cell B was subsequently constructed in 1988 for additional tailings storage capacity. The reclaimed water from the tailings impoundment flowed to a double-lined reclaim pond and was subsequently pumped to the plant. Reclaim water was recycled into the process facilities. The site facilities are shown on figure 1

A cyanide heap leach facility was constructed on top of deposited tailings solids in cell A in 1991. Pregnant solution from the heap leach facility was collected in a pond located near the center of the heap leach pad in cell A. During heap leach operation, reclaim solution from the tailings was used as barren make-up water for the heap leach operation. Pregnant solution was pumped to the CIL plant for gold extraction.

Cyprus Copperstone Mine was designed, constructed, and operated as a zero-discharge facility. Process solutions utilized for heap leaching or tailings management during operations were recycled and contained in the lined tailings impoundments, lined heap leach facility, curbed process facilities, and lined solution transfer channels for piped solution conveyance. During closure, to maintain the zero-discharge requirement, process solutions were pumped to the tailings impoundment for evaporation. Heap leach pad rinse solutions were detoxified and recycled prior to evaporation.

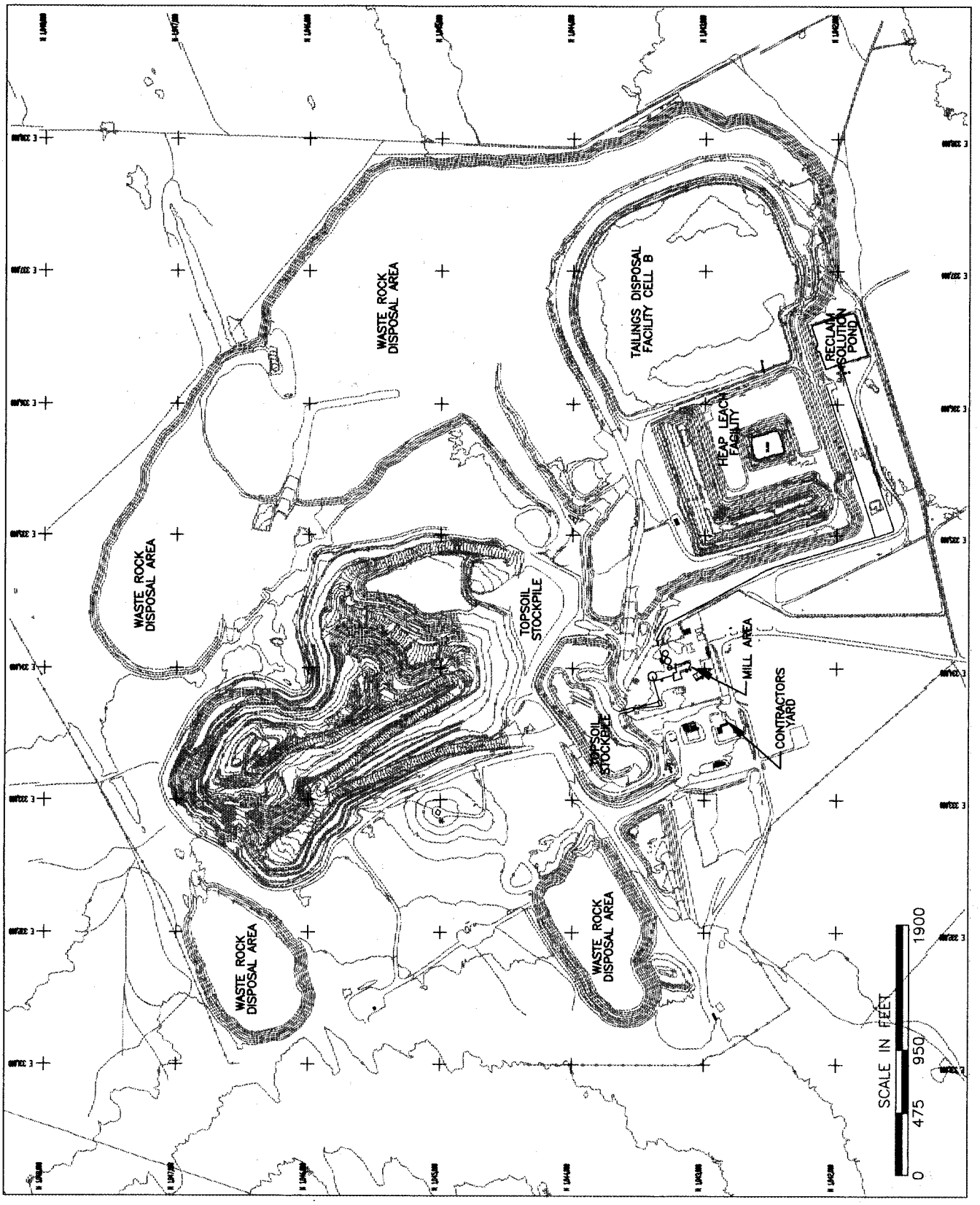

Figure 1. Site facility map.

Mine and Waste Rock Disposal Area Closure

The mine pit configuration near the end of operation is shown on figure 1. The pit wall has been excavated to between 47° and 63° slope angles. Some minor slope failures occurred during operation, mostly related to the geologic structure of the bedrock. Additionally the exposed slopes in the alluvium have failed locally. The bottom of the pit (at elevation 350 ft above msl) is approximately 20 ft above the local ground water level.

It is expected that the pit slopes will ultimately ravel to an overall 1.5H:1V in the alluvial overburden, while some future failures may occur in the structurally controlled rock faces. Because of the potential for future slope failures a rock berm was constructed on the surface around the predicted outer limits of the eventually stabilized pit rim. The berm was constructed of waste rock and excavated native soils. The berm is approximately 4 ft high with angle of repose sideslopes.

The waste rock disposal areas consist of a large contiguous rock pile on the east side of the pit, a north waste rock disposal area, and a south waste rock disposal area (fig. 1). These waste rock disposal areas were constructed in lifts through end dumping and dozing. The final lift was placed as loose "plug" dumps, creating a hummocky topography. The hummocky topography provides a more natural appearance as well as helping to collect wind-blown seeds, eolian silts, and moisture. Waste rock generated during the final stages of mining has been deposited in the southern part of the pit.

Geochemical Characterization

The mine pit overburden is comprised of both alluvium and bedrock. The bedrock is a quartz latite ranging from a massive to laminated texture and locally brecciated along faults. Adjacent to the ore zones, the quartz latite becomes sericitically or chloritically altered to various degrees. The altered zones contain minor amounts of barite, chrysocolla, hematite, and magnetite. The waste rock and ore contain only insignificant amounts of sulfide mineralization, and as such are not expected to have a potential for generation of acid drainage. A conformational geochemical testing program was developed to predict the geochemical behavior of the waste rock. This program consisted of the following four phases--

- Phase 1. - Identification of waste rock domains.
- Phase 2. - Selection of representative pit wall samples.
- Phase 3. - Acid-base accounting laboratory tests.
- Phase 4. - Meteoric water leach tests of waste rock samples.

The 57 million st of barren rock in the waste piles that will remain after closure were shown to be geochemically inert through the acid-base accounting and meteoric water testing program. Because these materials do not represent a potential source of contamination to surface or ground water, no treatment or discharge control is anticipated. No limitations on future land or water uses will be created as a result of the facility closure.

The closure plan presented for the mine pit and waste rock disposal areas is consistent with the State air quality and water quality permit requirements. This closure plan also meets the objectives established by the BLM including--

- Stabilized waste rock disposal areas against water and wind erosion.
- A confirmational geochemical evaluation determined no potential impact to ground water from infiltration of precipitation through the waste rock disposal areas
- Postmining land use consistent with the surrounding area except for the pit area.

Mine Contractor's Compound Closure

Cyprus Copperstone employed a private contractor to perform the mining operations. The contractor set up a compound with offices, maintenance facilities, refueling area, and storage yard in the contractor's compound area shown on figure 1. The fuel storage area consisted of a number of diesel tanks in a containment berm. The base of the contained area under the front end of the diesel tanks was lined with a 60-mil polypropylene liner.

The mine contractor's compound has been closed and reclaimed by removing equipment, followed by sampling and analysis, and finally by covering with topsoil. Some buildings will remain as the property of the claim holder, as these facilities have been purchased and bonded. All other equipment related to the mine contractor's compound was dismantled and removed for future use elsewhere.

Quantities of petroleum-contaminated soil from the mine contractor compound and plant area were identified based on the analytical results of a soil survey. The petroleum-contaminated soils have been excavated and are being bioremediated on-site.

Heap Leach Facility

The heap leach facility containing 1.2 million st of ore was constructed on the cell A tailings area (fig. 1), thus taking advantage of the existing buried liner under the tailings. Ten feet of waste rock was placed on the Cell A tailings impoundment with an overlying 20-mil PVC liner prior to construction of the heap. The heap was constructed in 20-ft lifts consisting of ore crushed to minus 5/8 in. Leaching was carried out with solution containing about 2 lb of free cyanide per ton of water delivered through drip emitters. The pregnant solutions were collected in a pond located in the center of the heap.

The heap leach pad closure requirements established in the operating permits are as follows: rinseate to be sampled from the pregnant solution pond should contain 0.2 mg/*l* or less total cyanide; the operator must assure that all solids will be properly capped (at least 2 ft of nontoxic native rock and solids) or that the constituent concentrations are less than or equal to the concentrations listed below.

Constituent	Limits, mg/*l*
Cyanide	20
Arsenic	5
Barium	100
Cadmium	1
Chromium	5
Lead	5
Nitrate	10
Selenium	1
Silver	5

The three options evaluated to potentially achieve the 0.2-mg/*l* total cyanide rinse effluent standard following detoxification included--

- Semicontinuous and partial low volume fresh water rinsing.
- Continuous rinsing with high volumes of recycled treated water.
- Natural attenuation using recycled water containing either indigenous or augmented microbial populations, both with possible nutrient addition.

A fourth closure option was considered that involved recontouring the 1.2-million-st heap without treatment and covering the solids in place with a cap. Although the treatment cost of this option was obviously less than the costs of the other three, it was less appealing owing to increased capping costs. As a result, the focus remained upon the three initial closure options.

Although the evaporation rate at the mine is high in comparison with precipitation, the use of large volumes of fresh water rinse and continuous rinsing to achieve the

desired effluent standard is not practical. Thus, the preferred approach involved rinsing and enhancement of natural attenuation biological treatment to either eliminate or reduce the residual total cyanide content.

The use of biological treatment for destruction of cyanide is well known and has been applied successfully in full-scale applications at both conventional vat and heap leaching operations (Smith and Mudder, 1991, Mudder and Whitlock, 1984, and Thompson, 1990). Although biological treatment of cyanide is generally less expensive than chemical treatment, it requires a longer period to initiate and complete. As a result, the benefits of reduced treatment costs are offset by the costs associated with leaving the operation open for a longer period. However, at Copperstone, time was less of a problem because of the need to allow the tailings pond surface to dry enough to permit access for covering with waste rock.

The climatic conditions at Copperstone are optimal with respect to initiating biological degradation of cyanide, using indigenous or augmented bacterial populations. A review of the chemical analyses of the reclaim and pregnant solutions suggested that biological degradation was already occurring, as indicated by the observed decrease in copper and cyanide levels and the corresponding increase in ammonia, nitrite, and nitrate concentrations. The resultant pH decrease is probably due to copper hydroxide precipitation and the destruction of carbonate alkalinity through nitrification.

Rinsing of the west half of the leach pad with fresh water was initiated in November 1992. Figure 2 illustrates the total cyanide degradation in the heap after the first fresh water rinse. A significant decrease, on the scale of two orders of magnitude, was observed. This suggested a strong, well-adapted population of bacteria was present and able to oxidize the available total cyanide very quickly. Total cyanide concentrations decreased from approximately 148.0 mg/*l* to 4.4 mg/*l* in 3 months.

As a result, biological treatment was used at Copperstone to reduce the cyanide level in the heap to the regulatory level of 0.2 mg/*l* total cyanide. The process designed for enhanced biological treatment consists of: production of bacteria proven to oxidize cyanide in spent ore and the pore solution in the heap; application of dilute solutions of the treatment culture; and, analysis of draindown solution and spent ore to verify biological treatment efficiency.

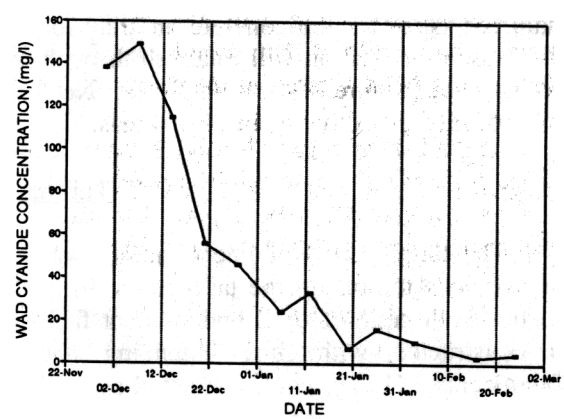

Figure 2. Decomposition of cyanide during rinse, west pad.

The rinsing process was operated as a closed system with no discharge to the environment. The bacteria populations and nutrients are natural and nontoxic.

The heap leach ore has been rinsed to the regulatory limit of 0.2 mg/*l* total cyanide for leachate, the next step is that rinsed ore will be collected for testing. Eight boreholes will be drilled and sampled and analyzed for Synthetic Precipitation Leaching Procedure (EPA method 1312). Only if the solids criteria identified above are exceeded will the heap leach material have to be graded and capped with 2 ft of waste rock.

After verification of rinsing and detoxification of the spent ore, the pregnant solution pond liner will be punctured to prevent the development of perched water in the heap. The center of the heap where the pond is located will be filled with spent ore, forming a low spot to the southwest corner. Rinsed spent ore from the east side of the heap leach area will be dozed and graded to cover the western part of the tailings impoundment.

No materials will be removed from the overall lined area as part of the heap leach closure. The chemical, physical, and biological characteristics of the heap leach facility will pose no potential environmental liabilities after the biological treatment is complete. Cyanide concentrations will be at an environmentally acceptable level, and the bacteria and nutrients are nontoxic. Active treatment will not be necessary after closure of the heap leach facility. No discharge control will be required after closure because of low precipitation and high evaporative losses. No limitations on future land or water uses will be created as a result of heap leach closure activities.

This closure plan presented for the heap leach pad is consistent with the State water quality and air quality permit requirements. This closure plan also meets the objectives established by the BLM including--

- All process fluids will be detoxified and evaporated from the site eliminating a potential for ground water contamination.
- The spent ore will be stabilized against wind or water erosion.
- The cover will be graded and compacted to minimize infiltration.
- The area will be returned to premining land use.

Plant Closure

The processing plant and facilities will be closed and reclaimed by removing buildings and equipment. Two buildings will remain as the claim holder will purchase and secure bonding. Should cyanide contaminated soils be identified, the material will be excavated and buried in the tailings impoundment. The only materials which will remain consist of broken concrete building foundations. These materials will be covered with waste rock and top soil. Natural vegetation will establish through invasion. No treatment or control of discharge will be required as a result of the closure of these facilities. No limitations on future land or water uses will be created as a result of mining or closure activities in these areas.

Tailings Impoundment Closure

The tailings impoundment facility was constructed with two cells to contain the tailings. A 40-mil PVC liner underlies both cells of the impoundment facility. Cell A was constructed with liner extending underneath the embankments. Cell B was constructed as a fully contained impoundment with liner extending up the embankment sideslopes on three sides. The west embankment of Cell B served as a center drainage core between cells A and B.

The tailings have been deposited as a slurry using thin-layer deposition techniques. The tailings were deposited in thin layers in a managed cyclic rotation to maximize consolidation and drying of the tails. Deposition in cell A started in the third quarter of 1987. In 1988 a downstream raise to cell A was constructed and cell B earthworks were also completed. The average production rate throughout the operating life was 2,900 st/d. Figure 3 graphically shows the tailings deposition history of cell B.

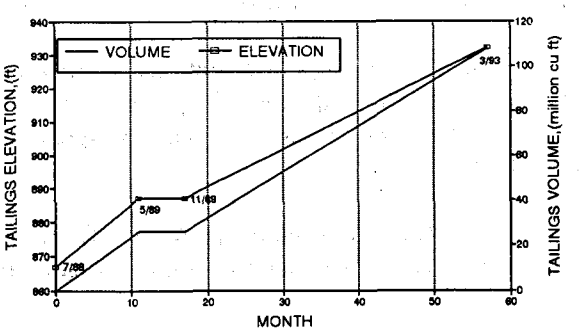

Figure 3. Tailings deposition, cell B.

The tailings facilities were constructed with internal drainage systems overlying the liner. Seepage collected in the underdrain system flows to the reclaim solution pond located outside the southeast corner of cell B. The tailings consolidate through self-weight and desiccation as water is decanted from an overlying pond, and by dewatering through the drainage system. The tailings deposition was managed to promote rapid drying of tailings, thus minimizing subsequent consolidation, and to allow placement of cover materials as soon as possible after project cessation.

In 1989 a net was placed over cell B to prevent avian mortality. This floating net consists of a polypropylene net suspended by cables. To allow permanent suspension of the net above the tailings, vertical risers were constructed. These were attached to polypropylene drums with a steel frame. These drums acted as "floats", raising the net as the tailings level rose. Maintenance activities were conducted on the net throughout the project life.

Closure and reclamation of the tailings impoundment started after milling ended. The polypropylene drums were punctured in March 1993 to allow them to be covered with tailings. After mill closure in June of 1993 evaporation of the excess tailings liquid evaporation began. It is expected that it will take at least six months to evaporate the remaining tailings and process solutions. The net will then be dropped on the tailings surface. Concrete scrap from the plant demolition and any cyanide contaminated soils will be placed on the net prior to covering it with about three feet of waste rock and spent heap leach material. The net will act as reinforcing while placing the cover thereby improving access.

The waste rock and spent ore will be spread and compacted with earthmoving equipment. Experience on site shows that these material break down readily under trafficking thereby forming a surface which will enhance runoff during the high intensity rainfall in the area.

Because of the expected settlement of the tailings surface over the first few years after cover placement it may be necessary to perform maintenance operations on the cap. Such maintenance may consist of regrading and reworking the cover surface to eliminate cracks and maintain positive drainage.

The reclaim solution pond liner system consists of a 30-mil XR-5 geomembrane liner and a 30-mil PVC geomembrane secondary liner. A leakage collection system between the primary and secondary liners includes a sand layer at the bottom of the pond and a drainage net in the pond sideslopes. Monitoring of the leak detection system located at the northwest corner of the reclaim pond is performed by sampling through a 4-in-diameter pipe.

The tailings impoundment closure requirements established in the State permit are as follows: the operator must assure that all solids will be properly capped with at least 3 ft of nontoxic native rock and solids; and, the area surrounding the tailing pond should be graded to preclude the migration of tailings off the impoundment during a 100-yr, 24-hr storm event.

In addition, any sludge or residue from the reclaim solution pond will be analyzed using U.S. Environmental Protection Agency approved methods for submittal to the agencies prior to burial or disposal.

Analyses of representative water quality samples from water collected from the tailings impoundment and water draining from the impoundment underdrain during operations indicated that free and weak acid dissociable cyanide are detected in significant quantities. These results indicate that the tailings water which ponds on the top of impoundment is of similar quality to the tailings pore water from the underdrain.

To determine the quantity and duration of water expected to drain from the tailings impoundment underdrain, a consolidation analysis was performed. During operations piezometers were installed at different depths and monitored in both cells A and B. A review of the piezometer data indicated that pore pressures during tailings deposition were less than the expected hydrostatic pressures at the piezometer locations. This indicates a downward

gradient in the tailings deposit, and that the tailings are normally consolidated. Because the tailings are normally consolidated, classical consolidation theory was used for the postoperational consolidation analysis.

This analysis evaluated settlement likely to be caused by the surcharge load provided by the cover material to be placed on the impoundment. These results suggest that the surcharge load would result in approximately 0.6 ft of settlement. Seepage from the tailings impoundment underdrain system is estimated to increase in response to the surcharge load. The initial seepage flow is estimated at 41 gpm during the first several months, decreasing to approximately 3 gpm within 1 yr of cover placement. It is recognized that classical consolidation theory is not appropriate for large strains and may over-predict the consolidation period. However, it is usually conservative and was deemed adequate for this project.

The performance of the engineered tailings cover was evaluated to estimate stormwater runoff and infiltration from the reclaimed surface. This evaluation was performed using the HELP model version 2.05. Site-specific evaporation and precipitation were used in this evaluation. Three cases were evaluated with the HELP model in which the hydraulic conductivities for a 3-ft-thick cover layer of $1x10^{-3}$, $1x10^{-4}$, and $1x10^{-5}$ cm/s were evaluated.

The results from the HELP model suggest that zero runoff is expected from the reclaimed tailings surface, and that 94% of the precipitation falling on this surface will be lost to evaporation for a $1x10^{-4}$cm/s cover layer. The remaining 6% will infiltrate the tailing deposit, where it would be collected in the tailings underdrain system. The average annual seepage rate for a $1x10^{-4}$cm/s cover is estimated as 0.16 gpm. When the hydraulic conductivity of the cover layer is reduced to $1x10^{-5}$cm/s, the surface evaporation is reduced to 77% of precipitation. For this case, surface runoff is estimated to be 23% of precipitation. A third case was evaluated in which the hydraulic conductivity of the cover layer is $1x10^{-3}$cm/s, resulting in 87% evaporation with zero runoff.

The results from the HELP model indicate that zero surface runoff is expected from the cover layer with a hydraulic conductivity of $1x10^{-4}$cm/s or less. The HELP model predicts that a peak daily precipitation for the site is 1.45 in. Zero runoff is also estimated for this peak precipitation event when the hydraulic conductivity of the cover is $1x10^{-4}$cm/s or less. Based on the texture of the cover material, it is unlikely that the hydraulic conductivity would be much lower than $1x10^{-4}$cm/s. Therefore, it can be concluded that very little runoff can be expected from the reclaimed tailings surface under average precipitation conditions.

A simplified water balance for the reclaim pond was evaluated to determine the volume of solution present in the pond during the postoperational and reclamation period.

Seepage resulting from consolidation will drain into the existing reclaim pond for evaporation during the first 2 yr. Based on on-site evaporation data (83 in lake evaporation per year) the evaporative capacity of the reclaim pond is 10.7 gpm. The initial seepage rate from the tailings impoundment is estimated to exceed the evaporative capacity of the reclaim pond for the first 6 months. During this period some buildup in solution may occur in the pond until a negative water balance is established. The pond has ample capacity to store this volume without overflowing. The netting covering the reclaim pond will be left in place until the reclaim pond is backfilled.

The reclaim solution pond closure will be conducted once the flow from the tailing impoundment drains drops below 10.7 gpm. As discussed above, this is the balance point between inflow and evaporation.

The pond will be reclaimed by covering the lined area with alluvium and waste rock. A standpipe will be installed in the infilled pond for water level monitoring. The seepage will infiltrate the cover materials and be retained as soil moisture content, or be lost to evapotranspiration.

The quantity of inflow into the reclaim solution pond is currently about 40 gpm. This inflow quantity is expected to diminish to approximately 3 gpm within 1 yr. Because of the potentially low quality of this water flowing into the reclaim solution pond, the liner will be left intact. The quantity of flow within 1 yr will be

insignificant. As such, filling in the pond with alluvium and waste rock will prevent the potential for wildlife exposure to the cyanide-bearing water.

In summary, no materials will be removed from the tailings pond during closure. The net will be dropped on the surface of the tailings after evaporation of excess tailings liquid is completed. Finally the tailings impoundment will be covered with 3 ft of waste rock and spent ore.

This closure plan also meets the objectives established by the agencies including--

- All process fluids will be detoxified and evaporated from the site, eliminating a potential for ground water contamination.
- The tailings will be stabilized against wind or water erosion.
- The cover will be graded and compacted to minimize infiltration.
- The area will be returned to premining land use.

Postclosure Monitoring

Postclosure monitoring by Copperstone will be performed to evaluate the success of the closure activities. The following monitoring activities will be performed:

- Water-level measurements will be recorded in the backfilled reclaim solution pond.
- A new groundwater monitoring well be installed downgradient of the tailings/heap leach area and sampled quarterly for total cyanide and metals for several years.
- Visual inspection of tailings impoundment cover.
- Visual inspection of stabilization and resistance of waste materials against wind and storm water.

Conclusions

The Copperstone Mine closure plan, as discussed above, is predicted to be successful for the following reasons: the mine closure activities result in a low-maintenance return to preexisting land uses; the mine closure activities comply with all State and Federal regulations; the site water management plan allows for detoxification and evaporation of all process solutions; and, the mine pit, waste rock disposal areas, heap leach facility, and tailings impoundment will all be stabilized physically and geochemically upon final closure.

Literature Cited

Mudder, T. and Whitlock, J., "Biological Treatment of Cyanidation Wastewaters", Minerals and Metallurgical Processing, pp. 161-165, August, 1984.

Smith, A. and Mudder, T., "The Chemistry and Treatment of Cyanidation Wastes", Mining Journal Books Limited, 1991.

Thompson, L.C., 1990. New technologies for mining waste management, biotreatment processes for cyanide, nitrates and heavy metals. In Proceedings of the Western Regional Symposium on Mining and Mineral Processing Wastes. (University of California at Berkeley, May 30-June 1, 1990.

Acknowledgements

TIMES, Ltd., Bozeman, MT, cooperated in developing the overall closure plan and more specifically Pintail Systems Inc., Aurora, CO, implemented the biological treatment system for heap decontamination.

THE GIBRALTAR NORTH PROJECT ASSESSING ACID ROCK DRAINAGE[1]

Robert J. L. Patterson[2] and Keith D. Ferguson[3]

Abstract: The Gibraltar Mine is a large open pit copper operation located north of Williams Lake , British Columbia. Acid rock drainage (ARD) was first discovered on the property in 1982. Since this period all drainage has been collected and pumped to the concentrator for neutralization in the lime circuit. Copper is also recovered from some of the waste rock dumps using sulfuric acid leaching followed by solvent extraction and electrowinning. The Gibraltar North project is a new ore body being considered for development. An extensive program of testing and analysis was conducted to determine the potential of the waste from the project to produce ARD and to develop mitigative measures. The quantity of potentially acid generating material was estimated in two ways. First, statistics for acid base accounting (ABA) data were used to estimate the percentage of waste rock and ore that would likely be acid generating. Second, the location of a pyrite "halo" was mapped using visual pyrite estimates and assay results; a sulfur criterion was developed to separate blocks that were potentially acid-generating. Estimates of the quantity of potentially acid generating material from the two methods were different because the ABA data base under represented the quantity of waste rock in the upper benches and over represented the quantity of waste rock in the lower benches. Results highlighted the need for careful selection of samples in ARD testing programs. The potentially acid-generating zones on the pit walls were mapped using the location of the pyrite halo. In this way the quantity and location of potentially acid and non-acid-generating walls were identified. The Gibraltar North tailing exhibited a significantly higher potential to generate ARD compared to the current tailing.

Additional Key Words: acid rock drainage (ARD), acid base accounting (ABA), acid-generation estimations, neutralizing potential, pyrite halo, sulfur plots, tailing acid generation, and pit wall acid generation.

Introduction

Location and Description of Operations

The Gibraltar Mine, which has been in operation since 1977, is located approximately 160 km south of Prince George, British Columbia, near McLeese Lake (fig.1). Access is by way of a 18 km paved highway that joins Highway 97 near the north end of McLeese Lake. The ore bodies occur as large low-grade copper-molybdenum porphyry deposits.

Ore is mined by the open pit method and is concentrated using conventional crushing, grinding, and flotation processes. Tailing is discharged to a impoundment area with 80% of the water recycled as process water. Additional copper is extracted from the waste dumps using sulfuric acid as a leach solution followed by solvent extraction and electrowinning to remove copper.

Ore reserves occur in five mineralized zones. These are the Gib West, Gib East, Polyanna, Granite Lake, and recently discovered Gib North zone. Mining has occurred in all zones except the Gib North, which is not being developed due to economic restraints.

---

[1]Paper presented at the International Land Reclamation and Mine Drainage Conference and the Third International Conference on the Abatement of Acidic Drainage, Pittsburg, PA, April 24-29, 1994.

[2]Robert J.L. Patterson, Sr. Environmental Engineer, Gibraltar Mines Ltd., McLeese Lake, British Columbia, Canada.

[3]Keith D. Ferguson, Environmental Manager, Placer Dome Canada, Vancouver, British Columbia, Canada.

Gibraltar North Pit Project - Description

The recently discovered Gib North Zone lies to the northwest of the Gib East pit and is intersected by the access road into the minesite. If developed, the projected pit dimensions will be 1,000 by 550 m by 230 m deep. Stripping will entail 7.2 million mt of overburden and 109 million mt of waste to produce 34.7 million mt of ore. As the zone contains a thick mantle of waste, stripping would take up to 4 yr to expose ore, followed by 3 yr of ore production.

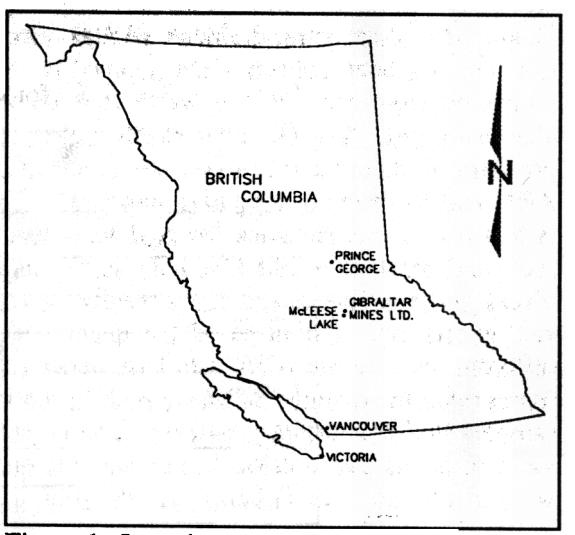

Figure 1. Location map.

Current Status of ARD

ARD was not detected at the minesite until several years after startup of mining. As early as 1975 copper-contaminated flows were detected coming out of rock fills on the property. It was not until 1982, an extremely wet year, that ARD manifested its presence throughout most waste fills on the property. The presence of this seepage prompted the construction of a property-wide collection and pumping system during the 1982 - 83 construction periods. All surface drainage was then treated and discharged to the tailing pond.

The present practice in regard to handling of wastes is disposal on a dump structure adjacent to the pit being mined. Each dump is surrounded by a ditch system for leach solution return where leaching is being practiced, as well as by a secondary ditch system to collect seepage out of the leach circuit. Reclamation steps have been execised on several dumps. Reclamation is geared more to aesthetic improvement than to ARD prevention, although the practice no doubt has had some mitigative benefits.

Acid-Base Accounting For The Gib North Zone

Sample Selection

A total of 27 vertical drill holes were chosen to obtain samples for acid-base accounting on the Gib North zone and were also used for metal analysis. These holes were all within the proposed open pit as currently planned and were distributed over as wide an area of the surface of the pit as possible. However, as limited drilling was conducted away from the ore body, fewer samples of waste rock were available from the upper benches distant from the ore zone.

Samples were composited over 13.7 m of core, which represents the proposed bench interval. The composites were made up from 3 m pulp samples. Each composite was comprised of five pulps with the fifth only half the mass of the other four. Four of the pulps were 50 g and the fifth was 25 g. A total of 395 samples were tested for ABA, including 151 ore and 244 waste rock samples.

Analytical Methods

Samples were tested for ABA according to the methods described in Sobek et al. (1978). The standard analyses for paste pH, total sulfur, sulfate sulfur, and neutralization potential (NP) were performed. In addition, a total carbon assay was obtained from the Leco furnace used for the total sulfur determination. The "fizz" rating and color of precipitate in the NP titration were also recorded. The acid potential (AP), net neutralization potential (NNP), equivalent NP from the carbon assay (assuming all the carbon was present as carbonate), and neutralization potential-acid potential ratio (NP/AP) were determined by calculation from the assayed ABA parameters.

An inductively coupled plasma metal scan was also performed on 326 samples (143 ore and 183 waste rock). Copper grade information, obtained from previous assays of the samples, was used to separate the samples into ore and waste, using a 0.18% copper cutoff.

ABA Results

ABA results for the waste rock and ore are summarized in tables and 2.

Table 1. ABA results for waste rock

Statistic	Paste pH	Total S, %	Potential, mt/kmt $CaCO_3$			NP/AP
			AP	NP	NNP	
Number	183	244	244	244	244	244
Mean	9.01	.66	20	24	3	5
Variance	.31	1.05	1023	284	1344	169
Std. Dev.	.55	1.02	32	17	37	13
Maximum	11.07	6.82	213	80	75	170
Upper quartile	9.43	.74	23	32	21	4.6
Median	9.07	.31	10	21	7	1.8
Lower Quartile	8.63	.14	4	10	-7	.7
Minimum	7.45	.01	0.3	3	-209	.02

In general the paste pH was neutral to alkaline. All of the sulfate sulfur assays were less than detection (not shown in table). These data suggest the samples had not oxidized significantly prior to testing and no acidic salts are present. The total sulfur was relatively low for waste rock with a mean of only 0.66%. The NP was very low with a mean of only 24 mt/kmt $CaCO_3$.

The paste pH was lower in the ore samples compared to the waste rock, with some relatively acidic paste pH recorded. Sulfate sulfur results were all below detection. Despite the low pH in some samples, very few oxidation products (acidic salts) had apparently accumulated. It is not clear if these oxidation products are present in situ in the ore or were formed after drill core recovery. The total sulfur and AP were substantially higher, and the NP slightly lower in the ore compared to the waste rock. In general the sulfur content (and AP) increased with copper grade (fig. 2) and is additional support for the existence of a pyrite halo around the ore body.

Table 2. ABA results for ore samples.

Statistic	Paste pH	Total S, %	Potential, mt/kmt $CaCO_3$			NP/AP
			AP	NP	NNP	
Number	143	151	151	151	151	151
Mean	8.03	2.98	93	17	-76	0.33
Variance	0.58	4.40	4296	146	4964	0.18
Std. Dev.	0.76	2.10	65	12	70	0.43
Maximum	9.31	11.5	359	62	39	2.7
Upper Quartile	8.62	3.54	111	26	-27	0.41
Median	8.15	2.47	77	14	-56	0.18
Lower Quartile	7.52	1.43	45	7	-106	0.08
Minimum	4.98	0.41	13	3	-355	0.01

The carbon assay results were converted to an equivalent NP, assuming all the carbon was present as carbonates. The actual NP and equivalent NP from the carbon assay agreed for most samples (fig. 3). About 10 to 15 samples had a higher carbon equivalent, suggesting that a portion of the carbon may not have been present as carbonate or that the NP was underestimated by the assay titration for a few samples.

An NP/AP of 1 (equivalent to NNP = 0) is sometimes used to separate potentially acid and non-acid generating samples. Plots of NP and AP relative to this criterion are shown in figures 4 and 5. About 35% of the waste rock and about 95% of the ore samples were potentially acid-generating. There was a slight trend to lower NP with a higher AP. Cumulative frequency plots for ABA parameters are shown in figure 6. The significantly lower acid production potential of the waste rock relative to the ore is apparent. Only about 5% of the waste rock was strongly potentially acid generating (NNP < -50 mt/kmt $CaCO_3$ or NP/AP < 0.2).

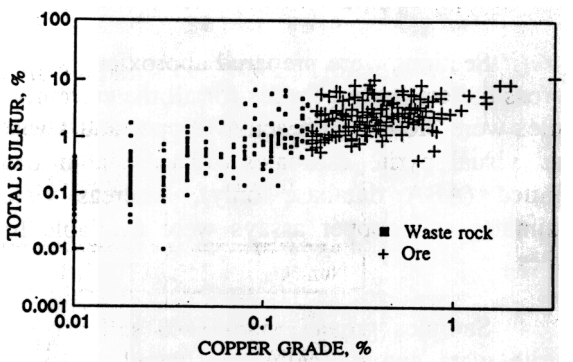

Figure 2. Sulfur versus copper grade

In general, the ABA characteristics of Gib North project waste rock are consistent with a low sulfur-very low NP system. A significant proportion of the waste rock according to ABA is potentially acid generating; however, the extent of acid production may not be large given the low sulfur content. The acid production potential correlates with the copper, and therefore the ore is much more strongly potentially acid producing than the waste rock.

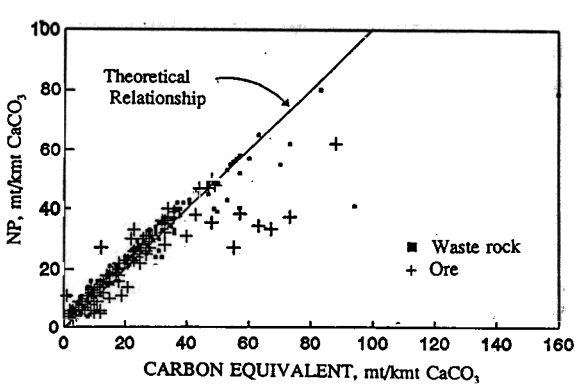

Figure 3. NP versus carbon equivalent.

Pyrite-Copper-Geology Database

An independent assessment of the quantity of material with a potential to produce ARD was made using visual pyrite estimates, copper assays, and the geological model of the Gib North deposit. The data indicate that there is a pyrite halo around the Gib North ore body, which should provide a reasonable estimate of the quantity of potentially acid-generating material. This halo can be identified by visual estimates of pyrite made by the geologists during core logging. Beyond the halo, the waste material is practically devoid of sulfide minerals.

The limit of the pyrite halo was chosen to be equivalent to a 0.6% total sulfur based on the following reasons:

1. Only 17% of the samples with less than 0.6% sulfur had a NP/AP less than 1, whereas 75% of the samples greater than 0.6% sulfur had a NP/AP less than 1 from the ABA database for waste rock.
2. At a 1:1 NP-AP ratio, 0.6% sulfur is equivalent to an NP of about 19 mt/kmt CaCO3, close to the median NP of 21 mt/kmt CaCO3 for the ABA database for waste rock.
3. Lappako (1991) found that rocks with less than 0.6% S did not produce ARD owing to neutralization by silicate minerals in long-term

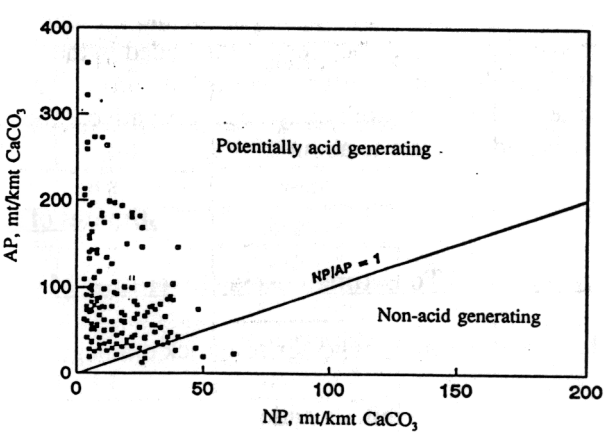

Figure 4. Ore AP:NP

field tests of low sulfur-containing rocks in Minnesota. This finding may not be universally applied to all minesites because of differences in sulfide mineral reactivity and climatic conditions at a particular site, however, it does serve as a useful guide.

4. From observation of drill core and sulfur data, a low sulfur value such as 0.6% S is a reasonable boundary to identify the extremity of the higher sulfur containing material.

Sections were prepared approximately every 18 m across the ore body. Traces for all the currently available holes were plotted with actual copper and sulphur assays and visual pyrite estimates. The sulphur dataset was limited (ABA database only), whereas visual pyrite estimates and copper assays were available for all the holes.

Samples greater than 0.6% sulfur or 1% visual pyrite were automatically considered to be within the pyrite halo. For values between 0.5% and 1.0%, the sulfur associated with the copper was added to the visual pyrite estimate assuming all the copper was present as chalcopyrite. Waste blocks were separated from the ore blocks using krigged copper estimates (0.18% Cu cutoff).

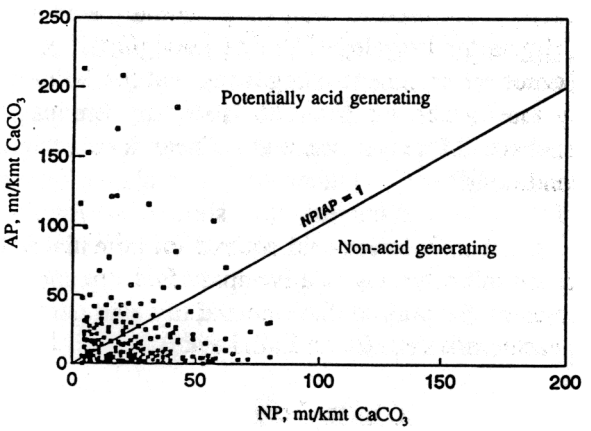

Figure 5. Waste AP:NP

The location of the pyrite halo on the drill hole traces was identified by the actual or calculated sulfur values. The geological model of the ore body was then used to identify the location of the pyrite halo between drill hole traces. The halo was assumed to follow the general outline of the ore body then contoured onto the section.

Finally the contoured sulfur halos on the sections were transferred to bench plans through the pit. The intersection of the bench level with the pyrite halo on each section was marked, and the resulting points were connected to identify the location of the halo on plan.

In general, there were very few discrepancies in the overall shape of the pyrite halo generated by the visual pyrite and by sulfur assay values; only small isolated pods of halo material in the upper part of the pit identified by the visual pyrite method were not included in the estimates based on the actual sulfur assay information. The visual pyrite method, therefore, may be conservative. The use of pyrite estimates to determine the location of the pyrite halo is believed accurate to about ±20%.

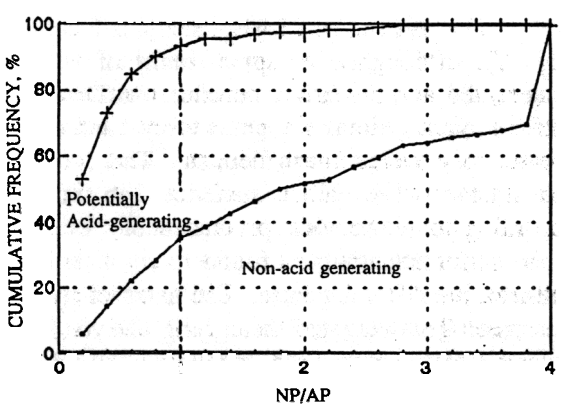

Figure 6. Cumulative frequency plots for NP:AP

Estimates of Acid-Generating Material

Criteria Used To Estimate Acid Generating Material

Three factors control whether acid rock drainage (ARD) is likely to be produced at a minesite:

1. The magnitude and variability in the maximum capacity of the rocks to produce and to consume acid.
2. The availability of potentially acid-producing and neutralizing minerals on particle surfaces.
3. The relative rates of acid production and neutralization.

Static methods such as acid-base accounting (ABA) directly assess the magnitude and variability of the maximum capacity of the rocks to produce and to consume acid. To make predictions, the results from ABA are compared with empirical criteria because mechanistic models of the acid production process are not available. The other two factors that control ARD production are included indirectly in these criteria. Separate criteria have been developed to classify homogeneous individual rock samples and heterogeneous rock dumps composed of several rock types with different acid production potentials.

Criteria for Individual Waste Rock Samples. Ferguson and Morin (1991) and Cravotta et al. (1990) both presented theoretical arguments suggesting that the NP/AP criterion could be about 2:1. However, in the database presented by the former authors, 166 laboratory leaching tests indicated no sample with a positive NNP produced acidic leachate. Moreover, there is no clear documented evidence of rock with a positive NNP producing ARD under field conditions.

A safety factor is required for mines in wet climates where carbonate minerals may be preferentially removed in the mine wastes relative to sulfide minerals. The precipitation at Gibraltar is only 500 mm/yr, therefore, the potential for preferential removal of carbonates should be low. A NNP = 0 (NP/AP = 1) should provide an adequate measure of safety for an initial evaluation of the ABA data.

Criteria for Tailings. Ferguson and Morin (1991) combined studies by Environment Canada of tailings deposits at 20 mines in British Columbia and by Lindahl (1990) at 15 mines in Sweden. Some of the Canadian mines were operating, whereas all the Swedish mines were abandoned. The authors found that the NP/AP = 1 criterion could be used to separate acid and non-acid-producing mines. This criterion was used for the Gib North project.

Acid Generating Waste Rock by ABA Dataset

The percentage of ABA samples from each bench generally follows the percentage of waste rock production (fig. 7), although the upper benches are somewhat under represented and the lower benches over represented. Since the sulfur content generally appears to increase with depth, the ABA dataset may overestimate the actual acid production potential of the waste rock. ABA statistics by bench were weighted according to waste rock production by bench. The weighted mean sulfur content was found to be 42% less than the mean sulfur of the ABA database. The two mean NP values are about the same. The weighted mean NNP and NP/AP indicate a lower potential to generate ARD, compared with the original database.

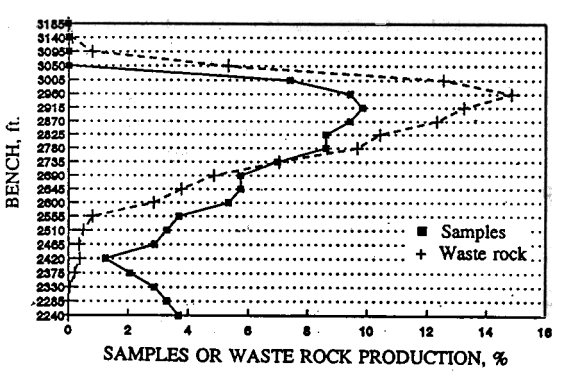

Figure 7. Percent samples and waste rock production by bench.

The weighted quantity of potentially acid-generating material was calculated by multiplying the percentage waste rock production per bench by the percentage of potentially acid-producing samples per bench according to the ABA dataset. The NP/AP < 1 criterion was used to identify the potentially acid producing samples. In general, about 28 million mt or 26% of the total waste rock production, is predicted to be potentially acid generating. This is 11% lower than the percentage of samples predicted to be potentially acid generating from the ABA database. The ABA database therefore was skewed because of too few samples in the upper benches and too many in the lower benches.

Most of the holes used for the ABA database were relatively close to the ore body and possibly were within the pyrite halo. Therefore, the weighted values calculated above may be conservative. This weighted value was compared to the quantity of material within the pyrite halos.

Acid-Generating Waste Rock Within the Pyrite Halo

The quantity of material within the pyrite halo (assumed to be potentially acid generating) was estimated by a block-counting method. A grid representing 15.2 x 15.2 m blocks was placed on top of each bench plan. The waste blocks within the pyrite halo and the pit boundary were counted, and the total for each bench was multiplied by 8,530 mt per block. This method is believed accurate, with the possible exception of errors introduced in counting partial blocks.

For some benches, the quantity of waste rock within the pyrite halo was apparently greater than the total quantity of waste from that bench; the error may arise from counting too many partial blocks. The percentage of potentially acid-generating material for these benches was simply adjusted to 100% and the tonnage recalculated. About 14.5 million mt of waste rock, or 14% of the total production, is predicted to be potentially acid generating using the pyrite halos method. This is about 13.5 million mt or 12% less than that calculated by weighting the ABA database. The pyrite halo method is believed more accurate because it accounts for smaller scale variations close to the ore body and is consistent with the geological model of the deposit.

Figure 8 shows the production of potentially acid-generating waste rock by bench using both the pyrite halo and the weighted ABA database. Both methods show most of the potentially acid-producing waste rock to be from benches 2960 to 2600. The weighted ABA database, however, indicated more potentially acid generating material would be produced from these benches.

Both methods of calculation indicated the percentage of potentially acid generating material would increase with depth, consistent with the increasing sulfur content. As the pit narrows with depth, more waste rock would be taken from within the pyrite halo, confirming that these percentages are consistent with the geological model. The percentage of potentially acid-generating waste according to the ABA dataset was higher than the pyrite halo for all but a few benches.

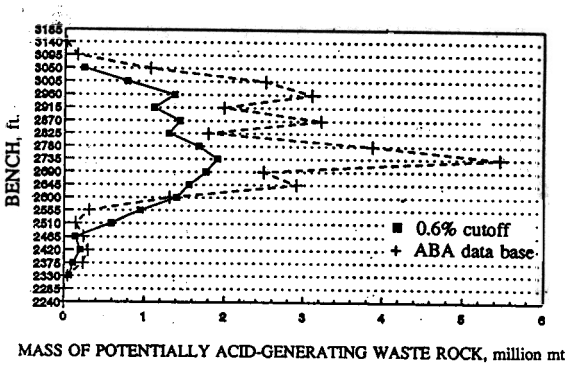

Figure 8. Production of potentially acid-generating rock by bench.

Pit Walls

The location of potentially acid-generating rock exposed on the ultimate pit walls was identified by projecting the pyrite halos onto the trace of the ultimate pit walls for each bench. As expected, pit walls remaining in the lower benches may be potentially acid generating, primarily below the 2600 level. Some potentially acid-generating material may also be left exposed at higher elevations on the south and east walls.

The exposed surface areas of potentially acid-generating and non-acid-generating pit walls were calculated for each bench by multiplying the running footage of the bench classified according to ARD potential by the cross-sectional length of the bench. The berm was assumed to be 14.6 m and the bench 15.2 m (overall angle 26.5°) for a total of 29.8 m. Overall, about 59% of the walls will be non-acid generating and 41% potentially acid generating. Less than 20% of the ultimate pitwall above the 2600 bench would be potentially acid generating. Below the 2600 level, more than 50% is potentially acid generating.

The pitwater originating from the upper portion of the pit should be alkaline with low metal concentrations. Runoff from the upper alkaline benches would flow over the potentially acid-generating walls. At least some neutralization of acidic drainage and coating of sulfide minerals should occur on these lower walls. Moreover, since

most of the potentially acid-generating walls will be exposed during the last stages of mining, they will have limited time to generate ARD prior to closure. Therefore, the pitwater should not be highly contaminated during mining.

At other minesites, pitwater is generally not as contaminated as seepage from waste rock dumps and abandoned tailings ponds because the surface area of exposed sulfide minerals is much less. The location of potentially acid-generating walls at lower levels in the Gibraltar North pit should further limit the potential for acid production.

Tailing

Ore Classification. Three types of ore were chosen for the metallurgical tests. These are:

Chlorite (GN-1) comprises only 1% of ore body. It is mainly a high level ore with distinctive dark green chlorite alteration; pyrite concentration are estimated at 2% to 4%; often elevated zinc.

Sericite-Chlorite (GN-2) comprises 80% to 90% of the orebody. It is hosted by a mixture of quartz-sericite, quartz-sericite-chlorite and chlorite; pyrite ranges from moderate to high; zinc is usually low.

Quartz-Sericite (GN-3) comprises 1% to 10% of the orebody. It is not always a good copper-silver host, particularly away from the ore zone.

Six head samples of ore were tested for ABA. These samples were chosen to represent specific types and characteristics of the ore and are not necessarily representative of the ore body as a whole. The ABA results are shown in table 3. The sulfur content of the metallurgical samples was high, corresponding to the 40th to over 80th percentile of the ore ABA database. The average was above the 80th percentile. The NP of these samples was low, corresponding to only the 15th to the 40th percentile, and therefore may represent a worst case ARD potential.

Weighted average ABA characteristics were calculated using the percentage of each ore type. The weighted average sulfur was relatively high (4.81%) and the NP very low (7 mt/kmt $CaCO_3$). The weighted average indicated the heads were strongly potentially acid generating.

Table 3. ABA data for ore head samples

Sample	Paste pH	Total Sulfur, %	SO_4, %	Potential, mt/kmt $CaCO_3$			NP/AP
				AP	NP	NNP	
GN-1	8.03	2.01	<.05	63	7	-56	.11
#1GN-2	7.44	3.52	<.05	110	5	-105	.05
#2GN-2	7.46	6.83	<.05	213	10	-203	.05
#3GN-2	7.36	3.44	<.05	108	6	-102	.06
#4GN-2	7.64	4.05	<.05	127	9	-116	.07
GN-3	7.51	8.23	<.05	257	4	-253	.02
Avg.	7.57	4.68	<.05	146	7	-139	.06
Std. Dev.	.22	2.15	0	67	2	67	.03
Max	8.03	8.23	NA	257	10	-56	.11
Min	7.36	2.01	NA	63	4	-253	.02

NA - Not applicable

Tailing. Eight separate scavenger and two cleaner tailings samples were analyzed for ABA. The cleaner tailings were from GN-2 ore, the largest ore type by mass. Three of the scavenger samples of the GN-3 ore type exhibited an acidic pH. These contained high sulfur (7% or greater) and very low NP. The low paste pH confirmed that scavenger tailings with high sulfur content would be acid generating. The sulfur content of the GN-1 ore type was much lower than that of the other two. NP levels of all samples were very low. All samples were potentially acid generating, although two were very marginal. In general, scavenger tailings from the GN-3 and some GN-2 ore types were strongly potentially acid generating.

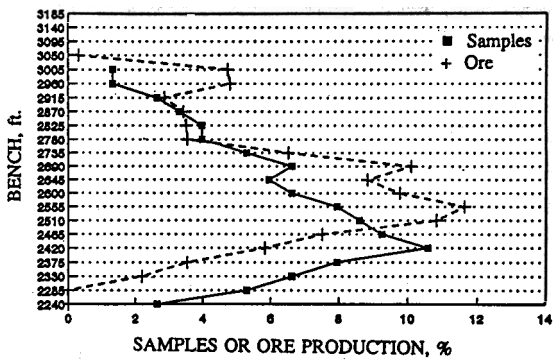

Figure 9. Percent samples and production by bench.

The ABA dataset for the Gib North ore samples was weighted according to ore production by bench in the same manner as for waste rock. In general, the percentage of samples and percent ore production by bench were in better agreement than for waste rock (fig. 9). The weighted mean values for the ABA characteristics were similar to the mean values from the raw data (table 4).

Table 4. Summary of weighted statistics for ore.

Statistics	Statistics for Gib North Ore			
	Sulfur, %	Potential, mt/kmt $CaCO_3$		
		AP	NNP	NP/AP
Absolute Mean	2.98	17	-76	.33
Weighted Mean	2.88	17	-73	.34

From results it is obvious that the Gib North ore is potentially acid generating. The finding of an acidic paste pH in some samples indicates acidic leachate would be expected from samples with elevated sulfur and very low NP. The metallurgical testing indicated the acid production potential of the ore would be reduced by about 27% due to milling. However, the scavenger, cleaner, and combined tailings are still expected to be potentially acid generating. Only the GN-1 ore type gave marginally acid-producing tailings, but that ore type comprises an insignificant proportion of the total ore feed. The Gibraltar North scavenger tailings have a significantly higher sulfur content and net acid production potential compared with the Gib East pit tailings currently being produced (table 5).

Table 5. Comparison of tailing from two ore zones

ABA statistic	Gib East[1]	Gib North[2]
Total sulfur	.81	3.46
NP	9	6
NNP	-16	-102

[1]Mean of 4 samples
[2]Weighted mean

The coarse fraction of the Gib North tailings is expected to have a higher acid production potential than the fines. Cycloned tailings, probably largely comprised of the coarse fraction, are currently used for am construction. The existing tailings dams could become potentially acid generating if the Gib North tailings were used for construction. The existing tailings pond slimes may also become potentially acid generating if Gib North tailings were deposited within the current basin. The tailings from the Gib North project need to be disposed of in a secure

location to ensure ARD will not become a problem.

Conclusion

On the basis of the test work the following conclusions can be drawn.

♦ This study illustrates the importance of conducting a thorough assessment of the potential to produce ARD prior to mining. Placing tailing from the Gib North project onto the beach or dam at the end of mining could have a significant impact on acid production.

♦ The goal of any program should be to establish consistency between geochemical test results, geological knowledge of the deposit, and water quality information. If consistency can be established, the conclusions developed from the program will have greater confidence.

♦ Collecting representative samples is not a simple task. Samples should be sorted by grade, occur within the pit boundary, cover the range of rock types, provide good spatial coverage, and be proportional to the waste quantities by bench and by rock type. A significant number of samples are often required to provide a reasonable dataset. Even in this study, weighting of ABA statistics by bench showed the raw dataset was somewhat skewed.

♦ Visible pyrite estimates are not always accurate, but when combined with metal assays and a geological model they can provide a check of geochemical test results and identify smaller scale versions in acid generation potential.

Literature Cited

Cravotta III C.A., K. C. Brady, M.W. Smith, and R.L. Beam. 1990. Effectiveness of the addition of alkaline materials at surface coal mines in preventing or abating acid mine drainage: Part 1. geochemical considerations. Proceedings of 1990 Mining and Reclamation Conference and Exhibition. (April 23-26, 1990, Charleston, WV)

Ferguson, K.D. and K.A. Morin. 1991. The prediction of acid rock drainage - lessons from the database. Proceedings of International Conference on the Abatement of Acidic Drainage. (September 16-18, 1991, Montreal, PQ).

Lapakko, K. 1991 Non ferrous mine waste characterization project status report. Minnesota Department of Natural Resources.

Lindahl, L.A. 1990. Acid mine drainage - research and remedial actions in Sweden.Proceedings of Acid Mine Drainage -Designing for Closure - GAC/MAC Joint Annual Meeting. (May 16-18, 1990, Vancouver, BC).

Sobek, A.A., W.A. Schuller, J.R. Freeman, and R.M. Smith. 1978. Field and laboratory methods, applicable to overburdens and minesoils. EPA 600/2-78-054, 203 p.

REGULATORY CONTROLLED DESIGN - LOUVICOURT PROJECT - A CASE STUDY[1]

Michel P. Filion[2], Frederick W. Firlotte[3], Michel R. Julien[3] and Pierre F. Lacombe[4]

Abstract: The Louvicourt Project, a base metal mining development near Val d'Or, Québec, Canada, is currently the largest new mining project under construction in Canada. The deposit discovered by Aur Resources Inc. in 1989 is a polymetallic orebody of copper, zinc, gold and silver. The tailings produced will have a high acid generation potential. Six potential sites for the future tailings basin were identified and compared against a series of criterion. The main objective in the site selection process was to identify sites that could permit flooding of the tailings from day one during and after operation. The selected site was retained on the basis that it satisfies sound environmental review, permits flooding of tailings during and after operation, facilitates closure and was not expected to cause delays during the approval process based on the current regulatory environment in the province of Québec. The construction of Phase 1 of the proposed basin was completed during the fall of 1993 and filling of the basin is currently underway.

Additional Key Words: tailings basin, water cover, acid mine drainage, site selection, regulatory environment.

Introduction

This paper discusses the site selection process and engineering design considerations for the new Louvicourt tailings area located near Val d'Or in northern Québec, Canada. The site selection process involved an examination of the various physical, environmental and permitting constraints related to the potential sites identified. An important factor in the overall site selection and engineering design was the environmental design philosophy established by the project participants during the early stages of project development. These factors resulted in the selection of a site which conformed to environmental requirements, minimized impact on the environment and fell within the economic constraints of the project.

The Louvicourt Project is a joint venture between the operator Aur Louvicourt Inc. (a wholly owned subsidiary of Aur Resources Inc.) (30%), Teck Corporation (25%) and Novicourt (a subsidiary of Noranda) (45%). The project is the most significant new base metal mine development in Canada with undiluted geological (in-situ) reserves in excess of 27 Mt averaging 4.3% Cu, 2.1% Zn, 27.4 g Ag/t and 1.06 g Au/t using an equivalent cutoff grade of 2% copper based on surface drilling data. The orebody was discovered in 1989 and start-up of the 4000 t per day mill is expected to occur in July 1994. The brief amount of time elapsed between discovery and start-up could not have been possible without the economic development policies of the Government of Québec and what we have termed regulatory controlled design. Total capital cost of the project has been estimated at 349M$ including working capital and capitalized interest, totalling 30M$. The mine will employ 340 people at full production and will be in operation for 18 years. Operational assumptions are summarized in Table 1. General design criteria for the tailings basin used in the tailings site selection study are given in Table 2.

---

[1]Paper presented at the Third International Land Reclamation and Mine Drainage Conference and the Third International Conference on the Abatement of Acidic Drainage, Pittsburgh, PA, April 24-29, 1994.

[2] Michel P. Filion, Director, Environmental Affairs, Teck Corporation, Vancouver, BC, Canada.

[3] Michel R. Julien, Geotechnical Engineer, Frederick W. Firlotte, Principal, Golder Associates Ltd., Pointe-Claire, PQ, Canada.

[4] Pierre F. Lacombe, Mill Superintendent, AUR Resources Ltd. - Projet Louvicourt, Val d'Or, PQ, Canada.

Table 1. Summary of operational data.

	Quantity
Reserves (assumed)	24.0 M t
Concentrates (18%)	4.3 M t
Tailings backfill (50%)	12.0 M t
Tailings disposal (32%)	7.7 M t

Table 2. Tailings area design capacity (assuming an in-place dry density of 1.7 t/m^3).

	Tailings (M t)	Volume (M m^3)	Percent (%)
Assumed reserves (24 M t)	7.7	4.5	55
Assumed additional reserves (3 M t)	1.0	0.6	7
Mine water sediments	0.5	0.3	4
Placement inefficiencies	-	1.7	21
Contingency	1.9	1.1	13
Total design capacity	11.1	8.2	100

Constraints

Tailings Properties

The typical mineralogical composition of the tailings is characterized by a sulphide content (mostly pyrite) that will be on average about 40% and a carbonate content which will vary from about 11 to 23%. Some acid base accounting tests have been carried out on samples of the future ore and waste rock. From these results and experience with similar tailings in the area, it is expected that the tailings will be a net acid generator. Depending on the zone of the orebody, it is believed that the theoritical acid production will vary from about 10 to 1000 kg/t and the buffer capacity will vary from 0.5 to 35 kg/t. The waste rock will also have variable theoritical acid production potential and buffer capacity (< 0.3 to 370 kg/t and 5.9 to 98 kg/t, respectively).

Physical Constraints

The area surrounding the mine site is characterized by low topographic relief, generally poor drainage, frequent swamps, and a few scattered, small, relatively shallow lakes. The main topographic relief through the area is a southwest-northeast esker ridge located on the east side of the mine site that is a local source of fresh water, sand and gravel.

The area has moderate net positive precipitation. The average annual precipitation for the Val d'Or area for the recorded period (1961 to present) is 954 mm. If the average annual evaporation or evapo-transpiration is subtracted, the net annual precipitation is about 413 to 465 mm.

The watershed boundaries and drainage patterns for the project area are shown on figure 1. The area is interesting because it contains the drainage divide for three principal watersheds. The mine site is located in the Harricana River watershed which flows northward toward James Bay. Immediately over the esker ridge to the east of the mine is the Nottaway River watershed which also flows to James Bay. About 11 km south of the mine is the drainage divide between northward-flowing rivers and the southward-flowing Ottawa river watershed, which eventually drains into the Saint-Lawrence River.

In the Val d'Or region, the Harricana River watershed has historically been heavily impacted by mining operations. Mining activity in the Nottaway and the Ottawa River watersheds has been minimal. West of the mine, in a radius of 20 km and within the Harricana River watershed, at least 6 old or active tailings basins can be identified. In particular, two rivers west and north of the mine site (Bourlamaque and Colombière) are known to have been seriously impacted over the years by mining activity.On this basis, the Harricana River watershed was the preferred one in which to locate a large tailings basin.

There are no towns or communities in the vicinity of the mine site. There are some cottages along the lakes located east and north of the mine site. The area does not contain exceptionnal habitats for wildlife. However, virtually all of the creeks and small rivers have been occupied by beaver communities. The recreationnal usage of the area is limited mainly to hunting and fishing.

Regulatory Considerations

At the beginning of the project, the design team met to discuss the permitting procedures in Québec and to delineate an overall schedule of activities. A major constraint to the project was set by the fact that the construction of the tailings dam and other major project components, such as the mill, had to begin during the spring of 1993 if the major project milestones were to be met on schedule. This therefore allowed a total of 14 months for the environmental assessment documents to be completed including baseline studies (which had been already initiated), feasibility studies and detailed engineering designs. Project start-up was scheduled for July 1994.

In Canada, major projects are subject to environmental requirements established by the Federal Government as well as the provinces. The laws and regulations for the federal and provincial jurisdictions contain a number of constraints which can trigger detailed environmental impact statements and full public consultation. Since these processes can result in time delays of at least 18 to 24 months in the overall permitting procedure, the design team set out to identify all possible triggers with the objective of designing an environmentally sound project while avoiding potentially lengthy delays in the process.

Federally, impact assessments are administered through the Environmental Assessment and Review Process (EARP). This process is currently under formal review and will be replaced by the Canadian Environmental Assessment Act (CEAA) probably in 1994. However, during the process of defining regulatory requirements it was assumed that the draft regulations based upon CEAA might apply in some form to the development. A thorough review of the draft regulations identified two potential triggers which might require that a detailed impact assessment be undertaken on the Louvicourt Project:

- diversion of a navigable water way; and
- building of a railway spur.

Environmental assessment requirements in the province of Québec are detailed in the Environmental Quality Act (Government of Québec, 1989, Q-2 r.1, Q-2 r.9). The triggers pertinent to the Louvicourt Project which would require, beside the necessary environmental study, the preparation of a detailed environmental impact statement with consequent possible public hearing, included:

- diversion of a named river;
- placement of waste materials in a lake;
- construction of a railway spur greater than 2 km in length;
- creation outside the main tailings basin of a pond greater than 5 ha in surface area; and
- construction of a permanent access road greater than 2 km in length.

At all stages during the planning and design of the project the above triggers were kept in mind and avoided.

The Québec Ministry of Environment (MENVIQ) has established several administrative regions or districts. Under the Environmental Quality Act, each regional director of the administrative districts has the authority to issue Certificates of Authorization for different phases of project development. For mine developments, environmental requirements and submissions are administered through Directive 019 (Government of Québec, 1989, Directive 019). The principal components of Directive 019 include:

- application of the provincial liquid effluent regulations at the final point of discharge; and
- detailed guidelines as to the information requirements to be submitted for the various types of Certificates of Authorization (COA) to be issued.

Four authorizations are specified as requirements in Directive 019; COA-exploration, COA-tailings site selection, COA-ore extraction and COA-mineral treatment. Of these four authorizations the two most significant to Louvicourt were approval of the tailings site selection document and mineral treatment. The COA for mineral treatment allows for the construction of the tailings area and milling facilities.

The Québec Government recognizes that the time frame for the development of new grass roots projects can be shortened by allowing the construction of certain aspects of the facilities in parallel with the environmental approvals process. Thus, separate approvals can be obtained for certain project components such as: exploration shafts and headframes; production shaft and headframe; mine surface facilities such as electrical substations, generator stations, wharehousing, hoist rooms, underground ventilation facilities, administration and maintenance facilities. In addition, with appropriate environmental documentation, it was possible to obtain phased approvals for clearing and logging a preferred tailings site; clearing and preparing borrow sites; construction of small access roads and pipelines; installation of construction camps prior to tailings dam construction; construction of the concrete foundation for the mill; and construction of Phase 1 of the tailings facility. All of these approvals were obtained prior to the issuance of the final certificate of authorization for mineral treatment. The resulting net benefit to the overall project was a time saving of over two years in relation to an impact assessment procedure which precludes any construction prior to completing the process. In the end, the total number of approvals required for the Louvicourt Project from inception to the beginning of operations totalled 46.

Environmental Design Philosophy

Because the environmental approval process allows for the expenditure of hundreds of millions of dollars prior to receiving operating approval, an aggressive position was taken with respect to the environmental design of the overall facilities. The fundamental design philosophy that was established for the project was intended to reduce regulatory uncertainties in receiving approval and to maximize protection of the environment. Upon review of the available technologies, it was considered that permanent storage underwater from day one could be an effective way to inhibite tailings oxidation as confirmed by recent works (Robertson, 1991; Morin, 1993 and Pedersen et al., 1993). Taking into account current and projected regulatory requirements in Canada, the design philosophy established for Louvicourt is summarized as follows:

- design for closure and operate for closure;
- tailings will be acid generating and will be managed as such; best available technology economically achievable (BATEA) will be used to prevent acid rock drainage (in the case of the Louvicourt project BATEA meant placement of fresh tailings under water in a man-made facility);
- minimize the quantity of ARD producing waste materials generated by the facility. (i.e. maximize the placement of waste materials underground);
- maximize water recycle; and
- use mother nature to advantage wherever possible.

When taken as a group, the design philosophy had a significant overall effect on all decisions related to site selection and design. In practice, this meant that a tailings site had to be selected so as to provide good topographic relief and hydrogeological containment sufficient to maintain a permanent water cover over the tailings; a watershed of sufficient size to ensure maintenance of a water cover even during drought conditions and to obtain seepage losses and flows through the tailings that were relatively small. The design philosophy also governed: dam design (geometry, slopes, erosion protection), the requirements for both operational and emergency water control structures and management of the upstream watershed.

Site Selection Study

A site selection study was carried out to identify possible sites that would allow flooding of tailings during and after operation. A total of 6 sites (sites 1, 2-A, 2-B, 3, 4, and 5) were identified in the area surrounding the mine site (figure 1). A list of selection criteria was prepared and each of the sites were evaluated and reviewed with respect to:

Technical and Economic Considerations

- minimum storage of 4.5 M m3 of tailings (7.7 M t at 1.7 t/m3) to accommodate at least the in-situ reserves;
- distance from the mill (the maximum distance - radius was set to 15 km);
- area of the tailings basin - to be minimized;
- expansion potential - to be maximized;
- maximum length of dykes - to be minimized;
- maximum elevation of the dykes - to be minimized;
- difference of elevation between the mill and the basin - to be greater than 0 if possible;
- accessibility around the basin with existing roads and with future roads; and
- mineral potential under the basin had to be shown to be poor or non existent;

Geology and Physical Features

- foundation conditions which effect dam stability; and
- topographical containment.

Hydrology and Hydrogeology

- location with respect to major watersheds;
- drainage area of the basin to allow flooding during and after operation;
- diversion required;
- length of diversion channels;
- flows to be diverted;
- tailings basin proximity to rivers or lakes;
- water recirculation potential; and
- ground water infiltration potential;

Ecological Considerations

- type of vegetation;
- clearing requirements;
- aquatic background;
- recreational use; and
- unique or exceptional habitats.

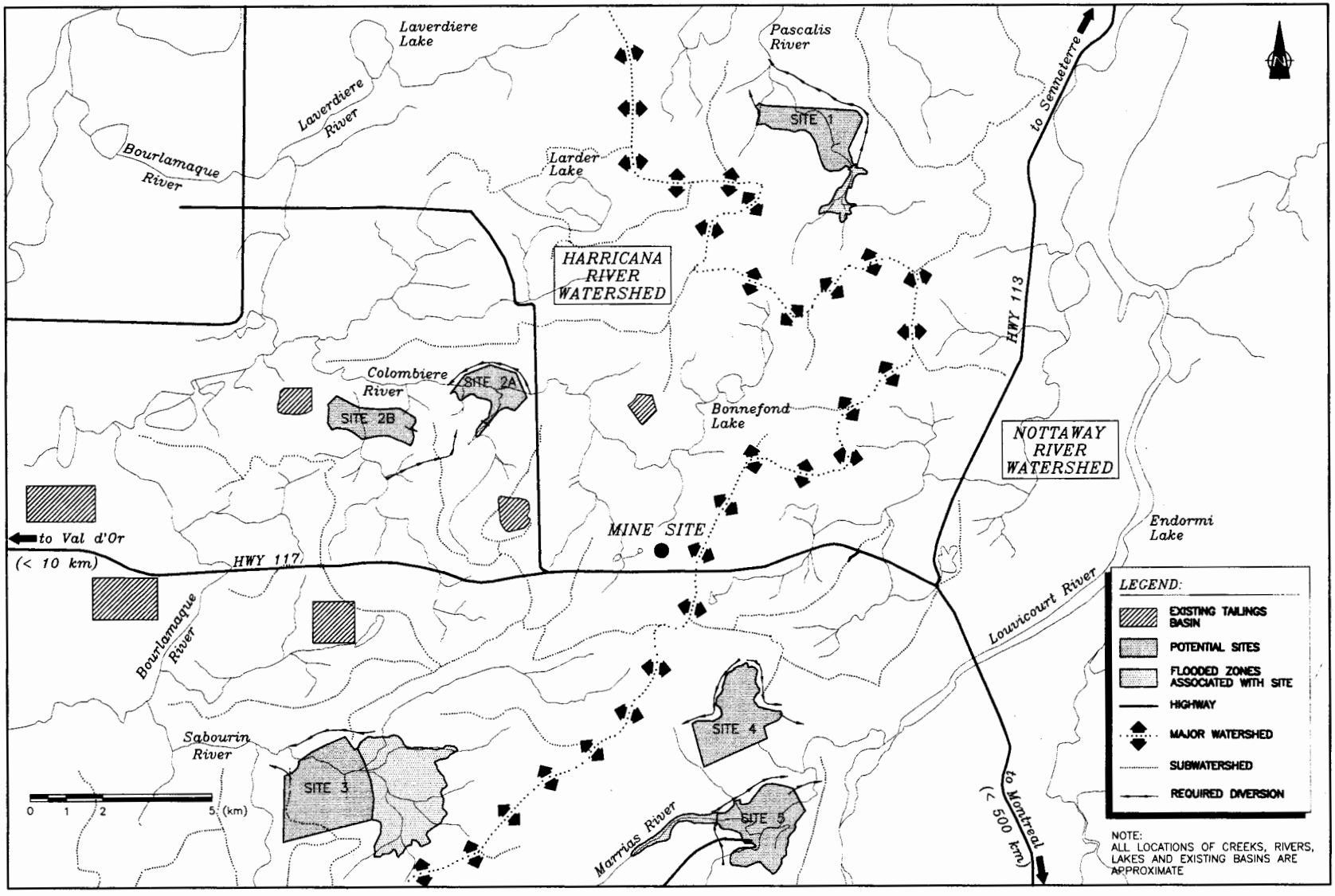

Figure 1. Location of six potential tailings basin sites in a 15 km radius of the Louvicourt Project. Also shown are major watershed and subwatershed limits as well as existing tailings basins.

Social Considerations

- distance from nearest houses;
- land use and ownership prior to operation;
- land use after operation; and
- aesthetic impacts;

Others

- mining rights on the properties;
- implications on pipeline path; and
- compliance with environmental design philosophy.

The following paragraphs review the characteristics of the 6 different sites and present a summary of the comparison between them.

Site 1 is far (13 km) from the mill. It is in the Pascalis river basin located in the Nottaway river watershed, which has not been much affected by mining operations. The area is swampy. Natural topographical confinement is good but the basin would have to be shallow. Therefore, long confining structures, most likely built through peat, would be required. The operator does not control mining rights in this area. Site 1 requires the diversion of the Pascalis river valley for a distance of 4.5 km.

Site 2-A is the closest to the mill and is situated in the Colombière River valley in the Harricana river watershed about 6 km from the mine. There are important upstream watersheds that could provide water for flooding in the post-operational period. Diversion of the Colombière river would be required as well as the development of a significant flooded area upstream of the basin. Topographical confinement is good, expandability is good, and this site is located on lands partially controlled by the operator.

Site 2-B is also located in the valley of the Colombière river about 8.5 km from the mill. The basin corresponds to a topographical low in the river sub-watershed. Topographic confinement is good and the subwatershed upstream of the basin can be diverted during and after operation. Expandability is good, a river diversion is not required, and the property is controlled by the operator.

Site 3 is located within the watershed of the Harricana river, more than 11 km from the mill, on property controlled by the operator. A large sub-watershed is present upstream of the basin to enable flooding at closure but because of a lack of topography the tailings placement would be shallow and therefore the site would be difficult to manage and would cover a large area. Development of site 3 could require the diversion of a river.

Site 4 is located about 6 km from the mine in the Nottaway river watershed which is currently not significantly affected by mining operations. The site offers poor topographical confinement. Upstream watersheds for future submergence of tailings are limited. The ground surface elevation of this site is about 13 m higher than the mill. The site is located on lands partly controlled by the operator.

Site 5 is located about 8 km from the mill in the Nottaway river watershed. The site has good potential for a small tonnage of tailings but is most likely too small to accommodate the design tonnage and offers little expandability without having to resort to extensive confining structures. The site would require the diversion of the Marrias River and the lands are not controlled by the operator.

Only Sites 2-B and 4 were considered to be compatible with the overall environmental design philosophy selected for the project.

Site Selection

Following the application of the previously described selection criterion, Site 2-B was considered to be the most attractive in terms of storage capacity, overall impacts, ease of closure, and compliance with the environmental design philosophy. The layout of the basin is given on figure 2. The main difficulty associated with this site was the diversion of the unnamed creek draining the area south of the basin. This creek, at the time of the design had a heavy contaminant load caused by acidic drainage from tailings south of the subwatershed limits. Diversion alignments to the east and west of the proposed tailings facility were examined.The option selected was the easterly diversion of the unnamed creek into the subwatershed to the east, resulting in the discharge of the unnamed creek into the Colombière River some 4 km upstream of the original location. A west diversion channel was also considered but the east diversion was found the most secure, since it offers natural topographic containment between the diversion channel and the basin. The west diversion would require the construction of a channel close to the proposed tailings basin and the existing Aurbel tailings basin west of the selected basin.

Despite the magnitude of the confining structures the site offers, with the available external watersheds, good potential for flooding during and after the operating life as well as acceptable foundation conditions under the basin and the dams; good expansion possibilities and no indication of important mineralization . It also allows construction of water control structures founded in rock which allows for more secure operation and simplifies the closure works. The final development scheme for the basin involves the development of the basin in two Phases. Phase 1 includes the construction of the east cell and the polishing pond. Phase 2 involves the construction of the west cell and the east diversion channel.

In order to minimize seepage losses to a level considered accepable, construction of low permeability dam cores and key trenches, and the construction of low permeability blankets and bedrock grouting were included in the design.

Construction of the east cell was completed on time and within budget during the fall of 1993. Flooding of the basin is currently underway. It is expected that the water cover will be adequate when operation starts to enable submergence of the tailings from day one. The water management strategy may require, for some years, short duration exposure of the tailings beaches during the coldest months of the year, December and January (average temperature -13.2 and -16.8°C). It is not believed that this short exposure during operation will be sufficient to trigger AMD generation. Table 3 provides a summary of the design characteristics of the tailings basin. An equivalent average infiltration rate is also provided for information.

Table 3. Summary of tailings basin characteristics.

	(Phase 1) East cell	(Phase 2) West cell	Whole basin
Total solid capacity (M t)	7.1	4.8	11.9
Total solid storage (M m^3)	4.2	2.8	7.0
Expected operating life (years)	12	8	20
Minimum water cover (m)	1.0	1.0	1.0
Free board of dykes(m)	2.0	2.0	2.0
Tailings basin area (ha)	96	68	164
External watershed draining to basin (ha)	76	50	126
Estimated seepage losses (M m^3/year)	0.4	-	0.5[1]
Average infiltration rate (m^3/m^2/year)	0.4	0.3	0.3
Discharge period (april to november - 8 months)	yes	yes	yes
Effluent discharged of the system (M m^3/year)	3.1	2.7	3.6[2]

[1] The estimated seepage losses include both east and west cells.
[2] During operational period only.

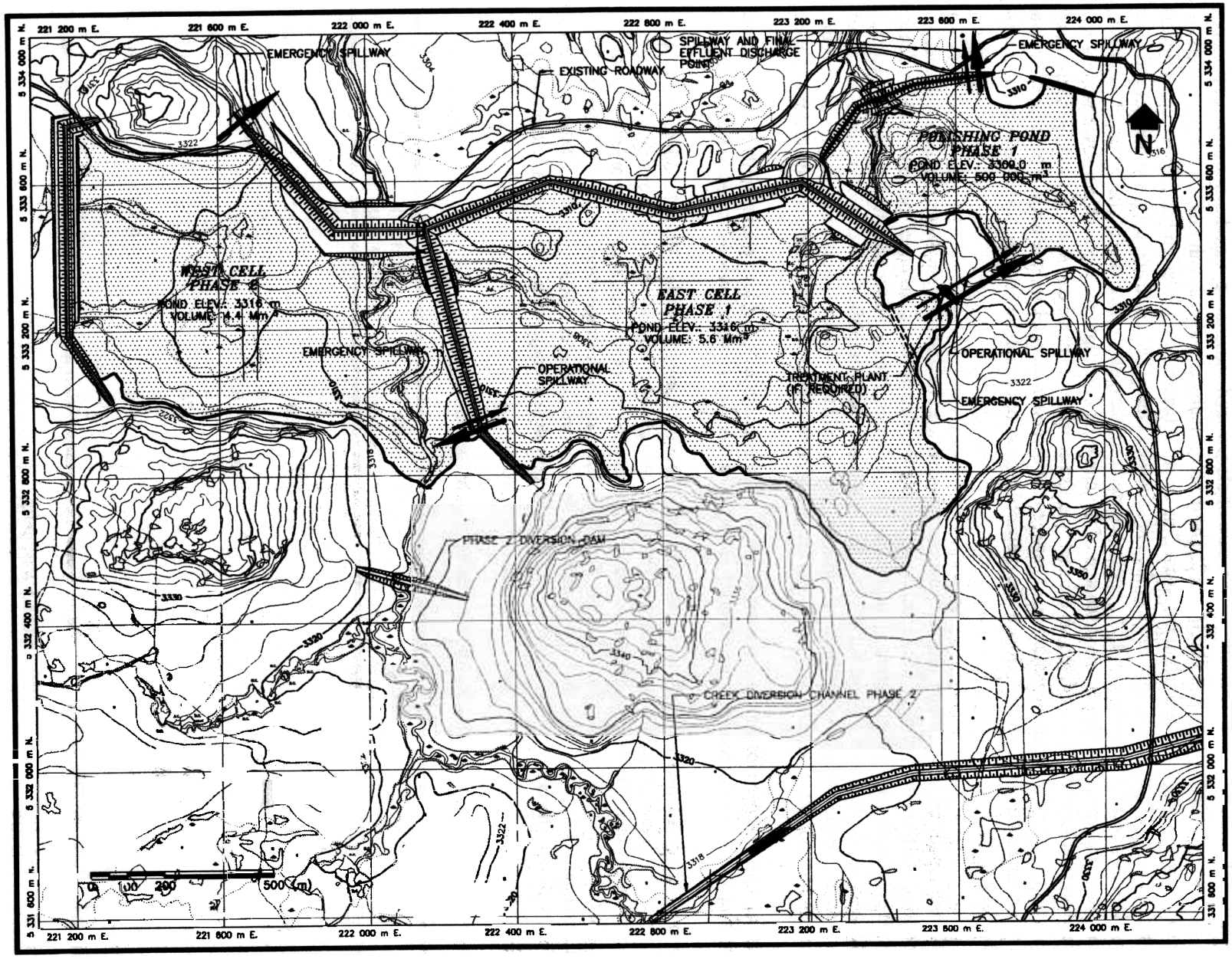

Figure 2. Louvicourt Project tailings basin (Site 2-B) configuration (Phase 1 & 2), with location of confining structures, operational and emergency spillways and the east diversion channel.

Conclusions

The Louvicourt Project is an example of a modern mine development designed to meet stringent environmental criteria established by both the regulators and the proponents. The design of the facilities has been undertaken using the best available technologies which have been established through operational experience and research conducted under the National Mine Environment Neutral Drainage (MEND) program. The speed with which the project was designed, approved and built could not have been achieved without the pro-active policies established by the Québec Government. These policies allow for the construction of key components of a project while permitting is underway. Since construction can proceed in parallel with the permitting process, the time frame for development of grass roots projects can be reduced by up to two years. This process requires significant commitments by the developers since the expenditure of hundreds of millions of dollars cannot be risked by submitting inadequate environmental design information. The process includes an expectation that approvals will be granted subject to conforming to environmental requirements and requires cooperation, faith, goodwill and trust of all participants. On the negative side, if operating approvals are not granted within established time limits the developers could be forced to accept conditions they would not otherwise agree to. In addition, the prescriptive approach provided in Directive 019 can reduce the flexibility in preparing environmental documents which address the site specific concerns of a facility. We believe that it is impossible for regulatory agencies to include in one regulatory document all of the potential variables which need to be considered, particularly with respect to the site specific nature of mine developments.

Literature Cited

Government of Québec (MENVIQ), 1989. Règlement relatif à l'administration de la loi sur la qualité de l'environnement L.R.Q. cQ-2, r.1.

Government of Québec (MENVIQ), 1989. Règlement sur l'évaluation et l'examen des impacts sur l'environnement, L.R.Q. cQ-2, r.9.

Government of Québec (MENVIQ), 1989. Directive 019, Industries minières.

Morin, K. A. 1993. Rates of sulfide oxidation in submerged envrionments:implications for subaqueous disposal. 17th Annual Mine Reclamation Symposium, Port Hardy, British Columbia, May 4-7, 1993.

Pedersen, T. F. , B. Mueller, J. J. Mcnee, and C.A. Pelletier, 1993. The early diagenesis of submerged sulphide-rich mine tailings in Anderson Lake, Manitoba. Can. J. Earth Sci. 30, 1099-1109 (1993).

Robertson, J.D. 1991. Subaqueous Disposal of reactive mine waste: An overview of the practice with case studies. p. 185-200. In Proceedings of the Second International Conference on the Abatment of Acidic Drianage. (Montréal, PQ, September 16-18 1991).

DECOMMISSIONING OF TAILINGS AND WASTE ROCK AREAS AT STEKENJOKK, SWEDEN [1]

Per G Broman and Torbjörn Göransson [2]

Abstract: The zinc-/copper deposits at Stekenjokk were discovered in 1918. Operations started in 1976 and continued until October 1988. The operation left a 110 ha tailings and clarification pond, a minor open pit, waste rock dumps and surface installations mainly comprising a head frame with ore bins and a combined concentrator, workshop and office building.

The tailings pond contained some 4,4 Mtons of tailings, grading approximately 20 % sulphur, making the material a potential AMD source.

A conceptual decommissioning plan for the area was approved in 1983. The detailed planning commenced in 1986 and took almost three years to complete. The solution selected was based on a flooding concept. The decommissioning was largely completed in 1991 with minor completion works in the two following years.

The paper describes the development of and the practical completion of the plan. It describes the reasons behind the selection of the method and reports practical experiences from the decommissioning work as well as the monitoring results so far.

Additional Key Words: acid mine drainage, tailings pond reclamation

Introduction

Stekenjokk is located in Sweden's southern Lapland Mountains (see figure 1). Copper and zinc mineralizations were localized in this area about 80 years ago.

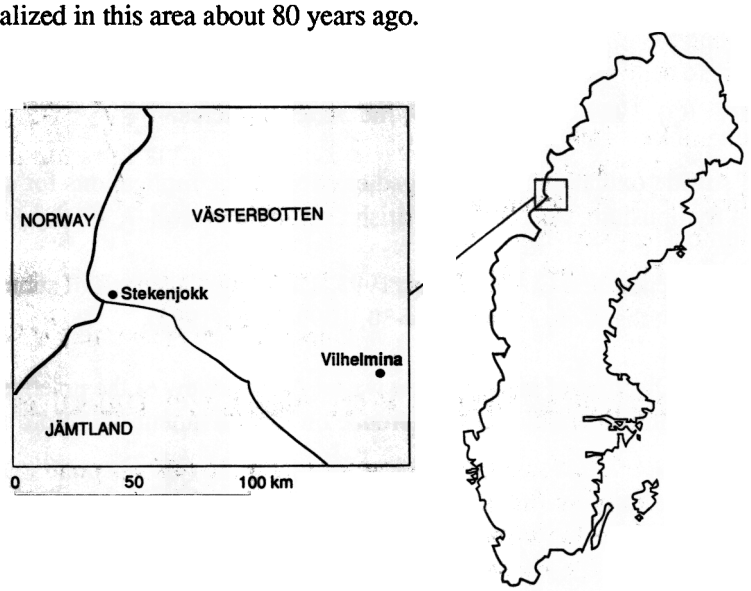

Figure 1. Localization map.

---

[1] Paper presented at the International Land Reclamation and Mine Drainage Conference and the Third International Conference on the Abatement of Acidic Drainage, Pittsburgh, PA, April 24-29, 1994.

[2] Per G. Broman, Vice President, Environment, and Torbjörn Göransson, Environmental Coordinator, Mines, Boliden Mineral AB, Boliden, Sweden.

From 1976 to 1988, Boliden Mineral AB mined and concentrated a total of approximately 8 million tons of ore in this area, of which the value components were copper, zinc and silver (see table 1).

The mining facilities were situated at approximately 800 meters above sea level in naturally beautiful but barren surroundings. The buildings were specially designed with climate and environment in mind. Practically all mining occured underground by means of cut-and-fill operations. A small amount of ore was mined in an open pit. Following autogenous grinding, the ore was subjected to flotation to produce separate copper and zinc concentrates. A substantial part of the tailings´ coarse fraction was used as backfill, with the slimes fraction deposited in a tailings and clarification pond immediately downstream from the concentrator. At its peak, 630,000 tons of ore were mined annually.

During the period of operation, a range of protective measures were adopted, including water recycling and strict control of pH values of the water in the tailings pond. Accordingly, this limited the environmental impact, enabling the ecological balance of the sensitive surroundings to be maintained.

Remaining in Stekenjokk after operations ceased were a small open pit, a 110-hectare tailings and clarification pond, a dike enclosing Stekenjokk´s raw water pond, rock dumps formed from ramp drifting and overburden stripping, and various, aboveground facilities (see figure 2).

Table 1. Tonnage and ore contents.

Tonnage	8 Mton
Copper content	1.5 %
Zinc content	3.5 %
Silver content	40 g/ton

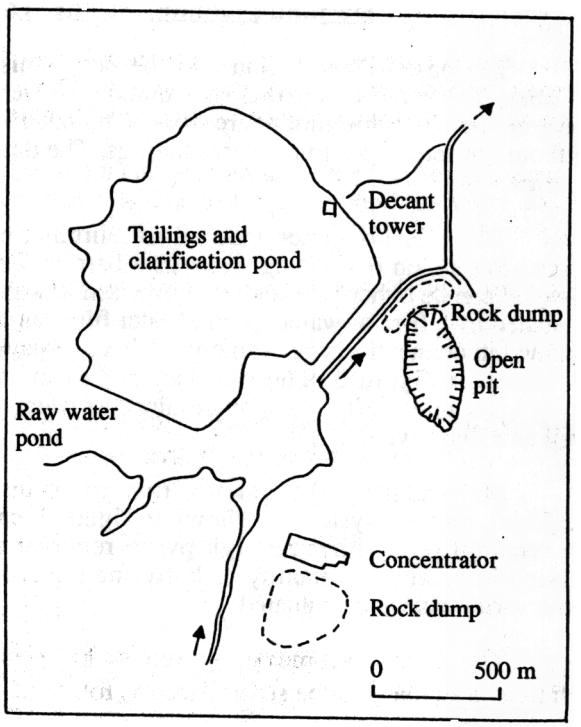

Figure 2. Mining facilities at Stekenjokk.

Decommissioning: General Prerequisites and Objectives

The decisive prerequisites of the decommissioning were that the tailings pond and segments of the rock dump contained significant amounts of sulfur-rich material. For example, the content of the sulfur in the tailings was about 20 %, and the content of the buffering minerals only about 1 % (see table 2). Accordingly, the residue products were potentially strong acid mine drainage (AMD) sources.

Another important consideration was that 2 years of operations remained at the time that detailed planning of the decommissioning started. Other important factors were the localization in a climatically harsh environment and the limited access to covering material, e.g., moraine.

The objectives of the decommissioning were largely the following:

- Preventing the area from becoming a major source of migrating metals and acidic components.
- Removal of facilities that could be hazardous to humans.
- Adapting the area to its natural state.

Table 2. Tailings pond features.

Area	110 hectares
Volume dumped	4.4 Mton
Sulfur content	20.0 %
Copper content	0.19 %
Zinc content	0.64 %
Buffering minerals	1 %

Decommissioning of the Tailings Pond: Studies of Alternatives

The basic phenomenon that the decommissioning must address is the oxygen-induced weathering of sulfides. There are two principal methods of overcoming weathering. One approach is to eliminate access to oxygen, thereby inhibiting the reaction. The other is to manipulate the composition so that weathering can occur without consequences to the surroundings. The detailed decommissioning plan began with a study of both these alternatives.

There is no better method of eliminating access to oxygen than using water as a barrier. The material can be either permanently immersed in water or sealed by a film of water. Such a water film can be attained in connection with a fine-particle cover layer as shown in figure 3. The capillary forces in the cover layer prevent it from being drained of water as well as reduce evaporation.

Manipulating the composition to form a buffering mineral system, as shown in figure 4, can be accomplished either through pyrite removal or mixing in a suitable quantity of buffering material. Both variations were evaluated.

The technical measures representing the different principles can be summarized as follows:

Flooding
Dry moraine covering
Depyritization
Buffering

As the term implies, flooding involves damming the water so that it covers the entire tailings area. The flooding must be permanent. Accordingly, the water level is not allowed to fall and thereby drain parts of the tailings pond, nor can any physical forces be permitted to resuspend the fine tailings particles in the water cover.

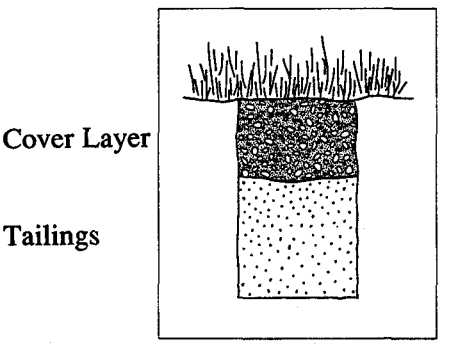

Figure 3. Cover layer.

Limiting weathering through changes in the composition

$$\cancel{FeS_2} + H_2O \rightarrow H_2SO_4 + FeSO_4$$

+ lime
etc.

Figure 4. Possibilities for limiting the effects of weathering.

Dry covering involves covering the entire tailings area with moraine of appropriate thickness and quality. Stekenjokk is remote from suitable moraine deposits. In the comparative study, it was supposed that moraine of dike-construction quality would be applied to a thickness of 0.5 m.

Depyritization, or the removal and separate disposal of pyrite, involves an extra step in the ore treatment process in the form of pyrite flotation. The open-pit mine would be a suitable site for dumping of the pyrite.

Finally, buffering involves opening an olivine quarry and adding coarse olivine to the concentrator's autogenous system in quantities corresponding to 15 % of the ore volume.

In comparing the four options, we attempted to take all conceivable and relevant parameters into consideration. A central parameter was, of course, the environmental protection effect. Other important parameters were:

- the requirement for methods development and other studies;
- the requirement that final dumping sites be determined;
- the time required for implementation;
- the necessity for supplementary protective measures;
- the consequences for other landscape preservation measures;
- the uncertainties and limitations of the various methods; and
- the most critical parameter cost.

A comparison of the different options, illustrated in table 3, yielded results that were very easily interpreted. Neither manipulation alternative was feasible due simply to the fact that the remaining time of operation was too short. It is essential that enough time be available to form a sufficiently thick layer of buffering tailings and thereby provide an adequate protection.

Ultimately, the choice was between the flooding and moraine-cover alternatives. In practically all respects, the evaluation favored the flooding method. Simply stated, flooding was judged to be safer and more effective, above all, eight times more cost-effective. The two manipulation options, which were eliminated, were judged to be two to three times more expensive than flooding.

Table 3. Comparison of the decommissioning options examined.

Parameter	Flooding	Dry moraine covering	Depyritization	Buffering
Environmental protection	+	-		
Methods development	+	-		
Other studies	+	-		
Requirements of the deposition		-		
Implementation time			Prohibitive circumstances	
Supplementary protection	+	-		
Other landscape preservation measures				
Uncertainty, limitations	+	-		
Approximate cost (MSEK, 1989 cost level)	15	120	45	30

Decommissioning of the Tailings Pond: Detailed Planning Phase

The decision was reached, in consultation with the appropriate government agencies, that the ongoing work should focus on the detailed planning of the flooding option. A number of consultants were hired for this work.

Flooding rests on two fundamental conditions. First, the flooding must be permanent. Accordingly, any droughts of the area must be prevented. Second, the water-immersed tailings not be subjected to movement. Any disturbance causing resuspension will break the thin film of oxidized material at the tailings surface and the shielding of other tailings particles.

Permanent flooding is, of course, a matter of water balance and is determined largely by precipitation and evaporation effects on the water surface, the runoff of surface water from adjoining land, inflow and outflow of ground water, and seepage through the dikes. A hydrogeological study indicated an assured water availability and, in the event of extreme drought occurring once every 1,000 years, that the water level would fall a maximum of 20 centimeters.

The question of the stability of the tailings surface is somewhat more complicated. This is almost exclusively a matter of the shear force exerted, i.e., the wave-induced lateral forces that affect the tailings layer. The shear force diminishes if the water cover thickness is raised, i.e., the water depth is increased, or if the wave fetch is decreased. The resistance to shear force increases if the tailings surface is stabilized by superimposing a layer of coarse material.

The solution that eventually was formulated required that all stabilizing possibilities be used. As figure 5 demonstrates, this comprehensive action plan includes a large number of interim steps. First, the water level was lowered, and the dykes were raised three meters, the extent permitted by the availability of construction material, mainly moraine. Attaining the required water depth required more than raising the height of the dikes, it also proved necessary to lower the surface of the upstream part of the tailings area. To obtain a decrease in wave force, it was required that a breakwater system be constructed. It was also deemed necessary to superimpose coarse material in the shallow parts for added resistance to shear forces. Other important features of the plan included the design and construction of erosion-stable dikes having a long-term safety factor and able to withstand an earthquake with an intensity of 6 on the Richter Scale, with an epicenter directly under the dikes. Of equal importance was the design of erosion-stable spillway arrangements. Prior to plan approval, we were also required to demonstrate the effect of the lake´s water freezing into a complete ice cover.

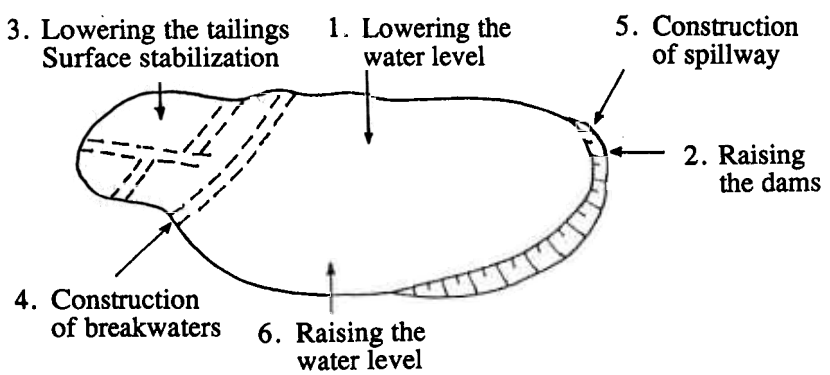

Figure 5. The working out of the flooding solution in detail.

After 3 years of studies (see reference list at end) and consultations with representatives of the National Environment Protection Board, Västerbotten´s County Council, Vilhelmina Municipality and the southern Lapp village of Vilhelmina (a total of nine consultations), the County Council approved the plan in 1990.

Deommissioning of the Tailings Pond and Waste Rock Areas: Implementation

The work was initiated in the summer of 1990 and was completed by late summer 1991. The work on the dikes, mainly the nearly 2-km-long downstream dike, provided an excellent opportunity for eliminating the existing sulfide bearing waste rock dumps (see figure 6). Large amounts of sulfide free waste rock were required to raise the dike and reduce its slope to a 1:3 proportion. An erosion-inhibiting, breakwater shelf was set in place on the dike´s inner side. Here, large amounts of sulfide-bearing waste rock were deposited to ensure safe underwater disposal during a long period. The breakwaters were constructed using similar type waste rock and, preferably, such material that required underwater deposition for safe, long-term disposal. The breakwaters were constructed somewhat in a checked pattern, which covered the shallow part of the future lake (see figure 7). The tailings were excavated and removed using the breakwaters as working and transport surfaces for excavators and hauling vehicles. The tailings´ ground water level proved to be higher than originally calculated, resulting in water saturation of the tailings surface occuring prior to the final depth being reached. Driving vehicles over such material was impossible. In this instance, the area´s plentiful supply of crushed waste rock turned a drawback into an advantage. By using waste rock, the surface could actually be made sufficiently stable for trafficability. Approximately 100 hectares, or one-tenth of the surface, were thus covered with waste rock. About 90,000 m^3 of tailings were excavated from other locations, hauled to the lower-lying areas, and deposited.

An erosion-stable spillway was built in the land area adjoining the dike.

Figure 8 shows the area when completed.

Figure 6. The completed downstream dike.

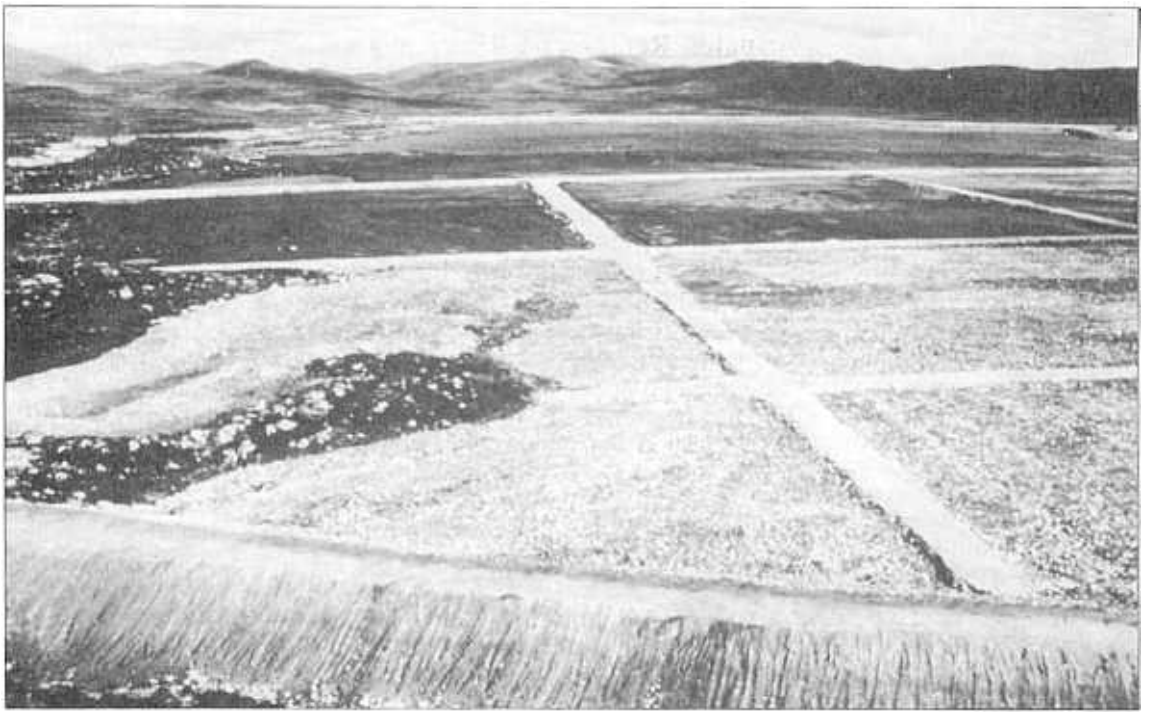

Figure 7. Breakwaters in the shallow part of the lake.

Figure 8. The tailings pond following flooding (the photo´s middle and background). Shown in the foreground is the raw water pond.

The water has risen to a level covering the adjoining land area on the lake´s western shore. The surface of the water remains undisturbed, except when strong winds blow, wherein the waves are broken along the breakwaters. In the event of a 1,000-year drought, the breakwaters would be visible, even during a calm. To the casual onlooker, this lake is indistinguishable from any other in the area. Eventually, normal biological life should develop in the lake.

Anticipated Results and Those to Date

The simulations of the lake's water quality development are shown in figure 9. In the figure, the anticipated development of the zinc content, under two assumptions, is shown. The simulations assume that a maximum zinc load of about 800 kg will be transported by overflow from the lake annually. This is the same level as when operations were underway. Ultimately, this transport will decline to very low levels.

The effect of the decommissioning will be followed by means of a monitoring program which primarily is focused on a 5-year period. Results to date have been positive. The zinc contents from samples taken from spillway water are also illustrated in figure 9 and are well within the anticipated range.

The monitoring has demonstrated that a certain level of metal migration occurs at some areas of the dike base. A review of the causes of this diffuse metal transport is presently underway. To date, two explanations have been formulated: (1) the transport originates from the "flushing" of the partially weathered rock that has been deposited on the inside of the dike; (2) the transport results from acid-generating rock fractions in the dike's outer support filling. The survey now in progress shall determine the extent to which actions are necessary, as well as those which are feasible and suitable.

Costs

The decommissioning at Stekenjokk has taken place largely according to plan. The overall cost has amounted to 25 million Swedish crowns in 1991, of which the tailings pond accounts for 15 million Swedish crowns. Table 4 summarizes the major cost items.

Table 4. Major cost items for decommissioning the tailings pond (1991 cost level).

Tailings dams	9 MSEK
Spillway arrangement	1 MSEK
Excavation of tailings	2 MSEK
Construction of breakwaters	2 MSEK
Others	1 MSEK

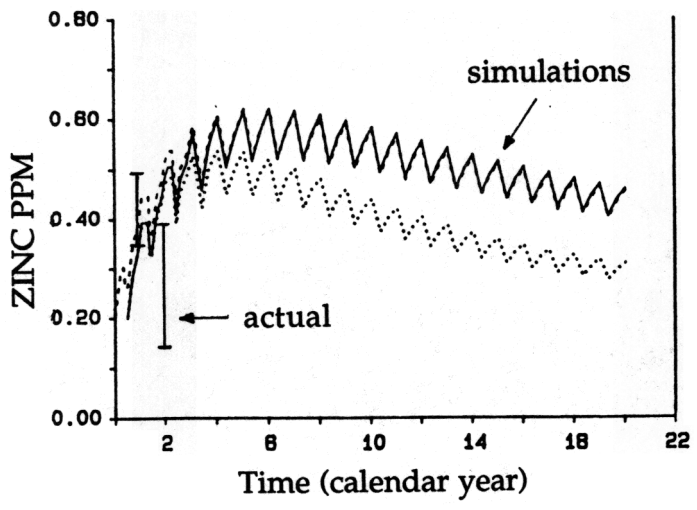

Figure 9. Simulated zinc concentration as a function of time and zinc concentration levels for 1992 (year 1) and 1993 (year 2).

References

Arnesen, R.T. 1987. Avslutning av deponi for avfallssand ved Stekenjokk gruve. Norsk institutt for vannforskning. Report no 2041. 41 p.

Axelsson, C.L. and Ekstav, A. 1989. Vattenbalansstudie för sandmagasinet vid Stekenjokkgruvan. Golder Geosystem AB. Report no 897-1170. 25 p.

Knutsson, S. 1989. Tjälens inverkan på sandmagasin i Stekenjokk. Tekniska högskolan i Luleå. 8p.

Kristiansen, Ø. and Dahl, T.E. 1989. Sandmagasin i Stekenjokk- nødvendig vanndybde. Norsk hydroteknisk laboratorium. Report no STF60 F89097. 17 p.

Markland, Å. and Eurenius, J. 1989. PM angående sandmagasinets anordning vid gruvans nedläggning. Vattenbyggnadsbyrån. Report R2151. 9 p.

Schönfeldt, T. 1989. Rapport över utförd grus- och moräninventering vid Stekenjokkgruvan. Edström & Schönfeldt, Bygg och Mark Konsulter AB. 7 p.

Schönfeldt, T. 1989. Mätning av grundvattennivåer i sandmagasinet. Edström & Schönfeldt, Bygg och Mark Konsulter AB. 5 p.

EVALUATION OF ACID PREVENTION TECHNIQUES USED IN SURFACE MINING[1]

Meek, F. Allen Jr., P.E.[2]

Abstract: Surface coal mining was conducted in a potentially acid producing region of central West Virginia between 1979 and 1986. Seven different surface mining operations were conducted at the complex with different acid preventative techniques employed at six of the operations. No acid preventative techniques were utilized on the first operation that serves as the control for this evaluation. Water quality, treatment reagents and acid preventative costs were closely monitored from the time the operations were started to several years after reclamation. The evaluation indicates that 50% to 70% of the control acidity was prevented by the techniques employed at the facility. The evaluation also indicates that the acid generation at these facilities has a defined life of 16 to 20 years. The economics of the evaluation indicates that the preventative techniques employed at the facility were more expensive than treating the drainage from the sites with no preventative techniques employed.

Additional Key Words: acid mine drainage, overburden, acid preventative technique.

Introduction

The Upshur Complex of Island Creek Mining Inc. consists of approximately 27,000 acres of both surface and deep mine reserves located in Upshur County West Virginia. The principle seams on the reserve are the Middle and Lower Kittanning. Other mining in the area during the late 1960's and early 1970's produced surface mines that exhibited severely acidic drainage characteristics both during the mining phase, and after reclamation was completed. The Buckhannon River, the principle drainage for the area, is a high quality, lightly buffered stream, that is periodically stocked with trout. Because past mining had caused post mining acidic discharges and the Buckhannon River was a valuable recreational resource, mining permits for the area were put on hold by regulatory authorities until solutions to the acid mine drainage questions could be addressed.

In 1978, the director of the West Virginia Department of Natural Resources appointed a Task Force consisting of Industry, Regulatory and Academic participants. This Task Force was charged with gathering information and evaluating field procedures used during mining to prevent acidic mine drainage. In 1979, the group published a document titled "Suggested Guidelines for Mining in Potentially Acid Producing Overburdens" which summarized material handling and mining procedures that could be employed to help prevent the occurrence of post mining acid mine drainage. In 1982,

---

[1]Paper presented at the AIME Conference in Denver, CO, February, 1991

[2]F. Allen Meek, Jr., Director of Environmental Affairs, Glenn Springs Holdings, Inc., Lexington, KY, USA.

a Technical Advisory Committee was appointed consisting of well known researchers in the field of acid mine drainage prediction and prevention. The group was charged with the task of conducting research in the field of acid mine drainage prevention.

Mining conducted at the Upshur Complex between 1979 and 1986 employed various acid mine drainage preventative techniques recommended in the suggested guidelines manual and techniques concurrently being researched by the Technical Advisory Committee. Costs for the various techniques were documented and the resulting post-mining water monitored.

Description of Site

The Upshur Complex is located on the western slope of the Allegheny Mountain Range. Average elevation at the site is 2200 feet. Topography consists of plateaus intersected with frequent valleys having moderate to steep slopes, with relief ranging from 300 to 500 feet.

The Kittanning Coal seams are located at the base of the Allegheny group of the Pennsylvanian formation. The Lower Kittanning occur in two splits, with 15 to 24 inches of shale parting material separating the seam. The Middle and Lower Kittanning seams have 4 to 15 feet of shale/bone coal interburden separating the seam, with only minimal portions in the Middle Kittanning seam itself. Total seam height mined at the property is typically 10 feet. Overburden encountered at the site has ranged from 60-80 feet, with those areas having less than 80 feet of cover mined by mountain top removal method, and those with higher cover are contour mined with an 80 foot highwall. The overburden consists of primarily sandstone with minor amounts of carbonaceous shale streaks and lenses.

Overburden removal at the site was conducted after blasting, by utilizing three 20 cubic yard electric shovels. Coal was mined using D-9 ripper tractors in combination with front end loaders and trucks. The interburden separating the seams was removed with 10 cubic yard backhoes and trucks. Annual production at the operation between 1979 and 1986 averaged slightly under one million TPY.

Methodology

All mining conducted at the Upshur Complex between 1979 and 1986 was within a two square mile area located in the central portion of the reserve. Prior to mining, each individual permit area (ranging in size from 150 acres to 400 acres) was core drilled and samples of individual strata were retained for laboratory analysis. The number of holes completed on each permit varied according to the size of the area to be mined. Holes were placed at a maximum of 1000 foot spacings.

Each stratum was analyzed for "Acid/Base Accounting" which consists of: paste pH, a total sulfur/pyritic sulfur ratio and neutralization potential.

Paste pH is an indication of the amount of sulphide oxidation present which in turn is an indication of the amount of weathering the stratum has been subjected to. Upon exposure, overburden having a low pH will produce acidic leachate until the soluble salts are leached from the material. The total pyritic sulfur analysis indicates the amount of acid producing material present in the rock being

analyzed. The higher the sulfur content, the more likely the material will produce acidic leachate upon exposure. The neutralization potential analysis is a measure of the amount of alkalinity or neutralizing material present in the stratum.

Both the total sulfur, (acidic potential) and the neutralization potential test results are expressed in Calcium Carbonate equivalents. The amount of alkalinity and acidic potential contained in each stratum is an indication of the quality of leachate the material will produce upon weathering. In addition to acid base accounting, simulated weathering tests were performed on selected cores on each permit. Simulated weathering tests were conducted by subjecting the material to alternating cycles of moist and dry air, followed by leaching the samples with water. The leachate water was collected and analyzed for acid and/or alkaline constituents.

Analytical results at Upshur indicate that the acid producing material is confined to the interburden, and about 15 feet of overburden directly above the middle Kittanning Coal seam. The more acidic components are associated with carbonaceous materials in the coal partings and interburdens. Although there are differences in overburden quality between boreholes and permit areas, for the purpose of this report, the acid producing potential of the areas under discussion was assumed to be equal. This is justified by the fact that statistically, with the standard deviation of laboratory procedures, there are no significant difference in the overall quality of the overburden mined within the study area. All sites have potentially acid producing material associated with the interburden and the overburden directly above the middle Kittanning, with the remainder of the overburden being neutral.

Acid Preventative Measures

Various acid preventative techniques were utilized at the Upshur Complex. A brief description of these are listed below.

Selective Handling and Placement

Selective handling and placement is a very basis approach to the prevention of acid mine drainage from surface mining operations. The technique involves the identification of acid producing material prior to mining, and placement of this material, during reclamation in a location which minimizes exposure to oxygen and water (fig. 1). The potentially acid producing material is placed off the pit floor, on a porous pad and a porous non-acid producing drain is placed against the highwall of contour operations. Groundwater entering through the highwall will move through the drain and porous material, without coming in contact with the acid producing material. In addition, acid material is covered with a minimum of 4 feet of non-acid producing overburden. The acidic material is also compacted prior to capping to further minimize ground water infiltration.

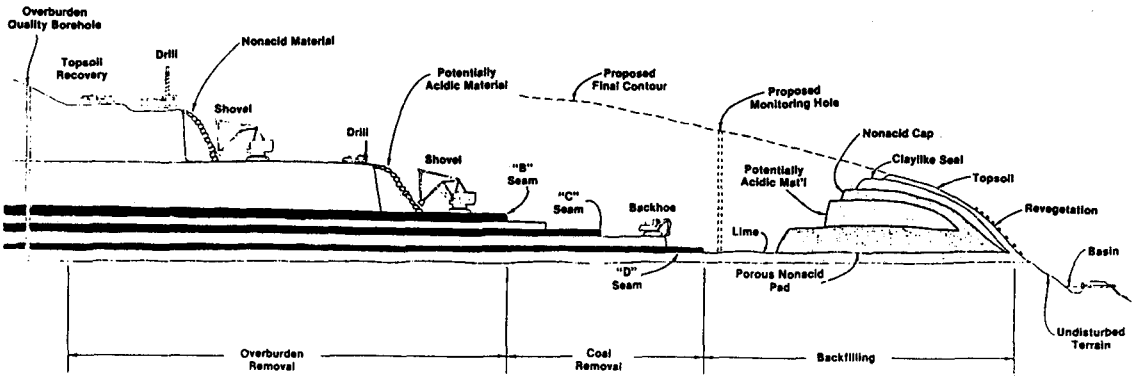

Figure 1. Backfill of Regrading Plan (section)

Sealing of Acid Producing Material

While selective handling and placement has been used as the only preventative technique in some cases, at Upshur a combination of a plastic liner placed over the acid producing material was studied at one 45 acre area. In utilizing this technique, the acid material was placed on a ten foot porous pad, brought up to final grade, and the surface prepared for liner placement. Thirty mil PVC was used for the liner. After installation, approximately 10 feet of non-acid producing overburden was placed on the liner. The area was then topsoiled and seeded. In this application, the mining method was mountain top removal, and no highwall drains were utilized.

Lime Addmixing

A method of acid prevention described in the Suggested Guidelines manual and utilized at the Upshur Complex is lime addmixing. In this technique, the acid spoil is selectively handled, as described above, but ground limestone is added to the backfill at specific rates and in specific locations. At Upshur, the limestone consisted of quarry by product called #10 block sand. This material ranged in size from 3/8" down to less than 200 mesh and is approximately 85% Calcium Carbonate. The limestone was placed at a rate of 5-10 tons/acre on the pit floor, prior to backfilling, blended into the acid spoil at a rate of 20 to 30 tons/acre, and placed on the surface at a rate of 5 tons/acre.

A slight variation to the technique was also used on a permit area at the site. In this variation, more soluble Quick lime was blended into the acidic spoil. Ground limestone was still placed on the pit floor and the surface, but 250 tons/acre of quick lime was blended into the acid spoil.

The alkaline material placed at specific locations of the backfill are intended to prevent acid formation by keeping the acid producing material in an alkaline environment. This alkaline condition helps to prevent bacterial oxidation of pyrite while neutralizing the pyritic material that is oxidized. In the process it is theorized that precipitated metal hydroxides coat the reactive surfaces of the pyrite thus slowing further oxidation.

Phosphate Addmixing

A relatively new acid preventative technique used at Upshur is the application of Apatite rock (Calcium FloroPhosphate) as an addmixed material to surface mined overburden. Phosphate ions in solution react to form highly insoluble Iron Phosphate compounds when in contact with pyrite oxidation products. Apatite rock is relatively insoluble at a neutral pH with increased solubility as the pH decreases. The technique requires that the Apatite rock be thoroughly blended with the acid producing material within the backfill. When pyrite begins to oxidize, and pore water within the fill becomes acidic, the Apatite rock will release phosphate ions into solution. The phosphate ions will then complex the oxidized iron ions on the pyrite surfaces to coat the reactive surfaces with iron phosphate compounds. Once the reactive pyrite surfaces are coated, further oxidation will be reduced. When oxidation and acid production is stopped, further solubilization of the Apatite rock will also cease.

At Upshur, when this technique was used, overburden was selectively handled as with the other techniques described above. Apatite rock was placed on the pit floor prior to backfilling and blended into the acidic overburden at the rate of 3 tons Apatite/1000 tons of acidic spoil. The gradation of the Apatite used was 28 mesh x 0, with most of the material being between 10 and 28 mesh in size.

Alkaline Addition

The acid producing spoil is selectively handled and segregated in the backfill area. The surface of the acidic spoil is then graded and a 2 foot thick compacted earthen seal is applied as a clay liner. The acid spoil is then covered with 4 feet of non-acid producing overburden, topsoiled and vegetated. In addition, at the toe of the clay liner, an alkaline trench is installed. This trench is 3 feet wide and 6 feet deep and is filled with different gradations of limestone and Soda Ash briquettes at the rate of 0.65 lb/sq. ft. The technique is designed to modify the hydrology of the backfill by limiting infiltration into the acidic region while directing surface runoff through the alkaline trench. In theory, the acidity that is produced within the acidic region of the backfill will be neutralized within the fill.

Evaluation

The techniques employed to reduce the amount of acidic mine drainage at the Upshur Complex are new to the surface coal mining industry. Many of the methods described above were tried for the first time at this site. All the techniques add significant costs to the mining operation while each benefited in reduced water treatment costs during and after the mining operation is completed to some degree. With the added cost, it became quickly apparent that a method of determining the effectiveness of each technique needed to be developed. One would expect that by comparing the water quality draining from the individual permit areas, a good determination can be made. However, because these measures were applied in sequence rather than concurrent, it became difficult to make direct comparisons because of the age differences of each reclaimed area. A study conducted by the Office of Surface Mining and subsequent report titled "Methodology For Water Quality Predictions" reported that the mineralization of surface mine leachate varied with time. Figure 2 graphically shows the mineralization of mine runoff with respect to the age of the operation.

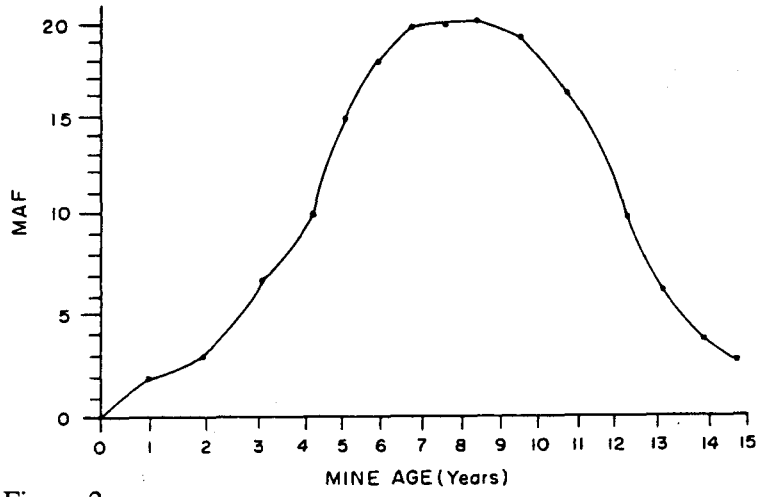

Figure 2.

The effectiveness of preventative techniques used at the Upshur Complex is measured by the resulting water quality of mine runoff at each of the mine areas. Flow measurements and acidity concentrations are taken on the untreated runoff at specific locations and at various times during the year. Measurements are used to double check acid production numbers generated from the amount of neutralizing agent used at our water treatment facilities throughout the complex. The amount of chemical used to neutralize the runoff is a direct correlation to the acid mine drainage being produced at each site and is measured on a continuous basis. The amount of neutralizing agent being used at each site is converted mathematically to acid production, and divided by the acres of coal extracted from each permit area. The resulting number is the acid production rate in pounds of acidity ($CaCO_3$ equivalents) per acre of area mined. The acid production rates of the mine areas having different preventative techniques employed are graphically shown in Figures 3-8. The numerical results are tabulated in Table 1.

Table 1.

PERMIT NO.	PREVENTATIVE TECHNIQUE	TOTAL ACID PROD/ACRE
163-76	None	100,000 lb/ac
112-78	Selective Plac. Lime Add. 35TPA	60,000 lb/ac
57-80	Selective Plac. Quick Lime 250TPA	50,000 lb/ac
S-12-82	Selective Plac. Alkaline Addition	50,300 lb/ac
S-108-82	Selective Plac. PVC Liner	27,500 lb/ac
S-91-83	Selective Plac. Phosphate Added	31,250 lb/ac

The results indicate varying degrees of success with the different techniques employed. None of the techniques were successful in eliminating the production of acid mine drainage completely. However, a reduction of greater than 70% over that of the control was demonstrated with the PVC liner technique. All preventative techniques reduced acid production to some degree.

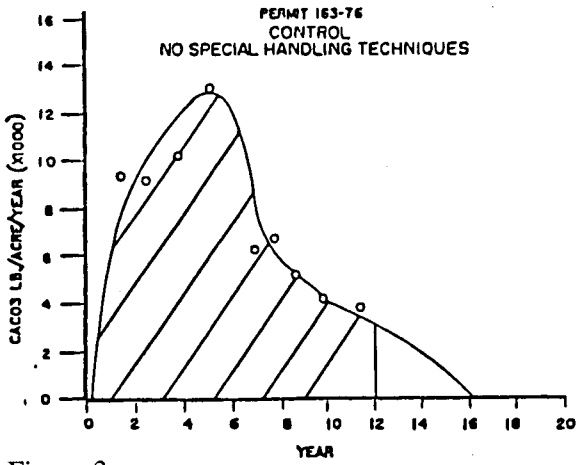

Figure 3.

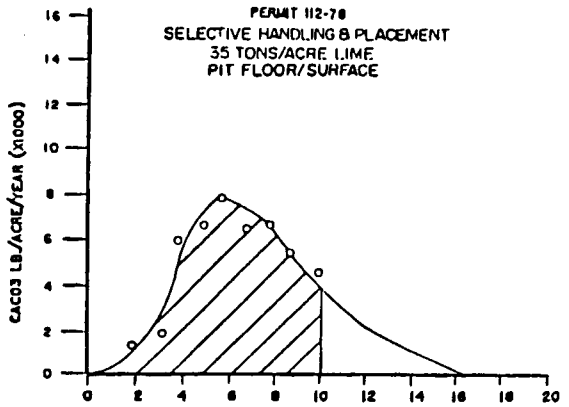

Figure 4.

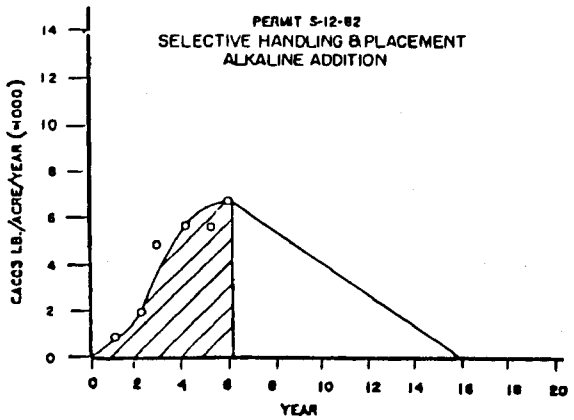

Figure 5.

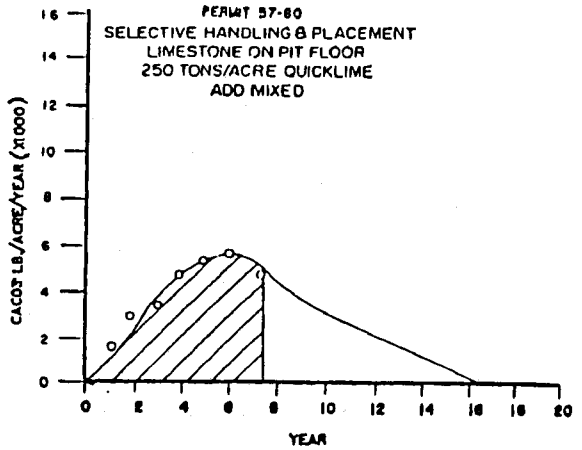

Figure 6.

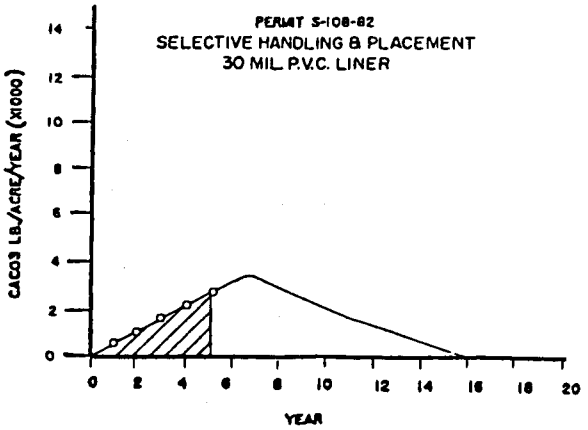

Figure 7.

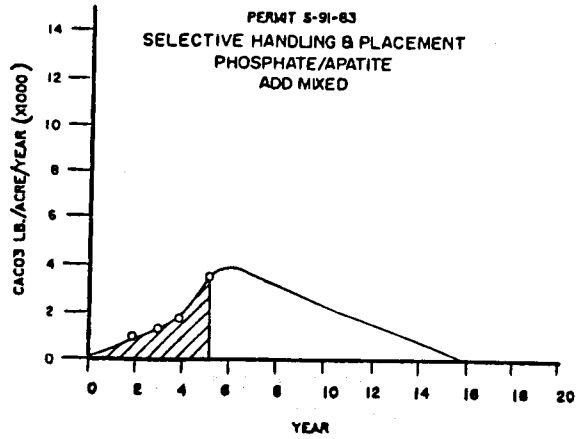

Figure 8.

Economic Considerations

From the time that mining began at the Upshur Complex, the environmental sensitivity of the area made it necessary to give serious consideration to the prevention of acid mine drainage. The area was known to produce acidic drainage upon mining, and it was thought the resulting water treatment requirement would go on indefinitely. Therefore, the costs incurred to prevent perpetual water treatment were considered a necessity. However, after years of monitoring, a trend of reducing acidity with time has become apparent. The evaluation indicates that over a period of 20 years or so, the raw water quality will reach levels similar to background and minimal, if any treatment will be required as shown in figures 2 and 3. Table no. 2 shows the costs of the acid preventative techniques, the difference in acidity produced from the control, and the treatment cost savings.

Table 2.

PERMIT IDENT.	PREVENT. TECH. COST	ACID PREVENTED	TREATMENT COST SAVING
163-76	Control	Control	Control
112-78	$15,300/ac	40,000 lb/ac	$2,000/ac
57-80	$25,500/ac	50,000 lb/ac	$2,500/ac
S12-82	$22,800/ac	40,700 lb/ac	$2,500/ac
S108-82	$16,300/ac	72,500 lb/ac	$3,600/ac
S91-83	$19,000/ac	68,750 lb/ac	$3,400/ac

The evaluation indicates the most cost effective acid preventative technique employed at the Upshur Complex has been the Selective Handling and Placement with Phosphate/Apatite Addmixed technique used on permit S-91-83. In conclusion, it can be said that none of the techniques attempted were entirely successful in the complete elimination of acid mine drainage. It is also apparent, considering the economics, that acid prevention can be more expensive than simply treating the drainage from a site. The most cost effective preventative technique cost $16,300/acre to prevent a potential of $10,880/acre of treatment costs. This evaluation indicates that this facility would have been better served by utilizing the capitol spent on preventative techniques to construct dependable, efficient treatment systems for treating the acid mine drainage produced.

REFERENCES:

Anon., 1979 "Suggested Guidelines for Surface Mining of Areas with Potentially Acid-Producing Materials" West Virginia Surface Mine Drainage Task Force.

Flynn, J.P. 1969. Treatment of earth surface and subsurface for prevention of acidic drainage from the soil. US Patent 3,443,882, May 13.

Meek, F.A. 1984. Optimization of apatite rock addition rates to acid producing mine spoils for the prevention of acidic drainage. West Virginia Surface Mine Drainage Task Force Symposium, Morgantown. Mar.

Sobek, A.A. 1978. Field and laboratory methods applicable to overburdens and mine soils. EPA-6001/2-78-054, U.S. EPA. Cincinnati, OH.

Stiller, A.H. 1982. A method for prevention of acid mine drainage. 3rd West Virginia Surface Mine Drainage Symposium. Clarksburg, WV. May 17.

LONG TERM BEHAVIOR OF ACID FORMING ROCK: RESULTS OF 11-YEAR FIELD STUDIES [1]

PAUL F. ZIEMKIEWICZ [2] and F. ALLEN MEEK JR. [3]

Abstract: The ability to predict long term acid mine drainage (AMD) under field conditions is limited by the near absence of long-term, well controlled and well documented field sites. Much of the literature on AMD derives from either uncontrolled, operational mine sites or from laboratory studies using a variety of simulated weathering methods.

In February 1982, Island Creek Corporation constructed eleven 400 ton rock piles on plastic lined pads at its Upshur County, WV coal mine. The piles ranged from 100% sandstone to 100% shale with several mixtures of the two rock types. Leachate waters were collected biweekly during the first year and subjected to chemical analysis. Because water volumes were also measured it was possible to estimates mass balances and flux rates for key constituents such as sulfur, calcium and acidity.

Eleven years after construction the piles were again sampled. Data are presented indicating the rates of sulfur flux from each of the piles and changes in water quality over the 11 years of the study. Of particular interest was the tendency of the sulfur flux rate to approximate that reported for pure pyrite under laboratory conditions.

Additional Key Words: Acid mine drainage, coal spoil, alkaline amendment.

Background

Acid Base Accounting.

Acid Base Accounting (ABA) was developed in the early 1970's by researchers at West Virginia University to identify and classify geologic strata encountered during mining (West Virginia University, 1971). A history of Acid Base Account is provided by Skousen et al. (1990).

Since its development, ABA has been used extensively in the United States and several other countries for premining coal overburden analysis. Its popularity largely stems from its simplicity. It uses two key parameters: maximum potential acidity (MPA) and neutralization potential (NP). MPA is estimated by multiplying the percent pyrite sulfur by 3.125 yielding the total acid produced. NP is the acid consumed by the rock in a titration. Both MPA and NP are given in calcium carbonate equivalents. ABA does not address the different rates of acid and alkali-generating reactions in rock.

Introduction

The long term behavior of acid producing rock under field conditions has been the subject of much speculation and modelling but relatively little systematic study.

DiPretoro and Rauch (1988) found poor correlations (reported R^2=0.16) between a volume-weighted acid base net neutralization potential (NP) and net drainage alkalinity near thirty mine sites in West Virginia. Erickson and Hedin (1988) showed similar low correlation among MPA, NP, net NP from ABA and net alkalinity from drainage

---

[1] Paper presented at the International Land Reclamation and Mine Drainage Conference and the Third International Conference on the Abatement of Acidic Drainage, Pittsburgh, PA, April 24-29, 1994.

[2] Director, National Mine Land Reclamation Center, West Virginia University, Morgantown, WV, USA.

[3] Glen Springs Holding Company, Lexington, KY, USA.

water. Both reports related that factors other than overburden characteristics were involved in predicting post mining water quality.

DiPretoro and Rauch (1988) found that sites with greater than 3% calcium carbonate equivalent (NP) in overburden produced alkaline drainages while at 1% or less acidic drainage resulted. Erickson and Hedin's results indicate that 2% calcium carbonate or less produced acidic drainage while 8% or more produced alkaline drainage. (In this later study there were no sampling points between 2% and 8%).

O'Hagan and Caruccio (1986) found that the addition of calcium carbonate at 5% by weight to a coal refuse containing 1% S produced alkaline drainage. In Minnesota, Lapakko (1988) found that 3% calcium carbonate neutralized an overburden material with 1.17% S.

Cravotta et al. (1990) reviewed the calculation of NP in ABA. In current ABA usage, 3.125 g calcium carbonate equivalent is required to neutralize acidity resulting from oxidation of 1 g S. Cravotta et al. (1990) argue that this ratio should double to 6.25:1. Volume-weighted maximum acidities are subtracted from NP giving a positive or negative net NP for the mined area. A negative, or deficient, net NP is interpreted to indicate the amount of calcite that must be added to equalize the deficiency and prevent AMD formation.

Other alkaline materials have higher NP's than calcite. Quicklime, kiln dust and hydrated lime all have higher activities than calcite, though it is not clear that the kinetics of pyrite oxidation favor readily soluble sources of alkalinity.

Brady et al. (1990) conducted a study of 12 sites where ABA data were available. They computed net NP based on both 3.125% and 6.25% to 1% S. Alkaline addition on the sites was conducted to abate potential AMD problems. When using 6.25%, the sign of the net NP (plus or minus) matched the sign of the overall net alkalinity of water at 11 of 12 sites.

The results of their study concluded that NP and traditional estimates of MPA (e.g. 3.125% to 1% S) were not equivalent and that overburden NP must be twice the MPA to produce alkaline mine drainage. They also concluded that mining practices (such as alkaline addition, selective handling, and concurrent reclamation) enhanced the effect of alkaline addition on reducing acidity. Lastly, they concluded that additional studies are needed to determine the rates, application and placement of alkaline material during mining.

Methods

Island Creek Corporation constructed a series of 11 test piles at its Upshur County, WV mining complex between January and March 1982. Rocks used in the trials were taken from the company's active mining operations on the site and were sized to exclude roughly +8 in. and -1 in. rocks. Treatments consisted of various combinations of sandstone and shale. Another series of treatments consisted of various amendments for controlling AMD.

About 400 tons of rock were placed in each test pile. Each rock mass was placed on a plastic liner with an 8 inch perforated pipe for collection of drainage to an automatic sampling station. The piles were flat-topped and were roughly 16m X 16m X 2m. The rock units were sampled on placement in each pile and ABA were developed for each. Table 1 describes the treatments and properties of each pile. Treatments can be summarized thus:

Table 1. Identification, summary of treatments and NP/MPA of the 11 test piles, Upshur County, WV.

PILE #	DESCRIPTION	CODE	NP/MPA
CONTROL, NO AMENDMENT			
PILE 1	100% sandstone	SS	3.94
2	100% shale	SH	0.08
3	sandstone/shale in layers	LAY	0.18
10	sandstone/shale blended	BLD	0.29
LIMESTONE AMENDMENT			
PILE 5	0.5% by mass	LS1	0.46
4	1.65% by mass	LS2	1.07
8	2.4% by mass	LS3	1.26
PHOSPHATE AMENDMENT			
PILE 7	0.15% by mass	RP1	0.15
6	0.3% by mass	RP2	0.31
CALCIUM OXIDE AMENDMENT			
PILE 9	0.62% by mass	CaO	0.15
BACTERICIDE AMENDMENT			
PILE 11	30 lbs. sodium lauryl sulfate +31 lbs Microwet #2 + impregnated pellets	SLS	0.41

Amendments were spread over one foot spoil layers during construction. A rain gauge was maintained on the site during the period of the study. Annual precipitation averaged 45 inches. The pH of the local rainfall averaged about 4.5.

Immediately following pile construction, water samples were collected and analyzed weekly, then later bi-weekly for roughly the first year. Sampling then halted for the next 11 years until January 1993. The following parameters were measured: flow, acidity, alkalinity, pH, sulfate, calcium, magnesium, iron and manganese. Since flow was measured it was possible to develop mass balances for various ions, particularly sulfate.

With the exception of pile 1 all of the piles were undisturbed when sampled in January 1993. About one half of pile 1 had been excavated and could not be sampled. The automatic samplers had been removed from each pile and it was not possible to estimate flows. Therefore, only chemical concentrations are reported for the January 1993 sample. Flow data were based on flow meters attached to the outlet of each pile. They did not always work and some of the flow data is inferential (e.g. calibrated against precipitation). Nonetheless, it was clear that flows varied little among piles at a given time interval.

A key parameter in developing the sulfur dynamics was sulfur flux (Sf). Sulfur flux was expressed as the percent of the original pyrite sulfur mass which had exited the pile as sulfate ion. Sulfur flux integrates both pyrite oxidation and sulfate leaching rates into a single, empirical parameter.

Results

The results are based on 400 ton test piles constructed in mid-winter 1982. Only one sample was taken of each rock unit during placement so that on a given pile NP and MPA are based on a one shale sample and/or one

sandstone. It is likely that the distribution of pyrite and alkalinity were neither homogeneous nor random and that reported NP/MPA ratios may be subject to error. It is also possible that the placement of alkaline amendments was not uniform. Results of the sampling program are presented in figures 1-6. Treatments are summarized in table 1.

Control, No Amendment. In piles SS and SH pH fell rapidly to about 4.2 over the first 7 months while sulfate rose from near zero to the range 2000 to 2500 ppm. Leachate sulfate concentrations from LAY and BLD rose to about 2700 ppm while pH fell less dramatically to 4.9 and 6.2 respectively. By January 1993, pH had changed little while sulfate concentrations dropped to less than 100 ppm. At least over the first year, blending seemed to improve the pH of the piles while there appeared to be little effect on sulfate generation. See figures 1 and 2.

Limestone Amendment. Addition of limestone had no effect on the rate of sulfate generation and, by inference, the rate of pyrite oxidation. Over the first year, the pH of LS1 AND LS2 remained above neutral while LS3 became acid. Nonetheless, 11 years later the final pH of LS1, LS2 AND LS3 were 5.2, 6.4 and 6.6 respectively. It is not clear why LS3, with the highest NP/MPA initially became acid. Sulfate generation was the same as the other piles so the difference must lie in the efficiency with which the available alkalinity was utilized. This could be a result of initial placing and mixing but records indicate no compelling cause for this result. It is also not clear how long LS3 remained acid. By year 11, at any rate, it had the highest pH.

Sulfate generation was the same as the control piles (SS, SH, LAY, BLD) and by year 1 sulfate concentrations had dropped to below 350 ppm. See figures 3 and 4.

Phosphate Amendment. Sulfate profiles of the two phosphate treatments over the 11 years of the study indicate that pyrite oxidation is not affected by phosphate addition. Effluent pH remained above or near neutral for the first year. The pH of RP1 AND RP2 then dropped to 4.7 and 3.8 respectively. It is not clear why the heavier phosphate application reached a lower pH or whether the difference is even significant. It is clear that phosphate does not control pyrite oxidation, but simply acts as a lime by neutralizing produced acidity. Mindful that it is usually much more expensive than limestone, it should if used, be applied at rates similar to those at which limestone is effective. See figures 5 and 6.

Calcium Oxide Amendment. Sulfate concentrations, like all of the other plots rose rapidly over the first 7 months of the study, reached a peak of about 2500. By year 11 sulfate concentration on this pile was less than 100 ppm. Over this period pH declined rapidly, and by year 11 was about 4.2, the pH of the local rainwater. See figures 5 and 6.

Bactericide Amendment. Sodium lauryl sulfate is a bactericide, meant to control the rate of pyrite oxidation by killing the Thiobacillus ferroxidans bacteria. The sulfate concentration profile for this treatment suggests that pyrite oxidation was little affected by the treatment and that the primary effect of the treatment was to increase the pH over the first year. By year 11 pH was about 4.2. The pH and sulfate profiles are consistent with an alkaline amendment applied at less than adequate rates. See figures 5 and 6.

Sulfur Flux. Sulfur flux through each pile ranged from 0.064% per day to slightly less than 0.01% per day. With only two exceptions all values fell between 0.01% and 0.03% per day (figure 7). For comparison, the literature value of Taylor et al. (1984) of 0.02% per day is presented. This is a surprising level of agreement given the inherent errors expected in estimating original pyrite sulfur contents of the rock masses.

When the results were ranked according to sandstone content (figure 8) it was apparent that sulfur flux is strongly influenced by the proportion of sandstone. Sulfur flux took about nine months to reach its maximum observed rate. Figures 9 and 10 indicate the acceleration of sulfur flux in selected piles.

Figure 1. LEACHATE pH-UNTREATED PILES

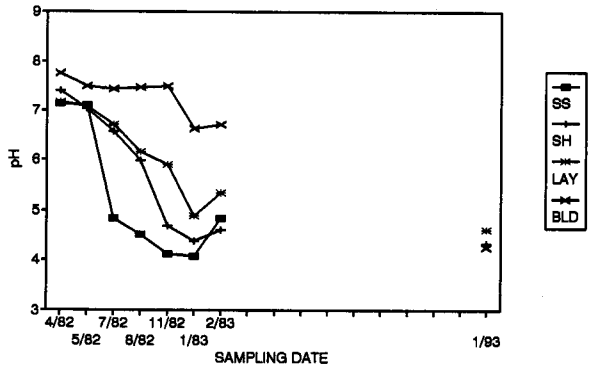

Figure 2. LEACHATE SULFATE (PPM) UNTREATED PILES

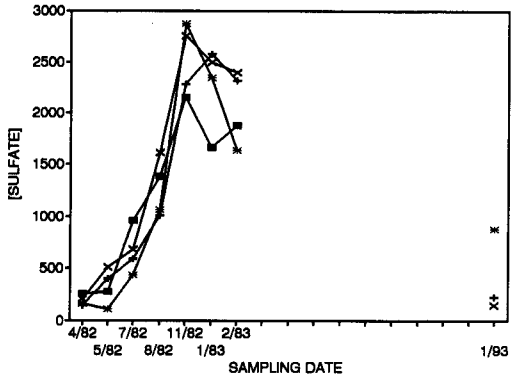

Figure 3. LEACHATE pH-LIMESTONE TREATED PILES

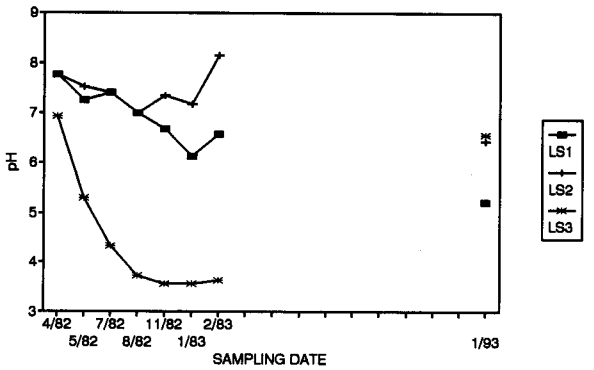

Figure 4. LEACHATE SULFATE (PPM) -LIMESTONE TREATED PILES

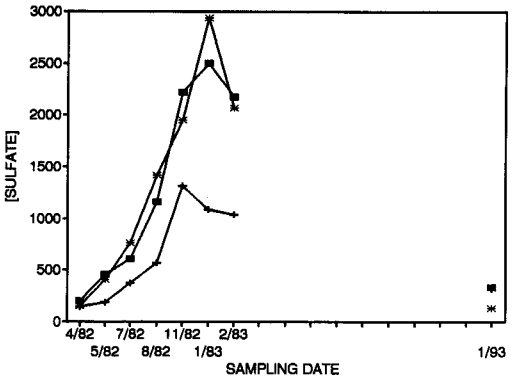

Figure 5. LEACHATE pH-PHOSPHATE, CaO, SLS TREATED PILES

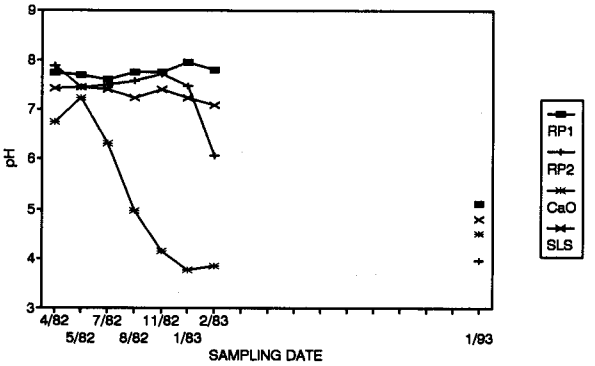

Figure 6. LEACHATE SULFATE (PPM) -PHOSPHATE, CaO, SLS TREATED PILES

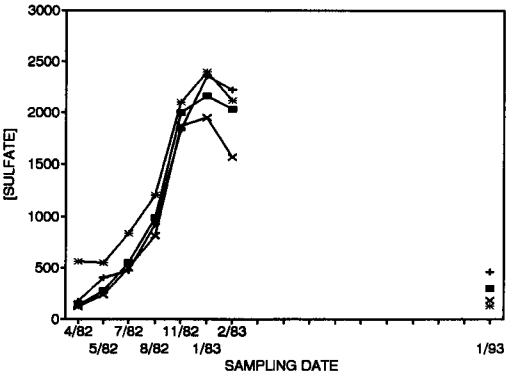

Figure 7. SULFUR LOSS RATES FROM THE 11 TEST PILES AND A LITERATURE VALUE (LIT)

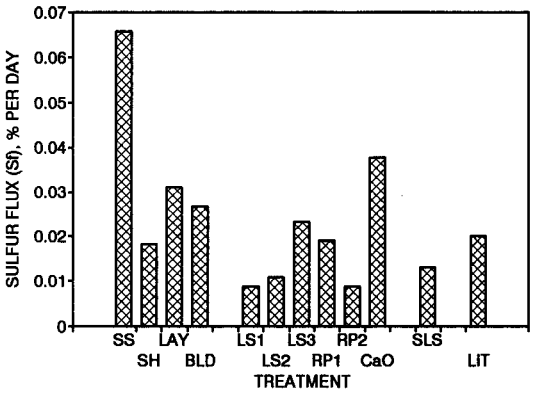

Figure 8. SULFUR LOSS RATES FROM THE 11 PILES RANKED BY SANDSTONE CONTENT

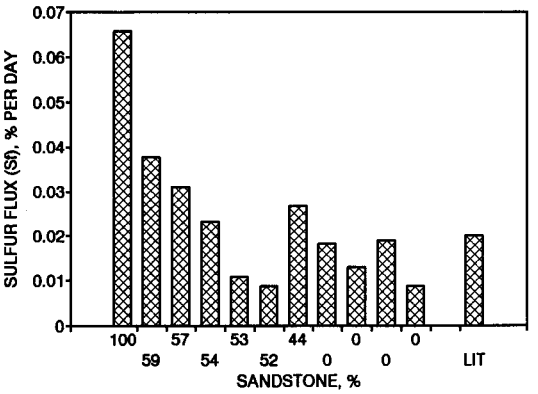

Figure 9. CHANGE IN SULFUR FLUX DURING THE FIRST YEAR, UNAMENDED PILES

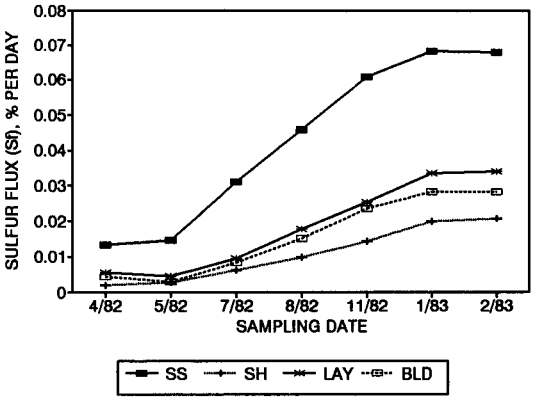

Figure 10. CHANGE IN SULFUR FLUX RATES DURING FIRST YEAR, AMENDED PILES

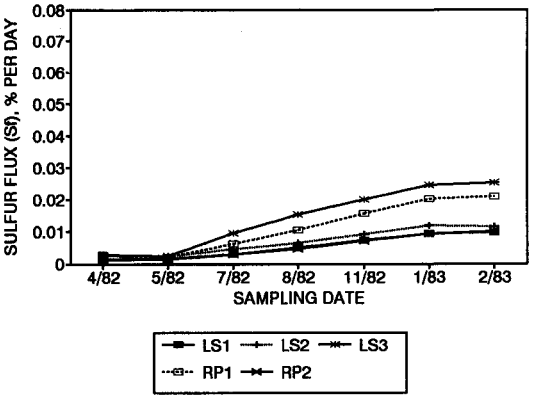

Conclusions

The following conclusions pertain to the results of observed leaching of eleven 400 ton piles of acid producing rock under field conditions in Upshur County, WV. The piles had a large surface area and were only 2 m thick. It is likely that leaching was optimized by this design and that storage was minimized. Sulfur flux rates would be much lower on a large, conventional rock dump. In the following discussion, therefore, sulfur flux is taken to estimate pyrite oxidation.

1. Pyrite oxidation in rock dumps is independent of overall leachate pH. While pH in the immediate vicinity of oxidizing pyrite grains would be low, circumneutral pore water pH will cause most metal ions to precipitate near the point of oxidation and the acidity to be quickly neutralized

2. At the rates tested in this trial pyrite oxidation was little affected by any of the following amendments: limestone, rock phosphate, calcium oxide and sodium lauryl sulfate.

3. There was no clear relationship between NP/MPA and pH performance of the piles. Since sulfate generation appeared to be consistent with estimated rock pyrite sulfur contents it is likely that substantial error occurred in the estimation of effective NP. The error could have had several causes: poor mixing of amendments and spoil types, inherent overestimation in the NP analysis procedure or sampling error.

4. It appears that gross physical phenomena, independent of pyrite forms, surface area, amendment, pH or micro properties of the rock control the rate of pyrite oxidation within relatively narrow limits. Since the rate increased with the proportion of sandstone, oxygen diffusion is the likely candidate.

5. In most, but not all cases, alkaline amendments tended to maintain a circumneutral pH over the first year while untreated piles quickly became acid.

6. In the two cases where limestone addition raised the NP/MPA above 1.65 a circumneutral pH was observed after 11 years. Untreated piles and those treated with rock phosphate, calcium oxide and SLS remained acid.

Literature Cited

Brady, K., M.W. Smith, R.L. Beam and C.A. Cravotta. 1990. Effectiveness of the use of alkaline materials at surface coal mines in preventing or abating AMD: Part 2. Mine site case studies. pp. 227-241. In: Proceedings of the 1990 Mining and Reclamation Conference, West Virginia University, Morgantown, WV.

Cravotta, C.A., K. Brady, M.W. Smith, and R.L. Beam. 1990. Effectiveness of the addition of alkaline materials at surface coal mines in preventing or abating AMD: Part I. Geochemical considerations. pp. 221-225. In: Proceedings of the 1990 Mining and Reclamation Conference. West Virginia University, Morgantown, WV.

diPretoro, R.S. and H.W. Rauch. 1988. Use of acid-base accounts in premining prediction of acid drainage potential: a new approach from northern West Virginia. pp. 2-10. In: Mine Drainage and Surface Mine Reclamation. USDI Bureau of Mines Information Circular 9183.

Erickson, P.M., and R.S. Hedin. 1988. Evaluation of overburden analytical methods as means to predict post-mining coal mine drainage quality. pp. 11-19. In: Mine Drainage and Surface Mine Reclamation. USDI Bureau of Mines Information Circular 9183.

Lapakko, K. 1988. Prediction of AMD from Duluth Complex mining wastes in northeastern Minnesota. pp. 180-190. In: Mine Drainage and Surface Mine Reclamation. USDI Bureau of Mines Information Circular 9183.

O'Hagan, M., and F.T. Caruccio. 1986. The effect of admixed limestone on rates of pyrite oxidation in low, medium, and high sulfur rocks. In: 1986 National Symposium on Mining, Hydrology, Sedimentology, and Reclamation. University of Kentucky, Lexington, KY.

Skousen, J., R.M. Smith, and J. Sencindiver. 1990. Development of the Acid-Base Account. Green Lands 20(1): 32-37.

Taylor, B.E., M.C. Wheeler and D.K. Nordstrom. 1984. Stable isotope geochemistry of acid mine drainage: Experimental oxidation of pyrite. Chemica et Cosmochimica Acta Vol. 48. pp. 2669-2678. Pergamon Press Ltd.

West Virginia University. 1971. Mine spoil potentials for water quality and controlled erosion. 14010 EJE 12/71. Contract with West Virginia University by the U.S. Environmental Protection Agency, Washington, D.C.

SURFACE CHEMICAL METHODS OF FORMING HARDPAN IN PYRRHOTITE TAILINGS AND PREVENTION OF THE ACID MINE DRAINAGE[1]

Syed M. Ahmed[2]

Abstract: This work was undertaken to identify conditions under which hardpan could be formed in pyrrhotite (FeS) rich tailings using surface chemical methods and to check the susceptibility of the synthetic hardpan to atmospheric oxidation and acid formation.

Pyrrhotite hardpan was first grown on a small scale (200 g) by surface chemical and electrochemical methods, after treating the FeS-rich tailings with a dilute solution of Fe^{2+}, pH adjustment, and curing for several weeks in the presence of air. This synthetic hardpan was similar to the phrrhotite hardpans formed under natural conditions, consisting of FeS grains embedded in iron oxyhydrate (goethite) matrix.

Attempts were then made to grow similar hardpans on a large scale with FeS columns of 3 ft length and 4 in diameter. The effects of surface oxidation of FeS in air, Fe^{2+} treatment, humidity, pH, and a water head (2 in) on the hardening of tailings and acid formation have been examined. Hardening was confined mainly to the outer layer of the tailings exposed to air; the inner core remained soft and retained most of the Fe^{2+} in the unoxidized form. The pH, dissolved iron concentration, and redox potentials of the percolant solutions were monitored. Most pronounced was the effect of maintaining 2 in of water head on the tailings, which prevented the oxidation of FeS and acid formation completely. The data have been examined in light of the Eh-pH diagram of the FeS_2-FeS-Fe_2O_3 system in equilibrium with water. It is inferred that the FeS system can be stabilized through formation of iron oxide and other less soluble compounds such as iron silicates on the surfaces. Methods of improving kinetics of hardpan formation have been suggested.

Additional Key Words: acid mine drainage, pyrrhotite, hardpan, sulfides.

Introduction

Natural formation of hardpans is often experienced in sulfide tailings that are exposed to air and water at the disposal sites. The hardpans normally consist of pyrrhotite (FeS) and pyrite (FeS_2) grains cemented in iron oxyhydrate (goethite) structure. This phenomenon has been attributed to the Fe^{2+} being oxidized to ferric oxyhydrates and forming hardpans in selective areas. Pyrite, being an electrocatalyst for oxygen reduction, undergoes little surface oxidation itself; hence pyrite hardpans are rare in nature.

In our earlier work (Ahmed and Giziewicz, 1992; Ahmed, 1990, 1991) in this field, the electrochemical and solid state properties of iron sulfides were examined, and the oxidative decomposition of iron sulfides was attributed to 'holes' or electron vacancies, formed as electrons are transferred from the substrate to oxygen or Fe^{3+}. The holes are electrically mobile and lead to bond breaking and decomposition. It was also reported that FeS and FeS_2 can be electrochemically passivated by growing iron oxide films on the sulfide surfaces. The oxide film would then protect the sulfide substrate from further oxidation. The Eh-pH diagram of the FeS-FeS_2-Fe_2O_3 system in equilibrium with water, as shown in fig. 1, indicates that iron sulfides under oxidizing conditions are unstable and produce acid and dissolved Fe^{2+} and Fe^{3+}. At sufficiently low pH, the dissolved Fe^{3+} in turn causes further oxidation and decomposition of the sulfides. The sulfide oxidation by air can occur even in a basic medium. On the contrary, iron oxides, being the oxidation products, can form a stable phase under oxidizing conditions as long as the medium is neutral or basic. Also, iron oxides can be further stabilized by converting the surface into less soluble compounds.

---

[1] Paper presented at the International Land Reclamation and Mine Drainage Conference and the Third International Conference on the Abatement of Acidic Drainage, Pittsburgh, PA, April 24-29, 1994.

[2] Research Scientist, Mineral Sciences Laboratories, CANMET, Natural Sciences, Canada, Ottawa, CANADA.

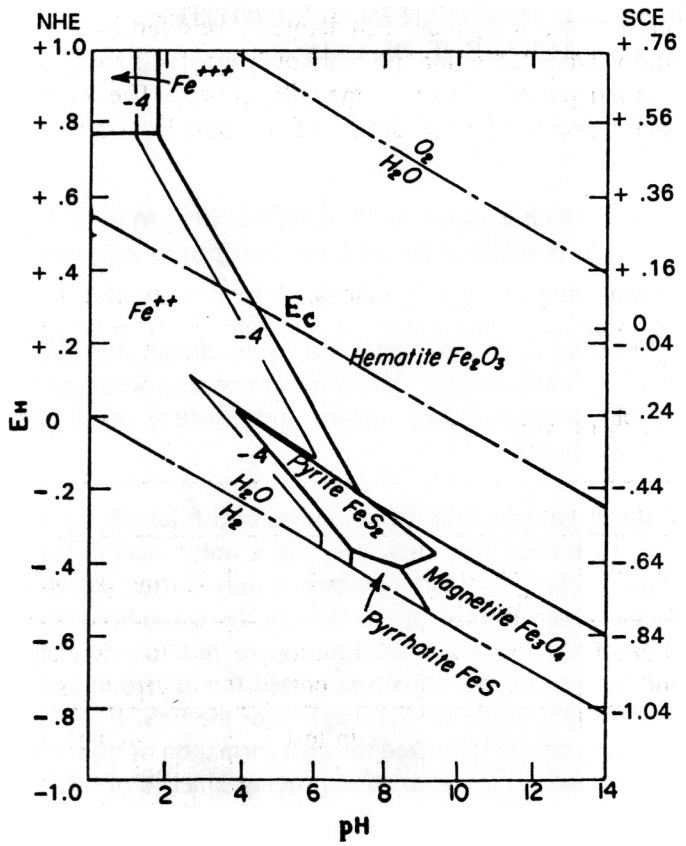

Figure 1. Eh-pH diagram showing the stability contours for pyrite, pyrrhotite and iron oxides in water at 25° C, when total $S=10^{-6}$ mol. Log of iron concentration is shown to be -4, the line indicating changes in solubility. The conduction band edge, E_c, of pyrite is also shown. The potentials relative to the saturated calomel electrode are shown on the right-hand side.

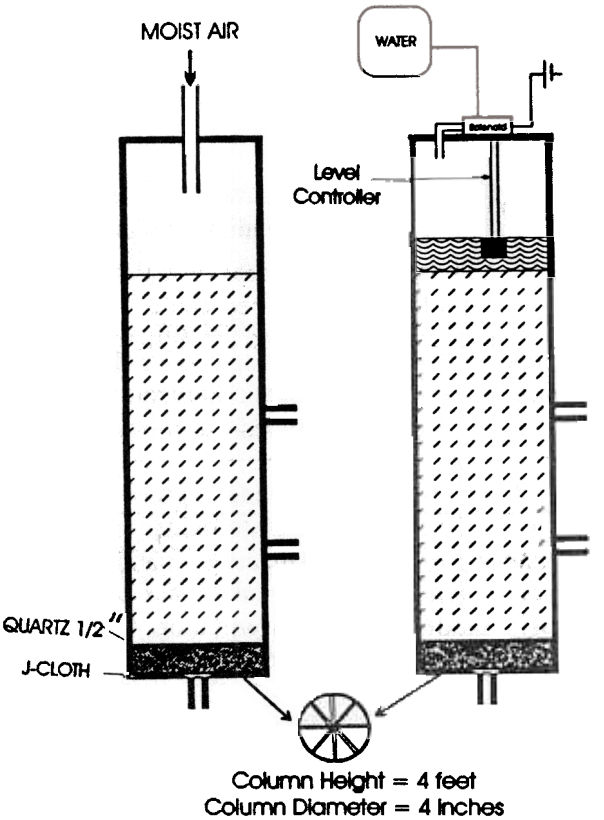

Figure 2. Diagram showing lysimeter design. Lysimeter 2 is provided with a solenoid valve to control water level to 2 in above the tailings.

It follows from the foregoing considerations that it may be possible to control and even prevent the atmospheric oxidation of pyrrhotite and the resultant acid generation by converting the sulfide into an oxide hardpan where each FeS particle is coated with an iron oxide film and the particles cemented together to form a goethite structure.

The following work was therefore undertaken to examine the formation of pyrrhotite hardpans by surface chemical methods and to test their stability and susceptibility to atmospheric oxidation and acid formation.

Experimental Methods

Materials and Equipment

Fresh pyrrhotite tailings in unoxidized form were obtained from the Sudbury (Ontario) area. From image analyses, these tailings were found to contain 78% pyrrhotite, 15% magnetite, 4% silicates, and 3% chalcopyrite, pentlandite, and other minor constituents. The tailings were first oxidized in a slurry form by bubbling air through the slurry for 12 h. These samples are henceforth referred to as "laboratory oxidized" tailings. Another batch of fresh tailings was exposed to air in a steel tray for two weeks in moist condition at room temperature. The tailings were raked frequently for uniform oxidation. These samples are referred to as 'naturally oxidized' tailings in the text to follow.

For large-scale experiments, five cylindrical lysimeters of 4 ft length and 4 in diameter were fabricated from clear plexiglass of 1/8 in wall thickness (fig. 2). A solenoid valve fitted to the top plate of lysimeter 2 and a water reservoir enabled control of the water level automatically to a depth of 2 in above the tailings bed. The following is a detailed description of the procedures. Figures 3 and 4 provide further details of the sample histories and treatment.

Oxidation and Loading

The lysimeters were loaded with tailings in slurry form using heavy duty pumps. It took about 48 h for the tailings to settle before the bed could be treated with Fe^{2+} solution. The treatment methods are summarized in table 1 in sequential form and are further described below.

Table 1 - Summary of work

	Treatment method					
Lysimeter	Tailings type	Laboratory oxidation	Treatment with Fe^{2+}	Curing period 1	pH	Curing period 2
1	Fresh, unoxidized	Yes	Soak and drain method	2 weeks	8.5 on top, 5.5 at bottom	6 to 8 weeks, kept moist
2	Fresh, unoxidized	Yes	Percolation	2 weeks	as in test 1	6 to 8 weeks, kept 2.5 cm solution head
3	Naturally oxidized	No	Soak and drain method	2 weeks	as in test 1	6 to 8 weeks, kept moist
4	As in test 1, without Fe^{2+} treatment					
5	Fresh unoxidized	Yes	Intimate mixing	2 weeks	as in test 1	Air

Treatment with Fe^{2+} Solution

Lysimeters 1, 3, and 4 were treated with a 0.01M solution of Fe^{2+} (2.78 g/L of $FeSO_4.7H_2O$) at a pH ~6, by a "soak and drain method" in which the column was first soaked with a solution head and then allowed to drain naturally until the percolant solution contained at least 0.001M of the ferrous salt. In the case of lysimeter 2, the Fe^{2+} solution was percolated from the top until the percolated solution at the bottom had acquired the required concentration (~0.001M) of ferrous salt. In the case of lysimeter 5, however, the tailings were intimately premixed with the Fe^{2+} solution in the drum itself before being transferred to the lysimeter. Lysimeter 4 was set up for a blank run without any treatment with the ferrous solution.

Tailings in lysimeter 2 were maintained under a constant head of water as described earlier, while column 5 was kept exposed to air under natural, atmospheric conditions.

Curing Period 1

After treatment with ferrous salt, the columns were left for an initial period of 2 weeks of curing to allow oxidation of ferrous to ferric iron take place under moist conditions. Extra moisture was maintained in lysimeters 1, 3, and 4 by bubbling air through water aspirators and circulating the moist air on the top of the tailings.

After 2 weeks of curing (period 1), tap water adjusted to a pH of 10.5 was allowed to percolate through the tailings until the percolant solution had reached a pH of at least 6. A pH of 6 was selected because the zero point of charge of iron oxides lies between pH 5.5 and 6.5, at which the solubility of iron oxides is minimum. Also Fe(OH)3-Fe_2O_3 starts precipitating at about this pH. The tailings were then left for a curing period of 8 to 10 weeks for the hardpan to form.

Since water in lysimeter 2 was kept under constant flowing conditions, the percolant solution in this case was monitored continuously during the 8 week period for pH, Eh, and dissolved iron concentration. The results obtained for all lysimeters at the beginning and at the end of the curing periods are presented in graphical form in figures 3 and 4, respectively.

Small Scale Experiments

Hardpans were grown by both surface chemical and electrochemical methods using 200 g samples of fresh pyrrhotite tailings in each test. In the former case, samples with and without being surface oxidized were subjected to surface chemical treatment separately in glass tubes of 1 in diameter. The rest of the treatment was the same as in lysimeter 5.

In the second method, the tailings were subjected to cathodic treatment in K_2SO_4 solution using a two compartment cell with a fritt glass junction. A graphite rod immersed in the tailings bed served as the cathode and an inert metal electrode was used as anode. A potential of -200 to -300 mV (SCE) was applied potentiostatically with a current of ~ 0.1 mA passing through the cell under steady state conditions. Further details may be seen elsewhere (Ahmed, 1991).

Results and Discussion

Small Scale Experiments

The electrochemically treated tailings (no Fe^{2+} added) and tailings treated with Fe^{2+} after oxidation with air hardened in about 6 weeks. The glass walls broke at this stage, most probably due to cementing of the iron oxide in the hardpan with the glass walls and subsequent contraction. No such breakage of walls occurred in plexiglass but shrinkage from the walls was observed. Fresh tailings treated with Fe^{2+}, without any surface oxidation, took longer to harden.

The hardpans from these experiments were examined by scanning electron microscopy. The backscattered electron image (BEI) and hardpan photographs are shown in figures 5 to 8. It is seen in figures 6, 7, and 8 that the FeS-FeS_2 grains in these hardpans are cemented in a goethite (+ lepidocrocite) structure and that the synthetic and natural hardpans of pyrrhotite have the same structure (figs. 7,8). The pyrite hardpan (fig. 6), however, is seen to be separated from the goethite phase by a third phase which seems to be a dehydrated form of iron oxide.

Lysimeter Tests

Probe tests with nails after the second curing period indicated that the hardening of tailings was confined mainly to the outer layer of the beds exposed to air; the inner core, which was not exposed to air (oxygen), remained soft and retained most of the Fe^{2+} in the unoxidized form. Obviously, the Fe^{2+} in the inner core of the tailings was not oxidized and not precipitated as ferric oxyhydrate. As a result, the excess of Fe^{2+} (~ 0.001M) drained out through columns 1, 3, 4, and 5 during percolation tests, as shown in fig. 4. The pH of the percolant solutions was between 5 and 6.

HISTORY

April 2	Tailings loaded
April 6	Initial settling
April 8	Solution clearing
	Fe^{2+} Addition started
April 29	Fe^{2+} Addition ended
May 4	pH adjusted; pH_i = 10.45
May 29	Fe^{2+} = added to lysmtr. #3

Redox Potentials

Fe^{2+} Soln. = 0.243 V

#5 = 0.046 V (SCE)
#2 = 0.120 V (SCE)
#1 = 0.186 V (SCE)

Flow Rates:
0.7 to 0.8 mL /mm

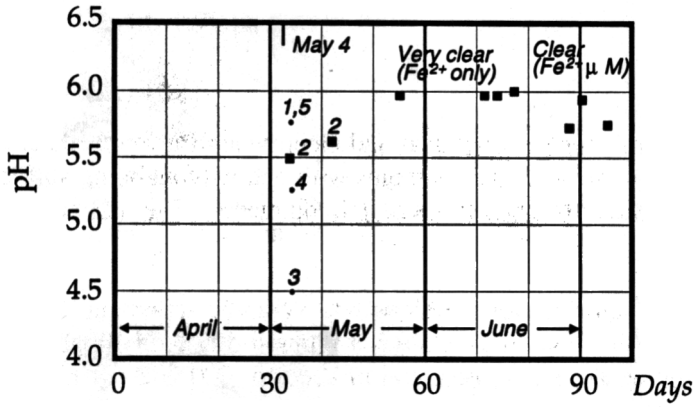

Figure 3. Diagram showing the history and a record of redox potentials, pH and Fe^{2+} concentration in the percolating solution, during the first 3 months. The numbers refer to different lysimeters and ● ■ refer to readings for respective lysimeters.

HISTORY

Aug 28, 1993
Lysimeter 1,2,3,4 and 5 filled with water & percolation tests carried out.
Redox Potentials :-

# 1	0.0640	V (SCE)
# 2	- 0.0230	V (SCE)
# 3	0.0834	V (SCE)
# 4	0.0653	V (SCE)
# 4X	0.1236	V (SCE)
# 5	0.0692	V (SCE)

FLOW RATES

#2	Uniform	1.07 mL /min
#1	Fast	27 mL /min
	Slow	0.18 mL /min
#3	Slow	0.26 mL /min
#5	Fast	33 mL /min
	Slow	0.6 mL /min

Fast and **slow** refer to flow rates through the annular space (between column and lysimeter wall) and through the tailings column, respectively.

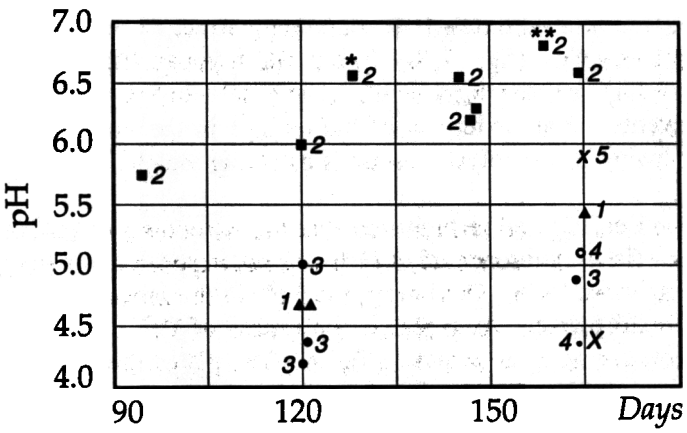

*2 After leaving dry for 1 week

**2 After leaving 2 in water head standing without flow.

Figure 4. Diagram showing the history and a record of redox potentials, pH and Fe^{2+} concentration in the percolating solution, during the last 3 months. The numbers refer to different lysimeters ● ■ refer to readings for respective lysimeters.

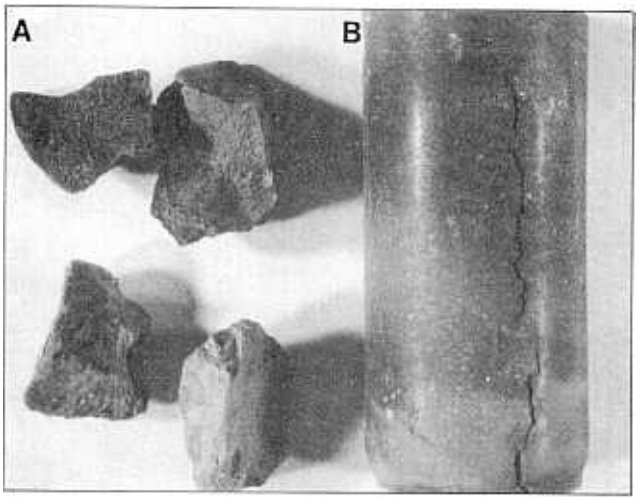

Figure 5A. Surface chemically formed pyrrhotite hardpan, obtained after a preoxidation step (pieces shown);
Figure 5B. Surface chemically formed pyrrhotite hardpan obtained without any pre-oxidation.

Figure 7. Synthetic hardpan showing pyrrhotite grains embedded in goethite matrix (+ some magnetite). White grains -- FeS.

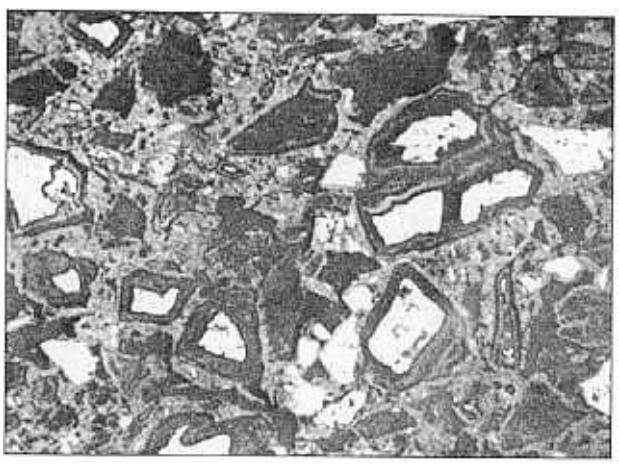

Figure 6. BEI photographs of natural, pyrite hardpan showing FeS_2 grains (white) coated with an iron oxide film, embedded in goethite matrix.

Figure 8. BEI photographs of natural, pyrrhotite hardpan showing FeS grains embedded in goethite matrix.

Although the presence of Fe^{2+} prevents the air oxidation of the tailings in the inner core, the Fe^{2+} in the leachate will eventually add to the acidity owing to hydrolysis reactions as shown below.

$$Fe(OH)_2 + H_2O = Fe(OH)_3 + H^+ + e^-. \quad \text{(in the presence of } O_2) \tag{1}$$

$$2\,Fe^{3+} + 6\,H_2O = 2\,Fe(OH)_3 + 6\,H^+. \tag{2}$$

$$Fe(OH)_3 = Fe[(OH)_2.O]^- + H^+. \quad \text{(acidic dissociation)} \tag{3}$$

$$Fe(OH)_3 = Fe[(OH).O_2]^{2-} + 2H^+. \quad \text{(etc. all in hydrated forms)} \tag{4}$$

The standard free energies of formation (Garrels and Christ, 1965) of the hydrated iron oxides from $Fe(OH)_2$ and $Fe(OH)_3$ are fairly negative (equations 5-8). Hence, these hydroxides are unstable and should decompose to hematite (goethite) and magnetite as found in the hardpan.

$$2\ Fe(OH)_3.nH_2O\ s \quad = \quad Fe_2O_3\ nH_2O\ s\ +\ 3H_2O. \tag{5}$$

$$\Delta\ F^0\ (Fe_2O_3) \quad = \quad -\ 15.17\ \text{kCal for reaction 5.} \tag{6}$$

$$3\ Fe(OH)_2\ s \quad = \quad Fe_3O_4 + H_2 + 2H_2O. \tag{7}$$

$$\Delta\ F^0\ (Fe_3O_4) \quad = \quad -\ 11.1\ \text{kCal for reaction 7.} \tag{8}$$

However, this decomposition will be slow because the activities of the reactants and products (solids) are unity. The hardpan formation is therefore time dependent, but the kinetics can be significantly accelerated by modifying the techniques of surface chemical treatment. The access of oxygen to sulfide tailings for surface oxidation is also kinetically controlled. Both these factors need to be considered in improving the kinetics of hardpan formation.

The Fe^{2+} concentration to be used needs to be optimized so that it does not contribute to the acidity significantly. Alternatively, the ferrous iron used should be completely oxidized and precipitated on the sulfides as oxyhydrates before loading the lysimeters. The latter procedure in particular will increase the kinetics of hardpan formation to a great extent.

Hardening Effect

The hardening was most pronounced in tailings that were preoxidized in the laboratory, treated with Fe^{2+}, and exposed to air with normal humidity (~50%). Except in lysimeter 2 (with a water head), tailings in all lysimeters had hardened from the top and sides to varying degrees, depending on the availability of oxygen in the bed. The most hardened column was 5, where the laboratory-oxidized tailings were intimately mixed with Fe^{2+} solution and exposed to air under atmospheric conditions. Tailings exposed to extra moist conditions (lysimeter 1, 3 and 4) by passing air saturated with water vapors, appeared to be less hardened; the least hardened column was 4 which was not treated or very little treated with ferrous iron. Hardening and self-compaction appeared to proceed simultaneously. As a result, the beds had developed cracks and detached from the walls at several places with water droplets condensing in the intermediate space. Water was condensing even in lysimeter 5 which was exposed to air under atmospheric conditions. Hence the condensed water was most probably originating from a dehydration process during hardening of the tailings.

E-redox, pH and Fe^{2+}-Fe^{3+} Concentration in the Percolant Solutions

The water percolation rates, pH, E-redox and concentration of dissolved Fe^{2+}-Fe^{3+} in the percolating solutions were measured at the beginning of the curing period 1 and at the end of the curing period 2 and the results are shown in graphical form in (figures 3 and 4), respectively. Before taking the end readings, (fig. 4), the trapped air was removed from the lysimeters (except #2) by slowly filling the units from the bottom with tap water having pH 6.5 to 7. The water was then allowed to percolate through the column.

In the case of lysimeter 2 with continuous waterflow, the flow rate, pH and ferrous-ferric concentration in the percolant solution were monitored for the entire period. These results are also shown in figures 3 and 4 for the beginning and the end periods of this work, respectively.

Because of the free space created between the tailing bed and the lysimeter wall, almost all of the water in percolation tests flowed through the column through this space readily in a short period of time (~400 mL in 10

to 15 min). The rest of the water percolated very slowly, most probably through the centre core which was not hardened and remained soft. These two rates are referred to as fast and slow flow rates in fig. 4.

At the starting stage prior to curing period 1 (fig. 3), the pH of the percolant solutions was between 5 and 6 for all columns except that lysimeter 3, with naturally oxidized tailings, had a pH of 4.5. This is because the tailings for this lysimeter were oxidized by exposing to open air in moist condition when much acid must have been produced. This acid was not washed out before lysimeter 3 was loaded and hence accounts for the low pH recorded. The iron content of the percolant solutions in all these runs was also high (0.01 to 0.001M) because the columns were freshly treated with Fe^{2+} solutions.

The pH values of the percolant solutions recorded at the final stage of the work and the redox potentials are given in fig. 4. These pH values range from 5 to 5.5 for lysimeters 1, 3, and 4, while column 5 shows a pH of 5.94 and the pH for column 2 (with a constant water head) continue to be well above 6. The lowest pH recorded was 4.92 for column 3, as before. Except for lysimeter 2, the dissolved iron concentration (almost entirely as Fe^{2+}) was rather high, in the range of 0.01 to 0.005M. As discussed earlier, this high concentration of iron in the leachate is originating from the inner core of the tailings as the adsorbed Fe^{2+} in this region is not oxidized and precipitated as $Fe(OH)_3$-Fe_2O_3 owing to insufficient oxygen supply.

Behavior of Tailings in Lysimeter 2, under 2 in of Water

The pH of the percolant solution from tailings under 2 in of water was initially 5.5 and became clear in about 6 days, the Fe^{2+} concentration being in the m mole range. The pH in later stages was between 5.5 and 6.0, and the Fe^{2+} concentration kept decreasing steadily to μ mole range (fig. 3). In the final stages of work, as shown in fig. 4, the pH was 6.6; E-redox was -0.023 V(SCE), which is highly reducing; and Fe^{2+} concentration was 10^{-8} M with no sign of Fe^{3+} present in the percolant solution. The percolant was practically pure water, once excess of Fe^{2+} (added initially) was removed. Although the bed had compacted well during the curing period, there was no sign of hardening or hardpan formation.

In one experiment, the pyrrhotite column in lysimeter 2, at the final stage of work, was left filled with water without draining it for a week, followed by draining the water and measurement of pH and dissolved iron concentration. In another experiment, the tailings in column 2 were left dry without any water head for a week, and water was then allowed to percolate through. In both these experiments, the pH of the percolant solution was still close to neutral while Fe^{2+} concentration continued to stay low (10^{-8} M). The untreated tailings under the same conditions would produce both acid and Fe^{2+}.

Redox Potentials

Redox potentials of 0.046, 0.120, and 0.186 V(SCE) were measured in solutions percolating from lysimeter 5, 2 and 1, respectively, at the beginning (fig. 3). These potentials, although fairly positive in relation to the standard hydrogen electrode, are still in the cathodic range in regard to charge transfer reactions with pyrite and pyrrhotite (Ahmed, 1990,1991). As a result, in this potential range, Fe^{2+} can still donate electrons and provide cathodic protection to the sulfide from the atmospheric oxidation.

The redox potentials shown in fig. 4 were measured in the percolant solutions at the final stage, after curing period 2. In general these potentials (fig. 4) are more negative than those at the beginning (fig. 3) and indicate reducing or cathodic conditions available at the FeS-solution interface with respect to Fe^{2+}-Fe^{3+} couple. There was experimental evidence to show that the redox potentials inside the bed were more negative than those measured outside, in the presence of air. Under these conditions, oxidation of sulfides by oxygen and Fe^{3+} by electrochemical mechanisms is not possible, although oxygen may still chemically attack pyrrhotite if it is not passivated and protected by iron oxide films.

Stability of Hardened Tailings

The hardened part of the tailings appeared to have good physical stability to withstand water percolation upto a pH of 4.5. In addition to the fully oxidized (type O) forms of the FeS hardpan which are porous and brownish in color, a gray type of unoxidized (type R) FeS hardpan was also encountered in the present work. The type R can be obtained by treating fresh and unoxidized FeS tailings with Fe^{2+} and exposing to air under moist or slightly wet conditions. After a few weeks, a hard and a very dense compact pan is formed which is gray in color and resistant to oxidation in dry or moist air because of the presence of Fe^{2+} in solid state. However, on immersion in water, surface reactions take place, leading to dissolution and precipitation of brown oxyhydrate of iron as a loose precipitate. The hardpans found in nature are usually a mixture of type O and type R hardpans. These hardpans can be completely stabilized by converting the iron oxide surface into less soluble compounds (solubility $< \mu M$) of iron such as silicates and carbonates, as suggested by phase diagrams (Garrels and Christ 1965).

Summary and Conclusions

1. Pyrrhotite hardpans can be prepared on a small scale by surface chemical treatment of the FeS tailings with Fe^{2+} under controlled conditions of pH, moisture, and oxygen supply. Such hardpans could also be made by cathodic treatment of the FeS tailings followed by exposure to air. The synthetic and natural hardpans were found to have the same structure, consisting of the FeS grains cemented in a ferric oxyhydrate matrix (goethite + lepidocrocite). The hardpan is formed as a result of the the oxidation of the adsorbed Fe^{2+} to the ferric state on FeS surfaces and precipitation of the oxyhydrates in the intergranular spaces. The ferric oxyhydrates then seem to consolidate into a hardpan on aging. Natural hardpans of pyrite are rare in occurrence and have slightly different structure at the pyrite-goethite interface.

2. In large scale experiments using lysimeters, formation of hardpans by surface chemical methods was restricted only to the outer layers well exposed to air. The inner core of tailings which was devoid of oxygen, remained soft and retained Fe^{2+} in the unoxidized form. The presence of ferrous iron provides cathodic protection to FeS from air oxidation. During water percolation, however, the excess Fe^{2+} ions drain out and contribute to the acidity of the percolant solution. Hence, the Fe^{2+} concentration to be used, the pH conditions and aeration methods need to be optimized in the hardpan formation.

3. The formation of hardpan is time dependent and is a slow process due to various factors such as low concentration of the dissolved oxygen in water and its slow diffusion to FeS, if immersed in water. Hence, the oxidation rates of FeS are known to be greatly enhanced in moist conditions where the oxygen has to diffuse through only a few molecular layers of water on the surface compared to tailings in wet conditions under several inches of water. The galvanic cells could be formed on FeS surfaces even in moist conditions. Formation of $Fe(OH)_3$-Fe_2O_3 is also kinetically slow (eqns. 5-8), as discussed earlier.

Fast methods of forming FeS hardpans can be developed by improving the reaction kinetics of the processes involved. In addition, the FeS-$Fe_2O_3.nH_2O$ hardpans can be further stabilized by converting the iron oxide surfaces into less soluble compounds of iron such as silicates, by surface chemical methods. This would greatly reduce the equilibrium concentration of the dissolved iron and hence the acidity in the percolant solutions.

4. Whereas the oxidation of pyrrhotite by oxygen is predominantly chemical, the oxidation of pyrite is mainly electrocatalytic in nature. Hence, formation of iron oxide films on pyrite is difficult without changing the surface composition significantly. The present, surface chemical methods therefore were not applicable to pyrite for hardpan formation.

5. The presence of an iron oxide layer on the FeS surfaces would substantially reduce the cross section of the sulfide exposed to oxygen attack. The use of Fe^{2+} would further reduce the oxygen flux by reacting with it and eventually forming the ferric oxyhydrate in the inter granular space.

6. The oxidative decomposition of the FeS and of the acid generation can be completely prevented by maintaining about 2 in of water head on the top of the tailings. This effect is not merely due to the lowering of the oxygen flux at the surface and its slow diffusion kinetics as discussed above, but also due to the formation of Fe^{2+} ions formed from FeS oxidation. The Fe^{2+} provides cathodic conditions to the surface in addition to reacting with oxygen directly as discussed above. Hence treating the tailings with a dilute solution of Fe^{2+} further helps in the protection of FeS from oxidation. However, the concentration of Fe^{2+} to be used needs to be optimized so that it does not contribute to the acidity of the percolant solution significantly.

In field conditions, the existing beds could be treated with the minimum amount of Fe^{2+} to prevent air oxidation and the bed could then be topped with a hardpan formed as above. The iron oxide in the hardpan need to be further stabilized by converting the surface into less soluble compounds of iron so as to completely prevent the dissolution of iron. For new tailings, the entire bed could be converted into a hardpan by applying a fast method of hardpan formation by treating with Fe^{3+} in low concentration, followed by hydrolysis. Certain optimization studies need to be conducted in this respect before a large scale method could be developed.

Acknowledgement

The help from M.T. Skaff in the initial treatment of tailings and setting up of the lysimeters was significant and is gratefully acknowledged.

Literature Cited

Ahmed, S.M. and Giziewicz, E., 1992. Electrochemical studies of iron sulfides in relation to the atmospheric oxidation and prevention of acid drainage, Part II. Proc. Third Intern. Symp., Electrochemistry in Mineral and Metal Processing, May 1992, St. Louis, ed. P. Richardson and Ron Woods, p. 403-415.

Ahmed, S.M., 1991. Electrochemical and surface chemical methods for the prevention of the atmospheric oxidation of sulfide tailings. Proc. Second Intern. Conf. on the Abatement of Acid Drainage, Montreal, Sept. 1991, Pub. MEND, Vol. 2, 305-320.

Ahmed, S.M., 1990. Electrochemical studies of semiconducting pyrite in relation to its atmospheric oxidation and chemical leaching. Electrochem. Soc. 178th Meeting, Seattle, WA, Oct. 14-19. Abstract No. 725.

Garrels, M.R. and Christ, L.C., 1965. Solutions, Minerals, and Equilibria. Harper and Row, New York, p. 182.

INTERNATIONAL PERSPECTIVE ON THE ROLE OF ACID GENERATION IN SELECTING DECOMMISSIONING TECHNIQUES FOR URANIUM MINING SITES IN EASTERN GERMANY[1]

D.G. Feasby[2], D.B. Chambers[3], J.M. Scharer[3], C.M. Pettit[3], R.G. Dakers[4] and M.H. Goldsworthy[5]

Abstract: The control of acidic drainage from uranium mine wastes in Germany is a significant component of mine site rehabilitation that began in 1992. Uranium was mined on a very large scale in the States of Thüringen and Sachsen from 1946 to 1991. Sulfide oxidation creates acidic drainage from waste rock piles at several mine sites and may occur in the future at two tailings impoundments. The extent of the problem of acidic drainage and methods to control acid production are reviewed from an international perspective. A central component of the rehabilitation plans in Germany is a proposal to fill a large open pit with acid-producing waste rock, allowing it to flood, and treating the overflow. This plan is assessed using a regional geological model in a probabilistic framework. This modeling has proven to be a useful tool in assessing management alternatives.

Background

Starting in 1946 and ending in 1991, uranium was mined on a large scale in the States of Thüringen and Sachsen in southeastern Germany. The scale of uranium mining in this area made it one of the world's largest uranium producers. The mining and uranium recovery was undertaken in the former East Germany by U.S.S.R.-German Democratic Republic company, Wismut. In addition to the recent mining for uranium, mining of these areas had been carried out since the Middle Ages for iron, silver, and other metals including bismuth (Wismut 1992). Following the reunification of Germany and the closure of the mines, major work and environmental assessment have been performed to decommission both the Wismut and historic sites. The authors have participated in assisting the Bundes Ministerium für Umwelt Naturschutz und Reaktorsicherheit (BMU) in their ongoing review of the Wismut decommissioning programs.

Over 1,600 sites in the mining region have been identified as having greater than background levels of radioactivity. Most of these sites have been linked to previous mining activity. The major mine waste sites of interest are those that resulted from the uranium mining, where approximately 200 million mt of mine tailings and 500 million mt of mine waste rock have been deposited on surface. The major uranium mining and mineral processing sites were those of the Wismut company; their locations are shown in figure 1.

An inventory of the major wastes remaining on surface is summarized in table 1. Acid generation resulting from the oxidation of sulfide minerals has been identified as a major concern in the mines and waste rock heaps on surface and underground at Ronneburg and is a potential concern at Königstein. In addition, there is a potential problem in two of the tailings basins at the Seelingstädt site, where ores were processed by acid and alkaline leaching to recover uranium.

---

[1]For presentation at the Third International Conference on Abatement of Acidic Drainage. Pittsburgh, Pennsylvania, U.S.A., 25-29 April 1994

[2] Mineral Sciences Laboratories, CANMET, Ottawa, Canada
[3] SENES Consultants Limited, Toronto, Canada
[4] Consultant, Ottawa, Canada
[5] Golder Associates, Celle, Germany

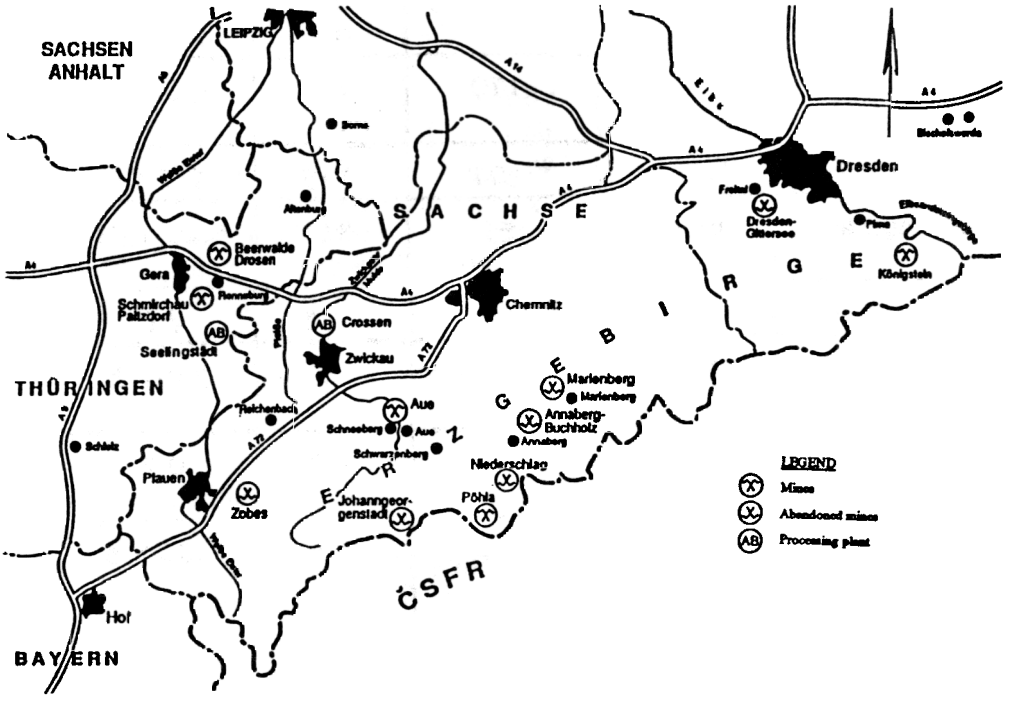

Figure 1. Location of Wismut mining works

ACKNOWLEDGEMENT

The authors gratefully acknowledge the permission of Wismut GmbH to publish this paper. The patient assistance of Dr. Daenecke and his staff in providing the needed information is very much appreciated.

TABLE 1 SUMMARY CHARACTERISTICS OF URANIUM MINE WASTES

Location	Waste type	Volume million m^3	Surface area, ha	Radium Bq/g	Pyrite, %
Ronneburg	Waste rock	170	409	0.3-1.5	3.3-4.8
Seelingstädt	Tailings	104	335	6.7-12	Variable*
Seelingstädt	Waste rock	59	519	0.25-1.65	NA
Crossen	Tailings	45	213	6.0	NA
Crossen	Waste rock	2	22	2.0-2.3	NA
Aue-Schlema	Waste rock	47	343	0.2	NA
Königstein	Waste rock, treatment sludges	3.3	25	0.34-5.6	1-2

NA Not available
Bq/g Becquerel/gram
* Acid leach tailings 0.8% to 5%, alkaline <1%,

Because of the very large quantities of these sulfide-bearing wastes, minimizing acid generation is a critical element in the decommissioning of the sites. The concerns are not only the production of acid waters and their effect on the environment per se, but also the leaching of radioactive species and heavy metals into ground and surface water and their subsequent dispersal in the environment. In addition, if significant acid generation continues to occur, there will be a need to collect and treat water for possibly hundreds of years. Ongoing water treatment also requires ongoing management of water treatment sludges, which contain radioactive and other heavy metals.

This paper describes the acid generation sources and magnitude of the problem and implications for decommissioning these former uranium mining areas.

The Impact Of Acid Generation in Uranium Mine Wastes

Experience in Canada and elsewhere has led to the conclusion that sulfuric acid generation is one of the major concerns associated with the decommissioning of sulfide-containing tailings and waste rock areas. Acid-leached uranium tailings are often significant acid producers even though the sulfide mineral content in the ore may originally have been very low. Strong acid generation can occur because most or all of any natural mineral alkalinity has been removed in the uranium extraction process by a hot sulfuric acid leach.

The chemistry of acid generation has been reviewed in detail (Nordstrum 1982) and can be summarized by the following reactions:

$$2\ FeS_2 + 7\ O_2 + 2\ H_2O \rightarrow 2\ Fe^{2+} + 4SO_4^{2-} + 4\ H^+, \quad (1)$$
$$2\ Fe^{2+} \rightarrow 2\ Fe^{3+} + 2e^-, \quad (2)$$
$$2\ H^+ + \tfrac{1}{2}\ O_2 + 2e^- \rightarrow H_2O, \quad (3)$$

Although these reactions can occur in a biologically sterile environment, chemolithotrophic bacteria, particularly Thiobacillus ferrooxidans, can accelerate the iron oxidation rate. Ferric iron in acidic solution can also oxidize metal sulfides (MS) according to

$$MS + 2\ Fe^{3+} \rightarrow M^{2+} + S^\circ + 2\ Fe^{2+} \quad (4)$$

Low pH (<4.0) seepage waters are often associated with mine wastes where sulfide oxidation is occurring, but frequently alkaline minerals such as calcite or dolomite present in the wastes can neutralize the acidity produced and near neutral conditions (pH ~ 7) can result *until the alkaline minerals are consumed or rendered unreactive by surface coatings.* Acidic drainage from mine wastes will solubilize many metals including aluminum, copper, zinc, nickel, manganese, and lead. For uranium-rich deposits, uranium and thorium are also dissolved. Blair et al. (1980) have identified metal contaminants mobilized by acid production as the most important concern in the management of pyritic uranium tailings. Also, acidic drainage has been identified at uranium mine waste rock sites in Australia by Ryan and Joyce (1991). Waste rock piles are very porous to water and oxygen, essential ingredients for sulfhide oxidation; because the piles are usual constructed on porous foundations, this "acid rock drainage" has been very difficult to prevent and control at sites around the world.

Acidic drainage is a significant environmental concern at the former uranium mining area in the States of Sachsen and Thüringen, Germany. High levels of acidity and dissolved metals are found in drainages at several locations. At one location, Ronneburg, autogenous combustion caused by rapid oxidation of sulfide sulfur and carbon (graphitic carbon) had caused additional problems in mining and waste disposal. Significant quantities of sulfide minerals (notably pyrite) are also present in the waste rock at Crossen, Aue, and Königstein. Although most drainages sampled to date indicate neutral drainage, elevated levels of dissolved calcium and magnesium sulfates indicate that the possibility of future acid generation in these wastes cannot be excluded.

Site Considerations

Ronneburg-Drosen

The Ronneburg-Drosen mines are in east Thüringen, Wismut's most important uranium mining area. In total, these mines produced over 170 million m^3 of waste rock, all of which is potentially acid generating. At present, over 100 million m^3 of waste rock are stored on surface (in 14 waste piles). One pile was subjected to in situ uranium leaching using mine water supplemented with sulfuric acid. The remainder had been placed in a large open pit. Like most of the waste piles in southeastern Germany, the waste piles are located close to villages and individual homes (within several hundred meters). In addition to the understandable concerns about environmental radioactivity, particularly radon emissions, there are concerns about contamination of surface water and ground water and physical access to the materials. A cross section of the most environmentally significant part of the mining area at Ronneburg is shown in figure 2. Mining ceased at Ronneburg in December 1991, and the lower levels of the mine are now being allowed to flood.

Current plans (Wismut 1992) are to fill the open pit with as much waste rock as possible. The most severe acid producers will be placed on the pit bottom, but about 30 million m^3 will remain above the water table. The final contouring and cover applied to these materials will be important factors in determining long-term acid production. Excess alkalinity, for example, lime and/or limestone, is being considered to help control acid generation, and studies were recently completed to determine the effect of submerging most of the waste rock under the water table in the open pit.

Until the mine workings are flooded, acid will continue to be produced from sulfide minerals in open spaces and fractured zones underground. In addition, in the long term after the mines are flooded, acid will continue to be produced in the fractured ground above the water table.

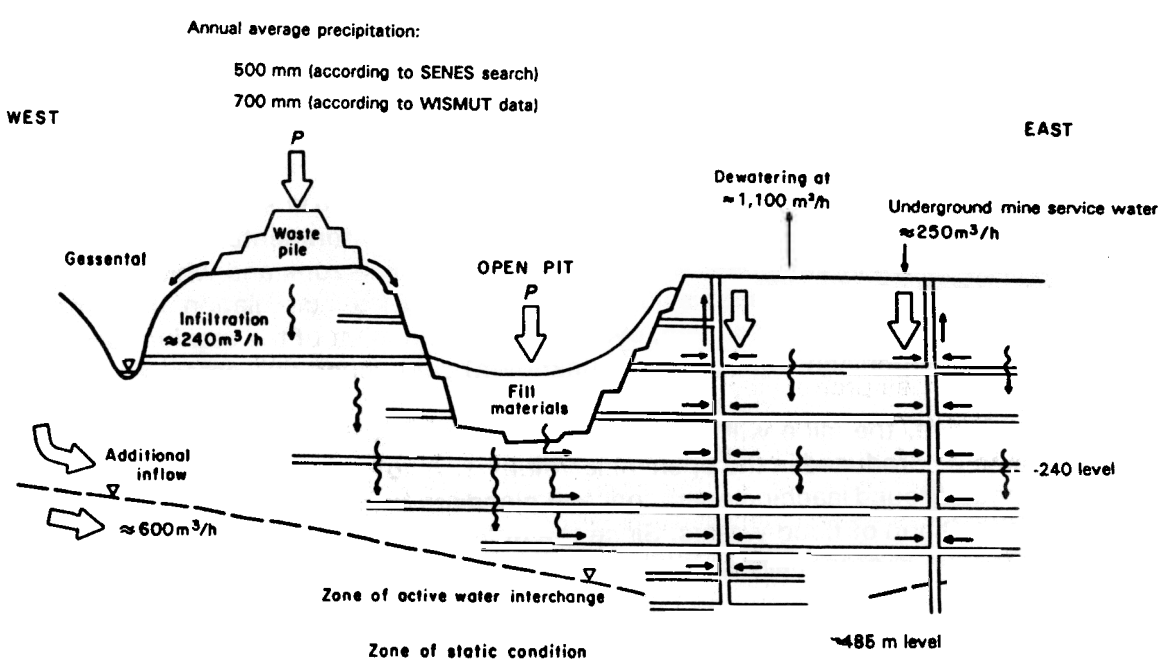

Figure 2. Wismut Decommissioning
Ronneburg Site Existing Hydrological Situation Typical Conceptual E-W Section

Seelingstädt

Seelingstädt was a central ore processing facility for the Wismut mines. Uranium was extracted from the ore in parallel circuits, one with alkaline sodium carbonate, and the other with sulfuric acid. The sulfuric acid circuit was used to leach uranium from high sulfide ores and pyrite concentrates. Tailings from the acid circuit are potential acid producers if dewatered and exposed to oxygen. The tailings from the alkaline circuit represent no acid generation potential because the pyrite was converted to soluble sulfate by the following reaction:

$$4FeS_2 + 15O_2 + 16Na_2CO_3 + 14H_2O \rightarrow 4Fe(OH)_3 + 8Na_2SO_4 + 16NaHCO_3. \quad (5)$$

Available data (Wismut 1992) indicate potential for acid generation in two large tailings basins at this site. At present, the basins are water saturated, and much of the formerly exposed tailings surface is covered with soil. The conceptual plan (Wismut 1992) is to dewater the tailings pond and to cover the balance of the dewatered tailings with a soil cover. Dewatering has the potential to result in increased oxidation and acidification of sulfide minerals, even though the pore fluids are currently alkaline from the mixing in of alkaline chemicals used in the milling process.

With respect to tailings and acid generation, the situation at Seelingstädt is unique; acid leached tailings are covered with alkaline water (pH 7.4 to 9.9) with high levels of dissolved sulphates (10 G/L). However, any residual mineral alkalinity has been removed in the acid leaching process, and if the tailings are dewatered as planned, infiltration of rainwater could flush out these buffering salts and permit acid generation to start. Based on the appearance of ferric iron salt coloration on exposed tailings beaches, this acidic generation potential appeared to be confirmed.

There is considerable international experience in predicting the rate of acid generation in pyritic mine tailings, and estimates of the rate of acid production by sulfide-bearing uranium tailings have been given by Halbert et al. (1983) and Scharer et al. (1991). Acid-base accounting on field samples (Wismut 1992) has shown that the acid-leached tailings are potentially acid generating; precise predictions cannot be made until the decommissioning scenario (eg., dewatering and covering) is established.

Königstein

The Königstein site in Sachsen has extensive underground workings, which were initially developed by conventional mining, and more recently by underground in situ leaching with sulfuric acid addition to leach solutions recirculated from surface. The key environmental concern at this site is the potential for contamination of an aquifer which overlies the mining zone and which is used for drinking water. About 1 million m^3 of acid leach solution has been lost from circulation and is presently in the pore space in the fractured rock. In addition, pyrite is present in most of the uranium-bearing zones, and these strata represent significant (but currently unknown) acid generation potential.

In the near future, the mine will be flooded, and acid production will cease, but until such time acid will continue to be produced in the open mine volumes. Also there will remain considerable residual acidity from the underground leaching operation, and plans are being developed to neutralize this acidity on surface by recirculation of flood waters. Since the underground workings cover 5 km^2, the effect of the natural acidification is potentially significant.

Also at Königstein, there exists a 3.2 million m^3 surface waste pile, which is composed of 2.0 million m^3 of heap leach waste rock and other wastes, principally uranium-barren waste rock and water treatment sludges. The main concern with respect to acid generation is the heap leach pile. Although it has been depleted in sulfide sulfur content by bacteria-catalyzed oxidation, oxidation of the estimated remaining 1% to 2% pyrite content could accelerate in the near future. Currently, the waste pile produces an acidic effluent, as shown in table 2

TABLE 2 ACIDIC DRAINAGE FROM KÖNIGSTEIN WASTE ROCK

Volume	3 to 10 m^3/h
pH	2 to 4
U	30 mg/L
Ra	0.5 Bq/L
Fe (total)	200 mg/L
SO_4	3000 mg/L

Technical Considerations for the Prevention and Control of Acid Production

Various interdependent geochemical, physical, and biological factors control the rate and quantity of sulfide oxidation in the waste rock and tailings. These factors include temperature, bacteria activity, oxygen profile, pore water composition, effective grain size of sulfide minerals, and acid neutralization potential.

As an example of currently available predictive techniques, the authors have recently completed an extensive review of the environmental impact of depositing acid-producing waste rock into the bottom of the open pit at Ronneburg. To develop a reference point for environmental assessment, a waste rock pile that had formerly been a heap leach for uranium recovery was selected for evaluation. A computer model (ACIDROCK) was used to simulate the placement and leaching history of the waste rock pile (SENES 1993a). The model was used to predict the long-term seepage quality for various management options (e.g., covered with an engineered soil cover, and uncovered). The results of modeling the 27-ha pile showed that -

- Acidity will be produced for more than 100 years, with or without cover;
- A state-of-the art earth cover will reduce acid production and water treatment requirements by an order of magnitude;
- Continuous care and maintenance of the site would be required.

A much more complex predictive modeling evaluation was completed on the option of placing the same waste rock pile into the bottom of the pit. Geochemical measures, such as the addition of lime to neutralize acidity contained in the waste rock, were considered as part of the evaluation. The first stage of the modeling was the development and application of a hydrological model that simulated the flooding process, the establishment of steady-state flows with all of the mine cavities filled with water, and the contaminated ground water emerging at a nearby stream valley (Brenk Systemplanung 1993). A filled pit in the flooded condition is shown in figure 3.

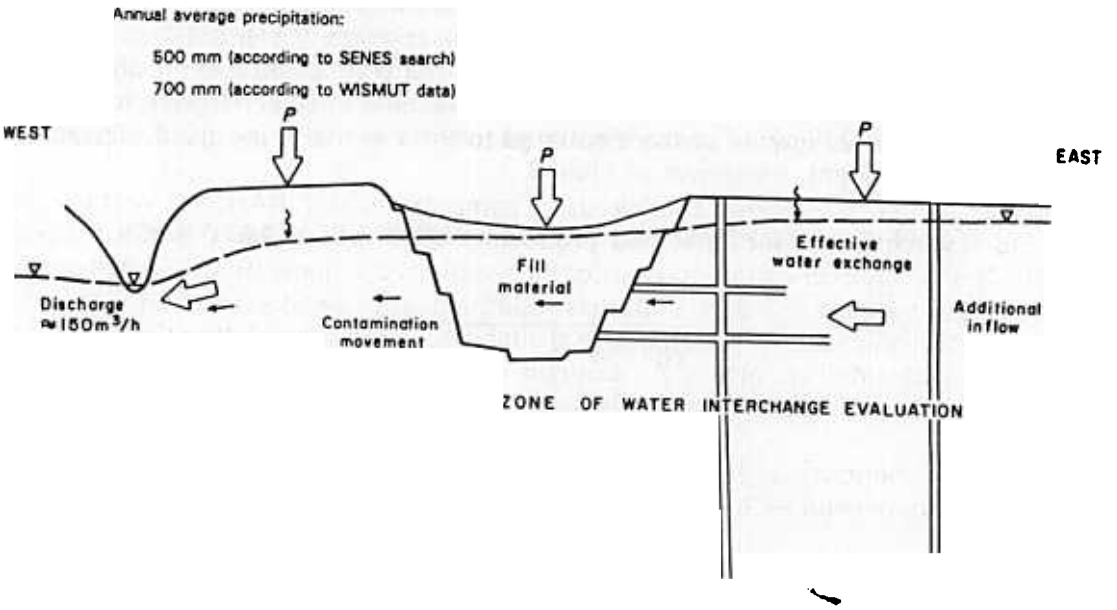

Figure 3. Wismut Decommissioning
Ronneburg Site Future Hydrological Situation Typical Conceptual E-W Section

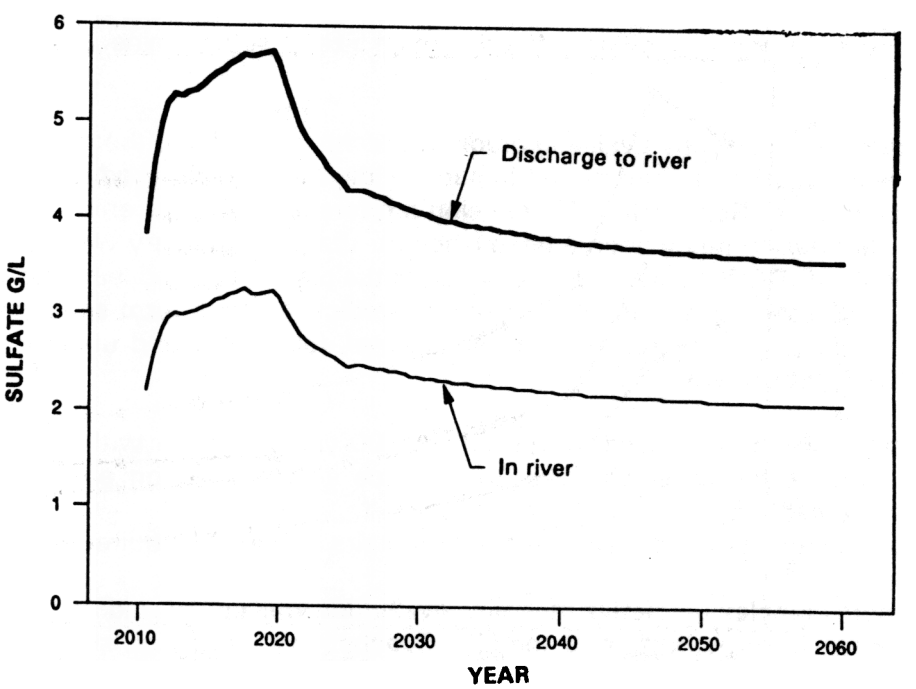

Figure 4. Predicted Sulfate

A computer model (ROCKSTAR) was used to simulate the geochemical processes occurring in the flooded pit materials and the associated underground mining areas (SENES 1993b). The model was used deterministically to predict the water quality within the pit fill and mining areas, as well as the water quality of the surface water body (river) that would receive the discharge from the mining region. Figure 4 shows the predicted quality of the discharge to the river, and the quality in the river.

Probabilistic modeling was also employed. A computer model (RANSIM) was used to randomly select many input values from the specified probability distributions for the key model parameters (SENES 1989). These values are substituted into the geochemical model (ROCKSTAR) to obtain a single value for each output variable. This procedure is repetitive, with each selection being referred to as a trial. Using the probabilistic approach, subjective probability distributions rather than single numbers will be obtained for the calculated variables. An example of the predicted water quality of the discharge to the river for 50 trials of the probabilistic model is shown in figure 5.

The predictive modeling assessment of placing the heap leach waste rock into the pit at Ronneburg can be summarized as follows:

- Nearby mine openings and underground broken rock zones control water flow patterns. (The underground mine excavations included over 1,800 km of tunnels).
- The contained acidity and stored oxidation products of the waste rock had a small impact on the emerging water quality.
- The addition of lime to the waste rock reduced the predicted impact of the waste rock to insignificant levels (reduced sulphate and metal mobility).

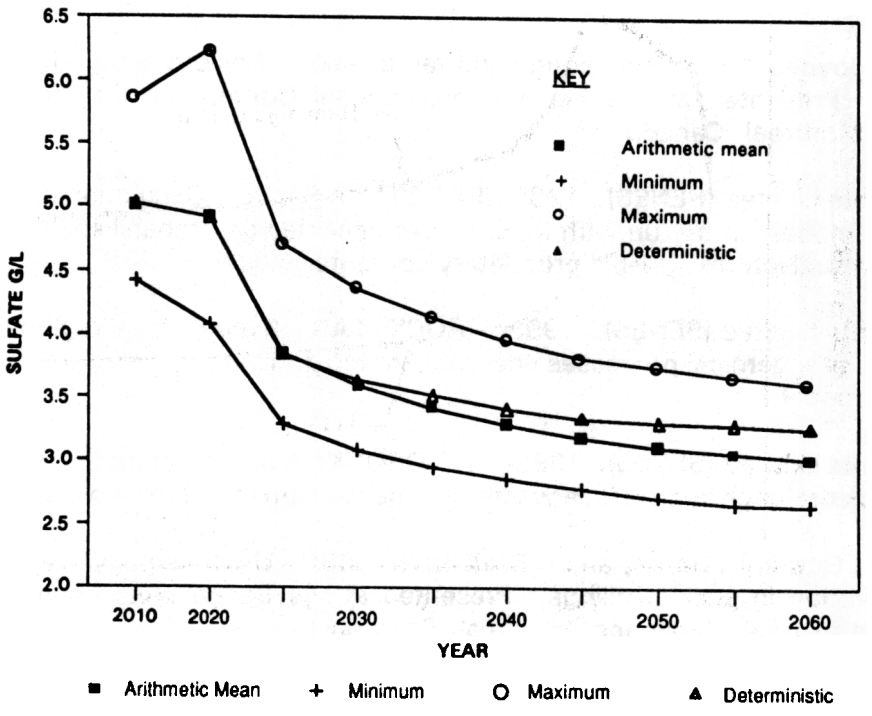

Figure 5. Predicted Water Quality for Discharge to River
Probabilistic Approach - 50 Trials

Summary

Control and treatment of acid rock drainage is a major focus of the decommissioning strategies being developed for the uranium mine sites in south eastern Germany.

Sophisticated mathematical models are being applied in the evaluation of mine decommissioning technology, which includes prevention and control of acidic drainage from waste rock and tailings. A major focus of the control measures for waste rock is depositing the rock into an open pit and then allowing the pit to flood with mine waters. Worldwide, the evaluation of options for dealing with acid-producing waste rock and tailings has led to the selection of the use of water covers and underwater disposal as the best technology.

References

Blair, R.D., J.A. Cherry, C.P. Lin, and A.J. Vivyurka. 1980. Groundwater monitoring and contaminant occurrence at an abandoned tailings area, Elliot Lake, Ontario. Presented at the First International Conference on Uranium Mine Waste Disposal, Vancouver, Canada.

Brenk Systemplanung. 1993. A three dimensional finite element model for simulating groundwater flows in a mining region.

Halbert, B.E., J.M. Scharer, R.A. Knapp, and D.M. Gorber. 1983. Determination of acid generation rates in pyritic mine tailings. Presented at the Annual Conference of the Water Pollution Control Federation, Atlanta, GA.

Nordstrum, D.K. 1982. Aqueous pyrite oxidation and the consequent formation of secondary iron minerals in acid sulphate weathering. Soil Sci, Soc, America, p. 37-55

Ryan, P. and C. Joyce. 1991. Prevention and remediation of acid drainage from mine waste rock in Australia. Presented at the Second International Conference on the Abatement of Acidic Drainage, Montreal, Canada.

SENES Consultants Limited (SENES). 1989. RANSIM: A Random Simulation computer model to allow FORTRAN models to be run with input values specified as probabilistic distributions rather than as constants. Non marketable proprietary computer model.

SENES Consultants Limited (SENES). 1993a. ROCKSTAR: A multi-nodal regional computer model for simulating geochemical processes occurring within a mining region. Non marketable proprietary computer model.

SENES Consultants Limited (SENES). 1993b. ACIDROCK: A computer model for simulating production of acid rock drainage in a surface waste rock heap. Non marketable proprietary computer model.

Scharer, J.M., V. Garga, R. Smith, and B.E. Halbert. 1991. Use of steady-state models for assessing acid generation in pyritic tailings. Presented at the Second International Conference on the Abatement of Acidic Drainage, Montreal, Canada.

Wismut. 1992. Umweltbewertung des gesamtkomplexes tagebau-flutung-halden (Environmental evaluation of the total complex - open pit). Wimsut 30.9).

EVALUATION OF ACID GENERATING ROCK AND ACID CONSUMING ROCK MIXING TO PREVENT ACID ROCK DRAINAGE[1]

Stephen J. Day[2]

Abstract: Mixing acid generating and acid consuming rocks is an attractive and potentially low cost alternative for in situ prevention of acid generation in waste rock piles at some mine sites. In addition to the practicalities of day-to-day management of mixed waste rockpiles, the success of the mixing will probably depend on the proportion of acid-consuming material, the availability of the acid consuming minerals, and the intimacy of mixing. A 5-yr column study for the Cinola Gold project, an epithermal gold deposit located in a cool, moist maritime area of northwestern British Columbia, Canada, was initiated in 1988 to evaluate limestone requirements to prevent acid and metal release from waste rock stockpiles. Limestone content in five columns varied from zero (control, net neutralization potential = -58 kg/mt $CaCO_3$) to 6.6% (NNP = 7 kg/mt $CaCO_3$). Four of the columns generated acid. The column containing the highest concentration of limestone did not release acid, although residues in the upper part of the column were acidic and sulfate concentrations in leachate were gradually increasing. It was concluded that (1) the actual quantity of limestone required to prevent acid drainage in perpetuity would probably be at least twice that determined by conventional acid-base accounting, (2) limestone availability was not reduced by ferric hydroxide coatings, (3) the time required for marginally acid generating rock to release acidity increased exponentially as the quantity of limestone increased, and (4) the time required for zinc release to begin increasing was linearly proportional to the neutralization potential. Limestone addition was therefore highly effective in delaying acid release but was less effective in delaying zinc release.

Additional Key Words: acid rock drainage, waste rock, alkaline addition.

Introduction

Many potentially economic mineral deposits contain high concentrations of iron sulfides and therefore waste rock, mine workings and tailings associated with such deposits are prone to acid generation. However, a significant number of deposits also have associated acid consuming minerals in the mineralization or nearby host and country rocks. In some situations, the possibility of mixing acid generating and acid consuming rocks is an attractive and potentially low cost alternative for in situ prevention of acid generation. When correctly engineered, mixing (or blending) may yield a long term waste management solution without the long term liability and maintenance of artificial structures such as dry covers, artificially flooded impoundments, or water treatment plants.

This paper presents results for a 5-yr column leaching study conducted on marginally acid-generating materials. The study was initiated by City Resources (Canada) Inc. to evaluate the inhibition of acid generation by adding limestone to stockpiles of potentially acid-generating rock at the proposed Cinola Gold Project in northwestern British Columbia (BC). The limestone is not naturally available at the site but is found on an island off BC.

General Background

A number of uncertainties remain regarding design of mixed rock waste piles. Although some of these uncertainties relate to the practicalities of day-to-day management of such piles under operating conditions, a more

---

[1] Paper presented at the International Land Reclamation and Mine Drainage Conference and the Third International Conference on the Abatement of Acidic Drainage, Pittsburgh, PA, April 24-29, 1994.

[2] Stephen J. Day, Senior Geochemist, Norecol, Dames & Moore, Inc. 500-1212 West Broadway, Vancouver, British Columbia, Canada, V6H 3V1.

fundamental issue relates to the amount of neutralizing material required to effectively consume acid produced by oxidation of iron sulfides.

The commonly used acid-base accounting procedure represented one of the first attempts to determine an acid producing-consuming balance in heterogeneous materials (Sobek et al. 1978). The theory was based on the assumption that neutralizing minerals (represented by calcium carbonate) are consumed completely to release carbon dioxide (gaseous or dissolved). In reality, the initial phases of acid generation occur under approximately pH-neutral conditions and carbonates neutralize acid incompletely, forming the bicarbonate ion (HCO_3^-). In natural rock mixtures, other considerations arise, such as the heterogeneous distribution of sulfide and carbonate minerals, the slow dissolution of carbonate minerals in the absence of acid, and the coating of carbonate grains by precipitated hydroxides. In recognition of these uncertainties, regulators in some jurisdictions (for example, California and British Columbia) require that blended rock mixtures at metal mines contain at least three times as much neutralizing material as acid generating material (both expressed in equivalent concentration units of calcium carbonate). Some support for these requirements can be found in the data from coal mines in the eastern United States which indicate that the ratio of neutralization potential to potential acidity in waste rock should be at least 2.4 to ensure acid is not released (Cravotta et al., 1990).

One of the difficulties in determining acceptable mixing ratios is that results from laboratory and field tests tend to be inconclusive. The success of a mixing approach is shown by the lack of acid generation. The problem is that most tests are not continued to a definitive end point which indicates that acid will not be produced. Ferguson and Morin (1991) showed that the time for acid to be produced increases exponentially as the ratio of neutralization potential (NP) to maximum potential acidity approaches 1. Any experiment designed to address marginal acid generating conditions must operate for an extended period (often several years) to demonstrate conclusively that acid will not be produced.

Cinola Project Background

The Cinola Gold Deposit is located on the Queen Charlotte Islands off the north BC coast. The deposit is classified as epithermal Carlin-type by Champigny and Sinclair (1982) owing to the small (<0.5 μm) particle size of gold, age of about 14 million years, presence of argillic alteration, association with faults and felsic intrusions, and porosity of the host rock. Disseminated, fine-grained (<25 μm) sulfide minerals (primarily pyrite, with lesser marcasite) occur throughout the mineralization and host rocks, generally in concentrations of a few percent. In contrast, calcite occurs sporadically, and in one important unit, the Skonun Sediments, is almost completely absent. Acid-base accounting indicated that the Skonun Sediments are potentially acid generating. Laboratory and field kinetic tests confirmed that acid would be produced.

The region hosting the deposit experiences seasonal weather patterns typical of coastal western Canada, that is, most precipitation occurs as rain during October to March. Annual precipitation ranges from 1,700 to 2,200 mm. Average monthly temperatures are never less than 0° C. As a result of the high precipitation rate, the potential for mobilization of acid weathering products from waste rock dumps composed of Skonun Sediments is high. Waste rock management was therefore planned to address perpetual prevention of acid generation. It was proposed that the potentially acid generating Skonun Sediments be stockpiled during operation and then backfilled and submerged in the open pit during mine decommissioning. To prevent extensive oxidation and the release of acid rock drainage from the stockpiles prior to submergence, it was proposed that limestone be added to the stockpiles in a controlled fashion. A column leach study was designed to evaluate such factors as limestone requirement, availability of limestone for reaction, and the effect of intimate mixing and layering of acid consuming and acid generating rock.

Experiment Design

Five columns were designed:

Column 1	Waste rock only (control test).
Column 2	Approximately 6.6% limestone intimately mixed with waste rock (theoretically sufficient to neutralize maximum potential acidity).
Column 3	Approximately 3.2% limestone mixed with waste rock capped with 1 cm of column 2 mixture (50% of maximum potential acidity). The cap was intended to investigate one dump design option.
Column 4	Approximately 0.84% limestone mixed with waste rock capped with 1 cm of column 2 mixture (acid neutralized for 10 weeks at a rate predicted from humidity cells).
Column 5	Approximately 1.2% limestone as five 1-cm thick layers of column 2 material alternating with four 10-cm layers of column 4 material to evaluate the effects of layering.

Materials and Methods

Test Materials

Waste rock for the columns was derived from composited reverse circulation drill cuttings from various subgroups of the Skonun Sediments. The composites were designed to approximate the expected composition of waste rock piles. Limestone for the experiments was obtained from Texada Island, the proposed source of limestone if the deposit were developed. The limestone was dried and crushed to a diameter of 0.6 mm or smaller. Limestone and waste rock were mixed on plastic sheets before placement in the columns.

Test Material Characteristics

The waste rock contained approximately 2.1% total sulfur and had a neutralization potential of 8 kg/mt $CaCO_3$. Net neutralization potential (NNP) was approximately -58 kg/mt $CaCO_3$. The limestone contained some sulfur (0.22%), and based on the neutralization potential of 932 kg/mt $CaCO_3$ had a high purity. The dominant carbonate mineral in the limestone was calcite. Dolomite was expected to be a minor component. The surface area of particles was estimated using size fraction analysis and assuming that particles were perfectly spherical. Waste rock and limestone had surface areas of 5.4 and 30.9 m^2/kg, respectively. These values are gross approximations but show that the reactive surface area of the limestone was about five times that of the waste rock. The limestone was deliberately crushed finer than the waste rock to yield a greater reactive surface area.

Acid-base accounts (ABA) for the four columns containing limestone (2 through 5) were determined using mass-weighting. Values for each parameter were determined using the formula

$$P_{weighted} = (P_{lst} \cdot M_{lst} + P_{rock} \cdot M_{rock})/(M_{lst} + M_{rock}) \quad (1)$$

where P is the parameter (e.g., neutralization potential, NP; maximum potential acidity, MPA), and M_{lst} and M_{rock} are the masses of limestone and waste rock in the column. Values for each column are summarized in table 1. Neutralization potential ratio (NPR) was determined as equal to $NP_{weighted}/MPA_{weighted}$. Since the quantity of limestone was relatively small, the MPA of the columns varied over a small range (62 to 65 kg/mt $CaCO_3$). Only column 2 was considered potentially acid consuming from conventional interpretation of ABA. The remaining columns had NNP<0 and NPR<1, implying a potential for net acid generation.

Test Procedures

Test materials were placed in 15-cm diameter plastic columns to a thickness of 0.5 m. Column tops were covered with a plastic plate to minimize evaporation. Holes in the plate allowed humidified air and de-ionized water (at a rate of 0.4 to 0.5 mL/min) to be continuously introduced into the column. The top plate was rotated daily so

Table 1. Acid-Base Accounting - Test Materials and Residues.

	Position in column	S, %	Sulfate, S, %	Sulfide, S, %	MPA	NP	NNP	NPR	Paste pH
					kg/mt, CaCO3				
Column 1, Control									
Pre-test	Bulk.....	2.10	NA	NA	66	8	-58	.12	6.90
Residue	Top, bulk.....	.53	.09	.44	17	-2	-19	.00	3.30
Residue	Middle, bulk.....	.55	.10	.45	17	-2	-19	.00	3.62
Column 2, 6.6% Limestone									
Pre-test	Bulk.....	1.98	NA	NA	62	69	7	1.11	NA
Residue	Oxidized, bulk.....	1.12	.05	1.07	35	3	-33	.07	5.30
Residue	Non-oxidized, bulk..	1.72	<0.01	1.71	54	57	2	1.05	7.80
Column 3, 3.2% Limestone									
Pre-test	Bulk.....	2.05	NA	NA	65	38	-27	.58	NA
Post-test	Top, bulk.....	.85	.05	.80	27	0	-26	.01	4.76
Post-test	Middle, bulk.....	.77	.11	.66	24	-2	-26	.00	4.05
Column 4, 0.84% Limestone									
Pre-test	Bulk.....	2.08	NA	NA	66	16	-50	.24	NA
Post-test	Bulk.....	.65	.11	.59	20	-2	-22	.00	4.06
Column 5, 1.2% Limestone in layers									
Pre-test	Bulk.....	2.08	NA	NA	66	19	-46	.29	NA
Post-test	Bulk.....	.68	.12	.56	21	-2	-23	.00	4.25

NA - Not analyzed.

Pretest results were calculated from mass-weighted averages of limestone and waste rock components

that the introduced water contacted different surface locations. In addition to the direct weekly measurement of conductivity and pH, leachates in the collection vessel were analyzed for sulfate (by a gravimetric method), alkalinity/acidity (by titration with sulphuric acid and sodium hydroxide, respectively), and dissolved (<0.45 μm) metals, which included iron, copper, zinc, arsenic, lead, and the major alkali and alkali earth metals. Metal concentrations were determined by several methods including atomic absorption, flameless atomic absorption and inductively coupled argon plasma (mass spectroscopy). After completion of the tests, the columns were dismantled and examined. Samples of the residues were collected for chemical analysis (acid-base accounting, carbonate and sulphur species) and preparation of polished thin sections for identification of secondary minerals.

Results

Leachate Chemistry

Leachate from all four columns containing some limestone was initially pH neutral (fig. 1). Column 1 (control) generated leachate with pH 3 for about 11 weeks. The pH then dropped to near 2. The pH of leachate from this column then steadily increased to greater than 3. Column 4 (low limestone concentration) and column 5 (layered limestone) both generated acidic leachate at week 33. For both columns, pH dropped to between 2 and 3 very rapidly, without intermediate plateaus. Column 3 (intermediate limestone concentration) generated acidic leachate after about 4 yr of operation. The transition to low pH conditions was not quite as rapid as for columns 4 and 5. The column containing the highest concentration of limestone (column 2) generated pH-neutral water throughout the 5-yr experiment.

Sulfate concentrations in the leachate from each of columns 1, 3, 4, and 5 followed similar trends (fig. 1). Sulfate loadings show the same trends because the water percolation rate was relatively constant. All columns

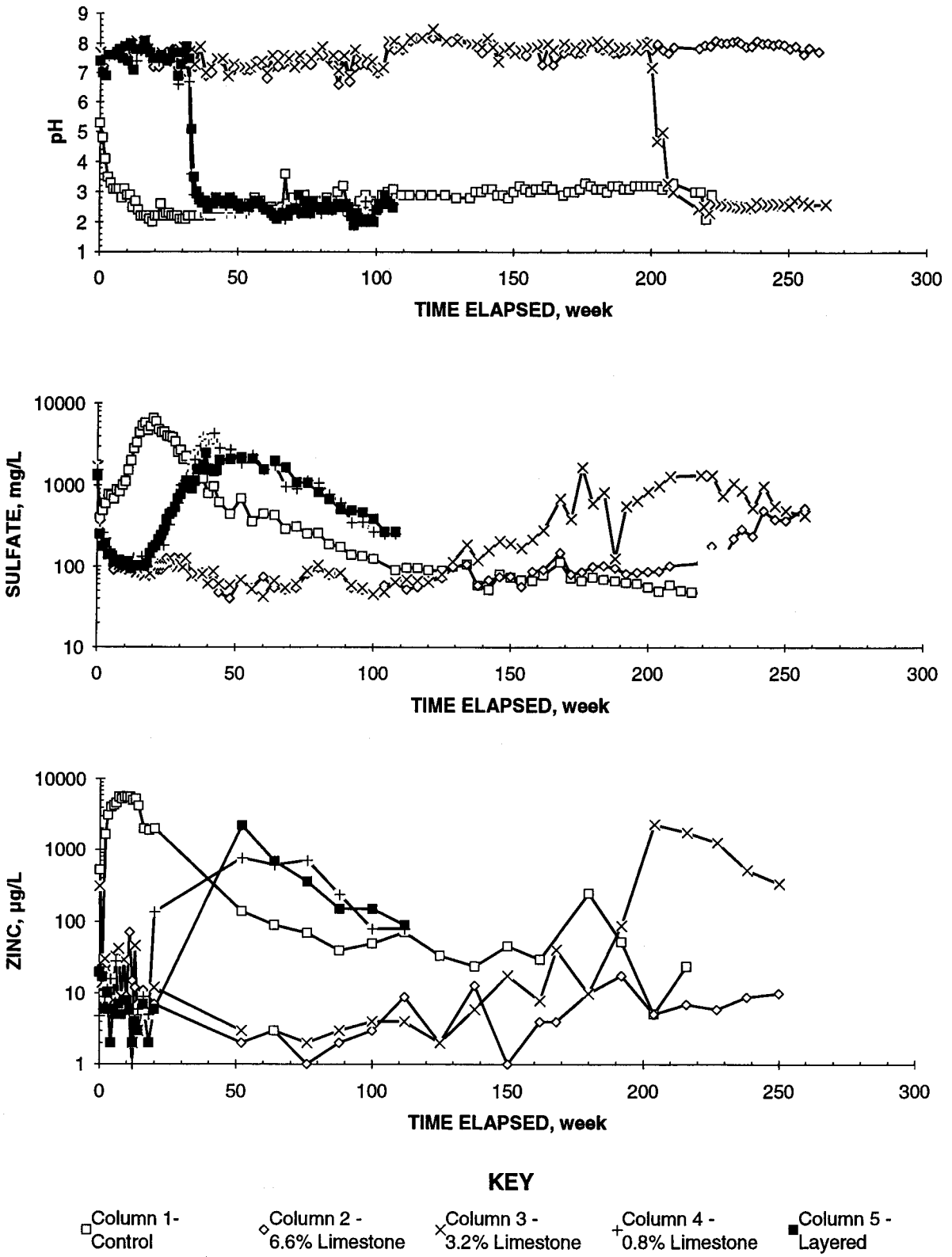

Figure 1. Trends in pH, sulfate, and zinc concentrations in leachates.

showed initially decreasing sulfate concentrations. Concentrations then increased several weeks before pH dropped to between 2 and 3, and peak sulfate release occurred several weeks after the pH dropped.

The observations can be summarized and correlated as follows:

- The time elapsed from a noticeable increase in sulfate concentration to the production of a low pH leachate increased with the proportion of limestone. For columns 4 and 5, 12 weeks elapsed. For column 3, 100 weeks elapsed. Although column 2 did not generate acidic leachate, the time elapsed would be expected to be greater than 180 weeks,

- The time elapsed from release of acidic leachate to peak sulfate concentration was between 9 and 21 weeks for all tests, including the control column,

- The intensity of the sulfate concentration peak decreased with increasing limestone concentration,

- The sulfate concentration peak became less well-defined with increasing limestone concentration, and

- The sulfate decay curve slopes appear to be similar on semilogarithmic graphs, indicating half lives (i.e. time taken to reach half the maximum sulfate concentration) of 5 (control) to 22 weeks.

Sulfate concentrations from column 2 were increasing when the test was terminated. Characteristics of the curve were similar to those of the other tests. Sulfate concentrations had not reached a level that might be expected prior to the onset of fully acidic conditions.

Trends in leachate alkalinity and calcium concentrations were very similar reflecting the dissolution of calcium carbonate. Calcium determinations were most useful for monitoring leaching of limestone because determinations were made regardless of pH. Alkalinity in leachate from column 3 began to increase about 20 weeks after sulfate concentrations increased and peaked at 110 mg/L $CaCO_3$ just before pH dropped. Calcium concentrations also increased during this period, and peaked at about the same time as sulfate concentrations. Once pH decreased, alkalinity also decreased very rapidly and could not, by definition, be measured once pH dropped to less than 4.5. Alkalinity in leachate from column 2 began increasing about 30 weeks after sulfate concentrations began increasing. Calcium also began increasing.

Dissolved iron was the most significant heavy metal in the column leachates. Sulfate and iron concentrations showed similar trends, although iron varied over a wider range. At low pH (less than 2.9), iron and sulfate concentrations (in mg/L) were comparable. At near neutral pH, iron concentrations were commonly less than the detection limit of 0.03 mg/L. Zinc concentrations (fig. 1) showed similar trends to sulfate. Zinc concentrations began increasing as sulfate increased, long before pH decreased. Peak zinc concentrations tended to precede peak sulfate concentrations by a few weeks.

Characteristics of Column Residues

Column residues were of two types: Columns 1, 3, 4, and 5 (acid generators) contained visibly oxidized (orange-coloured) rock. Column 2 residue was vertically zoned. The upper one third of the column contained oxidized material similar to that in the acid-generating columns. These residues also yielded low paste (de-ionized water) pH. Residue from the lower portion of this column were relatively unweathered (grey-colored), reacted strongly with dilute HCl (indicating readily available NP), and was pH neutral.

Several significant textural features were noted in polished thin sections. In residues from nonacidic columns, abundant fresh pyrite and marcasite grains were observed. These grains showed some in situ replacement by limonite along grain boundaries. By contrast, alteration of pyrite grains varied from negligible to complete in acidic material,

and in situ replacement of sulfide grains by limonite was common. Replacement had taken place along grain edges and along internal fractures and crystal boundaries. In both nonacidic and acidic material, limestone particles appeared fairly fresh and did not have significant limonite rinds. In summary, pseudomorphic (one-for-one replacement) of iron sulfide grains by limonite (primarily goethite, FeOOH) appeared to be common. Coating of limestone grains by transported limonite was not observed.

Acid-base accounting results for residues are summarized in table 1. Reproducibility of duplicate analyses was excellent and confirmed that differences in chemistry between column zones and experiments were significant. Columns 4 (0.8% Limestone) concentration) and 5 (layered) yielded very similar results for total sulfur and sulfate. Total sulfur concentrations decreased by about 1.3% over the 2-yr of weathering. All reactive neutralizing material was consumed, as shown by negative neutralization potentials. Column 1 (control) had slightly lower sulfur concentrations after 5-yr of leaching and similarly contained no detectable NP (the negative NP shown in table 1 indicates the presence of soluble acidity). Column 3 yielded slightly greater sulfur concentrations and no NP. Rock from the top part of column 2 (6.6% Limestone) contained higher concentrations of sulfur than any of the other well-oxidized material, and contained a small amount of NP. The deeper, less oxidized material contained about 0.3% less sulfur than at the start of the experiment. NP decreased by 12 kg/mt $CaCO_3$.

Discussion

Leachate Chemistry

Column leachate chemistries followed a series of stages. Initially, sulfate concentrations were elevated but then decreased rapidly as weathering products accumulated during sample storage were flushed from the columns. During stable pH neutral conditions, the dominant ions in solution were calcium and sulfate. The molar ratio of sulfate to calcium under these conditions was between 0.5 and 1 (fig. 2) which is consistent with general chemical theory for acid generation and neutralization. The usual reaction used to express overall acid generation at pH>3 is

$$FeS_2 + 15/4O_2 + 7/2H_2O \rightarrow 2SO_4^{2-} + Fe(OH)_3 + 4H^+, \quad (2)$$

Under strongly acidic conditions, the acidity will be neutralized by $CaCO_3$:

$$CaCO_3 + 2H^+ \rightarrow Ca^{2+} + H_2CO_3^{\circ}. \quad (3)$$

Under mildly acidic to mildly alkaline conditions, the reaction will be, as follows:

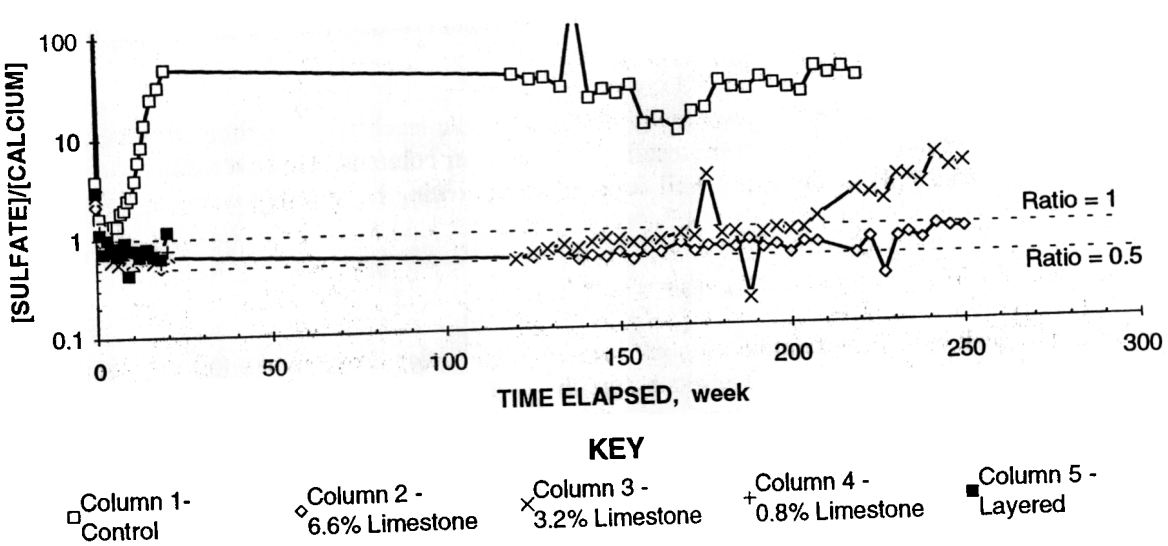

Figure 2. Molar sulfate to calcium ratios.

$$CaCO_3 + H^+ \text{ --> } Ca^{2+} + HCO_3^-, \quad (4)$$

Under acidic conditions, the molar ratio of sulfate to calcium should be equal to or greater than 1, whereas under less acidic conditions the ratio will be less than 1 owing to the formation of bicarbonate (Cravotta et al. 1990). Several months prior to generation of acidic leachate, this ratio steadily increased and gradually approached 1 (Columns 2 and 3, fig. 2). Once acidic leachate was produced, the ratio passed 1.

Consumption of Alkaline Minerals

Acid-base accounting results for columns generating acid leachate (1,3,4,5) indicated that no neutralization potential remained in the residues. Petrographic observations support the conclusion that all limestone was available for buffering of acidic leachate. Very few limestone fragments were observed in the residues from acidic columns. In the oxidized part of column 2 (highest limestone concentration), remaining limestone fragments were corroded and did not have a thick coating of transported limonite.

The lack of limonite rinds on limestone fragments is consistent with the low iron concentrations in leachate prior to generation of acid and the observed in situ one-for-one replacement of pyrite by limonite (goethite). During overall pH neutral conditions, iron probably remained at the source of oxidation as goethite and was not transported to limestone grains. This result is only observed when limestone and acid generating rock are relatively well mixed. If very acidic conditions are generated in isolated spots, allowing iron to move away from the oxidation site, the resulting iron would precipitate and cement limestone grains. This shows that the availability of calcareous material would probably decrease as the mixture becomes more heterogeneous and may explain the result observed for the layered column. For this column, the higher limestone concentration in the layers did not appear to be available, perhaps owing to cementing once the material above the individual layers became acidic.

Estimation of Alkaline Mineral Requirements

Four of the columns were predicted to be acid generating based on mass-weighted acid-base accounts, and all four columns produced acidic leachate during the course of the experiment. Column 2 (6.6% limestone) did not yield acidic leachate during 5 yr of weathering; however, the upper part of the column was clearly acidic (as shown by low paste pH and negligible neutralization potential), and sulfate and metal concentrations were increasing at the time the experiment was terminated. This column fits the relationship (fig. 3):

$$t_{SO4\ \text{increase begins}} = 2.9NP - 25. \quad (5)$$

Although based on only five points (fig. 3), the correlation coefficient (r=0.991) is statistically significant with a confidence level of better than 95%.

It is expected that column 2 would have eventually produced acidic leachate. The time required to produce acidic leachate for this column can be estimated from results from the other columns. However, since the time taken for column 1 leachate to become fully acidic is not well defined, the following relationship was determined instead (fig. 3).

$$t_{max\ SO4} = 11e^{0.079NP}. \quad (6)$$

For column 2, the peak sulfate concentration is predicted to occur after 2,600 weeks (50 yr). Leachate pH would be expected to drop to less than 3 about 20 weeks before the peak. The visual progress of the acid generation front suggests a much shorter time frame. If the rate of migration was constant, acid release would have been expected in about 15 yr. The sulfate peak would probably have been at a much lower concentration than for the other columns and would have been poorly defined.

Column no. and Limestone (LS)	NP, kg/mt	Sulfate release increasing, week	Leachate pH<7, week	Sulfate peak, week	Half sulfate peak, week	Sulfate released, % of total
1. Control.....	8	1	1	20	25	62
2. 6.6% LS.....	69	170	-	-	-	11
3. 3.2% LS.....	38	100	200	219	241	50
4. 0.84% LS.....	16	19	31	40	58	61
5. 1.2% LS, layers..	19	19	31	54	72	49

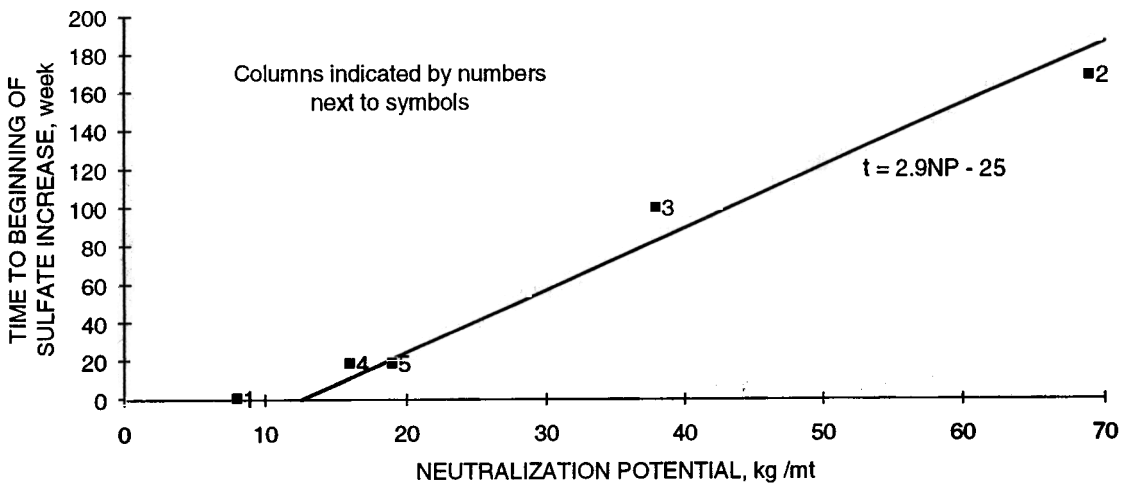

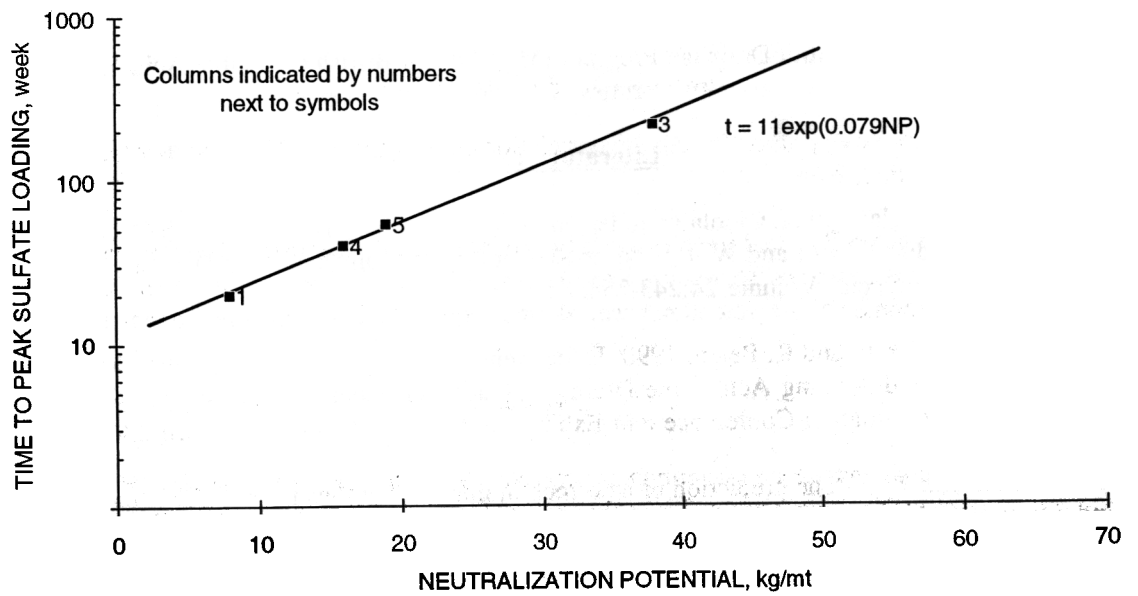

Figure 3 Relationships between beginning of sulfate increase, peak sulfate concentration and time.

The amount of limestone required to neutralize any acid for an indefinite period cannot be estimated from the above relationships since neither converges to a limiting value. However, the molar ratio of sulfate to calcium during the pre-acid leachate phase indicates the release of calcium in proportion to sulfate. The ratio is typically 0.5 to 0.6. As the conventional acid-base account assumes a 1:1 relationship, the actual NP required to prevent acid release is double the amount in column 2 (NP=69 kg/mt $CaCO_3$), or 138 kg/mt $CaCO_3$.

Mitigation of Metal Release by Calcareous Rock Mixing

Results indicated that under fully alkaline conditions where sulfate production is fairly uniform, metal and arsenic concentrations will remain low and stable. Once sulfate production begins increasing, metal release also increases. Zinc is the first to appear (at about the same time as increasing sulphate concentrations) followed by arsenic and copper (the latter being coincident with low pH conditions). This is consistent with commonly understood relationships between pH and dissolved metal concentrations. It appears therefore that limestone addition will only delay the release of zinc according to relationships of the form of equation (5), but will delay copper release for a much longer period (equation 6).

Conclusions

The following was concluded:

1. The actual quantity of limestone required to prevent acid drainage in perpetuity would probably be at least twice that determined by conventional acid-base accounting provided that the limestone and rock are intimately mixed (not thickly layered) and zinc release is not expected;

2. The time elapsed before marginally acid generating rock released acidity increased exponentially as the quantity of limestone increased; and

3. The time elapsed before sulfate and zinc release began increasing prior to release of low pH leachate was linearly proportional to the neutralization potential.

Acknowledgements

The Mine Environment Neutral Drainage Program (MEND) and British Columbia Acid Mine Drainage Task Force are gratefully acknowledged for granting permission to present this paper.

Literature Cited

Champigny, N. and A. J. Sinclair. 1982. Cinola gold deposit, Queen Charlotte Islands, British Columbia: A Canadian Carlin-type deposit. In Hodder, R.W., and W. Petruk (eds.), Geology of Canadian Gold Deposits, Canadian Institute of Mining and Metallurgy, Special Volume 24:243-254.

Cravotta, C., K. Brady, M. Smith and R. Beam. 1990. Effectiveness of the Addition of Alkaline Materials at Surface Coal Mines in Preventing and Abating Acid Mine Drainage: Part 1. Geochemical Considerations. In Proceedings of the 1990 Mining and Reclamation Conference and Exhibition. (Morgantown, WV, April 23-26, 1990).

Ferguson, K. and K. Morin. 1991. The prediction of acid rock drainage - Lessons from the Database. In Proceedings of the Second International Conference on the Abatement of Acidic Drainage. (Montreal, PQ, September 16-18, 1991).

Sobek, A. A., W. A. Schuller, J. R. Freeman and R. M. Smith, R.M. 1978. Field and laboratory methods applicable to overburden and minesoils. EPA 600/2-78-054, 203 pp.

MITIGATION OF ACID MINE DRAINAGE BY THE POROUS ENVELOPE EFFECT[1]

Luc C. St-Arnaud,[2] Bernard C. Aubé,[2]
Mark E. Wiseman,[3] and Steven R. Aiken[4]

Abstract: A porous envelope effect may occur in ground water systems when mine tailings of low permeability are placed within high-permeability soils. If the permeability contrast between the tailings and the natural soil is large, ground water will flow around the tailings mass rather than through it, and metal leaching will be minimal. A hydrogeological study at the Falconbridge Fault Lake tailings site suggests that conditions for porous envelope containment may be occurring. The tailings have been deposited in a kettle lake formed within glacial outwash sand and gravel. At present, the tailings are mostly above the water table, and surveys using a combination of electromagnetic geophysical methods and monitoring wells did not detect any presence of metals in the ground water. A 2-D finite-element numerical model was used to predict conditions that may occur if the water table would rise within the tailings. The model suggested that the contribution of tailings leachate to the regional ground water system would be small.

Introduction

In 1992, Noranda Technology Centre (NTC) undertook a hydrogeological investigation of the Fault Lake tailings site. The site is unique in that a "porous envelope effect" may be occurring. If this is the case, flow through the tailings mass is low enough, relative to the surrounding, more permeable till, that impact to the ground water by tailings oxidation is insignificant at the regional scale. The specific objectives of the investigation were to analyze the chemical and physical hydrogeology of the site, to delineate areas affected by acid mine drainage (AMD) generated from the tailings, and to verify the presence of the porous envelope effect.

Background

The Fault Lake tailings site is located northwest of the Falconbridge Sudbury operations, approximately 3 km north of Falconbridge and 0.5 km east of the Sudbury Airport. The tailings were deposited between 1965 and 1978 and were produced from the milling of nickel ore in the Sudbury area. Approximately 6.45 million mt of tailings containing as much as 50% pyrrhotite were deposited in a depression of a maximum depth of approximately 30 m. The tailings were contained by dams to the northeast and southeast of the site (referred to as north and south dams). The deposit has an approximate volume of 3.36×10^6 m^3 and a surface area of 22.2 ha (55 acres).

During the spring and fall, ponding occurs at the north dam, south dam, and various berms. The water slowly infiltrates into the tailings and evaporates from the ponds. During the summer, very little ponding has been observed. Tailings in areas where ponding has occurred are soft and gray, while the rest of the tailings are hard and crusty, showing orange traces of oxidation.

---

[1]Paper presented at the International Land Reclamation and Mine Drainage Conference and the Third International Conference on the Abatement of Acidic Drainage,Pittsburgh, PA, April 24-29, 1994.

[2]Luc St-Arnaud, Program Leader, Hydrogeologist, Bernard Aubé, Environmental Scientist, Noranda Technology Centre, Pointe-Claire, Québec, Canada.

[3]Mark Wiseman, Supervisor, Environmental Control, Falconbridge Limited, Sudbury Operations, Falconbridge, Ontario, Canada.

[4]Steven Aiken, Hydrogeologist, Elliot Lake, Ontario, Canada.

Surficial Geology

Overburden thickness varies within the studied area, from 36 m to more than 60 m. Overburden mainly consists of coarse to fine glacial outwash sands and gravels, with some large boulders and silt lenses. Kettles, fluvial terraces, discontinuous crevasse fillings, and eskers within the Fault Lake tailings area are evidence of a glacial meltwater channel, partly choked with stranded ice blocks. The small round kettle lakes were formed after the late melting of the stranded ice blocks which were caught among the mass of glacial sediments. The sediments are assembled in longitudinal formations which follow a northeasterly direction.

Investigative Methodology

Installation of Ground Water Monitoring Stations

The routes by which acid water could be transported from the Fault Lake tailings site were examined by electromagnetic surveys (Geomar Inc. 1991 and 1992), and probable seepage routes were identified leaving the tailings site at the base of the north and south dams. Thirteen ground water monitoring stations were placed to sample the ground water in the sediments directly below the tailings deposit and along the seepage routes. In addition, one station (FS-2) was located upgradient of the tailings to characterize background conditions. Figure 1 shows the locations of all the stations and also shows the outline of the original kettle lake as determined from aerial photographs taken prior to tailings deposition. Bedrock in the vicinity of the tailings site was not believed to have an important influence on ground water flow in the area.

Measurements of in situ hydraulic conductivity were conducted at most of the monitoring stations using the "falling-head test." Interpretation of the water level versus time data was conducted using the Hvorslev (1951) method for point piezometers. Ground water was sampled from monitoring wells in December 1992 and in March 1993. Sample pH, temperature, oxidation reduction potential (Eh), and electrical conductance were recorded. Acidified portions were later analyzed for dissolved metal and major ions, and the nonacidified portion was analyzed for chloride. Tailings pore water and the five kettle lakes in the Fault Lake tailings area (fig. 1) were also sampled in 1992.

Results

Physical Hydrogeology

Measurements indicated that the water table is 0 to 2 m below the base of the tailings, except at station FS-6, where there is evidence of a perched water table approximately 8 m above the base of the tailings. At station FS-12, which is the closest to the center of the original kettle lake, the measured water level was approximately 20 m below the tailings surface, near the base of the tailings. The fact that nearly all of the tailings are above the water table is surprising because water was visible in the kettle lake before tailings deposition. Low water infiltration in the tailings and changes in watershed configurations due to nearby quarry excavation are apparently causing the lowering of the water table. Regional ground water flow from the tailings watershed was determined to be northeast toward the small kettle lakes and southeast across the dam.

Hydraulic gradients were calculated for both vertical and horizontal directions. Vertical gradients were near zero at most of the monitoring stations surrounding the tailings deposit. Beneath the tailings deposit, significant vertical gradients indicate percolation. Upward gradients suggest partially confined conditions and/or localized flow paths below the tailings. Horizontal gradients were very small. At the north dam, the horizontal gradient was 0.0002; at the south dam, it was 0.007.

Measured hydraulic conductivities in the natural overburden were highly variable, ranging from 8×10^{-1} cm/s to 2.5×10^{-5} cm/s. The large variations in hydraulic conductivity are explained by the heterogeneity of the soil,

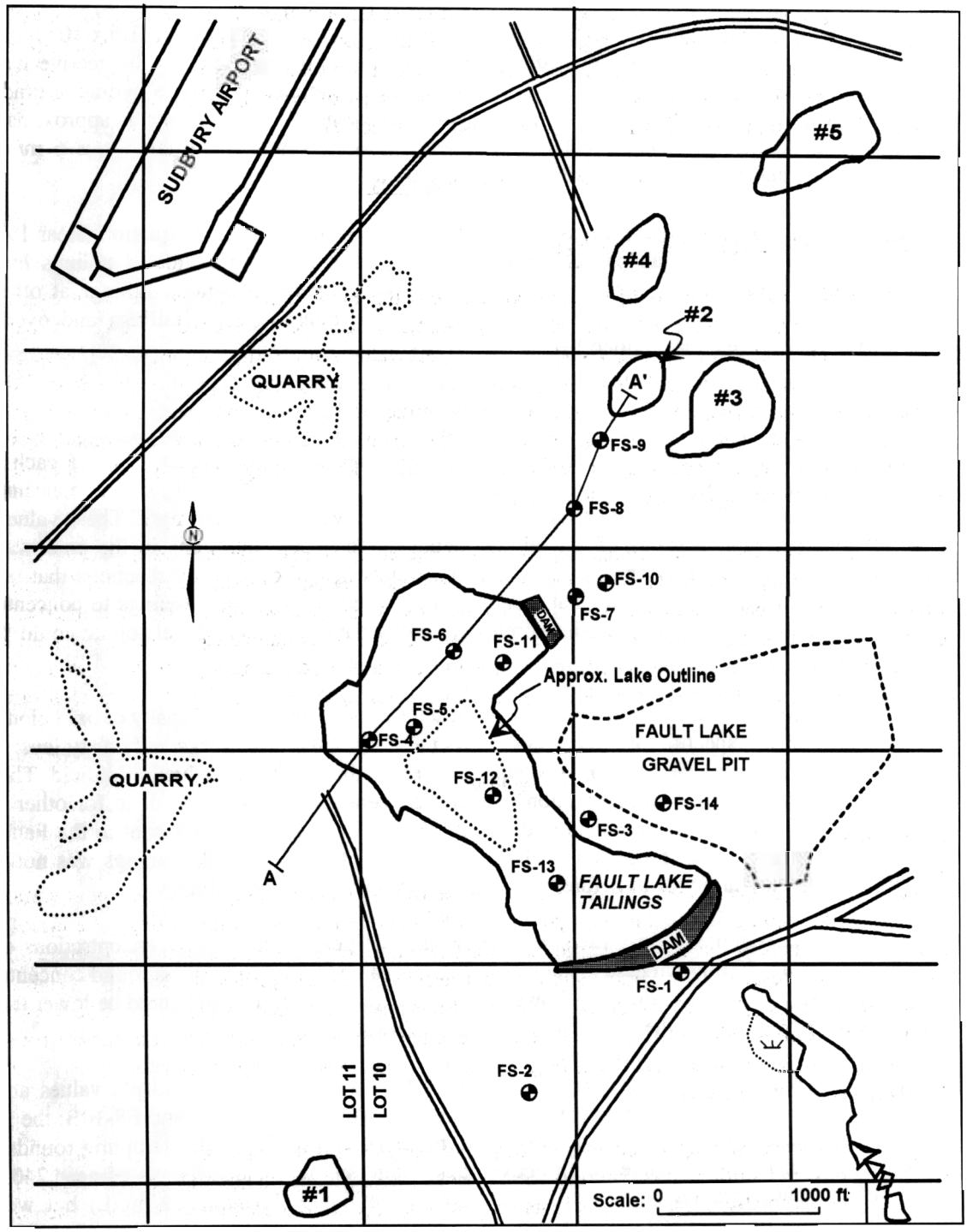

Figure 1. Fault Lake tailings.

typical of ice-contact deposits, which include silts, sands, gravels, and boulders. The higher hydraulic conductivities occur where fast meltwater flows have formed accumulations of well-sorted sands and gravels. The lower hydraulic conductivities occur where glacial abrasion and slow meltwater flows have left finer silts.

The geometric average of all hydraulic conductivity measurements in the overburden is 1.6×10^{-3} cm/s. This value is typical of a clean to silty sand and is considered to be representative of the overall effective hydraulic conductivity of the soils in which the tailings lie. Using the average hydraulic conductivity, a hydraulic gradient of 0.0002, and an estimated effective porosity of 0.30, the calculated velocity north of the tailings is approximately 30 cm/yr. With a horizontal gradient of 0.007, the calculated average velocity south of the tailings is 6 m/yr. This velocity is only approximate, and actual local velocities may vary by a factor of 10.

The hydraulic conductivity of the tailings was estimated using the Kozeny-Carman equation (Bear 1972), an estimated porosity of 0.45, and the median particle diameter, or d_{50}. The resulting estimated tailings hydraulic conductivities averaged 1.2×10^{-5} cm/s, which is consistent with measurements of similar tailings at other sites (Yanful and St-Arnaud 1992, for example). The measured hydraulic conductivities of tailings and overburden materials also agree with previous estimates done by Geocon (1985).

Chemical Hydrogeology

Water extractions were performed on six selected samples collected in November 1992 at each of the monitoring stations located on the tailings. Nickel concentrations ranged from 4 to 644 mg/L, sulfate concentrations ranged from 3,041 to more than 84,600 mg/L, and total iron concentrations were 0.5 to 466 mg/L. These values show evidence of sulfide oxidation within portions of the tailings deposit. Metal concentrations in the pore water are strongly influenced by downward water movement, chemical precipitation, and dissolution reactions that occur in the tailings mass. These effects seem to have attenuated nickel in the deeper parts of the tailings to concentrations of 5 to 8 mg/L. Thermodynamic calculations done on porewater quality data suggested nickel sulfate could be near saturation.

Differences in measured metal concentrations could be caused by variations in the intensity of oxidation across the surface of the tailings. Visual inspection of the tailings shows the development of cracks and crusty layers at the surface, which could locally influence water and oxygen entry as well as the resulting production of acid. Thorough investigations of the geochemical sources and evolution of metal concentrations have been done for other sulfide tailings sites (Blowes et al. 1988) and for the Falconbridge main pyrrhotite tailings site adjacent to the Fault Lake site (Nicholson and David 1991). The investigation of the geochemistry of the Fault Lake tailings was not part of the objectives of the present study and was therefore not pursued further than described above.

Background ground water monitoring station FS-2 showed a pH near 7 and nickel concentrations of 0.01 mg/L, iron 0.03 mg/L, and sulfate 30 mg/L. These metal concentrations can be accepted as background concentrations for ground water at the site since a second sampling showed similar results. Background pH could be lower than that measured at FS-2 (as low as 6) owing to the infiltration of acidic rainwater.

Ground water sampled near the tailings site in December 1992 and March 1993 had pH values above 6. Above-background concentrations of nickel were measured in wells FS-3A, FS-3B, FS-9C, and FS-10B; the highest of these concentrations was 0.5 mg/L (at FS-10) and was measured during only one of the sampling rounds. Only at FS-3 were the higher nickel levels associated with above-background sulfate concentrations of near 240 mg/L. Above-background sulfate concentrations were also encountered at station FS-1 (max 339 mg/L) but were not associated with any above-background metal concentrations.

Sampling results suggest that metal concentrations are not high enough to affect ground water quality. This is also suggested by the results of surface water quality sampling, which do not show the presence of any metal above background concentrations.

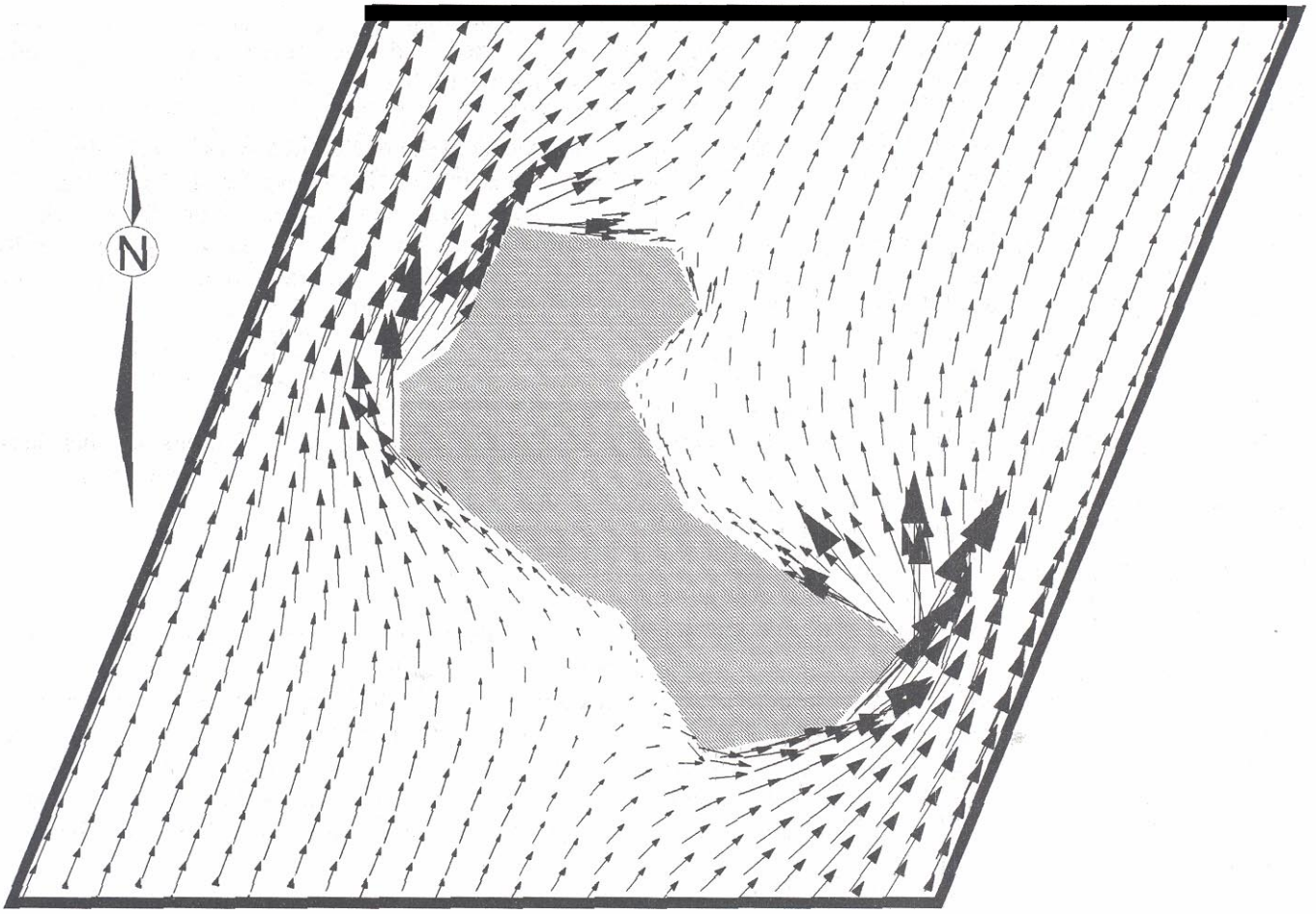

Figure 2. Plan **view** modeling results.

Ground Water Flow **Modeling**

Modeling Procedure

Ground water flow around the tailings was simulated using the saturated-unsaturated flow modeling program SEEPN (GEO-SLOPE International 1992). In order to determine the **flownet**, SEEPN requires the definition of i) a domain (finite-element grid), ii) soil hydraulic conductivities, and iii) boundary conditions.

Two models were defined in order to obtain a quasi-three-dimensional perspective of the ground water flows in the Fault Lake tailings area. The first model was a plan model and was defined as a rectangle with the long edges parallel to the main flow direction inferred from previous analysis. This model was conceptual only, representing the flow of water directly beneath the soil surface as affected by the hydraulic conductivity contrast between the tailings and the surrounding sediments. This did not include the effects of topography or infiltration.

The second model was a cross section across stations FS-4 to FS-9 (A-A' in fig 1). The model domain started southwest of **piezometer** FS-4, extended northeast of FS-9, and passed through FS-6 and FS-8. Elevations were taken from the monitoring well data where possible; otherwise, the topographic map was **used**. Representative hydraulic conductivities (K) for the soils and tailings were derived from the geometric mean of the field measurements, as described earlier.

Constant-head boundary conditions were defined at both ends of the model domains. In the first model, the constant-heads were set equal to the elevation of the nearest lakes: lake #1 in the south and lake #3 in the north.

In the second model, a water table elevation slightly higher than that measured at FS-4 was used at A; for A', the elevation of lake #2 was taken from the topographic map. The infiltration flux across the top boundary was determined using previous estimates from Yanful et al. (1993) obtained using the HELP (Hydrologic Evaluation of Landfill Performance) computer program of Shroeder et al. (1984). Different fluxes were used in the SEEP/W modeling, depending on the slope and nature of the ground surface. The tailings surface infiltration was set to 200 mm/yr, sloped till 250 mm/yr, and flat till 350 mm/yr. It was determined that infiltration into the till would be higher than that into the tailings since the hydraulic conductivity is higher and the water table is low. This would cause precipitation to be absorbed by the till and transferred away from the surface (to the water table), thereby limiting evaporation. On the tailings, evaporation is enhanced by surface ponding, thereby reducing infiltration.

Modeling Results

Flow vectors for the first model are shown in figure 2. The flow vectors illustrate the direction of flow, with their length being proportional to the flux. The figure clearly shows how the water would flow mainly in the till and around the tailings because of the higher hydraulic conductivity of the till. Figure 2 is only a conceptual illustration of actual conditions since this modeling procedure is highly simplified. For realistic results in a plan view, topography, depth of soils, and infiltration would need to be included into a three-dimensional modeling program.

Figure 3 depicts the flow characteristics for the cross-sectional model. The figures indicate that the horizontal flow is predominantly in the till and does not enter the tailings. The only water flowing through the tailings is the water that infiltrates from precipitation.

The flow vectors in figure 3 show a ground water divide left of the tailings (southwest). Although the general flow was calculated to be toward the northeast, it is possible that local gradients occur that cause some water to travel southwest. Such digression in the flow could be caused by manmade changes, such as the gravel pits in the area. From aerial pictures taken before tailings deposition, it is known that this area was once a lake. The fact that the water table is now below what used to be the lakebed suggests that local excavation may have greatly affected regional ground waters. A second influence to the water level is the tailings, which, by decreasing infiltration and promoting evaporation, reduce recharge to the aquifer. Other human disturbances, such as the building of roads, may have affected watersheds and ground water flow directions. It is also possible that the present conditions are temporary, and that the water table could eventually return to previous levels.

To verify the effects that would occur if the water table were to rise into the tailings and saturate the bottom portion of the impoundment, the constant-head boundary functions at either end of the section were raised. The results of this simulation showed that, although the bottom 5 m of the tailings are saturated, the flow within the tailings remains insignificant. This suggests that the increase in metal loading in the ground water due to the water table rise would not be important.

The use of a 2-D flow model to assess the conditions on the Fault Lake site has inherent limitations. In particular, any quantification of flow volumes is affected by the fact that all the water is assumed to move only in the reference plane, while in reality water also moves across the plane. Model predictions based only on ground water flow can also lead to overestimation of chemical loadings, since metal transport is usually slower than water velocity owing to chemical attenuation. The flow model can, however, be used to predict the worst-case scenario where no chemical attenuation takes place. Predictions that account for chemical attenuation are complex and were not part of the objectives of the present study.

Discussion

The glacial sediments surrounding the Fault Lake tailings site are characterized by their elongated formation and relatively high bulk hydraulic conductivities. This creates a flow system with a relatively flat and deep water table. Several favorable factors contribute to limit the observed metal concentrations downgradient of the tailings. These factors and their probability of occurring elsewhere follow:

1. Hydraulic conductivity contrast: Sediments of high hydraulic conductivities such as sands and gravels occur commonly in Canada. The ice-contact deposits surrounding the Fault Lake area possess a high average hydraulic conductivity, but are also characterized by a high variability due to the process by which they were deposited. Other sands and gravels may be more uniform, showing less heterogeneity in hydraulic properties and possibly a higher bulk hydraulic conductivity. As for tailings, measurements at several sites by Blowes et al. (1988) and Yanful and St-Arnaud (1992) have yielded values close to 10^{-5} cm/s, as measured at the Fault Lake tailings. Large hydraulic conductivity contrasts between tailings and surrounding sediments are therefore possible.

2. Deep water table: The water table in well-drained sand and gravel formations in temperate climates will usually be far below the ground surface. The depth to water table is also largely affected by topographical features. The hummocky terrain surrounding the Fault Lake site is largely controlled by the occurrence of the kettle lakes. In other similar glacial outwash areas, the coarse glacial deposits are commonly elevated, and deep water tables can result, depending on bedrock topography.

3. Limited infiltration: Infiltration of water through tailings surfaces is usually less than through natural soils. This is due to the relatively low bulk hydraulic conductivity of the tailings, the high potential for evaporation at the tailings surface, and the formation of dense crusts which can further reduce conductivity at the tailings surface. At the Fault Lake tailings site, infiltration could be reduced by encouraging runoff, thus preventing ponding along the dams.

4. Dilution by regional ground water flow: Large glacial outwash sediment formations normally have high ground water discharges, which are less susceptible to degradation by point contamination sources. In the case of the Fault Lake site, results from the second model (**A-A'** cross section) suggest that flow upstream of the tailings site would not be very large. The occurrence of much larger regional flow systems at other sites is possible.

5. Chemical attenuation: Some chemical attenuation in the form of precipitation and adsorption reactions occurs in most tailings. The degree to which these reactions take place depends on geochemical and mineralogical factors, in particular those that influence the neutralization potential of the tailings. Chemical attenuation in the Fault Lake tailings is suggested by the tailings pore water data and could also occur within the natural overburden deposits.

All five factors outlined above contribute to create the porous envelope effect; these factors could probably be present at other locations near mine sites. Tailings deposition in these types of environments could be done with little effect on ground water quality, if thorough site evaluations are performed and appropriate control is enforced at the time of deposition.

Conclusions

1. The piezometric elevations throughout the Fault Lake site, combined with lake elevations, suggest that the regional direction of subsurface flow is toward the northeast, along with the alignment of the kettle lakes. Some subregional flow systems could be moving ground water in other directions.

2. The base of the tailings is at the same level or higher than the water table across most of the site. Low water infiltration in the tailings and changes in watershed configurations due to nearby quarry excavation are suggested as causes for the apparent lowering of the water table.

3. The average bulk hydraulic conductivity of the soil surrounding the tailings is estimated at 1.6 x 10^{-3} cm/s. The hydraulic conductivity of the tailings was estimated using grain size correlations at 1 x 10^{-5} cm/s. These values agree with previous estimates.

4. Analysis of tailings pore water showed elevated values of nickel, iron, and sulfate, indicating the presence of sulfide oxidation products within portions of the tailings deposit. Metal concentrations are attenuated in the deeper parts of the tailings. Heterogeneity in measured metal concentrations could be caused by variations in the intensity of oxidation across the surface of the tailings due to surface effects such as ponding and cracking.

5. Water quality sampling in monitoring wells outside the tailings did not show any evidence of above-background metal concentrations, which suggests that leaching of metals from the tailings would be minimal. This is also suggested by the results of water sampling in nearby lakes.

6. Two-dimensional ground water models showed that the flow is diverted around the tailings mass owing to the hydraulic conductivity contrast between the tailings and the surrounding sediments. The models also showed that flushing of the tailings by ground water should not contribute significantly to the regional ground water flow system under present water table conditions, as well as under conditions of moderate rise in water table level.

Factors that contribute to limit metal concentrations downgradient of the Fault Lake tailings are:

- the large hydraulic conductivity contrast between the tailings and the surrounding sediments.
- the low position of the water table relative to the tailings bottom.
- the limited infiltration through the surface of the tailings.
- the dilution of metals flushed from the tailings by water flowing around and below the tailings.
- chemical attenuation of metals in the tailings and overburden.

8. These factors could probably be present at other locations near mine sites. Tailings deposition could be done at these sites with little effect on ground water quality if thorough site evaluations are performed and appropriate control is done at the time of deposition.

Acknowledgements

This project was funded by Falconbridge Limited and by the Ontario Ministry of Northern Development and Mines as part of the MEND program. Acknowledgements are owed to M. Woyshner for reviewing the paper and to B. Michelutti and B. Mikkila of Falconbridge Ltd. for providing useful comments and site information.

Literature Cited

Bear, J. 1972. Dynamics of fluids in porous media. American Elsevier, New York. p. 161-167.

Blowes, D. W., J. A. Cherry, and E. J. Reardon. 1988. The rate of geochemical evolution of the Heath Steele mine tailings, New Brunswick. p. 5-17. In C. L. Lin (ed.), Proceedings of the International Ground water Symposium on Hydrogeology of Cold and Temperate Climates and Hydrogeology of Mineralized Zones. International Association of Hydrogeologists, Canadian National Chapter, Halifax, NS.

Felmy, A. R., D. C. Girvin, and E. A. Jenne. 1984. MINTEQ—A computer program for calculating aqueous geochemical equilibria, U.S. Environmental Protection Agency, Athens, GA, EPA-600/3-84-032.

Freeze, R. A. and J. A. Cherry. 1979. Groundwater. Prentice-Hall, Inc., Englewood Cliffs, NJ.

GEOCON. 1985. Unpublished data submitted to Falconbridge Limited.

Geomar Inc. 1991. EM survey, Falconbridge operations, Fault Lake, Falconbridge, Ontario, Canada.

Geomar Inc. 1992. TEM survey, Falconbridge operations, Fault Lake, Falconbridge, Ontario, Canada.

GEO-SLOPE International. 1992. SEEP/W version 2 user manual. Geo-Slope International Limited, Calgary, AB, Canada.

Hvorslev, M. J. 1951. Time lag and soil permeability in ground water observations. U.S. Army Corps Engrs. Waterways Exp. Sta. Bull. 36, Vicksburg, Ms.

International Water Supply Ltd. 1971. Department of Transport ground water investigation, Sudbury Airport.

Nicholson, R. N. and D. J. David. 1991. Preliminary hydrogeological investigation of the Falconbridge new tailings impoundment: fall 1990. Final report. Waterloo Centre for Ground water Research report submitted to Falconbridge Limited.

Schroeder, P. R., J. M. Morgan, T. M. Walski, and A. C. Gibson. 1984. The hydrologic evaluation of landfill performance (HELP) model. U.S. Environmental Protection Agency, Office of Solid Waste and Emergency Response, Washington, DC.

Yanful, E. K. and L. C. St-Arnaud. 1992. Migration of acidic pore waters at the Waite Amulet tailings site near Rouyn-Noranda, Quebec, Canada. Canadian Geotechnical Journal, Vol. 29: 466-476.

Yanful, E. K., M. R. Woyshner, and B. C. Aubé. 1993. Field evaluation of the effectiveness of engineered soil covers for reactive tailings. Report for MEND, DSS contract 23440-0-9061/01-SQ.

POTENTIAL MICROENCAPSULATION OF PYRITE BY ARTIFICIAL INDUCEMENT OF $FEPO_4$ COATINGS

V.P. Evangelou

Abstract: A novel coating methodology was developed to prevent pyrite oxidation in mining "waste." The mechanism of this coating technology involves leaching mining "waste" with a phosphate solution containing hydrogen peroxide (H_2O_2); when this solution reaches pyrite surfaces, H_2O_2 oxidizes the surface portion of pyrite and releases Fe^{3+} so that iron phosphate precipitates and forms a passive coating on pyritic surfaces. This study demonstrated that iron phosphate coatings on pyritic surfaces could be established with a solution containing as low as 10^{-4} mol/L phosphate and 0.027 mol/L H_2O_2 and that the iron phosphate coating could effectively protect pyrite from oxidizing further. Development of this coating methodology could mean solution to production of acid mine drainage from certain types of mine "waste." Further investigations are being carried out to extend this methodology to practical use.

Introduction

Pyrite oxidation in mining "waste" or overburden is considered as the main cause for the production of acid mine drainage (AMD). The need to prevent AMD formation has triggered numerous investigations into the mechanisms of pyrite oxidation and its prevention (Singer and Stumm, 1970; Silverman, 1967; Nordstrom, 1982; Kleinmann et al., 1981; Ziemkiewicz, 1990).

It has been reported that pyrite in mining wastes or coal overburden is initially oxidized by the atmospheric O_2, producing H^+, SO_4^{2-}, and Fe^{2+} (Nordstrom, 1982). The Fe^{2+} produced can be further oxidized by O_2 into Fe^{3+}, which in turn hydrolyzes into amorphous iron hydroxide and releases additional amounts of acid into the environment (Nordstrom, 1982). In this initial stage, pyrite oxidation in pyritic "waste" is a relatively slow process (Ivanov, 1962). As acid production continues and the pH in the vicinity of the pyritic surfaces drops below 3.5, the formation of ferric oxide is hindered and the activity of free Fe^{3+} in solution increases. Under these conditions, the oxidation of pyrite by Fe^{3+} becomes the main mechanism for acid production in mining wastes since Fe^{3+} can oxidize pyrite at a much faster rate than O_2 (Singer and Stumm, 1970). Meanwhile, at low pH, an acidophilic, chemoautotrophic, iron-oxidizing bacterium, *Thiobacillus ferrooxidans*, flourishes; it can catalyze and accelerate the oxidation of Fe^{2+} into Fe^{3+} by a factor larger than 10^6 (Singer and Stumm, 1970) and thereby effectively recycle the iron released from pyrite as a major oxidant of pyrite or as an electron conductor between FeS_2 and O_2 (Kleinmann et al., 1979). *Thiobacillus ferrooxidans* is thus considered to be primarily responsible for the rapid oxidation of pyrite in mining wastes at low pH (Nordstrom, 1982).

So far the approaches to preventing pyrite oxidation are mainly based on the above mechanisms and are aimed at eliminating Fe^{3+} from pore waters. These approaches include the use of phosphate to precipitate Fe^{3+} in the insoluble form as $FePO_4$ (Ziemkiewicz, 1990) and the application of bactericides to inhibit the oxidation of Fe^{2+} into Fe^{3+} (Kleinmann et al., 1981). Both approaches have shown a certain degree of success in preventing pyrite oxidation and acid production in pyritic "waste"; however, they both have two weaknesses-they are costly and have a short span of effectiveness. The main reason for the failure of these methods is that the surfaces of pyrite particles in mining "waste" are still exposed to the atmospheric O_2 after treatment; as Fe^{2+} accumulates and *Thiobacillus ferrooxidans* repopulates on pyritic surfaces, pyrite oxidation by Fe^{3+} and acid production is initiated (Kleinmann and Crerar, 1979). To completely prevent pyrite oxidation, it appears essential to block the access of the atmospheric O_2 to pyritic surfaces.

The purpose of this study was to examine the feasibility of creating an iron phosphate coating on pyrite surfaces to prevent pyrite oxidation. The basic hypothesis for this coating approach was that by leaching pyritic mining "waste" with a phosphate solution containing a low concentration of H_2O_2, the Fe^{3+} released from pyrite by H_2O_2 will react with phosphate to form a passive $FePO_4$ coating on pyrite surfaces. Thus, at the expense of a small fraction of pyrite, oxidation of pyrite and production of acid could be prevented.

Theory

Pyrite Oxidation by H_2O_2

Pyrite oxidation by H_2O_2 can be described as follows (Huang and Evangelou, 1992):

Paper presented at the International Land Reclamation and Mine Drainage Conference and the Third International Conference on the Abatement of Acidic Drainage, Pittsburg, PA, April 24-29, 1994.

V. P. Evangelou, Department of Agronomy, Univ. of Kentucky, Lexington, KY 40546-0091.

$$FeS_2 + 7.5H_2O_2 = Fe^{3+} + 2SO_4^{2-} + H^+ + 7H_2O \qquad [1]$$

$$FeS_2 \underset{Fe^{2+}}{\overset{H_2O_2}{\rightleftarrows}}$$

According to equation 1, pyrite oxidation is an autocatalytic process because one of the oxidation products, Fe^{3+}, can also oxidize pyrite. The rate law corresponding to this oxidation mechanism can be written as

$$-dM/dt = (k_1[H_2O_2] + k_2[Fe^{3+}])KM, \qquad [2]$$

where M is the number of moles of pyrite in the system at any time t. $[H_2O_2]$ and $[Fe^{3+}]$ refer to concentrations of H_2O_2 and Fe^{3+}, while k_1 and k_2 refer to the rate constants of H_2O_2 and Fe^{3+}, respectively; K stands for the specific surface of pyrite.

By moving M in equation 2 to the left-hand side, integrating with respect to M and expressing it as log to the base 10, equation 2 becomes

$$-dlogM/dt = (k_1/2.3[H_2O2] + k_2/2.3[Fe^{3+}])K. \qquad [3]$$

According to equation 3, the first-order plot of log M versus t will be curvilinear even if $[H_2O_2]$ is kept constant. Whether the plot concaves down or up depends on whether the Fe^{3+} concentration in the system increases or decreases with time. However, if Fe^{3+} is prevented from oxidizing pyrite and $[H_2O_2]$ is kept constant, the plot will be a straight line.

Pyrite Oxidation by H_2O_2 in the Presence of Phosphate

Pyrite oxidation by H_2O_2 in the presence of phosphate can be described by:

$$FeS_2 + 7.5H_2O_2 + H_2PO_4^- = FePO_4 + 2SO_4^{2-} + 3H^+ + 7H_2O. \qquad [4]$$

The iron phosphate formed can precipitate either as a discrete phase or as a coating on pyritic surfaces, depending on the degree of the supersaturation of the solution on pyritic surfaces with respect to iron phosphate (Huang and Evangelou, 1992). If the degree of supersaturation is relatively low, the iron phosphate might not precipitate instantly and thereby exist as a discrete phase. In this case, equation 3 becomes

$$-dlogM/dt = Kk_1/2.3[H_2O_2]. \qquad [5]$$

This equation implies that the precipitation of iron phosphate as a discrete phase is characterized by the linear first-order plot of log M versus t if $[H_2O_2]$ is kept constant.

If the degree of supersaturation with respect to iron phosphate is high, iron phosphate will precipitate as a coating on pyritic surfaces. The rate of pyrite oxidation should be smaller than that predicted by equation 5 as pyrite oxidation is not only surface chemical reaction-controlled but also coatings-controlled. In this case, the kinetics of pyrite oxidation would be described by the shrinking core model (Huang and Evangelou, 1992; Nicholson et al., 1989):

$$t = 1/(Ds'C)\{1 - 3(1-X)^{2/3} + 2(1 - X)\} + 1 / (Ks'C) \{ 1 - (1 - X)^{1/3}\} \qquad [6]$$

where t is the time required for a specific fraction (X) of pyrite to oxidize in the system and C is the concentration of H_2O_2 in the bulk solution. Ds' is the apparent diffusion coefficient for H_2O_2 through $FePO_4$ coatings and Ks' is the first-order rate constant with respect to pyrite. The first term in equation 6 describes the effect of accumulation of iron phosphate precipitates on pyritic surfaces on the rate of pyrite oxidation. The second term describes the first-order kinetics with respect to pyrite itself. Note: The second term in equation 6 is the same as equation 5.

Materials and Methods.

The sample used in this study was a pyritic shale with 6.5% pyrite. The shale sample was pulverized, passed through a 60-mesh sieve, and stored in a plastic bag. Part of the pulverized sample was used to separate pyrite using a heavy liquid, 97% tetrabromoethane. The separated pyrite particles were washed with 4 mol/L hydrofluoric acid to remove silicate and iron oxides and then rinsed repeatedly with nitrogen-purged distilled water. The cleaned sample

was then dried and stored in a vacuumed desiccator. X-ray diffraction analysis indicated that the separated sample was pure pyrite and free of any crystalline impurities.

To prove the feasibility of coating pyrite with iron phosphate, we leached a mixture of 50 mg of the separated pyrite sample and 500 mg of 140-mesh sand with the following three solutions, using a chromatographic column (fig. 1) and a peristaltic pump at a flow rate of 0.5 mL/min and a temperature of 40°C: 0.147 mol/L H_2O_2, 0.147 mol/L H_2O_2 with 0.013 mol/L disodium ethylenediamine tetraacetate (EDTA), 0.147 mol/L H_2O_2 with 0.01 mol/L KH_2PO_4. All three solutions contained 0.1 mol/L NaCl as background electrolyte and were adjusted to pH 4 with 0.01 mol/L HCl. At pH 4, it was expected that the Fe^{3+} produced during pyrite oxidation was either completely complexed by EDTA or precipitated by phosphate as $FePO_4$. The pyrite-sand mixture in the column was pressed into a disc with a diameter of 10 mm and a thickness of 3 mm and preleached with 50 mL of 2 mol/L HCl to guarantee removal of free $FeSO_4$ and iron oxides. The leachate from the column was collected at 20-min. intervals with a fraction collector.

At the end of leaching, the residual pyrite particles in the pyrite-sand mixture were separated with 97% tetrabromoethane. The residual pyrite particles were further washed with acetone and dried in a vacuumed desiccator. The surface status of pyrite particles was then examined using scanning electron microscopy and diffuse reflectance infrared spectroscopy.

To determine the effectiveness of the coating approach in preventing pyrite oxidation, two columns with a mixture of 0.5 g of the pulverized shale and 0.5 g of 140-mesh sand were leached first with 50-mL of 2 mol/L HCl to expose pyritic surfaces and then with 500-mL of pH 4 solutions containing 0.1 mol/L NaCl, 10^{-4} mol/L KH_2PO_4, and 0.053 mol/L H_2O_2 to coat pyrite particles. The leachates were collected in a 500-mL bottles. One of the columns was leached again with 50 mL of 2 mol/L HCl to remove the iron phosphate coating. Both columns were then subjected to leaching at 40°C with a pH 4 oxidizing solution containing 0.1 mol/L NaCl and 0.088 mol/L H_2O_2 to test the effectiveness of the coating in preventing pyrite oxidation. Leachates were collected at 20-min intervals using a fraction collector. All the leaching experiments were conducted using the chromatographic column (fig. 1) at 40°C and a flow rate of 0.5 mL/min.

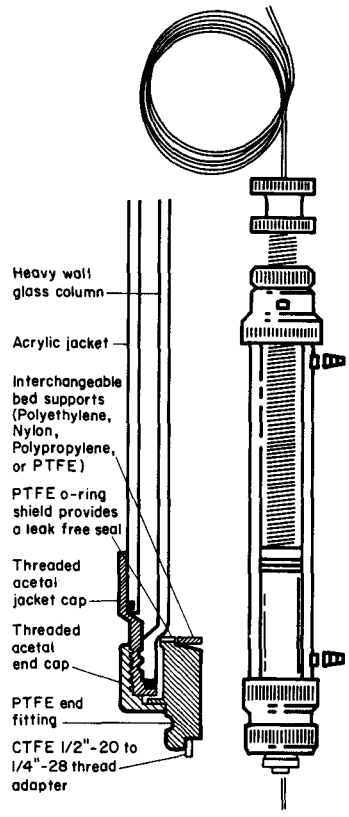

Figure 1. Chromatographic column for pyrite leaching experiments.

Sulfate concentration in the leachates was measured using turbidometry with $BaCl_2$. The amount of pyrite remaining in the column was calculated according to the FeS_2-SO_4 stoichiometry and the extent of pyrite oxidation was expressed as percent of remaining pyrite versus time.

Results and Discussion

Kinetics of Pyrite Oxidation During Leaching

Figure 2 shows the first-order plot of log (100 x M/Mo) versus t (Mo = original amount of pyrite, and M = amount of unreacted pyrite at any time t) for the data of pyrite oxidation when pyrite was leached with the three solutions listed in the caption. During leaching with 0.147 mol/L H_2O_2, pyrite rapidly oxidized and by the end of leaching, 70% of pyrite was oxidized. The first order plot was curvilinear and concaved up. Since the total volume of pores in the pyrite-sand column was small (the total volume of the column was 0.058 cm^{-3}), the concentration of H_2O_2 used was high, and the residence time of the leaching solution within the column was low, it was assumed that H_2O_2 concentration in contact with pyritic surfaces was always constant. With this assumption, the curvature of the first order plot can be attributed to oxidation of pyrite by Fe^{3+} (equation 3). The analysis of the iron in the leachate indicated that the amounts of the soluble Fe^{3+} released from pyrite decreased dramatically with time, and approximately 50% of iron released from pyrite precipitated as iron hydroxide within the column by the end of leaching (fig. 3A).

When pyrite was leached with the solution containing 0.147 mol/L H_2O_2 and 0.013 mol/L EDTA, the rate of pyrite oxidation decreased, especially during the initial stage of leaching, but it did not stop; at the end of leaching, approximately 65% of pyrite was oxidized, a value close to that for being leached with 0.147 mol/L H_2O_2. The first order plot was a straight line (fig. 2, curve B). This indicated that pyrite oxidation by Fe^{3+} had been completely inhibited by EDTA (equation 3). Analysis of iron in the leachates confirmed that 100% of the iron released from pyrite was instantly flushed out of the column (fig. 3, curve B).

When the pyrite was leached with the solution containing 0.147 mol/L H_2O_2 and 10^{-2} mol/L KH_2PO_4, almost 99% of the iron released from the pyrite was precipitated by phosphate (fig. 3, curve C). The precipitation of iron as $FePO_4$ might influence the rate of pyrite oxidation via two mechanisms: (1) by inhibiting the oxidation of pyrite by Fe^{3+} or (2) by forming a passive coating. As shown in figure 2, pyrite oxidation during leaching with the solution containing 0.147 mol/L H_2O_2 and 0.01 mol/L KH_2PO_4 was much slower than that during leaching with the solution containing 0.147 mol/L H_2O_2 and 0.013 mol/L EDTA (fig. 2, curve C). Before 300 min, the first-order plot was nearly parallel to that of EDTA treatment. This indicates that at the initial stage of leaching phosphate inhibited oxidation of pyrite by Fe^{3+} by precipitating Fe^{3+} as $FePO_4$, but not all the iron phosphate had precipitated as coating. After 300 min of leaching, pyrite oxidation nearly stopped. At the end of leaching, more than 70% of pyrite was preserved. The above results clearly suggest that by leaching with the phosphate solution containing H_2O_2, we can establish an iron phosphate coating on pyrite surfaces at the expense of surface portions of pyrite particles.

The growth of iron phosphate coatings on pyrite surfaces during leaching with phosphate solution containing H_2O_2 can be well explained with the shrinking core model. As indicated in the Theory section, the second term in equation 6 represents first-order kinetics with respect to pyrite. During leaching with the solution containing H_2O_2 and EDTA, pyrite oxidation by Fe^{3+} was inhibited and no coatings were supposed to form. Thus, the rate of pyrite oxidation by H_2O_2 is of the first order with respect to pyrite. This was clearly confirmed by the linearity of the plot of t versus $\{1-(1-X)^{1/3}\}$ (fig. 4) (deviation from straight line at around 700 min is believed to be due to the failure of the linear relationship between the surface area and the mole number of the remaining pyrite (Turner, 1960)). With the apparent first-order rate constant obtained from the plot in figure 4, we expressed the data of pyrite oxidation during leaching with the solution containing 0.147 mol/L H_2O_2 and 0.01 mol/L KH_2PO_4 as a plot of $t-1/(Ks'C)\{1-(1-X)^{1/3}\}$ versus $\{1-3(1-X)^{2/3} + 2(1-X)\}$ (fig. 5). The values of $t-1/(Ks'C)\{1-(1-X)^{1/3}\}$ represent the extra time required for H_2O_2 to oxidize a given fraction of pyrite due to iron phosphate coatings. As shown in figure 5, the plot followed a straight line after 200 min of leaching. The shrinking model requires that all the iron phosphate formed precipitate as a coating on pyritic surfaces. The deviation from linearity before 200 min indicates that some iron phosphate did not precipitate as coating. Part of the reason is that the concentration of acid produced by pyrite oxidation was relatively high during the initial stages of leaching (pH of the leachates was 2.7 in the first 200 min of leaching). The acid

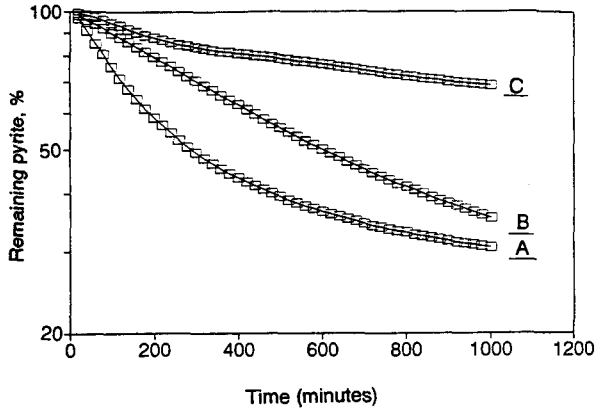

Figure 2. The first-order plot of log (100 x M/Mo) versus t for the data of pyrite oxidation when pyrite was leached with the following three solutions: A, 0.147 mol/L H_2O_2; B, 0.147 mol/L H_2O_2 plus 0.013 mol/L EDTA; C, 0.147 mol/L H_2O_2 plus 0.01 mol/L KH_2PO4.

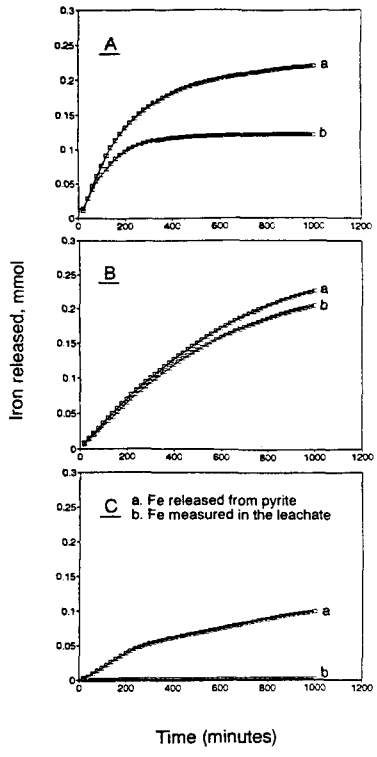

Figure 3. Release of iron as calculated according to the Fe-SO_4 stoichiometry and as measured in the leachates when pyrite was leached with the solutions listed in figure 2.

can inhibit formation of iron phosphate coatings owing to its influence on the degree of supersaturation with respect to $FePO_4$ and thereby increase the amount of pyrite oxidized to create iron phosphate coatings. The use of a buffer reagent will greatly decrease the amount of pyrite oxidized to create the coating.

Surface Analysis

Scanning electron microscope photos show that after leaching with 0.147 mol/L H_2O_2, the residual pyrite particles were coated with a layer of iron hydroxide. But the framboidal morphology of most pyrite particles were still distinguishable (fig. 6A). This indicates that iron hydroxide did not precipitate as a coating owing to its relatively high solubility, although 0.1 mol of iron hydroxide formed during leaching within the column. As expected, the residual pyrite particles leached with the solution containing 0.147 mol/L H_2O_2 and 0.013 mol/L EDTA were free of any coatings (fig. 6B). Most pyrite particles displayed a typical framboidal morphology. Nevertheless, after leaching with the solution containing 0.147 mol/L H_2O_2 and 0.01 mol/L KH_2PO_4, residual pyrite particles were so heavily coated with FePO4 that crystals constituting pyrite particles were barely identifiable (fig. 6C). In addition, pyrite particles were much smaller than was observed for residual pyrite particles after leaching with H_2O_2 or H_2O_2 plus EDTA. This indicates that leaching with the phosphate solution containing H_2O_2 will introduce an iron phosphate coating on any size of pyrite particles.

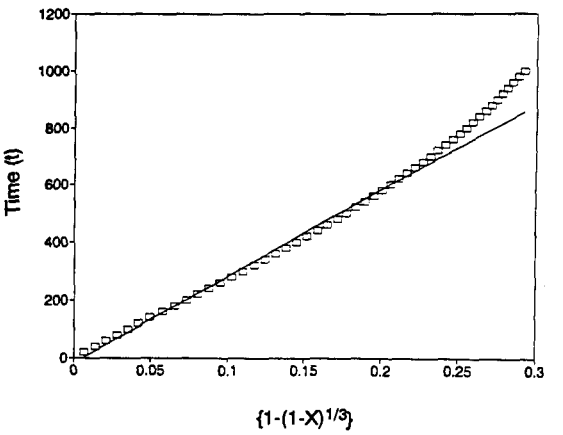

Figure 4. A model plot of t versus $\{1-(1-X)^{1/3}\}$ for the data of pyrite oxidation during leaching with the solution containing 0.147 mol/L H_2O_2 and 0.013 mol/L EDTA.

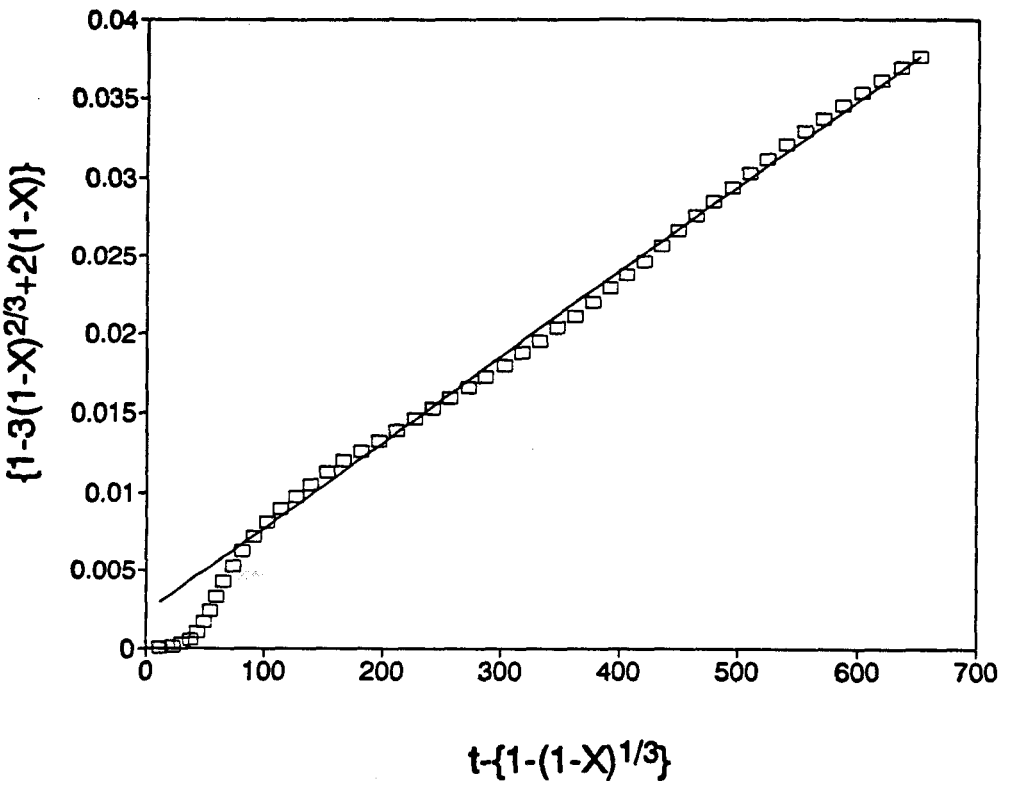

Figure 5. A model plot of $\{1-3(1-X)^{2/3}+2(1-X)\}$ versus $t-\{1-(1-X)^{1/3}\}$ for the data of pyrite oxidation during leaching with the solution containing 0.147 mol/L H_2O_2 and 0.01 mol/L KH_2PO4.

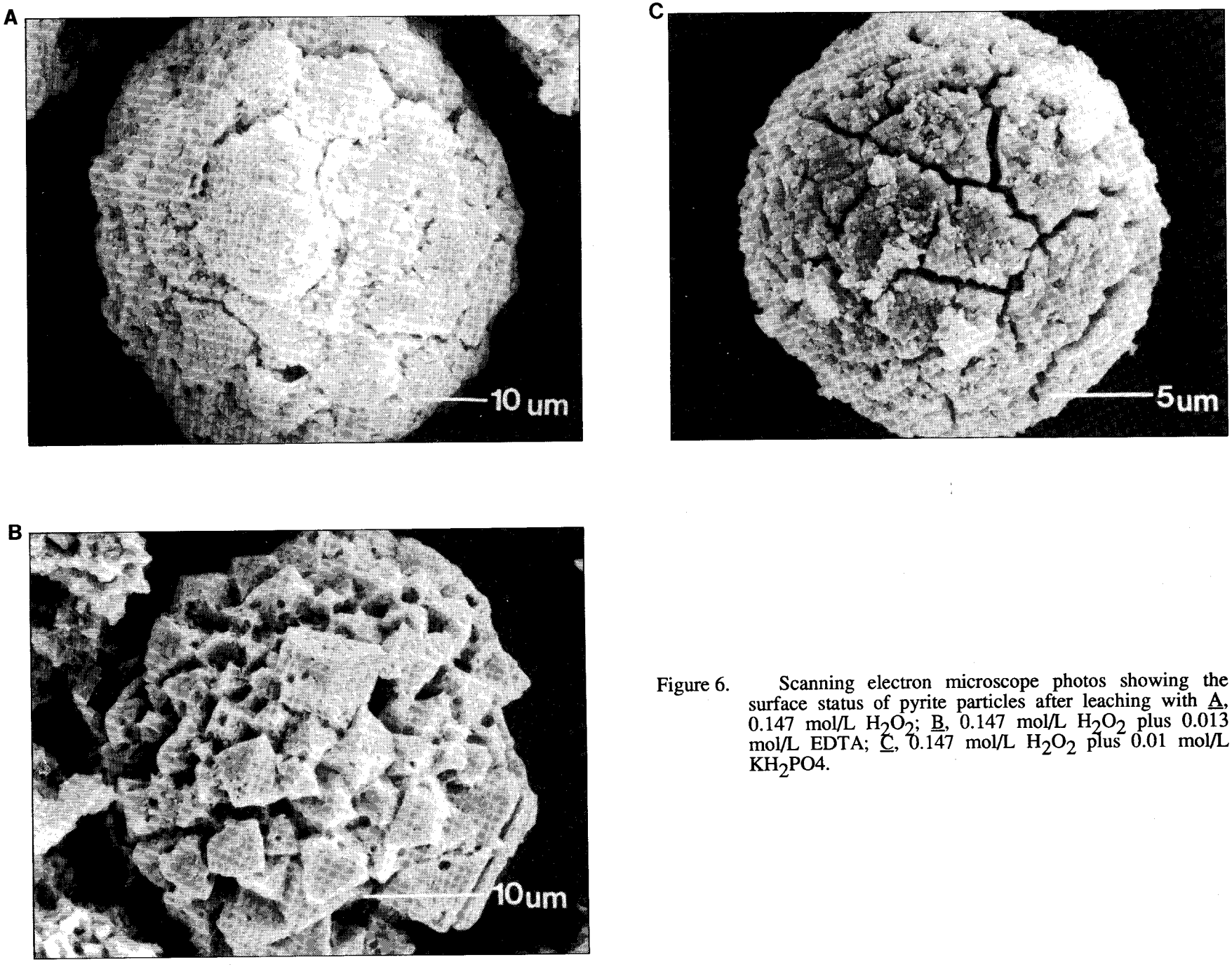

Figure 6. Scanning electron microscope photos showing the surface status of pyrite particles after leaching with A, 0.147 mol/L H_2O_2; B, 0.147 mol/L H_2O_2 plus 0.013 mol/L EDTA; C, 0.147 mol/L H_2O_2 plus 0.01 mol/L KH_2PO4.

Considering an $FePO_4$ precipitate of 0.1 mol with an $FePO_4$ gravity density of 2.73 g cm^{-3} and a pyrite specific surface of 7.3 m^2/g, its thickness was estimated to be approximately 188 Å (assuming that all the iron phosphate was precipitated as coating). Although the coating appears to be thin, the results in figure 2 indicate that once the coating was established H_2O_2 in the coating solution could no longer attack pyrite, and that iron phosphate coating was an effective H_2O_2-diffusion inhibitor.

To further understand the chemical properties of the iron phosphate coating, we repeated the leaching experiment with two columns of pure pyrite (50 mg pyrite and 500 mg sand) and the solution containing 0.147 mol/L H_2O_2 and 0.01 mol/L KH_2PO_4. At the end of leaching, one column continued to be leached with 50 mL of 2 mol/L HCl. The leachate was analyzed for iron and phosphate. We found out that the mole ratio of iron to phosphate was 1.0, indicating that the coating was $FePO_4$ and no hydroxyl entered the structure of iron phosphate. The pyrite in the other column was separated from the pyrite-sand mixture and its surface was examined using diffuse reflectance infrared spectroscopy (FT-IR). As shown in figure 7 (curve A), after leaching with the solution containing 0.147 mol/L H_2O_2 and 10^{-2} mol/L KH_2PO_4, the intensity of the IR absorption band at 439.7 cm^{-1} on the spectrum of the pyrite dramatically decreased. This absorption band was due to the vibration of the disulfide (S-S) in the lattice of pyrite; the decrease in intensity of this band strongly confirms the presence of the coating on pyritic surfaces. Three additional bands at 1624.3, 1184.7, and 1156.7 cm^{-1} and a broad band ranging from 3700 to 2800 cm^{-1} were also observed on the spectrum of the $FePO_4$-coated pyrite (Fig. 7A). The absorption band at 1624 cm^{-1} and the absorption hump around 3000 cm^{-1} are attributable to the bending vibration and rotation of water molecules either adsorbed on iron phosphate or within the structure of iron phosphate. The adsorption bands at 1184.7 and 1156.6 cm^{-1} are due to the P-O internal stretching vibration of PO_4 group (Nanzyo, 1986). Comparison of the spectra of $FePO_4$-coated pyrite and amorphous iron phosphate indicates that the iron phosphate coating is most likely amorphous material (Fig. 7A and 7C). However, the slight splitting of the P-O stretching vibration band at 1168 cm^{-1} suggests the tendency of iron phosphate coatings to become crystalline.

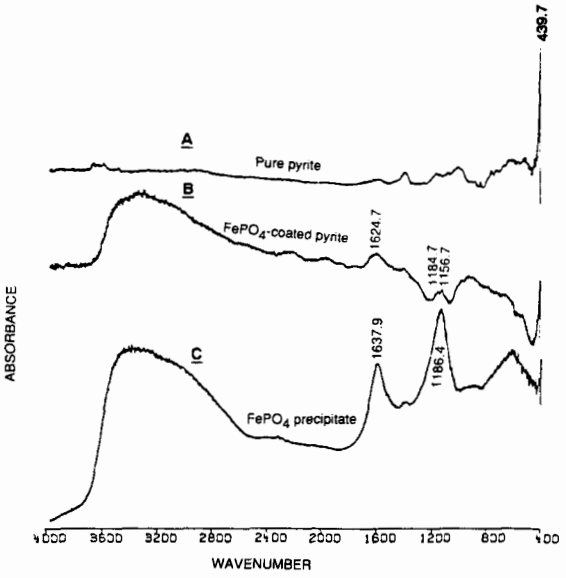

Figure 7. Infrared spectra of A, pyrite; B, $FePO_4$-coated pyrite and C, $FePO_4$ precipitate.

Effectiveness of the $FePO_4$ Coating in Preventing Pyrite Oxidation

We further tested the feasibility of this coating approach in preventing pyrite oxidation with the pulverized pyritic shale (the sample from which the pure framboidal pyrite was separated). We first leached the shale sample (500 mg) with 500 mL of a solution containing 0.053 mol/L H_2O_2 and 10^{-4} mol/L KH_2PO_4. This coating process consumed approximately 10% of the total amount of pyrite in the pyritic shale. The pyritic shale was then subjected to leaching with 0.088 mol/L H_2O_2 to test the effectiveness of the coating in preventing pyrite oxidation. As shown in figure 8, after leaching with 0.088 mol/L H_2O_2 for 800 min, only 15% of pyrite in the coated pyritic shale was oxidized, as opposed to more than 80% of pyrite oxidized in the uncoated pyritic shale. This result strongly suggests that the iron phosphate coatings can effectively protect pyrite from oxidizing.

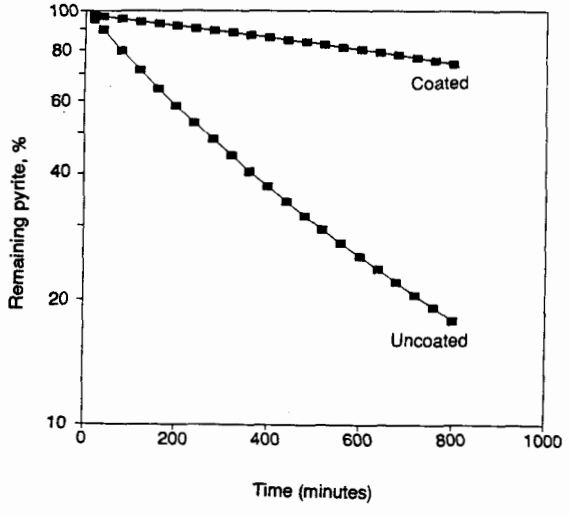

Figure 8. The plot of log (100 x M/Mo) versus t for the data of pyrite oxidation when the uncoated and coated pyritic shale samples were leached with 0.088 mol/L H_2O_2.

Conclusions

The results of this study demonstrate that an amorphous iron phosphate coating can be established on the surfaces of pyrite in mining "waste" by leaching with a phosphate solution containing H_2O_2 and that the iron phosphate coating could

effectively prevent pyrite oxidation.

The above conclusion sheds light on a possible solution to the long-unsolved problem of acid mine drainage. This coating approach or technology, if finally extended into practical use, has the following advantages over other approaches. First, due to the permanence of iron phosphate coatings on pyritic surfaces, pyrite particles in mining "waste" can no longer be oxidized and release acid; thus the prevention of the production of acid mine drainage could be permanent. Second, this coating approach does not require the physical mixing of coal wastes with ameliorants and thus can greatly simplify the operation. Third, the coating approach involves using only low concentrations of phosphate and hydrogen peroxide and can dramatically decrease the costs incurred in the operation.

The conclusions drawn in this study are mainly based on the small column experiments, where the effect of the acid produced during leaching with the coating solution on formation of iron phosphate coatings was minimized. It is expected that if we use the coating solution to leach large piles of coal "waste," the pH and concentrations of H_2O_2 and phosphate will decrease as the coating solution goes through the coal wastes. It has been proven in our laboratory that decreases in concentrations of H_2O_2 and phosphate will not significantly influence the efficiency of the coating solution. Nevertheless, the decrease in pH can pose a severe problem; when the pH of the coating solution drops below 4 or to 2, the solution no longer serves as a coating solution but becomes an oxidizing solution. Therefore, it seems essential to introduce a buffer in the coating solution to maintain the pH and the efficiency of the coating solution. Currently, in our laboratory, we are developing a coating solution with an optimal concentration combination of H_2O_2, KH_2PO_4, and a buffer reagent to prevent coal wastes from producing acid drainage.

Literature Cited

Singer, P.C. and W. Stumm. 1970. Acid mine drainage: the rate-determining step Science 167:1121-1123.

Silverman, M.P. 1967. Mechanisms of bacterial pyrite oxidation J. Bacteriology 94:1046-1051

Nordstrom, D.K. 1982. Aqueous pyrite oxidation and the consequent formation of secondary iron minerals. p. 46-53. In L.R. Hossner, J.A. Kittrick, and D.F.Fanning (eds.), Acid sulfate weathering: pedogeochemistry and relationship to manipulation of soil minerals, Soil Sci. Soc. America, Madison, WI.

Kleinmann, R.L.P., D.A. Crerar, and R.R. Pacelli. 1981 Biogeochemistry of acid mine drainage and a method to control acid formation Min. Eng. 3:300-305.

Ziemkiewicz, P. 1990. Advances in the prediction of and control of acid mine drainage. p. 51-54. In Proceedings of the Mining and Reclamation Conference and Exhibition, v 2. Charleston, WV.

Ivanov, V.I. 1962. Effect of some factors on iron oxidation by cultures of *Thiobacillus ferrooxidans*. Microbiology (Engl. Transl.) 31:645-648.

Kleinmann, R.L.P., and D.A. Crerar, 1979. *Thiobacillus Ferrooxidans* and the formation of acidity in simulated coal mine environments. Geomicrobiology J. 1:373-389.

Huang, X and V.P. Evangelou. 1992. Abatement of acid mine drainage by encapsulation of acid producing geologic materials. U.S. Bur. Mines Contract j0309013. 60 p.

Nicholson, R. V., R. W. Gillham, and E. J. Reardon. 1989. Pyrite oxidation in carbonate-buffered solution: 2. Rate control by oxide coatings. Geochim. Cosmochim. Acta 54:395-402.

Turner, R.C. 1960. An investigation of the intercept method for determining the proportion of dolomite and calcite in the mixtures of two. Can. J. Soil Sci. 40:232-241.

Nanzyo, M. 1986. Infrared spectra of phosphate sorbed on iron hydroxide gel and the sorption products. Soil Sci. Plant Nutri. 32:51-58.

SHOTCRETE AS A CEMENTITIOUS COVER FOR ACID GENERATING WASTE ROCK PILES[1]

C.E. Jones[2] and J.Y. Wong[3]

Abstract: A research program supported by both Westmin Resources and the Canada-British Columbia Mineral Development Agreement (MDA) has evaluated the use of cementitious dry surface covers for the prevention of water and oxygen infiltration into acid-generating waste rock piles. This paper presents the results of a field trial of a dry cover over a large test area on a waste rock pile at the Westmin Myra Falls site near Campbell River, BC, Canada. The objectives of this study were to apply the cementitious cover in the most cost effective manner and to evaluate the material properties and the long-term efficacy of the cover system. Approximately 3,500 m^2 area was covered using the shotcrete process. A robotic arm mounted onto a vehicle was used to apply the shotcrete onto the rock slope. The cementitious material used in the project incorporated high volumes of fly ash (a waste product) to reduce the material cost. The shotcrete mix also included the use of polypropylene fibers to control cracks. Costs of materials and application of the cover were determined. The test area was instrumented with survey markers to monitor settlement in the rock slope. The performance of the test area was monitored for 1 yr to evaluate the durability of this cover when subjected to field conditions. Compressive strength increased over the 1 yr period, and all samples achieved or exceeded the design criteria. Some plastic shrinkage cracks were observed in the shotcrete immediately after application but after 1 yr of exposure these cracks did not appear to have expanded.

Introduction

The Westmin Resources Limited, Myra Falls Operations is a 3,650 mt/d copper-zinc-gold-silver mine located in a narrow steep valley in the central region of Vancouver Island, BC. The climate of the site is classed as Marine West Coast by the Koppen system, with a mean annual precipitation of approximately 300 cm, with over 75% of the total precipitation occurring between October and March. Most of the waste rock from the mining operations has been placed in dumps constructed along the north valley wall, east of the inactive open pit. The waste rock dumps contain sulfide minerals and have been generating acid drainage with elevated metal loadings, particularly zinc, copper, and cadmium, for at least a decade. A water collection and treatment system is presently in place to protect the downstream environment; however, reclamation of the waste rock dumps and the eventual decommissioning of the mine will require a long-term control method for acid generation and drainage at the mine site. Ideally the long-term control method should restrict the availability and contact of oxygen and water, the primary ingredients of the acid generation process, with the reactive waste rock.

The mine's decommissioning plan recommended that the closure strategy for the waste rock dump focus on preventing acidic water from moving downward to the water table (C.E. Jones and Associates Ltd. 1992). Restricting the access of oxygen and surface water infiltration to reactive waste rock can be achieved using covers and seals. The restriction of water can potentially reduce the formation of acid and the subsequent transportation of the oxidation products away from the source (BC Acid Mine Drainage Task Force, 1989). A variety of materials have been proposed to provide covers for reactive waste rock or tailings, including soils, synthetic membranes, compacted clay and till, asphalt, and concrete. The draft ARD (Acid Rock Drainage)

---

[1]Paper presented at the International Land Reclamation and Mine Drainage Conference and the Third International Conference on the Abatement of Acidic Drainage, Pittsburgh, PA, April 24-29, 1994.

[2]Carol E. Jones, Principal, Northwest Geochem, a division of C.E. Jones and Associates Ltd., Victoria, BC, Canada.

[3]Joe Y. Wong, Materials Engineer, Powertech Labs, Surrey, BC, Canada.

Technical Guide (BC Acid Mine Drainage Task Force, 1989) and Malhotra (1991) discuss the relative advantages and disadvantages of the various types of covers.

A limiting factor governing the use of various materials proposed for use as covers is the cost associated with large-scale application (Malhotra et al. 1990). Conventional portland cement shotcrete is a well known technology for stabilizing vertical rock faces; however, this type of system becomes expensive for application on large areas where control joints, mesh reinforcement, and increased thickness are required.

Recent studies by CANMET and others (Morgan and McAskill 1990; Langley and Dibble 1990; Seabrook 1992) have shown that a fiber-reinforced, high-volume fly ash shotcrete can be used successfully in large-scale applications. The system incorporates discrete polypropylene fibers to increase toughness and inhibit cracking and uses large volumes of fly ash to lower material cost. A limited number of field trials have been conducted, but more data are required to determine the long-term effectiveness of the proposed capping systems.

Northwest Geochem, in conjunction with Powertech Labs Inc., has been researching, developing, and testing a cementitious cover that incorporates mine tailings. Laboratory trial mixes and limited small scale tests have indicated that there is great potential in this type of capping system (Gerencher et al. 1991). These trials also evaluated the effects of addition of fibers and fly ash to the shotcrete mix.

This paper presents the results of a large-scale test in which a shotcrete cover was applied to a portion of a waste rock dump. The primary objective of the test was to evaluate material properties and the long-term efficacy of the field-placed shotcrete. In addition, a large-scale test provides an opportunity to develop and use the best practicable technology to install a shotcrete cover material on reactive waste rock. This test site represents an open-ended system; therefore the effectiveness of large scale cover placement on restriction of acid generation and drainage was not evaluated, and detailed instrumentation to monitor ARD parameters was not installed.

Methods

Site Preparation

The shotcrete test was performed on an area of the waste rock dump which was not benched and had a slope between 37° and 39°. To facilitate this test, the upper 10 m of the dump was resloped to a grade of 22° (figure 1). After resloping, the test area was compacted using a vibrating Bomag roller. Although shotcrete can be applied to vertical slopes, the shallower grade was required for the use of the robotic arm shotcrete spraying equipment and subsequent placement of overburden and vegetation planned for the test area. An 8-m-wide access road was constructed at the base of the test slope. The approximate area of the test site was 3,500 m^2. The capping system was designed to connect with a diversion ditch that extends around the perimeter of the mine area.

Materials

One of the largest costs in using a cementitious dry cover is the transportation of raw materials such as aggregate and cement to the site. In a previous study by Northwest Geochem and Powertech (Gerencher et al. 1991), coarse mine tailings were used as an aggregate in the shotcrete mix and would eliminate the need to import aggregate from Campbell River (located 85 km from the mine site). That study indicated that mine tailings can be used effectively as aggregate in a cementitious dry cover. However, the coarse tailings are also used as mine backfill and may not be available for reclamation use. It is envisaged that during the final reclamation, the crushers at the mine will produce an aggregate to be used for shotcrete covers. The concrete can then be batched directly on site. For this field trial, it was not economical to set up a concrete batch plant on site. The proportioned aggregate along with the fly ash and water were trucked from Campbell River in

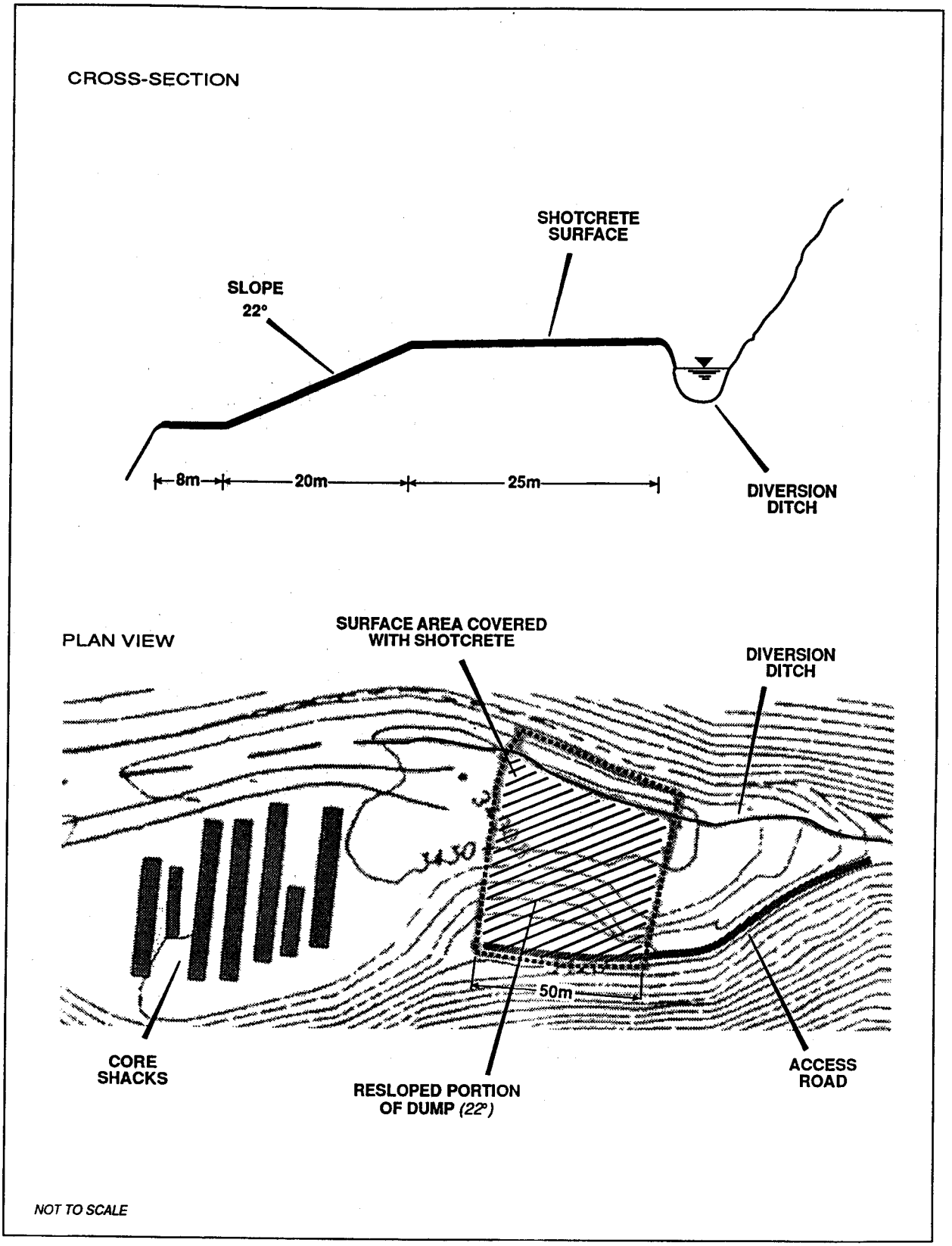

Figure 1. Schematic of large scale field application of shotcrete.

ready-mix trucks. Each truck contained 6 m^3 of aggregate. The cement was added to the truck on site. The mix proportions are given in table 1. The mix design was chosen with emphasis on optimizing the material costs. Since cement is an expensive material in a shotcrete mix, fly ash, a waste product from coal-fired power-generating plants, was used as a partial replacement for cement.

Approximately 100 m^2 of the test area were covered with a mix where coarse tailings were substituted for concrete sand (table 2). Since weighing facilities were not available on site, the tailings were added volumetrically, which resulted in a less accurate batch. The tailings did not blend well with the cementitious material and required a high water content to allow the mix to flow from the truck.

Equipment

Another major cost of this dry cover system is the application of the shotcrete. In Westmin's final closure plan, the approximate area required to be covered is 6 ha. Therefore it is imperative that equipment be used that can produce consistent quality shotcrete at very high production rates. The wet mix shotcrete in this project was applied using a robotic arm mounted on a rubber-wheeled carrier. The robotic arm is mounted on a turret with a 360° swing. The spray boom has a reach of 10.4 m. The shotcrete nozzle, attached to the end of the spray boom, is able to tilt 120° and has a rotation of 270°. The wet-mix concrete was pumped to the nozzle using a diesel-powered double-piston shotcrete pump through a 63.5-mm-diameter delivery hose. The arm is remotely controlled by an operator using a series of toggle controls.

Application of Shotcrete

The shotcrete was applied during August 1992. The crew consisted of one nozzleman, one helper, and one pumpman. The equipment did not require any major assembly and was mobilized in only a few hours.

The cement was added to the concrete trucks on site and was allowed to mix for at least 30 min. The concrete was then discharged into the hopper of the shotcrete pump. The pumpman controlled the amount of shotcrete supplied to the nozzle. The nozzleman controlled the shotcrete nozzle and the placement of the shotcrete onto the waste rock dump.

Table 1. Proportions for primary mix.

	kg/m^3
Type 10 cement	139
Fly ash	217
Concrete sand (<5 mm)	1,815
Water (water/cement ratio = 0.38)	138
Polypropylene fibers	4

Table 2. Proportions for tailings mix.

	kg/m^3
Type 10 cement	167
Fly ash	174
Tailings	1,500
Water (water/cement ratio = 0.76)	260
Polypropylene fibers	4

The common spraying sequence started with the boom fully extended at its maximum reach. The nozzle was usually positioned approximately 1 to 1.5 m from the surface. The boom was then swung side to side in a sweeping motion and was slightly retracted after each sweep. A nominal thickness of 75 mm of shotcrete was chosen for this test. Approximately 80 to 90 m^2 were covered without having to move the vehicle. Owing to the relatively smooth surface produced by the compaction of the waste rock, the thickness of the shotcrete cover was quite uniform.

The production rates achieved in this test program were higher than production rates achieved using conventional application methods. The entire test cover took approximately 5 days to install. The average rate achieved was 150 m^2/h. On some occasions production rates of 200 m^2/h were achieved. However, this type of equipment was originally designed for lining tunnels, and the movements of the boom are not suited for application on near-level grades. For example, the swinging motion of the arm resulted in wear on the clutch in the turret. Another improvement that would make the shotcrete application more efficient would be to use a smaller, more mobile vehicle that could easily traverse the shallow slopes.

There is potential to further enhance productivity by using a larger diameter delivery hose. For example, the use of a 75-mm-diameter delivery hose (versus the 63.5-mm hose used in this application) would increase production by at least 30%. The use of a larger hose would also reduce the plugging of the lines, which was a concern in this project.

Instrumentation

After the application of the shotcrete, a grid of survey markers was installed onto the cover at 5 m spacings and survey locations were determined.

Laboratory Testing

A number of laboratory tests were performed to characterize the quality of the shotcrete cover. Six shotcrete panels (1 m by 1 m by 150 mm) were prepared in the field for laboratory testing. Panels 4 and 5 were composed of the tailings mix; the others were shot from various batches of the primary mix.

Compressive strength tests were performed on cylinders 150 mm in diameter and 300 mm in length cored from the test panels at various stages of curing. The results of these tests are given in table 3 and illustrated in figure 2.

Table 3. Compressive strength of shotcrete (MPa).

	Age of cylinders			
	28 days	100 days	200 days	400 days
Panel 1	16.3	19.5	27.1	33.2
Panel 2	7.1	9.4	10.4	24.2
Panel 3	8.1	11.6	13.7	29.0
Panel 4 (tailings)	10.9	16.2	16.6	22.0
Panel 5 (tailings)	13.1	21.0	32.2	33.1
Panel 6	7.9	12.0	11.5	27.2

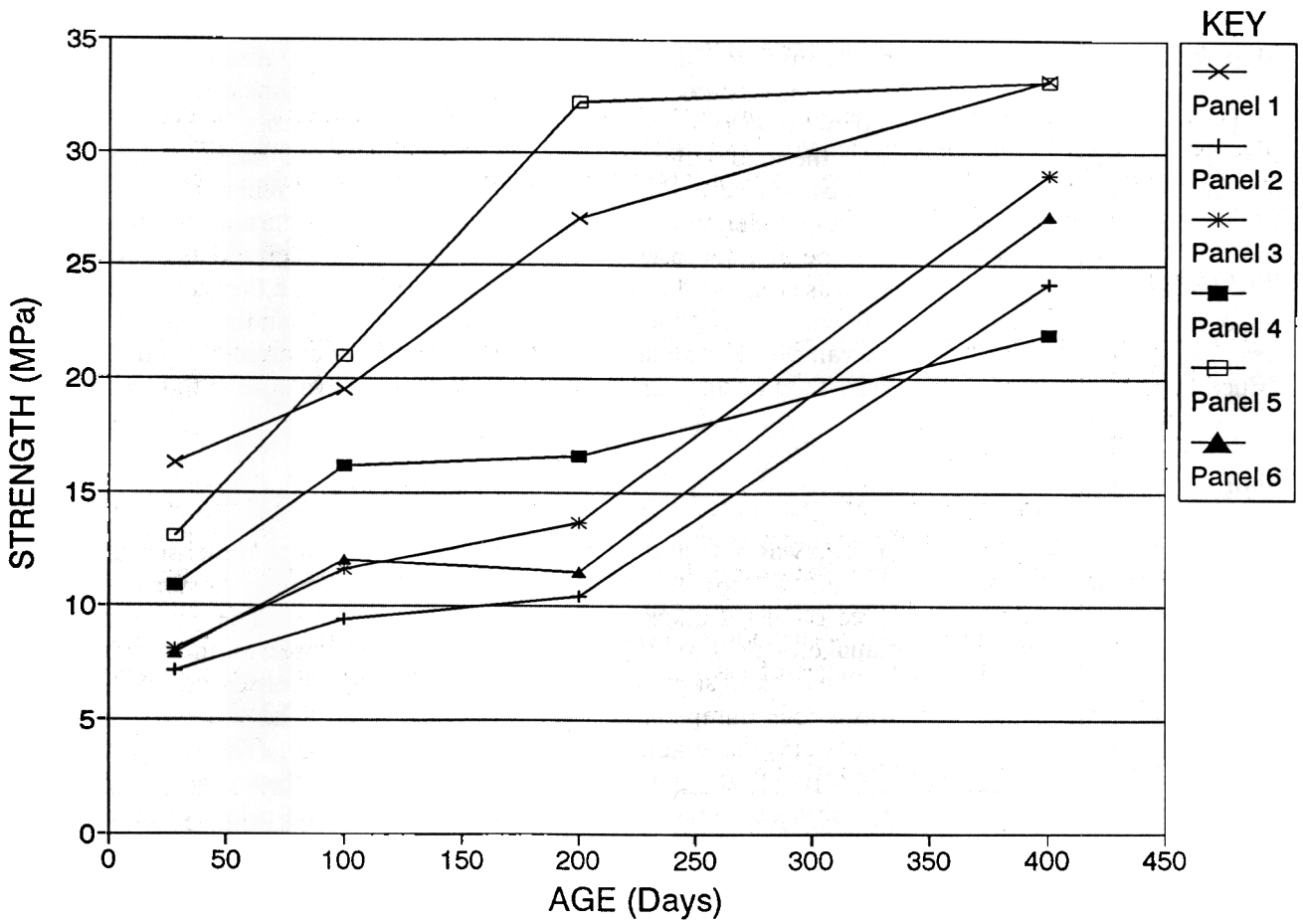

Figure 2. Compressive strength of shotcrete.

As a surface sealant, high-strength shotcrete is not required as long as it impedes infiltration of water and oxygen. The design objective was to achieve 15 to 20 MPa in compressive strength. After 400 days all of the panels achieved strength greater than the design objective. The strength gain was generally low over the first 200 days, during the winter period, but increased in the following 200 days during the warmer summer period. While all of the panels achieved the design objective for compressive strength, the values at 400 days range from 22.0 to 33.1 MPa. The inclusion of a superplasticizer would reduce this variability in the quality of the mix, but would increase the cost.

Concrete is typically a brittle material, exhibiting very low tensile strengths. Therefore, unreinforced concrete will tend to crack and separate following small deflections. Because the shotcrete material is designed for use as a surface sealant on a waste rock dump, the hardened concrete will require ductility to withstand local settlement within the waste slope. To evaluate the ductility of the test panels, toughness index tests were performed in accordance with ASTM C1018, Standard Test for Flexural Toughness and First-Crack Strength of Fiber Reinforced Concrete (Using Beam with Third Point Loading). Beams (100 mm by 100 mm by 350 mm) were cut from the shotcrete panels for flexural testing at 100 days' cure. Toughness of the shotcrete is defined as the total energy absorbed prior to complete separation of the specimen. This energy can be measured by calculating the area under the load deflection curve in flexure. The toughness in plain concrete is quite low and failure of the specimen usually occurs when the first crack develops. When fibers are present, the cracks cannot extend without stretching or debonding the fibers. As a result, considerable additional energy is required before complete fracture of the material occurs. The toughness index is defined as the ratio of the absorbed energy at various crack widths as compared to the absorbed energy when the first crack occurs. The results of the flexural tests (table 4) are variable, but the values are generally lower than the desired toughness indices of $I_5>3$ and $I_{10}>6$. These low values are not unexpected since a low fiber content (4 kg/m^3) was used to reduce the cost of the product. The field performance will be monitored to evaluate if this fiber content is adequate for this application.

Monitoring Program

No movement of the shotcrete cap was detected when the survey markers were remeasured in March 1993. A visual assessment was carried out in September 1993, and the overall durability performance of the cap was good. There was no evidence of major cracking or movement in the cap. The shotcrete did not appear to have suffered any frost damage or erosion. Some minor cracks were observed in two small areas where the shotcrete was thinner than the 75-mm standard depth. Iron staining was observed on these areas as a result of water flow from the waste rock dump through the shotcrete panel. The source of this flow is not certain, but it would appear to be lateral movement of water through the dump. The dump material is composed of a high percentage of fine particles and therefore retains moisture near the surface. Some plastic shrinkage cracks were observed in the shotcrete immediately after application. The primary cause of these cracks was the high rate of evaporation before initial set. In November 1992, cores were taken through a number of these cracks; some were found to extend through the cap, and others terminated approximately halfway through the cap. After 1 yr of exposure, these cracks did not appear to have expanded.

Cost of Shotcrete Cover

A major consideration in the design of the testing program was cost. Table 5 provides a breakdown of the cost of the project. It is apparent that the transportation of aggregate to the mine site is a substantial cost of the cover. If a local aggregate source, such as coarse tailing, were available, the unit cost per square meter of cover could be less than Cdn $12.

Table 4. Toughness tests of shotcrete at 100 days' cure.

	Primary mix	Tailings mix
Flexural strength MPa	1.5 - 2.0	2.9 - 3.1
Ductility:		
Toughness index I_5	1.6 - 2.7	1.4
Toughness index I_{10}	2.7 - 5	2.2 - 2.5

Table 5. Cost breakdown of shotcrete application.

	Cdn $/m^2
Cement	1.28
Fibers	1.88
Fly ash	1.40
Aggregate (includes transportation)	7.10
Labor	3.30
Equipment	3.50
Total	18.46

Conclusions

This study indicates that shotcrete dry covers can be a viable option for sealing prepared waste rock dumps. Prior to shotcrete application, the surface of the dump must be stabilized through resloping and surface compaction. The application using a robotic spray boom resulted in high productivity and therefore contributed to a low application cost. A major proportion of the cost involved the importation of aggregate. The use of a local aggregate source such as mine tailings would make this option more cost effective when compared to other types of covers. The shotcrete material exhibited good compressive strength and moderate ductility. One year after application the cover was intact and functioning well.

This study did not evaluate the effectiveness of the cover in restricting acid generation in a waste rock pile. It is recommended that this cover technology be applied in a controlled field trial on a designed waste rock test pile to evaluate its effectiveness in restricting the access of oxygen and surface water infiltration to reactive waste rock.

Literature Cited

BC Acid Mine Drainage Task Force. 1989. Draft acid rock drainage technical guide. Prepared by Steffen Robertson Kirsten (BC) Inc. in association with Norecol Environmental Consultants and Gormely Process Engineering.

C.E. Jones and Associates Ltd. 1992. Decommissioning plan prepared for Westmin Resources Limited, Myra Falls Operations, Vancouver, BC.

Gerencher, E.H., D.E. Konasewich, J.Y. Wong, and R. van Dyk. 1991. The use of mine tailings in concrete surface covers to control acid mine drainage in waste rock dumps. p. 69-84. In Second International Conference on the Abatement of Acidic Drainage, Volume 4. (Montreal, PQ, September 16-18, 1991).

Langley, W.S. and D. Dibble. 1990. Field trials of shotcreting polypropylene fiber-reinforced high-volume fly ash (ASTM Class F) concrete. Paper presented at the CANMET International Workshop on Fly Ash in Concrete, Calgary, AB.

Malhotra, V.M. 1991. Fiber-reinforced high-volume fly ash shotcrete for controlling aggressive leachates from exposed rock surfaces and mine tailings. p. 505-514. In Second International Conference on the Abatement of Acidic Drainage, Volume 1. (Montreal, PQ, September 16-18, 1991).

Malhotra, V.M., G.G. Carette, and A. Bilodeau. 1990. Fiber-reinforced high-volume fly ash shotcrete for controlling aggressive leachates from exposed rock surfaces and mine tailings. Paper presented at the CANMET International Workshop on Fly Ash in Concrete, Calgary, AB.

Morgan, D.R. and N. McAskill. 1990. Evaluation of polypropylene fiber-reinforced high-volume fly ash shotcrete. Paper presented at the CANMET International Workshop on Fly Ash in Concrete, Calgary, AB.

Seabrook, P.T. 1992. Shotcrete as an economical coating for waste piles. Paper presented at the Waste Management in the Cement Manufacturing Process Conference, Calgary, AB.

EVALUATION OF A COMPOSITE SOIL COVER TO CONTROL ACID WASTE ROCK PILE DRAINAGE[1]

Alan V. Bell[2], Mike D. Riley[3] and Ernest K. Yanful[4]

Abstract: Acid mine drainage (AMD) research under the MEND program has been ongoing since 1988 at the Heath Steele Mines waste rock piles including sulfide material, outside Newcastle, NB. In 1989 approximately 10,000 mt of waste rock was placed on a prepared sand base with an underlying impermeable membrane. The waste rock pile was heavily instrumented for oxygen concentrations and temperatures measures. In September 1991, a composite soil cover designed for the Heath Steele climatic conditions using local soils was placed over the pile, creating a totally enclosed system. Moisture content and oxygen probes were installed within the composite soil cover to monitor changes within the soils over time, while two large-size lysimeters were installed below the cover to monitor the hydraulic conductivity of the cover. The waste rock site has been monitored on a monthly basis since installation of cover for performance of both cover and waste rock. The monitoring shows very clearly that the placement of the composite soil cover has had a major impact on the generation of AMD. Major reductions in temperature and oxygen concentrations within the waste rock pile indicate that the cover has significantly inhibited the oxidation reaction that generates the AMD. Performance data have shown that the cover has maintained its integrity under the climatic conditions of the area.

Additional Key Words: acid mine drainage, acid waste rock pile cover, waste rock oxidation reduction.

Introduction

The Heath Steele Mine site in northeastern New Brunswick provides a unique opportunity to evaluate management techniques for acid waste rock under practical field conditions. The massive sulfide deposits at Heath Steele were developed in the late 1950's before the implications of acid drainage were fully appreciated. The highly pyritic waste rock encountered in the course of mining operations was stockpiled at various locations across the site and in some instances was used in the construction of haul roads and other infrastructure. Currently there are more than 20 acid-generating waste rock piles of various sizes and configurations located across the site.

A recent study of acid waste rock management at Canadian base-metal mines (Nolan, Davis 1987, Bell 1988) identified the need for field performance data on waste rock pile covers and other management systems. The Heath Steele Waste Rock Study is designed to address this need, as well as to aid in the development of practical reclamation measures for mine sites in northeastern New Brunswick, where the combination of massive sulfide ore bodies and the sensitivity of local salmon resources to acid and metal toxicity pose an especially difficult challenge to mine reclamation.

In 1989, a program was initiated by Brunswick Mining and Smelting Corp. Ltd. (BMS) to develop and test strategies for long-term management of several acid generating waste rock piles located at the Heath Steele Mine (HSM) site. The program was conducted in four phases under the auspices of Mine Environment Neutral Drainage

[1]Paper presented at the International Land Reclamation and Mine Drainage Conference and the Third International Conference on te Abatement of Acidic Drainage, Pittsburgh, PA, April 24-29, 1994.

[2]Alan V. Bell, President, ADI Nolan Davis (NS) Ltd., Halifax, N.S., Canada

[3]Mike D. Riley, Principal, ADI Environmental Management Inc., Fredericton, N.B., Canada

[4]Enerst K. Yanful, Associate Professor, University of Western Ontario, London, Ont., Canada

(MEND), Canada's national task force for acid rock drainage research. The four phases comprise the selection of several waste rock piles for field trials, definition of physicochemical characteristics of the selected piles, identification and evaluation of suitable candidate soils for a composite soil cover, and the design, installation, and monitoring of the composite soil cover on a selected pile.

This paper deals with the design, installation, and monitoring of the composite soil cover installed on selected waste rock pile 7/12. The results of 2 yrs. of monitoring both prior to and after placement of the cover are presented. The interpretation of the monitoring results indicate, how effective the cover has been in the control of acid rock drainage.

Project Setting

HSM site is located approximately 50 km northwest of Newcastle and about 60 km southeast of Bathurst, NB, within the drainage basin of the Northwest Miramichi River (fig.1). Presently, approximately 750, 000 mt of potentially acid-generating waste rock and reject ore are stockpiled in more than 20 piles at the HMS site. The total projected waste-rock inventory at closure in 1994 (including waste rock from active operations) is 2.3 million mt.

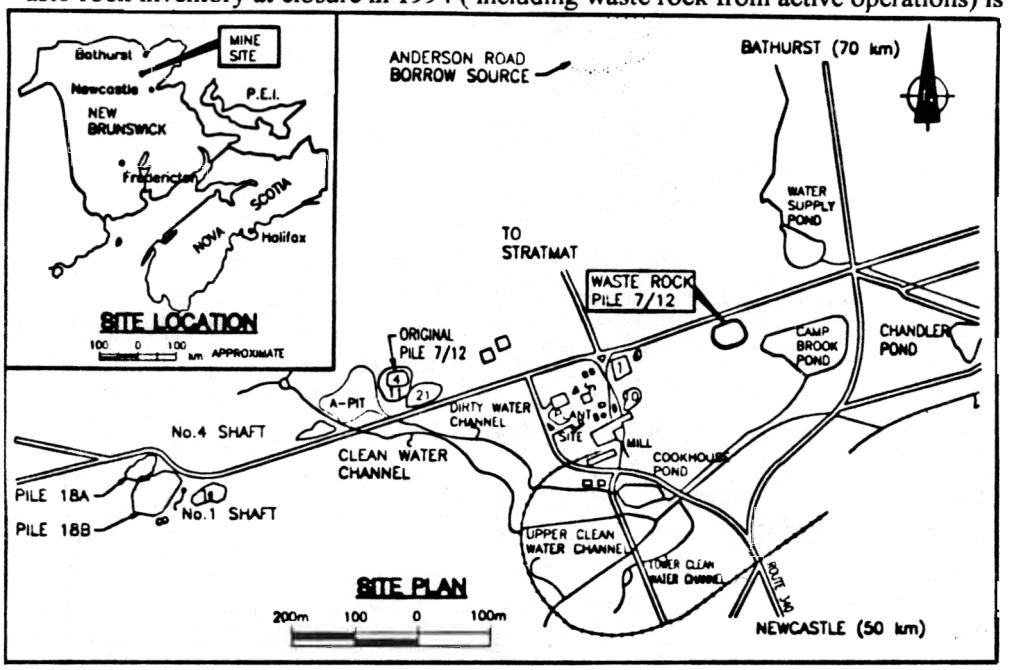

Figure 1. Site plan - Heath Steele Mines.

In 1989, approximately 10 000 mt of acid-generating waste rock was relocated from other areas of the HSM property to pile 7/12. Pile 7/12 is located approximately 1 km from the Heath Steele mill complex off the main haul road (fig.1) and has been sited so that it is isolated from the influence of any neighbouring topographical features. The relocated waste rock was placed on a prepared sand base, underlain by an impermeable membrane, by truck end dumping from the perimeter and pushing towards the middle with a loader. Pile 7/12, which covers an area of 0.25 ha in plan, has a maximum depth of 5 m. The pile was contoured to a uniform pile configuration having a maximum slope of approximately 3:1 (H:V). The final pile configuration is designed to minimize any shape-induced effects on the monitoring results and also to facilitate the placement of monitoring instrumentation.

Table 1. Physicochemical characteristics of relocated waste-rock pile 7/12.

Description	Value
Surface area	2 100 m2
Average depth	2.9 m
Maximum depth	5.0 m
Estimated volume	6200 m
Estimated tonnage	10 700 mt
Sulfide mineralogy,%	
Pyrite	7-10
FeS	5-7
Pyrrhotite	<1
Other sulfides (galena, sphalerite, etc.)	<1
Total sulfate	5
Theoretical acid production (as CaCO3)	210.7 kg/mt
Acid consumption (as CaCO3)	0.4 kg/mt

The predominant constituent sulfide mineral of pile 7/12 is pyrite (FeS_2), with total sulfur content averaging about 5%. The physicochemical characteristics of the pile are presented in table 1.

Pile 7/12 was instrumented with seven sets of thermocouples and six sets of pore-gas samplers. The typical instrumentation cluster at each sampling location consists of a piezometer installed to 5 m depth with a series of pore gas monitoring tubing (5 mm diameter nylon) attached to the exterior of the piezometer at various predetermined depths. Temperature probes, consisting of type K thermocouples, were installed at the same depths as the pore gas monitoring tubing in holes located within 1 m of the pore gas monitoring piezometers.

The underlying impermeable membrane has made possible the collection of leachate from the waste rock pile at the base of the pile both before and after placement of the soil cover. A perimeter ditch was constructed to allow for separate collection of surface runoff.

Composite Soil Cover Design

A soil cover for controlling acid drainage must effectively retain a high degree of water saturation as well as have a low hydraulic conductivity. While a saturated fine-grained soil layer, having a hydraulic conductivity of 10^{-7} cm/sec or less, can provide an effective barrier to the movement of both water and oxygen, studies indicate that a single soil layer that is initially saturated will, when placed on a waste rock pile, ultimately desaturate by drainage and moisture losses due to evaporation. As the soil desaturates, the diffusion coefficient of oxygen will increase with time, resulting in increased oxygen diffusion into the pile. Furthermore, a single soil cover designed to have a low hydraulic conductivity could dry out and crack over time, especially if the soil has a high clay content. As part of the Heath Steele Waste Rock Study, several soil-cover design scenarios were investigated for use on pile 7/12.

The design philosophy for the pile 7/12 soil cover, was based on the concept of the capillary barrier, where a coarse-grained soil layer, underlying a fine-grained layer, such as glacial till, is relied upon to reduce moisture loss in the latter by drainage. The underlying granular layer will drain faster and reach residual saturation long before the glacial till, thus maintaining saturation in the glacial till during summer dry conditions. At residual saturation, the hydraulic conductivity of the granular layer is minimum, so that it is no longer able to transmit negative pressures required to drain the till. If the glacial till is compacted at a moisture content slightly wetter than optimum, it can be expected to have a low hydraulic conductivity and hence to be an effective moisture barrier as well. To reduce evaporation and hence cracking of the surface of the fine-grained soil cover, an overlying coarse-grained granular layer is also required. In addition to acting as an evaporation barrier, the upper granular layer also promotes replenishment of moisture to the glacial till. During infiltration, the granular soil provides storage of water and reduces runoff, thus allowing more water to reach the glacial till.

The capillary-barrier concept, using a three-layer cover design, was evaluated in a series of detailed laboratory investigations at the Noranda Technology Centre (NTC). On the basis of the testing and analysis carried out, NTC proposed a composite soil cover for pile 7/12 consisting of a fine-grained saturated glacial till sandwiched between two coarse-grained granular layers. The thickness of the soil layers in the NTC composite soil cover design is 30 cm base

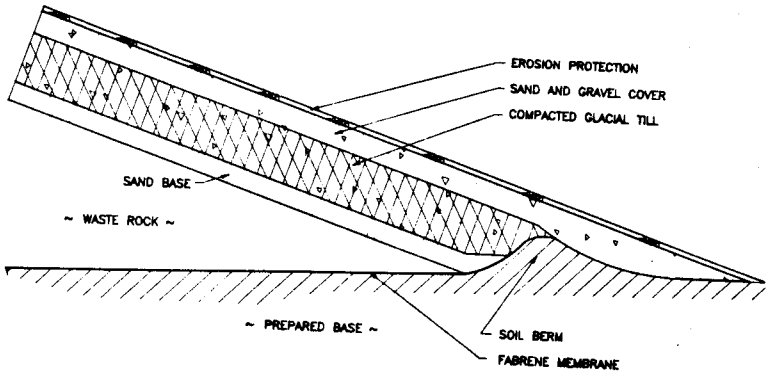

Figure 2. Cross section of composite soil cover.

granular layer, 60 cm saturated glacial till, and 30 cm overlying coarse granular layer. A final 10 cm thick surficial layer of coarse grained was also included for erosion protection. The proposed layer thicknesses, which are designed to keep the glacial till saturated for a minimum of 50 days without precipitation, provide effective oxygen and hydraulic barriers for the waste rock. A cross section of the completed composite soil cover is presented in figure 2.

Composite Soil Cover Construction

A 130 cm thick composite soil cover, consisting of a 30 cm thick sand base, 60 cm thick compacted glacial till, a 30 cm thick granular layer, and a final 10 cm thick erosion protection layer was placed over pile 7/12 during the period August 15-September 19, 1991. Following is a summary of the specific tasks associated with this cover construction.

Surface Preparation

The initial task in the placement of the cover was the preparation of the surface of pile 7/12 by levelling the top of the pile and removing high points on the side slopes. Voids and depressions were filled with excavated waste rock and non-acid-generating crushed rock. A total of 50 mt of crushed rock was used for surface preparation.

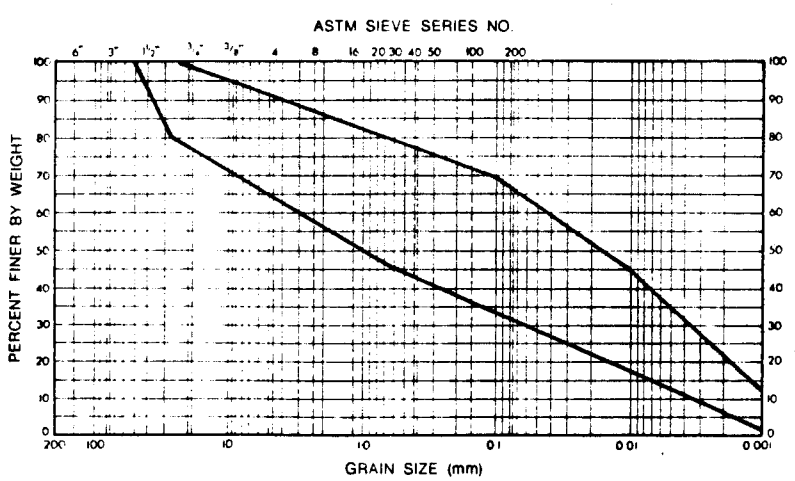

Figure 3. Grain size distribution - glacial till.

Sand Base

The prepared pile 7/12 surface was covered with a minimum 30 cm thick layer of medium to coarse sand consisting of 4% gravel particles, 90% sand, and 6% silt and clay-size particles and compacted to 95% of its modified Proctor density.

Glacial Till

The glacial till consisting of 10% to 33% gravel, 18% to 45% sand, 28% to 44% silt, and 7% to 23% clay-size particles was placed over the pile during the period September 4-14, 1991. The range of grain-size distributions obtained on several till samples is presented in figure 3. Atterberg limits of the glacial till ranged from 27% to 28% for the liquid limit and 5% to 6% for the plasticity index. The average optimum moisture content of the glacial till was 13.5% and a maximum dry density (ASTM D1557) of 1.96 mt/m^3.

The glacial till was placed in maximum 20 cm thick lifts and compacted with a 5 mt vibratory roller. A total of 94 in situ density tests were carried out on the compacted glacial till; results indicated that the degree of compaction ranged from 93% to 101% of the modified Proctor density at moisture contents ranging from 14.5% to 20.3%,

averaging 17.0%. Field hydraulic conductivity tests, performed in the till using a single-ring infiltrometer similar to the type described by Fernuik and Haug (1990), indicate hydraulic conductivity of 1.0×10^{-6} cm/s or less.

Granular Cover

A granular cover consisting of clean sand and gravel was placed over the entire pile and compacted to 95% of its modified Proctor density. Grain-size analyses indicated the granular cover to consist of 40% gravel, 58% sand, and 2% silt and clay-size particles.

Erosion Protection

A final 100-mm layer consisting of a well graded gravel was added to the covered pile to provide erosion protection.

Instrumentation/Monitoring Results

The evaluation of the effectiveness of the composite soil cover involved the performance monitoring of both the waste rock and the soil cover itself. For the covered waste rock, the temperature and oxygen concentrations within the pile were measured on a monthly basis, using the sample temperature and pore gas sampling ports and protocols used prior to placement of the cover. In addition, because the cover pile is an enclosed system, the total volume of leachate generated by the encapsulated waste rock was captured with the drains were installed beneath the pile and along the perimeter of the pile.

The performance of the composite soil cover itself was also monitored on a regular basis after placement, including measurement of soil suction, soil temperature, water content, and oxygen concentration at a number of points throughout the pile. Heat-dissipation sensors and electrical-resistance sensors (gypsum blocks) were used to measure soil suction, time-domain reflectometry (TDR) was used to measure water content, and thermocouple sensors were used to measure temperature. In addition, two large-size lysimeters located directly below the cover have been used to evaluate the hydraulic properties of the cover by collecting water that percolated through the cover.

Oxygen and Temperature Monitoring

The measurement of oxygen concentrations throughout pile 7/12 has been ongoing since 1988. Figure 4 presents the results of this monitoring for one of the six pore-gas-monitoring locations.

The results of oxygen measurement presented indicate the following:

1) Prior to placement of the cover, oxygen concentrations that station 3 ranged from 7.3% to 20.8%. The overall range of concentration in the other monitoring stations was 3.2% to 20.8%.

2) The oxygen levels, particularly near the surface of the pile, are influenced by the weather, decreasing in the winter.

3) In summer, as temperatures in the pile increase, thermal convection of oxygen into the pile causes oxygen levels to increase.

4) After cover placement in September 1991, there was a dramatic decrease in oxygen concentrations throughout the pile. At station 3 oxygen concentrations ranged from 8.2% to 14.5% immediately prior to cover placement. In October 1993, oxygen concentration at station 3 ranged from 0.2% to 0.7%.

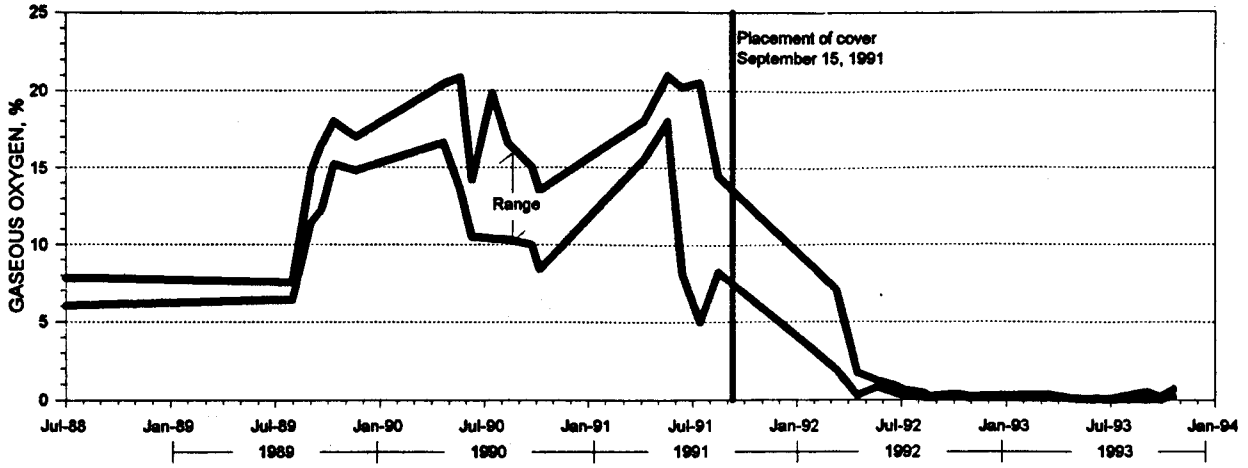

Figure 4. Gaseous oxygen versus time, pile 7/12, station 3.

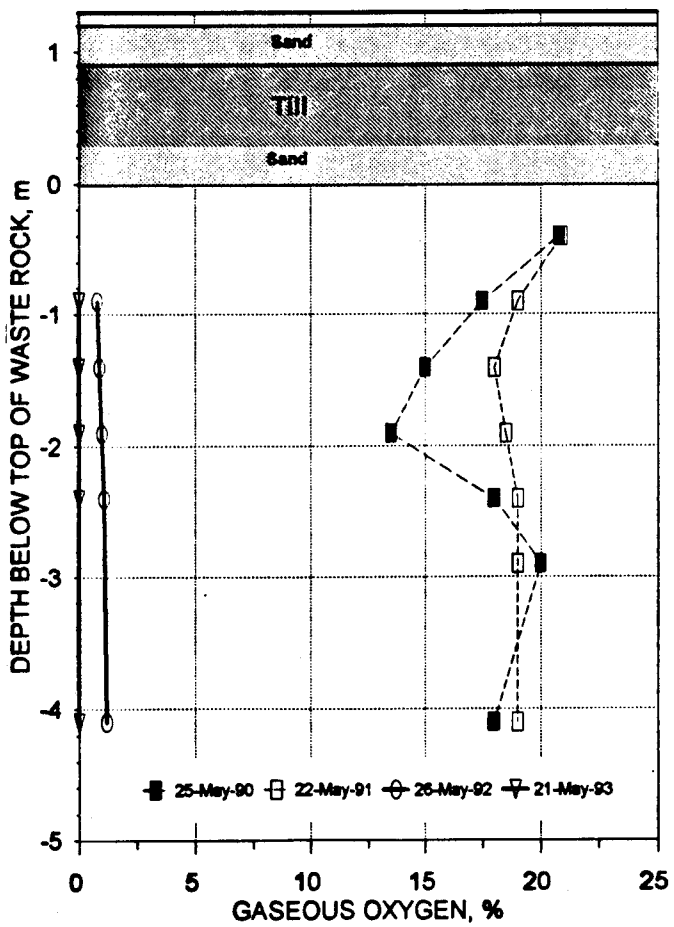

Figure 5. Gaseous oxygen profile pile 7/12, station 3. Cover placed Sept. 15, 1991.

The magnitude of the change in oxygen concentration is more clearly illustrated in figure 5, where the oxygen profiles are plotted for May 1990 and 1991 (prior to cover placement) and May 1992 and 1993 (after cover placement). It is apparent from figure 6 that the most significant decrease in oxygen occurred within several months after cover placement. However, monitoring results indicate oxygen within the system is still being depleted. The oxygen concentration dropped from 18.0% to 20.9% in May 1991 to 0.8% to 1.1% in May 1992 and 0.1% to 0.2% in May 1993.

The presented temperature monitoring results (figure 6) indicate the following:

1) In 1989 very high temperatures (50°C) were noted, which are indicative of the very rapid establishment of the endothermic oxidation process.

2) By 1990, temperatures decreased to under 40°C, indicating a stabilization of the reaction process.

3) There is a direct correlation between temperatures and weather conditions.

4) Temperatures at station 3 prior to placement of the cover ranged from 17.1°C to 24.0°C. One month after cover placement, temperatures dropped to 14.1°C to 18.3°C.

The magnitude of the temperature change prior to or after cover placement is more clearly illustrated in figure 7, which shows temperature profiles measured in May 1990 and 1991 before cover placement and May 1992 and 1993 after cover placement.

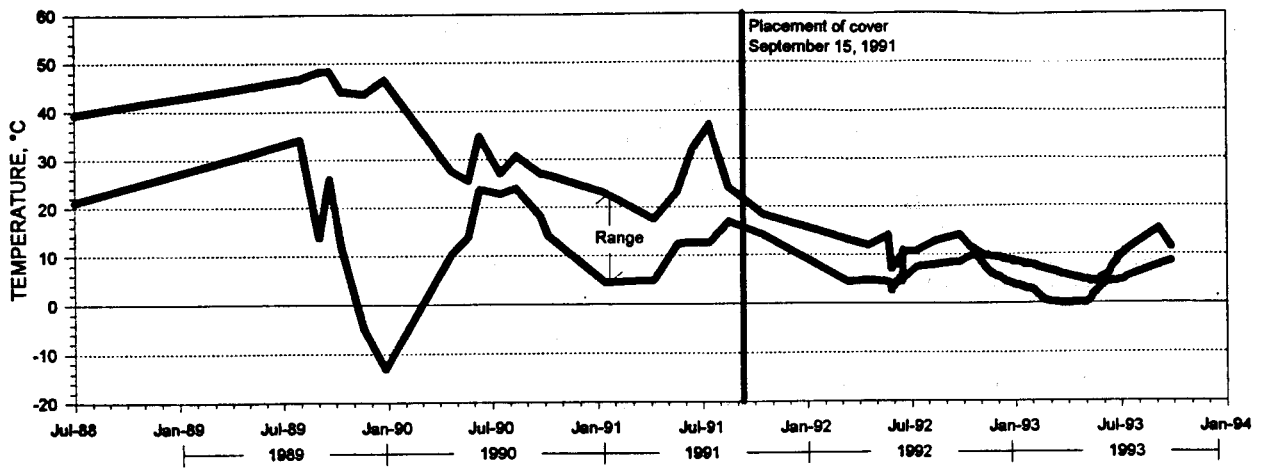

Figure 6. Temperature versus time, pile 7/12, station 3.

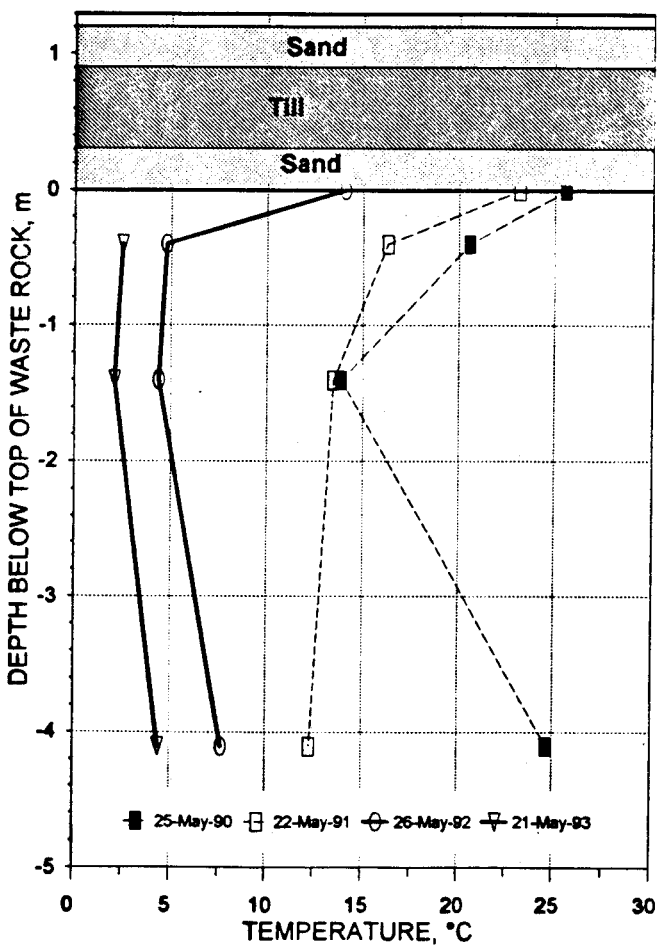

Figure 7. Temperature profile, pile 7/12, station 3. Cover placed Sept. 15, 1991

As with oxygen concentration, the most significant decrease occurred within several months after cover placement. However, temperatures are still decreasing throughout the pile but at a much reduced rate. For all temperature probes installed in pile 7/12 there has been a significant temperature decrease on a year to year basis since placement of the cover.

The results of analytical testing of leachate monitoring to date for pile 7/12 are presented in table 2. Since the system is closed system, the leachate collected after placement of the cover represents the total volume of leachate that has moved through the pile. In the 2 yrs since cover placement, a total of about 1,000 L has been recovered.

Performance monitoring of instrumentation to measure soil suction and moisture content in the composite soil cover has shown that the cover is performing as designed, with moisture content in the till showing little change from measurements taken immediately after cover placement. Soil suction measures show the expected evaporation rates from the surface of the cover.

The Lysimeter discharge data shown in table 3 indicate that only a small portion of the rainfall percolates through the cover.

Table 2. Water quality data for pile 7/12 leachate.

	July 1989 - Oct 1990	1992	1993
Ph	2.1 - 2.8	2.3 - 2.9	3.0 - 3.2
Acidity(CaCO3), mg/L	15,800 -73,250	15,800 - 54,450	NA
Sulfate, mg/L	12,700 - 43,440	5,140 - 71,042	9,970 - 73,854
Dissolved iron, mg/L	3,510 - 13,767	15,800 - 54,000	5,000 - 30,844

NA: Not available.

Table 3. Lysimeter measurements

	Rainfall		Lysimeters	
Date	Depth, mm	Volume, litre	Volume, litre	Ratio, %
June 24 - August 18, 1992	198	2455.2	50.3	2.0%
May 21 - July 13, 1993	188	2331.2	20.0	0.9%

Note : Total areal surface of lysimeters = 12.4 m^2

Discussion

The effectiveness of the composite soil cover based on the results of data collected to date is summarized below:

• Results indicate a reduction in gaseous oxygen concentrations in the pile from 20%+ before cover to less than 1% 2 yrs after cover placement. The decreased oxygen penetration implies reduced oxygen flux and acid production.

• Temperatures in the pile have decreased following cover installation but appear to be more influenced by climatic variability than by a decrease in heat production and hence sulfide mineral oxidation.

• Observed discharge from two lysimeters installed below the cover indicates infiltration of 2% of precipitation during a 55 day period when rainfall was heavy. In 1993, the infiltration was less than 1% of precipitation during a 53 day period.

• The quality of leachate shows signs of improvements with a definite trend toward increasing Ph, indicative that it has become less acidic since cover installation.

• There has been no noticeable change in the moisture content of the glacial till since cover placement.

Although pile 7/12 has a maximum height of only 5 m, precover temperature and gaseous oxygen data indicated behaviour similar to that of large waste rock dumps (of 20 m or more in height) such as those found at the Rum Jungle site in Australia (Harries and Ritchie 1981, 1985). Prior to cover placement, oxygen concentrations within the pile were high enough (20%) to allow oxidation to occur. Elevated temperatures tended to occur at locations where low oxygen concentrations were observed, confirming the exothermic nature of the oxidation process. In addition, thermal convection was found to be an important mechanism for oxygen transport into the pile through the base. The placement of the cover has resulted in a depletion of oxygen within pile 7/12 to less than 1%, thus stifling the oxidation process. Lower temperatures in the pile confirm this. Thus, while pile 7/12 is small compared with other

waste rock piles in the world, the results of this study show potential for developing effcive treatment for larger waste rock piles.

Acknowledgments

The project is being conducted as part of Canada's Mine Environment Neutral Drainage (MEND) program. Funding is provided by Noranda Minerals Inc., New Brunswick Department of Natural Resources, and Canada Centre for Mineral and Energy Technology (CANMET).

References

Bell, A.V. 1988. Acid waste rock management at Canada Base Metal Mines Proceedings International Conference on Control of Environmental Problems from Base Metal Mines, Norway.

Bennett, J.W.; J.R. Harries; and A.I.M. Ritchie, 1988. Rehabilitation of waste rock dumps at the Rum Jungle mine site. p. 104-108. Proceedings of Mine Drainage and Surface Mine Reclamation.

Ferniuk, N., and M.D. Haug, 1990. Evaluation of in situ permeability testing methods. ASCE Geotech Eng. 116(2):297-311.

Harries, J.R. and A.I.M. Ritchie, 1981. The use of temperature profiles to estimate the pyritic iron oxidation rate in a waste rock dump from an open cut mine. Water, Air and Soil Pollution 16:405-423.

Harries, J.R. and A.I.M. Ritchie, 1985. Pore gas composition in waste rock dumps undergoing pyritic oxidation. Soil Sci. 140:143-152.

Harries, J.R. and A.I.M. Ritchie, 1987. The effect of rehabilitation on the rate of oxidation of pyrite in a mine waste rock dump. Environ Geochem and Health 9(2):27-36.

Nolan, Davis & Associates. 1987. study of acid waste rock management at Canadian base metal mines. Report to Energy, Mines and Resources Canada (CANMET), Ottawa.

Nolan, Davis & Associates. 1990. Heath Steele waste rock study, phase II report. Report to Brunswick Mines and Smelting Corporation Limited.

CONTROLLING ACID MINE DRAINAGE USING AN ORGANIC COVER[1]: THE CASE OF THE EAST SULLIVAN MINE, ABITIBI, QUÉBEC

Robert L. Tremblay

Abstract: The East Sullivan site holds 15 million tonnes of tailings which generate significant acid mine drainage. The tailings pond covers a surface area of 150 hectares, and spillage extends over an additional 70 ha. The interstitial water at the centre of the pond is characterized as follows : ph= 2.3; Cu= 261 ppm; Zn= 23 ppm; SO_4= 13 500 ppm; and Fe= 3200 ppm. In order to stop acid drainage from being generated, plans have been made to cover the entire tailings pond with an organic blanket comprised of two metres of softwood and hardwood bark. This type of covering has proven effective in preventing oxygen from reaching the tailings. In fact, oxygen concentrations drop from 16.1 % near the surface to less than 1.5 % some 70 cm below it, while the CO_2 concentrations at the same depth rise from 8.2 % to 50.8 %. A grass cover is planted on top of the bark to reduce water seepage. Sludge from a municipal waters treatment plant is incorporated into the first 30 centimetres of the organic material as a conditioner and then seeded. A containment dike will be built around the entire site (6 km) to divert fresh water and carry drainage from the pond to a water treatment system. Studies have shown that some organic contamination results from bark decomposition. Phenol and tannin concentrations of 5.7 ppm and 95 ppm respectively have been measured to date. Tests are under way to determine the best passive treatment system for controlling both organic and mineral contamination caused by the tailings. A multimedia filter was installed a year ago and work will begin this year on experimental wetlands. The ultimate objective of the East-Sullivan mine site reclamation plan is to abandon the site as quickly as possible in an environnemtally benign manner. So far, 30 % of the mine site is under organic cover and the remaining 70 % should be covered within five years at most. The containment dike will be completed within the next three years, and the water treatment system should be operational the following year.

Additional Key Words: Reclamation, tailings, dry barrier, wood waste.

Introduction

Between 1946 and 1966, the East Sullivan mine, which lies 500 kilometers north of Montreal, produced 15 million tonnes of ore. From this ore 141,000 tonnes of copper, 73,000 tonnes of zinc, 3.9 tonnes of gold, 119 tonnes of silver were extract, and, between 1950 and 1956, 172,355 tonnes of pyrite were produced (Lavergne, 1985). Other sulfide minerals in the ore included chalcopyrite, sphalerite, galena, arsenopyrite, pyrrhotite, and marcasite; these were found in lenticular masses in the altered volcanic rock.

In 1980, after some clean-up work, the site was returned to the Provincial government. Since 1984, the tailings pond has been used for the dumping of wood wastes (bark), and, since 1985, sludge from septic tanks and from the Val-d'Or sewage treatment plant. In 1990, the serious management of these materials was undertaken within the framework of an overall trial reclamation plan financed, since 1992, through the Canada-Québec subsidiary agreement on mineral development.

---

[1] Paper presented at the International Land Reclamation and Mine Drainage Conference and the Third International Conference on the Abatement of Acidic Drainage, Pittsburgh, PA, April 24-29, 1994.

[2] Robert L. Tremblay, Engineer, Ministère des Ressources naturelles du Québec, Québec, Canada.

Description of the site

The site of the East Sullivan mine (fig. 1) covers an area of 228 hectares (ha) of which 205 ha are buried under mine waste (tailings and spillage). A waste-rock dump of 5 ha contains nearly 200,000 cubic meters of oxidized material. The area of mine buildings, of which only the concrete shaft head-frame survives, occupies 18 ha. The mill-tailings pond is a vast plateau whose rim rises about 5 m above a peat bog. The original dikes were built with tailings and extended according to the needs of the moment. The thickness of the tailings varies between 2 and 11.5 m.

The spillage, found especially on the south side, dates from the start of operations, when a pond was filled with tailings upon which the dike was later constructed. A break in this dike in 1980 contributed to an increase in the quantity of material spread beyond the tailings pond. This material covers an area of about 68 ha, but its thickness rarely exceeds 50 cm at a distance of 50 m from the original dikes. In the northeastern part of the site, one can observe the formation of dunes and ripples that bear witness to the importance of aeolian erosion. Clouds of dust reaching hundreds of meters in height are visible above the site on dry and windy days in the summer. The wind also sweeps the area in winter, so that very little snow rests on the tailings.

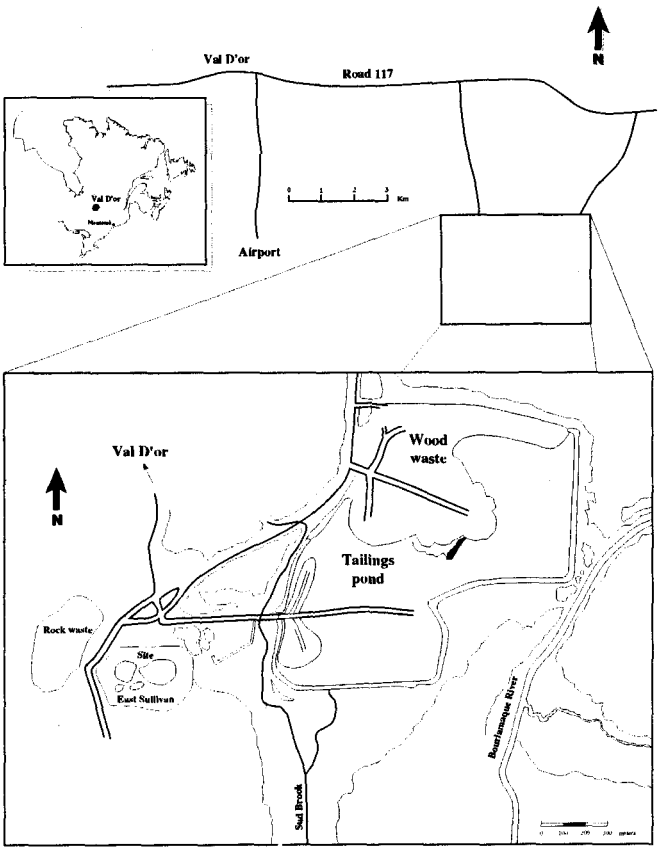

Figure 1. East Sullivan mine site.

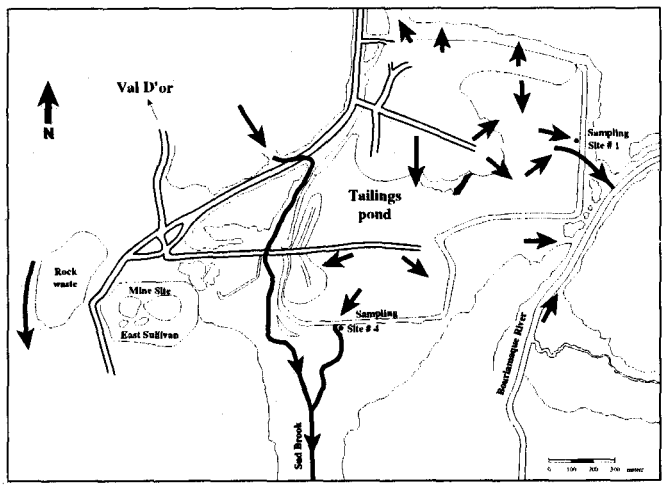

Figure 2. Drainage of the East Sullivan mine site.

The drainage of the site is mainly accomplished by Sud Brook, which runs along the west dike and crosses the zone of unconfined waste before joining the Bourlamaque River. Drainage on the north is by a small north-flowing brook, and a few gullies drain the east side of the area into the Bourlamaque River (fig. 2).

The granulometry of the tailings varies from fine at the centre of the area (50% silt and clay) to coarse-sand size near the edges, close to the dikes. At the surface, the material has a rusty color characteristic of the effects of oxidation. This color is found to depths of 30 to 40 cm in the fine material and to more than a meter in the coarser waste.

In 1990, the pH of the material was between 2.9 and 3.5 and the impact of the site upon the environment was considerable, based on the quality of runoff waters (Paquet 1991) (fig. 3). During a program of surface water sampling carried out regularly in April and May, 1990, the maximal values obtained for zinc were 540 times the acceptable limits defined by Directive 019 of the *ministère de l'Environnement* (270 mg/L vs 0,5 mg/L). Similar comparison can be made for iron (367 times : 1,100 mg/L vs 3

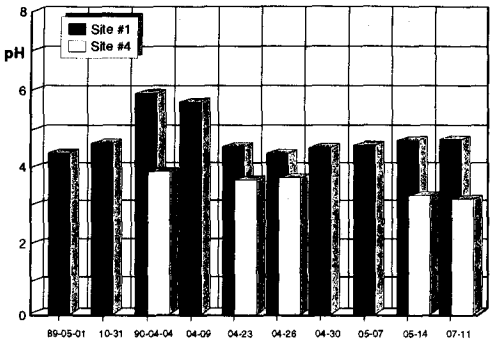

Figure 3. Variation of pH at the East Sullivan site.

mg/L), for material in suspension (292 times : 7,290 mg/L vs 25 mg/L) and for copper (97 times : 29 mg/L vs 0,3 mg/L). These results pointed up the urgency of proceeding with reclamation of the site in order to eliminate contamination of the Bourlamaque River. The interstital water at the center of the pond contained 261 mg/L of Cu, 23 mg/L of Zn, 13 500 mg/L of SO_4 and 3200 mg/L of Fe.

Reclamation plan

In February 1992, the *ministère des Ressources naturelles du Québec (MRNQ)*, in response to the results of numerous studies, prepared an overall program of reclamation trials for the East Sullivan mining site. The program had three principal phases : the construction of a watertight dike for the containment of the pond tailings and the spillage; the covering of the pond with ligneous waste, and the enrichment of the surface to permit the planting of a vegetal cover; and the establishment of a water-treatment system at the final outflow (fig. 4).

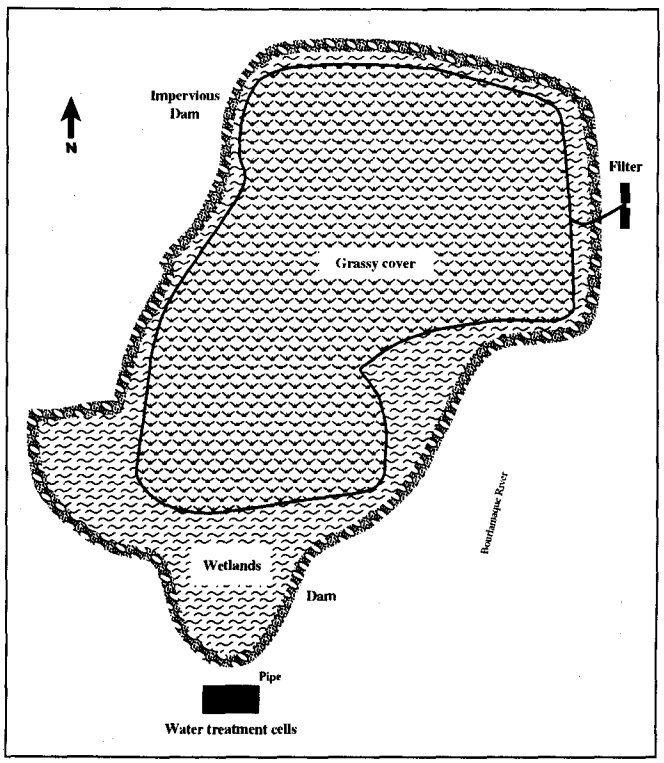

Figure 4. Draft of reclamation concept of East Sullivan tailings pond.

Construction of a watertight containment dike

In order to capture the runoff waters from the pond as well as the percolation waters that seep out at the base of the original dikes, the construction of a watertight dike to confine the tailings has been underway since 1992. With a total length of 6 km and an average height of 2 m, this dike will also confine all the waste that has flowed beyond the pond over the years. It contains a geosynthetic liner of bentonite, anchored in the underlying clay, which is found on the average a meter below the surface of the peat bog (fig. 5).

The dike will serve to divert clean waters from the site, and to channel the contaminated waters within the site towards a single point for treatment. The diffuse contamination of the Bourlamaque River by percolation waters from the pond will thus be significantly reduced.

A special arrangement will permit the containment, within the reservoir thus created, of all the water accumulating within the site over the period of a year. Thus, even though water treatment will be possible for only a few months each year, the dike will retain snow meltwaters as well as rainwater. A plantation within the reservoir will promote evapotranspiration and diminish the quantity of water to be treated.

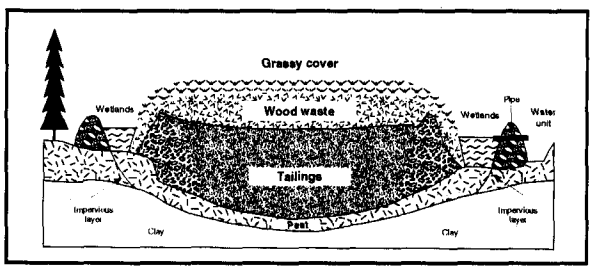

Figure 5. Section of reclamation concept of East Sullivan tailings pond.

Organic cover

The covering of the mine tailings with ligneous waste,

begun in 1984, will be continued through with more careful control of the material used. In 1989, the cover was approaching a thickness of 8 m in places, and fires were starting frequently in the waste material wich was composed of bark, fiber-board, pulp-wood, and sanding dust.

By 1990, the thickness of ligneous waste had been reduced to 2 m and the material was composed only of bark (85%), pulp-wood (10%), and sawdust and sanding dust (5%). In origin, the waste is about equally divided between coniferous species (mainly spruce) and leaf-bearing species (mainly aspen).

The ligneous waste is now being covered by sludge from a sewage treatment plant, which is being incorporated into the top 30 cm of bark, and seeded with grasses. The main purpose of this vegetal cover is to diminish the quantity of runoff, by promoting evapo- transpiration, but of course it also greatly improves the aesthetic quality of the site, and renders it useful to wildlife. Infiltration ponds for septic tank sludge have also been created on the site, in order to increase the quantity of material available for enriching the surface.

Water treatment

A water treatment system will be installed at the south end of the containment dike. Since the objective of the trial reclamation program is the earliest possible permanent abandonment of the site, only a passive system is envisaged. By «passive system», we mean a system needing little maintenance and capable of eventually purifying the water without human intervention. The design of these systems is still experimental, and since each site has its own characteristics, it will be necessary to verify the feasability of such a system at the East Sullivan site. A research project for the development of a passive system for the treatment of mine wastewaters has been completed. The project includes the preparation of plans and specifications for a pilot project integrating the chosen technology.

A multimedia filter was installed in 1992, but, after a month of satisfactory service, exfiltration problems began to compromise the effectiveness of the system. The filter will be relocated and used to treat water coming from the northern part of the tailings pond.

Effectiveness of the organic barrier

The covering of the tailings by an airtight blanket aims essentially at preventing the oxydation of sulfides by restricting the entry of oxygen. The use of bark and sawmill waste is an attractive alternative to the usual dry covers. The material is relatively abundant in many areas where the exploitation of both forest and mining resources is a major activity. The ligneous wastes can form an effective barrier while conserving a high level of humidity and consuming some of the available oxygen.

In 1991, a series of piezometers and thermocouples was installed on a limited portion of the ligneous waste to evaluate the effectiveness of the organic barrier in isolating the mine waste from the ambient air. The following graphs (figures 6 and 7) show the evolution of the pore waters since the beginning of the covering process. They are based on sampling by several workers, and illustrate a rise in pH that seems to be directly related to the organic cover. Thus, for the north part of the tailings pond, which is now about 50% covered by organic material, one notes relatively constant values of pH, around 4.5 for the month of May, whereas the values for the month of October increased from 4.5 in 1988

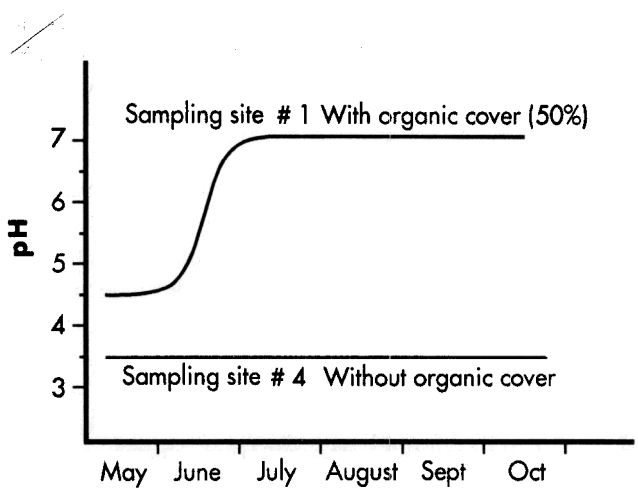

Figure 6. Monthly evolution of pH at the East Sullivan site during 1992.

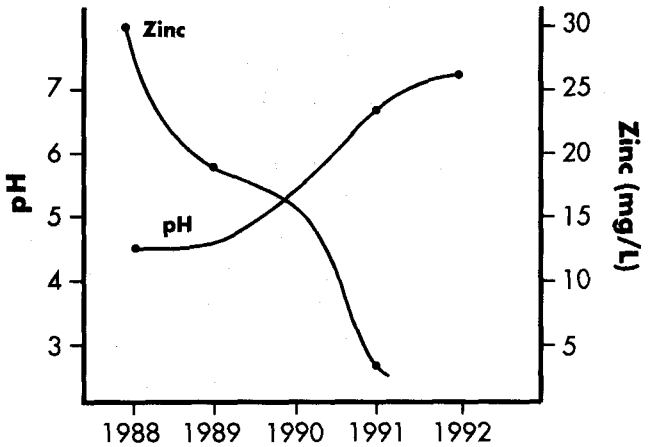

Figure 7. Annual pH and Zinc variations at East Sullivan sampling site #1 (october).

to 7.0 in 1992. In 1992, in fact, the pH was already at 7.1 in July.

In the southern part of the tailings pond, where no organic material was spread before 1992, the pH has remained stable, between 3.1 and 3.7, over the last three years. The metal content of the effluents has shown a similar pattern (fig. 7).

On-site plot instrumentation

In 1991, the MRNQ undertook an evaluation of the effectiveness of the cover at the East Sullivan tailings pond, within a plot some tens of meters from the southern limit of the ligneous waste (*Tassé et al.* 1993). The sampling in the ligneous waste was carried out in August and in October, using aluminum tubes. The content of free water in the samples was measured after extraction by centrifuge, and the total porosity obtained by calculating the volume of the interstices.

The contained gas was sampled by syringe and analyzed the same day. The gases detected were oxygen, methane, carbon dioxide, and nitrogen. The temperature of the waste was measured by four thermocouples installed at 40, 80, 120, and 150 cm below the surface.

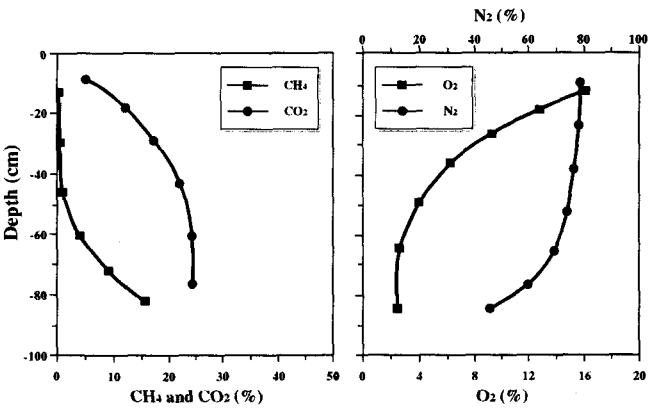

Figure 8. Proportion of gases in a 100 cm wood waste cover.

The results obtained demonstrate the effectiveness of a 100-cm-thick cover of wood chips (fig. 8). All the profiles show the same general tendency : diminution of the oxygen concentration from 16.1 % to 1.5 % an increase of carbon dioxide from 8 % up to 50 % and an increase of methane from 0 % to 15 % at a depth of 70 cm. Thus, the cover effectively blocked access of oxygen to the underlying sulfides. However, secondary reactions should be investigated in more depth before using the same technique at other sites (Germain *et al.* 1992).

Construction of supplementary plots

Following these observations, six experimental plots were constructed, in order to determine the effect of the cover on the process of acidification and on water quality. The *Centre de recherches minérales* of the *MRNQ* has coordinated the construction and supervision of the project (Paquet 1992). The plots were located in a sector of the tailings pond free from covering, in order to avoid any contamination. They were constructed as follows:

1 - **oxidized** tailings alone;
2 - **fresh** tailings alone;
3 - 1 m of conifer bark over **oxidized** tailings;
4 - 1 m of conifer bark over **fresh** tailings;
5 - 2 m of conifer bark over **oxidized** tailings;
6 - 1 m of conifer bark over **oxidized** tailings, with the addition of 30 cm of sewage plant sludge at the surface (fig. 9).

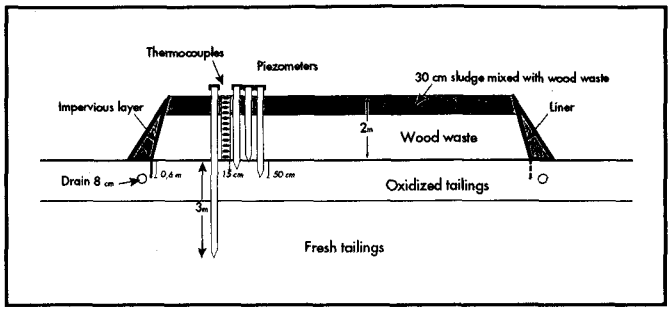

Figure 9. Scheme of #6 plot.

Each plot measures 20m X 20 m, and is separated from the next plot by 5 m. For each, a synthetic liner was installed on three sides, while a geotextile permits drainage to the south.

Plot 1 represents the present state of the site, 25 years after it was last used; plot 2 represents a site at the moment of its abandonment, at the end of mine exploitation. Plots 3 and 4 simulate an organic barrier covering an old and a recent tailings pond respectively; plots 5 and 6 represent possible variants on the technique of covering a tailings pond that is generating acid mine drainage.

Piezometers placed in each plot will permit the measurement of the physico-chemical quality of interstitial water and of ground water. They are installed so as to permit the sampling of the different levels of the plots. A program of gas monitoring is also being carried out in order to track the evolution of interstitial gasses over the next few years.

Observations and conclusions

Continuing observation of the experimental plots will permit the measurement of oxygen diffusion in the organic barrier, and its degradation in a controlled environment. If the various soluble organic compounds migrate into the mine waste, they could promote the reduction of sulfates and the fixation of metals in sulfide form, which could explain the observed decreases in dissolved metals and increased pH.

The present study will permit the measurement over the next few years of the effect of an organic cover used as a humid barrier to control acid mine drainage. The effectiveness of such a barrier would justify the extension of its use to other sites, particularly in regions like Abitibi-Témiscamingue, where both mining and forest exploitation are widely practiced. In addition the usefulness of organic wastes in reducing the impact of acid drainage from mine wastes merits consideration.

Acknowledgments

I wish to express my thanks to Claude Dufour and André Paquet of the *MRNQ*, who contributed greatly to the trial reclamation project at the East Sullivan mine site.

Literature cited

Germain, M. D., N. Tassé, and M. Bergeron. 1992. *Efficacité des copeaux de bois comme couverture pour les résidus miniers*; Government of Quebec, unpublished report on file, Ministère des Ressources naturelles, Quebec, 12 p.

Lavergne, C. 1985. *Gîtes minéraux à tonnage évalué et production minérale du Québec*; Ministère des Ressources naturelles, Québec, Rapport DV-85-08, 78 p.

Paquet, A. 1991. *Évolution physico-chimique des eaux de fonte printanière au parc à résidus miniers East-Sullivan*; Government of Quebec, unpublished report on file, Ministère des Ressources naturelles, Quebec, 37 p.

Paquet, A. 1992. *La conception d'une barrière humide à l'aide de résidus forestiers*; Government of Quebec, unpublished report on file, Ministère des Ressources naturelles, Québec, 24 p.

Tassé, N., M. D. Germain, and M. Bergeron. 1993. Composition of interstitial gases in wood chips deposited on reactive mine tailings: consequences for their use as an oxygen barrier; American Chemical Society, Symposium Series: *The Environmental Geochemistry of Sulfide Oxydation* (in press).

COLUMN TESTS INVESTIGATION OF MILLING WASTES PROPERTIES USED TO BUILD COVER SYSTEMS[1]

Mostafa Aachib, Michel Aubertin, and Robert P. Chapuis[2]

Abstract: Among the alternatives that can be used to control the production of acid mine drainage generated by reactive tailings (milling wastes), the use of so-called dry covers appears to be one of the most practical. The purpose of such covers is to limit the flow of water and/or oxygen to the tailings, so that reactions leading to acid generation can be stopped. Various types of materials have been considered to build such covers, including geomembranes and fine-grained soils. Because these materials are not always economically available, the authors have proposed the use of fine tailings that do not contain sulfide as a capillary material in a multilayer cover system. To investigate the potential efficiency of milling wastes, a research project is presently underway. It includes different types of tests on homogenized tailings to determine some of their hydrogeological properties, such as hydraulic conductivity, capillary curves, and effective diffusion coefficient. In this paper, the authors briefly review the basic principles behind the design of multilayer cover systems to control acid production. Then some of the main components of an ongoing laboratory investigation are presented. The emphasis is placed upon column tests procedures used to evaluate various cover configurations. Some analytical and numerical solutions to specific problems related to cover design are finally given.

Introduction

Canada is one of the largest mineral producers in the world. This activity provides an important input to the country's economy, but it is also a source of concern regarding environmental protection. Among the various potential problems linked to the mining industry, it is usually acknowledged that acid mine drainage (AMD), resulting from the oxidation of sulfide minerals, represents the most serious threat to the ecological balance of natural habitats. In Canada, over 12,000 ha of tailings (milling wastes) and about 350 million mt of waste mine rock have been identified as acid-generating material, resulting mainly from the last four or five decades of base metal mining (Itzkovitch and Feasby 1993). A preliminary estimate of the reclaiming cost amounts to more than Can$ 5 billion, considering the presently available technology.

When one considers the various alternatives for stabilizing reactive wastes and reclaiming the land, the installation of covers (or caps) appears to be one of the most practical solutions, albeit often very expensive. The goal of such covers is to limit the flow of water and/or oxygen to the sulfidic wastes, which are the essential elements for the production of AMD. Various types of materials can be used to build such covers. Water cover to submerge tailings is certainly one of the most promising ways to control the production of AMD, as oxygen diffusion is considerably reduced (e.g., SRK 1989). The construction of an artificial water basin over an existing tailings pond can cause some difficulties, however, because of topography limitations, possible long-term stability problems, and of uncertainties regarding the actual effectiveness of water covers to stop an ongoing reaction of acid production and metal solubilization (e.g., Ritcey 1991).

Different types of processed materials can also be used in covers, such as geomembranes, bitumen, cement, etc., but it now appears that one of the most appealing techniques relies on the use of natural soils and other particulate media. In this case, it is generally considered that the main objective of the cover design is to ensure

---

[1]Paper presented at the International Land Reclamation and Mine Drainage Conference and the Third International Conference on the Abatement of Acidic Drainage, Pittsburgh, PA, April 24-29, 1994.

[2]Mostafa Aachib, PhD Student, Michel Aubertin, Professor, Robert P. Chapuis, Professor, Mineral Engineering Department, École Polytechnique, Montréal, Qc, Canada.

that it will be an efficient barrier to oxygen transport. To do so, it is essential that at least part of the cover remains close to saturation. This can be accomplished by using a capillary barrier system (e.g., Nicholson et al. 1989, Collin and Rasmuson 1990, Aubertin and Chapuis 1991a).

Traditionally, fine-grained soils have been used to build the capillary layer in a complex cover made of different superimposed materials. Recently, it has been suggested that tailings themselves, that ideally would not produce AMD, could be used for that purpose (Aubertin and Chapuis 1990, 1991a). There are various advantages in using tailings which are often located close to (if not on) the site. For instance, existing mills could treat sulfide-free ores in order to produce part of the cover system for an existing tailings pond generating AMD.

In this paper, the authors present the core of an ongoing research project aimed at investigating the behavior of tailings used as a capillary barrier in a multilayer cover system. The general approach of the project is described. It makes use of various laboratory experiments that provide the main hydrogeological properties of the material, such as hydraulic conductivity, capillary characteristic curves, and effective diffusion coefficients for oxygen, together with physical models and numerical modeling calculations. The main elements of the research program and some preliminary findings are presented and briefly discussed. Because the basic geotechnical properties of tailings have been presented elsewhere (Aubertin and Chapuis 1991b, Aubertin et al. 1993a, Chapuis et al. 1993), they are not presented in this paper.

Capillary Barrier Concept

A capillary barrier can be generated when a porous material located above the water table maintains a water content close to saturation. This phenomenon can be advantageously controlled when a fine-grained material layer is placed between two coarser grained material layers. In this case, the middle layer will tend to maintain a high water content while the coarser materials will dry more easily.

Capillary Characteristics

To quantify the actual behavior of a layered system, one has to investigate the ψ-θ_w relationship of the different materials, where ψ represents the negative water pressure (or suction) and θ_w is the volumetric water content. This relationship is given by the capillary characteristic curve, which provides very important information for the cover design because θ_w largely influences the hydraulic conductivity K and the effective diffusion coefficient for oxygen D_e. Various methods have been used to measure the capillary characteristic curves of particulate media (e.g., Kovács 1981, Fredlund and Rahardjo 1993), and ensuing curves obtained from these tests have been described by different models (e.g., Bear 1972, Arya and Paris 1981).

On figure 1, one can see schematical ψ-θ_w relationships for a sand and a silt. When the elevation above the water table (or equivalent negative pressure) is below ψ_a (often called "Air Entry value - AEV"), the material remains close to saturation; in this case, the capillary forces acting in the largest pores are sufficient to resist the effect of the potential energy. As elevation is increased above ψ_a, the suction pressure increases (in absolute value), and water content decreases gradually as smaller pores are progressively drained until the residual water content θ_r is reached at an elevation corresponding to ψ_r (Kovács 1981).

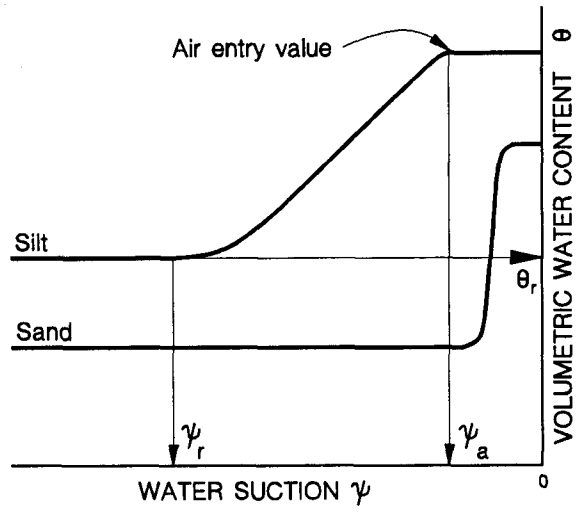

Figure 1. Typical moisture characteristic curves.

The AEV (or ψ_a) value is a very important parameter for capillary barriers because it indicates the height above the water table associated with nearly full saturation for a porous medium. It has been found experimentally that this value is about 10 to 50 cm for sands, between 100 to 300 cm for most silts, and above 5 to 10 m for clays (e.g., Lambe and Whitman 1979, Todd 1980).

The value of the main parameters of the suction curve (ψ-θ_w), that is, ψ_a, ψ_r, and θ_r, appears to be controlled by some of the basic properties of the material, such as grain size and porosity. A few relationships have been proposed to express the effect of these influence factors. A general formulation for that purpose, which would encompass most of the existing equations, could be expressed as follows:

$$\psi = f\ (D_x,\ n,\ Y\ ), \tag{1}$$

where D_x is the grain size, n is the porosity, and Y represents a complementary function (usually omitted in most formulations) introduced to take into account specific effects that could be expressed from other basic properties such as specific surface area S, viscosity of water μ, plasticity index I_p, and so on. In actual expressions proposed in the literature for ψ_a, equation 1 is generally given as a linear (Bear 1972) or nonlinear (Yanful 1991) function of the effective diameter D_{10}, while the porosity function is often expressed as (1-n)/n (e.g., Bear 1972, Kovács 1981). After investigating existing models, wide disparities have been found between the obtained results (Aubertin et al. 1993a, Aachib et al. 1993). Thus, one of the goals of this ongoing project is to develop a more appropriate expression (Ricard, in preparation).

By using the ability of different types of materials to maintain different water content as a function of height, it is possible to conceive a layered system in which a capillary layer (made of a fine-grained material that has a high ψ_a value) remains close to saturation. In a well-designed system, the thickness L of the capillary layer that could be maintained close to full saturation is given by (Nicholson et al. 1989):

$$L = |(\psi_a)_f| - |(\psi_r)_c|, \tag{2}$$

where $(\psi_r)_c$ represents the equivalent suction pressure corresponding to the residual water content of the coarse material, and $(\psi_a)_f$ is the AEV of the fine material layer placed above. As an example, using $|(\psi_r)_c| = 80$ cm for a sand (which is often about twice the value of $(\psi_a)_c$ according to Kovács 1981) and $(\psi_a)_f = 180$ cm for fine tailings, one obtains L=1 m. Interestingly, preliminary calculations on the efficiency of a layered system to decrease the oxygen flow show that there is not much gain to be made in increasing thickness L above 1 m (Nicholson et al. 1989, Aachib et al. 1993); this aspect will be discussed further later on.

The concept of a multilayer cover system placed well above the water table and in which the fine layer can maintain a high degree of saturation has been confirmed by some laboratory tests (Yanful 1991) and by numerical modeling calculations (Akindunni et al. 1991, Yanful and Aubé 1993).

Unsaturated flow

During and after a water inflow from the top, coarse material layers placed above and below the fine material layer serve to drain the cover. However, when these coarse materials themselves have been drained and their volumetric water content reaches θ_r, then they help to maintain a high θ_w value in the in-between layer because their hydraulic conductivity is considerably reduced. Thus the water will not tend to flow downward, nor will it move upward because the coarse material placed above the fine material also serves as a non-capillary barrier preventing capillary rise.

To better understand the behavior of a layered cover, one has to study different properties of the materials used in the system. As the hydraulic conditions play a key role, it is worth discussing the matter further.

The well-known Darcy's law is generally used to describe the flow of water in a porous medium under saturated conditions. However, when the degree of saturation S_r is less than 100%, one has to express the water flow equation as a function of ψ and θ_w. One popular approach in this instance is to use a modified version of Darcy's law in which the hydraulic conductivity is given as a function of the water content. Following numerous experimental investigations, different models have been proposed to describe the relationship between the unsaturated hydraulic conductivity $K(S_e)$ and θ_w (e.g., Mualem 1986). One of the most popular was proposed by Van Genuchten (1980); it can be written as follows:

$$K(S_e) = K_s \, S_e^{0.5} \left(1 - (1 - S_e^{1/\gamma})^{\gamma}\right)^2 \tag{3}$$

with

$$S_e = \frac{\theta_w - \theta_r}{\theta_s - \theta_r}, \tag{4}$$

where S_e = effective degree of saturation ($0 \leq S_e \leq 1$),
K_s = saturated hydraulic conductivity,
θ_s = volumetric water content at saturation,
and γ = constant parameter for curve adjustment.

According to this model, $K(S_e)$ becomes zero when θ_w reaches θ_r, and it tends toward K_s when θ_w approaches θ_s; such limiting values are in accordance with most experimental measurements.

Experimental Program

The behavior of tailings used in cover systems as a capillary barrier is studied using various experimental devices. Consolidation behavior is investigated with standard oedometer tests on homogenized tailings, while hydraulic conductivity is studied by performing constant-head and falling-head permeability tests in oedometric cells and in rigid-wall permeameters (Aubertin et al. 1993a). Capillary characteristic curves, on the other hand, are established by using various techniques, including the pressure plate vessel (Aubertin et al. 1993b), while the transport of oxygen in a humid porous material is presently studied with different approaches including one device used previously by Yanful (1993). All these basic experiments provide inputs into a numerical model that will be used to predict the actual behavior of a cover system.

The numerical model is calibrated and validated by performing two types of column tests (Aachib et al. 1993). The first type of column, called the drainage column (fig. 2), is used to estimate the water conditions existing in the cover. It is a plexiglass column having an internal diameter of 15.5 cm and a height of 110 cm . The column is instrumented with tensiometers and TDR (time domain reflectometry) probes to measure, respectively, suction pressure and volumetric water content along its length. The column design was adapted from Yanful (1991).

This column is used to investigate the behavior of various layered systems under different water boundary conditions. Although upward flow is sometimes considered, most experiments are performed under downward flow. Results of the drainage column tests are compared with those obtained on individual materials in capillary tests and with numerical calculations.

The other type of column test is performed in the control columns used to evaluate the performance of cover systems placed over sulfide tailings (fig. 3, B). These columns serve to evaluate the reduction in oxygen flow through the cover and toward the reactive tailings. Ten columns have been built for long-term tests, which started in October 1993 and will last until November 1994. These columns are also made from plexiglass, and eight of them have a height of 1.7 m. Two identical columns are made for each system, one being instrumented with TDR probes and thermocouples and the other one free of any instrument perturbation. The cover layers, which are placed over a layer of tailings containing about 20% iron sulfide, include a layer of sand (30 cm in thickness), a non-reactive tailings layer (50 cm in thickness), and a final layer of sand (20 cm in thickness). The sand used in the covers is a concrete sand, and the capillary barriers are made from three different tailings free of sulfide minerals. Another tailing containing a small amount of pyrite is also investigated in the last two columns. Two smaller columns have also been built with reactive tailings without any cover in order to evaluate the effect of the cover (fig. 3, A). In all the columns, water is added from the top periodically, and the percolating water reaching the bottom of the column is analyzed; electric conductivity, pH, sulfate, and metal contents are determined. These provide indication of the possible reactions happening in the system. Temperature measurements in the column also serve as indirect evidence of chemical reactions in the column.

The RETC program (Van Genuchten et al. 1991) is used to evaluate the conditions in the cover system. Numerical calculations are compared with measured performance in the control columns to validate the basic calculation approach.

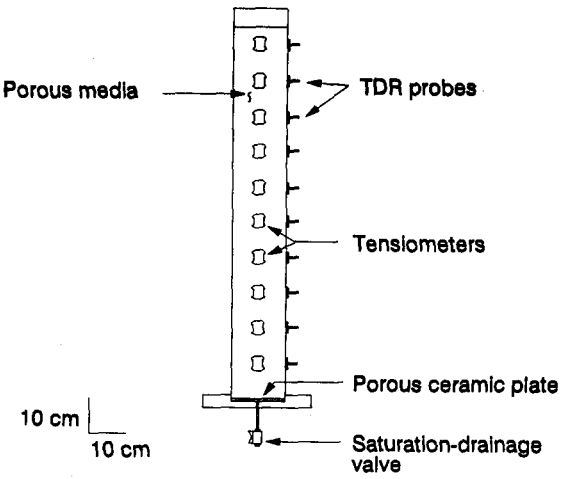

Figure 2. Schematical representation of the drainage column.

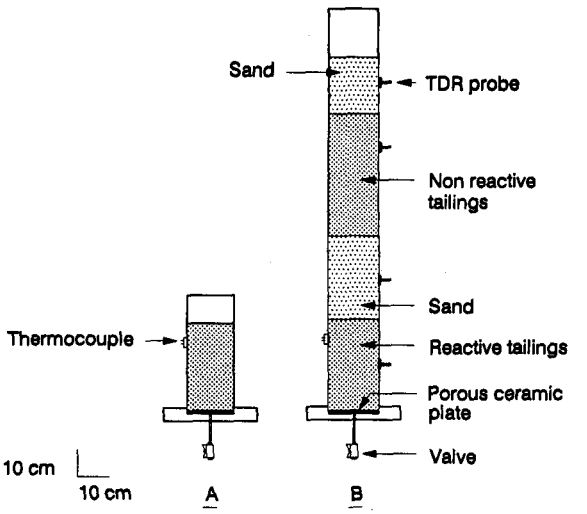

Figure 3. Schematical representation of the control columns;
A: reference column for reactive tailings without covers;
B: reactive tailings covered by a layered system.

Preliminary Calculations for Two Cover Systems

In covers made from partly saturated materials, it is often considered, at least for preliminary calculations, that oxygen transport is controlled by molecular diffusion in the gaseous or liquid phases, as temperature and pressure gradient effects are neglected (Collin 1987, Nicholson et al. 1989). Such oxygen diffusion is associated with concentration gradients between conditions found in the atmosphere and those of the porous media.

Using the presently available information, the authors have performed some simple calculations in order to compare the efficiency of two cover scenarios; more details are given in Aachib et al. (1993). The first case is that of a single layer cover having a thickness L. The starting points of the calculations are Fick's laws given by Bear (1972) and Shackelford (1991):

$$F(t) = \theta_g D_e \frac{\partial C(t)}{\partial z} \tag{5}$$

and

$$\frac{\partial C(t)}{\partial t} = \frac{\partial}{\partial z}\left(D_e \frac{\partial C(t)}{\partial z}\right) - k_r C(t) , \tag{6}$$

with

$$\theta_g = \frac{V_g}{V} , \tag{7}$$

where $F(t)$ = diffusive flux of oxygen (kg/m²/s),
D_e = effective diffusion coefficient of oxygen (m²/s),
$C(t)$ = oxygen concentration in the gaseous phase at time t (kg/m³),
z = depth (m),
t = time (s),
θ_g = volumetric gas content of the porous media, also called gas-filled porosity (m³/m³),
V_g = gas volume (m³),
V = total volume (m³),
and k_r = reaction rate constant (for sulfide oxidation).

In this equation θ_g is related to the degree of saturation S_r and porosity n :

$$\theta_g = n(1 - S_r) . \tag{8}$$

Analytical solutions to these equations have been given by Crank (1975), for $k_r = 0$ (non-reactive cover system):

$$F(t) = 2C_o\theta_g \sqrt{\frac{D_e}{\pi t}} \sum_{m=o}^{\infty} \exp\left[-\frac{(2m+1)^2 L^2}{4D_e t}\right] \tag{9}$$

and

$$C(z,t) = C_o \ \mathrm{erfc}\left(\frac{z}{2\sqrt{D_e t}}\right), \tag{10}$$

where

$$\mathrm{erfc}\ (u) = 1 - \frac{2}{\sqrt{\pi}} \int_o^u \exp(-v^2)\ dv , \tag{11}$$

and m is an integer variable. These are obtained for the following limiting conditions:

$C = 0$ for $t = 0$ and $z \geq 0$,
$C = C_0$ for $t \geq 0$ and $z \leq 0$,
and $C = 0$ for $t \geq 0$ and $z \geq L$,

where C_0 is the atmospheric oxygen concentration. These conditions imply a decreasing oxygen concentration in the cover until it is reduced to zero at the top of the reactive tailings, where the oxygen consumption is very rapid. In these equations, D_e is calculated from the modified Millington-Shearer model given by Collin (1987) and Aubertin et al. (1993a):

$$D_e = (1 - S_r)^2\ [a(1-S_r)]^{2x}\ D_o + S_r^2\ (a\ S_r)^{2y}\ H\ D_w , \tag{12}$$

where D_o = diffusion coefficient of oxygen in air (m²/s),

D_w = diffusion coefficient of oxygen in water (m^2/s),
H = solubility constant of gas in water,
and a,x,y = material parameters, expressed as function of n and S_r.

To estimate the value of D_e, results of Reardon and Moddle (1985) were used to calibrate the above model. Typical parameters values for the sand and tailings are thus obtained. Calculation results are shown in figure 4. As one can see, $D_e \approx D_w$ when $S_r \approx 90\%$. Having a D_e value for the humid porous system practically equal to that of water is very advantageous because water covers have often been considered the most efficient way to control production of AMD (e.g., SRK 1989). In the case of dry covers, however, one is somewhat less concerned with stability problems of the retaining structures.

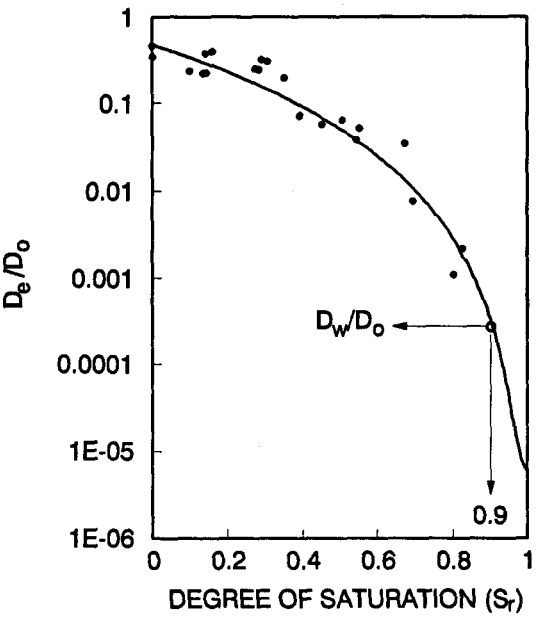

Figure 4. Effective diffusion coefficient expressed as a function of the degree of saturation (see equation 12); data taken from Reardon and Moddle (1985).

Using these equations, a first calculation is made for steady state flow in a simple layer using typical parameters for the cover material (i.e., C_o=21%, n=0.41, S_r=0.87, L=1.1 m, D_e=4.61x10^{-9} m^2/s); this calculation gives F(t)=0.036 $kg/m^2/yr$ O_2.

Using the same set of equations, one could also calculate the efficiency of the cover layer, as defined by Nicholson et al. (1989):

$$E_c = \frac{F_r}{F_c} = \frac{\sqrt{k_r (D_e)_r}}{(D_e)_c} L + 1 , \qquad (13)$$

where F_r = oxygen flux through the reactive tailings without a cover,
F_c = oxygen flux through the cover,
and $(D_e)_{r,c}$ = effective diffusion coefficient in the reactive tailings (r) and cover material (c).

Figure 5 shows some calculated E_c values as a function of L and S_r, for k_r = 300 yr^{-1}. These results compare well with those of Nicholson et al. (1989) obtained for slightly different conditions. These show that increasing the thickness of the cover above about 0.5 to 1 m does not much change its efficiency. Also, these show that a cover 1 m thick with S_r = 90% is more efficient than one of 4 m having an S_r = 80%. As expected, the degree of saturation is thus found to be a critical parameter for cover design.

For a complex cover made from different horizontal layers, one can also calculate the oxygen flux with the first Fick's law for steady-state flow, equating the flux at each interface, which gives the following equation (Yanful 1991):

$$\left(\frac{D_i}{L_i}\right) C_{i-1} + \left(\frac{D_{i+1}}{L_{i+1}} - \frac{D_i}{L_i}\right) C_i + \left(\frac{D_{i+1}}{L_{i+1}}\right) C_{i+1} = 0 , \qquad (14)$$

where index i is given for layer i. Again, assuming atmospheric oxygen concentration at the surface and a zero concentration at the top of the reactive tailings, one calculates that the same flux of oxygen is obtained for the single

layer cover with L = 1.1 m, and for a three-layer system in which the capillary barrier (n = 0.41, S_r = 90%) is only 0.5 m thick. Table 1 compares the two scenarios. This result is possible because the layered system helps to maintain a high degree of saturation in the capillary barrier, which in turn reduces the value of the effective diffusion coefficient that largely controls the oxygen flux.

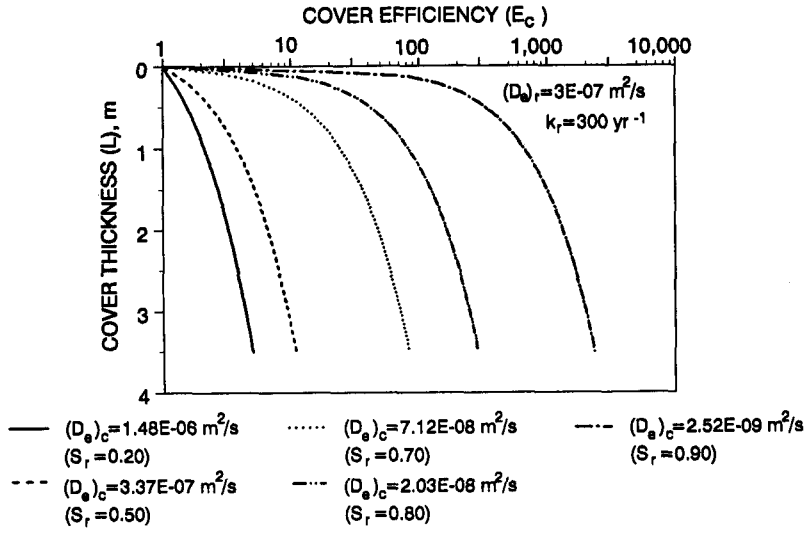

Figure 5. Relationship between the cover thickness and its efficiency to reduce the oxygen flux (after Aachib et al. 1993).

Table 1. Oxygen flux calculations for two cover systems.

Cover	Material	n	S_r	L, m	D_e, m²/s	Oxygen flux, kg/m²/yr O_2
One layer	Tailings	0.41	0.87	1.10	4.61×10^{-9}	0.036
Three layers	Sand	0.39	0.10	0.30	1.87×10^{-6}	
	Tailings	0.41	0.90	0.50	2.52×10^{-9}	0.036
	Sand	0.39	0.10	0.30	1.87×10^{-6}	

Conclusion

After briefly reviewing the basic principles behind the use of covers made from particulate media to control the production of acid mine drainage (AMD), the authors have presented the core of a laboratory research effort to investigate the properties of milling wastes used in a multilayer cover system. The emphasis is placed upon the two types of column tests used to calibrate and validate a model in which the input parameters are obtained from basic laboratory tests, such as hydraulic conductivity, capillary characteristic curves, and effective diffusion coefficients of oxygen. The description of the experimental devices is followed by some preliminary calculations on the efficiency of a layered cover system to reduce oxygen flow, based on analytical solutions of Fick's laws. Using these, it is infered that the critical parameter in the design of a cover system is the volumetric water content, which (as may be expected) should be maintained as high as possible in the capillary layer in order to reduce the flow of oxygen. A degree of saturation of 90% in a porous material produces a layer that has about the same effective diffusion coefficient as that of water. So far, this fairly broad research project has shown that tailings present some very interesting properties as a constitutive material in a multilayered system, considering their relatively low hydraulic conductivity, high water retention characteristics and capacity to reduce the flow of oxygen.

Acknowledgements

The main financial support for this research project has been provided so far by the MEND program, through the NEDEM-Quebec branch managed by the Centre de recherches minérales.

References

Aachib, M., M. Aubertin, and R.P. Chapuis. 1993. Étude en laboratoire de la performance des barrières de recouvrement constituées de rejets miniers pour limiter le DMA - un état de la question. Report EPM/RT-93/32, École Polytechnique de Montréal, 180 p.

Akindunni, F.F., R.W. Gillham, and R.V. Nicholson. 1991. Numerical simulations to investigate moisture-retention characteristics in the design of oxygen-limiting covers for reactive mine tailings. Can. Geotech. J. 28:446-451.

Arya, L.M. and J.F. Paris. 1981. A physicoempirical model to predict the soil moisture characteristics from particle-size distribution and bulk density data. Soil Sci. Soc. America J. 45:1023-1030.

Aubertin, M. and R.P. Chapuis. 1990. Projet de recherche, Parc à résidus miniers Manitou-Barvue, Devis Technique, Report submitted to Centre de recherches minérales, Project C.D.T. P1537, École Polytechnique de Montréal (Sept. 1990), 30 p.

Aubertin, M. and R.P. Chapuis. 1991a. Considérations hydro-géotechniques pour l'entreposage des résidus miniers dans le nord-ouest du Québec. p. 1-22. In Proceedings of the Second International Conference on the Abatement of Acidic Drainage. (Montréal, PQ, September 16-18, 1991).

Aubertin, M. and R.P. Chapuis. 1991b. Critères de conception pour les ouvrages de retenue des résidus miniers dans la région de l'Abitibi. p. 113-127. In Proceedings of the First Canadian Conference on Environmental Geotechnics (Montréal, PQ, May 14-16, 1991).

Aubertin, M., R.P. Chapuis, B. Bussière, and M. Aachib. 1993a. Propriétés des résidus miniers utilisés comme matériau de recouvrement pour limiter le DMA. p. 299-308. In Arnould, M., M. Barrès, and B. Côme (eds), Balkema, Rotterdam, Géoconfine 93.

Aubertin, M., R.P. Chapuis, B. Bussière, M. Aachib, J.F. Ricard, and L. Trembley. 1993b. Propriétés des rejets de concentrateur utilisés pour la construction de barrières de recouvrement multicouches. p. 155-175. Colloque sur le programme de neutralisation des eaux de drainage dans l'environnement minier, NEDEM 93, Val d'Or.

Bear, J. 1972. Dynamics of fluids in porous media. Dover Publications, Inc. New York, 764 p.

Chapuis, R.P., M. L'Ecuyer, and M. Aubertin. 1993. Field permeability tests in mine tailings. p. 51-59. In Proceedings of the 46th Canadian Geotechnical Conference, Saskatoon.

Collin, M. 1987. Mathematical modelling of water and oxygen transportation in layered soil covers for deposits of pyritic mine tailings. Ph. D. Thesis, Royal Institute of Technology, Sweden.

Collin, M. and A. Rasmuson. 1990. Mathematical modelling of water and oxygen transport in layered Soil covers for deposits of pyritic mine tailings. p. 311-333. In Acid mine drainage: designing for closure. GAC-MAC Annual Meeting.

Crank, J. 1975. The mathematics of diffusion. 2d ed. Clarendon Press, Oxford, UK.

Fredlund, D.G. and H. Rahardjo. 1993. Soil mechanics for unsaturated soils. Wiley, New York, 517 p.

Itzkovitch, I.J. and D.G. Feasby. 1993. Le programme de neutralisation des eaux de drainage dans l'environnement minier. p. 1-16. Colloque sur le programme de neutralisation des eaux de drainage dans l'environnement minier, Val d'Or, NEDEM 93.

Kovács, G. 1981. Seepage hydraulics. Elsevier Scientific Pub. Cie, Amsterdam, 730 p.

Lambe, T.W. and R.V. Whitman. 1979. Soil mechanics, SI version, Wiley, New York, 553 p.

Mualem, Y. 1986. Hydraulic conductivity of unsaturated soils: Prediction and formulas. p. 799-823. In A. Klute (ed.), methods of soil analysis. Part 1. Physical and mineralogical methods. Agron. Monogr. 9 (2d ed.). Am. Soc. Agronomy, Madison, WI.

Nicholson, R.V., R.W. Gillham, J.A. Cherry, and E.J. Reardon. 1989. Reduction of acid generation in mine tailings through the use of moisture-retaining cover layers as oxygen barriers. Can. Geotech. J. 26(1):1-8.

Reardon, E.J. and P.M. Moddle. 1985. Gas diffusion coefficient measurements on uranium mill tailings: implications to cover layer design. Uranium 2:111-131.

Ritcey, G.M. 1991. Deep water disposal of pyritic tailings - a simulation for acid Prediction. p. 421-442. In Proceedings of the Second International Conference on the Abatement of Acidic Drainage. (Montréal, PQ, September 16-18, 1991).

Shackelford, C.D. 1991. Laboratory diffusion testing for waste disposal. A review. J. Contam. Hydrol. 7:177-217.

SRK (Steffen, Robertson & Kirsten). 1989. Draft acid rock drainage guide. BC AMD Task Force, V. 1.

Todd, D.K. 1980. Groundwater hydrology. 2d edition, Wiley, New York, 535 p.

Van Genuchten, M. T. 1980. A closed-form equation for predicting the hydraulic conductivity of unsaturated soils. Soil Sci. Soc. America. J. 44:892-898.

Van Genuchten, M. T., F.J. Leij, and S.R. Yates. 1991. The RETC code for quantifying the hydraulic functions of unsaturated soils. EPA/600/2-91/065, 85 p.

Yanful, E.K. 1991. Development of laboratory methodologies for evaluating the effectiveness of reactive tailings covers. Final Report (Draft), Centre de Technologie Noranda (Québec), 81 p.

Yanful, E.K. 1993. Oxygen diffusion through soil covers on sulphidic mine tailings. J. Geotech. Eng., ASCE 119(8):1207-1228.

Yanful, E.K. and B. Aubé. 1993. Modelling moisture-retaining soil covers. p. 273-280. In Proceedings of the Joint CSCE-ASCE National Conference on Environmental Engineering (Montréal, PQ, July 12-14, 1993).

FIELD AND LABORATORY PERFORMANCE OF ENGINEERED COVERS ON THE WAITE AMULET TAILINGS[1]

Ernest K. Yanful,[2] Bernard C. Aubé,[3]
Mark Woyshner,[4] Luc C. St-Arnaud[3]

Abstract: The Waite Amulet Covers Project was initiated in 1990 under the MEND (Mine Environment Neutral Drainage) program to evaluate the effectiveness of engineered soil covers in reducing acid generation in reactive tailings. Two three-layer soil covers (60 cm compacted clay placed between two 30 cm sand layers) with gravel crusts were designed and installed on the partially oxidized sulfidic tailings at the decommissioned Waite Amulet site, near Rouyn-Noranda, PQ. Another test plot was installed in which a 2 mm thick, high density polyethylene replaced the compacted clay. The three covered test plots and a control plot without a cover were instrumented to measure gaseous oxygen concentrations, water contents, pressure heads, temperature, and water quality. Laboratory experiments were also installed to simulate the soil-covered test plots. The laboratory tests contained unoxidized tailings recovered from the saturated zone of the Waite Amulet tailings impoundment. Field and laboratory results indicated that the compacted clay layer in the composite cover remained near saturation (≥93%) even during dry conditions. The soil covers in the laboratory reduced oxygen flux and acid generation by 99.9% and 95.4%, respectively. Infiltration into the covered field plots was equal to 3.9% of total precipitation. The hydraulic conductivity of the clay did not change from its placement value of 1×10^{-7} cm/s during 3 yr of monitoring. Field lysimeters placed beneath each test plot showed a 70 to 91% reduction in sulfate concentrations and an 80 to 93% reduction in iron concentrations, compared with the control plot. These concentrations do not show the same cover effectiveness as the oxygen data because of mixing with surrounding ground water, as the water table rose higher than the top of the lysimeters during spring 1992.

Introduction

A large number of Canadian metal and uranium ore bodies contain sulfide minerals which, when milled, produce tailings which are generally deposited in exposed environments. When iron-bearing sulfide minerals (particularly pyrite and pyrrhotite) contained in the tailings are exposed to oxygen and water, they oxidize and turn receiving surface waters acidic if sufficient alkaline minerals are not present. The solution resulting from this oxidation is characterized by low pH and high concentrations of ferrous iron and sulfate. The overall process of sulfide oxidation may be summarized by the following equation:

$$FeS_2(s) + \frac{15}{4}O_2 + \frac{7}{2}H_2O \rightarrow Fe(OH)_3(s) + 2SO_4^{2-} + 4H^+$$

Naturally occurring bacteria, notably the genus *Thiobacillus ferrooxidans*, catalyze the oxidation reaction (Nordstrom 1982). The ferric iron generated may either be hydrolyzed and precipitated as ferric hydroxide [$Fe(OH)_3$] or oxidize other heavy metal sulfides present such as galena [PbS], sphalerite [ZnS], and chalcopyrite [$CuFeS_2$]. Acid drainage may therefore also contain high concentrations of heavy metals. Rainfall and snowmelt flush the acidic solutions from

---

[1]Paper presented at the International Land Reclamation and Mine Drainage Conference and the Third International Conference on the Abatement of Acidic Drainage,Pittsburgh, PA, April 24-29, 1994.

[2]Associate Professor, Department of Civil Engineering, The University of Western Ontario, London, Ontario Canada.

[2]Bernard Aubé, Environmental Scientist, Luc St-Arnaud, Program Leader, Hydrogeologist, Noranda Technology Centre, Pointe-Claire, Québec, Canada.

[4]Mark R. Woyshner, Consulting Hydrologist, MW Hydrologics Inc., Montreal, Québec, Canada.

the tailings sites into the downstream environment. If acid drainage is not collected and treated, it could contaminate ground water and local water courses, damaging the health of plants, wildlife, fish, and possibly humans.

Current major tailings management practices for decommissioning are flooding, revegetation of the tailings dam, and treatment of the acid drainage from the tailings area. Flooding requires construction and long-term maintenance of engineering structures such as dams and dikes. Treatment of acid drainage involves the addition of lime to neutralize the acidity and precipitate heavy metals and calcium as hydroxides and sulfates in the form of sludge. Although lime treatment plants effectively prevent adverse environmental impacts from occurring, acid generation may occur for several hundred years following mine closure, therefore necessitating the operation of these treatment plants in near-perpetuity. In 1989, the Canadian Mine Environmental Neutral Drainage (MEND) program began to investigate other technologies, such as engineered soil covers for preventing and controlling acid drainage, in an attempt to find permanent and cost-effective solutions. This effort resulted in a laboratory investigation into the design and construction of soil covers, which was later followed by a field evaluation at the Waite Amulet tailings site, near Rouyn-Noranda, PQ, Canada, during the summer of 1990.

The Waite Amulet Covers Project consisted of a combined field and laboratory study. The main objective of the field program was to evaluate the effects of meteorological changes (such as freezing and thawing), hydrology, and hydrogeology, which are difficult to adequately simulate in the laboratory. The objective of the laboratory study was to evaluate cover performance in a controlled environment where material placement, installation of instrumentation, and monitoring are more convenient.

Methods

The design of the composite soil cover focused on the curtailment of oxygen and water to the tailings.To curtail oxygen, cover moisture must remain near saturation, and to inhibit infiltration, the cover must have a low hydraulic conductivity. One method of achieving these two objectives above the water table is by incorporating a capillary barrier in the design of the cover. In a capillary barrier, a saturated, fine-grained soil layer with a low hydraulic conductivity is placed on top of a coarse-grained soil layer (Rasmuson and Eriksson 1986, Nicholson et al. 1989). When the sand base is drained, capillary suction forces prevent drainage of the fine-grained soil cover.

To reduce evaporation from the clay, a layer of sand is placed over the clay. This sand cover also reduces runoff and provides storage of water following infiltration, thereby allowing more water to reach the fine-grained cover to alleviate moisture losses. For maximum reductions in oxygen fluxes, the design aimed at placing the fine-grained cover at a high water content (as close to saturation as practicable). The near-saturation requirement ensures that the diffusive flux of gaseous oxygen through the cover is very low since the diffusion coefficient of gaseous oxygen decreases with moisture content (Yanful 1993).

A gravelly sand layer was selected for the sand base, a compacted varved clay for the fine-grained soil cover, and a fine to medium sand for the sand cover. In the field, a 10 cm thick gravel crust was placed on the sand cover to reduce erosion.

Field Test Plots

Four 20 by 20-m test plots were designed as follows: (1) control plot without a cover, (2) composite plot consisting of upper and lower sand layers and a middle varved clay layer compacted at 93% modified Proctor and a water content of 25%, (3) composite plot consisting of upper and lower sand layers and a middle varved clay layer compacted at 91% modified Proctor and a water content of 26%, and (4) composite plot consisting of upper and lower sand layers and a middle 80-mil (2-mm-thick) high-density polyethylene (HDPE) geomembrane. This design enabled a direct comparison between the performances of the clay and HDPE covers. Each test plot was designed with 3:1 (H:V) end slopes and perimeter drainage ditches to conduct surface runoff away from the plots. The design specified that the slopes be lined with 40-mil HDPE sheets at the clay-upper sand contact to prevent lateral

transfer of gaseous oxygen into the covers. For the same reason, a similar lining was specified for all the perimeter ditches.

Based on results of oxygen flux modeling conducted prior to construction of the test plots, the cover was designed with a 60-cm-thick compacted fine-grained layer placed between two sand layers, each 30-cm-thick. A 10-cm gravel crust was placed on top of the covers for erosion protection. It was estimated that this design would reduce oxygen fluxes to very low values.

An integral component of the test plot design was the installation of instrumentation to assess the performance of the covers. The critical parameters for this assessment were identified to be (1) the moisture content of the cover, particularly that of the clay layer and the sand base, (2) the hydraulic heads in the cover and tailings, (3) the concentration of gaseous oxygen in the cover and tailings, (4) the water quality of the tailings porewater, and (5) the temperature of the cover and tailings. Hydrometeorological parameters, such as rainfall and pan evaporation, were also monitored.

To provide information on changes in water quality in the short term, a collection basin lysimeter was installed in the existing tailings directly beneath the cover. The lysimeter was filled with unoxidized tailings recovered

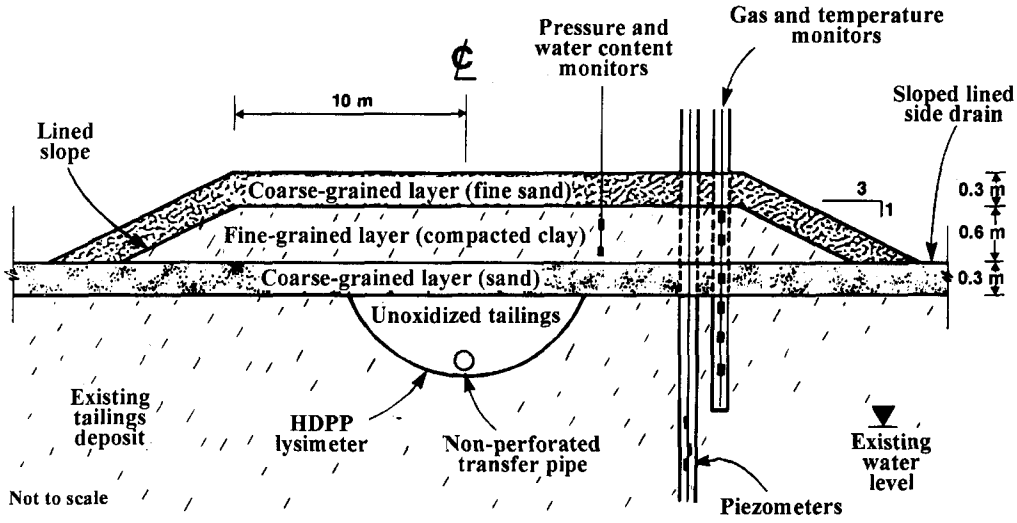

Figure 1. Test plot soil cover.

from the southern section of the existing impoundment. Each lysimeter wasconnected to a manhole by means of a transfer pipe. The transfer pipe wasconnected to the manhole at a lower elevation to promote drainage by gravity. The field installation was completed in September 1990 and the test plots were monitored from that time until September 1993.

Cover Simulation Columns

The effectiveness of the three-layer cover in reducing tailings oxidation was investigated by comparing covered tailings with uncovered tailings in laboratory columns. The cover design and soils used in the simulation columns were the same as those used in the field test plots and the drainage column. Tailings used in the evaluation were recovered from the same area as the lysimeter unoxidized tailings. These tailings are rich in sulfides, consisting predominantly of pyrite (15%), pyrrhotite (6%), chalcopyrite, and marmatite.

The columns used in the evaluation consisted of square plexiglass columns (28 cm per side) of 105-cm length. Four such columns were fabricated and installed with soil and tailings materials as follows: (1) two test columns

packed with 45 cm of unoxidized tailings overlain sequentially with 15 cm coarse sand, 30 cm clay, and 15 cm fine sand and (2) two control columns packed with 90 cm of unoxidized tailings. Each column was instrumented to measure gaseous oxygen concentrations in the soil voids, soil moisture content, and temperature. The ports were sampled by means of a percent oxygen analyzer with a hand-held sampling trigger and a syringe needle.A detailed description of the column installation is presented by Yanful (1993).

It was soon evident that oxygen was diffusing through the instrumentation in the test columns since the tailings surrounding the sampling ports were oxidizing. Oxidized tailings are easily recognized by their reddish-yellow color, as opposed to the dark-gray color of fresh tailings. Two new test columns were subsequently installed, approximately 200 days after the first set was constructed. These new columns were fabricated from one piece of clear plexiglass with a reduced number of sampling ports, and packing was rigorously controlled to minimize preoxidation of the tailings.

Rainfall and snowmelt were simulated by periodically adding water. Drainage water collected from the two control columns (without covers) was sent for metal and major cation analysis for physicochemical analysis, and [SO_4^{2-}] determination. The test columns (with covers) did not produce any drainage water because the clay layer essentially prevented infiltration. To have a basis for comparison between the control and test columns,the tailings in the test columns were flushed by bypassing the cover and the acidity was measured. The tests were conducted over a period of 760 days.

Results

Water Drainage and Percolation

Cover Simulation Column. The water content profiles in the control columns indicated that the water content of the surface tailings was highly dependent on rainfall and that the deeper tailings were essentially saturated throughout the experiment. The water contents for the test columns showed that the fine sand layer was dependent on rainfall events, while that of the clay remained constant at (or near) saturation (≥95%). The coarse sand below the clay stayed essentially dry except when the columns were flushed to measure acidity. The tailings below the coarse sand layer remained at a constant water content of 30% to 35% until the first column flush, when they became saturated and remained so to the end of the experiment. This data confirm the effectiveness of the upper sand as an evaporation barrier that prevents the clay from losing moisture by evaporation. The bottom sand remained near residual water content, thus preventing the clay from draining by gravity and illustrating its efficiency as a capillary barrier (Nicholson et al. 1989).

The three-layer cover was effective in preventing percolation to the tailings. When precipitation was simulated, most of the added water reported as runoff, some water filled the pores of the sand cover, and no water was collected as drainage. Since the clay presented such an efficient water barrier, it was necessary that flush water bypass the cover in order to obtain acidity results to be compared with the control columns. The columns were flushed four times during the experiment.

Field Results. The data taken from three years of testing show that the clay remained close its construction water content, with a degree of saturation greater than or equal to 93% throughout the entire experiment. The coarse sand remained at residual water content, and the fine sand varied with precipitation and evaporation. Table 1 presents the 1993 volumetric water contents for the two soil covers and underlying tailings and the sand base and tailings underneath the HDPE cover. These results support the 1990-1992 data and are in complete agreement with results obtained from laboratory and modeling analysis. The water content data of the tailings are probably too high and may be explained by the high ionic strength of the tailings pore water which made it difficult to obtained a well-defined TDR wave for interpretation (Yanful et al. 1993)

The percolation through one of the soil covers was estimated by measuring the discharge from the lysimeter during an eleven-month period (October 1992 to September 1993). It was possible to obtain an good estimate of the

infiltration because, unlike the spring of 1992, the water table did not rise above the top of the lysimeters. The collected volume was 82 L, which was equivalent to 37 mm of precipitation. This represents 3.9% of the total precipitation (958 mm) for that period. Duplication of the results was not possible as the transfer pipe from the lysimeter below the other soil cover seemed to have ruptured during the third year. The infiltration in the control plot was estimated to be five times that of the test plot.

Table 1. Volumetric water contents of test plots at Waite Amulet (1993).

Test Plot	Material	Depth (cm)	May 21	June 11	August 19
Soil cover 1	Clay	30-60	43	43	42
	Clay	60-90	46	45	46
	Sand Base	90-120	9	9	9
	Tailings	120-150	50	50	49
	Tailings	150-180	60	60	56
Soil cover 2	Clay	30-80	45	45	44
	Clay	60-90	44	45	43
	Sand Base	90-120	8	9	8
	Tailings	120-150	52	52	52
	Tailings	150-180	57	57	54
HDPE cover	Sand Base	30-60	9	9	--
	Tailings	60-90	53	53	--

Hydrologic Modeling. The Hydrological Evaluation of Landfill Performance (HELP) model is a deterministic water balance model that uses climatic, soil, and design data to determine the water budget of a landfill (Schroeder et al. 1984). The HELP model simulates four hydrologic processes on a daily account: (1) runoff, and hence infiltration, (2) percolation (i.e., saturated and unsaturated vertical flow), (3) lateral drainage, and (4) evaporation. The HELP model was utilized in this project to evaluate the amount of percolation that is expected through the composite soil covers. A small amount of percolation is required for the clay to remain near saturation; however, a large amount of percolation will tend to promote the dispersion of AMD.

The HELP model was run with 20 yr of synthetically generated climatic data. Percolation (39 mm/yr) is slightly greater than the hydraulic conductivity of the clay ($1x10^{-7}$cm/s or 32 mm/yr). This is possible only when free water is ponded at the surface of the clay. The monthly results indicated these conditions existed and that the predicted soil water content at the end of the 20-yr modeling period was similar to the initial value of 44%.

To validate the HELP modeling, the flow model SEEP/W was used to simulate flow through the composite soil cover at Waite Amulet. The test plot was modelled as a two-dimensional system under steady-state conditions. The top boundary condition was specified as a constant flow of water equivalent to the precipitation minus the runoff and evaporation (240 mm/yr). The results of steady-state flow modeling are only an indication of what one might expect as the average annual flow condition. The transient effects of the system are not depicted.

SEEP/W flow modeling determined that 34.4 mm would percolate through the cover. HELP modeling determined that 39 mm would percolate through the cover. Both modeling programs also indicate that the clay will remain saturated by a perched water table in the upper clay and lower fine sand layers. In the eleven-month period mentioned above, 37 mm of percolation was measured.These converging results between the two modeling methods and the field data confirm the validity of the modeling programs.

Freeze-Thaw. Since the method of measuring water content (time domain reflectometry, or TDR) measures only water and not ice, it can be used to indicate when soils are frozen. The results indicated the tailings under the soil covers did not freeze, while the uncovered tailings froze during the winter. The clay cover also showed freezing during winter. These data agreed with the temperature data, which showed below zero temperatures in the cover and the top 25 cm of uncovered tailings during the winter.

The effects of freeze-thaw on the integrity of the compacted clay layer in the composite cover were investigated. The results showed that most of the negative effects occur during the first two freeze-thaw cycles. Laboratory hydraulic conductivities increased by one to two orders of magnitude after the first two freeze-thaw cycles and then remained steady. Field hydraulic conductivity was measured yearly from 1991 to 1993, and the results indicated a value of ~1.0 x 10^{-7} cm/s, similar to the initial design value. Based on these results and those of the laboratory freeze-thaw studies, it is concluded that freezing and thawing have not adversely affected the cover and that no future negative effects need be anticipated.

Oxygen Diffusion

Field Results. The diffusion of oxygen in water is a very slow process, compared with its diffusion in air (2.5×10^{-9} m^2/s in water and 1.8×10^{-5} m^2/s in air). This implies that a layer of water placed above tailings could severely limit the available oxygen for tailings oxidation. The oxygen diffusion coefficient in a saturated soil is equal to the diffusion coefficient in water multiplied by the tortuosity factor of the soil, since the oxygen must travel through the water in the pores of the soil. Since a tortuosity factor is smaller than 1, the diffusion of oxygen through a saturated soil is therefore lower than that in water.

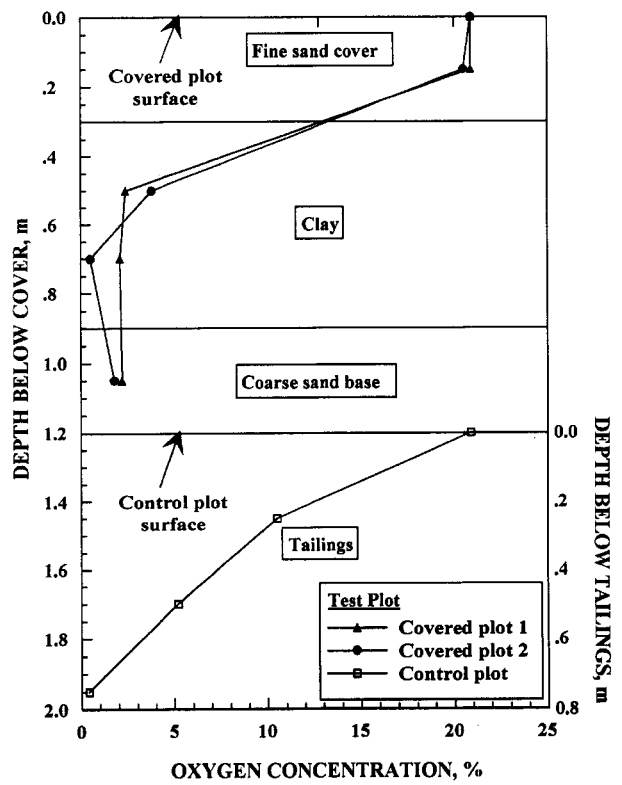

Figure 2. Field O_2 concentrations.

The computer program POLLUTE (Rowe and Booker 1990) was used to determine the flux of oxygen into the covered and uncovered tailings. Modeling results showed that, in July 1992, the flux of oxygen into the uncovered tailings was 2.76 g $O_2/(m^2 \cdot day)$, compared with 4.96×10^{-4} g $O_2/(m^2 \cdot day)$ for the covered tailings. This represents a cover effectiveness of over 99.9%.

Figure 2 presents gaseous oxygen profiles measured in July 1992 on both covered test plots as well as the uncovered control plot. These profiles show that the covers have a significant effect on the oxygen concentration at the surface of the tailings. When the tailings are not covered, the oxygen at the surface of the tailings is at atmospheric conditions (20.9% O_2). When the three-layer cover is placed over the tailings, the oxygen concentration is reduced to 2.0%. This represents a 90% efficiency in reducing oxygen availability.

The bacteria that catalyze the oxidation reaction are aerobic and may therefore not be capable of survival where oxygen concentrations are low. Below a soil cover, this would represent a greater decrease in oxidation rate than that due to the reduction in oxygen concentration alone, since biological oxidation is eliminated. For example, a 90% decrease in oxygen availability could conceivably imply a 97% decrease in tailings oxidation rate.

During 1992, oxygen measurements at the membrane-covered test plot were consistently 20.9% above, and 6% below, the geomembrane. The fact that the concentration was not lower than 6% below the geomembrane

indicated a constant supply of oxygen in the sand base layer. Horizontal inflow of oxygen from the edge of the cover was most likely responsible for the oxygen observed in the sand base.

Simulation Column Results. In the test columns, the oxygen concentration in the fine sand at the surface remained essentially constant near atmospheric value (20.9%). In three of the four test columns, the oxygen concentration beneath the soil cover remained below 1%. In the fourth test column the concentration ranged from 6% to 15% oxygen. As the cover was intact and the tailings in the fourth column did not oxidize (the tailings remained gray and very little acidity was measured), the sampling port was considered defective. The oxygen concentrations measured in all covered tailings were always below 1%.

In the control columns, an oxydation front was formed and gradually descended farther into the tailings as the upper layers oxidized. The oxidation rate decreased with time because the oxygen had to diffuse through the upper layers of oxidized tailings to reach the fresh tailings below. Near the end of the test period (~650 days), oxygen concentrations greater than 2% were observed at the 31-cm depth. This suggests that the tailings above the 30-cm depth must have been oxidized.

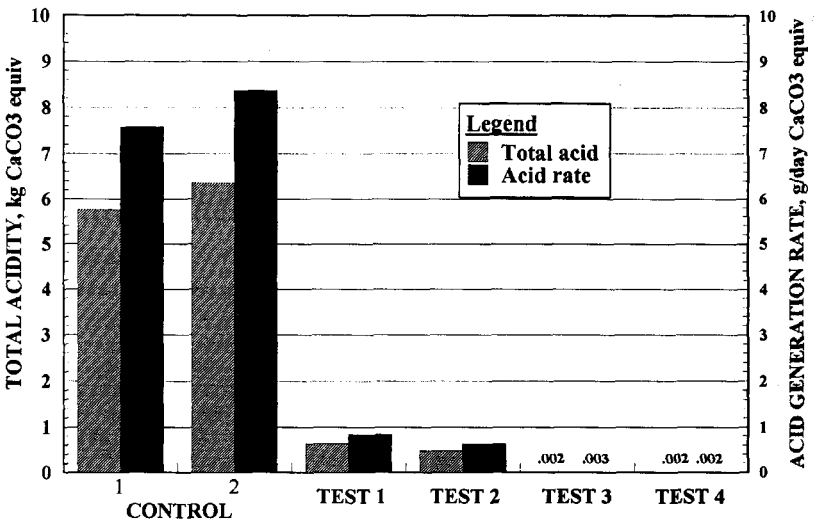

Figure 3. Total acidity and acid production rate in laboratory columns.

Chemistry

Simulation Column Results. Total acidity was used as a basis for assessing soil cover effectiveness during the simulation column experiments. The total acidity was determined as the product of the acidity as $CaCO_3$ equivalent, in grams per liter, and the respective volume of drainage water through the columns. For the control columns, this included both simulated rain and flush water. For the test columns, only flush water was measured since the simulated rain water did not permeate through the clay. The acidity data are presented in figure 3 for the uncovered and covered tailings. The data indicate that the soil cover decreased acid production from the tailings by an average of 95.4%. Reduction of acid production in test columns 1 and 2 was not as high as in columns 3 and 4, because of oxidation resulting from test artifacts, as previously mentioned.

The oxidation rate calculated for the uncovered tailings was about 10 mg/(d·cm^2) of $CaCO_3$. This oxidation rate could not be related to field oxidation rates since laboratory conditions were almost optimal for microbial activity (22° C). However, the laboratory results provide an estimate of the maximum acid flux generated by a tailings with similar mineralogy.

At the end of the tests, solid tailings samples were removed from the columns and sent for analysis. Pyrite content was

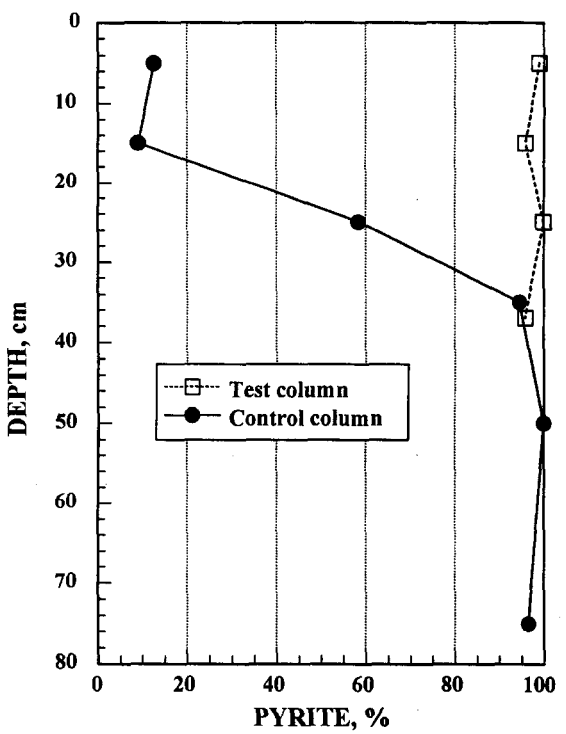

Figure 4. Percentage of initial pyrite.

considered to be a good basis for verification of the degree of oxidation since it is quickly oxidized and represented 12% to 18% of the fresh tailings. The results in figure 4 were obtained by dividing the final concentration of pyrite at the specific depths by the initial concentration of the tailings taken when the columns were packed. These results clearly show that the control column tailings had been mostly oxidized in the first 20 to 30 cm of depth, and that the covered tailings were virtually intact.

Porewater samples were extracted (by squeezing) from approximately 200 g of tailings and analyzed for pH and for metals and sulfur by the inductively coupled plasma method. The results showed that iron concentrations in the control columns were more than 100 times higher than iron concentrations in the test columns. The oxidation front in the control columns was also well defined at around 30 cm, with iron concentrations of 15 g/L compared with 5 g/L near the surface. Table 2 presents some water quality data for the uncovered (Control 1) and covered (Test 4) tailings. Details of the water quality data from the columns are presented and discussed in detail in the MEND report on the project (Yanful et al. 1993).

Bacteria count was also performed on tailings samples to evaluate the population of iron-oxidizing microorganisms such as *Thiobacillus ferrooxidans*. The results indicate that the bacterial population in the covered tailings (test columns) ranged from $1x10^2$ to approximately $1x10^5$ cells, while the uncovered tailings (control columns) showed a maximum number of cells of $1x10^7$ near the oxidation front, at a depth of 30 cm.

Table 2. Post-testing pH and species concentrations (mg/L) in tailings pore water.

Depth (cm)	pH	Fe	Fe^{3+}	Zn	Cu	SO_4^{2-}	Al
Uncovered Tailings (C1)							
5	1.87	4,970	3,590	13.5	80.7	22,380	1,300
15	1.89	4,150	4,130	15.7	136	21,240	1,300
25	2.02	15,800	14,270	67.2	158	49,500	2,700
36	2.87	11,600	11,680	184	52.2	34,500	2,240
50	3.31	9,230	9,320	432	15.9	27,690	1,730
75	4.06	1,330	70	72.5	<0.02	3,840	5.3
Covered Tailings (T4)							
5	4.12	5.31	2.31	11.6	0.1	2,610	1.87
15	5.45	1.42	0.7	2.48	0.03	1,950	0.58
25	5.41	7.58	0.7	8.31	<0.02	1,980	0.69
37	5.29	0.9	1.75	12.4	<0.02	2,250	0.51

Field Results. The chemistry of the drainage water from the control lysimeter indicated rapid oxidation of the exposed tailings in the uncovered lysimeter. Immediately following installation in October 1990, the pH of drainage water decreased from 3.78 to 3.33 within a month. Concentrations of Fe and other heavy metals (Zn, Cu, and Cd) were higher than those observed in the saturated tailings surrounding the lysimeter. After the initial flushing of the tailings, the concentrations of sulfate and metals apparently decreased in 1991. Further oxidation during the following summers produced more acid, and concentrations of sulfate and metals have increased in 1992 and 1993.

The lysimeters underneath the soil covers did not produce any drainage water until after a year of monitoring. Unoxidized tailings were placed in the lysimeters at residual saturation prior to covering. Following installation, it was calculated that the lysimeters underneath the soil covers would not report water until after 14 months, based on

the hydraulic conductivity of the compacted clay and the residual water content of the tailings. When the lysimeters finally reported water, the water table below the test plots was found to have risen above the level of the lysimeter as a result of high rainfall. This was evident from hydraulic head data, ponding observed on the control test plot and water collected from the lysimeter below the geomembrane. Analysis of the lysimeter water and pore water of the surrounding tailings supported the inference that ground water had contaminated the fresh tailings inside the lysimeters by rising above the the sand base and into the lysimeters. This contamination would affect the collected water from both the control and the soil covered test plots. Ferric ions (Fe^{3+}) in the tailings pore water could subsequently oixidize the fresh tailings below the covered plot and worsen the water quality in the lysimeter, before collection. The chemistry of the lysimeter drainage water was therefore not considered a useful measurement of the acid generation rate. A different design for the lysimeter system could have averted the problem associated with the water table elevation. Also, the problem would not occur in a full-scale soil cover application, in which covering of the entire tailings deposit would lower the net infiltration in the tailings, and hence lower the water table.

The tailings from the two soil covered and control test plot lysimeters were removed and examined after 3 yr of monitoring, to assess the extent of oxidation. The tailings from the control lysimeter showed some discoloration due to oxidation, whereas the samples removed from beneath the covered tailings were gray and seemingly unoxidized. Chemical analysis for sulfate and metals indicated oxidation in the control tailings but little or no oxidation in the covered tailings. For example, total Fe concentration in the uncovered tailings pore water ranged from 5,000 to 20,000 mg/L, compared with 1,000 to 1,500 mg/L in the covered tailings. Sulfate concentrations in the uncovered tailings pore water were about 16,000 to 63,000 mg/L compared with 5,000 to 5,700 mg/L in the covered tailings. These data do not indicate the same soil cover effectiveness as the gaseous oxygen and hydraulic data and are believed to be influenced by mixing from surrounding ground water which overtopped and contaminated lysimeters hosting the tailings. It is estimated that, at the time of sampling, the ground water that had contaminated the covered lysimeters had not yet been flushed from the lysimeter pore water. In fact, only about 1/6 of the total tailings pore volume (in the soil-covered lysimeters), had been flushed. Details of the water quality data are presented by Yanful et al. (1933b).

After three years of monitoring, pore water sulfate concentrations in soil-covered tailings (lysimeters) were 9 to 30% those of uncovered tailings. Total iron concentrations in the covered tailings were 7 to 20% of those observed for the uncovered tailings.

Conclusions

The three-layer soil cover, consisting of one fine-grained (clay) saturated layer placed between two coarse-grained (sand) layers, is an efficient method of inhibiting acid mine drainage generation. Field and laboratory tests have shown that the clay barrier will remain near saturation (≥93%) even under dry conditions. Oxygen profiles measured in the laboratory and the field showed that the oxygen flux could be reduced by up to 99.9%. The reduction in oxygen flux in the laboratory columns reduced the activity of the bacteria which catalyze the oxidation reaction by 99.0%. The curtailment of oxygen and biological oxidation resulted in a reduction of the rate of acid generation of 95.4% in the laboratory.

Field water balance measurements indicated that only 3.9% of precipitation percolated through the cover. This was confirmed by hydrologic modeling. This infiltration is equal to approximately one fifth the infiltration into uncovered tailings. After three years of monitoring, the hydraulic conductivity of the compacted clay had not changed from the initial value of 1.0×10^{-7} cm/s.

Literature Cited

Nicholson, R.V., R.W Gillham, J.A. Cherry, and E.J. Reardon. 1989. Reduction of acid generation in mine tailings through the use of moisture-retaining cover layers as oxygen barriers. Can. Geotech. J., 26(1): 1-8.

Nordstorm, D.K. 1982. Aqueous pyrite oxidation and the consequent formation of iron minerals. p. 37-56. In Acid Sulphate Weathering. Soil Sci. Soc. America. Spec. Pu. 10.

Rasmuson, A. and J.C. Eriksson. 1986. Capillary barriers in covers for mine tailings dumps. National Swedish Environmental Protection Board Report 3307.

Rowe, R.K., and J.R. Booker. 1990. POLLUTE v.5.0 1-D pollutant migration through a non-homogeneous soil—user manual. Geotechnical Research Centre, Faculty of Engineering Science, University of Western Ontario. Report GEOP 90-1.

Schroeder, P.R., J.M. Morgan, T.M. Walski, and A.C. Gibson. 1984. The hydrologic evaluation of landfill performance (HELP) model. U.S. Environmental Protection Agency, Office of Solid Waste and Emergency Response, Washington, DC.

Schroeder, P.R., and R.L. Peyton. 1984. Verification of the hydrologic evaluation of landfill performance (HELP) model using field data, U.S. Environmental Protection Agency, Washington, DC.

Woyshner, M.R. and E.K. Yanful. Hydrologic analysis and prediction in a composite soil cover. Joint CSCE-ASCE National Conference on Environmental Engineering (Montreal Canada, July 12-14, 1993)

Yanful, E.K. and L.C. St-Arnaud. 1992. Migration of acidic pore waters at the Waite Amulet tailings site near Rouyn-Noranda, Quebec, Canada. Canadian Geotechnical Journal, Vol. 29: 466-476.

Yanful, E.K, 1993. Oxygen diffusion through saturated soil covers on sulphidic mine tailings. ASCE J. Geotech. Eng., Vol. 119, No. 8, pp. 1207-1228.

Yanful, E.K., M.R. Woyshner, and B.C. Aubé. 1993. Field evaluation of the effectiveness of engineered soil covers for reactive tailings.Report for MEND, DSS contract 23440-0-9061/01-SQ.

COMPOSTED ORGANIC WASTES AS ANAEROBIC REDUCING COVERS FOR LONG TERM ABANDONMENT OF ACID-GENERATING TAILING[1]

W.G. Pierce[2], N. Belzile[2], M.E. Wiseman[3], and K. Winterhalder[2]

Abstract: While organic amendments have been well documented for revegetation of acid-generating tailing and waste rock, it is recognized that they do not prevent tailing oxidation and therefore are not a permanent solution to the acidic drainage problem. Laboratory research presented here compared three compost cover layer models that employed fresh and mature municipal solid waste compost. Fresh compost covers on tailing established low redox potential under anaerobic conditions that not only prevented further tailing oxidation, but also reversed the processes that generate acidic mine drainage. Reductive dissolution of previously oxidized and precipitated trace metals was seen, but this may be a transient phenomenon. Further laboratory studies and preparations for a field research program are ongoing.

Additional Key Words: acid mine drainage, compost, municipal solid waste, oxygen barrier

Introduction

The prevention or treatment of acid mine drainage (AMD) resulting from the oxidation of sulphides in waste rock and tailing is one of the most significant environmental problems facing the mining industry and various government agencies. In Ontario, Canada, recent amendments to the provincial Mining Act requiring the filing of long term Rehabilitation Plans with financial assurance to complete them, has added impetus to the efforts to find more cost effective and permanent strategies to prevent AMD. Revegetation efforts improved the aesthetic qualities of mine wastes but have done little to ameliorate the AMD problem (Davé and Michelutti 1989).

It is recognized that metal sulphides in tailing and waste rock react with oxygen and water to produce sulphuric acid and release associated trace metals. Some of the strategies currently being investigated to stop the AMD processes include preventing oxygen, water, or both, from contacting the tailing. It is also recognized that the bacterium *Thiobacillus ferrooxidans* plays a significant role in accelerating the tailing oxidation process. Thus, stopping oxygen penetration into the tailing will reduce the activity of *T. ferrooxidans*.

One of the promising areas of research by industry and government is the use of various covers to prevent the oxidation of tailing sulphides. Unfortunately, most effective cover designs have proven to be prohibitively expensive to implement (Davé and Lim 1989, Nicholson *et al.* 1989). Recently, a number of studies have recognized that there are natural conditions of low oxygen concentration and redox potential that could be adapted to stop the AMD processes and perhaps actually reverse it (Pierce 1992). Anaerobic conditions found in landfills and wetland organic sediments are populated by reducing bacteria that produce methane gas and reduce dissolved sulphate, nitrate and metals, returning them to a solid state as sulphide precipitates. Other organic materials, such as Municipal Solid Waste (MSW) compost, share many of the characteristics of landfills and wetland sediments and it is hypothesized that a designed

---

[1]Paper presented at the International Land Reclamation and Mine Drainage Conference and Third International Conference on the Abatement of Acidic Drainage, Pittsburgh, PA, April 24-29, 1994.

[2]W. Glenn Pierce, Research Associate, Centre in Mining and Mineral Exploration Research, Nelson Belzile, Assistant Professor of Chemistry, and Keith Winterhalder, Associate Professor of Biology, Laurentian University, Sudbury, ON, Canada.

[3]Mark E. Wiseman, Manager Environmental Projects, Falconbridge Ltd., Falconbridge, ON, Canada.

compost cover may also be able to maintain reducing conditions in acidic tailing.

The disposal of municipal wastes is a major environmental problem and cost facing many urban centres. The organic fraction can be 30% of MSW but its use in the production of clean, high-grade compost can be ten times more expensive for a municipality to manufacture than the present cost of landfilling the MSW. Land reclamation uses by the mining industry may represent a large and reliable market for MSW compost, especially if the compost could be less mature and contain gross contaminants such as glass, ceramics, plastics, wood chips, concrete and other wastes that are difficult and expensive to remove in making agricultural-grade compost. Large quantities of low-grade compost could be diverted from a MSW compost plant early in the manufacturing process and would therefore be much cheaper to produce and dispose of -- at a significant saving to the municipal taxpayers. Recognizing the potential "win-win" situation for municipalities and the mining industry, Falconbridge Limited initiated a research program to study the benefits of using MSW compost as an ameliorative cover layer on acidic tailing sites.

Benefits of a Compost Cover Layer

A literature review of what is known about the physical and chemical characteristics of MSW compost and other organic materials (Pierce 1992), revealed that a compost layer on sulphide tailing could be beneficial in five ways in the suppression of tailing oxidation and acidic mine drainage. First, the compost could maintain sufficient water saturation to produce a physical oxygen barrier. Second, the continued decomposition of compost would create a large biological oxygen demand that acts as a sink for atmospheric oxygen or dissolved oxygen. Third, compounds and decomposition products in the MSW compost that leach into the tailing may inhibit the growth and metabolism of sulphate-producing bacteria. Fourth, organic constituents and reducing bacteria in the MSW compost could cause the reductive dissolution of ferric oxides and prevent indirect ferric sulphide oxidation and acid generation. Fifth, compaction of the compost layer could reduce the hydraulic conductivity and prevent infiltration of precipitation, thus decreasing tailing groundwater flow.

Project Objectives

Three major lines of investigation were undertaken during the laboratory phase of the research program-

1. Determine the potential leachate characteristics of fresh and mature compost.
2. Evaluate the physical characteristics of compost that determine its ability to maintain water saturation and anoxic conditions.
3. Evaluate the chemical processes and changes within compost and tailing when compost is placed on acidic tailing.

In this paper we present the results of a six month laboratory simulation experiment comparing the effects of fresh and mature compost used in three cover layer designs on oxidized acidic mine tailing.

Methods

Tailing material utilized in this research was obtained from the Nickel Rim site of Falconbridge Ltd., near Falconbridge, ON, Canada where it was deposited in the early 1950s (Blowes *et al.* 1991). The material was taken from the oxidized tailing zone approximately 10-30 cm below the surface layer of sandy, revegetated soil. Mature and fresh MSW compost was obtained through Dr. Lambert Otten at the University of Guelph, and was produced in a pilot plant from source-separated, organic, kitchen and yard waste collected from 900 suburban homes (Otten 1993). The fresh compost obtained was four weeks old, had a strong odour, and contained numerous twigs, stones and bits of plastic that had passed through a 7.5 cm screen sieve. The 14-week-old mature compost was sieved through 12 mm screen and had a fine texture like potting soil and very little odour.

Compost Leachate Composition

Several tests were done to evaluate the risk of using MSW compost on mining lands. Standard

chemical leachate analyses on compost to satisfy regulatory requirements of Ontario Regulation 347, Environmental Protection Act, regarding waste classification. The analyses included Ni, Cu, Pb, Zn, Cd, As, Cr, Co, Mo, Se, Hg, and the organics PCB, Aldrin, Dieldrin, Chlordane, DDT, Endrin, Heptachlor epoxide, Methoxychlor, Toxaphene, 2,4-D and Silvex. The Toxicity Characteristic Leaching Procedure was also performed on compost to determine the leachate characteristics under simulated acid rain conditions. Both Regulation 347 and TCLP procedures were repeated on compost that was spiked with ten times greater a concentration of organic chemicals and trace metals than that allowed by the Ontario Compost Quality Guidelines (Ontario Ministry of the Environment 1991) in order to simulate worst case conditions for MSW compost contamination.

Chemical Processes and Changes in Tailing

The physical and chemical characteristics of the tailing were determined before and after compost cover layer treatments. The investigations included-

1. Characterization of the crystallinity of oxidized tailing and the distribution of adsorbed trace elements with the tailing by x-ray diffraction.
2. Evaluation of the effects of redox potential and acidity changes on solid phase chemical speciation and the composition of tailing pore water and leachate through a standard sequential leaching analysis (5 fractions), and by mixing tailing with standard solutions of chemical reducers, such as sodium dithionite. Trace metals were analyzed by Inductively-Coupled Plasma spectrophotometry (ICP).
3. Determination of the effects of compost on solid phase chemical speciation and the composition of tailing pore water and leachate. This was accomplished by mixing compost with a slurry of tailing, followed by ICP analysis on filtrate (0.2 μm membrane), and analyses of samples obtained from the compost cover layer simulation experiment (see below).

Compost Cover Layer Simulation

Leaching columns were employed over several months to investigate the potential benefits that were suggested for three compost cover layer models, using fresh and mature compost treatments. The objectives of the simulation experiment were-

1. Study the effects of compaction pressure and compost maturity on the physical properties and water retention by the compost layer. The physical measurements included degree of compaction, water saturation, dry bulk density, porosity, and saturated hydraulic conductivity.
2. Measure the oxygen concentration profiles within the compost-tailing columns to determine the extent of anoxic conditions.
3. Determine any changes in tailing and compost pore water and gas quality through the simulation period, including relative measurements of redox potential, oxygen, carbon dioxide, carbon monoxide, methane, and dissolved sulphate, nitrate, iron, nickel, copper, zinc, cobalt, and manganese.

Experimental Treatments. Three cover layer designs were investigated using leaching columns to contain a vertical column of tailing and compost. The simplest cover treatment, called the Compost model, was a 95 cm layer of compost placed directly on a homogeneous layer of oxidized tailing (fig. 1A). In the Ploughed model (fig. 1B), a 20 cm layer of compost mixed with tailing (1:1 ratio by volume) was first placed on the tailing layer, followed by a 30 cm layer of compost. The Sand model consisted of a 5 cm layer of coarse aquarium sand on tailing to hydraulically isolate an upper 30 cm layer of compost from the tailing layer (fig. 1C). All columns contained an 88 cm layer of oxidized tailing to simulate the drainage characteristics of the tailing site. Two grades of compost (agricultural-grade, mature, 14-week-old compost, and coarse, fresh, 4-week-old compost) were used as contrasting treatments to investigate the relative benefits of compost maturity and quality. The six types of treatments were constructed in triplicate, giving a total of 18 leaching columns. The compaction pressure of a layer of revegetation medium was simulated by placing a weighted piston on the top of each compost layer (fig. 1).

Leaching Column Design. Leaching columns were constructed from clear acrylic plastic tubes 185 cm high and 10 cm outside diameter with 3 mm walls (fig. 1). The clear tube walls allowed examination of the quality of packing of tailing and compost in the tube, as well as monitoring of visible changes in the material during the simulation experiment, such as porosity and colour changes in the compost, and inthe

oxidized tailing as a result of reduction of iron oxides. Compaction of the compost in the leaching columns was achieved using a piston made of a 9.4 cm diameter disk of 13-mm-thick acrylic plastic attached to a pine post that reached above the top of each tube. Each disk had eighteen 3 mm holes drilled through it to allow the free passage of gases and water. Lead fishing net weights were attached to the top of the pine posts. In the Compost model (fig. 1A), a 9-Kg lead weight applied a pressure of approximately 12.5 KPa (0.125 atm) to the top of the compost in order to simulate the weight of a revegetation layer of about 50 cm. In the Ploughed and Sand models (fig. 1B-1C), 36 Kg of lead weights were attached to the top of each post by chains to give a pressure on the compost of 50 KPa (0.5 atm). This amount of weight was applied to simulate the effect of a surface revegetation layer of about 2 m of gravel and sandy soil.

After the compaction pistons were inserted, all columns were flooded with distilled water. The leaching columns were mounted vertically inside a 2.5 m-tall plywood cabinet and seated into polyethylene funnels supported on a bottom shelf. Each column was supported near the top by sticking through a hole in an upper shelf. Doors on the cabinet were closed during the experiment to keep the experimental material in darkness.

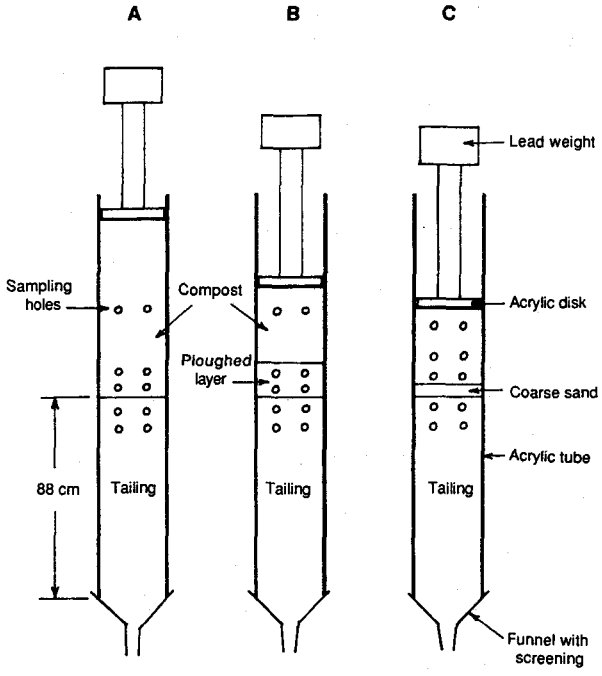

Figure 1. Diagrammatic view of the leaching columns used in the compost cover layer simulation, showing: (A) Compost model, (B) Ploughed model, and (C) Sand model.

To gain access to the compost and tailing material inside the leaching columns, two vertical lines of sample holes were previously drilled through the tube walls and sealed with rubber stoppers. The vertical lines of holes were separated by 90 degrees around the circumference of the tube. These holes were used to extract compost and tailing material for chemical and gas analyses. Another vertical line of six sampling holes was made on the backside of each tube at the level of the compost layer, with the holes mid-way between the other sampling holes. These holes were used near the end of the experiment to extract cores of compost in order to determine the degree of water saturation, bulk density, and gas-filled porosity.

Sampling Methodology. During the simulation experiment, small samples of tailing and compost were taken periodically for gas analysis and relative redox potential (Eh) measurement. To avoid the introduction of atmospheric oxygen into a column when a stopper was removed from a sampling hole, it was necessary to establish an anoxic atmosphere around a portion of the column before removing the rubber stopper. An acrylic plastic glove box was constructed to fit half-way around the column and provide access to the two sampling holes at each level (fig. 1). Inside the glove box were placed a 4 mL glass vial, a 15 mL plastic tube (containing 5 mL of distilled, deoxygenated water), a redox potential probe and a cork borer with wooden plunger. Both containers were pre-weighed. The glove box was flooded with nitrogen gas fed into a port on the top for about a minute before sampling to establish anoxia in the box. Using the cork borer, the experimenter extracted a 1- to 2-cm core of material. Half of the material was put in the glass vial and sealed with a rubber septum and screw cap. The rest of the material was inserted into the plastic tube containing deoxygenated water. The tube was gently agitated for about 30 s before a redox potential probe was inserted into the liquid. The Eh was recorded after three minutes, and then the tube was capped. Both containers were removed from the glove box and reweighed. After gas

analyses were completed, the glass vial and solid sample was oven dried at 75°C overnight to determine the dry weight of material sampled.

The Eh measured is a relative redox potential value since the redox transformations in the compost-tailing system would be complex and thus could not be calibrated against a redox potential standard. The redox probe was checked periodically against a standard solution to guard against malfunction and drift in its response. The redox probe was too fragile to insert directly into compost or tailing material so the method to measure an equilibrium Eh between a solid sample and deoxygenated water was devised. Therefore, the redox potential measurements made in the compost and tailing material are a relative Eh, consistent between experimental samples. Similarly for acidity measurements, since pore water was not being extracted, an accurate measurement of in situ sample pH could not be obtained. However, a relative pH was measured in the deoxygenated water used to determine relative Eh for the solid core samples. We are assuming that a similar equilibrium situation existed between the solid phase and the deoxygenated water in all the core samples.

Gas Analysis Technique. The glass vials containing compost or tailing samples were transported to another lab for gas chromatography and ion chromatography analyses. To avoid the possibility of contamination error, only as many samples were collected from the columns as could be analyzed the same day, and vials were stored in the refrigerator until shortly before starting gas analysis to minimize further chemical changes. A precision syringe was used to sample 100 μL of gas in the vial. This sample was injected into a gas chromatograph equipped with a thermal conductivity detector and a column designed for low molecular weight gases. Gases of interest to this study that could be measured with this instrument include oxygen, carbon dioxide, carbon monoxide and methane.

Anion Analysis. The levels of nitrates and sulphates were analyzed in each sample of deoxygenated water using a high pressure liquid chromatography system controlled by the Millenium 2010 software.

Results and Discussion

Unfortunately, space limitations permit presentation of only some results of the cover layer simulation portion of the project. Major conclusions of the compost leachate analyses and the characterization of chemical processes and changes in oxidized tailing are presented. A complete presentation of data and analyses for the project is available in a detailed report to MEND Ontario (through the Ontario Ministry of Northern Development and Mines) entitled "Reclamation of Sulphide Tailing Using Municipal Solid Waste Compost: Laboratory Studies Final Report".

Compost Leachate Composition

All fresh and mature compost samples met the Ontario Compost Quality Guidelines. No detectable concentrations of common toxic organic compounds were found in either the fresh or mature compost. Both the Regulation 347 and TCLP leaching tests showed similar patterns in the availability of trace metals and nitrogen compounds. Trace metals in compost leachate met the latest Municipal Industrial Strategy for Abatement (MISA) regulatory concentration standards for discharge from mining lands in Ontario. While the tests indicated elevated concentrations of nitrogen compounds, it is expected that these will not be of concern in the compost-tailing system where nitrate-reducing bacteria are active and will produce harmless nitrogen gas. Compost quality standards for agricultural use must be stringent to prevent uptake of toxins into the human food chain . However, this study suggests that leachate from contaminated compost will not be a risk to water quality outside the tailing site. As such, the application of MSW compost to mining lands would involve a low level of environmental risk.

Chemical Processes and Changes in Tailing

The sequential extraction analyses of oxidized tailing material before treatment by a compost cover layer showed that high concentrations of Fe and Ni that are associated with amorphous or recently formed oxyhydroxides. These elements could be released from the solid phase under reducing conditions since iron oxides and oxyhydroxides can be dissolved and release Fe(II) and the trace metal adsorbed onto

them. A significant proportion of Cu and Zn was associated with organic or sulphide solids. Mn, Cu and Zn show a strong presence in the residual component of the extraction procedure, and thus would not be expected to mobilize under oxidizing conditions. Other metals, such as Cr, Co and Pb were extracted only in relatively low concentrations. These elements adsorbed or precipitated in the oxidized tailing may be resolubilized as iron changes from the ferric precipitate to the soluble ferrous state under reducing conditions. Strong reducing conditions, however, may recreate stable sulphides thus immobilizing most trace metals. Sequential extraction analyses of tailing following the compost cover layer treatment are not complete at the time of this report. Preliminary compost-tailing slurry experiments using mature compost as a reducing agent in oxidized tailing material suggest that chemical interactions with mature compost will produce weak reducing conditions.

Compost Cover Layer-Tailing Simulation

The transparent walls of the leaching columns provided a view of the chemical changes that were occurring in the compost-tailing system during the simulation. At approximately three weeks into the experiment, a blackening of the tailing and compost material appeared near the compost-tailing interface in the fresh compost treatments. This material was identified as iron sulphide precipitate. Similar darkening from iron sulphide also appeared several weeks later in some of the mature compost treatments. These visual observations confirm that anoxia became established, especially under the fresh compost, and created reducing conditions strong enough for the formation of iron sulphide precipitate.

Compost Layer Physical Changes. Fresh compost layers compacted 10% to 20% more than those of mature compost, although fresh compost showed a significantly higher total porosity and lower dry bulk density under the same compaction treatment. Fresh compost maintained a higher water content than mature compost as a result of its greater porosity. Since gas-filled porosity was found to be strongly correlated to total porosity and inversely correlated to bulk density, the variability and importance of pore water volume were relatively small. Therefore, we concluded that a compaction pressure of 50 KPa, approximately equivalent to a two metre cover of soil, was not effective in squeezing pore space out of the compost matrix under these experimental conditions. However, as the experiment progressed, voids developed in all the fresh compost layers, presumably due to the accumulation of decomposition gases.

Saturated hydraulic conductivity for the different compost-tailing systems ranged over several orders of magnitude (fig. 2), from a maximum of 4.4 x 10^{-4} cm/s in mature compost to a minimum of 2.2 x 10^{-6} cm/s for fresh compost columns. By contrast, tailing and ploughed (mixed) layers had much higher saturated hydraulic conductivities of 1.3 x 10^{-3} cm/s and 0.6 x 10^{-3} cm/s, respectively. Three fresh compost columns still held a shallow head of water above the compost layer 48 days after rewetting, indicating that their conductivities had dropped to a value near zero. Buttler *et al.* (1991) concluded that the low hydraulic conductivity of peat is determined by the blockage of pore space by trapped methane gas bubbles. We could not determine the basis for the low hydraulic conductivities in the fresh compost in this case. If a fresh compost cover layer could be kept wet and in a state of anaerobic decomposition, it is possible that this extremely low conductivity could be maintained. The result would be very poor water flow through the compost layer and the maintenance of near-saturated conditions and anoxia.

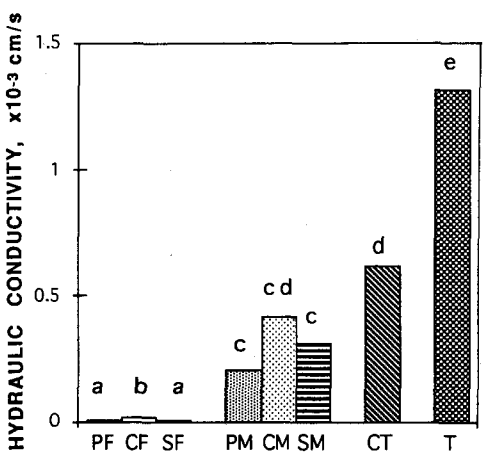

Figure 2. Saturated hydraulic conductivity of the compost cover layer-tailings system. Each bar is the average of three replicates and the same bold letter indicates no significant difference at the p=0.2 level. (treatments: PF - Ploughed Fresh, CF - Compost Fresh, SF - Sand Fresh, PM - Ploughed Mature, CM - Compost Mature, SM - Sand Mature, CT - Compost and Tailings mixture, T - Tailings).

Chemical Changes. Oxygen concentrations measured through the simulation experiment (fig. 3) indicate that the mature and fresh compost covers led quickly to anoxic conditions in all cover models studied. None of the oxygen concentrations measured was zero; however, the low concentrations detected are believed to be the result of oxygen contamination due to sampling technique, and not due to the presence of detectable amounts of oxygen inside the columns. The few high oxygen concentrations measured are believed to be the result of either an error in sample handling or an air leak into the column past an improperly seated stopper.

The creation of anoxia led quickly to a large decrease in Eh. The relationship between Eh and water content for all the samples of the simulation run is shown in figure 4. It is clear that the highest water contents and lowest Eh were found in the fresh compost layer (fig. 4, solid squares), and the lowest Eh in tailing was produced under this cover (fig. 4, solid circles). The ploughed layer, with an equal mixture of compost and tailing (fig. 4, triangles), shows an Eh-water relationship intermediate between the compost and tailing. Some of the tailing treated under fresh compost had Eh values as low as those in fresh compost samples. This suggests that the properties of the cover layer, rather than just chemical processes, produced the low Eh in the tailing layer.

The progress of Eh in the tailing layer is shown in figure 5. Tailing under the fresh compost treatments showed a continuous Eh decrease from one sampling period to another, while the tailing under the mature compost cover layer demonstrated little decrease until much later. The water content of the tailing samples was little modified by the rewetting of the columns or by the drying periods.

Analyses of gas samples in equilibrium with the solid phase samples revealed patterns that were consistent with the relative redox potential and oxygen concentration results. In all three cover layer models employing fresh compost, methane and carbon dioxide production showed a general increase with time in the compost and tailing regions of the profile. Profiles of methane concentration in the Compost model are shown in figure 6 at three sampling points during the simulation. Methane concentration increased in the tailing layer during the run, but was virtually absent in the

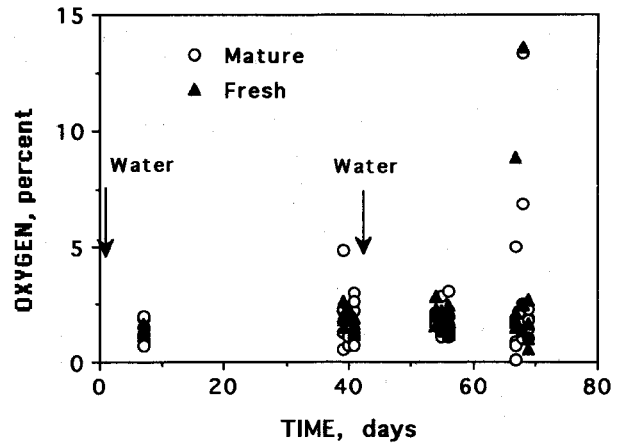

Figure 3. Oxygen concentrations measured in compost and tailings samples during the first four sampling periods of the simulation experiment. Arrows indicate days when water was added to the columns.

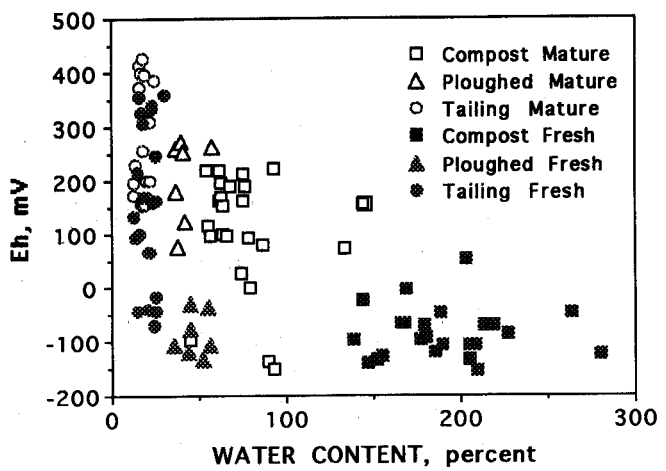

Figure 4. Relationship between relative redox potential (Eh) and water content for the six cover layer treatments.

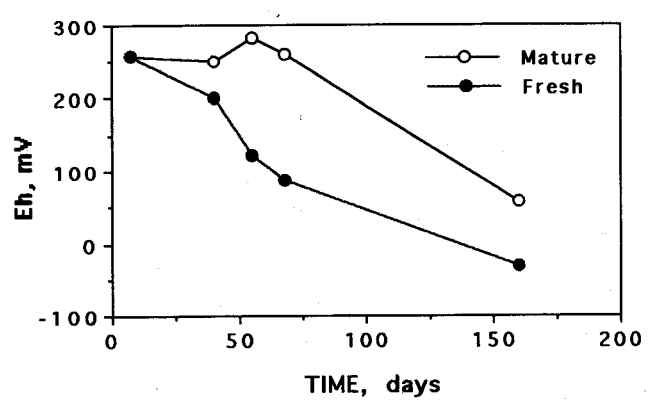

Figure 5. Changes in tailing layer relative redox potential (Eh) during the simulation under fresh and mature compost treatments.

mature compost treatments. These patterns are consistent with the decrease in Eh found in the tailing layer and the establishment of sufficiently strong reducing conditions for the observed methane and iron sulphide production. Carbon dioxide concentrations were greater in 80% of the fresh compost samples than in the matching mature compost samples. Methane and carbon dioxide are both decomposition products of anaerobic bacterial breakdown of organic substrates that are provided here in abundance by the compost and its leachates. Our gas chromatography system could not measure hydrogen sulphide, however, since the iron sulphide observed is formed from the reaction of hydrogen sulphide with Fe (II), it is certain that H_2S gas was present in the tailing-compost interface zone where iron sulphide precipitate was found. Hydrogen sulphide is produced by anaerobic sulphate-reducing bacteria that utilize small organic molecules as substrates.

Acidity and Trace Metal Analyses. Under aerobic conditions, iron and other trace metal sulphides in the oxidized tailing are mobilized due to oxidation by oxygen or ferric ion to produce sulphuric acid. In the sequential extraction analyses of the Nickel Rim oxidized tailing material, iron and nickel were associated with amorphous or recently formed oxyhydroxides that can easily dissolve to release Fe (II) and any metals adsorbed onto them. Copper and zinc were also present in significant amounts, probably as sulphides or associated with organic matter. Under anoxic conditions, sulphate-reducing bacteria use small organic molecules as substrates to reduce sulphate and produce hydrogen sulphide (Stumm and Morgan 1981). Hydrogen sulphide reacts readily with iron and other metals to form sulphide precipitates, and in the process, consumes acidity. Thus, the pH of the tailing should rise as Eh decreases when an anaerobic, reducing environment is established in the tailing.

Figure 7 shows that an inverse relationship exists between relative pH and relative Eh for the compost and tailing samples taken on day 160 of the simulation experiment. The Ploughed model samples showed the highest acidity and Eh. This trend is consistent with the expected rise in pH as reducing conditions become established. We conclude from these patterns that decomposition products in the fresh compost were fuelling a high rate of sulphate and iron reduction by sulphate-reducing and

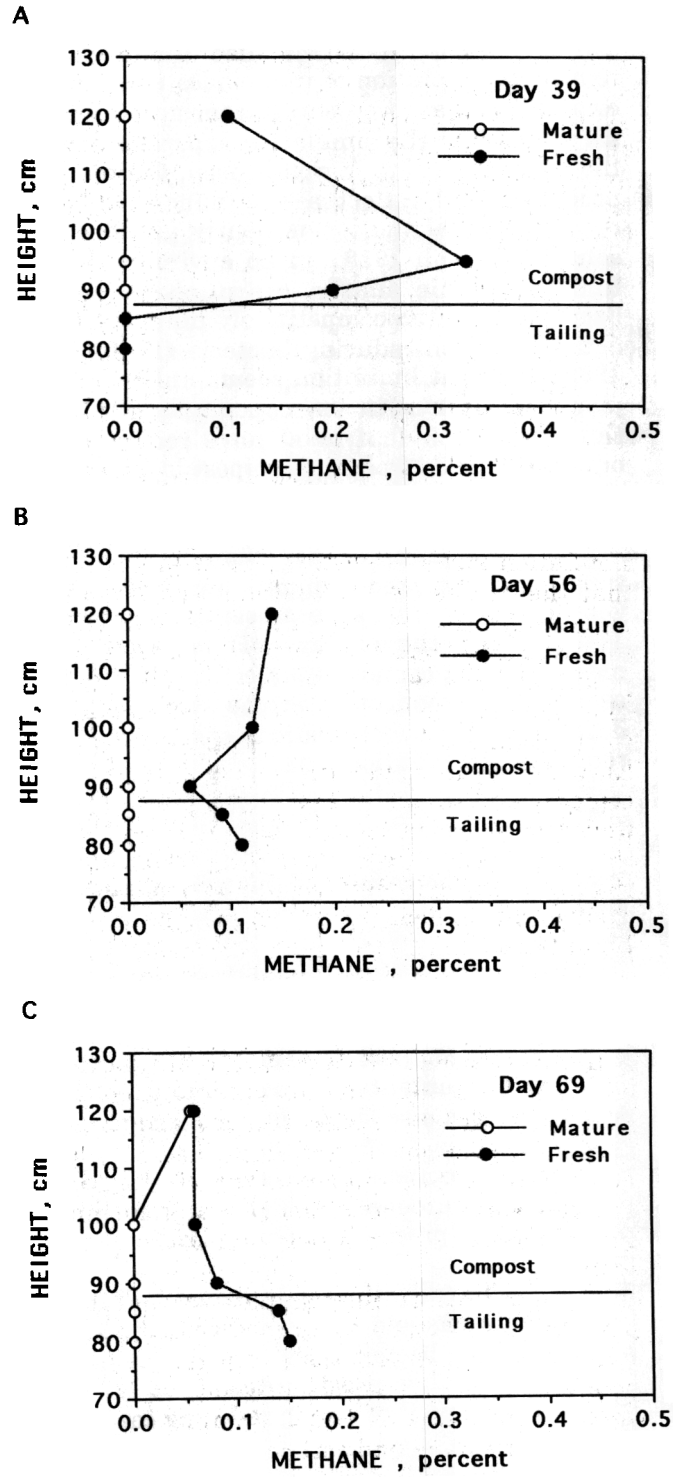

Figure 6. Profiles of methane in the Compost model mature and fresh compost treatments during the simulation experiment. (A) Day 39, (B) Day 56, (C) Day 69. (Note: The tailing-compost interface is at 88 cm)

iron-reducing bacteria. The formation of iron sulphide precipitate seen in the region of the tailing-compost interface also indicates that reductive dissolution of iron oxides and sulphate compounds was proceeding from approximately six weeks into the simulation experiment. Since the oxidized tailing is rich in iron, the reductive processes will reflect a dominance by Fe(III) reduction until the ion is nearly all gone from solution (Rowell 1988). In an environment with limited organic substrates, sulphate-reducing bacteria are often competitively inhibited by the activity of iron-reducing bacteria (Hedin *et al.* 1989), but that limitation seems unlikely in the ploughed layer or in the upper tailing layers in this simulation that must have received some organic leachate from the compost layer above it.

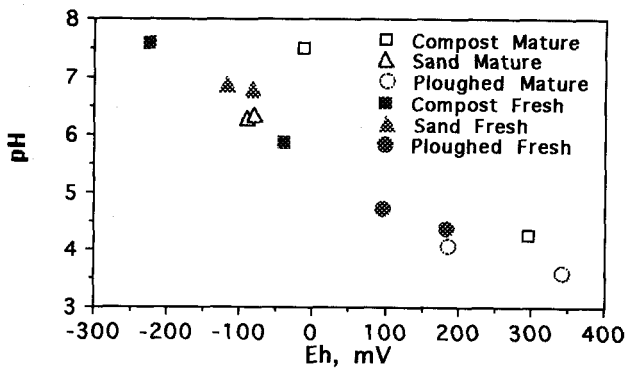

Figure 7. Relationship between relative redox potential (E_h) and relative acidity (pH) for tailing samples in the six cover layer treatments on day 160 of the simulation.

Trace metals other than iron were found only in low concentration in the six cover layer treatments and predominantly under acidic conditions and at high redox potentials. Five trace metals Ni, Cu, Zn, Co and Mn were present at somewhat higher concentration only when the relative Eh is above 100 mV and the relative pH is below 6. The magnitudes of these relative pH and relative Eh measurements cannot be directly applied to the in situ conditions in the column, but it seems clear that, as reducing conditions become stronger and pH rises under a compost cover layer, we can expect a decrease in the concentrations of trace metals in the tailing pore water as reductive dissolution shifts to reductive precipitation.

Conclusions

From the results of this preliminary study of compost cover layers on acid-generating tailing we have concluded-

- The Compost and Sand cover layer models were better at maintaining anoxic or other ameliorative conditions in the tailing than was the Ploughed model, during the six month simulation.
- Fresh compost treatments are much more effective than mature compost in maintaining high water content and strong reducing conditions in the region of the compost-tailing interface, and this was also shown by the formation of iron sulphide precipitate and methane.
- Fresh compost cover layers showed a great resistance to the conduction of water, that along with the maintenance of high water content, would seal off the tailing from infiltration of atmospheric oxygen, precipitation and surface water, thus forming a physical oxygen barrier.
- The mobilization of iron and sulphate was enhanced by the establishment of strong reducing conditions and the availability of organic substrates for the reductive dissolution of iron oxides by reducing bacteria. This may be a transient condition until iron and sulphur become immobilized as less soluble precipitates, such as sulphides. Trace metals become less mobilized with the development of strong reducing conditions and low acidity.
- Compost quality tests show that leachates from mature and fresh compost present a low environmental risk for use on mine lands. The cover layer simulation results indicates that in the compost-tailing system nitrates and metals will be quickly reduced. Additionally, the very low hydraulic conductivity of the fresh compost cover layer will inhibit vertical water flow through the compost layer and thus reduce the potential for the leaching of nitrogen compounds, acids, and metals from the compost-tailing system.

The experimental work has shown that a cover layer of MSW compost can be of benefit in the reclamation of oxidized tailing. However, the conclusions that we reached were based on a relatively short-term laboratory experiment that lacked natural environmental conditions and variability. Comprehensive, long-term field work should now be done to follow up on the potential benefits identified, and also those benefits that may have been overlooked by the current study.

References

Blowes, D.W., W.D. Robertson, and J.A. Cherry 1991. Nickel Rim Mine tailings investigation. Progress report, Nov. 30, 1991. Waterloo Centre for Groundwater Research, University of Waterloo.

Buttler, A.J., H. Dinel, M. Levesque, and S.P. Mathur. 1991. The relation between movement of subsurface water and gaseous methane in a basin bog with a novel instrument. Can. J. Soil Sci. 71:427-438.

Davé, N.K. and T.P. Lim 1989. Wetlands and their role in treating acid mine drainage - a literature review. Report MRL 89-107 LS, Elliot Lake Laboratory, CANMET.

Davé, N.K., and R.E. Michelutti 1991. Field evaluation of wet cover alternatives of high sulphide tailings. Final Report. In Proceedings of the Second International Conference on the Abatement of Acidic Drainage, Montreal, Sept. 16-18, 1991. Vol. 3. pp. 61-81.

Hedin, R.S., R. Hammack, and D. Hyman 1989. Potential importance of sulphate reduction processes in wetlands constructed to treat mine drainage. In Hammer, D.A. (ed.), Constructed wetlands for the treatment of acid mine drainage. Report of the U.S. Bureau of Mines. p. 508-514.

Nicholson, R.V., R.W. Gillham, J.A. Cherry, and E.J. Reardon 1989. Reduction of acid generation in mine tailings through use of moisture-retaining cover layers as oxygen barriers. Can. Geotech. J. 26:1-8.

Otten, L. 1993. Experimental and theoretical study of the Guelph pilot scale solid waste composter. RAC Project 501G. Report prepared for the Ontario Ministry of the Environment and Energy by the School of Engineering, University of Guelph. May 1993.

Pierce, W.G. 1992. Reclamation of sulphide tailings using municipal solid waste compost: literature review and recommendations. Report prepared for Falconbridge Ltd. by the Centre in Mining and Mineral Exploration Research, Laurentian University, Sudbury, ON. July 1992.

Rowell, D.L. 1988. Flooded and poorly drained soils. In A. Wild (ed.) Russell's soil conditions and plant growth. Eleventh ed. Wiley, New York. p. 899-926.

Stumm, W. & J.J. Morgan 1981. Aquatic chemistry. Second ed. Wiley, New York.

Acknowledgements

We would like to acknowledge the financial support of Falconbridge Limited and the MEND program of the Ontario Ministry of Northern Development and Mines, and the Canadian federal government. The Ontario Geological Survey Geoscience Laboratory provided laboratory space in the Willet Green Miller Centre and use of other facilities for the project. We would like to thank Dr. Hugh DeSouza (Section Chief), Dr. Jean Richardson, Ms. Natalie Vigneault, and Dr. Bonnie Blackwell for the many forms of help they have given our project. The University of Guelph Compost Study group under Dr. Lambert Otten has also been extremely helpful in providing both advice and compost for our study. Rodney Stuparyk did the compost preparation and characterization as part of his M.Eng. project. Lakefield Research of Falconbridge Ltd. did the analyses of compost quality. Terry Dinsmore and Monica Illescas provided technical assistance at Laurentian University.

COMPACTION BEHAVIOUR OF LIGHTLY CEMENTED SANDSTONE AS A RESULT OF DEWATERING[1]

Hamid R. Nikraz[2], Martin E. Press[3], and Anthony W. Evans[4]

Abstract: Deep mining in the Collie Basin has suffered from a high level of water flow and sediment in-rushes throughout its century long history. A major source of these problems is the very extensive system of weak, saturated, sandstone aquifers. As a result, past underground operations have been limited to room and pillar extraction achieving 30 to 40 percent recovery. In order to increase the recovery to approximately 70%, the Wongawilli method of short-wall mining has been introduced. Extensive aquifer dewatering was carried out to enable this mining method to be applied. The porous and weak nature of the aquifers provides a potential source of subsidence with a significant risk of environmental instability on a large scale. This is particularly critical adjacent to town sites and industrial complexes and therefore an enhanced understanding of strata mechanics to enable confident application of engineering design. Controlled strata deformation was required for safe operations and limit surface subsidence.

A triaxial technique has been adapted to evaluate the compaction characteristics of the sandstone aquifer in the Collie Basin under conditions anticipated during dewatering operations. This technique, which allows the strata stress regime to be reproduced by triaxial loading with zero lateral strain, also provides a precise evaluation of lateral stresses and consequently Poisson's ratio under in situ conditions.

The paper contains a description of the equipment commission, test techniques, results, analysis, and interpretation of the data obtained.

The testing evaluation techniques are general in nature and can be applied to field situations in locations where similar weak sandstones occur.

Introduction

The Collie Basin lies nearly 200 km south-south-east of Perth in Western Australia and is 27 km long by 13 km wide, covering an area of approximately 230 km^2 (fig 1). It contains extensive reserves of good steaming coal, which is currently being mined by both open cut and underground methods.

The Collie Coalfield has a long history of strata control problems. They manifest themselves in the form of localized poor roof control, surface subsidence, slope instability, and mine abandonment (due to a sand-slurry inrush). Major sources of these problems include the very extensive, weak, saturated, sandstone aquifers. As a result, underground operations have been limited to room- and pillar- extraction, presently carried out by continuous miners and road-heading machines. Approximately 30% to 40% recovery by volume is being achieved by this method.

---

[1]Paper presented at the International Land Reclamation and Mine Drainage Conference and the Third International Conference on the Abatement of Acidic Drainage, Pittsburgh, PA, April 24-29, 1994.

[2]Hamid R. Nikraz (BE, MSc, PhD, MIEAust, CPEng), Lecturer, School of Civil Engineering, Curtin University of Technology, Perth, Western Australia

[3]Martin E. Press (BE Hons, FIEAust, FAusIMM, FASCE, CPEng), Head of Graduate Studies, School of Civil Engineering, Curtin University of Technology, Perth, Western Australia

[4]Anthony W. Evans (JP, MSc, DIC, FIMinE, C Eng, FIMM, FIEMS, FMVS), Head, Collie Federated School of Mines, Curtin University of Technology, Collie, Western Australia

To increase the recovery to approximately 70%, the Wongawilli method of short-wall mining has been introduced. Caving of this immediate roof is integral with this method. Extensive aquifer de-watering was carried out to enable this mining method to be applied. The porous and weak nature of the aquifers provides a potential source of subsidence (due to pore closure) and strata failure (due to increasing the effective stress), as a result of pore pressure reduction upon de-watering. The proposed development of multiple seam extraction below areas sensitive to surface subsidence has increased the need to establish the strata mechanical properties. This will assist in confident application of rock mechanics principles for predictive modeling of strata behaviour.

The roof dewatering-depressurization procedure involved a combination of in-mine vertical roof drainage holes and conventional dewatering bores constructed from the ground surface above the mining area. A full account of the dewatering strategy may be found elsewhere (Humphreys and Hebblewhite 1988, Dundon et al 1988).

Of prime concern is the effect of pore pressure reduction upon strata compaction. To simulate those effects, it is necessary to perform tests under triaxial conditions of the same order as experienced in situ. The pore pressure effect phenomenon is not a new concept. However, investigation of the effect under triaxial conditions is relatively new. Although rock bulk compressibility figures are generally larger for high porosities, simple compressibility porosity correlations do not exist. Furthermore, compressibility data reported for poorly consolidated sandstone differ greatly. This paper describes the equipment and the techniques and procedures used in carrying out deformation studies of poorly-consolidated sandstone in Collie Coal Basin.

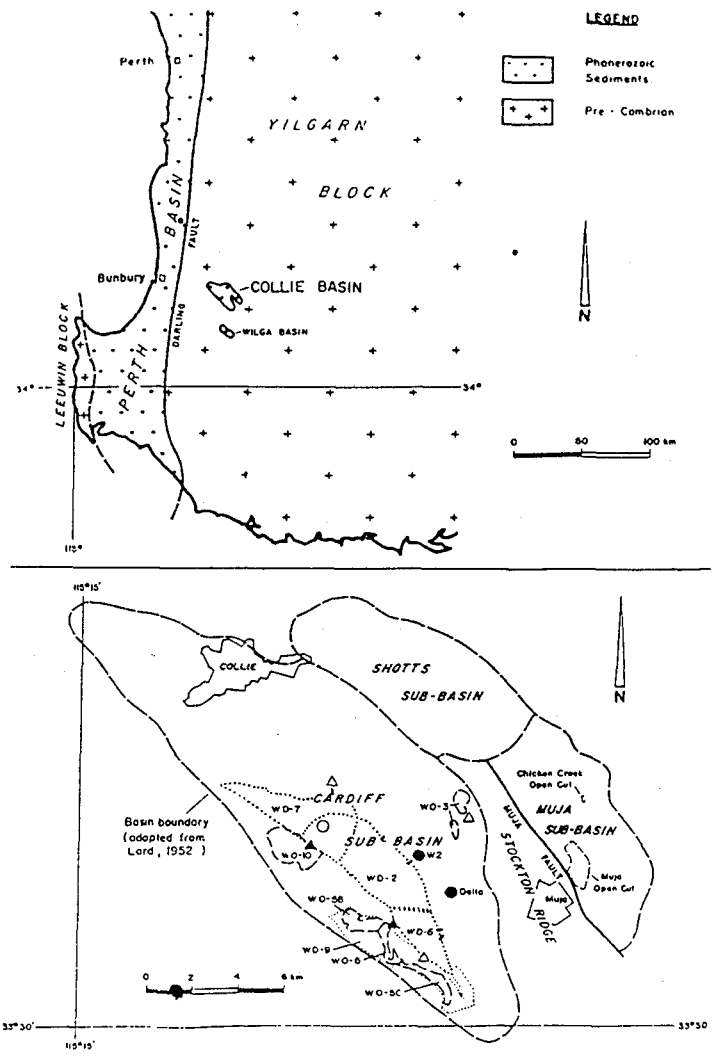

Figure 1. Collie Coal Basin, location and regional geological setting.

Regional Geology and Hydrology

The Collie Basin is comprised of two unequal lobes in part separated by a fault-controlled, basement high known as the Stockton Ridge. The basin itself consists of three sub-basins, the Cardiff, Shotts, and Muja (fig 1).

The Collie Basin sediments are mainly cyclic, high-energy fluviatile sandstones with thin gravel and conglomerate lenses. Siltstones and shales occur as overbank, lacustrine, or paludal deposits. Coal seams are remarkably uniform in thickness and composition over considerable distances.

The Collie Basin sediments can be described as saturated and weak, and have been altered through weathering or post-depositional processes. Lowry (1976) estimated that the coal measures were composed of 65% sandstone, 25% shale and claystone, and 5% coal.

The whole Collie Basin can be thought of as an interrelated groundwater system of Permian coal measures bounded by Archaean basement.

Permeable aquifers comprise fine to granular quartzose sandstones with little fines content. Moderately permeable material consists of silty-clayey sandstones. Siltstones represent the low to moderately permeable aquifers; whilst mudstone, shale, and coal layers form the system aquitards.

All coal seams in the deep mines are bounded by aquifers. In some locations aquifers are situated directly above or below the seams; however, most areas have aquitard barriers of variable thickness separating the mining seam from neighbouring aquifers (fig 2).

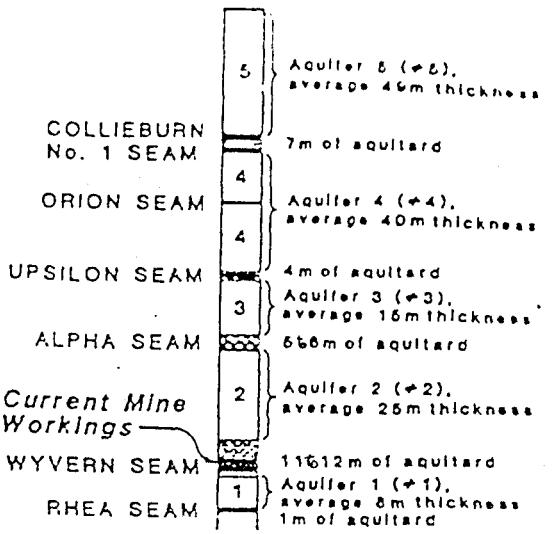

Figure 2. Generalised hydrostratigraphy.

Geomechanical Properties of the Coal Measures

The geology of the Collie Basin can vary within short intervals, both vertically and laterally. There are also marked variations within the major lithologies (sandstones, shales, siltstones, laminites). Each has a wide range of engineering properties, dependent on past and present geological processes. Table 1 below lists typical ranges of compressive strengths, elastic moduli, cohesive strengths, and friction angle for each major lithology of the Collie coal measures (Humphreys and Hebblewhite 1988). This table highlights the weak and plastic nature of Collie sediments and also illustrates that coal strengths are about two to three times greater than those of non coal lithologies. In terms of subsidence, the resistance to movement of non coals is small, and thus there is the possibility that coal seams will deform differentially and lead to bed separations at coal contact.

Table 1. Typical mechanical properties of Collie coal measures.

Lithology	UCS, MPa	Elastic modulus, MPa	Cohesive strength, MPa	Friction angle, deg
Sandstone	5.2	300	0.5	32
Siltstone	4.7	600	0.6	25
Laminite	4.7	700	0.7	25
Shale	7.0	1,200	0.8	22
Wyvem coal	19.8	2,000	2.0	42

Rock Movements Caused by Dewatering in Poorly Consolidated Sandstone

Land subsidence is caused by a number of mechanisms. Two such mechanisms are the withdrawal of fluid and the collapse of underground openings. This study is concerned with subsidence that results from the withdrawal of fluid.

The deformations resulting from equilibrium disturbance of the saturated lightly cemented sandstone aquifer due to water pressure decline are either elastic or non-elastic. Elastic deformations are mostly of a negligible extent with respect to both the involved surface subsidence and the reserve of the stored water, being only of importance in respect to the variation of the rate of flow.

The extents of the non elastic deformations are due to compaction or migration of the lightly cemented rock material. The former depends on the geotechnical characteristics of the rock, and on the extent of the pore pressure reduction. The extent of migration, on the other hand, depends on the pressure gradient (the flow velocity). The compaction may cause regional subsidence, while the migration of the granular particles causes local displacement, both phenomena being dependent upon the characteristics of the aquifer rock and the extent of dewatering.

Several techniques are available for predicting subsidence due to fluid withdrawal. They have been classed by Poland (1984) into three broad categories: empirical, semi theoretical, and theoretical. Empirical methods essentially plot past subsidence versus time and extrapolate into the future based on a selected curve fitting technique. However, empirical methods suffer from the lack of well documented examples to establish their validity. Semi theoretical methods link on going induced subsidence to some other measurable phenomenon in the field. Theoretical techniques require knowledge of the mechanical rock properties, which are either obtained from laboratory tests on core samples or deduced from field observations. Essentially, however, theoretical techniques use equations derived from fundamental laws of physics, such as mass balance. Thus, the method described in this paper may be classified as a theoretical technique.

Geertsma (1973) has shown in a theoretical analysis that reservoirs deform mainly in the vertical direction and that lateral variations may be discarded if the lateral dimensions of the reservoir are large compared with its thickness. For the one-dimensional compaction approximation, the vertical deformation of a prism of the aquifer material can be computed by (Geertsma 1966)

$$\Delta h = C_m \, h \, \Delta P \tag{1}$$

where Δh (mm) is the change in the prism height, C_m $(MPa)^{-1}$ is the one-dimensional compaction coefficient, h is the prism height, and ΔP (MPa) is the change in pore fluid pressure. Readers interested in limitation of equation 1 are referred to the original work of Geertsma (1966, 1973).

A similar approach to that used by Geertsma (1966, 1973) was adapted by Martin and Serdengecti (1984). Martin and Serdengecti (1984) report that in most cases C_m is the most difficult of the three one-dimensional compaction parameters to determine and suggest that the best way to obtain values of C_m is to measure it on core samples in the laboratory.

The one-dimensional compaction coefficient 'C_m' of friable sandstones can be measured by different methods: (1) indirect measurement by measuring rock compressibility 'C_b' under hydrostatic load and estimating Poisson's ratio of the rock and (2) direct measurement by equipment that simulates the aquifer boundary condition of zero lateral displacement (such as Oedometer cell test or a modified triaxial cell test). Although the triaxial test method is laborious and time consuming, its unique experimental conditions make it essential because they reproduce aquifer stress quite well. In addition, the triaxial setup has the advantage that the circumferential pressure needed to prevent lateral stain is measurable. The Poisson's ratio of the rock sample can therefore be determined independently from the ratio of lateral to vertical stresses.

Laboratory-determined Compressibilities

The cores taken from the Collie Basin show marked variations in both porosity and grain correlation. Medium to high porosities are found in consolidated and semi consolidated sections. In addition, the nonhomogeneous appearance of the cores suggests that the rock's properties vary over short distances. Consequently, compaction is expected to vary considerably with depth, implying that the cores must be sampled systematically at short intervals to obtain a reliable compaction profile. As this involves compaction measurements on a large scale, a simple, rapid, but nevertheless reliable measuring technique must be adopted.

The earlier studies by Grassman (1951), Biot (1941), Geertsma (1957), and Van der knaap (1959) resulted in the theory of pore elasticity. They demonstrated that the compaction behaviour depends only on the effective frame stress, i.e., the difference between external and internal stresses. Furthermore, the results obtained by Nikraz (1991) confirmed that the effective stress theory is applicable to Collie sandstone. Therefore, to

simulate aquifer compaction in a laboratory experiment requires the application of the stress difference instead of the actual pressures. Thus, experimentally the most attractive approach is to load the samples externally, keeping the pore water pressure constant and atmospheric.

Thus, a triaxial technique was adopted to predict the compaction behaviour of strata due to dewatering, in particular for the weakly cemented Collie sandstone. This technique, which allows the strata stress regime to be reproduced by triaxial loading with zero lateral strain, also provides a precise evaluation of lateral stresses and consequently Poisson's ratio under in situ stress conditions. The condition of zero lateral strain during triaxial compaction test was achieved both by preventing any volume change in the cell-water system surrounding the specimen and by using the modified piston and top cap (fig 3). This piston was of the same diameter as the sample; it therefore induced the triaxial stress in the sample, but not the deviator stress. Because bulk volume change was detected from pore volume changes, the pores of the specimens had to be completely saturated. A full detail of the equipment design may be found in Nikraz (1991).

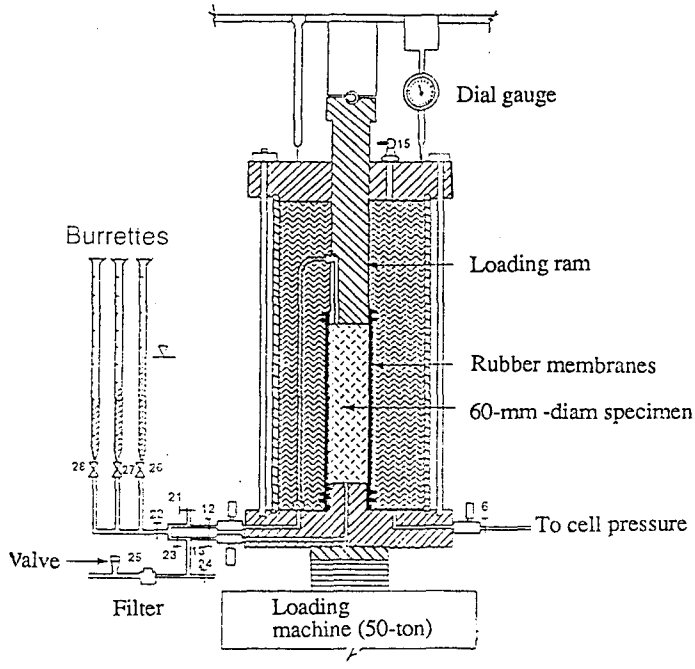

Figure 3. Arrangement of apparatus for compaction test.

The experimental procedure comprised two stages: (1) the preparatory stage, in which the specimen was brought into an "initial" loading state prior to the test, and (2) the test itself, which further compacted the specimen.

To eliminate possible membrane penetration effects during the test and thereby avoid errors in test results, the specimens were first loaded hydrostatically to a pressure of 1.25 MPa. The volume change related to this pressure was assumed as a reference point. The axial stress was then measured continuously at a constant rate until the desired axial stress was achieved. The cell pressure was adjusted simultaneously to prevent any lateral strain. However, the maximum axial stress level was confined within cell pressure limitation (maximum cell pressure limited to 12 MPa).

Therefore to check the zero lateral strain, the following relationship had to be satisfied:

$$\Delta V = (A\ X)/1000 \qquad (2)$$

where ΔV = volume change (mL),
A = cross sectional area of the specimen (mm^2),
and X = axial deflection (mm).

To determine the effect of loading history on compaction, the axial stress was released incrementally to approximately 1.5 MPa. Consequently, the confining pressure was adjusted to satisfy equation 2. The loading and unloading were repeated for another two cycles.

A total of six tests were made on specimens at strain rate of $2 \times 10^{-4} min^{-1}$.

Results Analysis and Interpretation

Measurements were made on six core samples taken from four locations in the Collie Coal Basin (table 2).

Table 2. Sandstone properties.

Sample	Location	Depth, m	UCS, MPa	Initial porosity, %	Permeability, 10^{-8} m/s
1	D156	286.00	3.351	20.50	36.22
2	D157	262.88	5.895	17.65	18.33
3	D157	264.26	5.201	18.05	20.62
4	D157	266.70	4.783	18.78	21.64
5	D158	259.30	3.481	22.09	34.07
6	Western 6	125.00	2.311	23.10	41.311

Typical axial stress-uniaxial compaction and lateral stress-uniaxial compaction are shown in figures 4 and 5 respectively. Similar behaviour was observed in five other specimens.

The three significant features of the stress-uniaxial compaction curves are their non linearity, hysteresis, and irrecoverable compaction on loading. Microstructural changes that produce permanent strain are a likely source of cycling effects. For example, assume that a microstructural element such as an asperity contributes to the elastic response of a rock by separating two grains. If the asperity is crushed subsequently at a high pressure, then later strain curves will be different because of the absence of the asperity. The unloading to atmospheric pressure is believed to have a significant role in stress cycling effects. When cracks are created and asperities crushed, they are probably pinned because of the high confining pressure. However, when the confining pressure is released, the microstructure can deform along new degrees of freedom and thus behave differently when reloaded. Other likely mechanisms that produce permanent strain are displacement of fines and clay minerals, and frictional sliding on grain contacts (Brace et al 1966, Batzle et al 1980).

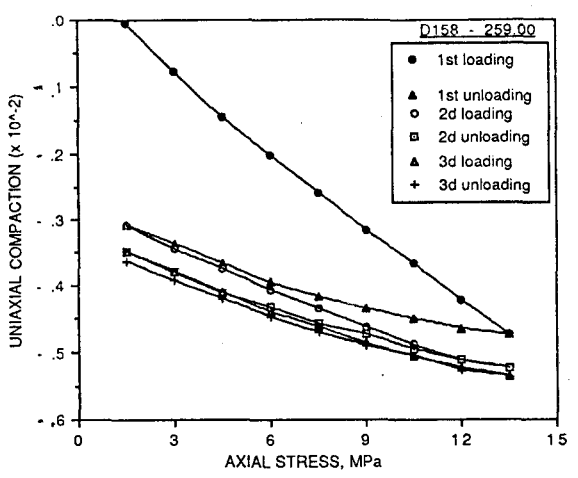

Figure 4. Typical axial stress-strain compaction relationship with three loading cycles.

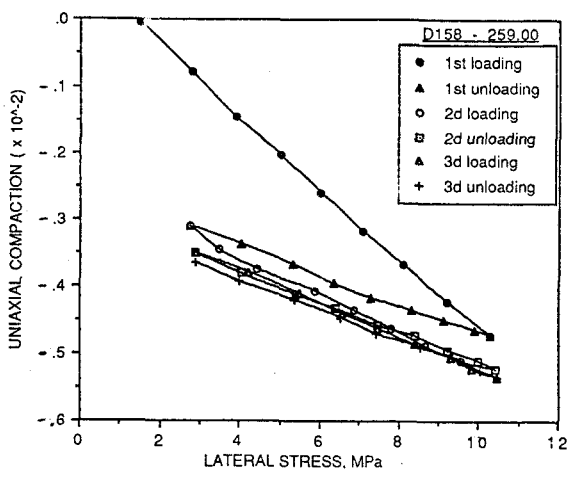

Figure 5. Typical lateral stress-strain compaction relationship with three loading cycles.

The problem of choice of loading cycle for field application has been studied by Knutson and Bohor (1963), van Kesteren (1973), Mattax et al (1975) and Mess (1978). The work of Mess (1978) suggests that for fully undisturbed unloaded core material, compressibility values derived in laboratory tests should be lower than in situ values for reservoirs that are not overconsolidated. For overconsolidated reservoirs they could be either too low or too high for in situ application, depending on the degree of overconsolidation of the reservoir rock.

It is suggested by Knutson and Bohor (1963) that a reasonable compressibility value may be obtained by averaging values from the first and subsequent cycle. However, in extensive laboratory and in situ tests on relatively soft rock, Mattax et al (1975) suggested that the first cycle compressibility is the most realistic measure of in situ response to changes in effective pressure that occur during reservoir depletion. It was mentioned, however, that erroneously high values of first cycle compressibility are obtained in laboratory tests on unconsolidated sands because of systematic experimental error (caused by freezing and thawing of the sample and some grain crushing). It was therefore recommended that about two thirds of the first cycle compressibility be taken as representative of in situ compaction.

The uniaxial compaction curves representing the six samples tested are plotted for figure 6 for the first loading cycles. The graph shows an almost linear compaction-stress relationship for higher stresses, so that average compaction per unit stress can be calculated for this range. Further, it is noted that the compaction curves are parabolic. Thus, there is an observed relationship:

$$\varepsilon_1 \alpha \sqrt{\sigma_1'} \tag{3}$$

where ε_1 = axial strain

and σ_1' = axial effective stress.

To demonstrate the observed relationship, the axial strains have been replotted against σ_1' as shown in figure 6. This plot provides strain lines, although it is noted that some points deviate slightly from linearity. By using the linear relationship as shown in figure 7, the uniaxial compaction coefficient, C_m, may be calculated over the relevant stress interval.

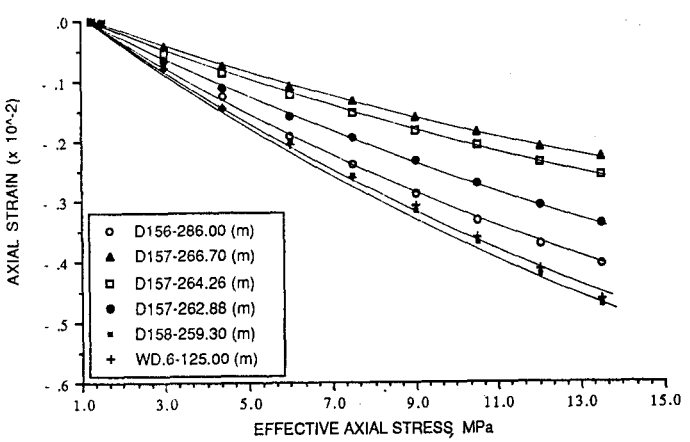

Figure 6. Relationship between axial strain and effective axial stress for first loading.

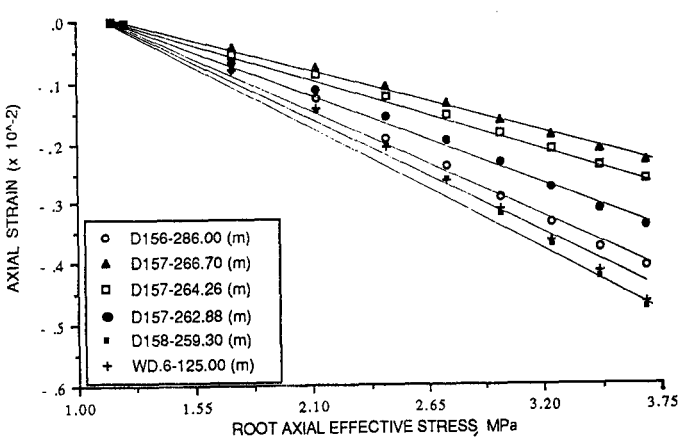

Figure 7. Relationship between axial strain and root of effective axial stress for first loading.

Consider the simulation of dewatering operations for a typical specimen such as D156-286. Assuming an average overburden density of 2.5 st/m^3, the initial in situ hydrostatic effective stress 7 MPa would increase to 9 MPa to simulate the effects of dewatering. Hence the uniaxial compaction can be calculated by

$$C_m = \frac{(e_1)_9 - (e_1)_7}{9 - 7} \tag{4}$$

where $(e_1)_7$ and $(e_1)_9$ are axial strain at hydrostatic effective stresses of 7 and 9 MPa, respectively.

$$C_m = \frac{(0.288 - 0.277) \times 10^{-2}}{2} \tag{5}$$

The uniaxial compaction coefficient data corresponding to first, second, and third loading cycles are plotted as a function of initial porosity in figure 8. It appears that compaction is greater for the first loading, indicating loading history influences on compaction. However, those correlations serve to assess a reliable average field value of the uniaxial compaction coefficient, which is required for a prediction of field compaction.

In an early study (Nikraz, 1991), the average porosity obtained from 105 samples tested as 20.77% of bulk volume, although variation in porosity between holes was considered to be minor. This and the near-linear relationship between uniaxial compaction and porosity prompted the acceptance of 20.77% porosity for the determination of an average value of the uniaxial compaction coefficient.

Based on the first loading cycle, figure 8 indicates a uniaxial compaction coefficient of 3.124×10^{-4} $(MPa)^{-1}$. The effects of stress relief upon sampling are accommodated within this value. However, the second and third loading cycles exhibit elastic compaction characteristics and provide an average value of uniaxial compaction coefficient for the second and subsequent loading cycles of 1.6409×10^{-4} $(MPa)^{-1}$.

The difference between two values indicates the elastic component of compaction. Considering the strain hardening and core disturbance arguments one may expect the true compaction to be somewhere in between. In view of the quite small difference between maximum and minimum values, the most practical approach seems to be to take the average as a working value, thus reducing the uncertainty to an acceptable limit. Thus, a mean value of 2.382×10^{-4} $(Mpa)^{-1}$ was used to represent the in situ compaction coefficient.

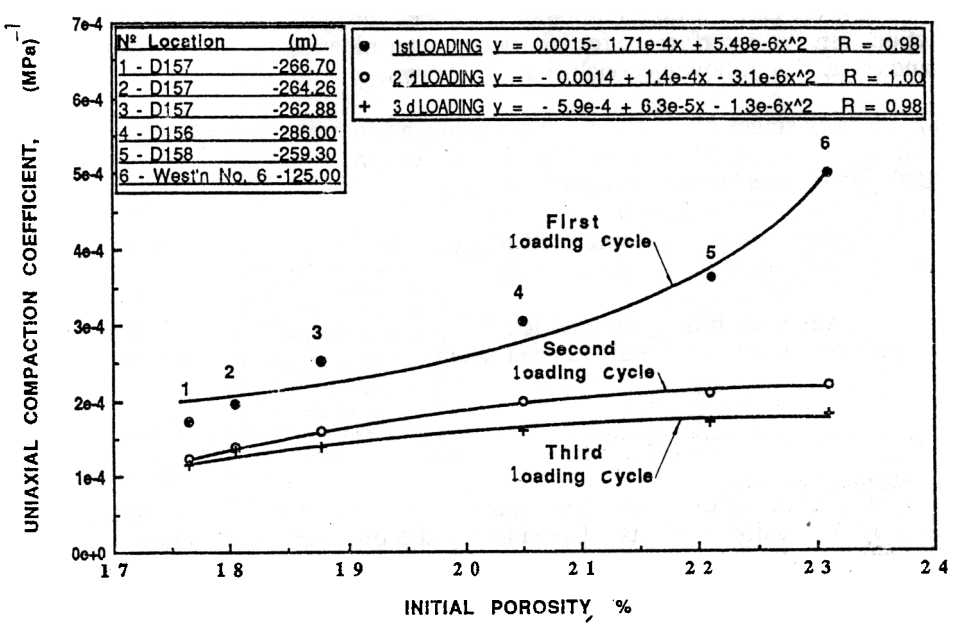

Figure 8. Relationship between uniaxial compaction coefficient and initial porosity for first, second and third loading.

Applying these results to a 12.5 m thick aquifer above the Collieburn No. 2, with an ultimate reduction in pore water pressure of 2.0 MPa, could produce a vertical compaction of

$$\Delta h = C_m h \ \Delta P \tag{6}$$

$$= 2.382 \times 10^{-4} \times 12.50 \times 10^{3} \times 2.0$$

$$= 5.96 \text{ mm}$$

The Poisson's ratio of the specimens tested can be determined independently using the ratio of lateral to vertical stresses. The ratio of lateral to vertical stresses under isotropic conditions suggested by Teeuw (1971) is

$$\frac{\sigma_h}{\sigma_v} = \left(\frac{\nu}{1 - \nu}\right)^{1/n} \tag{7}$$

where ν is the Poisson's ratio and n is the exponent in relationship of the uniaxial compaction-axial pressure in figure 4. The exponent reflects the deformation of the contact points and/or contact areas between grains (Brandt 1955). According to Hertz's theory (Timoshenko et al 1951) for perfect spheres $\nu = 2/3$, while for linear elastic media such as nonporous quartz and steel, $\nu = 1$, reducing equation 7 to the well known equation,

$$\frac{\sigma_h}{\sigma_v} = \frac{n}{} \tag{8}$$

For ideally elastic materials, a variation in ν thus reflects a change in grain sphericity at the point of contact between adjoining grains. The values of n for the specimen tested range from 0.869 to 0.982. This range is higher than the value of 0.677 for spheres and indicates flatter contact surfaces.

Conclusion

Special purpose - designed triaxial testing equipment has been designed, tested, and commissioned. A series of uniaxial compaction tests were performed for laboratory determination of compressibilities and in situ behaviour of the Collie sandstone. The following conclusions are drawn.

While recognizing the early stages of development of subsidence prediction, some deformation has been postulated based on laboratory observations. In situ monitoring of strata deformation will be required for verification of the actual deformation mechanisms at work.

It has been observed that the uniaxial compression of Collie sandstone is characterized by significant nonlinearity, hysteresis, and an irrecoverable strain on unloading.

Uniaxial compaction curves have been presented for the sandstone aquifer in the Collie Basin. It was found that the uniaxial compaction curves were parabolic over the major part of the stress range. This yielded the expression

$$\varepsilon_1 \ \alpha \ \sqrt{\sigma_1'} \tag{3}$$

A good correlation was found to exist between uniaxial compaction coefficient and porosity. The correlation was quantified by regression analysis. Considering the different compaction behaviour of the specimens in the first and subsequent loading cycles, an average value for uniaxial compaction coefficient equal to 2.382×10^{-4} $(MPa)^{-1}$ was obtained for an average porosity of 20.77%.

Literature Cited

Batzle, M.L., G. Simmonds, and R.W. Siegfried. 1980. Microcrack closures in rocks under stress: direct observation. J. Geophys. Res. 85:7072-7090.

Biot, M.A. 1941. General theory of three-dimensional consolidated ion. J.App.Phys. 12:155-162.

Brace, W.F., B.W. Paulding, and C. Scholz. 1966. Dilatancy in the fracture of crystalline rocks. J.Geophys Res. 71(16):3939-3958.

Brandt, H. 1955. A study on the speed of sound in porous granular media. J.Appl.Phys. 22:479.

Dundon, P.J., D. Humphreys, and B. Hebblewhite. 1988. Roof depressurisation for total extraction mining trials, Collie Basin, Western Australia. p. 743-752. In 3rd International Mine Water Congress (Melbourne, Australia).

Grassmann, F. 1951. "Uber die Elastizitat Poroser Medien", Vierteljahrschrift der Naturforschenden Gesellschaft in zurich, 96(1): Sec. 1-51.

Geertsma, J. (1957). The effect of fluid pressure decline on volumetric changes of porous rock. Trans.AIME. 210:331-430.

Geertsma, J. 1966. Problems of rock mechanics in petroleum production engineering. p. 584-594. In Proceedings, First Congress of the International Society of Rock Mechanics, Lisbon, Vol 1.

Geertsma, J. 1973. Land subsidence above compacting oil and gas reservoirs. J.Petrol.Technol. 25:734-744.

Humphreys, D., and B.K. Hebblewhite. 1988. Introduction of total extraction mining in conjunction with strata dewatering at Collie, Western Australia. Coal. Australian Coal Min.Tech. and Res. 19:45-56.

Lowrt, D.C. 1976. Tectonic history of the Collie Basin, Western Australia. Geol. Soc. Australia J. 23:95-104.

Knutson, C.F., and B.F. Bohor. 1963. Reservoir rock behaviour under moderate confining pressure. In Rock Mechanics, Proceedings, 5th Rock Mechanics Symposium. Macmillan, New York.

Martin, J.C., and S. Serdengecti. 1984. Subsidence over oil and gas fields. p. 23-34. In T.L. Holzer. (ed), Man-induced land subsidence. Rev.Eng. Geol. VI, The Geol Soc. of America.

Mattax, C.C., R.M. McKinley, and A.T. Clothier. 1975. Core analysis of unconsolidated and friable sands. J.Petrol.Technol. p.1423.

Mess, K.W. 1978. On the interpretation of core compaction behaviour. p.76-91. In K.S. Surendra (ed), Evaluation and prediction of subsidence. Am. Soc. of Civil Eng.

Nikraz, H.R. (1991). Laboratory evaluation of the geotechnical design characteristics of the sandstone aquifer in the Collie Basin. Ph.D. Thesis, Curtin University of Technology, p. 317.

Poland, J.F. 1984. Guide to the study of land subsidence due to ground-water withdrawal. United National Educational, Scientific, and Cultural Organisation, Paris.

Timoshenko, S., and J.N. Goodier. 1951. Theory of elasticity. McGraw-Hill, New York.

Van der Knaap, W. 1959. Non-linear behaviour of elastic porous media. Trans. AIME. 216:179-187.

Ven Kesteren, J. 1973. Estimate of compaction data representative of the Groningen Field. Verhandelingen Mijnbouwkundig Genootschap. 28:33-42.

ASSESSMENT OF ACID MINE DRAINAGE REMEDIATION SCHEMES ON GROUND WATER FLOW REGIMES AT A RECLAIMED MINE SITE[1]

M. A. Gabr[2], J.J. Bowders[3], and M. S. Runner[4]

Abstract: Ground water modeling and a field monitoring program were conducted for a 35-acre (150,000 m^2) reclaimed surface mine site that continues to produce acid mine drainage (AMD). The modeling effort was focused on predicting the effectiveness of various remedial measures implemented at the site for the abatement of AMD production. The field work included surface surveys and monitoring of ground water levels with time, seepage areas, and sedimentation ponds located on the site. The surveys provided the physical and topographic characteristics of the site. Pump tests conducted at the site provided general hydraulic conductivities (k) for two major areas of the site; undisturbed area ($k \simeq 2.9 \times 10^{-5}$ ft/s or 8.7×10^{-6} m/s) and disturbed area ($k \simeq 3.3 \times 10^{-4}$ ft/s (1×10^{-4} m/s) to 2.0×10^{-3} ft/s (6.2×10^{-4} m/s)). The monitored ground water data indicated rapid change in ground water levels during recharge events. Such behavior is indicative of flow regime that is dominated by fracture flow. Modeling of an approximately 700 ft by 1500 ft (213 m x 457 m) area of the site was achieved using the US Geological Survey code MODFLOW, and ground water field measurements were used to calibrate the model. A hydraulic conductivity of approximately 1.15×10^{-3} ft/s (3.5×10^{-4} m/s) was estimated for the undisturbed area and 1.15×10^{-2} ft/s (3.5×10^{-3} m/s) was estimated for the reclaimed area. Remedial measures for diverting the ground water away from the areas of spoil included the use of a subsurface seepage cutoff wall and discrete sealing techniques. Modeling results indicated that the most effective remedial technique for this site is the use of a subsurface seepage cutoff wall installed at the interface (highwall) between the disturbed and undisturbed zones. Using this scheme caused a dewatering effect in the reclaimed area and therefore reduction in the volume of the AMD generated at the site.

Additional Key Words: acid mine drainage, coal refuse, ground water, grouting

Introduction

AMD poses a serious environmental problem in the United States. Kleinmann (1989) estimated that abandoned coal and metal mines and the mine waste that accompanies them adversely affect water quality in 12,000 miles of streams and rivers and 180,000 acres of lakes and reservoirs. AMD forms due to the oxidation of sulfide minerals and subsequent hydrolysis during and after the mining process. Chemical reactions associated with the production of AMD were presented by Stumm and Morgan (1970). The presence of pyrite material (FeS_2), water, and air is required for generation of AMD. The AMD pollution leads to low pH values, increased turbidity, and increased concentration of metals such as iron, and manganese and elements such as sulfates. The advent of clean water standards mandated by Federal laws such as the National Pollutant Discharge Elimination System (NPDES) and Wetlands Mitigation necessitates the development of cost effective and innovative remedial measures for regulatory compliance.

One of the emerging remedial techniques for abatement of AMD is the use of subsurface grouts to encapsulate and divert ground water from areas containing the pyrite material. Harshberger (1991), Almes (1991), and Baker (1993) investigated the development of grout mixtures for formation of subsurface low permeability hydraulic

---

[1]Paper presetned at the International Land Reclamation and Mine Drainage Conference and the Third International Conference on the Abatement of Acidic Drainage, Pittsburgh, PA, April 24-29, 1994.

[2] Assistant Professor, Dept. of Civil Engineering, West Virginia University, Morgantown, WV 26505-6101.

[3] Associate Professor, Dept. of Civil Engineering, West Virginia University, Morgantown, WV 26505

[4] Civil Engineer, United State Geological Survey, Jackson, MS (formerly, Graduate Research Assistant).

barriers. In general, the function of these barriers is twofold; (1) control of AMD migration to stream reaches and rivers and (2) encapsulation of the spoil material to minimize exposure to water and air and therefore to minimize AMD production. As part of the ongoing research program for development of low permeability subsurface barriers, a 35 acres test site near Waynesburg, PA, was selected for field demonstration. Application of subsurface grout mixes to this test site was performed by US Bureau of Mine, Pittsburgh Research Cnetere, in cooperation with the authors.

The research presented in this paper includes the modeling of the ground water flow regime before and after subsurface grouting. The simulation model is developed using the computer code MODFLOW by the US Geological Survey (USGS). Monitored ground water wells installed at the site were used to calibrate the computer model. Various modeling scenarios for simulating the placement of low-permeability grouts were conducted. Recommendations regarding the various grouting schemes and the most effective one for abatement of AMD are presented.

Research Site

The study site is located in Greene County, PA. The site encompasses 35 acres of reclaimed surface mine that currently produces approximately 20 gal/min of AMD under steady-state conditions. Figure 1 shows an overview of site area.

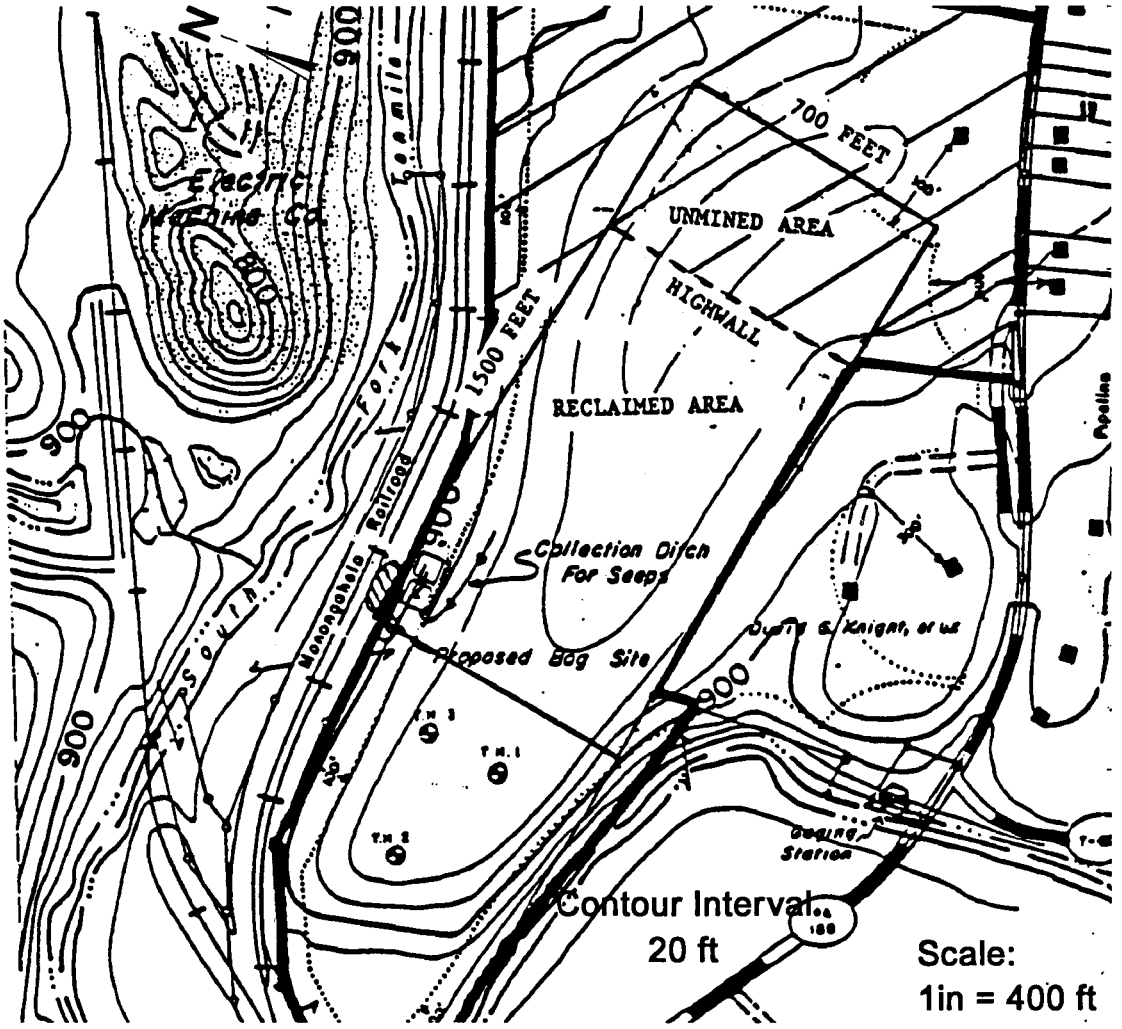

Figure 1. General overview and surface elevations of the study site

The AMD discharge exits the site in the form of seeps at several locations. These seeps are routed to aeration and sedimentation ponds and then pumped to a central location for lime treatment. The main coal seam on the site is the Waynesburg Coal. The coal seam is overlain by the Cassvile Shale and approximately 30 to 60 ft of Waynesburg Sandstone.

Fourteen monitoring wells were installed in the disturbed and undisturbed areas at the site. The general hydraulic conductivities (k) of the site were established using slug tests that were conducted by researchers at the U.S. Bureau of Mines. The results of the slug tests indicated that k values are approximately 2.85×10^{-5} ft/s for the undisturbed area and range from 3.3×10^{-4} to 2.0×10^{-3} ft/s for the disturbed area. These values are localized in nature, and variability in the hydraulic conductivities for both the disturbed and undisturbed areas should be expected. As discussed by Hawkins and Aljoe (1991) the hydraulic conductivity for disturbed areas can vary several orders of magnitude throughout the mine site.

As described by Harshberger (1991), magnetometry and conductivity surveys were performed at the site. Based on the results of these surveys, four separate areas were delineated as having material with high potential for producing AMD. However, subsurface exploration conducted during the installation of the monitoring wells indicated that the spoil material is randomly located over the whole site.

Monitored ground water levels indicated that the average ground water head difference between the undisturbed and reclaimed areas is approximately 8 ft with the higher heads within the undisturbed area. This head difference induces flow gradient across the site and results in recharge across the highwall from the undisturbed area to the reclaimed area. A second source of recharge to the reclaimed area is leakage from three AMD aeration and settling ponds. These ponds are lined with the sludge produced during the treatment process. The recharge rate from each pond was estimated by measuring the water depth and sludge thickness along with the permeability of the sludge material. Laboratory tests on the sludge material indicated that the average permeability of the sludge material is approximately 4.9×10^{-7} ft/s.

The estimated recharge rates from the treatment ponds are presented in table 1. Recharge from precipitation was minimal on the site. The greater portion of the reclaimed area is steeply sloped, and runoff trenches were installed. Water ponded in the runoff trenches after storm events is routed underground away from the site. Field data from monitoring wells around the run-off trenches indicated that these wells exhibit a significant increase in water levels after precipitation events.

Table 1. Recharge rates from the three treatment ponds at the site

Pond	Water depth, ft	Sludge thickness, ft	Permeability of sludge, ft/day	Hydraulic gradient	Discharge per unit area ft/day
1	1.0	4.2	2.8×10^{-2}	0.24	6.7×10^{-3}
2	3.0	1.0	2.8×10^{-2}	3.00	8.4×10^{-2}
3	7.7	0.6	2.8×10^{-2}	13.00	3.6×10^{-1}

Analysis Model

The computer program MODFLOW by McDonald and Harbaugh (1988) was used in this study. The flow regime is modeled as a 3-D nonhomogeneous media using the following steady-state governing differential equation:

$$\frac{\delta}{\delta x}\left(k_{xx}\frac{\delta\phi}{\delta x}\right) + \frac{\delta}{\delta y}\left(k_{yy}\frac{\delta\phi}{\delta y}\right) + \frac{\delta}{\delta z}\left(k_{zz}\frac{\delta\phi}{\delta z}\right) - w = 0 \qquad (1)$$

where: k_{xx}, k_{yy}, and k_{zz} = hydraulic conductivities along the x, y, and z axes,
ϕ = piezometric head at any point, and, w= flux per unit volume representing source or sink.

Solution of equation 1 is obtained using a block-centered finite difference method. The flow domain representing the site aquifer system is discretized into node and elements as shown in figure 2. The program allows for the simulation of confined and unconfined aquifers or a combination. External stresses such as recharge events can be incorporated in the model. Solution of the finite difference scheme is achieved using implicit procedure with successive relaxation technique.

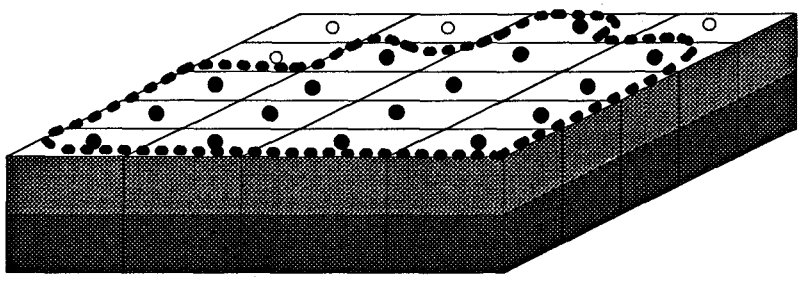

Key

• - Active cell ○ - Inactive cell ••••• - Aquifer boundary

Figure 2. Representation of flow regime in MODFLOW

In general, the characterization of ground water flow through mine spoils is rather challenging. As discussed by Hawkins et al. (1991), ground water flow through mine spoil exhibits bimodal characteristics that include those similar to flow through porous media as well as pseudokarstic flow. The difference between the pseudokarstic flow and porous media flow is distinct. Conventional porous media flow is generally laminar and can be described by Darcy's law. Pseudokarstic flow is characterized by turbulent with multiple primary flow paths, extreme ranges of hydraulic conductivity, and rapid response to recharge events. The analysis model used in this study is based on assuming the dominance of porous media flow. Using this assumption, the hydrogeologic parameters of the site can be averaged over the flow domain and porous media flow can be simulated.

Site Characterization and Analysis Domain

The analysis domain for the research site is shown in figure 3. The modeled area of the site is approximately 700 ft wide and 1500 ft long. A part of the undisturbed area that is 300 ft long was incorporated in the model. This was necessary in order to simulate recharge events from this area and include into the model the presence of the highwall. The site was modeled as unconfined aquifer wit the bottom of the aquifer at the elevation of the pavement. The bottom of the aquifer was estimated to be at El. 915.

Domain Discretization and Boundary Conditions

A grid measuring 18 cells by 25 cells was used to discretize the site as shown in figure 4. The cell width (in the y direction) ranged from 20 to 50 ft, and the length ranged from 25 to 100 ft. Boundary conditions for the flow model were selected in accordance with observed field conditions. A boundary located at the interface between the undisturbed and reclaimed area was modeled as a general constant head boundary with ground water flow allowed across it. The head levels for this border boundary were interpolated from the monitoring well data.

The north and south boundaries were set as no flow boundaries except where drains and ponds were located. The field location of the south boundary was set along the fence line at the edge of the mine site, as shown in figure 3. The field location of the north boundary was selected in the model to be off the reclaimed site such that its effect on the predicted ground water regimes is minimal. The simulated abatement techniques consisted of the installation of a 5-ft thick subsurface cutoff wall and the grouting of discrete spoil pockets as shown in figure 4. The permeability of the grout to form the wall was assumed equal to 3.3×10^{-8} ft/s. Seeps on the sites represented the primary source of discharge. Measurement of total seep volume indicated base flow of approximately 15 to 20

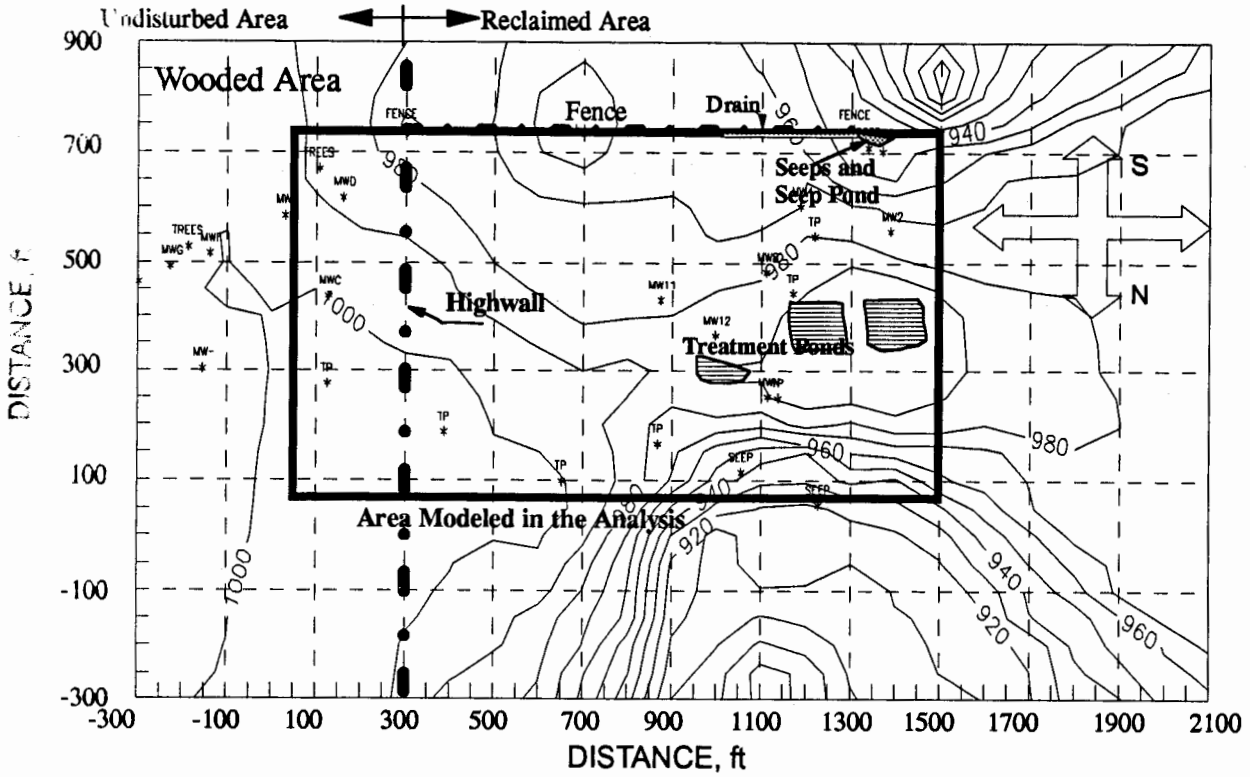

Figure 3. Area of the site used to model the ground water flow regime and remedial measures (North is Downward)

gallons per minute (gpm), or 2900 to 3900 ft^3/day. The seeps on the site were modeled as drains. In addition, an existing interceptor drain on the south side of the site that was installed to prevent seeps from flowing to property adjacent to the mine was included in the model. The treatment ponds were represented as constant recharge nodes with the recharge rates as shown in table 1.

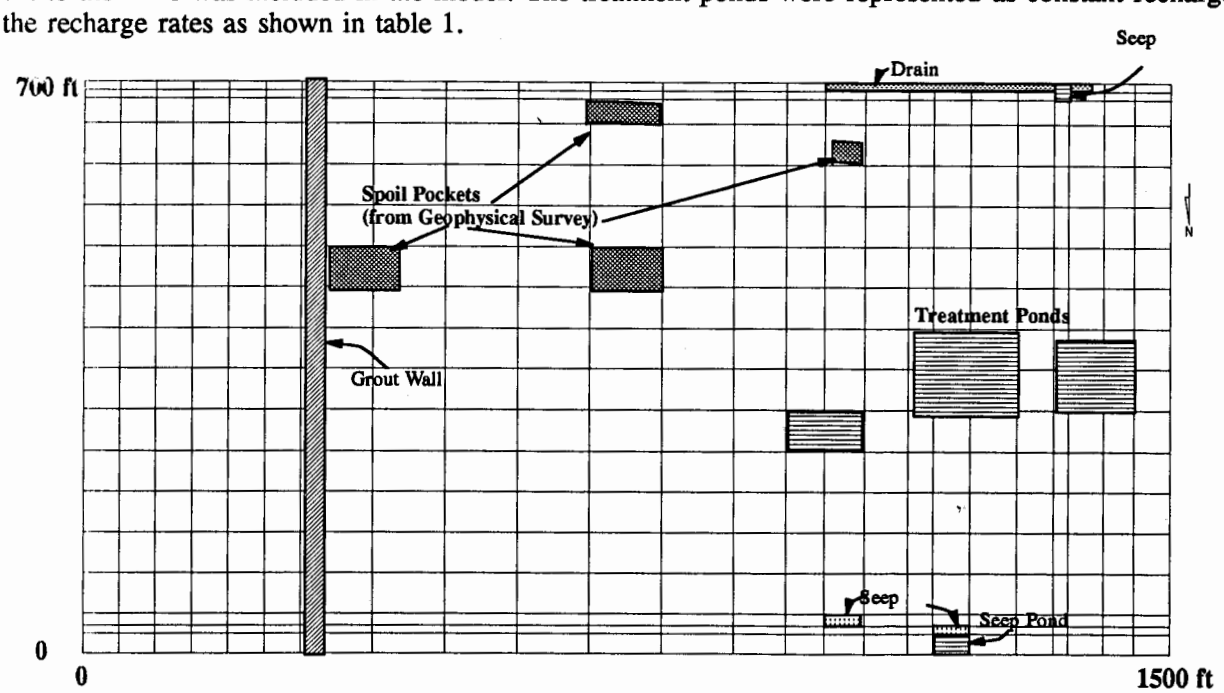

Figure 4. Domain discretization and boundary conditions

Model Calibration

A steady-state trial and error calibration study was performed using the monitored well data from measurements taken on June 24, March 5, and March 31, 1992. The June 24 data are representative of a time when seeps flow was minimum and precipitation did not occur for several days prior to that date. The March 31 data represent the highest water levels for the wells at the upgradient edge of the model as well as high-seep condition. The March 5 data were chosen to represent midlevel data between the low and high water levels.

The initial k values used for the model were those estimated from the slug tests as 2.85×10^{-5} ft/s for the undisturbed area and 3.3×10^{-4} ft/s to 2.0×10^{-3} ft/s for the disturbed area. Model simulations were conducted, and the predicted piezometric heads were compared with monitored well data. Adjustments were made to the k values until the differences between measured, and predicted piezometric heads in all wells were within 10% from each other. Figure 5 shows the results of the calibrated model and the difference in ft between measured and predicted heads.

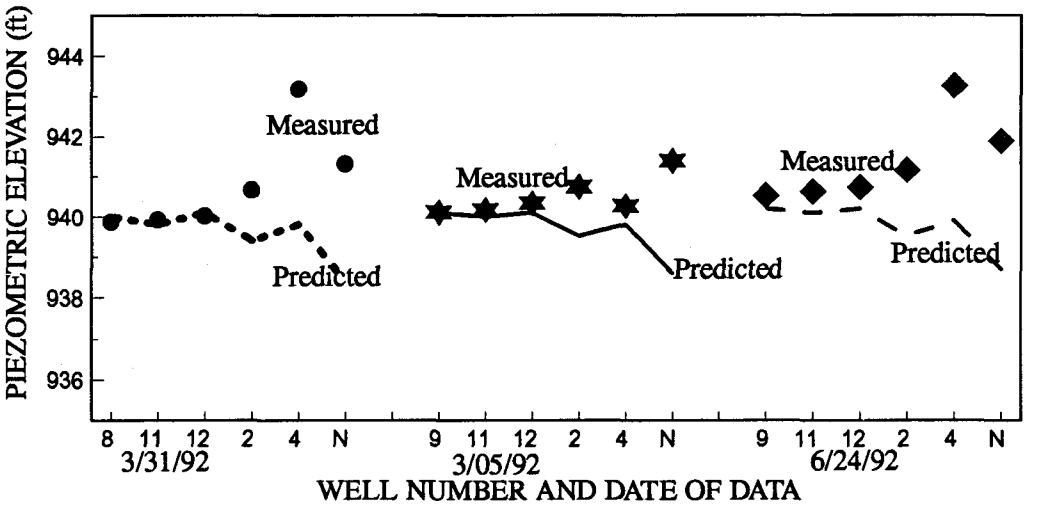

Figure 5. Measured and predicted piezometric levels from the calibration study.

Predicted piezometric heads at wells 2, 4, and N were consistently lower than the measured field values but within the 10% closure tolerance.

A possible explanation for the lower levels in these wells is the fact that the analysis did not account for rainfall recharge. The k-distribution shown in figure 6 was obtained such that these closure values were achieved. These permeabilities are 1 ft/day for the unmined area, and 10, 20, and 40 ft/day for zones in the reclaimed areas.
A volumetric budget generated for the site indicated a recharge flow of 785 ft^3/day from the unmined area and 4517 ft^3/day from the treatment ponds. Discharge from the reclaimed site was estimated at approximately 5290 ft^3/day into the seeps, drains, and seep collection ponds. This value is 1.8 times the measured value from seeps based on June 24 data. However, it is possible that water on the site is discharged via other field means, such as eavpotranspiration and possible vertical leakage, that were not represented in the analysis model. Based on the result of this analysis, approximately 85% of the seep water is from the treatment ponds.

Grout Wall: Simulation and Results

The use of subsurface grout wall is one of the most promising abatement techniques for AMD. In this study, the primary function of this wall is to block the inflow from the undisturbed area. The wall was extended along the length of the highwall with a thickness of 5 ft. The analysis was conducted for the days of June 24, March 5, and March 31. Two scenarios were assumed for the analysis. In the first scenario, the south seep pond remained at a constant head which artificially held the water level constant in this area.

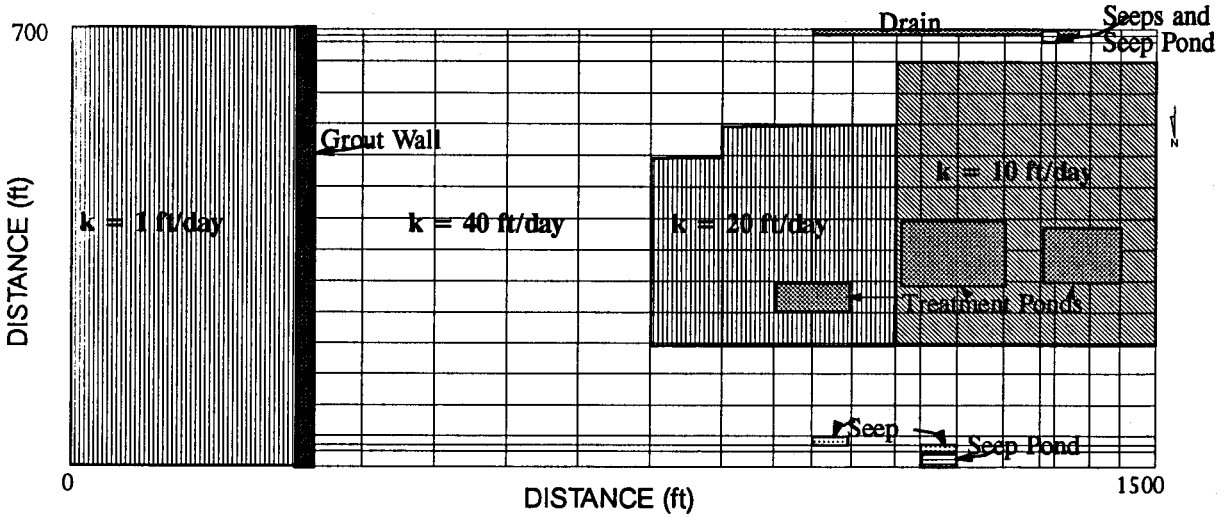

Figure 6. Distribution of permeabilities based on the results of the calibration study.

In the second scenario, the head at the south seep pond was set according to the initial conditions but was then allowed to vary in accordance with the analysis computations. As shown in figure 7A, the presence of constant head caused mounding of the ground water table.

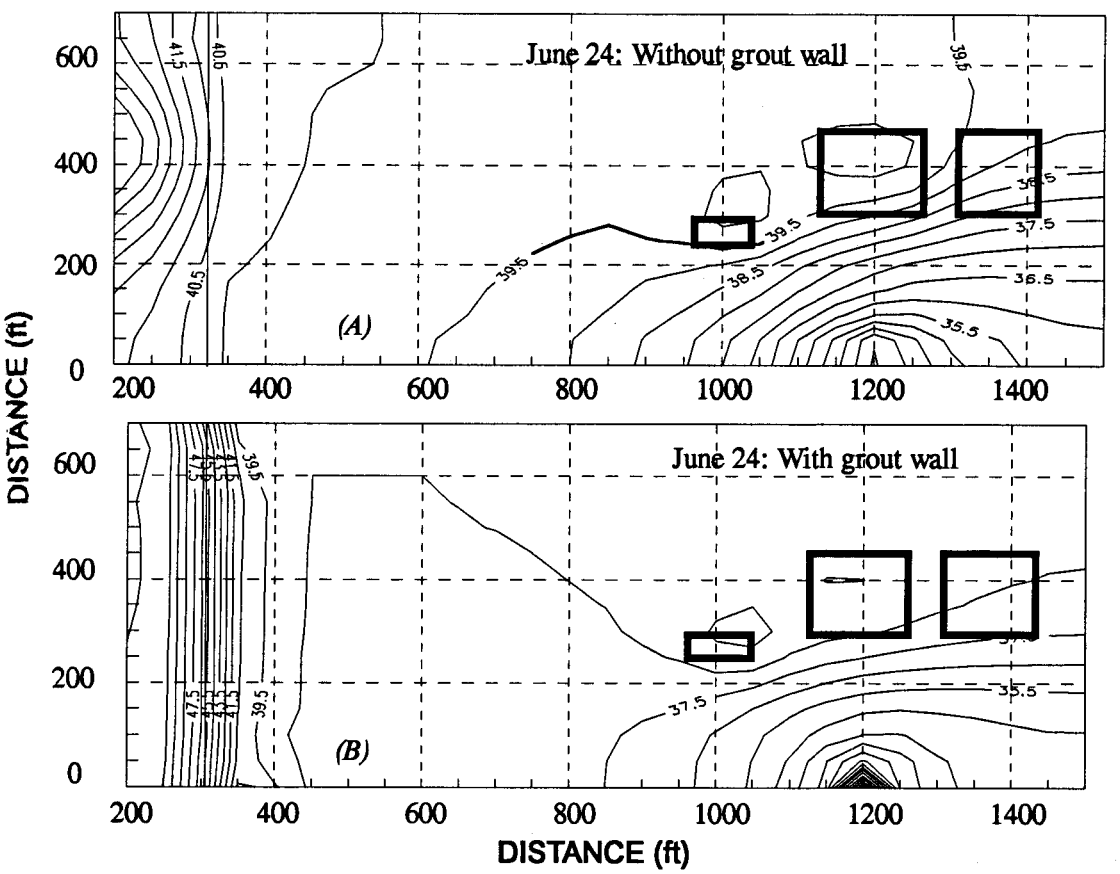

Figure 7. Piezometric contours (900+) from the ground water model : A, no grout wall; and B, grout wall installed.

This mounding dictated that the flow from the undisturbed area be routed around the south pond with the higher quantity flowing to the north boundary.

The installation of the grout cutoff wall caused a large head loss across the wall, as shown in figure 7B. The head loss occurred almost entirely within the grouted zone. As shown in figure 8 (section through the middle of the reclaimed area), the piezometric head drop across the grout wall is from El. 948 ft to El. 942 ft. Before the wall installation, the piezometric head was relatively constant and at about El. 940 at the edge of the reclaimed area.

After the installation of the grout wall the water level at the south seep collection pond was predicted below the initial level of El. 939.4 ft. As shown in figure 8, the piezometric level in the undisturbed area at the highwall boundary was predicted to increase from El. 941.9 without the wall to El. 951.9 (an increase of 10 ft) with the wall installed. In addition, a significant change was predicted in the direction of the flow in the reclaimed area as shown in figure 7. Before the installation of the wall, most of the flow from the unmined area was predicted to be around the treatment ponds. This flow was the result of the mounding effect induced from the recharge by the treatment ponds. The flow in this case was basically split between the north and south seeps. After the wall was installed, the piezometric head across the reclaimed area was reduced to an average of El. 939.5 with the entire flow routed to the location of the north seep. Accomanying this flow routing was a reduction of approximately 1.5 ft in the water level within the reclaimed area and therefore a reduction in the amount of saturated material. Results using the March 5 and the March 31 data were similar to those obtained using the June 24 data.

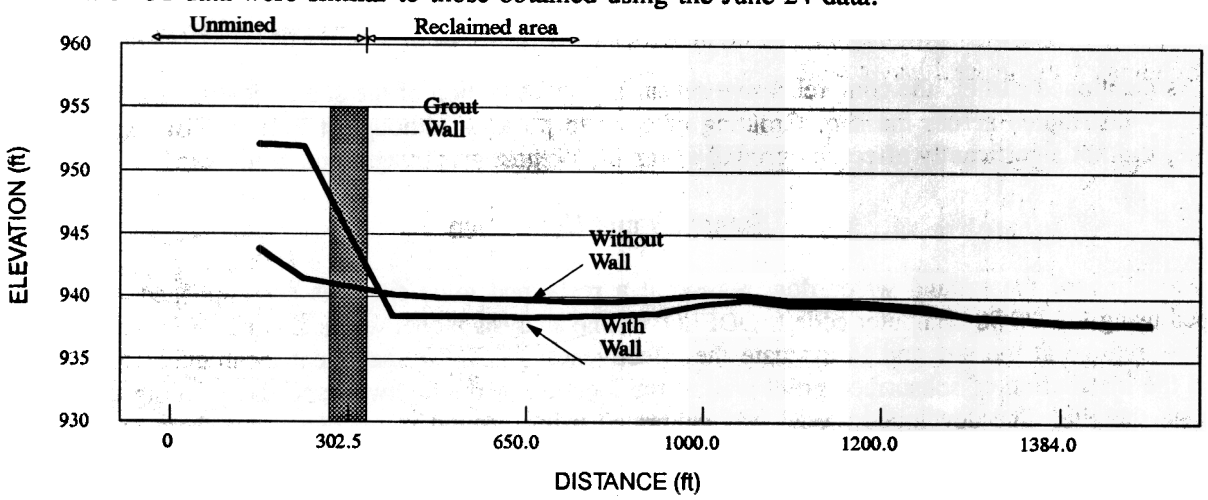

Figure 8. Profile of predicted piezometric heads based on June 24 data.

The volumetric budget for the grout wall simulation indicated that recharge from the unmined area was reduced to approximately 170 ft^3/day. The total recharge from the aquifer was estimated to be approximately 4700 ft^3/day. These discharge values correspond to 80% reduction in the amount of recharge from the undisturbed area and 10% reduction in the overall discharge from the aquifer. Based on the assumption used to formulate the model and the analysis conditions, approximately 97% of the amount of recharge to the reclaimed area was predicted to be from the treatment ponds after the cutoff grout wall was installed.

Grouted Pockets: Simulation and Results

The second abatement technique that was suggested for the site consisted of grouting isolated pockets of mine spoil that were identified from the geophysical surveys. The merit of this technique is to encapsulate the spoil material within the grout matrix and therefore minimize the generation of AMD. Ground water analysis was conducted with the spoil locations, shown on figure 4, grouted and thereby the cells were assigned a k value of 3.3×10^{-8} ft/s. The June 24 data were used to conduct the simulation. In general the grouting of pockets resulted in a slight increase in the predicted water levels (figure 9).

The increase in water levels ranged from 0.2 to 0.4 ft with the highest increase observed at the north side of the treatment ponds. In addition, and because of the location of the grouted pockets on the south side of the

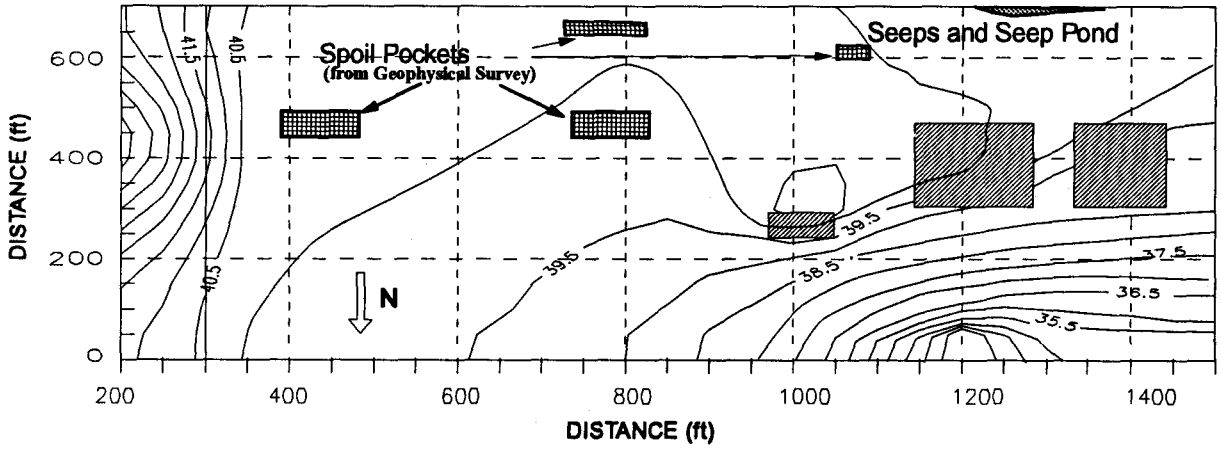

Figure 9. Ground water flow regime and discrete grouted spoil pockets

treatment ponds, increase in the flow to the north seeps was noted due to the routed recharge from the treatment ponds.

As mentioned earlier, the comprehensive subsurface investigation of the site indicated that the spoil material is randomly distributed across the site. Grouting of discrete pockets, although it may improve the quality of the discharge, did not significantly affect the ground water flow regime and magnitude at the site.

Summary and Conclusion

Modeling of the ground water flow regime at a reclaimed mine site was accomplished. The model was developed using the USGS computer code MODFLOW. The analysis model was used to predict the general ground water flow regime at the site and to evaluate the effectiveness of AMD abatement techniques. These techniques included the installation of subsurface grout wall at the location of the highwall and the grouting of discrete spoil pockets on the site. The developed model was calibrated using ground water elevations from monitoring wells. Closure between measured and predicted piezometric heads was approximately 10%. Modifications to measured permeability values were introduced to obtain close agreement with the monitored ground water heads. Based on the results of this study the, following conclusions can be advanced:

1. Installation of a grout wall at the location of the highwall provided for a significant reduction in the amount of recharge from the undisturbed area. A reduction of approximately 80% was predicted from the developed model.

2. After the installation of the wall, the main source of recharge to the reclaimed area, without accounting for precipitation, was the treatment ponds. The predicted flow pattern after the wall installation was radially outward from these ponds.

3. Due to the installation of the grout wall, the water levels near the south seep dropped to a level below the elevation of the south seep. This may cause the flow at the location of this seep to cease and therefore limit flow from the seeps to those on the north side of the site.

4. Grouting of discrete spoil pockets did not significantly affect the ground water flow regime. However, this area needs further investigation to evaluate whether improvements in the water quality may be realized due to encapsulating the spoil material within the grout matrix.

5. The most effective means for reducing the quantity of water flowing into the acidic spoil at this site is the use of subsurface grout wall. Predictions from this study indicated that this technique may eliminate the south seeps and therefore lead to a reduction in the volume of AMD. Consequently this reduction will lead to the downsizing of the treatment ponds which, after the installation of the grout wall, are the main source of recharge.

Acknowledgement

Financial support for this study was provided by the National Mine Land Reclamation Center and the authors appreciate the support of Dr. Paul Ziemkiewicz, the director of the center. The authors greatly acknowledge, Mr. Jay Hawkins, Mr. Terry Ackman, and Mr. Robert Kleinmann of the U.S. Bureau of Mines, Pittsburgh Research Center, for their valuable input to this research as well as their significant contribution to the field study. Mr. Jay Hawkins provided several significant and helpful comments to this work. A special thank you is due to Mr. Jim Burnell of Monongahela Power Company for providing fly ash for the grouting work.

Literature Cited

Almes, W. S. 1991. Development of an amended fly ash barrier for surface infiltration control applications. M.S. Thesis, Department of Civil Engineering, West Virginia University; Morgantown, WV. 210 p.

Baker, R. C. 1993. Engineering evaluation of amended fly ash for low hydraulic conductivity barriers. M.S. Thesis, Department of Civil Engineering, West Virginia University; Morgantown, WV. 110 p.

Harshberger, K. L. 1991. Fly ash grouts to control acid mine drainage. M.S. Thesis, Department of Civil Engineering, West Virginia University; Morgantown, WV. 216 p.

Hawkins, J. W. and W. W. Aljoe 1991. Hydrologic characteristics of a surface mine spoil aquifer. In Proceedings, Second International Conference on the Abatement of Acid Mine Drainage. (Montreal, PQ, September 16-18, 1991).

Hawkins, J. W., T. E. Ackman, and W. W. Aljoe. 1991. The effect of grout injection on mine spoil ground water hydrology. In Proceedings, National Meeting of the Society of Surface Mining and Reclamation. (Denver, CO, May 14-17, 1991).

Kleinmann, R. L. 1989. Acid mine drainage. Engineering and Mining Journal. 190: 16I-K+

McDonald, M.G., and A. W. Harbaugh, 1988. A modular three dimensional finite difference ground water model. U.S. Geological Survey Open File Report 88-875, book 6.

Stumm W., and J. Morgan. 1970. Aquatic chemistry, an introduction emphasizing chemical equilibrium in natural waters. J. Wiley, New York.

HYDROLOGIC AND WATER QUALITY CHARACTERISTICS OF A PARTIALLY-FLOODED, ABANDONED UNDERGROUND COAL MINE[1]

By William W. Aljoe[2]

Abstract: The hydrologic and water quality characteristics of a partially flooded, abandoned underground coal mine near Latrobe, PA, were studied to support the development of techniques for in situ abatement of its acidic discharge. A quantitative understanding of the conditions affecting discharge flow was considered to be very important in this regard. Statistical analysis of hydrologic data collected at the site shows that the flow rate of the main discharge (a borehole that penetrates the mine workings just behind a set of portal seals) is a linear function of the height of the mine pool above the borehole outlet. Seepage through or around the portal seals is collected by a set of french drains whose discharge rate is largely independent of the mine pool elevation. This seepage was enhanced after a "breakthrough" that occurred during a period of unusually high pool levels. The mine pool recharge rate during winter is about 2.5 times greater than that of any other season; recharge rates during spring, summer, and fall are approximately equal. Mine pool and discharge water quality information, along with bromide tracer tests, suggest that the original main entries discharge primarily to the french drains, while the borehole carries the discharge from an unmonitored set of entries northwest of the mains. The water quality of the east french drain discharge may have been improved substantially after seepage through the alkaline materials used to construct the portal seals.

Additional Key Words: acid mine drainage, mine pools, statistical analysis

Introduction

Small-scale mine site hydrology is one of the most poorly understood aspects of the acid mine drainage (AMD) problem. This makes it difficult to achieve in situ control of AMD and increases the uncertainty associated with disposal of waste materials such as AMD treatment sludge and fly ash into abandoned underground mine voids. This paper describes how the hydrologic and water quality data from a partially-flooded underground mine near Latrobe, PA, were used to characterize the "mine pool aquifer" and delineate probable flow paths through the mine. The study site, located within Keystone State Park, was described previously by Aljoe and Hawkins (1993). The mine pool (figures 1 and 2) was formed when the portals of an updip, free-draining underground coal mine were sealed in the early 1970's. The pressure of the impounded water eventually caused a breakout through the land surface approximately 45 m behind the seals. A borehole was installed at this point to allow a relatively unimpeded outlet for the mine discharge, thus limiting the further buildup of water within the mine. The open mine entries serve as a basal drain system which carries most of the flow; the orientation of the entries and the slope of the underclay governs the direction of flow. Flow toward the discharge occurs not because of a measurable hydrologic potential gradient within the mine pool, but because the pool is connected to the atmosphere (via the borehole) at an elevation that is lower than that of the pool surface. Seepage through or around the portal seals is collected by two french drains, providing another outlet for the mine discharge.

Mine Pool Elevation and Discharge Characteristics

In the initial hydrologic investigation at this site (October 1989 through December 1990), it appeared that the total mine discharge was related linearly to the elevation of the mine pool (Aljoe and Hawkins 1993). This suggested that the pool elevation could serve as a good predictor for the discharge rate using simple linear regression. Such a predictive capability would be valuable for long-term data collection because pool elevation can be measured and recorded easily in a borehole with a pressure transducer and datalogger. Conversely, direct measurements of mine discharge are typically more labor-intensive to obtain over the long term because the primary discharge structure (weir, flume, calibrated pipe, etc.) requires frequent cleaning and other maintenance, especially in AMD environments where iron hydroxide buildup is rapid.

A nonparametric line-fitting technique first described by Theil (1950) and refined by Conover (1980) was found to be more appropriate than the more commonly used ordinary least squares (OLS) technique for developing a linear

---

[1]Paper presented at the International Land Reclamation and Mine Drainage Conference and the Third International Conference on the Abatement of Acidic Drainage, Pittsburgh, PA, April 24-29, 1994.

[2]William W. Aljoe, Environmental Engineer, U. S. Department of Interior, Bureau of Mines, Pittsburgh, PA 15236.

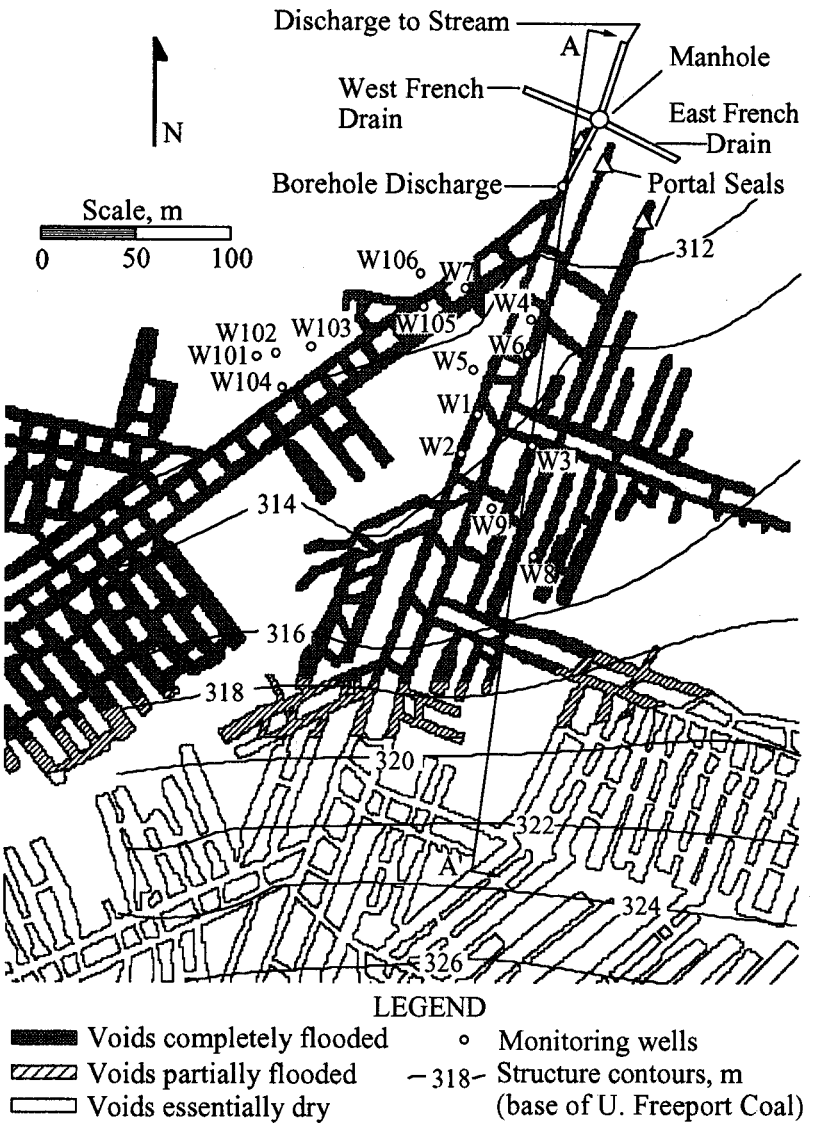

Figure 1. Map of study mine and discharge features

equation relating the discharge rate (Q) to the pool height (h). Although the OLS technique yielded a regression coefficient of 0.96 using the initial Q and h data, its validity was questionable because the position of the regression line was strongly controlled by four data points with very large Q and h values. Attempts to reduce the influence of these points by transforming the data (logs, square roots, etc.) were unsuccessful. Helsel and Hirsch (1991) provide an excellent discussion of the problems associated with this situation, and recommend the use of nonparametric techniques when it occurs. The slope of the Theil line (β_1) is defined as the median of all the n*(n-1)/2 pairwise slopes associated with a data set of n pairs:

$$\beta_1 = \text{median}\,(Q_j - Q_i) / (h_j - h_i) \quad (1)$$

for $i < j$; $i = 1, 2, \ldots (n-1)$; $j = 2, 3, \ldots n$.

The intercept of the Theil line, β_0, is

$$\beta_0 = [\text{median}\,(Q)] - [\beta_1 * \text{median}\,(h)]. \quad (2)$$

For the data collected in the initial investigation, the values of β_0 and β_1 were 4.28 and 13.91 respectively, with Q expressed in L/min and h in cm, referenced to the top of the discharge borehole. The resulting linear regression equation using the Theil slope and intercept was

$$Q = 4.28 + (13.91 * h). \quad (3)$$

However, equation 3 proved to be a poor predictor of the subsequent discharge flows because the hydrologic behavior of the mine pool appeared to change substantially after equation 3 was developed.

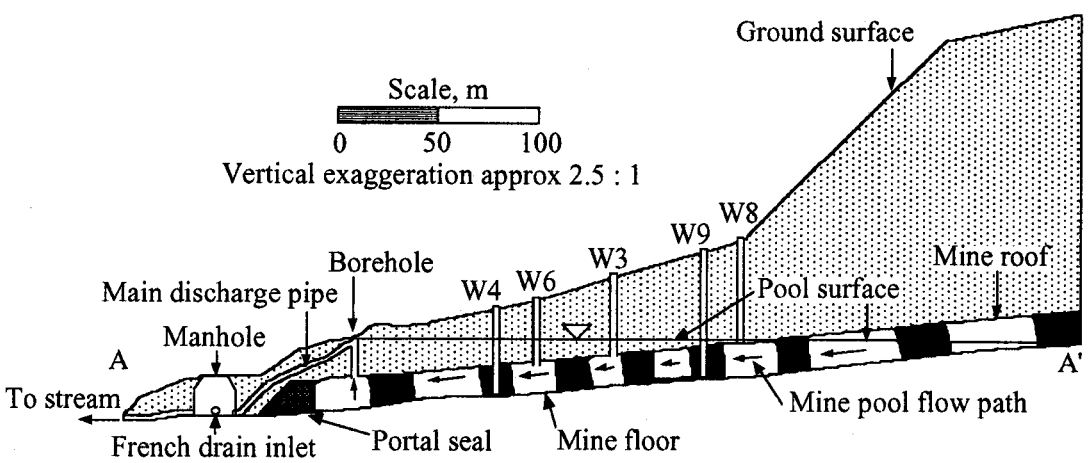

Figure 2. Cross-section of mine pool study site.

As shown in figure 3(a), the pool elevation dropped far below the top of the borehole in the late summer and fall of 1991 and 1992, but had not done so during 1989 and 1990. Also, the maximum pool elevations reached during the winters of 1991-92 and 1992-93 were more than 24 cm below the maxima of the two preceding winters. These changes could not be traced to precipitation differences; it was therefore postulated that they were related to a significant change in the mine discharge conditions.

Note in figure 3(a) that an anomalous data period occurred during December 1990-January 1991. This period is magnified in figure 3(b); a detailed discussion of these events is provided by Aljoe (1992) and is summarized here. Hourly water levels obtained from a pressure transducer in one of the mine void monitoring wells (W2) revealed several very sharp declines and rises in the pool elevation during this period. On two occasions, the pool elevation actually dropped below the top of the discharge borehole, although flows were consistently greater than at any time during the study period. Independent measurements of the pool elevation in wells 1, 6, and 8 confirmed that the W2 hydrograph was indicative of the overall pool elevation, and that the observed rapid fluctuations were not related to the subsequent transducer failure on January 19. The erratic pool behavior was interpreted as a breakthrough in the portal seal area, resulting in a permanent increase in flow to the french drains; this interpretation was supported when, in the fall of 1991, flows from the french drains became visibly discernable for the first time during the study period.

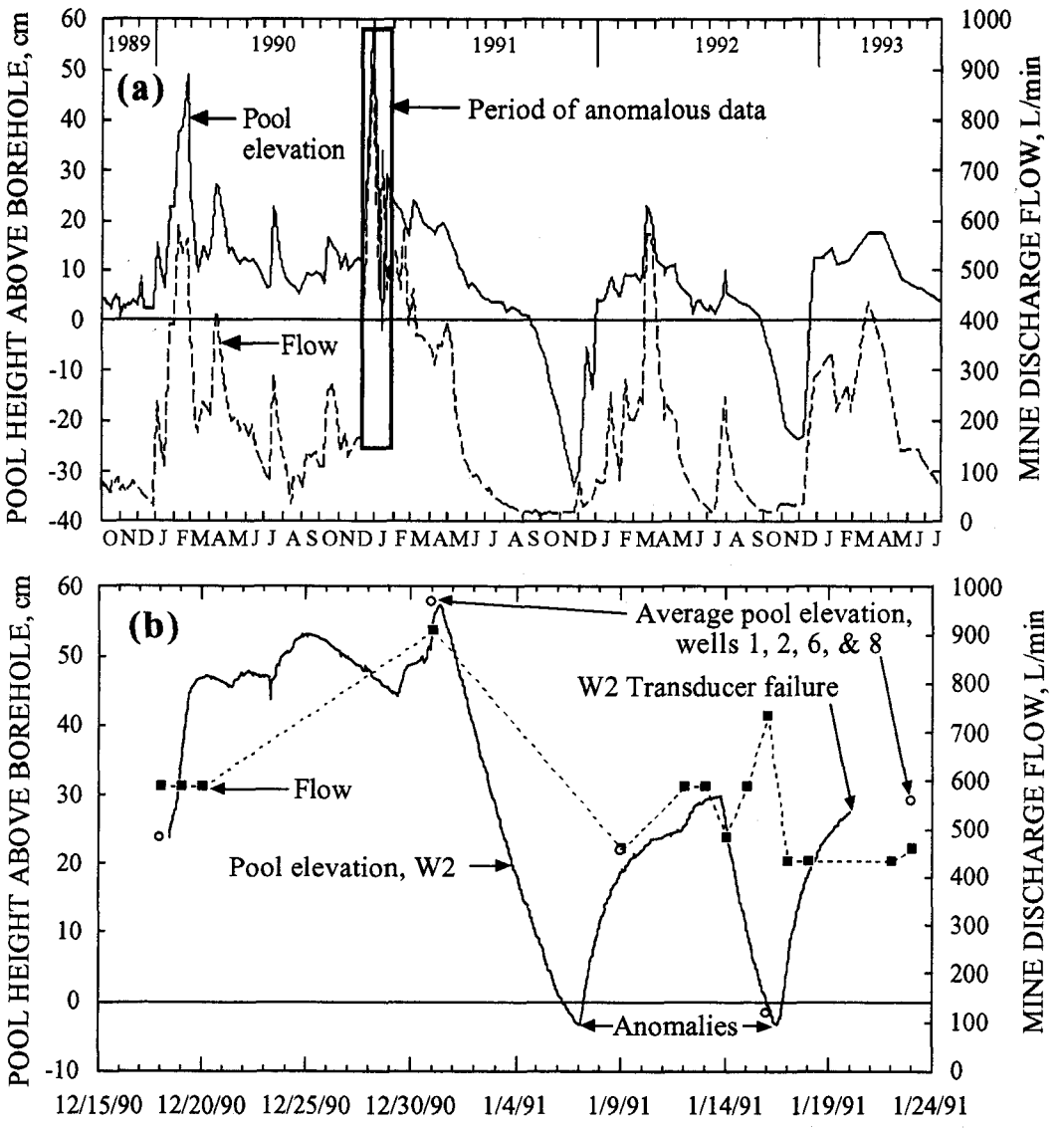

Figure 3. Mine pool elevation and discharge hydrographs:
(a) entire study period; (b) period of anomalous data

The data collected after the breakthrough still appeared to follow a linear pattern (at h>0) with a few high, very influential values; however, equation 3 proved to be a very poor predictor of the discharge flow rate. The change resulting from the breakthrough event can be quantified by defining the "conductance" of the mine discharge area as:

$$C_t = Q_t/h \mid h>0 \tag{4}$$

where C is the conductance of the mine discharge area, and the subscript t denotes the parameters of the total mine discharge. If the breakthrough did indeed increase the total conductance of the mine discharge area, the value of this parameter after the breakthrough (C'_t) should be statistically greater than its value before the breakthrough (C_t). Considering that the total flow is the sum of the flows from the borehole (Q_{bh}) and the french drains (Q_{fd}), expressions for the borehole and french drain conductances can be written as:

$$C_t = (Q_{bh} + Q_{fd})/h = C_{bh} + C_{fd}, \text{ where } C_{bh} = Q_{bh}/h \text{ and } C_{fd} = Q_{fd}/h. \tag{5}$$

where the subscripts bh and fd refer to the borehole and french drain flow paths. Before the breakthrough, all the discharge was observed to have come from the borehole, so $C_t = C_{bh}$ and $C_{fd} = 0$ for the pre-breakthrough period. After the breakthrough, the conductance of the flow path to the french drains (C'fd) would increase while that of the borehole (C'_{bh}) would remain unchanged. Therefore, while it would be impossible to quantitatively compare the french drain conductances before and after the breakthrough ($C_{fd} = 0$), the difference between the borehole conductances before and after the breakthrough (C_{bh} and C'_{bh}) should be statistically insignificant.

Direct measurements of the post-breakthrough borehole flow (Q'_{bh}) as required to compute C'_{bh} could not be obtained due to the logistics of the pipe entry to the manhole. However, in November 1992, provisions were made to measure the french drain flows directly, and these were subtracted from the total flows to yield values for Q'_{bh}. The relationship between Q'_{bh} and the total flow Q'_t was almost perfectly linear; the associated Theil regression equation

$$Q'_{bh} = -29.0 + (0.97 * Q'_t) \mid h>0 \tag{6}$$

was used to produce estimates of Q'_{bh} and equation 5 was used to estimate C'_{bh} for most sampling dates (except for dates when h<0) between March 1991 and November 1992.

The three conductance groups of interest were C_t (which is also C_{bh}), C'_t, and C'_{bh}; their median values were 1.54, 2.00, and 1.58 m^2/min, respectively, and their distributions were non-normal but similar in shape. To test the significance of the differences between the groups, the rank-sum test (also known as the Mann-Whitney test) was employed. This nonparametric test, first developed by Wilcoxon (1945), determines whether one data set has significantly larger values than another. In each test, a null hypothesis H_o (the values in the two groups do not differ) is compared to an alternative hypothesis H_1 (the values in the groups differ in a specified manner), and a test statistic W_{rs} is computed. The value of W_{rs} determines whether H_o should be rejected in favor of H_1 at a predetermined level of confidence. The test results (table 1) support the hypotheses relating to the breakthrough, i.e., the total conductance of the mine discharge increased significantly while the borehole conductance remained unchanged.

Table 1. Results of rank-sum tests on mine discharge conductances

Null hypothesis H_o	Alternate hypothesis H_1	Test significant at 95% confidence level?	Test statistic W_{rs}	p-value[1]	Interpretation
$C'_t = C_t$	$C'_t > C_t$	Yes	8495	<0.0001	Reject H_o: Total conductance of discharge area increased significantly after breakthrough
$C'_{bh} = C_{bh}$	$C'_{bh} \neq C_{bh}$	No	5409	0.9081	Cannot reject H_o: Borehole conductance did not change significantly after breakthrough
$C'_t = C'_{bh}$	$C'_t > C'_{bh}$	Yes	8403	<0.0001	Reject H_o: After breakthrough, total conductance is significantly greater than borehole conductance

[1]probability that the computed test statistic, or one even less likely, would have been achieved if H_o were true

The final model for predicting the future mine discharge flows from the pool elevation should be based only on data collected after the breakthrough period of January 1991, since these data more accurately represent the discharge conditions that are likely to exist in the future (assuming that no future breakthroughs occur). At positive h values, the total flow, Q'_t (in L/min), can be estimated from the pool height above the borehole, h (cm), by employing the Theil regression equation developed solely from the post-breakthrough data:

$$Q'_t = 20.5 + (22.0 * h) \mid h>0. \tag{7}$$

The borehole flow, Q'_{bh}, can be estimated by using equation 6, and the french drain flow is the difference between Q'_t and Q'_{bh} at the given pool elevation. Figure 4 shows the post-breakthrough data graphically and includes plots of equations 3, 6, and 7 for comparison. The french drain discharge rate (median flow about 30 L/min) did not appear to depend on the pool height at either negative h values, when flow occurred entirely through the french drains (see figure 4), or at positive h values, when borehole flow was dominant. This was attributed to the relatively small pool height fluctuations in comparison to the high resistance (low hydraulic conductivity) of the portal seals and fractured strata which comprised the flow path to the french drains. It is likely that a positive correlation would be found if flow and pool height measurements were made more frequently and accurately and if pool height fluctuations were greater.

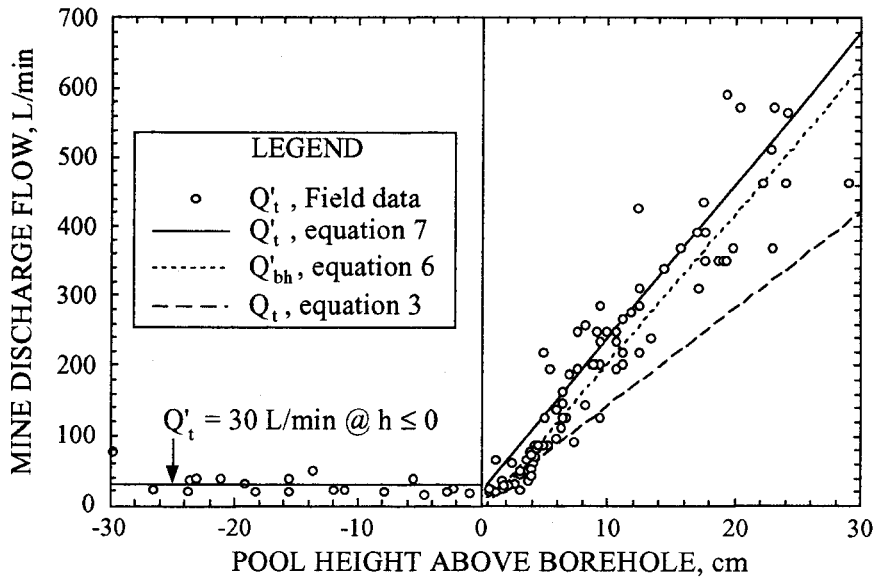

Figure 4. Relationship between mine pool height and discharge, post-breakthrough period

Mine Pool Recharge and Storage Characteristics

Previous reports on this study site (Aljoe, 1992; Aljoe and Hawkins, 1993) provided qualitative evidence that the mine pool recharge was greater in the winter and early spring than in the summer and fall. The availability of mine discharge and pool elevation measurements over a period of more than three years made it possible to quantify the seasonal recharge differences directly, without having to estimate the effects of related parameters such as soil type, soil moisture, and evapotranspiration rate, as would be required in a typical water-balance analysis. The key consideration in the analysis described here is that the change in the volume of water stored in the mine pool (ΔS) is equal to the difference between the total amount of water recharging the pool (ΣR) and the amount discharging from the mine (ΣD) over a given time period:

$$\Delta S = \Sigma R - \Sigma D. \tag{8}$$

If time periods are chosen such that the mine pool elevation (hence storage) is the same at the beginning and end of the time period, then $\Delta S = 0$ and $\Sigma R = \Sigma D$. The mine pool elevation hydrograph of figure 3 was divided into 43 "recharge periods" for which $\Delta S=0$; for each time period, the total discharge ΣD was computed as the area under the mine discharge hydrograph (figure 3), and the recharge ΣR was expressed as a function of precipitation such that

$$\Sigma R = f*A*\Sigma p, \tag{9}$$

where Σp is the sum of the daily precipitation falling on the mine area, A is the mine area over which recharge occurs (approx. 250 acres), and f is the "recharge factor," the fraction of precipitation that reaches the mine pool over the specified period. Recharge factors for each period were obtained by combining equations 8 and 9 and solving for f.

The 43 selected recharge periods ranged from 4 to 54 days in length, and each period was categorized as occurring entirely during one of three "seasons" -- winter (December 21-March 31), spring (April 1-June 30), or

summer/fall (July 1-December 20). If recharge is dominated by seasonal effects, there should be significant differences in the recharge factor distributions for different seasons. Figure 5 shows the boxplot representations of the seasonal recharge factor distributions. Although the absolute values of the recharge factors in figure 5 reflect the errors associated with the estimation of ΣD, A, and Σp, these errors do not affect the validity of seasonal comparisons.

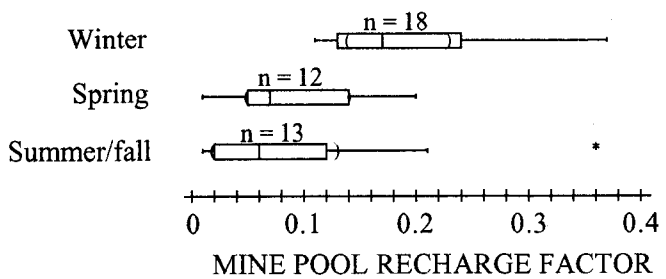

Figure 5. Boxplots of seasonal mine pool recharge factors. The width of each box represents the central 50% of the data; the vertical line within the box is the median; the parentheses represent the 95% confidence interval on the median; the horizontal lines at each end of the box extend to the last data point within 1.5 times the box width from the box end; outliers are denoted with an asterisk; n = number of observations in each group.

Differences between seasonal recharge factors were tested for significance using the rank-sum test, since the recharge factor distributions were found to be nonnormal. Table 2 summarizes the results of the rank-sum tests. As expected, winter recharge was significantly greater than that of the other two seasons; the median recharge factor was about 2.4 times higher (0.17 versus 0.07). However, spring recharge was not significantly different than that of the summer/fall.

Two long periods that were characterized by steady declines and subsequent rises of the mine pool elevation (late summer through early winter of 1991-92 and 1992-93, see figure 3) could not be included in the above analysis because the declines and rises took place during different seasons. For these periods, the change in mine pool storage (ΔS) was estimated by computing the mine void volume associated with the pool elevation change. Equations 8 and 9 were then used to calculate recharge factors for the two "decline" periods, which took place during the summer and fall, and the two "rise" periods, which occurred during the winter. Although the absolute values of the recharge factors were somewhat lower than the median values for the respective seasons (probably because of the error in estimating ΔS), the factors for the two "rise" periods were 2.5 to 3.7 times greater than those of the "decline" periods. This was generally consistent with the seasonal differences in recharge noted above.

Table 2. Results of rank-sum tests on seasonal recharge factors. f_w, f_{sp}, and $f_{su/f}$ represent the recharge factors for winter, spring, and summer/fall, respectively.

Null hypothesis H_o	Alternate hypothesis H_1	Test significant at 95% confidence level?	Test statistic W_{rs}	p-value[1]	Interpretation
$f_w = f_{sp}$	$f_w > f_{sp}$	Yes	359	0.0004	Reject H_o: Winter recharge factor is significantly greater than spring recharge factor
$f_w = f_{su/f}$	$f_w > f_{su/f}$	Yes	370	0.0006	Reject H_o: Winter recharge factor is significantly greater than summer/fall recharge factor
$f_{sp} = f_{su/f}$	$f_{sp} \neq f_{su/f}$	No	167	0.5679	Cannot reject H_o: Recharge factor is not significantly different in spring than in summer/fall

[1]probability that the computed test statistic, or one even less likely, would have been achieved if H_o were true

Water Quality Variations

Mine Void Wells

Figure 1 shows that three of the monitoring wells at the study site (W1, W2 and W6) penetrated the original main entries of the mine, W3 penetrated a submain, and W8 penetrated an isolated room. Aljoe (1992) showed that a significant degree of stratification existed in all five of these wells, i.e., the water sampled near the mine roof was much less contaminated than water at the center or bottom of the entries. This suggested that the flow through all the monitored entries was relatively slow. Comparatively minor differences in AMD contaminant concentrations existed at the bottoms of the voids, suggesting that flow between the monitored entries, if any, was occurring at a level close to the mine floor. It is also possible, however, that flow through the entries was occurring preferentially through other portions of their cross sections, effectively bypassing the portions penetrated by the monitoring wells.

Mine Pillar Wells

All wells in figure 1 except W1, W2, W3, W6, and W8 penetrated solid coal between or adjacent to the mine voids. The five "pillar wells," that were surrounded by mine voids (W4, W5, W7, W9 and W105), had water elevations that were almost identical to those in the voids (Aljoe, 1992), indicating a reasonable degree of hydrologic interconnection. However, AMD contaminant concentrations in the pillars and voids were vastly different. For example, the median concentrations of acidity and sulfate in W4 (613 and 1980 mg/L, respectively) were two to three times higher than those of the voids. Conversely, W7 and W9 were consistently alkaline with very low contaminant concentrations; W5 and W105, while acidic, also had much lower contaminant concentrations than the voids. Geochemical analyses of the drill cuttings obtained from the pillar wells showed no correlation between AMD contaminant concentrations in the wells and the net acid production potential of the overburden immediately above them. Therefore, it appears that the water quality in the pillars is controlled primarily by local geochemical conditions in the immediate vicinity of the wells rather than by the transfer of water from the adjacent voids or the overlying strata.

Water quality in the five wells located in the barrier coal on the downdip side of the mine workings (W101, W102, W103, W104, and W106) also exhibited wide variations, but the differences could be explained more readily by hydrologic considerations. The two wells closest to the mine (W104 and W106) had similar AMD contaminant concentrations (e.g., about 300 mg/L acidity and 1,000 to 1,100 mg/L sulfate). Although the concentrations of some of the AMD contaminants in these two wells were statistically different (rank-sum tests significant at 95% level), they compared more closely to each other than any other two monitoring wells completed in coal. Slug tests in W104 and W106 showed that these two wells had much higher hydraulic conductivities than the other pillar wells. Water quality data collected during pumping tests in these two wells suggested that they were both connected to strong AMD recharge sources, presumably the adjacent mine entries (Aljoe and Hawkins, 1992). Some degree of hydrologic connection with the mine may also exist at W101 and W102, both of which were consistently alkaline but had relatively high concentrations of sulfate and all cations unique to AMD. No such connection appeared to exist at W103, which had circumneutral pH and acidity and very low contaminant concentrations.

Mine Discharge Sources

The most striking and important water quality variations at this site were found at the mine discharge. Table 3 lists the median values of ten AMD-related parameters for the three discharge sources, the mine voids (bottom samples only), and the two "barrier wells" (W104 and W106, see figure 1) which were believed to represent the water quality in the unmonitored set of entries to the northwest of the original mains. Figure 6 shows the boxplot representations of eight of these parameters. For each parameter, significant differences in the median values exist where the 95 % confidence intervals at any two locations do not overlap in figure 6. Note in particular that: (1) most contaminant concentrations were significantly higher in the borehole discharge than in the two french drain discharges; (2) the east french drain discharge had a very high pH and was net alkaline, although its sulfate and AMD-cation concentrations showed that it had undoubtedly come from the mine; (3) the west french drain discharge was similar to the borehole discharge in sulfate concentration but had a higher pH and significantly less acidity, iron, and aluminum; (4) the borehole and west french drain discharges were generally more contaminated than the monitored mine voids; (5) the borehole discharge quality was similar to that of W104 and W106; (6) the calcium concentrations were higher in the two french drains than in the other locations; and (7) the concentrations of three relatively "conservative" AMD ions -- sulfate, magnesium, and sodium -- were about the same in the mine voids as in the east french drain.

Table 3. Median AMD-related water quality parameters in mine pool and discharge.

Parameter	Borehole Discharge	East French Drain	West French Drain	Wells 104 and 106	Voids (Bottom)
Number of Samples	141	56	57	20	84
pH	3.11	6.37	3.99	3.03	3.31
Net Acidity	365	-45.5	208	303	187
Total Iron	93.8	28.9	69.4	104.5	60.3
% Ferrous	72.3	99.0	100.0	97.9	97.1
Sulfate	1125	868	1074	1025	840
Calcium	185	248	224	184	162
Magnesium	74.4	56.6	69.5	70.4	53.8
Sodium	7.5	13.5	8.2	6.6	13.1
Aluminum	18.9	3.7	12.6	15.9	9.6
Manganese	13.6	12.7	12.8	13.4	5.9

pH in standard units; % Ferrous in percent; all other data in mg/L

These water quality patterns suggest that there are two largely independent internal flow paths within the mine pool. The set of entries near W104 and W106 constitutes the primary flow path; this path discharges mostly through the borehole, which is located where the flow path intersects the west main entry. This would explain the similarities in water quality noted in (5) above. The original main entries of the mine, in which the portal seals were constructed,

constitute a secondary flow path whose water quality is represented by the void wells. A portion of the primary flow path mixes with the secondary path in the west main entry, and the mix is chemically altered as it passes through the portal seals to the french drains. A report on the mine sealing project (Chung, 1973) shows that the seals contained large amounts of limestone aggregate and cement grout, which would account for the higher calcium concentrations in the french drain discharges. The west french drain represents the preferred flow path through the portal seals; its flow rate was consistently four times higher, its AMD contamination was much greater, and its calcium concentration was significantly lower than those of the east french drain. During periods of high pool elevation, diffuse seepage of AMD emanated from the ground immediately above and adjacent to the west french drain. These characteristics suggest that the west portal seal and the surrounding strata are more heavily fractured than elsewhere in the discharge area. Note also (figure 1) that the west portal seal is situated at the structural low point of the mine, and would therefore be subject to greater hydrostatic pressure than the other portal seals. The high degree of neutralization evidenced in the east french drain is the result of very slow seepage through the portal seals. Because of its location and the chemical similarities noted in (7) above, the east french drain probably derives most of its discharge from the secondary internal flow path.

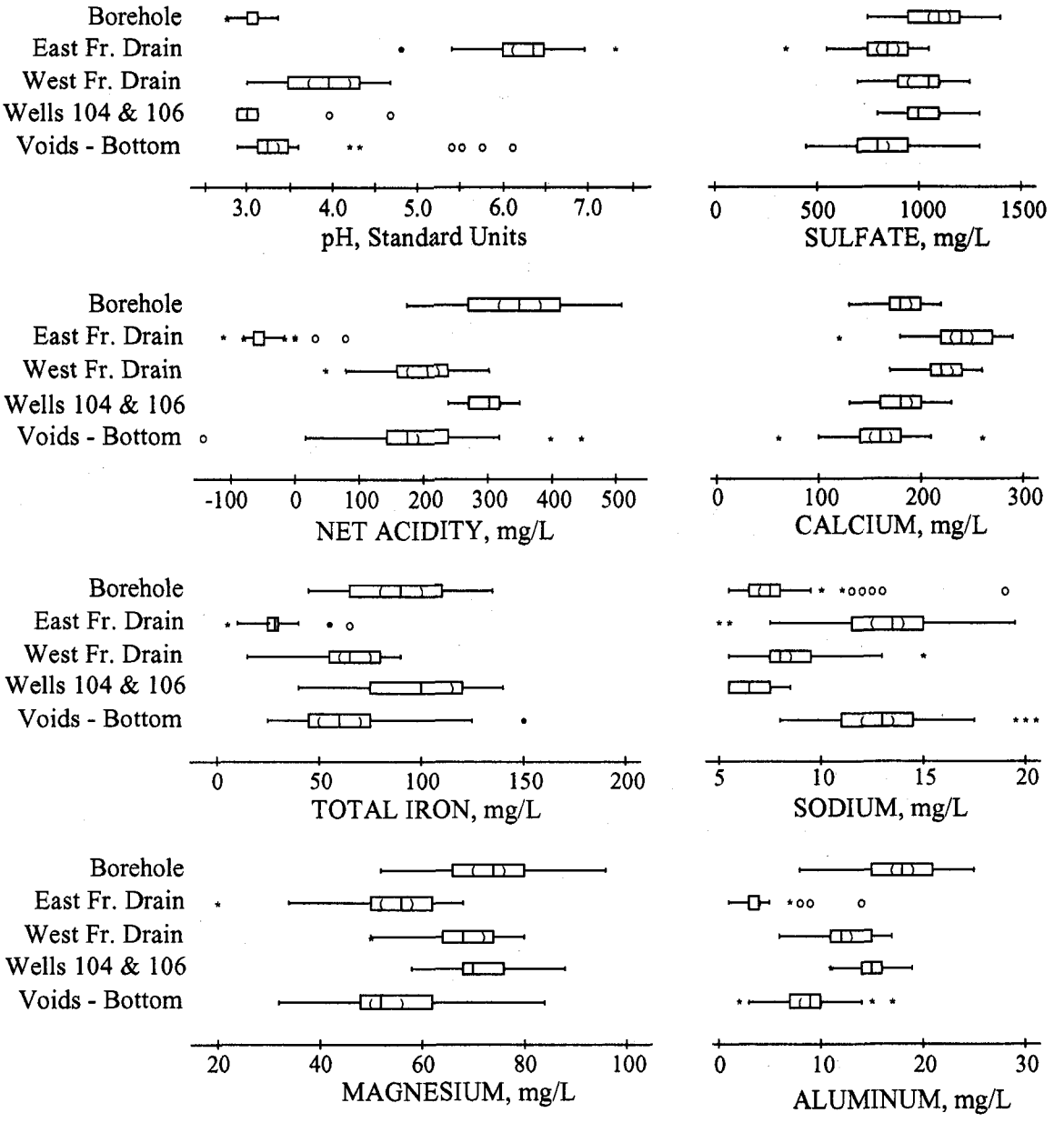

Figure 6. Boxplots of mine pool and discharge water quality parameters. See figure 5 for explanation of symbols; medians and confidence intervals are not shown when they coincide with the box ends; circles denote extreme outliers.

Tracer Tests

Aljoe and Hawkins (1992) described the results of a bromide tracer test, using W6 for tracer injection, which confirmed the hydrologic connection between the original main entries and the french drains. The highest bromide concentration in any discharge sample (6.8 mg/L) occurred in the west french drain on the third day after tracer addition; concentrations at this location decreased consistently thereafter. Conversely, bromide concentrations in the east french drain increased steadily during the first 17 days after tracer addition, remained relatively constant (close to 1.0 mg/L) through the 54th day, and continued at just above the detection limit (0.1 mg/L) for almost a year after tracer injection. This suggested a slower flow path to the east french drain, with greater opportunity for chemical change. Bromide concentrations in the borehole discharge were negligible. Tracer migration away from the injection well was more than three times as rapid at the bottom than at the top of the mine void, supporting the earlier inference of a higher flow rate along the mine floor.

Discussion and Conclusions

For mine pools with reasonably well-defined "spillover points" (e.g., boreholes or open fractures), the pool elevation can provide a reasonable estimate of the mine discharge rate. This can be an advantage in long-term monitoring because of the lower maintenance costs associated with pool elevation measurements. While the functional relationship between elevation and flow is linear, the predictive equation should be generated by non-parametric rather than parametric regression techniques in order to reduce the influence of high outliers. Data on both parameters should be collected for several water years before relying on pool elevation as a predictor, and discharge conditions should be field-checked periodically. This is especially important during high-pool periods, which can create or enhance discharge paths other than the one for which the predictive equation was developed. If this occurs, a new round of data collection for all discharges will be necessary, and new predictive equation(s) must be generated.

The efficiency of recharge to the mine pool, as defined by the "recharge factor" (recharge per unit precipitation input) was generally more than twice as high during the winter months compared to the rest of the year. This can be attributed primarily to the low temperatures and lack of plant activity during the winter, which combine to reduce evapotranspiration. In addition, snowmelt represents a gradual, widespread application of water to the land surface, which would tend to favor recharge versus runoff. Conversely, intense spring and summer rainstorms would tend to favor runoff over recharge. The lack of significant differences in recharge during the spring, summer, and fall can be explained by the offsetting effects of plant activity and temperature. During the spring, plant activities are relatively high while temperatures are low; during the summer and fall the reverse is true. Also, the accumulated effects of warm temperatures and plant activity create an undersaturated condition in the soil and overburden in the summer and fall. This moisture demand must be met before accelerated recharge to the mine can begin. This demand was apparently met on at least one occasion during the summer/fall period (outlier in figure 5); this event occurred at the end of a long period (1-2 weeks) of cool temperatures and consistent, heavy rainfall.

The wide variations in water quality that existed among the mine voids, pillars, and discharges can be attributed to several hydrologic and geochemical factors. Water quality in mine voids was vertically stratified, indicating a relatively slow flow velocity at the monitoring points. The vast differences in pillar water quality could not be explained by vertical or lateral flow from adjacent overburden or voids, and it was postulated that local pillar geochemistry was responsible. However, water quality patterns in four of the five wells in the barrier pillar immediately downgradient of the mine could be related to recharge from the adjacent voids. Differences in water quality at the three mine discharge points were attributed to the partial mixing of two internal flow paths through the mine prior to discharge, coupled with varying degrees of chemical alteration upon seepage through the calcareous portal seal materials. The apparent complexity of the internal flow and discharge patterns was somewhat surprising, given the close proximity of the discharges to each other and the relative simplicity of the deep mine itself (only a few open mine entries with no evidence of collapse). This implies that multiple flow paths will exist at any flooded deep mine, and a comprehensive definition of these paths would be necessary prior to implementing any type of in situ AMD treatment scheme. Conversely, the apparent existence of "natural" AMD amelioration at the east french drain provides encouragement that in situ treatment may be possible at the study mine if the neutralizing agents can be introduced along the primary flow path. Efforts are currently underway to develop a passive AMD treatment scheme that takes advantage of the observed hydrologic and geochemical characteristics of the mine pool.

Literature Cited

Aljoe, W. W. 1992. Hydrologic characteristics of a ground water reservoir in an abandoned underground coal mine. Unpublished M. S. project report, University of Pittsburgh, Dept. of Civil Engineering, 156 p. (Copies available from U. S. Bureau of Mines, Pittsburgh Research Center.)

Aljoe, W. W. and J. W. Hawkins. 1992. Application of aquifer testing in surface and underground coal mines, p. 541-555. In Proceedings of the Focus Conference on Eastern Regional Ground Water Issues. (Boston, MA, October 13-15, 1992).

Aljoe, W. W. and J. W. Hawkins. 1993. Neutralization of acidic discharges from abandoned underground coal mines by alkaline injection. BuMines Report of Investigations 9468, 37 p.

Chung, N. 1973. Investigation of use of gel material for mine sealing. U.S. Environmental Protection Agency, EPA-R2-73-135. 67 p.

Conover, W. L., 1980. Practical Nonparametric Statistics, Second Edition. John Wiley and Sons, 493 p.

Helsel, D. R. and R. M. Hirsch. 1991. Statistical Methods in Water Resources. Elsevier Publishers, 489 p.

Theil, H. 1950. A rank-invariant method of linear and polynomial regression analysis, 1, 2, and 3: Ned. Akad. Wentsch Proc. 53:386-392, 521-525, and 1397-1412.

Wilcoxon, F. 1945. Individual comparisons by ranking methods. Biometrics. 1:80-83

THE HYDROGEOLOGY AND HYDROGEOCHEMISTRY OF THE STAR FIRE SITE, EASTERN KENTUCKY[1]

David R. Wunsch and James S. Dinger[2]

Abstract: The Kentucky Geological Survey is directing an applied research program to determine the potential water supply for future property development at the Star Fire site. It is anticipated that an aquifer constructed in mine spoil could provide base flow to streams that could feed water-supply reservoirs. Dye tracing, water-level measurements, and chemical analyses of water samples indicate that ground water moves slowly in the spoil's interior, where it must flow into surrounding hollow fills before discharging out of the spoil. Two water tables have been established: one in the spoil's interior, and the second in the hollow fills below the main spoil body. Based on an average saturated thickness of 6.4 m, the saturated spoil stores an estimated 5.2 x 10^6 m^3 (1.37 billion gal.) of water. Hydraulic conductivity (K) values derived from slug tests range from 7.0 x E-5 to > 9.0 x E-4 cm/sec. All of the waters are a calcium-magnesium-sulfate type, differing mainly in the total concentration of these constituents. Saturation indices calculated using the geochemical model PHREEQE indicate that most of the ground water at the site is near equilibrium with gypsum. Nearly all of the samples had pH measurements in a favorable range between 6.0 and 7.0, indicating that the spoil at the site does not produce highly acidic water.

Additional Key Words: ground-water movement, conceptual model, hydraulic conductivity, mineral equilibria.

Introduction

Areas of Appalachia dependent on mining economies are finding out that economic diversification is hampered by the lack of water supplies and flat usable land. Although significant areas of relatively flat land are continuously being created by surface-mining operations throughout Appalachia, the question remains as to the availability of water resources to sustain alternative land uses such as industrial development or agriculture. This study by the Kentucky Geological Survey evaluates the potential development of water resources in a thick and extensive spoil at the reclaimed site owned and operated by Star Fire Coal Co., a subsidiary of Cyprus Minerals, Inc. The results of this study should (1) contribute to the basic understanding of the hydrogeology and hydrogeochemistry of the Star Fire site and (2) create baseline data and transferable technology that may be applicable to other reclaimed mine areas in the Appalachian Coal Field.

Geologic and Hydrologic Setting

The Star Fire Mine encompasses portions of Breathitt, Perry, and Knott Counties in eastern Kentucky (fig. 1). The coals being mined include the Hazard Nos. 7, 8, 9, and 10 seams, all of which are included in the Breathitt Formation of Pennsylvanian age. These seams consist of high-volatile bituminous coal ranging in thickness from 1.0 to 2.1 m. Several of the seams contain rider coals that are also mined. The overburden consists of interbedded sandstones, shales, siltstones, and underclays. In the process of mining, spoil up to 91 m thick is being created.

Analyses of sandstone samples taken from cores revealed the following average mineral percentages: quartz, 47%; feldspar, mainly K-spar, 29%; rock fragments, 11.9%; mica, 5.4%; and heavy minerals (pyrite, siderite), 0.5%. The majority of the cement was determined to be ferroan-calcite (Weinheimer 1983). Abundant authigenic kaolinite was found to fill pore spaces and form reaction rims around feldspar grains. The occurrence of dolomite in Breathitt rocks was rare. Shales and claystones in the Breathitt Formation contain illite, kaolinite, and chlorite (Papp 1976). The overburden should not produce acid mine drainage problems. All pre-mining overburden analyses show a potential acidity (PA) of less than 5. If PA < 5, the stratum is generally considered a non-acid producer, regardless of the neutralization potential (Sobek et al., 1978).

Ground-Water Considerations

Aquifer Framework

Several previous papers have described, in detail, components of the spoil and their interpreted implications toward controlling the movement and storage of ground

---

[1]Paper presented at the International Land Reclamation and Mine Drainage Conference and the Third International Conference on the Abatement of Acidic Drainage, Pittsburgh, PA, April 24-29, 1994.

[2]David R. Wunsch, Hydrogeologist, and James S. Dinger, Section Head, Water Resources Section, Kentucky Geological Survey, University of Kentucky, Lexington, KY, USA.

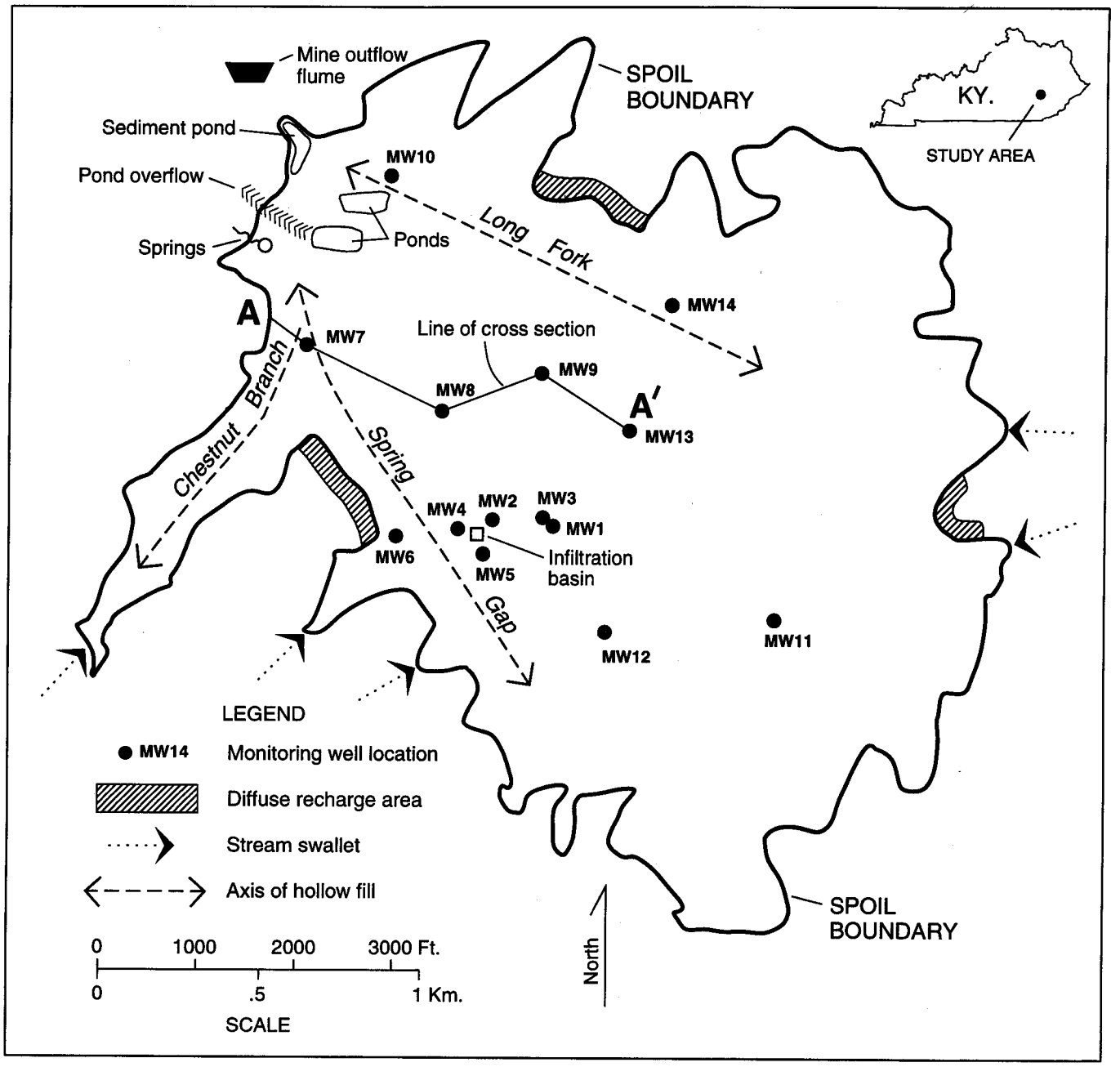

Figure 1. Location map, showing sigificant features at the site.

water at the site (Wunsch et al. 1992; Dinger et al. 1990). Therefore, these points are discussed only briefly here.

The spoil at the site, which approaches 91 m in thickness, consists of a heterogeneous mixture of broken clastic sedimentary rocks. A continuous coarse boulder zone exists on top of the pavement rock that lies below the No. 7 coal seam, which is the lowest seam in the section presently being mined. This boulder zone, and similar boulder zones that are found in hollow fills, should permit the storage and rapid movement of ground water. Because of their thick and continuous nature, these zones are anticipated to be the most capable of providing significant ground-water quantities.

A surface-water infiltration basin with a continuously penetrating rock chimney was constructed to create a direct connection to the rubble zone resting on top of the No. 7 coal underburden. The rock chimney was constructed to bypass all intermediate compacted zones within the spoil that might tend to perch percolating ground water.

Water Monitoring Methods

Monitoring Wells

Fourteen monitoring wells ranging in depth from 16.7 to 72.8 m were installed in the spoil. Several monitoring wells are equipped with data loggers at alternate times to record changes in the water table for extended periods of time.

Slug Tests

Based on methods first described by Hvorslev (1951), falling-head slug tests were performed in monitoring wells to determine the hydraulic characteristics of the spoil. The hydraulic conductivity values were then calculated by using the computer program TIMELAG (Thompson 1987). Nine tests were performed by injecting water (ground water derived from the spoil) as quickly as possible into the monitoring wells (injected at 3.2 liter/second) until the water level reached the top of the plastic casing. In most cases, the well casing could be filled with water in less than a minute. An equilibrium water level was maintained for several seconds while any trapped air bubbles were allowed to escape from the water column.

The instantaneous drop in head when the water flow was cut off was recorded by a submerged pressure transducer and digital data logger. These tests violate the assumption that instantaneous change in water level occurs at the initiation of the test. Even under ideal conditions this method is not precise, but it is generally considered as an appropriate means of estimating the order of magnitude of hydraulic conductivity (Thompson 1987).

In some cases, wells took more water than could be supplied by the pump. In these wells, the hydraulic conductivity calculated represents a minimum value based on a water injection rate of 3.2 liters/second. The static head level used in calculations was the maximum head level (top of casing) for each well, which provided for a minimum hydraulic conductivity value that would sustain the flow rate.

Water-Quality Sampling and Analysis

Water samples from the largest spring, monitoring wells, and the deep infiltration basin were collected to establish water-quality characteristics and determine changes in water quality that occur between recharge and discharge points. Field variables determined in most samples were temperature, specific electrical conductance, Eh, and pH. These parameters were collected utilizing a flow-through cell with water supplied by a 5 cm submersible pump. Laboratory analyses of water samples included dissolved concentrations of 30 major and trace metals and major anions.

Dye Tracing

Ground-water dye traces using Rhodamine WT were conducted to define flow paths and travel times through the the spoil. Dye traces were performed to determine the flow path of water entering the spoil at various points. Dye trace data from previous studies (Kemp 1990; Wunsch et al. in press) were also used to aid in the determination of ground-water flow paths.

Ground-Water Movement

Ground-water movement within the spoil will be controlled by the gradients that form as a function of the interaction of recharge and discharge zones, by the topography of the relatively impermeable pavement that underlies the lowest coal seam being mined (Hazard No. 7), and the drainage patterns that existed before mining began. The major streams that drained the pre-mined area (Fig. 2) (Chestnut Branch, Spring Gap, and Long Fork) eroded valleys whose bottoms are at elevations well below the elevation of the No. 7 coal. These drainage valleys became hollow fills as contour-cut mining occurred along the valley walls.

Knowledge of ground-water movement and saturated thickness has been gained by examining discharge hydrographs and dye tracing to the springs, by water-level measurements in the spoil monitoring wells, by direct field observations, and through ground-water quality determinations made at springs, ponds, and wells.

Results and Discussion

Recharge

Field reconnaissance of the study area revealed numerous places where streams and storm runoff recharge the spoil aquifer. Several streams were observed to flow directly into swallets (i.e., disappearing stream channel) at the toe of spoil slopes. The largest of these streams is Chestnut Gap Branch, a first-order stream with a watershed area of 0.85 km^2.

A number of recharge zones were observed on the spoil during storm runoff events. These occur where the spoil adjoins highwalls or natural bedrock slopes, or where spoil handling resulted in boulder zones being locally exposed at the surface. Storm runoff flows into these areas and then rapidly disappears into the spoil. Likewise, the deep infiltration basin has been functional in this regard, although its present watershed is limited. Numerous small cracks and fissures in the spoil surface were observed to capture lesser amounts of storm runoff. These discrete recharge points or "snakeholes" usually occur where rubble or boulders are exposed or intersect the surface.

Infiltration through the spoil surface is not thought to account for a significant amount of recharge owing to

the compacted nature of the graded spoil. A percolation test performed at the site revealed very low infiltration rate (0.47 cm/h) for water entering the spoil through the graded, compacted surface.

Spring Discharge

The most significant area of observed discharge is a group of three springs located at the northern toe of the Spring Gap Branch hollow fill (fig. 1). The springs crop out at an elevation of approximately 1,040 ft. (317 m). This discharge area is located at the toe of a 39.6-m-thick lift of end-dumped sandstone spoil that overrides a 13.7-m-thick lift of end-dumped shale that is believed to have a lower permeability than the sandstone spoil (Kemp 1990).

Discharge was not observed from the toe of the Long Fork hollow fill. Based on observations made by mine personnel, ground water is flowing through this hollow fill, but discharges directly into the sediment pond located at the bottom of this fill below the surface of the pond.

Ground water also discharges from the spoil into the active dragline pit when the pit is at the level of the No. 7 coal bed, requiring pumping on a daily basis. On occasion pumping rates have reached an estimated 1,360 m^3/d.

Two ponds have been created to store water for dust control. These ponds, shown on figure 1, are located at the northwest corner of the spoil, above the spoil springs. The bottom surface of the northern pond is on the underclay of the Hazard No. 7 coal. The bottom of the second pond has been excavated into the shale unit that is below the No. 7 coal and underclay. Both of these ponds are fed by water from the saturated spoil. Evidence for this observation is (1) the water levels in the ponds are very similar to those observed in the nearest monitoring wells that are located on the buried plateau, (2) although these ponds are pumped to fill 38 m^3 water trucks, the water is never depleted, (3) the ponds do not freeze in the winter, and (4) the electrical conductance (2,100 microsiemens) of the water flowing out of the overflow is similar to that of the spoil-fed springs that crop out below (Kemp 1990). Water overflows from the lower pond during wet periods and cascades down the spoil face by way of a riprap-lined drainage channel, and contributes to the total mine outflow.

A large-capacity flume was installed below the sediment pond to gage the total water outflow. Data collection from the flume has not been continuous owing to periods of freezing conditions and vandalism. However, for the 1992 water year, data were collected for 255 days. The monthly mean discharge data show a range of 0.13 to 0.29 m^3/s. Mean and median discharge are both approximately 0.16 m^3/s.

Ground-Water Occurrence

Figure 2 shows the outline of the spoil complex with a contoured surface of the present buried basal topography. The bottom surface of the interior is dominated by a gently undulating plateau capped by the underclay and shale that underlie the No. 7 coal. This "buried plateau" is bordered by the pre-existing stream drainage (shaded areas) formed by Long Fork to the northeast and Spring Gap-Chestnut Branch to the southwest. A considerable drop in elevation occurs from the plateau level to the bottom of the old stream drainages. Maximum relief (approximately 45.7 m) occurs in the northwest corner of the spoil where the the two buried drainage valleys converge.

A contour map of the water table within the spoil (fig. 3) was created from water elevation data from all 14 monitoring wells on the site, ponds, Chestnut Branch, and spring 1. Water-level elevation data for the wells were collected in June 1991. This map was produced without regard to the basal topography revealed on figure 2. A northwesterly sloping water table is shown with a relatively low gradient in the central plateau of the spoil bottom. Generally, the slope of the water table in this area follows the structure of the bedrock plateau. A structural low exists at approximately the center of the plateau (as shown by the nearly closed 1,110-ft. (335.3 m) contour line(*see* fig. 2). The gradient of the water table increases drastically near the northwest section of the plateau. The steep gradient is interpreted as representing the boundary between two sep-

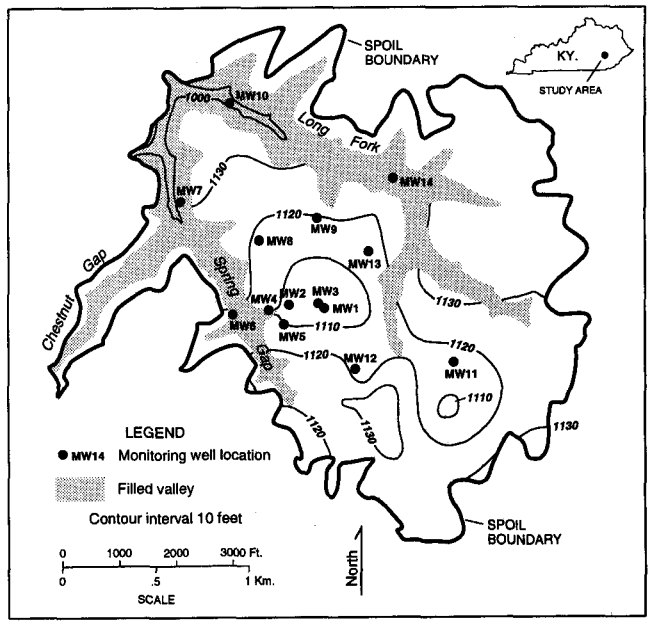

Figure 2. Map showing the contoured bedrock surface after removal of the No. 7 coal.

arate but interconnected saturated zones, separated by the increasing elevation difference toward the northwest between the buried plateau and the bottom of the pre-mining valleys. The structural contour map (fig. 2) shows that the interior basal plateau has roughly a "spoon" shape; thus, the slopes formed by the bedrock along the edges of the plateau may form the barriers that retard water movement in the plateau region.

The overall picture of the distribution of water within a section of the spoil is more clearly illustrated in figure 4, which is a cross section of the spoil through monitoring wells 7, 8, 9, and 13 along the line A-A' shown on figure 1. Two saturated zones are shown: one relatively shallow zone perched on the buried plateau formed by the removal of the No. 7 coal, and the other in the hollow fill of the Chestnut Branch drainage. The water levels in wells on the northern side of the spoil suggest that a similar configuration exists in the Long Fork hollow fill. The saturated zones should be connected at the southeast reaches of the spoil, where the elevation of the buried valleys approaches the elevation of the base of the No. 7 coal.

The apparent lack of direct connection suggests that the water system in the spoil's interior is somewhat stagnant, and that the majority of ground water must flow into either of the two buried valleys before finally discharging in the northwestern corner of the spoil. Additionally, some ground water from the spoil's interior discharges into the two ponds on the northwestern corner of the spoil and contributes to the total mine discharge through the pond's overflow.

Based on an average saturated thickness (6.9 m) determined from water levels taken from the 14 wells dur-

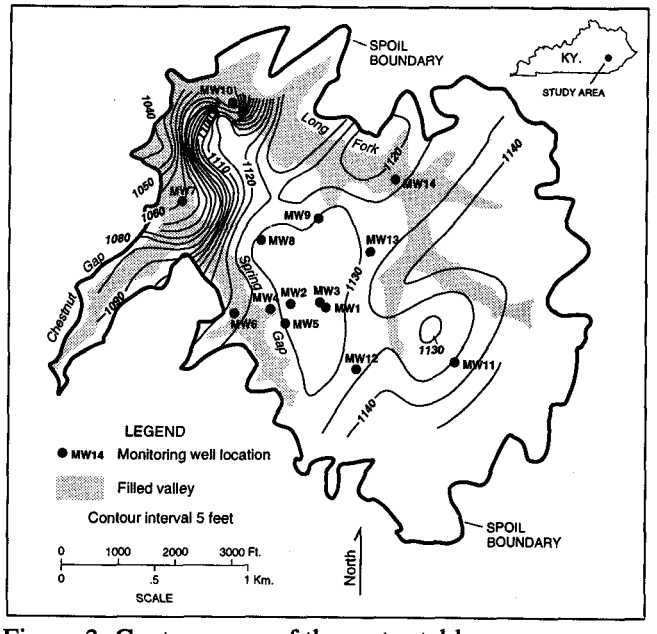

Figure 3. Contour map of the water table.

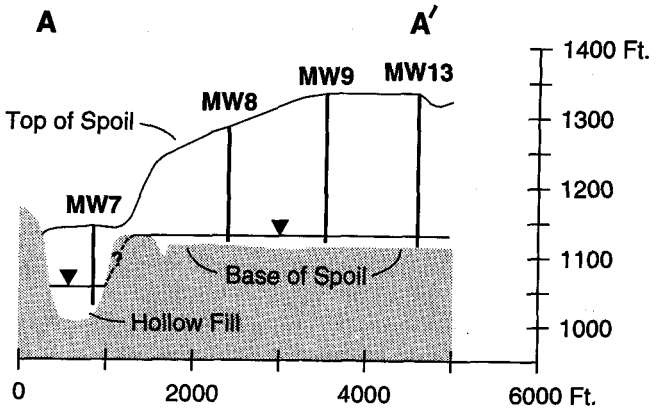

Figure 4. Cross section through line A–A' showing two water tables.

ing April 1991, and an estimated porosity of 20%, there would be approximately 5.2 x E^6 m^3 (1.37 billion gal.) of water stored within this 4 km^2 acres of spoil. Diodato and Parizek (1994) found that the porosity of mine spoil ranged from 30.1 to 57% in shallow, unsaturated boreholes. However, because of the greater spoil thickness, compaction, and saturated conditions at the Star Fire site, the 20% porosity estimate used here seems reasonable.

Slug Tests

Falling-head slug tests were performed in nine monitoring wells at the site during the fall of 1992 (table 1). The hydraulic conductivity (K) values ranged from 7.0 x E-5 to > 9.0 x E-4 cm/s. These values are comparable to those for silty sand (Freeze and Cherry 1979). These values are also consistent with hydraulic conductivity values determined by other researchers in mines that employ similar mining methods. For example, Oertel and Hood (1983) found K values in the range from 4.6 x E-5 to 2.1 x E-2 cm/s and Herring and Shanks (1980) found a range from 4.6 x E-5 to 4.8 x E-2 cm/s.

Table 1. Slug test data—hydraulic conductivity.

Well	cm/sec	ft./sec
MW 4	7.0 X E-5	2.0 X E-6
MW 5	> 8.2 X E-4	> 2.7 X E-5
MW 7	2.0 X E-5	8.0 X E-6
MW 8	> 7.3 X E-4	> 2.4 X E-5
MW 9	4.0 X E-5	1.0 X E-6
MW 10	> 9.0 X E-4	> 2.9 X E-5
MW 12	4.0 X E-4	1.0 X E-5
MW 13	> 5.8 X E-4	> 1.9 X E-5
MW 14	2.0 X E-4	8.0 X E-6

Because some wells (Nos. 5, 8, 10, and 13) were able to take water at a rate that exceeded injection capabilities, only a minimum hydraulic conductivity could be calculated. The actual K's for these wells may be significantly higher than the values given. In addition, high K's may be representative of spoil that exhibits turbulent or non-darcian flow, rendering dubious results.

Infiltration Basin

Water entering the basin probably flows in the direction of well 4 (southwest) toward the Spring Gap hollow fill (Wunsch et al. in press). Therefore, the Spring Gap hollow fill is probably capturing the water infiltrating the spoil through the infiltration basin, from where it most likely moves downslope to the Chestnut Branch hollow fill and discharges from the spoil at one of the springs located on the spoil's outslope. The structure contours shown on figure 2 support this hypothesis. The 1,110-ft. contour and surrounding intervals indicate a structural low in the base of the No. 7 coal beneath the infiltration basin, which slopes in the direction of the Spring Gap hollow fill.

Dye Tracing

A dye trace performed by Kemp (1990) involved injecting dye into monitoring well 1 (fig. 1). This dye was not recovered in the springs in the northwest corner of the spoil. Dye was still visible in well 1 after several months, indicating that ground-water movement is sluggish in the center of the interior spoil area. No discernible difference in hydraulic conductivity appears to exist between the wells tested in the hollow fills or the spoil interior. Therefore, the apparent sluggish nature of the ground-water movement in the spoil interior must be related to gradients induced by recharge-discharge relationships. The spoil interior, lacking any major direct recharge from the surface, remains stagnant, whereas the ground water in the hollow fills receives recharge from the streams that disappear into the base of the spoil, from adjacent bedrock aquifers, and from surface water that seeps in near the bedrock-spoil interface.

Additional dye tracing using Rhodamine WT was performed during the spring of 1991 to determine the flow path of recharge water that enters the spoil through the infiltration basin. Three dye-trace positives were detected to the west of the infiltration basin, which is consistent with the direction of flow as determined by hydraulic gradients and basal topography (Wunsch et al. in press). One positive trace was located in a pit excavated along the highwall-hollow fill contact near well 6. Additional positive traces were found where water flowed from the spoil's face below the elevation of the infiltration basin during wet periods. This indicates that not all of the water that flows into the infiltration basin penetrates to the base of the spoil; instead it may travel along highly conductive paths or be diverted by low-permeability horizontal barriers within the spoil.

Conceptual Model for Ground-Water Flow in the Spoil

Figure 5 shows a map of the spoil body with arrows indicating the assumed direction of ground-water flow. Water that slowly accumulates in the spoil interior flows toward the head of the buried valleys that now are hollow fills. This is evidenced by (1) dye trace data, (2) head data, and (3) bottom structure of the buried plateau.

Water contained in the hollow fills flows toward the northwest, where it discharges. Some of the water stored in the spoil's interior supplies the water to the ponds used for dust control that are situated above the springs. The pond water, in turn, discharges through the overflow down the face of the spoil, where it joins with the spring discharge before entering the lowermost sediment pond.

In summary, this model presents a scenario where the majority of water contained in the spoil moves through the hollow fills from the main spoil body and discharges at the northwest corner of the spoil. Recharge enters the spoil mainly along the edges of the hollow fills, and at discrete points on the reclaimed surface, which includes the infiltration basin.

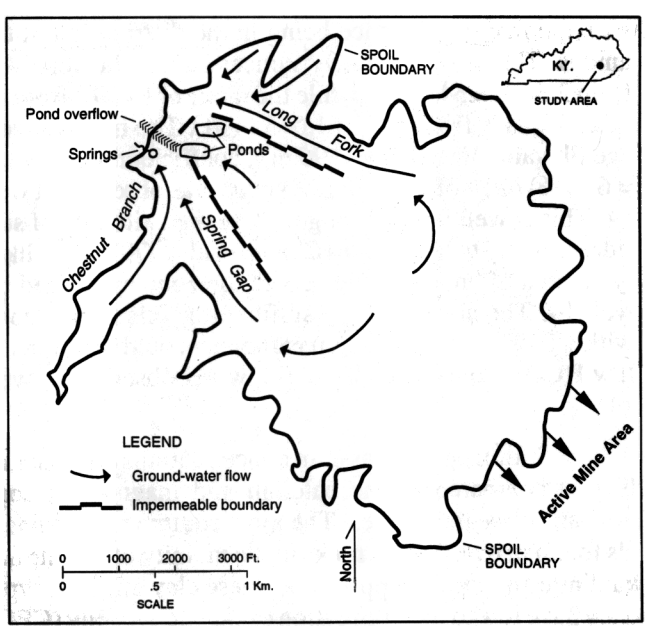

Figure 5. Conceptual model of ground-water flow at the Star Fire site.

Hydrogeochemistry

Interpretation of Spoil Water-Quality Data

Figure 6 shows water samples plotted as a function of the normalized percentage of the samples' major cations and anions. Sixty-eight water samples are represented on the diagram, which includes all samples taken from April 1991 through June 1992 and represent five sampling events. A complete list of data for samples collected from the Star Fire site can be found in Wunsch et al. (in press). All of the samples plot close to a single location on the diamond-shaped field of the diagram, indicating that calcium and magnesium are the major cations and sulfate is the dominant anion. The most likely origin for the Ca-Mg-SO_4 water type found at the site is the oxidation of iron sulfide minerals with the contemporaneous dissolution of calcium carbonate. The data shown here represent four sampling events spanning 14 months, indicating that the water-quality type has little temporal variation.

Figure 7 shows the distribution of pH values for all monitoring wells and spring 1. Monitoring wells show maximum, median, and minimum pH values greater than 6.0 with the exception of wells 6, 11, and 14. Overall, the majority of pH data collected at the site indicate that the mine spoil does not produce highly acidic water.

All samples from well 14 have pH's less than 4.5, which represents the lowest pH encountered on the site. Samples taken from MW 14 are somewhat separated from the group of other samples plotted on the Piper diagram (fig. 6). The samples from well 14 show that the distribution of cations (mainly calcium and magnesium) is consistent with the percentages found in other wells' samples, with the major difference being in the distribution of the anions. The range of HCO_3^- concentrations in well 14 is from 3.66 to 8.54 mg/L, while the range of HCO_3^- from all other wells is from 185 to 1,045 mg/L. The highest average Eh value (mean Eh = 196 mV, coefficient of variation = 6.97%) of all of the wells surveyed was observed at well 14. This is well into the range where the oxidation of sulfides is likely to take place (Champ et al. 1979). Most likely an area of "hot" spoil exists in the zone monitored by well 14. The abundance of sulfide minerals in this zone with a deficiency of calcium carbonate could result in the low HCO_3^- concentrations and low pH observed in well 14.

Sodium and potassium concentrations are generally low compared to the calcium and magnesium concentrations in all samples. The most common clay minerals found in overburden rocks in the vicinity of the site are kaolinite and illite (Papp 1976). These clay minerals typically have low to medium cation exchange capacity (CEC) (Bohn et al. 1985). Therefore, it is unlikely that cation exchange is an important factor in controlling the distribution of cations in the spoil ground water. The release of divalent cations from the dissolution of carbonate minerals appears to dominate the water chemistry reactions, such that any effect of cation exchange is insignificant.

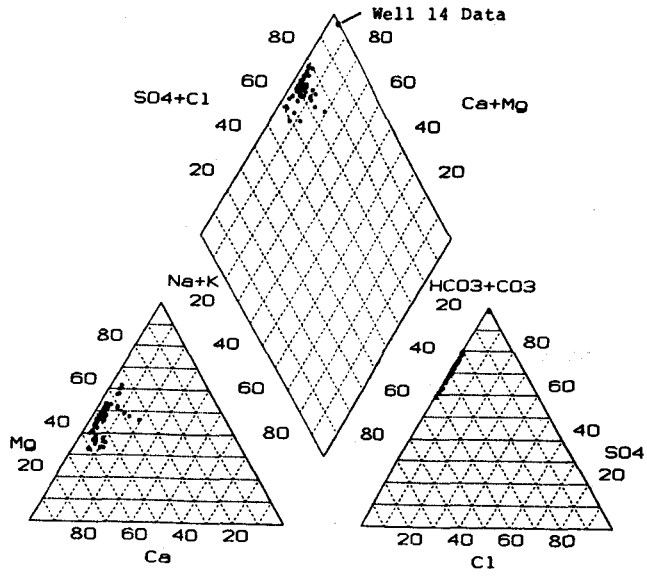

Figure 6. Piper diagram showing water types of groundwater samples from monitoring wells and the main spring.

Based on April 1991 data, the total dissolved solids (TDS) of water samples from wells in the spoil interior are higher than the TDS of wells located over hollow fills. Wells located in the interior section of the spoil (monitoring wells 2, 3, 5, 8, 9, 11, 12, and 13) have a mean TDS of 2,812 mg/L (std. dev. = 457), whereas hollow-fill samples (wells 4, 6, 7, 10, 14, and spring 1) have a mean of 1,128 mg/L (std. dev. = 766). The higher TDS values character-

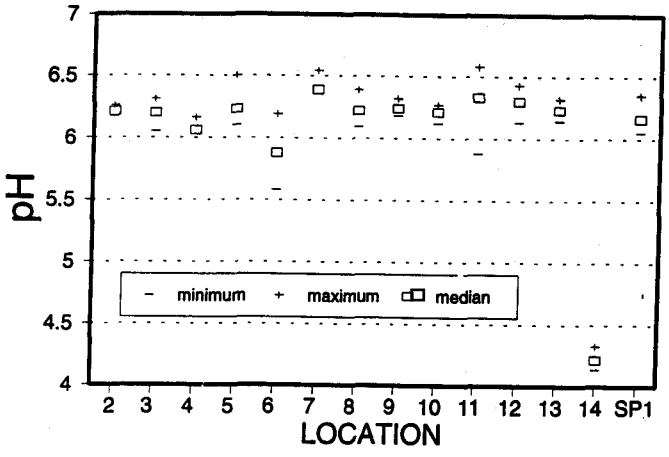

Figure 7. Distribution of pH values for water samples collected from monitoring wells and the spoil spring (SP1).

istic of wells located in the interior of the spoil are most likely the result of longer contact time between ground water and spoil due to slow ground-water movement. The extended contact time allows for greater water-rock interaction and leaching of soluble and reactive rock materials, therefore increasing the concentration of the dissolved constituents.

The TDS for samples taken from the springs and monitoring wells in the northwest area of the spoil (MW 7 and MW 10) are very similar to the TDS of the discharge water exiting the mine site through the flume. TDS values are 2,608 and 2,116 mg/L for wells 7 and 10, respectively, and 2,127 mg/L for the flume discharge water. These preliminary data suggest that the major source of the water discharging from the entire mine site is ground water derived from the mine spoil. If surface-water runoff at the site were making a significant contribution to the total mine outflow, it would be expected that the TDS would be considerably less than that observed. Water from the stream at Chesnut Branch and water entering the infiltration basin have TDS concentrations that are generally less than 500 mg/L (Dinger et al. 1990).

Saturation indices for minerals thought to impart a significant control on the water chemistry were calculated using the geochemical model PHREEQE (Parkhurst et al. 1980). Data used in the calculations are from water samples collected on June 16, 1992. The equilibrium data (table 2) indicate that all water samples are undersaturated with respect to both calcite and dolomite and suggest that these minerals, if present, should dissolve. Dolomite is not abundant in the rocks that comprise the overburden, and probably does not make a significant contribution to the magnesium content of the ground water at the site.

The carbonate cements in the sandstones indigenous to the overburden rocks were determined to be ferroan calcite, which may also contain magnesium and could provide calcium, iron, and magnesium to the ground water. Chlorite is abundant in the overburden, based on mineralogical assessments performed by Papp (1976), and is probably the main source of magnesium. Powell and Larson (1985) found chlorite to be a probable source of magnesium in ground water derived from rocks that are stratigraphically and lithologically similar to the rocks that comprise the overburden at the site. Table 2 shows that all of the water samples are undersaturated with respect to chlorite.

The water from nearly all wells is at or near equilibrium with gypsum ($CaSO_4 \cdot 2H_2O$), with the exception of monitoring wells 4, 6, and 14 (table 2). Each of these monitoring wells is located in an area of the spoil where surface water can easily influence the ground water. The effect of dilution by surface water and lower residence time is the most likely explanation for the degree of undersaturation with respect to gypsum in these three wells. The average total dissolved solids calculated for these wells was the lowest observed from all wells at the site, but the distribution-percentage of cations and anions remained consistent with that of all other ground-water samples.

Table 2. Saturation indices for selected minerals shown in log IAP/K using the model PHREEQE (Parkhurst et al. 1980). IAP=ion activity product, K=equilibrium constant, TDS=total dissolved solids (calculated).

Well	Calcite	Dolomite	Gypsum	Chlorite	TDS
MW 2	–0.3618	–0.8095	0.0116	–10.9561	2412
MW 3	–0.2230	–0.6151	0.0364	–10.8265	2796
MW 4	–1.2823	–2.4945	–0.8279	–15.3130	874
MW 5	–0.2750	–0.6708	–0.0378	–10.2089	2380
MW 6	–1.5691	–3.0704	–0.8140	–17.2109	726
MW 7	–0.2747	–0.3551	0.0095	–7.3621	2608
MW 8	–0.0049	–0.1510	0.0754	–7.8246	3409
MW 9	–0.2792	–0.5369	–0.0681	–9.2461	2812
MW 10	–0.4647	–0.8510	–0.1012	–10.3842	2117
MW 11	–0.5093	–0.9636	0.1195	–12.3585	3596
MW 12	–0.2738	–0.7338	0.1251	–11.3047	2574
MW 13	–0.4078	–0.8301	–0.0217	–9.9278	2521
MW 14	–4.5345	–9.0036	–0.4288	–34.2911	926
SP 1	–2.4520	–4.9492	–0.0336	–11.5458	1591

Wells 8, 11, and 12 show saturation with respect to gypsum. Each of these wells is located in the interior area of the spoil. Two of these wells (8 and 11) contain some of the highest TDS contents observed at the site (table 2). The degree of gypsum saturation in these wells correlates well with the increased mineralization of the ground water in the spoil's interior.

Summary

A ground-water resource evaluation has been initiated to monitor the development of the water table in the spoil, assess the effect of infiltration basins on ground-water development, perform tests to determine the hydraulic properties of the spoil, and delineate ground-water quality over time.

Water-table elevation data from the monitoring wells, springs, and ponds indicate that separate saturated zones exist in the spoil, one in the interior section of the spoil, and two additional at lower elevations in the two adjoining hollow fills (Spring Gap/Chestnut Branch and Long Fork). Most likely these saturated zones are in hydraulic connection in the upper reaches (southeast area) of the spoil body, but are separated by elevation due to the topography of the basal aquitard in the northwestern section of the spoil.

Based on an average saturated thickness of 6.9 m for the site, an estimated 5.2×10^6 m^3 (1.37 billion gal.) exists in the 4 km^2 acre spoil at the Star Fire site.

Slug tests performed in monitoring wells at the site show the range of hydraulic conductivity (K) values encountered in the spoil is from 7.0 x E-5 to > 9.0 x E-4 cm/s. The upper limit of K for spoil could not be determined because of equipment limitations and could be significantly higher than reported.

All waters at the site are a calcium-magnesium-sulfate type. The pH of most ground-water samples fell into a favorable range of 6 to 7. The TDS values for wells located in the spoil interior are significantly higher than those for wells located in the hollow fills. Higher mineralization of the water samples from the interior spoil area probably reflects the longer contact time of ground water with reactive spoil material. These data are consistent with the gentle gradient of the water table and dye-tracing data. Lower TDS values for the hollow-fill wells probably results from a greater contribution of less mineralized surface water into the ground-water flow system and a lower residence time.

Ground-water chemistry appears to be controlled by the dissolution of carbonate minerals and the oxidation of sulfide minerals, resulting in a Ca-Mg-sulfate water type for both ground and surface water at the site. Most of the ground water in the spoil is at or near equilibrium with the mineral gypsum. This may inhibit the use of ground water from the spoil for certain industrial or agricultural applications. Therefore, monitoring of water quality will continue to measure any changes in dissolved mineral equilibria with time.

Two saturated zones occur in the spoil. The interior of the spoil contains a relatively thin and stagnant saturated zone from the accumulation of water from discrete infiltration, the infiltration basin, and the active mining area where uncompacted or reclaimed spoil is present.

Water in the hollow fills is a combination of spoil seepage and ground water from the adjacent unmined bedrock highwall and surface water that accumulates and later percolates into the hollow fills along the spoil/bedrock contact.

Total mine outflow measured in the northwest area of the reclaimed spoil produces a base flow of approximately 0.16 m^3/s (3.9 mgd). Variations in water quality observed at the site are related to the flow system described by this conceptual model.

The initial water-quality and -quantity data measured at the Star Fire Mine demonstrate that ongoing mining techniques can provide the physical framework for an aquifer in the extensive mine spoil. Although the ground water stored in the spoil is not potable at this time, it is likely that it could serve for various agricultural and industrial uses. Development of a useful water supply from within the spoil will be a key factor in future land use and economic diversity of the site and other similar sites in eastern Kentucky.

Literature Cited

Bohn, H. L, B. L. McNeal, and G. A. O'Connor. 1985. Soil chemistry. 2nd ed. John Wiley and Sons, Inc., New York. 341 p.

Champ, D. R., J. Gulens, and R. E. Jackson. 1979. Oxidation-reduction sequences in ground water flow systems. Canadian Journal of Earth Science 16:12–23.

Dinger, J. S, D. R. Wunsch, and J. E. Kemp. 1990. Occurrence of ground water in mine spoil, a renewable resource: Star Fire tract, eastern Kentucky. Mining and Reclamation Conference and Exhibition. (Charleston, West Virginia, April 23-26, 1990).

Diodato, D. M., and P. R. Parizek. 1994. Unsaturated hydrogeologic properties of reclaimed coal strip mines. Ground Water 32(1).

Freeze, A. R., and J. A. Cherry. 1979. Groundwater. Prentice-Hall, Inc., Englewood Cliffs, N. J. 604 p.

Herring, W. A., and T. J. Shanks. 1980. Hydraulic conductivity of cast overburden. EOS 61(48):1193.

Hvorslev, M. J. 1951. Time lag and soil permeability in groundwater observations. U.S. Army Corps of Engineers Waterways Experiment Station Bulletin 36.

Kemp, J. E. 1990. Hydrogeologic characterization of surface mine spoil, Star Fire Mine, eastern Kentucky. M.S. Thesis, University of Kentucky, 102 p.

Oertel, A. O., and W. C. Hood. 1983. Changes in ground water quality associated with cast overburden material in southwest Perry County, Illinois. p. 73–78. In Proceedings of the 1983 Symposium on Surface Mining, Hydrology, and Reclamation. (University of Kentucky, Lexington).

Papp, A. R. 1976. Extractable cations from claystones and shales of the Pennsylvanian Breathitt Formation in eastern Kentucky as related to depositional environments. M.S. Thesis, Eastern Kentucky University, Richmond, Kentucky, 153 p.

Parkhurst, D. L, D. C. Thorstenson, and N. L. Plummer. 1980. PHREEQE, a computer program for geochemical calculations. U.S. Geological Survey Water-Resources Investigations 80-96. 210 p.

Powell, J. D., and J. D. Larson. 1985. Relation between ground-water quality and mineralogy in the coal-producing Norton Formation of buchanan County, Virginia. U.S. Geol. Surv. Water-Supply Paper 2274.

Sobek, A. A., W. A. Schuller, A., J. R. Freeman, and R. M. Smith. 1978. Field and laboratory methods applicable to overburdens and minesoils. Environmental Protection Agency, EPA-600/2-78-054.

Thompson, D. B. 1987. A microcomputer program for interpreting time-lag permeability tests. Ground Water 25(2):212–218.

Weinheimer, R. L. 1983. Vertical sequence and diagenesis in Breathitt sandstones in Eastern Kentucky: M.S. Thesis, University of Cincinnati, 147 p.

Wunsch, D. R, J. S. Dinger, and P. B. Taylor. 1992. Design, construction, and monitoring of the ground-water resources of a large spoil area: Star Fire tract, eastern Kentucky. Kentucky Geological Survey, ser. 11, Report of Investigations 6. 16 p.

Wunsch, D. R, J. S. Dinger, P. B. Taylor, D. I. Carey. in press. The hydrogeology and hydrogeochemistry of a large mine spoil area: Star Fire tract, eastern Kentucky. Kentucky Geological Survey Report of Investigations.

HYDROGEOLOGICAL EVALUATION AND WATER BALANCE OF A THICKENED TAILINGS DEPOSIT NEAR TIMMINS, ON, CANADA[1]

Mark R. Woyshner[2] and Luc St-Arnaud[3]

Abstract: Recent literature suggests that the thickened tailings deposition method has the potential to reduce acid generation and seepage, compared to conventional methods. A commonly studied site is the Kidd Creek deposit, located in northern Ontario. The present study was aimed at providing in-situ verification of the hydrology of that site. The field program included measurements of moisture content, hydraulic head and hydraulic conductivity. Precipitation, pan evaporation, and tailings water evaporation were monitored during the period 1991-93. Water balance components during average conditions (runoff 42% of precipitation, evaporation 51% and infiltration 7%) were similar to published predictions. Hydraulic gradients indicated that pore water in the saturated zone tended to move longitudinally with low average linear pore-water velocities (12 cm/y). The capillary fringe at the top of the tailings cone was observed to be less than 1 m from the surface of the tailings. Normally, the tailings are near 100% saturation after spring snowmelt; summer drying is replenished during the fall and with the following spring snowmelt. Dewatering during a drought year is predicted to have little impact on long-term saturation. When tailings disposal discontinues, the degree of saturation and water-table position are expected to resemble that presently observed in areas of the cone where deposition is not active. These conditions are favorable for decommissioning because the depth of oxidation is limited due to the sustained presence of near-surface saturated conditions. Release of metals and acidity from the tailings site to the environment should be slow because pore-water velocities are slow.

Additional Key Words: cone-shaped thickened-tailings deposit, tailings oxidation, acidic drainage, tailings decommissioning, high moisture retention, low hydraulic conductivity, energy balance and water balance.

Introduction

The use of the thickened-tailings disposition (TTD) method for tailings disposal was originally proposed by Robinsky (1975) for specific advantages such as low initial capital investment, low operational costs, good storage capacity, and the elimination of high perimeter dams, slime ponds and decant systems. The method involves the thickening of tailings slurry which is typically discharged in an elevated central spigot line, thereby producing a large cone-shaped deposit.

At the Second International Conference on the Abatement of Acidic Drainage, Robinsky et al. (1991) argued that the TTD method has the potential to reduce acid generation and seepage, compared to conventional deposition methods. This would be achieved by the creation of a relatively homogeneous tailings mass of low hydraulic conductivity and high moisture retention characteristics in which oxygen entry and the resulting tailings oxidation are very limited. The paper presented laboratory, field, and seepage modeling results from a study of the Kidd Creek thickened-tailings deposit, located in northern Ontario, near the town of Timmins. In a collaborative paper with the present authors, Barbour et al. (1993) subsequently reviewed the TTD method and compiled results of field and laboratory testing of hydraulic and geotechnical characteristics of the Kidd Creek tailings. Conclusions stated that the tailings tended to remain saturated to the surface above the water table, a favorable condition with respect to decommissioning of the tailings. The authors also concluded that the ingress of oxygen is minimized, reducing the long term potential for oxidation and the resulting development of acid drainage.

---

[1]Paper presented at the International Land Reclamation and Mine Drainage Conference and the Third International Conference on the Abatement of Acidic Drainage, Pittsburgh, PA, April 24-29, 1994.

[2]Mark R. Woyshner, Consulting Hydrogeologist, MW Hydrologics Inc, Montreal, PQ, Canada.

[3]Luc C. St-Arnaud, Program Leader, Noranda Technology Centre, Pointe-Claire, PQ, Canada.

The present paper describes the field testing in detail, and presents some of the findings to date. The program commenced in the summer of 1991 and included measurements of moisture content, hydraulic head, and hydraulic conductivity. Field monitoring included precipitation, pan evaporation, and evaporation from the tailings surface by the Bowen Ratio energy balance method. A monthly water balance was assembled for 1992 and calibrated to the measured water-table elevation. The water balance was estimated for average (i.e., steady state) conditions by using monthly meteorological normals from the Environment Canada meteorological stations. Extreme conditions were analyzed by substituting precipitation from the driest year of record and evaporation from the highest year of record. Results give insight to the degree of tailings saturation and therefore a sense for the likelihood of tailings oxidation.

Site Description

The regional topography is generally flat and forested, featuring elevated bedrock exposures rising above broad, wet lowlands. Since 1975, approximately 50 million mt of sulfide-mineral tailings have been deposited at a high point in the Porcupine River watershed, using the thickened-tailings disposal method. The thickener underflow density was gradually increased from 50% in 1976 to 61.5% at present (Yeomans 1985). The resulting tailings cone presently covers a circular area of 1,215 ha and at its center extends 23 m above the perimeter diking. It has a slight concave slope of about 1.5%. The Porcupine River flows along the west side of the site, to the north, and then shifting south to pass the east side of the site, almost encircling the entire deposit before reaching Nighthawk Lake to the southeast.

Beneath the tailings cone, the dominant overburden material is a varved clay, constituting part of a sequence deposited some 8,000 to 10,000 yr ago during the last phase of glacial Lake Ojibway (Quigley 1980). The clay is overlain by a thin layer of organic soil (peat) and underlain by uneven till and bedrock. A bedrock ridge exists underneath the present main embankment, where spigoting has taken place.

Field and laboratory testing of the tailings have been conducted by several researchers, most of which are reviewed by Barbour et al. (1993). The average hydraulic conductivity is 5×10^{-8} m/s. Porosity is about 46%, varying by $\pm 7\%$ with depth owing to alternating summer and winter deposition. In the summer, evaporation dewaters the surface of the tailings, thereby increasing the matric suction and consolidating the material to a lower porosity. The dry bulk density is about 1.7 g/cm^3 and specific gravity is 3.1. The tailings surface is nonvegetated and shows polygonal shrinkage cracks.

Regional Climate

The climate of northern Ontario may be classified as modified continental. The modification is mainly due to the presence of the Great Lakes on the south and, to a lesser extent, to Hudson Bay on the north (Chapman and Thomas 1968). A pattern of relatively low winter and high summer precipitation prevails in northern Ontario, although not to the degree that this occurs in the Prairie Provinces. This seasonal contrast decreases from northwest to southeast. Cold polar air masses producing dry, clear weather generally persist much of the winter. In the summer, a continuing succession of cyclonic storms sweeps over the area from west to east; warm, humid air masses from the south alternate with cooler and drier air from the north. This produces a typical pattern of 2 or 3 days of clear weather followed by warmer, more humid weather, often with changeable winds and rain for a day or two. The climate of the Kidd Creek region is particularly modified by Lake Superior; air masses generally track across the lake, which results in higher precipitation and a seasonal lag, retarding the onset of spring. The average annual precipitation at Timmins Airport is approximately 860 mm.

Investigative Methodology

Hydrometeorological Monitoring

A data-logger-driven monitoring station was installed on the tailings to measure precipitation, pan evaporation, and the evaporation of water from the tailings surface. Precipitation was measured with a tipping-bucket rain gage and pan evaporation was measured with a U.S. class A evaporation pan. Tailings evaporation was deduced from measurements of net radiation, soil heat flux, and vertical gradients of air temperature and vapour pressure. An energy budget by the Bowen ratio partitioning method of surface energy was used to calculate the latent heat flux from the tailings surface. The latent heat flux was then converted to a mass flux of water with the latent heat of vaporization. A summary of the method is found in Oke (1987). A snow density survey was conducted at the end of March to determine the water content of the snow pack before melting.

Hydrogeological Measurements

Instrumentation for measuring hydrogeologic parameters primarily consisted stations of 2 to 4 piezometers of different lengths. Several piezometer stations were located in the tailings (fig. 1): (1) along Section A-A', northwest from the top of the cone; (2) at Station B1, the hydrometeorological station; and (3) along Section C-C', southwest from the top of the cone. Section A-A' was selected to determine the horizontal hydraulic gradient in a portion of the site where tailings were not actively being deposited. At Section C-C', tailings were being deposited and the piezometer stations were located in the flow path of tailings slurry. C1 was located in an entrenched channel, above the point where the flow begins to spread and form a depositional fan, and C2 was located approximately 300 m downstream of C1 at the right (north) edge of the fan, where sheet flow had been actively depositing tailings. Station B1 included tensiometers which measured the hydraulic head above the water table.

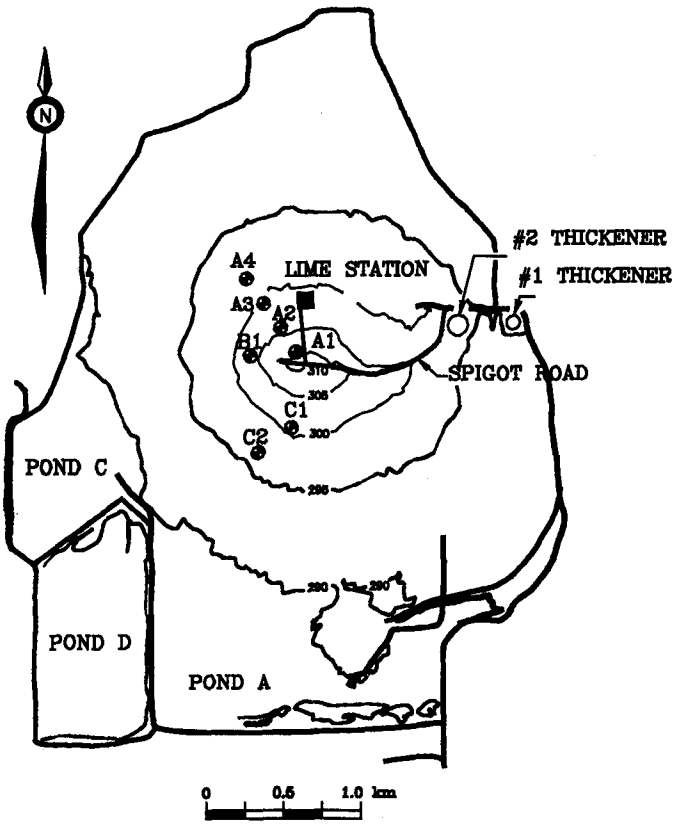

Figure 1. Piezometer nest location map.

Weekly water-level measurements were conducted in the spring, summer and fall. Monthly measurements were conducted in the winter. Continuous monitoring of the water level at B1 was conducted with submersible pressure transducers, connected to the data logger. Hydraulic conductivity measurements were conducted in each piezometer by the falling head method (Hvorslev, 1951). During 1991, soil-moisture content was measured at A1.

Available Data

Precipitation has been measured at Timmins Airport, ON since April 1955, and since 1968, pan evaporation has been measured at Amos, PQ, about 200 km to the east. Data from these stations were correlated to Kidd Creek data. Water-level measurements in a borehole network has been measured on a monthly basis by Kidd Creek personnel, since March 1991. A westwardly cross section of four boreholes were selected to illustrate the annual

changes in water-table elevation. Each borehole was installed with a piezometer which had a screened section that extended the entire depth of the saturated zone. These piezometers averaged the pore-water pressures of the entire saturated zone; therefore, they measured the water-table elevation where vertical hydraulic gradients were small. Concurrent with the present study, a runoff and erosion study had commenced in 1991 (Paul Wisner and Associates et al. 1993). A runoff coefficient (C=R/P) was determined for each runoff event and each month.

Findings and Discussion

Hydrogeology

Pore-water Flow. Figure 2 shows interpolated hydraulic head contours along Section A-A' following the largest rainfall of 1992. Flow is perpendicular to the contours and therefore primarily lateral, along the length of the cone. Tendencies for downward flow are apparent at the top of the cone. Upward flow is presumably past A4, further down the cone, although no well defined seepage face is observed. Percolation from the base of the tailings is likely restricted by the underlying clay soil. The average lateral hydraulic gradient is 0.017 which is similar to the slope of the tailing surface (0.015). Using Darcy's law, a porosity of 0.46, and a hydraulic conductivity of 1 x 10^{-7} m/s, the calculated flow velocity is 0.12 m/y. This velocity is quite low. Specific discharge is 0.054 m/y, which is also quite low.

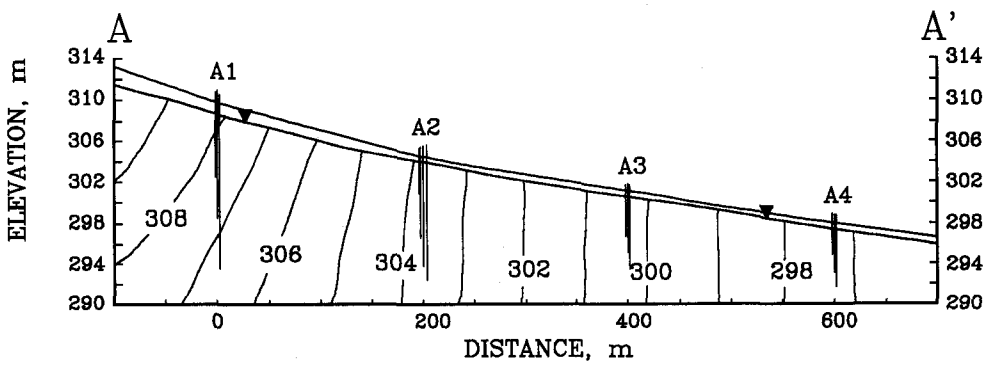

Figure 2. Hydraulic head contours at section A-A'.

Figure 3 shows the monthly water-level measurements in boreholes along a westwardly cross section from BH1 to BH4. These data indicate that the water table is high after snowmelt and during the fall, and low during the summer and winter. Figure 4 illustrates hydraulic heads at piezometer nest B1 during the summer and fall of 1992 and 1993. The hydrograph generally depicts the trend that was observed at all stations where the lowered summer water table rises in response to precipitation and a waning evaporation rate, to remain at a high level through the autumn and early winter. The advent of the recharge period was earlier in 1992 because August 1992 was much wetter than August 1993. The upward gradients shown in figure 4 may be caused by local flow within the cone; at other stations they are less frequent.

Hydraulic heads readily responded to individual rainfall events, rising as much as a meter, only to fall again during the dry period that followed each storm. These large fluctuations in water table levels typically occur in fine-grained soils, a process which has been described by Abdul and Gillham (1984). It is related to the fact that the water table can rapidly rise through the capillary fringe (i.e., the tension-saturated zone) after an infiltration event of minor intensity.

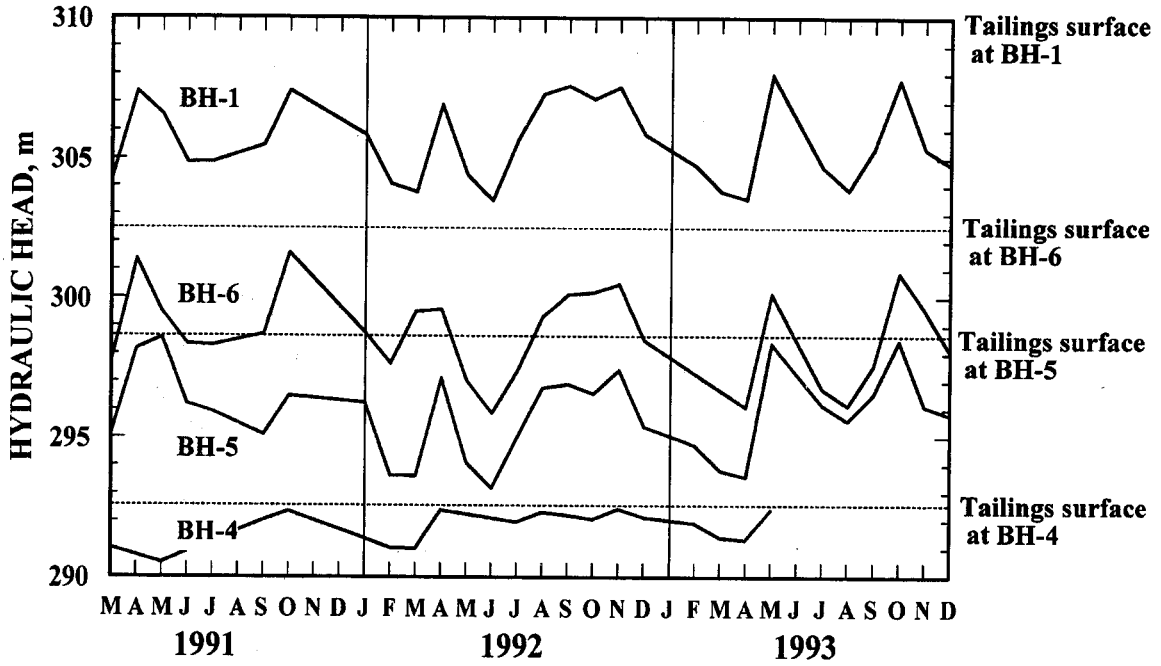

Figure 3. Borehole water-table elevations.

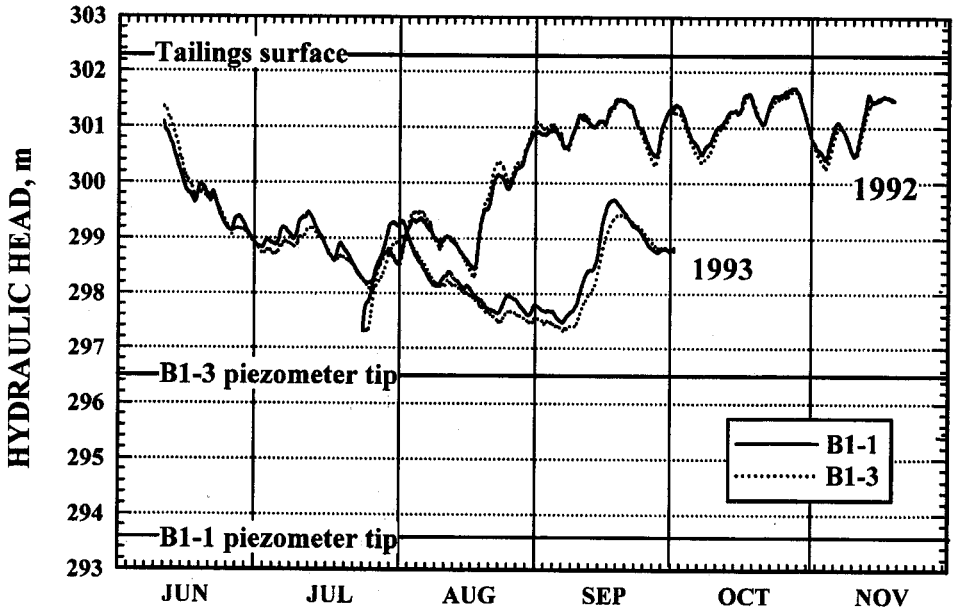

Figure 4. Hydraulic head hydrograph at B1.

The Capillary Fringe. Figure 5 shows soil-moisture content and water-table elevations at A1. Since this station is located near the top of the cone, the water table is farthest from the surface and the vadose zone is more developed than at other places on the cone. The water content profile shows the density layering from alternating summer and winter deposition. Full saturation is therefore depicted as a range from 22% to 27% (w/w). Figure 5 features a rising water table and capillary fringe, which is responding to infiltration. Most significantly, the thickness of the capillary fringe, the tension-saturated zone that extends above the water table, is delineated at approximately 4 m and is within 1 m of the tailings surface.

The capillary fringe is not always the same thickness. When the water table drops, the capillary fringe elongates, and when the water table rises (as in fig. 5), it retracts. The capillary fringe is held by surface tension, which causes its top to fluctuate with less magnitude than that of the water table. A plot of suction versus water content (drainage curve) best illustrates this phenomenon.

Figure 6 shows the drainage curve for the Kidd Creek thickened tailings (Yang et al, 1992). Matric suction is the force with which soil holds water by surface tension; it is equivalent to the negative pressure head, but expressed as a positive number. Pressure head is zero at the water table, positive below and negative above. Figure 6 indicates that up to a suction of about 6 m of water (60 kPa), significant drainage does not occur. Since this is the suction exerted at the top of the capillary fringe, 6 m is the predicted maximum thickness of the capillary fringe. If the water table drops below this, the larger voids at the top of the capillary fringe drain and therefore fracture the continuous water column. Recharge of water from infiltration causes the water table to rise and the thickness of the capillary fringe to diminish, as in figure 5. The larger voids at the top of the capillary fringe require significantly larger amounts of recharge to completely fill, which therefore limits the ability of the top of the capillary fringe to rise. Therefore, the thickness of the capillary fringe fluctuates, which is accompanied by the water-table fluctuation.

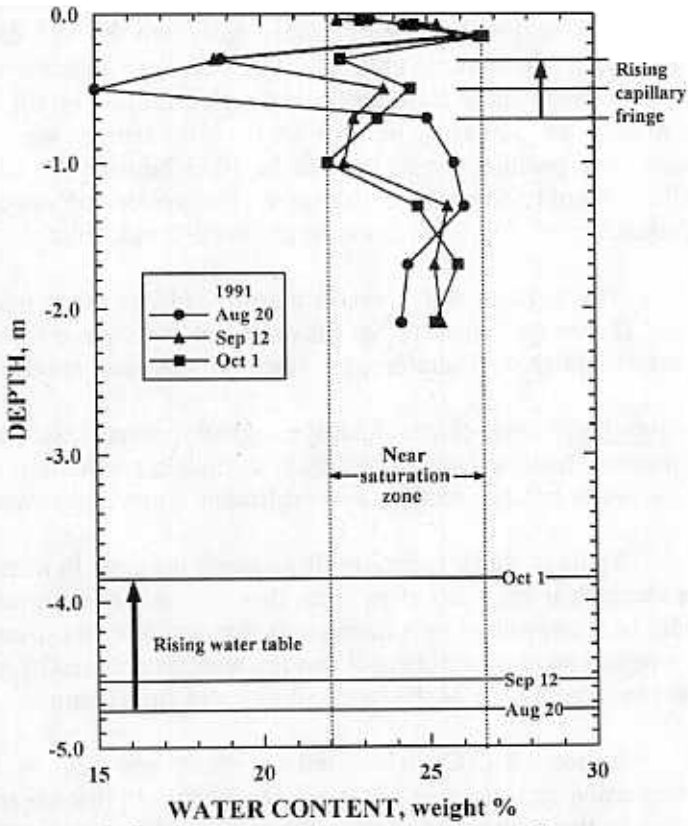

Figure 5. Recharge conditions at station A1.

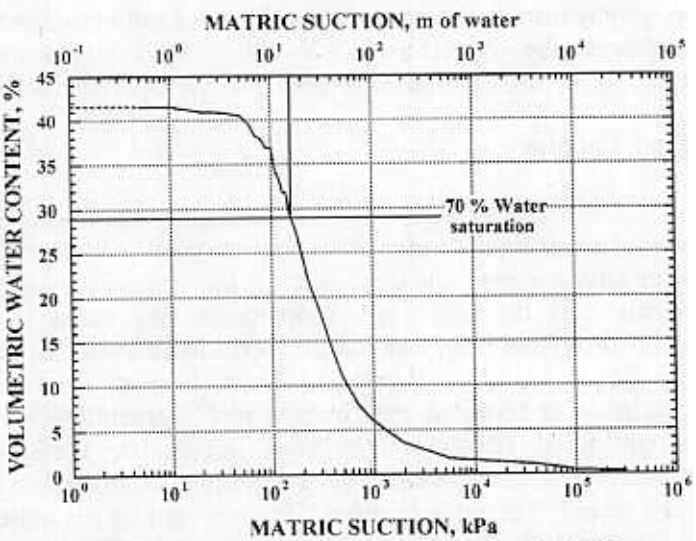

Figure 6. Drainage curve of the Kidd Creek tailings.

Oxygen Diffusion. In soils with a high degree of water saturation, the diffusion coefficient of oxygen (D_e) is the principal control on the rate of oxygen entry into the soil. Experiments using a well sorted till indicate that D_e does not significantly increase until the degree of water saturation drops below 70% (Yanful 1993). Applying this factor to the drainage curve from the Kidd Creek tailings (fig. 6), D_e would not increase until the matric suction is about 16 m of water (160 kPa). In other words, if the tailings were allowed to drain under gravity (and not evaporate), the water table position would have to be 16 m beneath the tailings surface before the rate of oxygen entry into the tailings would increase significantly. The results of ongoing diffusion experiments will help to confirm the applicability of this 70% factor on the Kidd Creek tailings.

The depth to water was between 6 and 7 m at the top of the cone and between 1 and 2 m at the base of the cone. Therefore, if it were not for drying at the surface by evaporation, the flux of oxygen into the soil would be constant and slow. Therefore, for practical purposes, gravity drainage will not promote oxidation.

Infiltration. One of the hydrogeological concerns is whether the water-table elevation is sustained by the infiltration. Infiltration is caused by precipitation and tailings-slurry water. Infiltration from precipitation is addressed in the water balance section, and infiltration from slurry water is adressed in this section.

Tailings slurry generally flows down the cone in a small braided channel. When the flow reaches the end of the channel, it spreads out as sheet flow, about 500 m down the cone where the grade decreases. The increase in width is accompanied by a decrease in depth and velocity, causing deposition of tailings and the formation of a fan. The wetted areas of the channel and fan were determined by planimetry of infrared areal photographs (1:5000 scale), and consisted of 1% of the total tailings area (maximum).

At section C-C', where tailings slurry was actively flowing, the water table fluctuated and responded to precipitation and dry spells in a similar manner to that observed at the other stations. Vertical gradients were also similar to those observed at the other stations. These data indicate a control of the tailings pore-water flow beneath the channel and fan area by the pressure dynamics of the cone. However, the water-table fluctuation was about 1.5 m, much less than that at the other station, and the depth to water table was shallower (0.4 to 1.8 m at C1, and 0 to 1.2 m at C2) in comparison to the other piezometer nests. At C1 and C2 water levels are controlled more by the topography than by the ponds. These facts suggest some contribution of water by tailings slurry discharge. However, considering the channel areas constitute only 1% of the tailings, infiltration by thickened tailings discharge is negligible in the water balance (less than 1% of precipitation).

Water Balance

The water balance was used to quantify infiltration and analyze its affect on water-table position. Monthly water balances were assembled for three separate conditions: (1) for the studied year 1992, which was calibrated to the measured water table elevation; (2) for average (i.e., steady state) conditions by using monthly meteorological normals from the Timmins Airport station and Amos station; and (3) for extreme conditions by substituting precipitation from the driest year on record at Timmins Airport and from the highest evaporation on record at Amos.

Description of Data. In the Timmins area, it generally rains from May through October and snows from November through March. The snow cover, which accumulates during winter, melts mostly during April. Monthly runoff was estimated with runoff coefficients. Environment Canada data was correlated to site measurements to extend the Kidd Creek record. The ratio of runoff (R) to rainfall (P) is defined as the runoff coefficient (C=R/P). Monthly runoff coefficients were determined on site for the year 1992 (Paul Wisner and Associates et al. 1993). These coefficients were adapted for average and extreme conditions by considering the monthly precipitation and season. Both pan evaporation and evaporation from the tailings surface were measured on site. Evaporation coefficients ($C_E=E_{tailings}/E_{pan}$), the ratio of tailings water evaporation to pan evaporation, were calculated for each month (table 1). The average C_E for each month was applied to the pan evaporation to estimate the evaporation of water from the tailings surface.

Table 1. Monthly evaporation coefficients at Kidd Creek thickened tailings site.					
Year	June	July	August	September	October
1991	no data	no data	0.37	0.66	0.46
1992	no data	no data	no data	no data	no data
1993	0.56	0.69	0.45	0.65	no data
Average	0.56	0.69	0.41	0.65	0.46

Infiltration (I) is quantified in the water balance by subtracting runoff and evaporation from precipitation (i.e., rainfall and snowmelt), leaving drainage (D) and the change in tailings moisture storage (ΔS) as unknowns. ΔS is the change in water-table elevation and tailings saturation. By arbitrarily setting ΔS to zero at the end of snow melt, negative values for succeeding months indicate a loss of moisture and a lower water table, and positive values indicate a gain of moisture and a higher water table. Water-table measurements during 1992 were used to calibrate the water balance. D (unknown) is adjusted to match ΔS to the water-table position. The specific discharge (54 mm/y) was used as D and gave reasonable values of ΔS.

Results. Figure 7 shows the monthly water balance results and table 2 summarizes the annual results. 1992 was a year of normal precipitation and normal evaporation. Evaporation, was high during May, and precipitation was high during August. Storage decreased during May and June and increased through the rest of the year. The position of the water table during 1992 confirmed the predicted trend. In December, a storage deficit was 35 mm. The water table position was observed to drop about 2 m by the end of 1992 (fig. 3), accompanied by the 35-mm deficit in the water balance. This gives a calculated specific yield (S_y) of 0.02 (35 mm/2 m). Since the usual range of S_y in unconfined aquifers is 0.01-0.3, a value of 0.02 seems reasonable for a soil (like the Kidd Creek tailings) with a high moisture retention capacity.

For average conditions, as in 1992, storage decreases following snowmelt and increases after summer. However, ΔS decreases less for the 3-month period May through July, is low during August, and increases from September through November. By the end of November, ΔS is at its original level. During winter (December-March), ΔS decreases slightly, only to be replenished by spring snowmelt. No annual deficit of ΔS was found. Infiltration during average conditions is similar to the 9% that was predicted with the Hydrological Evaluation of Landfill Performance (HELP) model by Robinsky et al. (1991).

For extreme dry conditions, storage decreased from May through August and stayed low for the remainder of the year. Furthermore, from August through the end of the year, ΔS was similar to that of July 1992. Therefore, the moisture conditions observed during July of 1992 reflected those of an extreme dry year. Since moisture was nearly replenished by the end of 1992, the dewatering following an extreme dry year should be replenished with normal rainfall. However, also considering that an additional year of evaporation would follow, average conditions may sustain the dry condition; above-normal rainfall would be necessary for replenishment.

Table 2. Water balance summary expressed as percent of precipitation.			
Hydrologic Component	1992	Normal Conditions	Extreme Dry Conditions
Runoff	48	42	39
Evaporation	51	51	72
Infiltration	1	7	-11

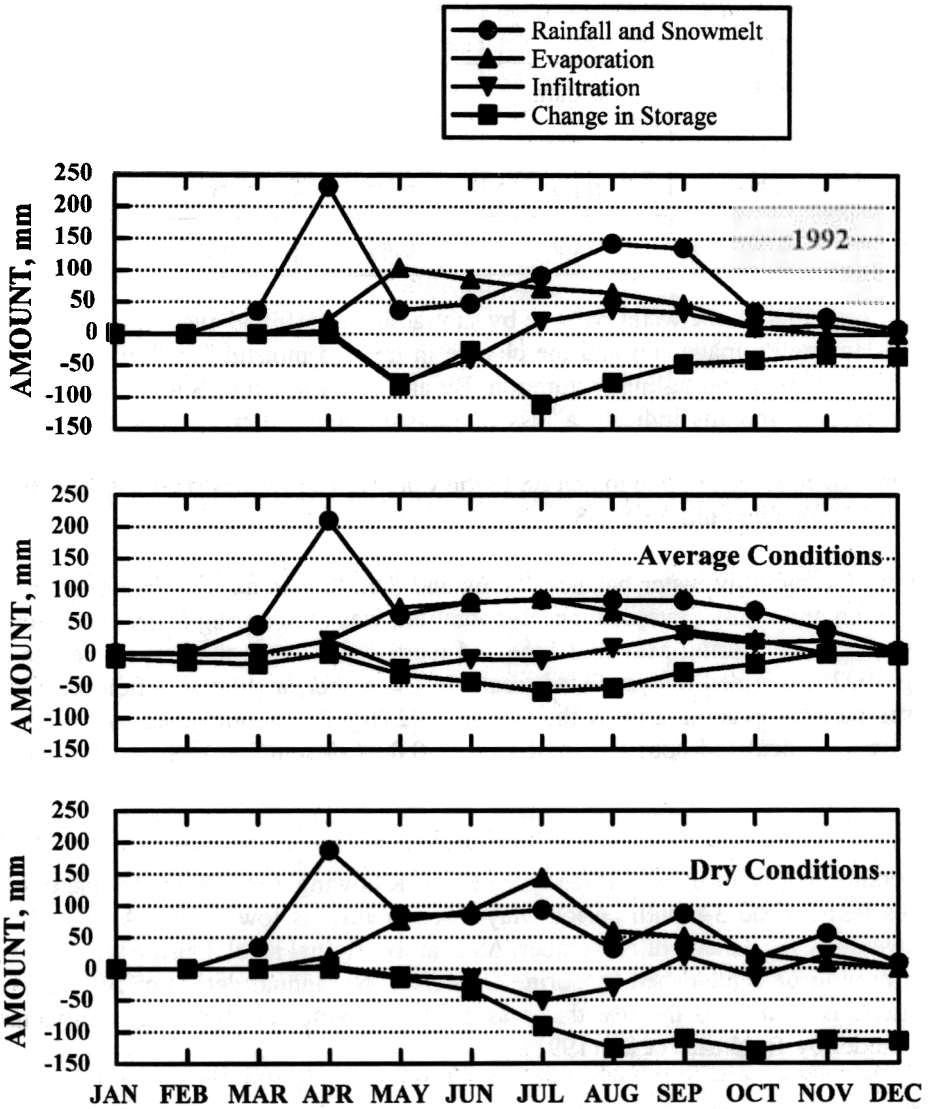

Figure 7. Water balance of the Kidd Creek tailings cone.

Summary and Conclusions

This paper reviewed hydrologic and hydrogeologic field data collected at the Kidd Creek thickened-tailings site. The findings confirm that very little slurry water contributes to water-table recharge, and if tailings deposition presently discontinues, then tailings saturation and water table position are expected to resemble that presently observed in areas of the cone where deposition is currently not active. Observations at the top of the cone, where the unsaturated zone is more developed, indicated near-saturated conditions within 1 m from the tailings surface. In this upper 1 m zone, where the top of the capillary fringe fluctuates, oxygen diffusion is predicted to be slow owing to the water saturation. Water balance modeling indicated that dewatering during a dry year is expected to have little impact on long-term saturation of the tailings. These conditions are favorable for decommissioning because the depth of oxidation is limited due to the sustained presence of near-surface saturated conditions. Release of metals and acidity from the tailings site to the environment should be slow because pore-water velocities are slow.

Acknowledgements

The authors thank the staff of Environment Control and Services at the Kidd Creek Division, in particular B. Swarbrick and M. Casper, for their invaluable assistance. The work could not have been realized without the technical contributions by the staff of the Noranda Technology Centre (NTC). Technical discussions with E. Yanful (NTC), L. Barbour and W. Wilson (Univ. SK), D. Blowes (Univ. Waterloo) and E. Robinsky and R. Salvas (E. Robinsky and Associates) were appreciated. K. Wheeland (NTC) and D. Bordin (Kidd Creek) provided project management. Funding for this work was provided by Falconbridge Ltd., Kidd Creek division, Environmental control and services.

Literature Cited

Abdul, A.S., and R.W. Gillham. 1984. Laboratory studies of the effects of the capillary fringe on streamflow generation, Water Resour. Res. 20(6):691-698.

Barbour, S.L., G.W. Wilson, L.C. St-Arnaud, R.J. Salvas, and D. Bordin. 1993. Aspects of environmental protection provided by thickened tailings disposal. p. 725-736. In Bawden and Archibald (eds), Innovative Mine Design for the 21st Century. Balkema, Rotterdam, ISBN 90 3410 325 6.

Chapman, L.J., and M.K. Thomas. 1968. The climate of northern Ontario, Climatological studies, No. 6. Can. Dep. Transport, Ontario. UDC: 551.582(713). 58 p.

Hvorslev, M.J. 1951. Time lag and soil permeability in groundwater observations. U.S. Army Corps Engrs. Waterways Exp. Sta. Bull. 36, Vicksburg, MS.

Oke, T.R. 1987. Boundary layer climates. Routledge, New York. 435 p.

Paul Wisner and Associates Inc. and W-E-R Engineering ltd. 1993. Tailings area surface hydrological study Falconbridge Ltd Kidd Creek division. Phase I final report presented to Falconbridge Ltd., Kidd Creek Division, Environmental Control and Services.

Quigley, R.M. 1980. Geology, mineralogy and geochemistry of Canadian soft soils: a geotechnical perspective. Can. Geotech. J. 17:261-285.

Robinsky, E.I. 1975. Thickened discharge -- a new approach to tailings disposal. Bull. Can. Inst. Min. and Metallur., p. 47-59.

Robinsky, E.I., S.L. Barbour, G.W. Wilson, D. Bordin, and D.G. Fredlund. 1991. Thickened sloped tailings disposal: an evaluation of seepage and abatement of acidic drainage. In Proceedings of the Second International Conference on the Abatement of Acidic Drainage. (Montreal, PQ, September 16-18, 1991).

Yanful, E.K. 1993. Oxygen diffusion through soil covers on sulfidic mine tailings. J. Geotech. Eng. 119(8):1207-1228

Yang, N., S.L. Barbour, and G.W. Wilson 1992. A laboratory characterization of the properties of the Kidd Creek thickened tailings required for evaporative flux modelling. Univ. SK, Dep. Civil Eng., Geo-Environmental Eng. Group, 74 p.

Yeomans, T.J., 1985. Tailings disposal at Kidd Creek Mines Ltd. p. 184-223 In Proceedings of the Canadian Mineral Processors 17th Annual Meeting. (Ottawa, ON, 1986).

THE PORE-WATER GEOCHEMISTRY OF THE Cu-Zn MINE TAILINGS AT KIDD CREEK, NEAR TIMMINS, ONTARIO, CANADA[1]

Tom A. Al[2], David W. Blowes[2], and John L. Jambor[3]

Abstract: The Kidd Creek Cu-Zn sulfide deposit near Timmins, ON. has been in operation since 1966, with current production of approximately 10,000 tpd. Tailings from the deposit contain 10 to 25 wt % pyrite and are disposed of as a thickened slurry in a 12- to 15-m high cone-shaped deposit in a 1,200-ha impoundment. Approximately 2.5 wt % natrojarosite residue from the zinc concentrate refining circuit has been disposed of with the tailings since 1985. The natrojarosite residue is limited to the upper 4.5 m of tailings. Three geochemical zones are defined by the pore-water concentrations of metals and SO_4. In the deepest zone, concentrations of most metals and anions are below detection and Na, K, Mg, Mn, Fe, Zn, HCO_3, and SO_4 are low, reflecting the mill discharge-water released with the tailings. In this zone, gypsum precipitation controls the concentrations of Ca and SO_4, the dominant elements in the pore water. Higher concentrations of Na, K, Mg, Mn, Fe, Zn, Pb, As, HCO_3, and SO_4 occur in an intermediate zone coincident with detectable natrojarosite in core samples. These increases indicate that some natrojarosite deposited with the tailings has dissolved. Higher Zn concentrations in the intermediate zone than in the deep zone are attributed to minor substitution of Zn in natrojarosite and to residual aqueous Zn-sulfate in the natrojarosite residue that is co-disposed with the tailings. A surficial zone with visible signs of sulfide oxidation contains high concentrations of Na, K, Mg, Mn, Fe, Zn, Pb, Cu, Ni, Co, Cd, Al, As, NO_3, and SO_4. Oxidation reactions, and the consequent pH decrease, have increased the concentrations of metals and SO_4 in the shallow pore-water.

Additional Key Words: mine tailings, tailings geochemistry, sulfide oxidation, jarosite, jarosite disposal, Kidd Creek.

Introduction

The Kidd Creek Cu-Zn deposit is approximately 25 km north of Timmins, ON, (fig. 1). The ore consists mainly of chalcopyrite, sphalerite, galena, and pyrite in massive ore, and chalcopyrite in stringers. In production since 1966, peak production of 12,400 tpd in 1985 has declined to approximately 10,000 tpd. Tailings are deposited as a thickened slurry in a 12- to 15-m high conical pile within a 1200-ha impoundment (Robinsky et al. 1991). The tailings consist of 10 to 25 wt % pyrite, 1 to 2 wt % pyrrhotite, 1 to 2 wt % combined sphalerite and chalcopyrite, 75 to 85 wt % gangue minerals, dominated by quartz and various silicates, 1 to 5 wt % carbonate minerals, and traces of numerous other minerals.

---

[1]Paper presented at the International Land Reclamation and Mine Drainage Conference and the Third International Conference on the Abatement of Acidic Drainage, Pittsburgh, PA, April 24-29, 1994.

[2]Waterloo Centre for Groundwater Research, University of Waterloo, Waterloo, Ont., Canada, N2L 3G1

[3]Mineral Sciences Laboratories, CANMET, Energy Mines and Resources Canada, 555 Booth St., Ottawa, Ont., Canada, K1A 0G1: Current Address: Waterloo Centre for Groundwater Research, University of Waterloo, Waterloo, Ont., Canada, N2L 3G1

The zinc-refining process used at Kidd Creek removes dissolved Fe from acidic Zn- and Fe-SO_4 solutions by precipitating natrojarosite ($NaFe_3(SO_4)_2(OH)_6$) (Scott and Dienstbach 1990). This natrojarosite residue was deposited in a settling pond until the pond reached capacity in 1985; since then the residue has been blended with the mill tailings prior to disposal. The natrojarosite residue, which averages 2.5 wt % of the tailings solids, is confined to the upper 1- to 4.5-m of the tailings impoundment.

In this study, pore-water geochemical data were collected through the vadose and saturated zones at several locations in the Kidd Creek impoundment (fig. 1). Coincident core samples of the tailings were collected for mineralogical analysis to identify the solid phases in contact with the pore water. These data and geochemical modeling were used to assess and interpret the geochemical mechanisms controlling the composition of the tailings pore water.

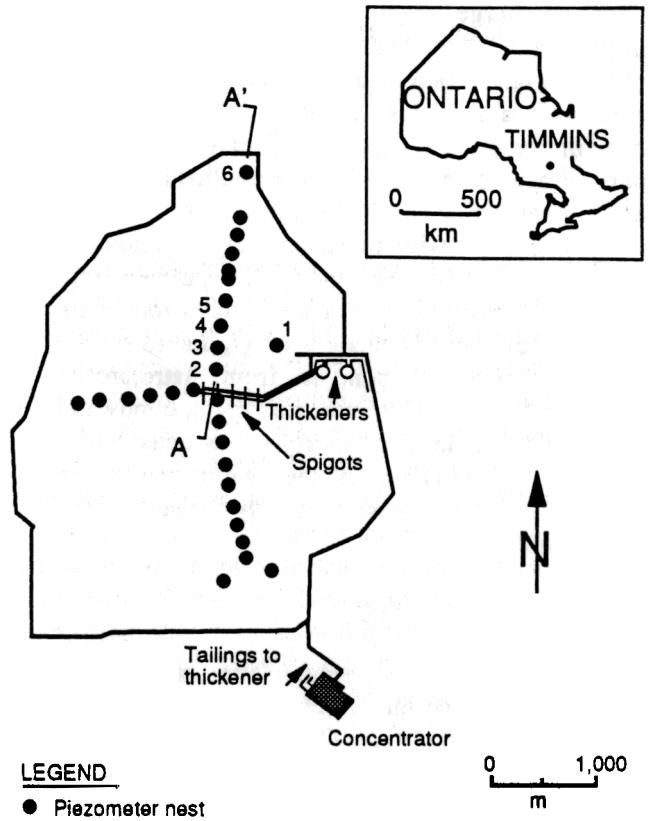

Figure 1. Location of the study area and piezometer nest sites.

Methods of Investigation

Pore water from the vadose zone at all sites (fig. 1) was sampled by collecting cores in thin-walled aluminum casing, 7.62-cm in diameter. The cores were cut into lengths of 20- to 25-cm, and pore water was squeezed from each section. Pore water from the saturated zone was collected with a peristaltic pump, in polyethylene lines, from polyethylene-lined stainless steel or PVC, single-completion drive-point piezometers installed at regular intervals between the water table and the base of the tailings. All piezometers were bailed dry prior to sampling. Groundwater temperatures were measured with a thermistor probe in the piezometer tip after the sample was collected. Determinations of pH and E_H of the vadose-zone pore-water were made at least three times during the collection of each sample. Measurements of pH and E_H of the saturated-zone pore-water were made in a sealed flow-through cell, maintained at the groundwater temperature. The Ross combination pH electrode was calibrated with standard buffers at pH 4 and 7, and the platinum redox electrode was checked regularly with Zobell's solution (Garrels 1960). All samples were filtered through 0.45-µm cellulose acetate filters, then split into two volumes. One was acidified with 12N, analytical-grade HCl to a pH of less than 1 for cation analysis, and the unacidified subsample was used for anion analysis. All samples were refrigerated until analysis. Cations were determined by atomic absorption spectroscopy, and anions by ion chromatography. Pore-water alkalinity was measured in the field on subsamples of 3- to 10-mL for vadose zone samples and 25- to 100-mL for saturated-zone samples using methyl red, bromcresol green indicator and a digital titrator or potentiometric titrations.

Results and Discussion

Pore-water data from two piezometer-nest sites (1 and 3 on fig. 1) are used to illustrate the pore-water geochemical evolution that followed tailings disposal. Limited tailings deposition has occurred at site 1 for the past 5 to 7 years. This site was chosen because the tailings near the surface display the most advanced oxidation observed within the impoundment. The maximum depth of sulfide oxidation at site 1 is only 20- to 40-cm. Site 3 is closer

to the discharge road, and nearly continuous deposition has limited the extent of sulfide oxidation. Profiles of concentrations of dissolved constituents at sample sites along cross section A-A' (fig. 1) are shown in figure 2. Three zones of distinct pore-water chemical composition can be outlined from the data: a deep, mill discharge-water like zone, an intermediate zone with increased concentrations of Fe, Na, K, Pb, Zn, As, and SO_4 resulting from natrojarosite dissolution, and a surficial zone with high concentrations of metals and SO_4 due to sulfide oxidation. The components from natrojarosite dissolution have been transported by groundwater from the deepest level of natrojarosite detection at the upper dashed line, to the depth where ion concentrations decrease significantly (lower dashed line in figure 2).

Table 1. Mill discharge-water composition.

	1991	1992	Average
Cations, mg/L			
Ca	654	684	669
Mg	10.5	12.7	11.6
Mn	0.95	3.08	2.11
Na	47.3	50.3	48.8
K	25.7	20.4	23.1
Al	<0.02	<0.02	<0.02
Fe	0.05	<0.05	<0.05
Zn	0.55	9.06	4.81
Cu	0.07	0.31	0.19
Ni	0.07	0.15	0.11
Co	0.05	0.10	0.08
Cd	1.23	0.16	0.70
As, µg/L	<3.0	3.5	1.8
Anions, mg/L			
SO_4	1520	1780	1650
Cl	24.4	24.6	24.5
HCO_3	15.0	50.4	32.7

Notes. - Samples collected from the tailings thickener overflow. Natrojarosite is added to the tailings prior to thickening.

Mill Discharge-Water Zone

Nearly continuous accumulation of tailings at site 3 has minimized the effects of sulfide oxidation by atmospheric oxygen. Consequently, observed changes to the pore-water chemistry, relative to the mill discharge-water, can be considered to result from reactions between the tailings solids and the pore water. From 6- to 10-m depth, the pore-water composition is similar to the mill discharge-water. Pore-water concentration profiles are shown in figure 3. Geochemical equilibrium calculations conducted using MINTEQA2 (Allison et al. 1991) indicate that the water in this interval of site 3 approaches or attains saturation with respect to calcite and siderite, and is undersaturated with respect to dolomite (fig. 4). Mineralogical analyses confirm the presence of calcite, dolomite, and siderite in the tailings solids. The pore water in this interval is consistently undersaturated with respect to jarosite, natrojarosite, and hydronium jarosite, thus indicating that if these phases are present, conditions are favorable for their dissolution. None of these jarosite-group minerals have been detected within this interval. The pore water in this zone is supersaturated with respect to ferric hydroxide ($Fe(OH)_3$), goethite (α-FeO(OH)), lepidocrocite (γ-FeO(OH)), and akaganeite (β-FeO(OH,Cl)). The pore water from surface to the base of the tailings is saturated with respect to gypsum. Gypsum has been detected by X-ray diffraction throughout most of this interval (Jambor et al. 1993).

The pore water from 3- to 9-m at site 1 also reflects the mill discharge-water composition. Most metals in this zone are below detection limits (fig. 3). Geochemical calculations indicate that the pore water below 3-m is slightly supersaturated with respect to calcite, is saturated with respect to dolomite, and one sample indicates saturation with respect to siderite. In the one sample with a significant iron concentration, the pore water is undersaturated with respect to jarosite, natrojarosite, and hydronium jarosite, and is supersaturated with respect to the ferric oxyhydroxide minerals (fig. 4). The pore water throughout the tailings at site 1 is saturated with respect to gypsum, and gypsum has been detected by X-ray diffraction throughout the core-sampled interval (0- to 1.65-m). The similarity between the deep pore water and the current mill discharge-water at sites 1 and 3 indicates that the water in this deep interval has been relatively unreactive with the tailings solids.

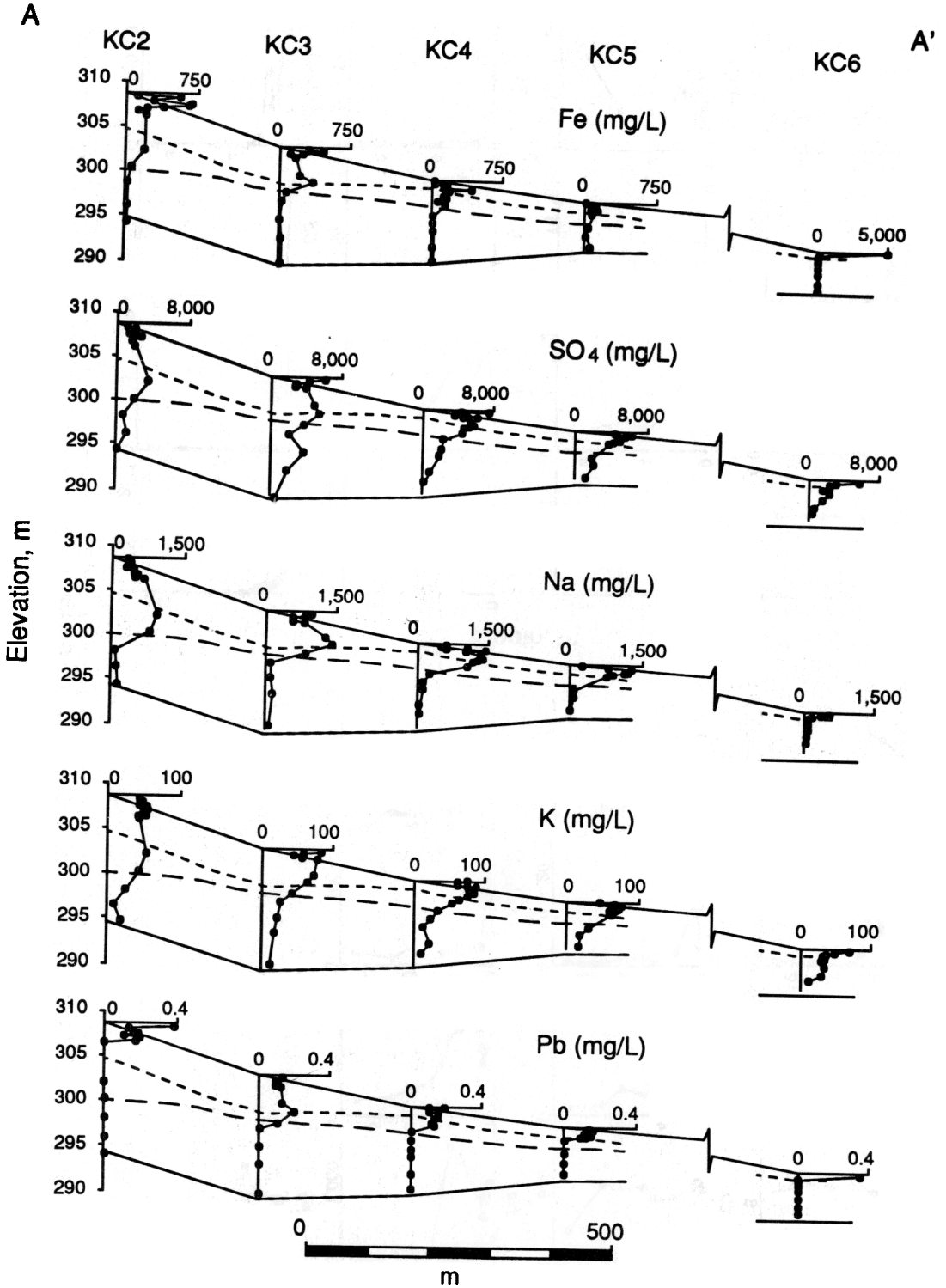

Figure 2. Cross section of pore-water concentration profiles.

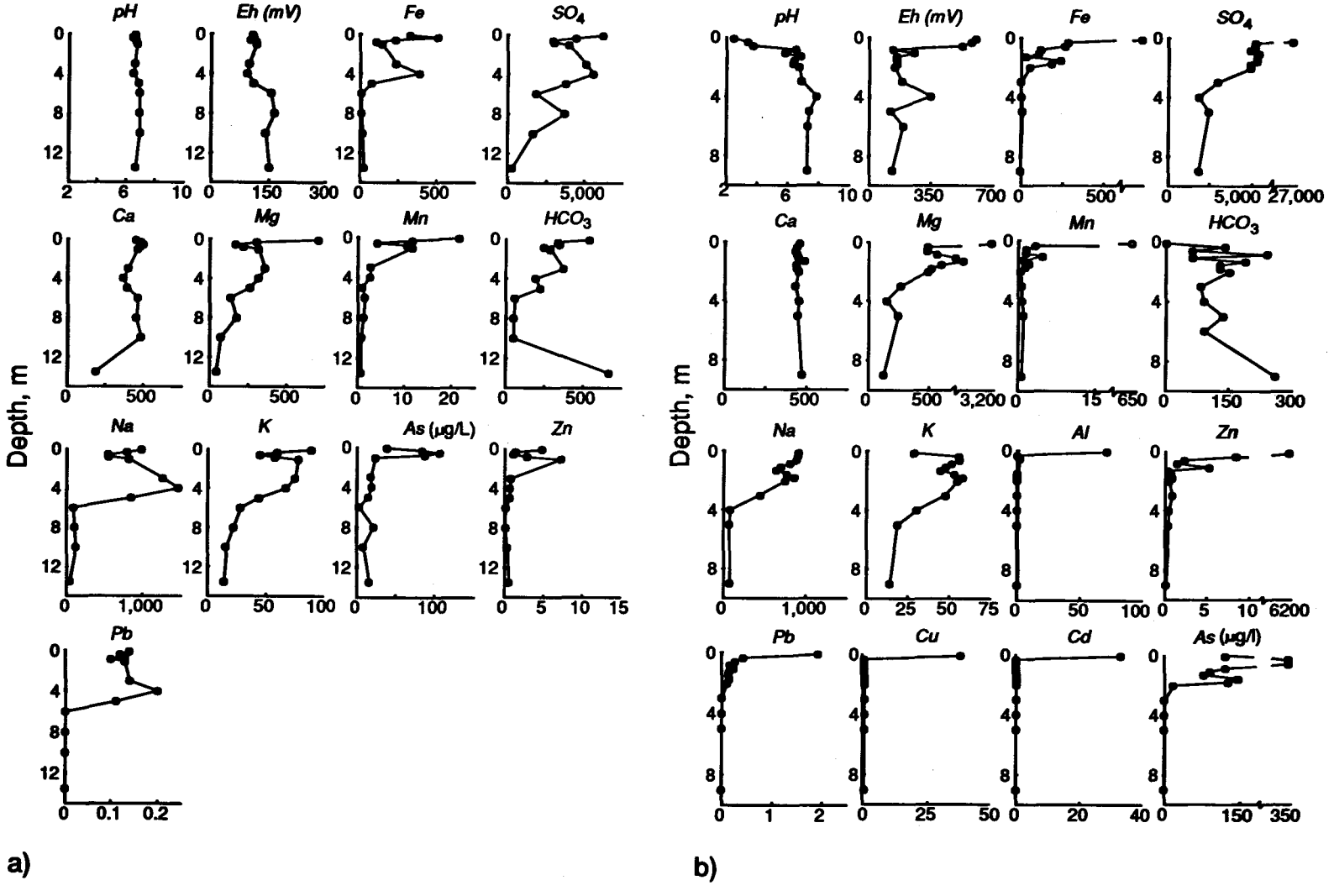

Figure 3. Pore-water concentration profiles for a) site 3 and b) site 1.
All concentrations are in mg/L unless shown otherwise.

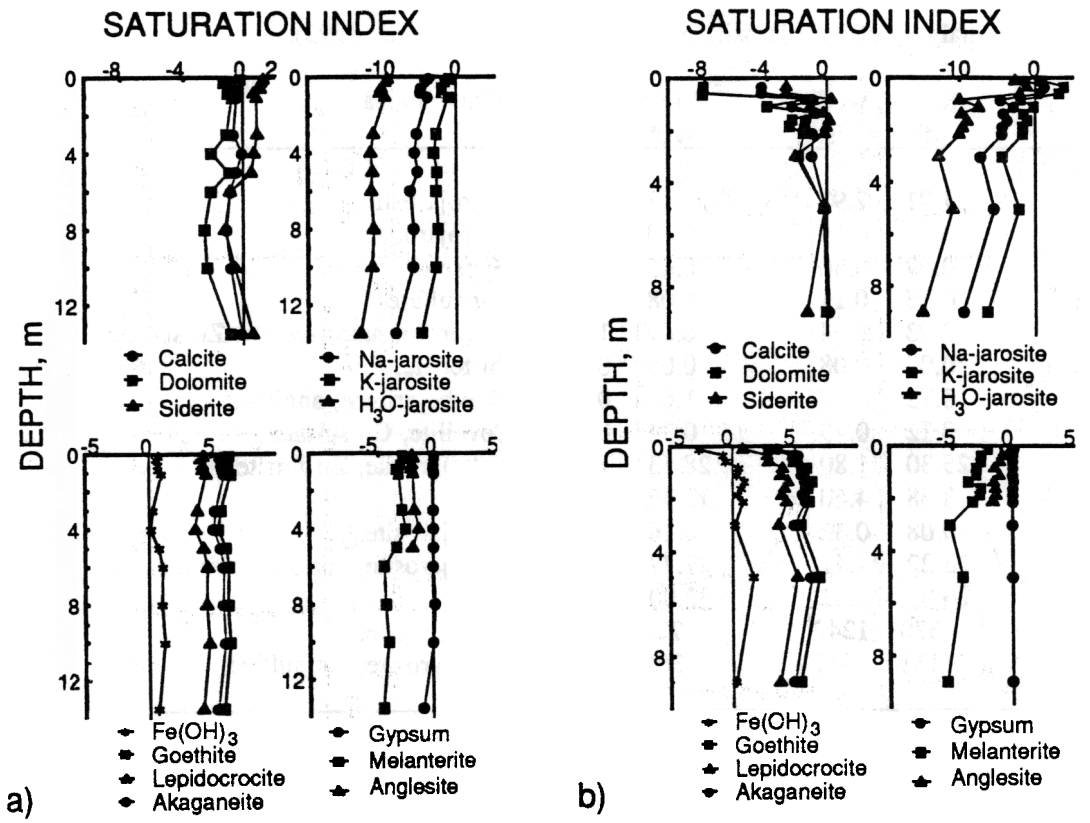

Figure 4. Saturation-index profiles for a) site 3, and b) site 1, calculated with MINTEQA2.

Natrojarosite Disposal Zone

The concentrations of Na, K, Fe, Pb, Zn, As, and SO_4 increase above 6-m depth at site 3 (fig. 3). Sodium, K and H_3O are the principal components in the monovalent cation site of the natrojarosite produced at Kidd Creek (table 2), and the high concentrations of Na and K at this depth interval are best explained by the dissolution of natrojarosite. Tailings pore water above 6-m depth has Na/K = 10 to 20, similar to the average Na/K ratio of 23.7 in natrojarosite from the jarosite pond (Jambor and Owens 1992). Similarly, the increased concentrations of Fe, SO_4, and Pb can be attributed to natrojarosite dissolution. The higher As concentrations in the pore water at this depth also may have resulted from natrojarosite dissolution, as minor solid-solution incorporation of As is documented in jarosite (Dutrizac and Dinardo 1983, Dutrizac and Jambor 1987). Increased concentrations of Zn may be attributed to retention of $ZnSO_4$ in the aqueous phase during co-disposal (Jambor and Owens 1992). Most other metals in this interval remain at or below their detection limits. Increased alkalinity can also be attributed to the dissolution of natrojarosite (reactions 1 and 2.).

$$[Na_{0.75}K_{0.01}(H_3O)_{0.24}]Fe_3(SO_4)_2(OH)_6 + 3H_2O \rightarrow$$
$$3/4Na^+ + 1/100K^+ + 24/100H_3O^+ + 2SO_4^{2-} + 3Fe(OH)_3 + 3H^+ \quad (1)$$

$$H^+ + (Ca,Mg,Fe,Mn)CO_3 \rightarrow HCO_3^- + (Ca,Mg,Fe,Mn)^{2+} \quad (2)$$

Above 6-m depth, the decrease of pH (fig. 3) may be a result of natrojarosite dissolution and ferric iron hydrolysis (reaction 1). In the tailings impoundment, the dominant redox-sensitive species are Fe^{2+} and Fe^{3+}. The decrease in

Table 2. Analyses of natrojarosite residue (Jambor and Owens 1992).

	Range, wt % Min	Max	Mean wt %	σ	Mineralogical Site
Na	1.91	2.97	2.37	0.25	Natrojarosite.
K	0.06	0.16	0.10	0.03	Natrojarosite.
Ca	0.07	0.30	0.15	0.05	Gypsum.
Mg	0.05	0.11	0.08	0.02	Mg sulfate.
Zn	3.93	8.04	6.69	1.21	Zn ferrite, natrojarosite, Zn sulfate.
Cd	0.03	0.08	0.05	0.01	Zn ferrite.
Pb	0.72	2.97	1.63	0.54	Plumbojarosite, anglesite.
Cu	0.12	0.49	0.34	0.09	Covellite, Cu sulfate.
Fe	25.30	31.80	28.53	1.65	Natrojarosite, Zn ferrite.
S	8.58	24.60	12.36	4.82	S^o.
As	0.08	0.32	0.16	0.06	Natrojarosite.
SO_4	25.22	31.41	27.77	1.83	Natrojarosite, various sulfate salts.
H_2O	26.06	36.82	32.00	2.97	
In[1]	370	1242	728	210	Natrojarosite.
Ag[1]	151	511	308	90	Natrojarosite, Ag sulfate.

[1] Concentration in grams per kilogram

Notes. - n = 17
- Small amounts of Mn, Sn, Al, and SiO_2 occur in the residue and are derived from MnO_2 and Mn-sulfate, cassiterite, natrojarosite, "silica gel", and quartz, respectively.
- Silica gel is the amorphous hydrated-alumina-silica product of acid leached chlorite.

E_H may be caused by increased activities of Fe^{2+} that result from natrojarosite dissolution followed by the oxidation of pyrite:

$$14[Na_{0.75}K_{0.01}(H_3O)_{0.24}]Fe_3(SO_4)_2(OH)_6 + 3FeS_2 \rightarrow$$
$$21/2Na^+ + 7/50K^+ + 84/25H_3O^+ + 34SO_4^{2-} + 45Fe^{2+} + 36(OH)^- + 24H_2O \quad (3)$$

Calculated saturation indices (SI) in this zone indicate undersaturation with respect to calcite and dolomite, and slight supersaturation with respect to siderite (fig. 4). These conditions are consistent with the inference of Morin et al. (1988) that precipitation of siderite occurred as a consequence of calcite dissolution in an aquifer affected by acidic Fe- and SO_4-rich tailings drainage water near Elliot Lake, ON. Calculated SI also indicate that the pore water is undersaturated with respect to jarosite, natrojarosite, and hydronium jarosite, suggesting a tendency for the natrojarosite to dissolve, with reaction 1 or 3 favored. This water is supersaturated with respect to goethite, lepidocrocite, and akaganeite, and is very close to saturation with respect to $Fe(OH)_3$. Goethite was the only ferric oxyhydroxide mineral detected by Jambor et al. (1993).

At site 1, a similar zone of high concentrations of Na, K, Fe, Pb, Zn, As, and SO_4 occurs above 3-m depth. As at site 3, the mechanism most likely to be responsible for the increased concentrations in this zone is dissolution of natrojarosite. Increased concentrations of Zn are probably due to adsorbed or aqueous-phase Zn within the natrojarosite residue. Within this interval, Cu, Ni, Co, Cd, Se, Cr, Ag, Ba, Al, NO_3 and PO_4 remain at or below their respective detection limits. Calculations for the interval from 0.6- to 3-m depth at site 1 indicate that the pore water

is undersaturated with respect to calcite and dolomite (fig. 4). Undersaturation with respect to siderite occurs from 0.6- to 1.0-m, and saturation to slight supersaturation occurs from 1.0- to 3.0-m. Between 0.6- and 3-m in depth, the pore water is undersaturated with respect to all jarosite phases, is saturated with respect to $Fe(OH)_3$, and is supersaturated with respect to other ferric oxyhydroxides. The zones of increased Na, K, Fe, Pb, Zn, As, and SO_4 concentrations above 6-m depth at site 3 and above 3-m depth at site 1 are characteristic of similar zones at all sites where natrojarosite has been added to the tailings. The pore water affected by natrojarosite occurs below the depth of natrojarosite occurrence (short dashed line, figure 2) as a result of solute transport with the advecting groundwater.

Sulfide Oxidation Zone

High concentrations of SO_4 and metals not associated with natrojarosite occur in the pore water of the upper 0.2-m at site 3. Sulfide oxidation (reaction 4) near the tailings surface is the most likely mechanism for these

$$FeS_2 + 15/4O_2 + 7/2H_2O \rightarrow Fe(OH)_3 + 2SO_4^{2-} + 4H^+ \quad (4)$$

observed increases. Sulfate is released directly to the pore water by sulfide oxidation. Sulfide oxidation generates H^+ ions, which are neutralized by carbonate-mineral dissolution (reaction 2). These reactions contribute Ca, Mg, Fe, Mn, and HCO_3 to the pore water. MINTEQA2 calculations indicate supersaturation with respect to siderite, and undersaturation with respect to calcite and dolomite in the top 0.2-m at site 3. These calculations support the inferred mechanism for increased Mn, Mg, and alkalinity in the pore water at this depth: up to 5.2 wt % Mn occurs in solid solution within siderite, dolomite, and ankerite, and up to 9.7 wt % Mg occurs in solid solution with these minerals (Jambor et al. 1993). The tailings water within this interval is undersaturated with respect to jarosite, natrojarosite, and hydronium jarosite, indicating that conditions are favorable for the dissolution of these minerals. The pore water is saturated with respect to $Fe(OH)_3$ and gypsum, and is supersaturated with respect to goethite, lepidocrocite, and akaganeite, suggesting that $Fe(OH)_3$ and gypsum may control the pore-water concentrations of Fe and Ca through precipitation-dissolution processes.

The pore water from the surface to 0.6-m depth at site 1 contains high concentrations of metals and SO_4 (fig. 3), reflecting the effects of sulfide oxidation: the H^+ released by pyrite oxidation (reaction 4) has decreased the pore-water pH to between 2.5 and 4, and the E_H has increased to between 525- and 600-mV because of the increased solubility of Fe^{3+} at low pH. Sulfide oxidation near the surface releases H^+ ions, which are neutralized by carbonate-mineral dissolution, causing increases in the concentrations of Ca, Mg, Fe, and Mn. The high concentrations of Mg and Mn (fig. 3) suggest that dissolution of dolomite is occurring. Also released by sulfide oxidation are Fe, Zn, Pb, Cu, Ni, Co, and Cd, which are relatively soluble under low pH conditions. Where the pH decreases below 5, Al concentrations increase, probably because of pH buffering reactions involving dissolution of aluminum-silicate minerals such as chlorite, muscovite, and albite. The alkalinity of the pore water decreases from 52 to 0 mg/L HCO_3 between 0.6-m depth and the surface, suggesting either depletion of the carbonate-mineral acid-neutralization capacity, or that the rate of carbonate-mineral dissolution is too slow to maintain measurable alkalinity concentrations. Mineralogical study indicates the latter since dolomite and siderite are present in this interval. The high concentrations of Cd, Co, Cu, Ni, Cr, and Al in the pore water distinguishes the effects of sulfide oxidation from the effects of natrojarosite dissolution. Geochemical modeling for the zone 0- to 0.6-m at site 1 indicates that the pore water is undersaturated with respect to all of the carbonate minerals (fig. 4). The pore water is saturated to supersaturated with respect to jarosite, is saturated with respect to natrojarosite, and is undersaturated with respect to hydronium jarosite. The SI of the ferric hydroxide and oxyhydroxide phases decrease in this interval. The pore water also approaches saturation with respect to anglesite ($PbSO_4$) in the upper 0.2-m, suggesting a possible control on the near-surface pore-water Pb concentrations.

Comparison with Mill Discharge-Water Chemistry

The geochemical data from site 1 and site 3, normalized to their respective concentrations in the mill

discharge-water, show changes in pore-water composition that have occurred since the tailings were deposited (fig. 5). Below the natrojarosite disposal zone there are slight increases of Mg, Na, Fe, and SO_4 relative to the discharge water, but except for Fe, these differences could be a result of variation in the discharge-water composition. The pore water in the zones affected by natrojarosite disposal displays similar patterns at sites 1 and 3. Concentrations of Na, K, Fe, Zn, Pb, Mn, As, and SO_4 are sharply increased relative to the discharge water. The concentrations of metals are highest at the surface where tailings have been affected by sulfide oxidation. Sulfide oxidation is associated with increased concentrations of Mg, Fe, Zn, Pb, Cu, Ni, Co, Cd, Mn, As, Cr, Al, and SO_4.

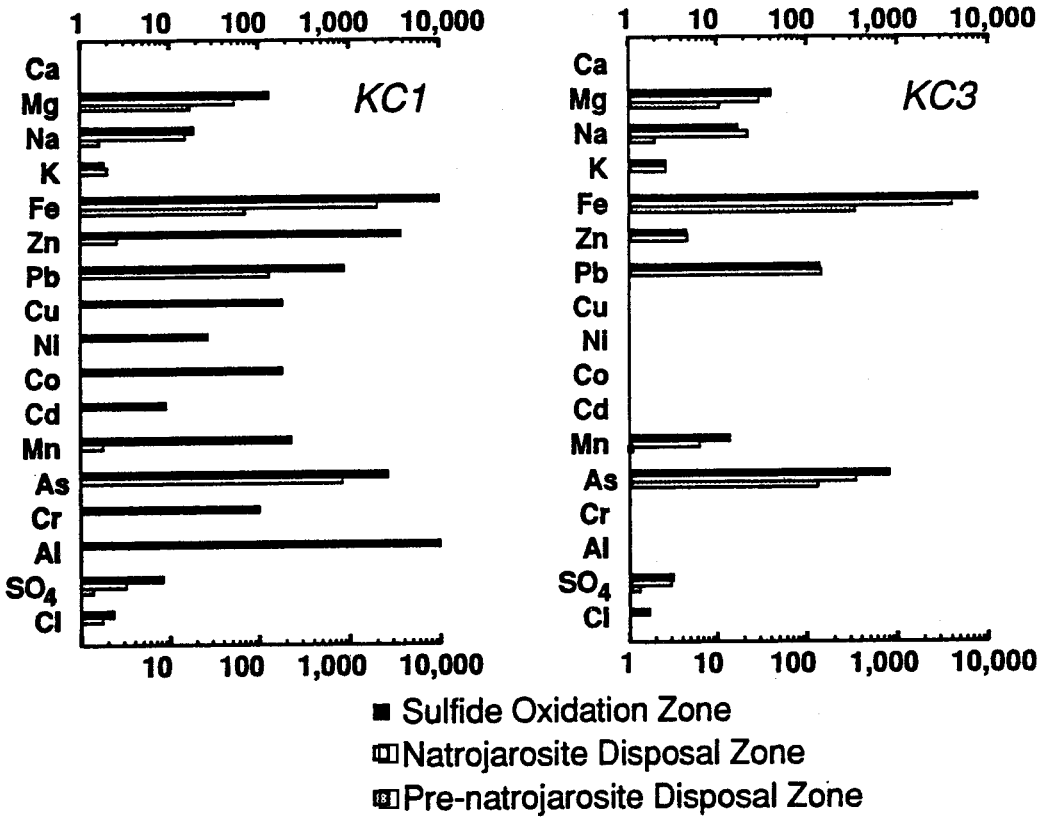

Figure 5. Average concentrations from the zones affected by sulfide oxidation and by natrojarosite dissolution, and the deep, pre-natrojarosite zone, all normalized to the average mill discharge-water concentrations from table 1.

Conclusions

The data define three geochemical zones, the deepest zone displaying pore-water concentrations of metals and sulfate similar to the present mill discharge-water concentrations. Intermediate depths display elevated concentrations of Na, K, Fe, Mg, Mn, Pb, Zn, As, HCO_3, and SO_4 relative to the present mill discharge-water. These increases are a result of the dissolution of natrojarosite that has been co-disposed with the tailings since 1985. Mineralogical studies indicate that a significant mass of natrojarosite remains in the tailings. Pore water near the surface contains high concentrations of Mg, Mn, Fe, Zn, Pb, Cu, Ni, Co, Cd, As, Cr, Al, and SO_4 that are the result of sulfide oxidation near the tailings surface, causing the release of metals and sulfate to the pore water. Both sulfide oxidation and natrojarosite dissolution cause the dissolution of carbonate minerals, consuming the acid-neutralization capacity of the tailings. Acidity is contributed to the pore water through increased pore-water Fe^{2+} concentrations related to

related to natrojarosite dissolution and sulfide oxidation.

Acknowledgements

Funding for this study was provided by Falconbridge Limited, Kidd Creek Division and by the Mine Environment Neutral Drainage (MEND) program of Ontario. We would like to thank Falconbridge Limited, particularly G. Marrs and J.D. Scott, for their help and cooperation in publishing this work.

Literature Cited

Allison, J. D., D. S. Brown and K. J. Novo-Gradac. 1991. MINTEQA2/PRODEFA2, A geochemical assessment model for environmental systems: version 3.0 user's manual. U.S. Environmental Protection Agency Report 600/3-91/021

Dutrizac, J. E. and O. Dinardo. 1983. The co-precipitation of copper and zinc with lead jarosite. Hydrometallurgy 11:61-78.

Dutrizac, J. E. and J. L. Jambor. 1987. The behaviour of arsenic during jarosite precipitation: arsenic precipitation at 97 °C from sulphate or chloride media. Canadian Metallurgical Quarterly 26:91-101.

Garrels, R. M. 1960. Mineral equilibria at low temperature and pressure. Harper and Brothers, 254 pp.

Jambor, J. L. and D. R. Owens. 1992. Mineralogical characterization of process products and secondary phases in the Kidd Creek jarosite impoundment, Timmins, Ontario. CANMET Division Report, MSL 92-29 (CR).

Jambor, J. L., D. R. Owens, P. Carrière and R. Lastra. 1993. Mineralogical investigation of tailings and associated waste products, and the distribution of natrojarosite in the Kidd Creek main tailings cone, Timmins, Ontario. CANMET Division Report, MSL 93-20 (CR).

Morin, K. A., J. A. Cherry, N. K. Dave, T. P. Lim and A. J. Vivyurka. 1988. Migration of acidic groundwater seepage from uranium tailings impoundments, 1. Field study and conceptual hydrogeochemical model. Journal of Contaminant Hydrology 2:271-303.

Robinsky, E., S. L. Barbour, G. W. Wilson, D. Bordin and D. G. Fredlund. 1991. Thickened sloped tailings disposal - an evaluation of seepage and abatement of acid drainage. *In* Second International Conference on the Abatement of Acidic Drainage, Vol. 1 pp. 529-550.

Scott, J. D. and U. Dienstbach. 1990. Circuit optimization, with silver recovery options and deportment, in the Kidd Creek zinc plant. *In* Lead-Zinc '90, *edited by* T.S. Mackey and R.D. Prengaman. The Minerals, Metals and Materials Society, Warrendale, Pennsylvania, pp. 121-134.

Walker, G. W. and G. W. Mannard. 1974. Geology of the Kidd Creek mine, a progress report. Canadian Institute of Mining and Metallurgy Bulletin 67:41-57.

LABORATORY TESTING OF COATINGS FOR PREVENTION OF ACID DRAINAGE IN UNDERGROUND COAL MINES[1]

Ronnie L. Adams, Judy J. Ninesteel, and Henry W. Rauch[2]

Abstract: Laboratory research has been conducted to develop tough chemical and mineral coatings for the prevention of acid mine drainage (AMD) in unsubsided underground coal mines. Specially designed sprayed coatings have the potential for substituting for initial rock dusting, preventing AMD in unsubsided mines, and opening up more acid-producing coal reserves for mining. Fifteen liquid chemicals were sprayed onto acid-producing mine rock samples for laboratory testing of coating durability in water tanks. Eight chemicals that passed the durability tests, and 4 of these were judged suitable for further tests. These 4 chemicals were mixed with water and apatite dust and sprayed on mine rock samples for more tests involving short-term bubbler tank, soxhlet, and long-term bubbler tank procedures. Two coating types, for chemicals code-named I and G, passed these tests. These 2 chemicals were then mixed with limestone dust and water and further tested as sprayed mine rocks using the same testing procedures. These coatings also worked well in retarding AMD products. For most tests coating G (an epoxy resin) worked the best but is most expensive; coating I (a latex) worked second best. The optimum G and I limestone coatings are ones composed of a 10% (by volume) chemical to 90% water solution mixed as a slurry with 30% by weight of limestone dust. These 2 coatings are economical, durable, and should be tested in an underground mine.

Additional Key Words: acid mine drainage, underground coal mines, mine coatings, apatite, limestone

Introduction

We thank Mr. James Laurita Jr. of MEPCO, Inc., the National Mine Land Reclamation Center and the National Research Center for Coal and Energy at West Virginia University, and Mr. William (Randy) Williams of Kiss Engineering for their financial support of collaboration on this research.

One costly and long-term consequence of coal mining is often acid mine drainage from underground mines. Current methods to remedy the problem have had limited success. Consequently, alternative techniques for mediating acid formation continue to be investigated. This report details preliminary research results for evaluating polymer-mineral coatings as inhibitors of pyrite oxidation and the generation of AMD in underground coal mines. Such inhibitions could possibly be achieved through spraying coating barriers on mine rock surfaces, to retard movement of mine air, water, and bacteria to rock and to keep the pH of adsorbed water high on rock surfaces. Successful coatings would likely target active mines for preventing AMD prior to mine abandonment and flooding.

Hart et al. (1990) have shown that phosphates reduce the oxidation of pyrite, possibly by forming iron phosphate on exposed pyrite. Texasgulf Inc.'s Code 31 apatite (about 95% apatite), was found to be very effective in suppressing AMD from mine wastes. Highly soluble at pH values below 5.5, apatite may react with ferric iron leached from pyrite to precipitate iron phosphate, disrupting acid generation. Although this theory for apatite is disputed by some, apatite was found to ameliorate AMD. Only one Appalachian area study was found in which phosphate rock was applied in an underground setting to inhibit acid mine drainage. Hause and Willison (1986) reported that a West Virginia coal mine was sealed and flooded with alkaline water, after above-high-water-table areas were dusted with ground apatite. The mine effluent required no additional treatment 14 months after treatment.

---

[1]Paper presented at the International Land Reclamation and Mine Drainage Conference and the Third International Conference on the Abatement of Acidic Drainage, Pittsburgh, PA, April 24-29, 1994.

[2]Ronnie L. Adams, Geology Graduate Student, Judy J. Ninesteel, Geology Graduate Student, and Henry W. Rauch, Professor of Geology, West Virginia University, Morgantown, WV, USA.

A 1990-91 study of potential mine coatings was funded by James Laurita, Jr. and supervised by Randy Williams and Henry Rauch. They found that two chemicals were successful in binding powdered apatite to mine rocks and that these coatings were durable and did not allow AMD during short-term laboratory testing. These two coating chemicals were also incorporated into our reported research here. In another mine-coating study, Franklin and Nuzum (1975) assessed the suitability of 46 chemicals in suppressing radon gas emissions from uranium mines. Several of these chemicals were later field-tested in an underground coal mine to try preventing the weathering of mine roof shales, and proved effective for at least 1.5 years (Franklin et al. 1977).

Materials for Study

Chemicals for coating mixes were chosen from chemical manufacturers, mine stabilization companies, and previous research. Future use of the chemicals in underground mines was a major consideration in developing criteria for suitable chemicals for study. These criteria included the ability to be applied under high relative humidity conditions, nonflammability, ease of spraying application, lack of adverse environmental effects, and reasonable cost.

Fifteen chemicals were chosen for initial testing. These polymer chemicals were first tested for adhesion on rock surfaces by dunking and short-term bubbler tests. The chemicals were then diluted with water and mixed with powdered apatite (Texasgulf Inc. Code 31) in varying percentages to prepare coatings for laboratory testing. After short-term testing, chemicals for the 3 most successful apatite coatings (J, a petroleum extract; G, an epoxy resin; and I, a latex) were mixed with cheaper limestone dust (agricultural lime) and water for further coating tests.

For testing coating effectiveness, rocks were obtained from an Upper Freeport coal deep mine of northern WV, a major AMD producer. Where possible, fresh roof, coal, and pavement rock were obtained from small areas (few square feet) and small volumes of rock in the mine, to minimize effects of prior weathering and lithologic heterogeneity. Coal was the greatest soxhlet acid producer, averaging 1.16% sulfur and -34.19 net neutralization potential (NNP). Roof and pavement rock averaged respectively 0.06% and 0.03% sulfur, and 0.45 and 1.33 NNP; these rocks were at most moderate acid producers, with roof rock being the greatest acid producer from bubbler tank tests. These rocks were reduced to convenient pieces for testing, and their surface areas were estimated using wrapped aluminum foil. Surface areas for rocks ranged 50-100 cm^2 and averaged about 80 cm^2 for soxhlet tests, and ranged 570-1,750 cm^2 and averaged about 1,100 cm^2 for the 1 to 4 rock pieces per bubbler tank test.

The tested coating mixes were slurries that were applied thin enough to be economical but thick enough to cover the rock. For tested apatite coatings, coating A was prepared by adding by volume 10% A (a latex) to 90% distilled water, supplemented by 25% by weight of apatite dust (AD); this mixture is abbreviated 10% A, 25% AD. In similar fashion, coating G was 25% G, 25% AD; coating I was 10% I, 25% AD; and coating J was 20% J, 25% AD. For the tested limestone dust (LD) coatings, coating G had three versions: 15% G, 0% LD; 10% G, 30% LD; and 20% G, 60% LD. Coating I LD versions were 10% I, 0% LD; 10% I, 30% LD; and 10% I, 60% LD.

The typical thickness of wet sprayed coatings varied with composition, with thicker coatings being associated with more mineral dust. From glass plate spray tests, wet chemical-mineral coatings ranged about 0.1-0.2 mm thick. Dry coatings were less than 50% the thickness of wet coatings. The dry coating weight percentages were 71-93% for apatite mixed with chemicals A, G, I, and J, and 88-96% for limestone mixed with chemicals G and I. Both minerals (especially limestone) are cheaper than the tested chemicals per unit quantity. From glass plate tests, the estimated expense of spraying chemical-limestone coatings in a mine is 2-4 cents/ft^2 for chemicals I and G, with G being more expensive. Labor costs are most of this expense. Our wet coatings would be considerably thinner and somewhat more expensive than a single typical limestone rock dusting in an underground mine.

Laboratory Methods

Dunking tests served to identify coatings for further testing by evaluating the short-term adherence of each tested chemical to painted mine rocks under submerged conditions. Polymers that remained intact on the rock

surfaces were subjected to additional tests. Short-term bubbler tank tests were next conducted to evaluate the short-term adhesion of applied coatings to mine rocks; these tests simulated flooded mine conditions using plastic tanks with 2.5 liters of distilled, aerated water. Mine rock samples about 3-8 cm in size and about 70 cm^2 in average surface area were coated with undiluted polymers, cured in a high-humidity chamber, and submerged in bubbler tanks for 5-7 days. Coating chemicals showing little or no change were used to formulate chemical-apatite coatings. These coating mixes of chemical, water, and mineral were sprayed onto more rocks, cured, and then tested submerged as before except that pH was held at 2.5 ± 0.1 by HCl addition, to simulate a harsh AMD environment. Coatings remaining durable after 5-7 day tests were visually identified. Of 8 coatings remaining intact after testing, the 4 cheapest and most convenient chemicals (A, G, I, and J) were further tested in apatite coating mixtures.

Following these further tests, various limestone dust mixtures with water and chemicals G, I, and J were tested as coatings using 5-day acid water bubbler tank tests as described above. Chemical A was not tested again because it was least successful in the apatite coating tests. Chemical J failed to be durable during these tests, so only chemicals G and I were further tested in limestone coating mixtures.

The soxhlet method (Renton et al. 1988) with modifications was used to evaluate acid-suppression ability of the coatings. Chemical-apatite coatings for chemicals A, G, I, and J, followed by 2 chemical-limestone coatings for chemicals G and I were tested. Coated mine rock samples averaging about 80 cm^2 in surface area and control specimens of uncoated rocks, chemical-coated glass marbles, and peels of chemical-limestone coatings (for chemicals G and I) were soxhlet tested in duplicate through 5 leaching and oven-warming cycles. Each leaching cycle consisted of 24-hour hot-water leaching followed by leachate collection for analyses. After each leaching cycle, the sample thimbles were oven heated at 37° C for 1 week under humid conditions (with a water tray), to increase leaching potential of sulfide minerals in the rocks and yet to not further dry and crack the coatings and to preserve any pyrite-oxidizing bacteria possibly present. After 5 leaching cycles, visual observations were made of coating durability.

The chemical-apatite and chemical-limestone coatings tested by soxhlet leaching were later subjected to long-term bubbler tank tests. One to 4 coated roof, coal, and pavement rocks, averaging about 1,100 cm^2 in total surface area, were placed in tanks containing 7 L (for apatite tests) and 8 L (for limestone tests) of continuously bubble-aerated, distilled water. The tanks were innoculated with 0.5 mL of fresh AMD from a mine source to ensure the presence of AMD bacteria. An initial tank water sample was chemically prior to test-rock immersion. Thereafter, pH readings were taken weekly and 60 mL water samples were collected at 2-week intervals for iron and sulfate analyses; a descriptive log of specimen appearance was also kept. These tests were run for a several months.

Water samples from the soxhlet and tank tests were tested for pH, total iron, and sulfate because these are the 3 primary chemical parameters indicative of AMD and pyrite weathering reactions. Elevated values of iron and sulfate concentrations and lower values of pH relative to background (initial) values indicate that AMD-generating reactions are occurring. Of these 3 parameters, sulfate is considered the most definitive indicator of AMD generation owing to its persistence, in contrast to pH and iron which change after AMD neutralization. Sulfate was measured by the turbidimetric method for the apatite-coating experiments and by ion chromatography for the limestone-coating tests. Total iron was measured by atomic absorption spectrophotometry on preacidified water samples. pH was measured with a pH meter, in water of tanks or tank samples just after sampling.

Results and Discussion

The soxhlet test results are summarized in Table 1, which contains data as hydrogen ion activity and sulfate concentration per cm^2 of exposed rock, for the first (A), fifth (E), and 5 cycles (cumulative total). Higher values may mean higher AMD leaching potential from the tested rocks. Of the control (uncoated) rocks, coal allowed the greatest acid and sulfate contents, producing a pH of about 4 for cycle 5 and about 60-100 mg/L of cumulative sulfate. Pavement rock allowed the least acid and sulfate, with a pH of about 7-8 for cycle 5 and about 15-79 mg/L of cumulative sulfate. Roof rock was intermediate in acid and sulfate, with about 7-7.6 for pH for cycle 5 and about 32-81 for cumulative sulfate. Apatite coatings allowed more sulfate than limestone coatings, probably because Code

Table 1. Hydrogen and sulfate results from soxhlet experiments.

APATITE DUST MIXTURES	CYCLE A		CYCLE E		CUMULATIVE	
	(H+)/cm2	SO4 Conc. mg/l/cm2	(H+)/cm2	SO4 Conc. mg/l/cm2	(H+)/cm2	SO4 Conc. mg/l/cm2
Roof Rock Tests						
Coating A	6.48E-11	3.59E-01	5.20E-10	2.09E-01	3.13E-09	9.07E-01
Coating G	4.17E-11	2.57E-01	5.97E-11	6.44E-02	2.33E-07	5.06E-01
Coating I	1.22E-10	4.95E-01	6.62E-11	1.04E+00	5.20E-09	1.97E+00
Coating J	2.80E-08	6.34E-01	5.24E-11	1.08E+00	3.13E-08	2.38E+00
Control Roof	**1.75E-05**	**2.73E-01**	**2.30E-09**	**1.33E-01**	**1.76E-05**	**9.99E-01**
Coal Tests						
Coating A	5.36E-11	3.70E-01	7.16E-11	1.71E-01	1.06E-05	6.75E-01
Coating G	7.87E-11	2.18E-01	4.02E-09	1.30E-01	3.47E-08	7.01E-01
Coating I	4.54E-09	4.92E-01	4.51E-11	1.15E+00	7.14E-09	1.83E+00
Coating J	9.47E-08	5.14E-01	2.26E-11	1.05E+00	9.52E-08	1.97E+00
Control Coal	**1.17E-05**	**1.85E-01**	**2.00E-06**	**2.86E-01**	**1.86E-05**	**1.13E+00**
Pavement Rock Tests						
Coating A	4.96E-11	4.21E-01	5.43E-11	2.14E-01	5.31E-10	8.76E-01
Coating G	7.19E-11	2.63E-01	8.57E-11	1.26E-01	3.78E-06	7.33E-01
Coating I	8.71E-11	4.74E-01	5.13E-11	1.28E+00	1.85E-09	2.16E+00
Coating J	2.95E-08	4.88E-01	3.11E-11	9.52E-01	2.98E-08	1.75E+00
Control Pavement	**5.93E-06**	**4.02E-01**	**1.62E-08**	**7.47E-02**	**6.14E-06**	**9.63E-01**

LIMESTONE ROCK DUST MIXTURES	CYCLE A		CYCLE E		CUMULATIVE	
	(H+)/cm2	SO4 Conc. mg/l/cm2	(H+)/cm2	SO4 Conc. mg/l/cm2	(H+)/cm2	SO4 Conc. mg/l/cm2
Roof Rock Tests						
10% Coating I Pure	1.02E-08	2.14E-01	4.88E-09	6.68E-02	1.59E-08	5.19E-01
10% Coating I/30% RD	2.67E-12	9.80E-02	7.56E-12	3.13E-02	2.91E-11	2.35E-01
10% Coating I/60% RD	5.24E-12	1.18E-01	2.40E-12	3.40E-02	1.50E-11	2.78E-01
15% Coating G Pure	1.70E-08	1.63E-01	3.45E-10	4.59E-02	4.27E-08	3.57E-01
10% Coating G/30% RD	2.49E-12	1.71E-01	5.88E-12	5.00E-02	2.16E-11	4.08E-01
20% Coating G/60% RD	4.28E-12	2.02E-01	4.28E-12	9.58E-02	1.92E-11	6.74E-01
Control - Roof	**1.37E-08**	**2.88E-01**	**5.23E-10**	**7.03E-02**	**2.41E-08**	**6.43E-01**
Coal Tests						
10% Coating I Pure	4.03E-09	7.96E-02	5.09E-09	2.16E-02	1.09E-08	1.47E-01
10% Coating I/30% RD	5.78E-12	9.74E-02	5.61E-12	2.03E-02	2.51E-11	1.75E-01
10% Coating I/60% RD	1.54E-12	8.19E-02	7.18E-13	1.46E-02	6.02E-12	1.49E-01
15% Coating G Pure	1.20E-09	1.29E-01	6.21E-10	1.66E-02	7.12E-09	2.03E-01
10% Coating G/30% RD	1.90E-12	8.32E-02	4.60E-12	2.15E-02	1.45E-11	1.61E-01
20% Coating G/60% RD	1.55E-12	1.12E-01	3.70E-12	1.12E-01	1.64E-11	5.28E-01
Control - Coal	**1.68E-08**	**1.75E-01**	**1.09E-06**	**1.30E-01**	**3.40E-06**	**6.67E-01**
Pavement Rock Tests						
10% Coating I Pure	9.89E-10	9.22E-02	1.32E-10	3.46E-02	1.39E-09	2.62E-01
10% Coating I/30% RD	4.64E-12	9.74E-02	4.10E-12	2.58E-02	2.82E-11	2.75E-01
10% Coating I/60% RD	2.90E-12	1.03E-01	3.17E-12	2.90E-02	1.12E-11	2.53E-01
15% Coating G Pure	1.77E-10	8.66E-02	9.75E-11	2.73E-02	1.60E-09	2.34E-01
10% Coating G/30% RD	2.15E-12	7.34E-02	4.67E-12	2.68E-02	1.92E-11	2.01E-01
20% Coating G/60% RD	2.98E-12	7.69E-02	3.48E-12	2.75E-02	1.36E-11	1.99E-01
Control - Pavement	**1.58E-10**	**9.29E-02**	**1.49E-10**	**2.44E-02**	**5.90E-10**	**2.12E-01**

(H+)=Hydrogen ion activity, in moles/kg, and SO4=sulfate concentration, in mg/L. All values are reported as ratios of activity or concentration to surface area of their respective tested rock samples. All values shown are averages of duplicates tested for each group of treatments and rock types. Number interpretations: 6.48E-11 = 6.48x10exp(-11).

31 apatite contains 1.2% sulfur. For the apatite tests all coatings showed less acid than control rocks. Coatings I and J allowed more sulfate than controls, perhaps because of the sulfur in apatite dust. Overall, coating G performed best, having the least acid and sulfate. For limestone tests the coal coatings performed better than the coal control, and most coatings performed better than the roof rock control. The coatings appear to be least successful for pavement rock, but this rock showed little acid (pH about 8) or sulfate (about 15 mg/L). Both 30% LD and 60% LD coatings performed well, and I coatings overall appear to have worked slightly better than G coatings.

Fig. 1 displays the results of the apatite-coating bubbler-tank leaching tests through April, 1993. For the control rocks, the roof rock allowed the most acid and sulfate and the coal was least associated with these chemicals. These rocks apparently varied in composition compared to those used in the soxhlet tests. The control roof, pavement, and coal rock produced respectively pH's of about 5, 5, and 6, and sulfates of 204, 99, and 80 mg/L on April 26th. The initially higher hydrogen ion and sulfate ratios for the first tested control samples of some bubbler tank tests cannot be readily explained and may be from experimental error; the only acid and sulfate sources for initial samples should be the 0.5 mL of AMD added to the tanks. In general, apatite coatings allowed less acid and sulfate than control rocks. Overall, coatings G and I performed very well, and better than coatings J and A. Coating J and especially coating A developed concentrated fungus growth after several months of tank testing, indicating that these chemicals are fungus-culture mediums and should not be used in mines. Also, coating J showed significant wear. Based on chemical results and visual appearances, coatings G and I performed best.

Fig. 2 and Fig. 3 show results of the limestone-coating bubbler-tank tests up to October, 1993, for coating types G and I respectively. For control rocks, the roof rock allowed the most acid and sulfate, while the coal also showed much acid and sulfate. The pavement exhibited the least AMD products. For the last reported October date, the control roof, coal, and pavement rocks allowed respectively pH values of about 3, 3, and 6.5, and sulfate values of 151, 67, and 12 mg/L. In general, the G and I coatings worked well in preventing sulfuric acid compared to the control rocks, with the exception of pavement rocks whereby the control allowed about as much acid and sulfate as the average G and I coated rocks; however, the control pavement rock allowed very little acid and sulfate and is considered an alkaline rock. Overall, G coatings worked better (with less sulfuric acid) than I coatings. The 30% LD G coatings worked better than 60% LD and 0% LD G coatings for 2 out of 3 tested rock types, with the exception of the alkaline pavement rock. The 0% LD I coating allowed more acid and sulfate than did 30% LD and 60% LD I coatings. Although 60% LD I coatings worked better than 30% LD I coatings with less AMD products, 60% LD I coatings tended to spall from tested rocks, probably because they are thicker and have less chemical cement. Therefore 30% LD G and I coatings are preferred over 60% LD G and I coatings to prevent AMD.

References

Franklin, J. and L. Nuzum. 1975. Polymeric materials for sealing radon gas into the walls of uranium mines. U.S. Bureau of Mines RI 8036. 26 p.

Franklin, J., K. Weverstad and R. Marquardt. 1977. Polymeric sealant used to stop shale degradation in coal mines. U.S. Bureau of Mines, Technical Progress Report 103. 8 p.

Hart, W., A. Stiller, T. Rymer and J. Renton. 1990. The use of phosphate refuse as a potential AMD ameliorant. In Proceedings of the 1990 Mining and Reclamation Conference and Exhibition. (Charleston, WV, April 23-26, 1990). p. 43-49.

Hause, D. and L. Willison. 1986. Deep mine abandonment sealing and underground treatment to preclude acid mine drainage. In Proceedings of the Seventh Annual West Virginia Surface Mine Drainage Task Force Symposium. (Morgantown, WV, April 1-2, 1986). 5 p.

Renton, J., T. Rymer and A. Stiller. 1988. A laboratory procedure to evaluate the acid producing potential of coal associated rocks. Mining Science and Technology 7:227-235.

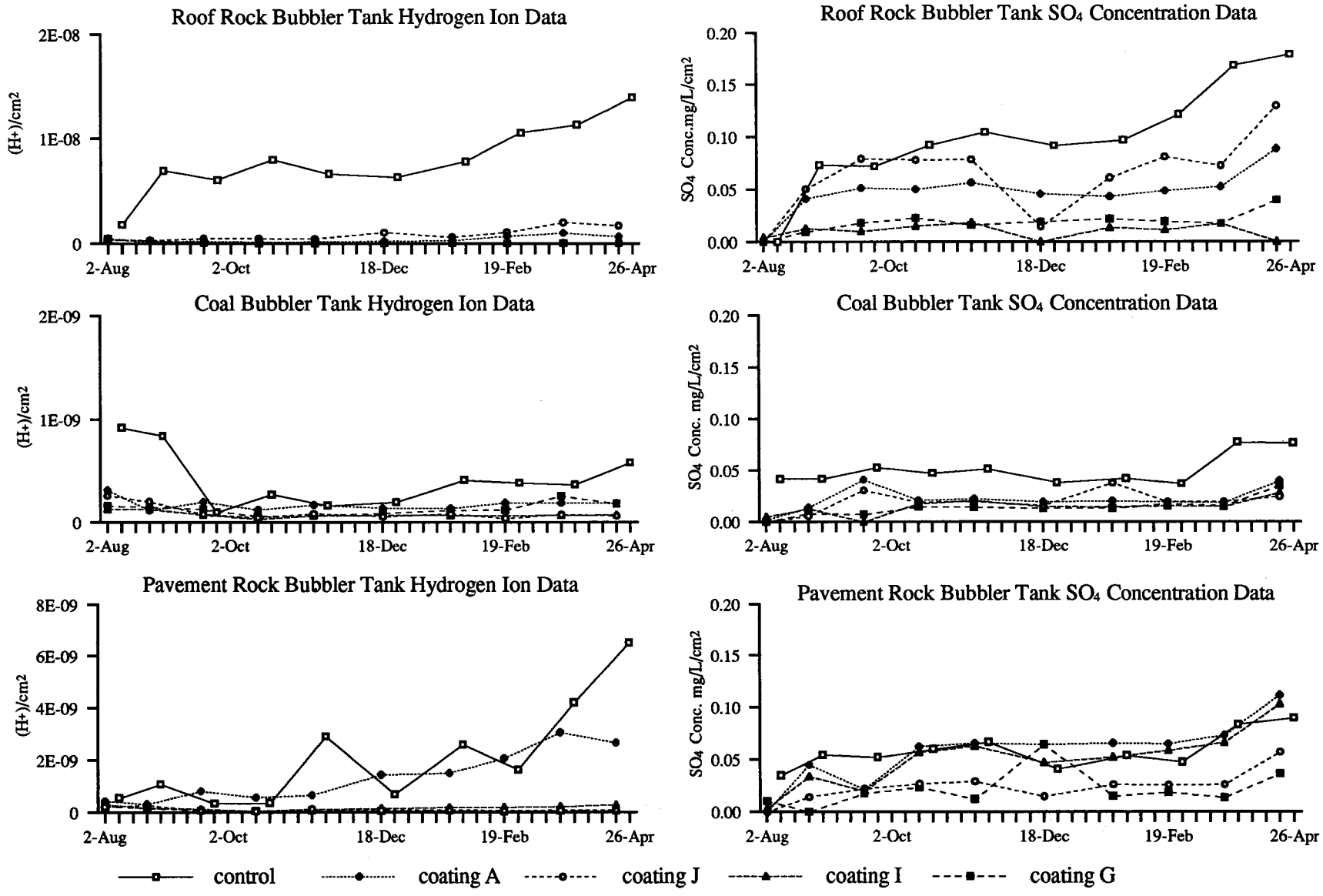

Figure 1. Graphs of water quality data for bubbler tank experiments performed on mine roof, coal, and pavement rock samples treated with various coating chemicals mixed with apatite dust. Hydrogen ion activity (H+) and sulfate (SO_4) concentration are reported in ratios to their respective rock sample surface areas. Control test bubbler tanks were started 1 week after all of the coating test bubbler tanks. The first water samples were taken prior to rock sample submersion.

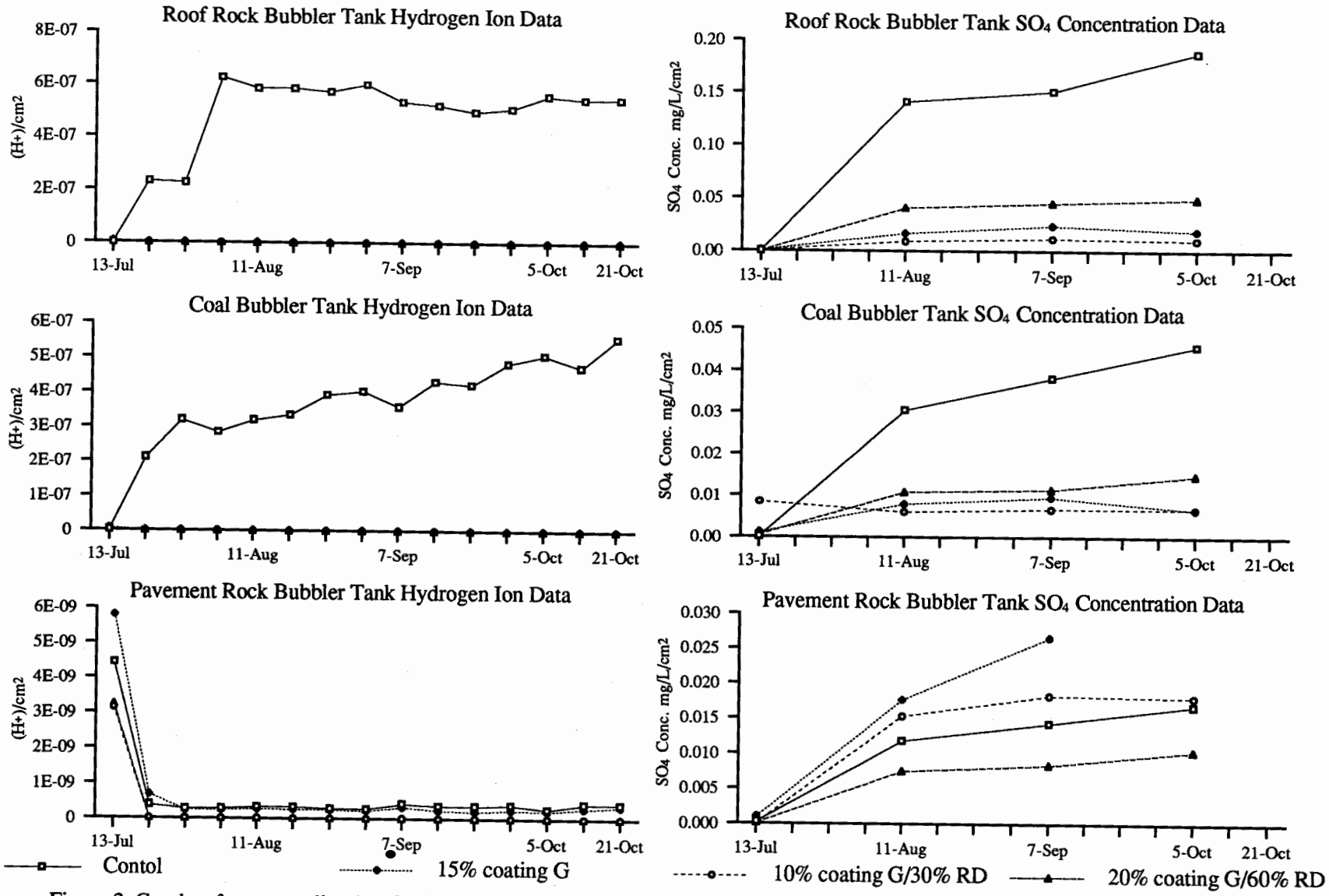

Figure 2. Graphs of water quality data for bubbler tank experiments performed on mine roof, coal, and pavement rock samples treated with mixtures of coating G and limestone rock dust (RD). Hydrogen ion activity (H+) and sulfate (SO_4) concentration are reported in ratios to their respective rock sample surface areas. The hydrogen ion activity ratio is shown for each week, while the sulfate ratio is shown for each month. The first water samples were taken prior to rock sample submersion.

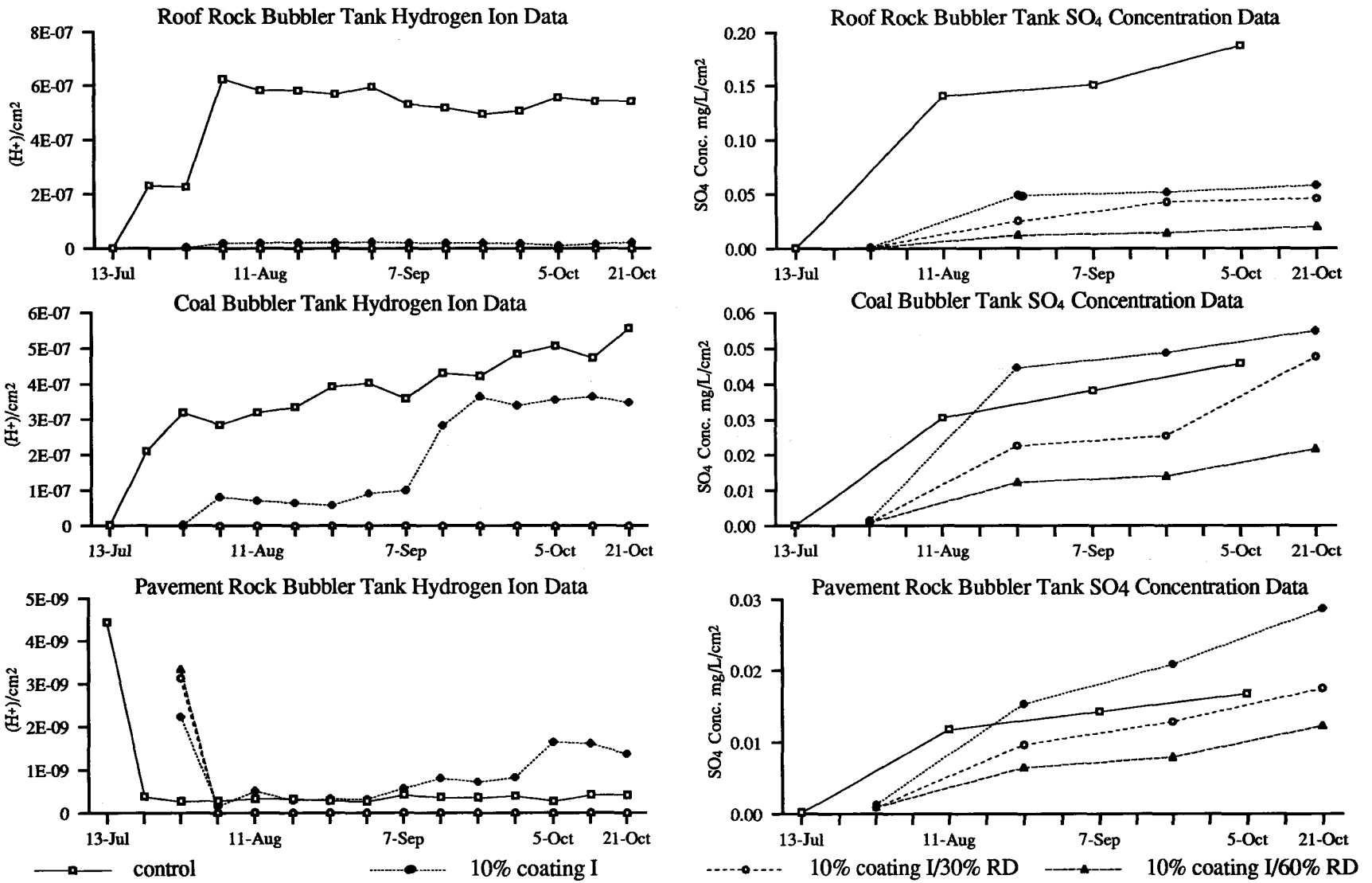

Figure 3. Graphs of water quality data for bubbler tank experiments performed on mine roof, coal, and pavement rock samples treated with mixtures of coating I and limestone rock dust (RD). Hydrogen ion activity (H+) and sulfate (SO4) concentration are reported in ratios to their respective rock sample surface areas. The hydrogen ion activity ratio is shown for each week, while the sulfate ratio is shown for each month. Coating I bubbler tanks were started 2 weeks after the control bubbler tanks. The first water samples were taken prior to rock sample submersion.

ENGINEERING EVALUATION OF AMENDED FLY ASH FOR HYDRAULIC BARRIERS[1]

John J. Bowders, Jr,[2] Mo A. Gabr,[2] Ellis M. Boury,[2] and Robert C. Baker[3]

Abstract: A laboratory investigation was conducted to determine the potential for producing low-hydraulic conductivity ($k<10^{-7}$ cm/s), amended fly ash barriers. The objective is to control sources of water which now leach and transport products of oxidization from mine spoil and overburden materials -- the result of which is acidic drainage. The surface barrier evaluation program consisted of blending a Class F fly ash, clay and sand at varying dry weight percentages and water contents and analyzing the resulting mixtures' physical and engineering properties. Optimum water content for the mixes ranged from 16.7% for 10% clay to 13.8% for 30% clay. Specimens were prepared at water contents from approximately -4% to +4% of optimum for each mix ratio. Over this range, the hydraulic conductivity typically varied by one order of magnitude. The lowest hydraulic conductivity achieved during the project was 1.5×10^{-7} cm/s for a mix containing 40% fly ash, 30% clay, and 30% sand.

Additional Key Words: acid mine drainage, hydraulic conductivity, permeability fly ash, reclamation

Introduction

Numerous abandoned and reclaimed surface mines continue to discharge acidic drainage. New technologic and economic methods to prevent or reduce the acidic drainage are required in order to improve and safeguard surface and groundwater. In many instances, reclamation budgets have long been exhausted. Continued control and treatment attempts by the owner or agency push budgets further into deficit. Thus, it is important to find effective, economic means for controlling and reducing acidic drainage from these sites.

Seepage cutoff systems using traditional materials, whether they are applied at the surface (infiltration barriers) or subsurface (grout curtains), have been effective when applied in well characterized materials (Bowman 1968, Powell and Morganstern 1985); however, this project involves developing nontraditional materials (fly ash, AMD sludge) to be placed in uncharacterized, highly heterogeneous material (surface mine backfill) for the purpose of controlling and reducing AMD. The abundance of fly ash leads to excessive disposal costs, and its proximity to existing acid drainage sites makes it an attractive material for hydraulic barriers, provided the ash can be engineered to have the necessary behavioral properties. This must be accomplished in an economic manner to allow the technique to be used throughout the mining and reclamation industry.

The work reported herein is the laboratory phase of a larger project whose objective is to demonstrate at-source control or reduction of AMD from surface mined sites through the utilization of combustion waste materials in subsurface grouts and surface barriers. The objectives of the laboratory phase include refining the surface barrier mixtures to optimize engineering and economic properties, including: minimizing hydraulic conductivity through constituent

---

[1]Paper presented at the International Land Reclamation and Mine Drainage Conference and the Third International Conference on the Abatement of Acidic Drainage, Pittsburgh, PA, April 24-29, 1994.

[2]John J. Bowders, Associate Professor of Civil Engineering, Mo A. Gabr, Assistant Professor of Civil Engineering, and Ellis M. Boury, Graduate Research Assistant, West Virginia University, Morgantown WV, USA.

[3]Robert C. Baker, Project Engineer, GAI Consultants, Inc., Monroeville, PA, USA.

proportioning, characterizing elemental constituents that leach from the mixtures, and determining the nature (pH, acidity, alkalinity) of any resulting flows from the mixtures.

Hart et al. (1992) showed that diffusion of oxygen to unreacted pyrite controls the rate of formation of oxidation products. When water is kept from the reacted material, a buildup of oxidation products occurs. These deposits not only slow diffusion of oxygen to the unreacted pyrite but also increase the resistance of subsequent leaching due to reduced pore size and tortuosity of the remaining flow paths. Results using a simulation model by Hart (1992) showed that system porosity was the second most important parameter controlling the generation of acid mine drainage. Acid transport rate is inversely proportional to the amount and size of the pores in the formation. These findings indicate two potential modes for controlling acidic drainage from exisiting sites: (1) cut off or reduce the supply of oxygen to the reaction system or (2) cut off or reduce the supply of water to the leaching system. A third potential control mode is to precipitate the Fe^{2+} during the final stage of the reaction. While this is done during treatment processes, it is the least efficient mode to implement in situ at existing sites.

Controlling the flow of water to the leaching process is the easiest mode to implement in situ. Two techniques for water control are possible: elimination and rate reduction. The first technique, elimination, reduces the quantity of water entering the volume of oxidized material, thereby reducing the volume of acidic drainage emanating from the oxidized volume. This reduction is obtained by placing a seepage cutoff barrier around the oxidized material. Barriers can be in the form of surface barriers or subsurface grout curtains. The second technique is to actually grout the matrix containing the pyritic material. This technique reduces the porosity of the matrix, thus slowing the rate of both the oxygen reaching the unreacted pyrite and the leaching and subsequent transport of the oxidation products.

For either water control technique to be effective requires that a low-hydraulic-conductivity material be available in significant quantities. Although clays or clay-rich soils can be ideal candidates, their lack of availability in mining areas is a limiting factor. Additionally, significant deposits of clay may be developed for more economical applications. Thus, an alternate source of material is required, and for many AMD sites in the Appalachian region, fly ash from the coal combustion process provides an attractive alternative (American Coal Ash Association 1991). However, the ash must first be amended with other agents to provide the needed engineering properties - low hydraulic conductivity and constituent retention during permeation. In this article we report on our laboratory efforts to characterize and optimize the physical properties through the addition of various amendments.

Program of Investigation

The primary parameter for the success of a surface barrier is that it possess and maintain a low hydraulic conductivity. In solid waste disposal applications this means maintaining a hydraulic conductivity at or below 10^{-7} cm/s. While this hydraulic conductivity does not exclude all flow, it can reduce the volume of flow passing through the barrier by up to 80% of the impinging water provided adequate drainage is supplied (Bowders and Chiado 1990). In the reclamation industry, a barrier possessing a higher hydraulic conductivity could be implemented while still reducing the volume of water entering a pyritic zone.

It was the intent of this investigation to minimize the hydraulic conductivity of the fly ash by adding clay and/or sand while maintaining the ash as the principal constituent. Several factors were analyzed to determine their effect on producing low-hydraulic-conductivity material: molding water content, percentages of sand and clay, clay type, hydraulic gradient during test, and grain-size distribution of mixtures.

Index properties of the materials used in the investigation are shown in table 1. Twelve test mixes were prepared with varying percentages of fly ash,

clay, and sand. Mix ratios are provided in table 2. Both the clay and sand were air-dried prior to mixing with the fly ash, which was at a nominal moisture content of 10%. Distilled de-ionized water was added during mixing to bring the mixtures to the desired moisture contents. Use of the fly ash and sand in conjunction with the low-plasticity clay were believed to produce a mixture that was not particularly sensitive to permeant liquid chemistry; thus, the distilled de-ionied water was used. Mixtures were placed in sealed plastic bags, and moisture equilibration was permitted for 24 h after which specimens were compacted using ASTM D698, standard Proctor compaction procedures (ASTM 1993a).

Hydraulic conductivities of the compacted specimens were measured in double-ring, rigid-wall permeameters (fig. 1). Hydraulic conductivities were calculated using the constant-head analysis (ASTM 1993b). Calculations of hydraulic conductivity were made for inflow volume and for outflow volumes for both the inner and outer rings. Termination of tests was based on the following: minimum of 3 pore volumes of flow and inflow hydraulic conductivity falling within 25% of the average hydraulic conductivity measured after 2 pore volumes (Peirce and Witter 1986).

Table 1. Index properties of materials.

Material	Specific Gravity	Max Dry Density Mg/m^3	Optimum Water Content %	Atterberg Limits LL	Atterberg Limits PI	Grain Size Parameters, Cu	Clay Fraction %	Unified Soil Classification
BBL	2.71	1.71	18.0	46	23	XXX	79.0	CL
LMS	2.73	1.68	17.3	40	19	XXX	67.8	CL
OR	2.69	1.78	XXX	NP		3.15	0	SP
AFA	2.29	1.45	20.4	NP		4.10	14.2	ML

BBL = Big Bear Lake Clay
LMS = Lake Monongahela Sediment
OR Sand = Ohio River Sand
AFA = Albright Fly Ash

LL = Liquid Limit
PI = Plasticity Index
Cu = Coefficient of Uniformity
NP = Non Plastic

Upon completion of the permeability tests, each test specimen was sectioned, water content was measured, and degree of saturation was calculated. In addition, grain-size distribution was measured to assess the effect of constituent material proportioning on the gradation of the test mixes.

Results and Discussion

Sixty-one specimens were prepared, and their hydraulic conductivities were measured at two hydraulic gradients. For each mix ratio shown in table 2, five specimens were compacted ranging from approximately 4% dry of optimum moisture content to 4% wet of optimum. After the specimens were compacted into the rigid-wall molds, end platens were added and permeation was initiated at a hydraulic gradient of 59. After steady flow and hydraulic conductivity was achieved, the gradient was increased to 118. A response, typical of that shown in figure 2, for hydraulic conductivity at the various molding water contents was exhibited for all mixes tested. As molding water content increased, the hydraulic conductivity decreased, reaching a minimum value for specimens prepared 2% to 4% wet of optimum. The hydraulic conductivity measured at the higher gradient (i=118) typically exceeded that at the lower gradient (i=59) when the specimens were compacted dry of optimum. When samples were compacted wet of optimum, the permeabilities measured at the higher gradient were lower than those at the lower

gradient. The measured permeabilities typically differed by a factor between 0.5 and 1.75 (table 2, col. 8).

A summary of the compaction and hydraulic conductivity results is given in table 2. The minimum hydraulic conductivities for each mix design at both hydraulic gradients are presented. Examination of the data indicates that an increase in sand percentage produced a subsequent reduction in mixture hydraulic conductivity for all clay contents tested. However, the effectiveness of the increased sand percentage diminished as the clay contents increased, as shown in figure 3.

Table 2. Compaction and hydraulic conductivity results for compacted fly ash, clay and sand mixtures.

Mix	γ_{dry} Mg/m^3		w, %		$Kmin_{i1}$, cm/s x10^{-7}	$Kmin_{i2}$, cm/s x10^{-7}	$Kmin_{i1}/Kmin_{i2}$	$Kmin_{avg}$, cm/s x10^{-7}
AS/CL/SA (1)	Max (2)	Mix (3)	Opt (4)	Mix (5)	(6)	(7)	(8)	(9)
100/0/0	1.45	1.42	20.4	23.0	150.0	200.0	1.33	180.0
80/10/10	1.60	1.59	16.7	18.0	17.0	21.0	1.24	19.0
75/15/10	1.63	1.60	16.0	17.8	7.0	6.5	0.93	6.8
70/20/10	1.64	1.59	16.0	19.0	5.5	2.4	0.44	4.0
60/30/10	1.64	1.58	15.3	20.0	2.5	2.0	0.80	2.3
70/10/20	1.64	1.62	15.2	17.2	9.0	8.0	0.89	8.5
60/20/20	1.67	1.66	14.8	17.0	2.8	2.6	0.93	2.7
50/30/20	1.68	1.64	14.6	17.0	1.8	1.6	0.89	1.7
60/10/30	1.74	1.67	13.8	17.0	5.0	5.0	1.00	5.0
50/20/30	1.77	1.66	14.1	18.0	1.9	1.8	0.95	1.9
40/30/30	1.77	1.68	14.2	17.5	1.5	1.4	0.93	1.5
80/L10/10	98.4	97.7	16.2	18.5	40.0	70.0	1.75	55.0
70/L20/10	98.9	97.0	16.9	19.5	20.0	30.0	1.50	25.0

(1) Fly Ash/Clay/Sand proportion by dry weight.
(2) Maximum dry unit weight for the mixture.
(3) Dry unit weight of specimen for reported hydraulic conductivity.
(4) Optimum water content (gravimetric) at max unit weight.
(5) Water content of specimen for reported hydraulic conductivity.
(6) Minimum hydraulic conductivity at i1= 29.5 for tests 1-3 and i1= 58.9 for tests 4-13.
(7) Minimum hydraulic conductivity at i2= 58.9 for tests 1-3 and i2= 117.8 for tests 4-13.
(8) Ratio between K measured at different hydraulic gradients.
(9) Average minimum hydraulic conductivity for the two testing gradients.

This is also illustrated in the hydraulic conductivity ratios given in table 3. The values in table 3 indicate the factors by which the hydraulic conductivity decreased as the sand percentage was increased above 10% for a constant clay content. At the low clay content (10%) the reduction due to the addition of 30% sand is nearing an order of magnitude. At the 30% clay content, the reduction in hydraulic conductivity due to the addition of 30% sand is about one-half order of magnitude.

Traditional thinking supposes that hydraulic conductivity decreases as the percentage of fines increase in a soil mass; however, the results of this investigation show this is not necessarily true when the primary constituent is fine, noncohesive particles, i.e., fly ash. The postpermeation grain-size distribution curves for fly ash-10% Big Bear Lake Clay-sand are shown in figure

4. The decrease (from 80% to 60%) in the percentage of fines (sizes less than 0.074 mm) is readily evident as the percentage of sand was increased from 10% to 30%. The corresponding coefficients of uniformity (Cu), a measure of the gradation of the mixture, are given in table 3. For the mixtures shown in figure 4, the Cu values increase from 8.0 for the mixture with 10% sand to 30 for the mixture with 30% sand. An increase in Cu indicates that the mixture is trending toward a more well-graded mixture, i.e., one containing a wide range of particle sizes.

Table 3. Hydraulic conductivity ratios, dry unit weights and coefficients of uniformity as a function of sand percentage for constant clay contents.

	10% Clay	20% Clay	30% Clay
10% Sand			
Kratio	1	1	1
γ_{dry}, Mg/m^3	1.58	1.58	1.58
Cu	8.0	11.0	17.3
20% Sand			
Kratio	0.45	0.68	0.74
γ_{dry}, Mg/m^3	1.62	1.66	1.64
Cu	18.3	24.2	41.7
30% Sand			
Kratio	0.26	0.48	0.65
γ_{dry}, Mg/m^3	1.67	1.66	1.68
Cu	29.8	32.0	51.9

Kratio = K @ X% sand/K @ 10% sand. Cu = coefficient of uniformity.
γ_{dry} = dry unit weight of specimen.

From compaction theory, we know that maximum densities are achieved when the material being compacted has a blend of particle sizes rather than having particles of a uniform size. Such a blend promotes dense packing, with the smaller particles filling in the interstices of the matrix of larger particles. This is also borne out by the data shown in table 3. The dry unit weights increase as the percentage of sand increases for a constant clay content. For example, at a clay content of 10%, the dry unit weight increases from 99 to 104 lb/ft^3 for a 20% increase in the sand content. From this increase in density, we can infer a decrease in the hydraulic conductivity of the compacted mixture. Indeed, this has been shown in tables 2 and 3. Thus, the addition of sand to the fly ash resulted in significant decreases in the hydraulic conductivity of the fly ash mixtures by permitting the mixtures to be compacted to greater densities than possible with mixtures of fly ash and clay alone.

Conclusions

The work reported herein was aimed at optimizing engineering properties of fly ash mixtures for surface hydraulic barrier applications. For the surface barrier mixture, the minimum hydraulic conductivity (1.5×10^{-7} cm/s) was obtained for a compacted mixture containing 40% ash, 30% clay and 30% sand. The addition of sand to the ash-clay mixtures resulted in a decreased hydraulic conductivity-about an order of magnitude for ash with 10% clay and one-half order for ash with 30% clay. The addition of sand widened the grain-size distribution of the mixtures, thereby allowing the mixtures to be compacted to greater densities, resulting in decreased hydraulic conductivities. A surface barrier at 10^{-7} cm/s, with adequate drainage for the repelled water, can exclude up to 80% of the potential infiltrating water. Hydraulic conductivities of the surface barrier

mixtures are in the range that makes it a candidate for hydraulic barriers at acid mine drainage sites.

Acknowledgements

The authors appreciate the many helpful and insightful comments of the reviewers. The support and continued involvement of the following individuals in our research into ash utilization and AMD abatement is gratefully appreciated: James D. Burnell, Ash Consultant, Monongahela Power Co., Brian M. Osborn, Engineer, Laurita Energy Corp., and Dr. Paul Ziemkiewicz, Director, National Mine Land Reclamation Center (NMLRC). Many thanks to Patricia Schnitzer for assistance in preparing this manuscript. Funding for this work was received though grant WV28 from the NMLRC.

References

American Coal Ash Association, Inc. 1991. Coal combustion by-product production and consumption fact sheet for 1990. Washington, DC.

ASTM. 1993a. Standard test method D698, Laboratory compaction characteristics of soil using standard effort. American Society for Testing and Materials annual book of standards, Section 4, 04.08, Soil and Rock; Dimension Stone; Geosynthetics.

ASTM. 1993b. Standard test method D5084, Measurement of hydraulic conductivity of saturated porous materials using a flexible wall permeameter. American Society for Testing and Materials annual book of standards, Section 4, 04.08, Soil and Rock; Dimension Stone; Geosynthetics.

Bowders, J.J., Jr. and E.D. Chiado. 1990. Engineering ealuation of waste phosphatic clay for producing low permability barriers. p. 11-15. In Proceedings of the Mining and Reclamation Conference and Exhibition. (Pittsburgh, PA, April 1990).

Bowman, W.G. 1968. Record grout curtain seals Nile's leaky bed. Eng. News Record 180(Feb. 28):22-24.

Hart, W.M., K.I. Batarseh, G.P. Swaney and A.H. Stiller. 1992. A rigerous model to predict the AMD production rate of mine wast rock. In Proceedings of the Second International Conference on the Abatement of Acidic Drainage. (Montreal, PQ, September 16-18, 1991).

Hart, W.M. 1992. A model incorporating the effect of leach rate for the prediction of AMD. Ph.D. Dissertation, College of Engineering, WV Univ., Morgantown, WV.

Peirce, J.J. and K.A. Witter. 1986. Termination criteria for clay permeability testing. J. Geotech. Eng. ASCE 112(9):841-854.

Powell R.D. and N.R. Morganstern. 1985. The use and performance of seepage reduction measures. p. 158-182 In: Volpe, R.L. and W.E. Kelly, eds. Seepage and Leakage from Dams and Impoundments. New York: American Society of Civil Engineers.

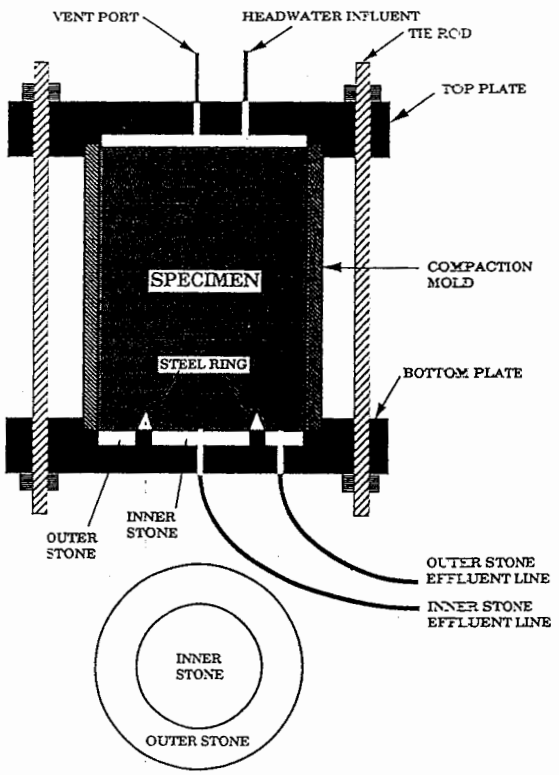

Figure 1. Double-ring, rigid-wall permeameter.

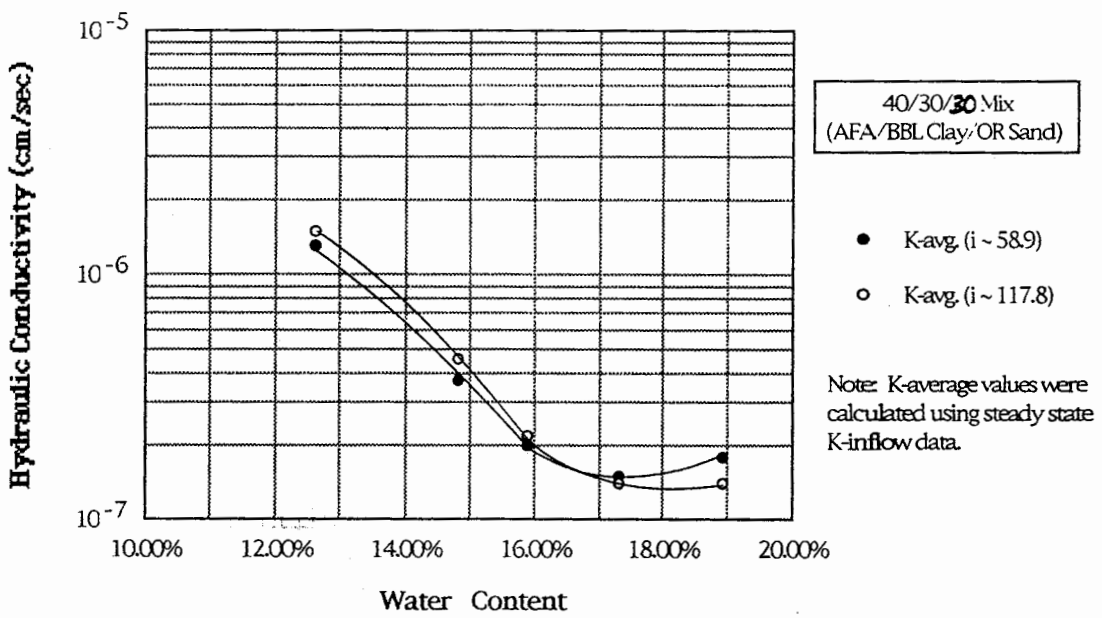

Figure 2. Typical hydraulic conductivity vs. molding water content for compacted fly ash-clay-sand mixtures (40%Ash/30%BBL-Clay/30%Sand).

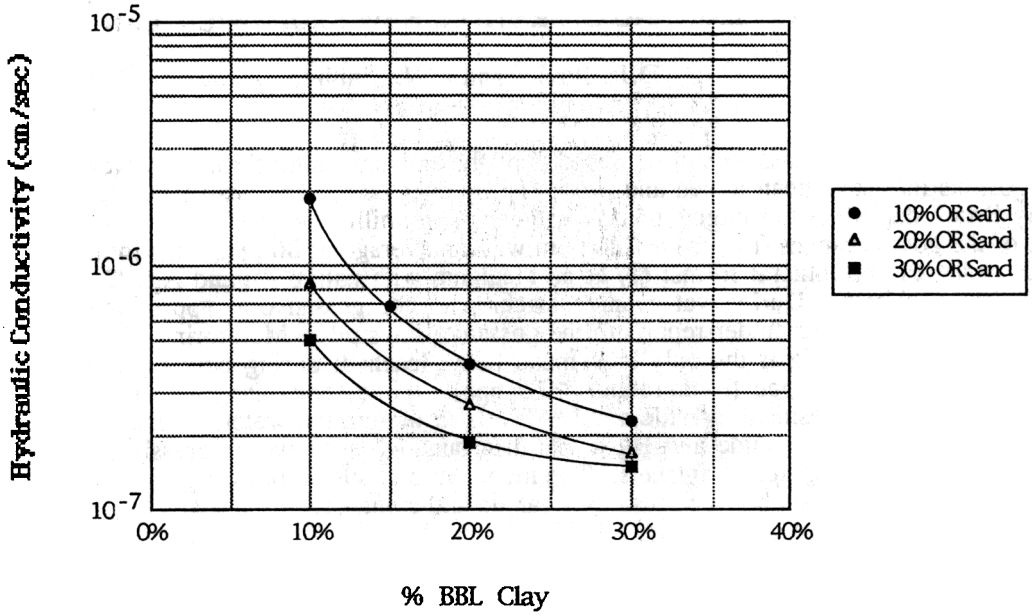

Figure 3. Hydraulic conductivity vs. percent BBL-clay and percent sand for all mixtures.

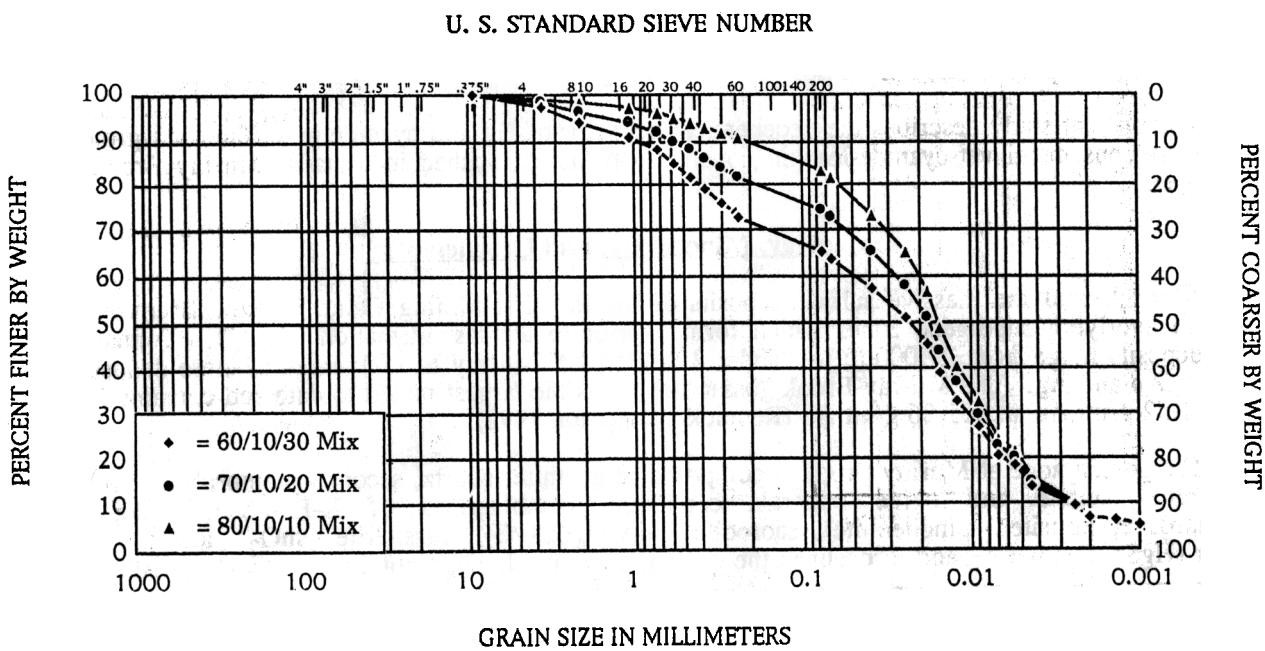

Figure 4. Postpermeation grain-size distribution curves for 10 percent BBL clay specimens.

MOBILIZATION OF MERCURY FROM A GOSSAN TAILINGS PILE, MURRAY BROOK PRECIOUS METAL VAT LEACHING OPERATION, NEW BRUNSWICK, CANADA[1].

D.R. Boyle[2] and C.N. Smith[3]

Abstract: A number of the massive sulfide deposits of the Bathurst mining camp in New Brunswick have well-developed gossans that have been mined and processed by cyanide vat and heap leaching to recover Au and Ag. The Murray Brook deposit is the largest of these gossans (1.9 million mt; 1.52 g/mt Au; 65.86 g/mt Ag). The Hg content of the gossan ranges from 10 to 220 ppm with an average of 36 ppm. Hg in the Murray Brook gossan is present in at least three mineral forms: (1) as an amalgam with native Au and Ag, (2) in cinnabar, and (3) in Sb-Bi-As hydroxy-sulfates. During vat cyanide leaching of the gossan ore, approximately 12% of the Hg is recovered by retorting; the remainder reports to the gossan tailings pile. Monitoring of the ground waters around the tailings pile shows that Hg is the only base metal being leached; during operation, levels of this element in ground waters reached 8,390 ppb (background <0.5 ppb). Time series analyses for monitoring wells show a strong correlation between residual cyanide and Hg levels in the ground waters. Since cessation of vat leaching operations, both the residual cyanide and Hg levels in ground waters have progressively decreased, with minor perturbations occurring during spring freshets. The mobilization of Hg from the gossan tailings pile is thought to be due to a slow kinetic reaction between residual cyanide and cinnabar.

Additional Keywords: mercury, cyanide, cinnabar, gossan, gold, ground water, vat leaching.

Introduction

During cyanide leaching operations at Au-Ag mining operations, special attention is given to the possible concentration and mobilization of such elements as Cu, Pb, Zn, Hg, Ni, Fe, and Co within the environments of these sites. This is because these elements form relatively stable complexes with cyanide and generally occur in the group of cyanicide minerals (base-metal sulfides) that often plague the efficiency of cyanide leaching as well as effluent treatment. With the exception of Co^{3+} and Fe^{3+}, Hg forms stronger complexes with cyanide than the metals mentioned above, and given the presence of numerous mineral forms in which this element can occur and its potential bioaccumulative toxic effects in the environment it is important to understand fully the factors that control the concentration and mobilization of Hg in cyanide leaching operations, especially heap and vat leaching waste disposal piles where residual cyanide often remains for some time. Problems with Hg mobilization in these environments may also be compounded by the fact that Hg does not respond to traditional lime neutralization-precipitation processes.

The present study describes the geochemical behavior of Hg and cyanide in surface and ground waters at the first precious metal vat-cyanide-leaching operation to be established in Canada (Murray Brook Mine, New Brunswick).

Geology, Mineralogy, and Geochemistry

A number of the massive sulfide deposits of the Bathurst Mining Camp in New Brunswick have well developed overlying supergene zones which formed prior to the last glaciation (fig. 1). Tonnages for these gossan deposits range from 20,000 to just under 2 million mt (Murray Brook); three of these deposits have been mined for Au and Ag. The Murray Brook gossan deposit is the largest mined to date and contains 1.7 mt tonnes grading 1.52 g/mt Au and 65.86 g/mt Ag (Rennick and Burton 1992).

The gossan zone at Murray Brook is composed of goethite, quartz, secondary amorphous silica, a number of hydrated sulfate and oxide minerals containing combinations of K-Fe-Pb-As-Sb-Ag (beudantite, plumbojarosite, jarosite , bindheimite), scorodite [$FeAsO_4 \cdot 2H_2O$]), cassiterite (SnO_2), and trace amounts of cinnabar (HgS). Native Ag and Bi occur in the gossan, and Au, although not directly, is also assumed to

[1]Paper presented at the International Land Reclamation and Mine Drainage Conference and the Third International Conference on the Abatement of Acidic Drainage, Pittsburgh, PA, April 24-29, 1994.

[2]D.R. Boyle, Geological Survey of Canada, 601 Booth St., Ottawa, Ontario, Canada, K1A 0E8

[3]C.N. Smith, NovaGold Resources Ltd, 774 Main St., Beresford, New Brunswick, E0B 1H0

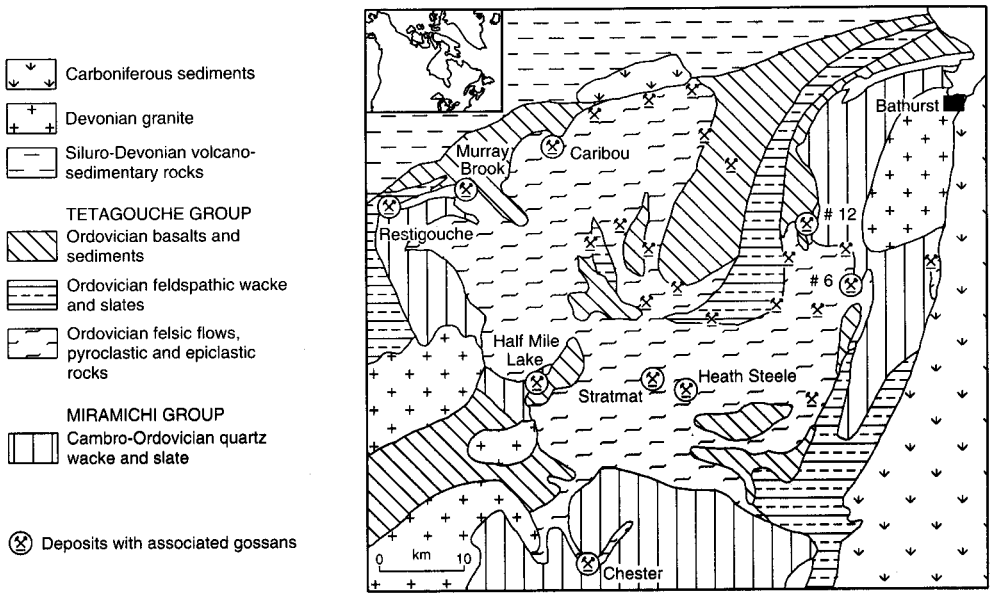

Figure 1. Geology of Bathurst Mining Camp showing locations of massive sulfide mineral deposits with associated supergene ore zones.

be in the native form (Boyle 1992). Pyrite in the gossan is only present in trace amounts at the gossan-supergene sulfide zone contact.

Mercury in the gossan has an average concentration of 36 ppm and a range of 10 to 220 ppm. Most of the Hg is present in the form of cinnabar (HgS), which occurs as submicron grains and veinlets in goethite, often associated with void structures. Some of the Hg is associated with native silver and presumably native gold. On average, the cyanide leaching process extracts 12% of total Hg, most of this is considered to be associated with native Au and Ag. Trace amounts of Hg are also associated with the hydrated sulfates, particularly beudantite.

Geochemistry and Mineralogy of Mercury

In the primary environment Hg may be present as a significant component in a wide variety of sulfide minerals (Jonasson and Boyle 1979). In the supergene oxidizing environment Hg is mainly present as cinnabar formed as the result of oxidation of Hg-bearing sulfide minerals. This mineral is perhaps the most stable of all sulfides in oxidizing environments, with solubilities of 5, 15, and 120 μg/L at pH values of 3.0, 7.0, and 9.0, respectively (Schwartzenbach and Widmer 1963). In weathered materials that make up the ore for many heap and vat cyanide leaching operations, cinnabar is the most common Hg-bearing mineral.

In the secondary environment, Hg is of great concern as a toxicant because during methylation processes, in both aerobic and anaerobic environments, it will readily form methyl-Hg complexes which are easily concentrated in the flesh of many forms of biota (Jonasson and Boyle 1979). In addition, Hg is a strong bioaccumulator in the aquatic food chain and may therefore accumulate in fish to such an extent that their consumption is hazardous to human health and the viability of fishing industries is jeopardized.

Physiography, Climate, and Hydrology

The Murray Brook deposit is located on the side of a hill with a 10° slope (fig. 2). The mill site, tailings pile, and treatment ponds are located at the base of the deposit with the entire operation forming the headland region of Gossan Creek valley. Overburden at the site varies in thickness from 1 to 2 m and consists mainly of sand and gravel glacial till. Bedrock underlying the overburden is strongly weathered and fractured.

The ground water table in the area varies from 2.5 to 5 m and generally follows surface relief; most of the overburden in the area is located in the vadose zone. Both surface and subsurface drainage in the area is channeled into Gossan Creek, which eventually flows into the Eighteen Mile Brook-Upsalquitch River system. Along its course, Gossan Creek receives surface drainage from two significant streams and many ground water springs (fig 2).

The mean annual precipitation in the area is approximately 980 mm, of which about 240 mm falls as snow and thus contributes to the spring freshet.

Mining and Milling Processes

The mining and milling process at Murray Brook began in September 1989 and continued without interruption until April 1992. Mining is carried out using opencast methods with ore being initially stored in a primary ore stockpile (fig 2). The gossan ore is crushed to minus 0.75 cm, and the fines are agglomerated with lime and cement before leaching. The leach material is placed in four indoor vats each with a capacity of 900 mt. Leaching by continuous sprinkling is carried out for 24 h using a free cyanide concentration of 0.7 to 1.0 g/L. The pregnant solution is processed for Au and Ag using the Merrill Crowe zinc dust precipitation method. Mercury, which reports to the precipitate during this process, is recovered by retorting. Because Cu, Zn, and sulfide concentrations are very low in this ore and Fe is not in the sulfide form, cyanide and process water recirculation at this site are optimum.

After vat leaching, the barren ore is washed with clean water for 4 to 6 h. The washed barren ore from the vats is then transported by front end loader to the tailings disposal area, where it is graded.

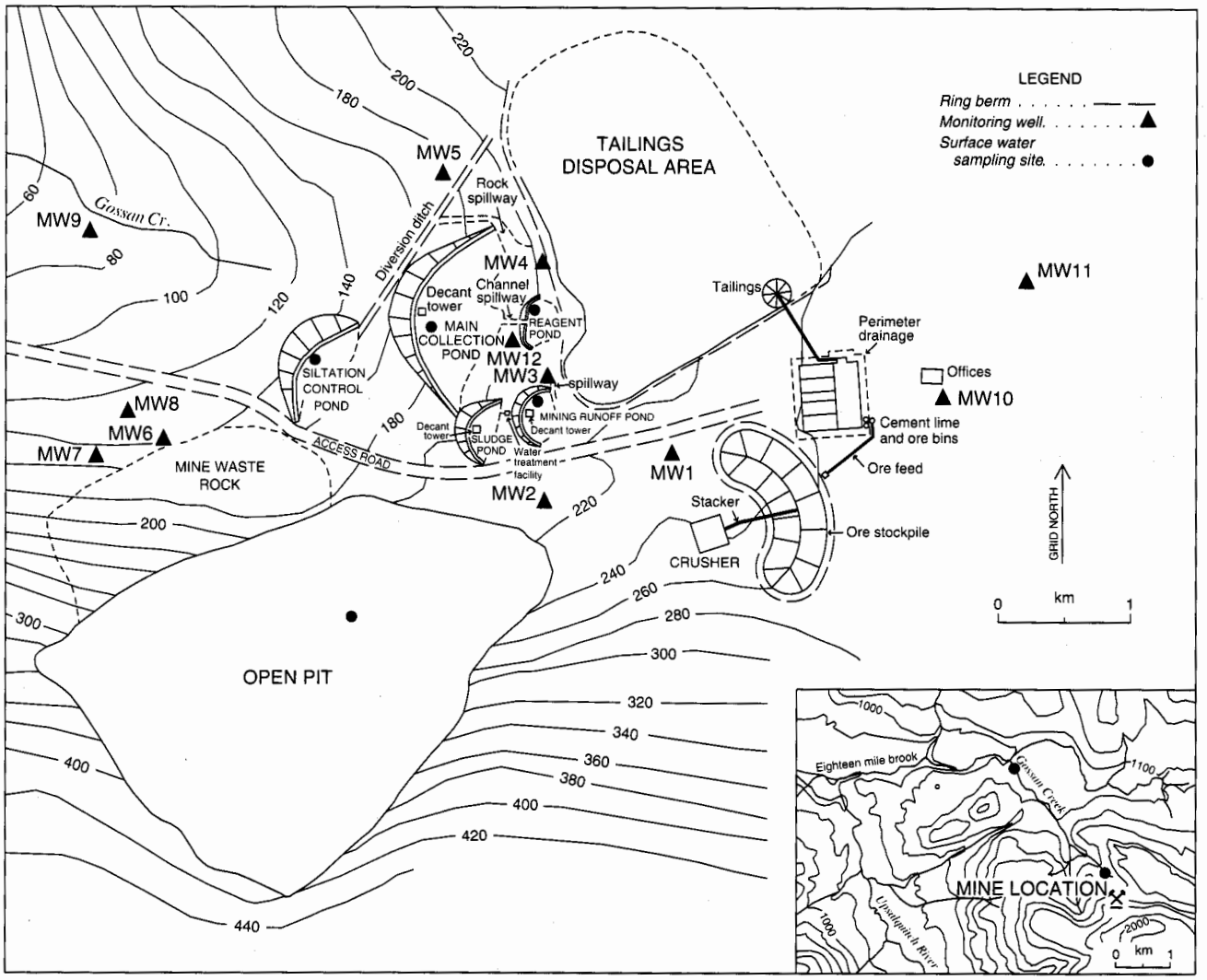

Figure 2. Murray Brook mining operation showing locations of surface and ground water monitoring sites for mine area and baseline study (inset).

Environmental Monitoring Program

Three years prior to mining, a baseline monitoring program was set up on the Gossan Creek-Eighteen Mile Brook-Upsalquitch River system (see insert, fig. 2). Shortly before mining commenced in September 1989, surficial and ground water monitoring networks were established on the site (fig 2). Surficial sampling was aimed at monitoring the composition of open pit water, runoff from various units of the mine site (tailings pile, ore stockpile, mill area), and various pond effluent waters. Twelve ground water wells were established to monitor composition of ground waters associated with the tailings disposal area (MW-4, MW-5, MW-9), the effluent pond environments (MW-3, MW-12), the waste rock pile (MW-6 to 8), the open pit area (MW-2), the ore stockpile (MW-1), the mill and office area (MW-10), and a background area just to the west of the operation (MW-11). All of the ground water monitoring wells are finished in bedrock with the overburden section sealed off from possible surface contamination. In all cases the water levels in these wells were within bedrock.

Surface drainage on the site is channeled through various drainage ditches to the collection ponds near the tailings disposal area, where it can be used as makeup water in the mill and eventually treated if necessary.

Monitoring sites were sampled biweekly from the start of site preparation in September 1989 and will continue to be sampled until the area is reclaimed and considered to be "chemically stable". It is expected that this will be a 'walk away operation' after reclamation.

Water samples from monitoring sites were analyzed consistently for pH, total cyanide, Cu, Pb, Zn, Fe, and Hg, and periodically for As. The pH was measured on site. Total cyanide was measured by a distillation-titrimetric method (method 4500-CN-C of Standard Methods for the Examination of Water and Wastewater, SMEWW), base metals by atomic absorption techniques, As by a hydride atomic absorption method, and Hg by cold-vapor atomic absorption spectrometry (method 3112-B of SMEWW). Ground water samples were not filtered and thus results for cyanide and Hg represent total concentrations.

Results and Discussion

Baseline Monitoring and Regulations

Results from the premining baseline monitoring program established low and high levels in the Gossan Creek-Eighteen Mile Creek watershed as follows: Cu, <0.01 and 0.033 μg/L; Pb, <0.01 and 7.9 μg/L; Zn, 0.025 and 0.169 μg/L; Fe, 0.027 and 0.963 mg/L, and pH, 7.17 and 8.01. At present the pH and concentrations of these metals at the regulatory environmental receiving site (mouth of Gossan Creek) are all within the premining baseline levels mentioned above. Although total cyanide and Hg were not included in the baseline studies, their levels at the receiving site have remained at <0.1 mg/L and <0.5 μg/L, respectively, since monitoring began at time of mining. The Federal and provincial regulatory levels imposed on this operation for total cyanide and total Hg at the receiving site are 1.0 mg/L and 10 μg/L respectively.

Tailings Pile Characteristics

The tailings pile at Murray Brook covers an area of approximately 3 km^2, has a maximum thickness of about 12 m, and constitutes about 1.1 million mt of gossan. Because of coarse crushing and the original porosity of the ore (average 21%), the pile is highly permeable to waterflow and O_2 diffusion.

The paste pH (using 0.01M $CaCl_2$ adjusted to pH 7.0) of 21 representative samples of the unleached gossan from the open pit averaged 5.20 with a narrow data range of 4.72 to 5.73, indicating that the gossan material will not be significantly acid generating once the lime-cement agglomerating material is dissolved out of the pile. The Hg concentrations of these pH paste solutions were all <1.0 μg/L.

To determine the amounts, variation with depth, and interrelationship of labile cyanide and Hg in the pile, five profile samples of the gossan material were sampled at 1-m intervals to a depth of 6.5 m and leached in the laboratory. The staticleaching method consisted of adding 2 kg of gossan to 1.5 L of de-ionized water that had been purged of dissolved oxygen by bubbling N_2 gas through it for 24 h. The gossan was leached without shaking for 48 h, and the leachates were then decanted, filtered (0.45 μm), and stabilized with NaOH solution to pH 12 for total cyanide determination and with concentrated nitric acid to pH 2 for mercury analysis. The results of this experiment (table 1) indicate that total cyanide has degraded considerably in the upper 2 m of the pile compared with lower depths. Roughly half of the cyanide in the 0 to 2 m depth interval has either oxidized in situ or been mobilized by meteoric precipitation, or a combination of both. Using an average total cyanide

concentration for the lower depths of the pile (>2 m) of 5.0 mg/kg and a date of April 1992 for last addition of material to the pile,

a degradation rate for cyanide of about 2.5 mg/kg/yr can be calculated. Given the fact that degradation is probably not linear with depth, this would have to be considered a maximum rate. Using this rate, it would take about 2 yrs for the cyanide in the pile to degrade to nondetectable levels. This compares well with the investigations of Engelhardt (1985), who found that 85% of the free cyanide in a heap leach operation in Arizona was destroyed within 15 months of shutdown.

The data in table 1 show an almost one to one correlation between labile total cyanide and labile mercury in the pile. For the highly stable $Hg(CN)_4^{2-}$ complex, the stoichiometric ratio of Hg to cyanide is 2:1. About half of the cyanide present in the pile can therefore be accounted for as a cyanide-mercury complex. The other half is probably present as other metal-cyanide complexes, particularly $Fe(CN)_6^{3-}$. The pH of ground waters leaving the pile ranges from 5.8 to 7.2, depending on climatic conditions; any free cyanide in solution will therefore be in the HCN form.

Table 1. Results of static leaches, Murray Brook gossan tailings.

Sample depth, m	Total cyanide, mg/kg	Mercury, mg/kg
0.5	2.4	2.7
2.0	2.1	3.6
3.0	7.0	6.4
4.5	4.0	4.2
6.5	5.6	3.0

Surface Water Chemistry

Throughout the monitoring program at Murray Brook, the concentration of total cyanide in stream waters at the head of Gossan Creek has remained consistently below 0.1 mg/L. The Hg concentration at this site remained at background levels until December 1991 and then began to rise steadily to peak at a level of 75 μg/L in March 1993, after which it has been steadily decreasing (fig. 3). At the time of peak Hg concentration in stream waters at the head of Gossan Creek, the concentration at the environmental receiving site (mouth of Gossan Creek) remained at baseline levels of <0.5 μg/L, well below the regulatory level of 10 μg/L. Based on the Hg results and the response of other elements in this system, waters (surface and ground waters) entering the head of Gossan Valley are diluted before reaching the receiving site by a factor of at least 200.

During the mining operation, the concentration of Hg in the open pit water remained below 0.5 μg/L even when the pit water went strongly acid (pH 2.5) when the gossan-sulfide contact was reached. The low concentration of Hg in pit water agrees well with the results for Hg in the pH paste solutions of fresh unleached gossan material.

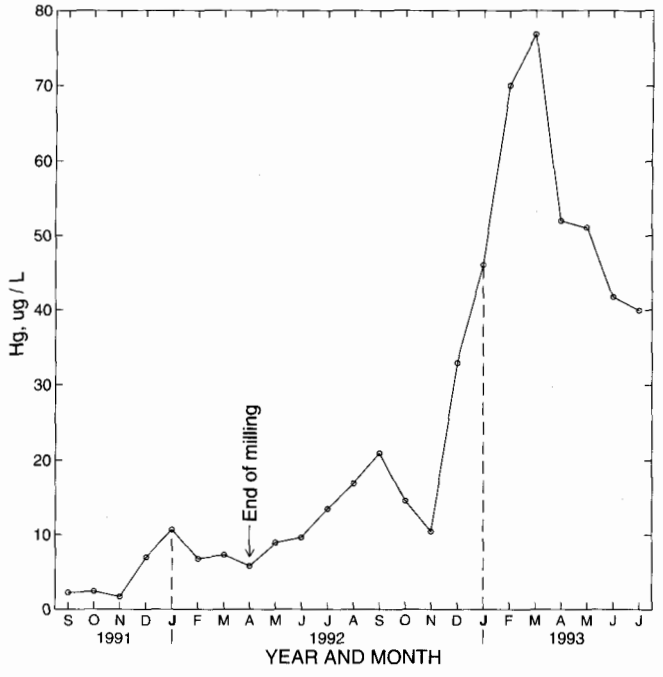

Figure 3. Monthly averages for Hg in stream water at the head of Gossan Creek. Total cyanide was consistently below 0.1 mg/L over this period.

Ground Water Chemistry and Flow

For ground waters representing subsurface flow from the ore stockpile (MW-1), the open pit (MW-2), the mine waste rock pile (MW-6 to 7), the southern portion of Gossan Creek valley (MW-9), and background lithology away from mining (MW-11), the Hg and total cyanide concentrations have been consistently at background levels from start of mining until the present (<0.5 μg/L and <0.1 mg/l, respectively). Ground waters in monitoring wells associated with the effluent and runoff pond environments (MW-3, MW-12) show sporadic increases in Hg and total cyanide, consistent with the times at which these ponds were used to store effluent before recycling to the mill or before liming, cyanide destruction, and passage into the collection and siltation control ponds. In these wells, Hg and total cyanide concentrations reached levels of 850

μg/L and 1.8 mg/l, respectively, but generally decreased within a few months to background levels after introduction of effluents into the ponds was stopped.

Of main concern to this study are the waters associated with baseflow from the tailings disposal area (MW-4, MW-5). Well MW-4 receives baseflow from tailings material deposited in the first two years of operation and MW-5 from material deposited mainly over the last year of mining. The monthly averages for total cyanide and Hg in MW-4 ground waters are plotted in figure 4. Apart from an obvious strong correlation between cyanide and Hg, there is a gradual decrease in the yearly averages for these two parameters from 1990 to 1993. After the end of milling (April 1992), there is a significant decrease in cyanide and Hg compared to the mining period, with a peak increase occurring only at the time of the spring freshet in 1993. Present levels for MW-4 are at background for total cyanide (<0.1 mg/L) and are approaching background for Hg (now about 250 μg/L).

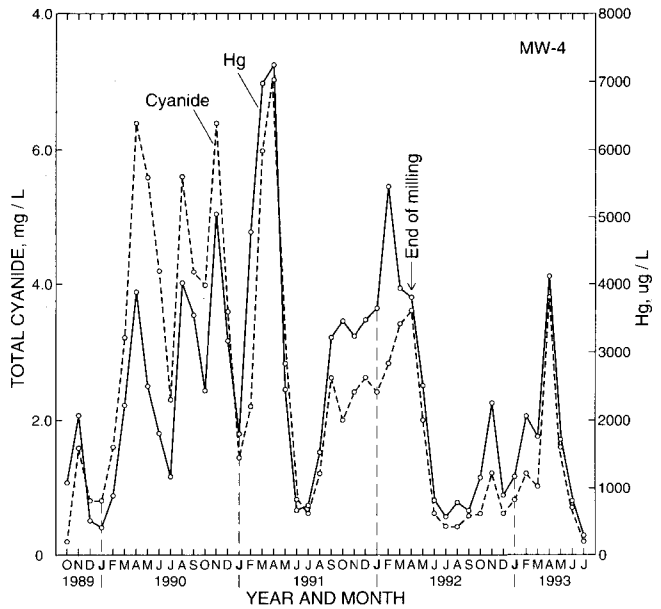

Figure 4. Monthly averages for total cyanide and Hg in ground waters of monitoring well MW-4.

For MW-5 ground waters (figure 5) there is also a strong correlation between total cyanide and Hg, but levels of both these parameters have remained high from late 1990 to the present. The differences between the concentration patterns for total cyanide and Hg in MW-4 and MW-5 ground waters are most likely due to a longer period of time for cyanide destruction for the portion of the pile monitored by MW-4. The comparative data between these two wells suggest that concentrations of Hg in pore waters within the pile and dispersion of this element out of the pile are controlled by the destruction and mobilization rates of residual cyanide. In figure 5 there is a slight offset in the times that cyanide and Hg initially reach MW-5. This is probably due to almost total destruction of free and complexed cyanide during the initial stages of baseflow from the northern portion of the tailings pile.

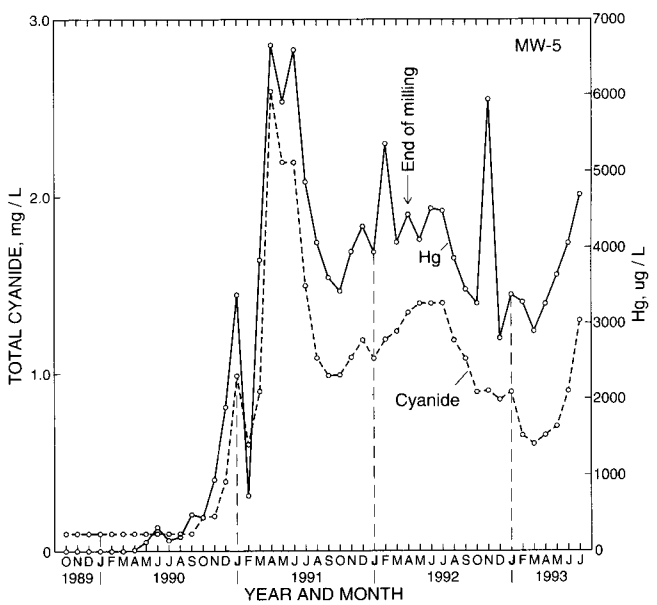

Figure 5. Monthly averages for total cyanide and Hg in ground waters of monitoring well MW-5.

From the breakthrough time of Hg into monitoring well MW-5 (fig. 5), the time of travel for ground waters in bedrock downslope from the tailings pile is estimated to be about 40 m/yr. This would result in an initial influx of ground waters from the pile into the headwaters of Gossan Creek at the end of 1992, which correlates quite well with results for Hg monitoring of this creek (fig. 3). The decrease of Hg in Gossan Creek after early 1993 probably represents overall increased destruction of free cyanide and cyanide-Hg complexes, with greater partitioning of Hg into the solid phases of the overburden-bedrock environment. Figure 6 shows the correlation between total cyanide and Hg for all analyses of ground waters at the site. Also shown on this plot is the line for stoichiometric $[Hg(CN)_4^{2-}]$. Many of the ground waters at Murray Brook contain more Hg than can be accounted for as a Hg-cyanide complex; this is especially so for the ground waters at MW-5. With greater destruction of the cyanide-Hg complex, by both inorganic and organic agents, more of the Hg is free to enter into solid adsorption

processes. Provided the supply of Hg from the pile is attenuated by cyanide destruction within the pile, solid phases should not become saturated and the influx of Hg into the Gossan Creek streamflow system will not reach critical proportions. Given the fact that the environmental receiving site is at the mouth of Gossan Creek and there is an almost 200:1 dilution factor along this creek, the influxes of Hg should be environmentally manageable. However, if this operation had been much larger, with a greater mined tonnage or higher Hg content, the mobilization of Hg could conceivably have been a serious problem.

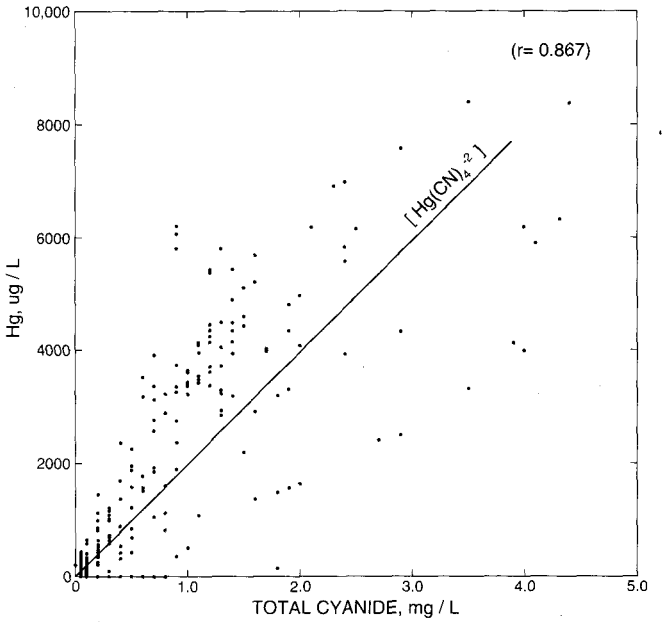

Figure 6. Plot of Hg versus total cyanide for all ground water analyses at Murray Brook. Line of stoichiometric composition of dominant $[Hg(CN)_4^{2-}]$ complex also given.

Behavior of Cinnabar in Cyanide Solutions

To determine if cinnabar, which is the principal Hg-bearing mineral in this deposit, was the major contributor of Hg to ground waters, a literature search was made for information on the behavior of cinnabar in cyanide solutions. Nothing was found and it was then decided to run some preliminary experiments. Results of three leaches of cinnabar using 1, 10 and 250 mg/L free cyanide solutions are presented, together with controls, (table 2). Considerable amounts of Hg can be leached from cinnabar in even weak cyanide solutions. Depending on the concentration of cyanide, the solubility of cinnabar in cyanide solutions (tables 1 and 2) is 270 to 800 times greater than in neutral noncyanide waters.

Table 2. Cyanide leaching of cinnabar (HgS)[1].

	Leaching solution		
Conditions	Cyanide, ppm	Hg, ppb	Hg leached, mg/g
Control 1	0	81	0.020
Control 2	0	94	0.024
Leach 1	1	2,150	0.538
Leach 2	10	4,350	1.090
Leach 3	250	12,200	3.050

[1]Leaches carried out on 1 g of cinnabar (Almaden Mine, Spain) with 250 mL of NaCN solution for 48 h with gentle agitation every 12 h. Control leaches carried out using de-ionized water. Both cyanide and control leach solutions were adjusted to pH 10 using NaOH.

Although the kinetic rates of this reaction still need to be determined, it would appear from the mill recovery of Hg (12% of total contained Hg), the strong correlation between cyanide and Hg in ground waters (fig. 6), and the constant uptake of Hg in pore waters of the tailings pile, that the dissolution rate of cinnabar in even weak cyanide solutions is high enough to be of environmental concern.

Conclusions

The following conclusions can be drawn from this research:

1. At Murray Brook Mine, the concentration of Hg in pore waters of mill tailings containing significant amounts of cinnabar (HgS) is related to the amount of residual cyanide remaining in the pile and, more importantly, to cyanide mobilization and cyanide destruction within the pile and along ground water flowpaths.

2. Clearly more research is required on the behavior of cinnabar in the cyanide leaching of various types of oxidized ores, especially since cinnabar is a common mineral in these ores and Hg is a very difficult element to remove from effluents.

3. Consideration should be given to methods of accelerating the rate of cyanide destruction in vat and heap leaching waste materials containing high concentrations of Hg (generally greater than 10 to 20 ppm) as cinnabar.

4. In Canada, indoor vat cyanide leaching methods will be the method of choice for certain types of Au-Ag ores owing to the severe climatic conditions of the country. For oxidized and volcanic epithermal Au-Ag ores, in which Hg is present in significant amounts as cinnabar, future vat leaching operations should utilize lined catchment reservoirs for mill tailings.

Acknowledgments

The authors would like to thank T. Smith of NovaGold Ltd. for collating much of the monitoring data for the site. P. Kondos of CANMET, Natural Resources Canada is greatly thanked for his diligent, but unfortunately fruitless, attempt at trying to find reference material on the behavior of cinnabar in cyanide solutions.

Literature Cited

Boyle, D.R. 1992. Transport and deposition of gold during formation of the Murray Brook Au-Ag-Hg gossan deposit, Bathurst Camp, New Brunswick. p. 647-653 In M. Pagel and J.L. Leroy (Eds), Source, transport and deposition of metals, , A.A. Balkema, Rotterdam.

Engelhardt, P.R. 1985 Long-term degradation of cyanide in an inactive leach heap. p. 539-547 In D. Van Zyl (Ed), Proceedings of Conference on Cyanide and the Environment (1984), Colorado State Univ. Publ.

Jonasson, I. and R.W. Boyle 1979. The biogeochemistry of mercury. p. 28-49 In Effects of mercury in the Canadian environment. National Research Council Canada Publication 16739,

Rennick, M.P. and D.M. Burton. 1992. The Murray Brook deposit, Bathurst Camp, New Brunswick: Geologic setting and recent developments. Exploration and Mining Geol, 1(2):137-142.

Schwartzenbach, G. and M. Widmer. 1963. p. 80-H-3. K.H. Wedepohl (Ed), In Handbook of Geochemistry, section II-5, Springer Verlag, New York..

Stott, W.G. 1985. Handling cyanide at Superior Mining Company's stibnite heap leaching operation. p. 231-248 D. Van Zyl (ed), In Proceedings of Conference on Cyanide and the Environment, Colarado State Univ Publ.

GEOCHEMICAL AND GEOHYDROLOGICAL CHARACTERISTICS OF BEDROCK AND SPOIL FROM TWO METHODS OF MINING AT A RECLAIMED SURFACE COAL MINE, CLARION COUNTY, PA, USA[1]

Charles A. Cravotta III[2], Keith B.C. Brady[3], Linda C. Gustafson-Minnich[2], and Michael R. DiMatteo[3]

Abstract: Two methods of mining caused subtle differences in geochemical and geohydrological characteristics of spoil at a reclaimed surface coal mine in western Pennsylvania. A dragline was used in the southern area of the mine, and bulldozers and front-end loaders were used in the northern area. Mining methods used in the intervening, middle area are uncertain. In general, overburden at the mine consisted of sideritic gray shale and siltstone. Calcareous zones were laterally discontinuous. However, a 1.2-m thick stratum of pyritic shale above the mined coal was laterally continuous and had total sulfur (S) concentrations >2.5 weight percent (wt %). Regardless of mining methods, pyritic material in backfill is inverted relative to its stratigraphic sequence in bedrock. Where bulldozers and front-end loaders were used, the pyritic shale was selectively handled and buried in compacted layers above the water table, and only low-S (<0.2 wt %) material was buried near the pit floor. Where the dragline was used, high-S (≥0.5 wt %) material was placed near the surface, but above intermediate-S material. In the middle area, where mining methods are uncertain, high-S material was randomly distributed, near the surface and on the pit floor, within the zone of water-table fluctuation. In the northern and middle areas, mass-weighted average S in spoil was comparable to that in premining bedrock. In contrast, average neutralization potential of spoil was about one-third of that of premining bedrock, possibly because of preferential weathering of carbonates in shallow bedrock (premining) or spoil. Despite differences in mining methods, hydraulic conductivities for spoil were similar among the northern, middle, and southern areas, ranging from $10^{-8.2}$ to $10^{-3.0}$ meters per second (m/s), with median hydraulic conductivities from $10^{-3.8}$ to $10^{-3.6}$ m/s. Hydraulic conductivities for spoil were not always greater than those for underlying bedrock.

Introduction

Geochemical and geohydrological characteristics of spoil at surface coal mines can vary because of differences in mining methods and equipment. This paper describes the geochemical and geohydrological characteristics of bedrock and spoil at a reclaimed surface coal mine in the bituminous field of western Pennsylvania and evaluates effects of two different mining methods on these characteristics.

The study area is a reclaimed surface coal mine in southern Clarion County, Pa. (fig. 1) that consists of 44.5 hectares covering two adjoining hilltops. The middle and lower Kittanning coals were mined during 1980-86 (Glover 1987). In the southern area of the mine, where calcareous materials were widespread, a dragline with a 34.4-m^3 bucket was used to remove overburden and to backfill the mine. In contrast, in the northern area, where calcareous strata were present only locally, bulldozers and front-end loaders were used for mining and backfilling, and in particular to selectively handle a 1.2-m thick stratum of pyritic, carbonaceous shale overlying the lower Kittanning coal. The selectively handled pyritic material was compacted with the mining equipment in layers, or pods, on lifts composed of low-S spoil at least 3 m thick on the pit floor, so that the pods would be above the anticipated post-mining water table. In addition, in the northern area, a total of 56 megagrams (tonnes) of limestone per hectare was added to the backfill near the surface and to the pit floor. The boundary between areas where the different mining methods were used is not known precisely. Hence, a middle area, between the southern and northern areas, was included in the investigation. The middle and northern areas are separated by an unmined hilltop. This unmined area is a 60-m-wide right-of-way for a natural-gas pipeline, which runs north-south through the mine (fig. 1).

Methods

Initially, records were reviewed from Pennsylvania Department of Environmental Resources (PaDER) and C&K Coal Company files, which included premining geologic logs, geochemical data for drill cuttings, and mining activities. Later, subsurface drilling, sampling, and testing were conducted to evaluate variations in geochemical and geohydrological characteristics of bedrock and spoil across the reclaimed area. Premining boreholes were drilled by

[1]Paper presented at the International Land Reclamation and Mine Drainage Conference and the Third International Conference on the Abatement of Acidic Drainage, Pittsburgh, PA, April 24-29, 1994.
[2]Hydrologist, U.S. Geological Survey, 840 Market Street, Lemoyne, PA 17043.
[3]Hydrogeologist, Pennsylvania Department of Environmental Resources, Harrisburg, PA 17105.

diamond-coring methods, and postmining boreholes by air-rotary methods, to collect rock samples and install ground-water monitoring equipment. Six boreholes (18-1, 23-6, 23-7, N1, CK3, and CK4 in fig. 1) were drilled in bedrock in or near the northern area through zones of maximum overburden thickness along a hilltop. Holes at locations CK1 and CK2 (fig. 1) were drilled in 1985, after mining. Clusters of boreholes identified with prefixes N, M, and S (fig. 1) were drilled in 1991, mostly through spoil, in the northern, middle, and southern areas, respectively. Rock samples from boreholes through spoil and bedrock were collected as composites over 1.5-m depth intervals.

Lithology of rock samples was determined, and most rock samples were analyzed for concentrations of total S and neutralization potential (NP) by methods of Sobek et al. (1978) for acid-base accounting. Mass-weighted averages for NP, maximum potential acidity (MPA), and net neutralization potential (NNP=NP-MPA) for each borehole and each of the three areas of the mine were calculated by methods of Smith and Brady (1990). Data for rock samples collected at the same depth at a borehole cluster were averaged for areal estimates. Major minerals in samples from borehole N1 (fig. 1) were identified by X-ray diffractometry (XRD; Whittig and Allardice 1986), which has a detection limit of about 1 to 5 percent. Lithostratigraphic correlation diagrams were constructed with premining and postmining data for lithology and rock chemical concentrations by use of the computer program StratiFact (Rosenlund et al. 1993). To facilitate correlation of horizons, the borehole data were adjusted to a common datum, the base of the lower Kittanning coal.

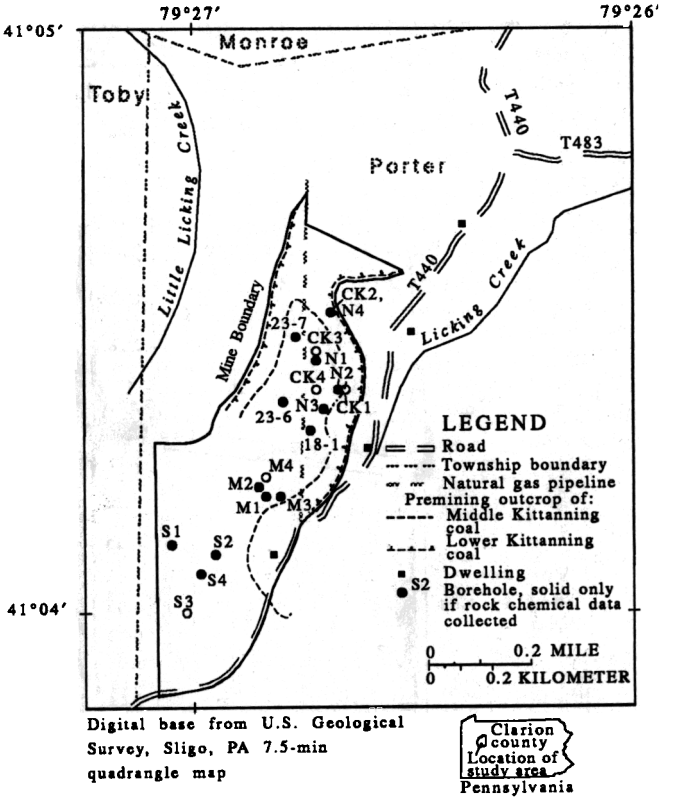

Figure 1. Location of boreholes at surface coal mine in southern Clarion County, PA.

Monitoring wells were installed in most boreholes. Wells were constructed of 5.1-cm diameter polyvinyl chloride pipe with a minimum of 3-m length slotted screen (Cravotta et al. 1994). Static water levels in wells were measured monthly by use of an electrical tape. Hydraulic conductivities were estimated for saturated intervals of the screened zones by use of slug-test methods of Bouwer and Rice (Bouwer 1989). A solid cylinder (slug) was submerged below the static water level in each well, and changes in hydraulic head during slug injection and withdrawal were measured with a submerged pressure transducer and recorded with a data logger. Methods of hydraulic testing and data reduction were reported by Hawkins and Aljoe (1991).

Geochemical Characteristics

Lithostratigraphic correlations, before mining (fig. 2), show vertical and lateral differences in overburden chemistry. Locally, the middle and lower Kittanning coalbeds dipped gently west-northwest and were separated by about 18 to 20 m of medium- to dark-gray shale that graded upward to siltstone and claystone. The middle Kittanning coal had a thickness of 0.6 to 0.8 m, and the lower Kittanning coal had a thickness of 0.45 to 0.6 m. A 1.2-m-thick stratum of high-S, pyritic, carbonaceous shale was immediately above the lower Kittanning coal (fig. 2, table 1). The shale and lower Kittanning coal had concentrations of total S >2.5 wt % and NP <10 grams as calcium carbonate per kilogram (g/kg $CaCO_3$). Most overburden horizons had concentrations of total S <1 wt % and NP <25 g/kg $CaCO_3$; however, some shale and siltstone were calcareous. High values of NP, up to about 125 g/kg $CaCO_3$, were associated with fossiliferous (brachiopods), gray shale between the lower and middle Kittanning coalbeds.

Bedrock samples from borehole N1 were further analyzed for major minerals and concentration of total carbon to indicate possible mineralogic forms of S and NP (table 1). Pyrite (FeS_2) was the predominant S-bearing mineral and siderite ($FeCO_3$) was the predominant carbonate mineral. Some siderite-bearing shale and siltstone also contained

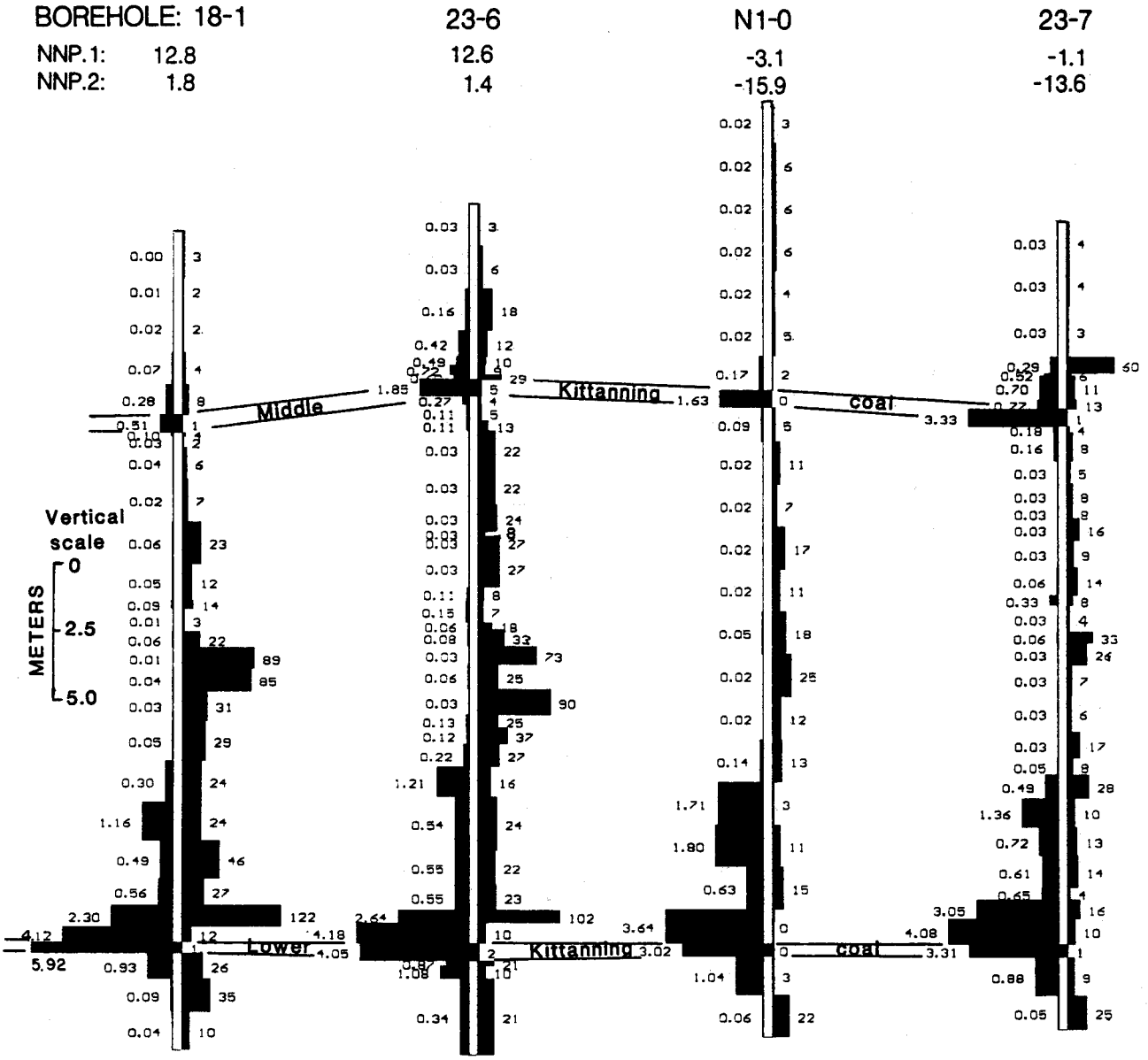

Figure 2. Lithostratigraphic correlations and rock-chemical variations for premining conditions. Datum is base of lower Kittanning coal. Values for column-weighted net neutralization potential computed using a factor of 31.25 (NNP.1) and of 62.5 (NNP.2) are shown below borehole number (see footnote 3 in table 2). Borehole locations shown in figure 1. For explanation of symbols, see "KEY" in figure 3.

manganosiderite [$(Fe,Mn)CO_3$], calcite ($CaCO_3$), and dolomite [$CaMg(CO_3)_2$]. Overburden and coal in the upper 12 m penetrated by borehole N1 lacked detectible sulfide and carbonate minerals and had lower concentrations of total S and NP than deeper strata, probably as a result of near-surface weathering. High concentrations of total S in the middle Kittanning coal at 11-m depth were probably from organic-S forms, because S-bearing minerals were not detected by XRD.

Regardless of the mining method used, backfilled spoil at the mine tends to be inverted relative to the stratigraphic sequence in bedrock, and unweathered material containing substantial concentrations of total S and NP commonly was placed near the land surface (fig. 3). Substantial lateral variations in total S concentrations also were produced, as indicated by cuttings from adjacent boreholes N2-0 and N2-2, N3-0 and N3-2, M1-0 and M1-2, and M2-0 and M2-2 (fig. 3), which were drilled about 1.5 m apart for installation of nested lysimeters and wells (Cravotta et al. 1994). In the northern area, where bulldozers and loaders were used, high-S (≥0.5 wt %) materials were placed near

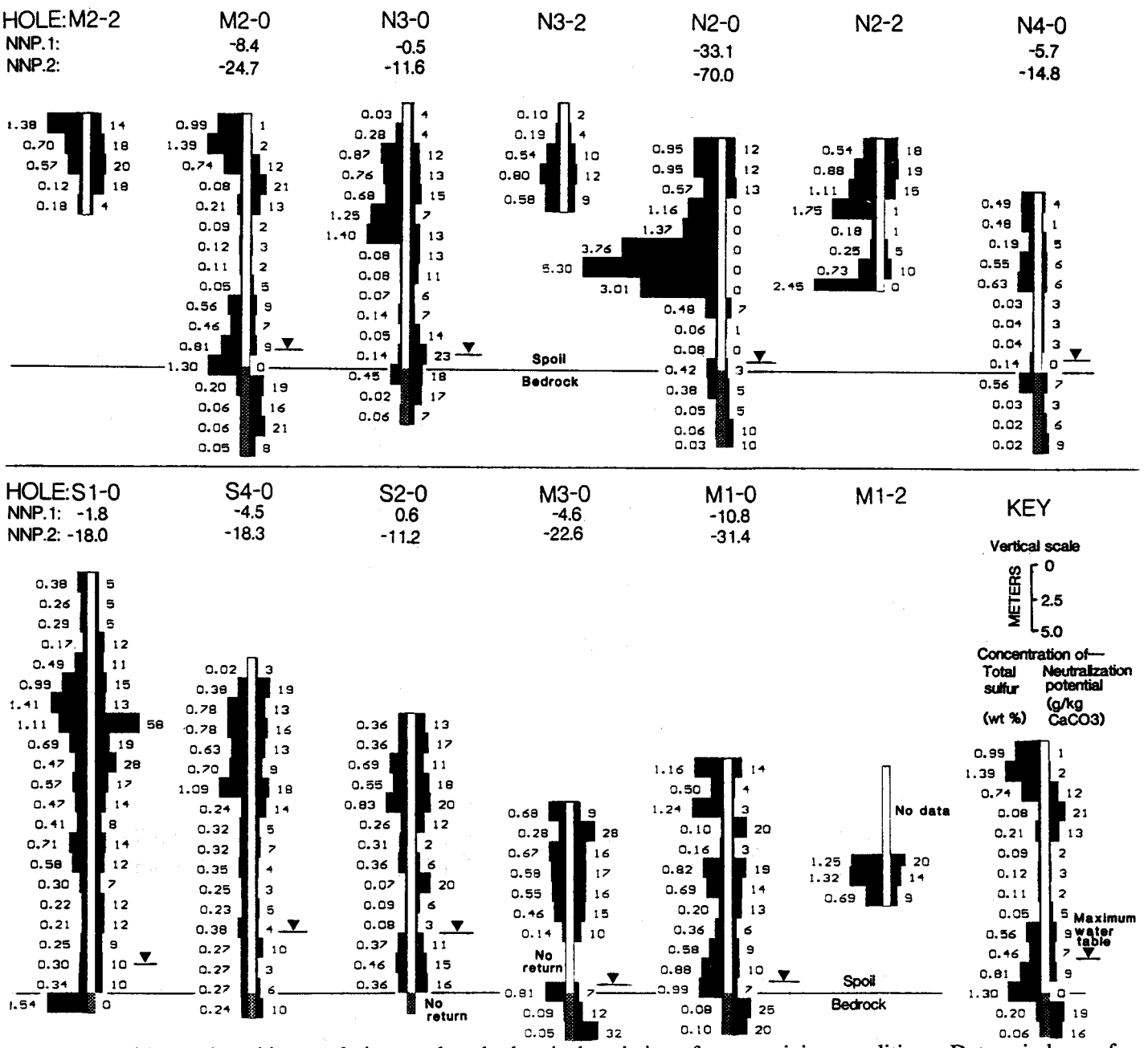

Figure 3. Lithostratigraphic correlations and rock-chemical variations for postmining conditions. Datum is base of lower Kittanning coal. Values for column-weighted net neutralization potential computed using a factor of 31.25 (NNP.1) and of 62.5 (NNP.2) are shown below borehole number (see footnote 3 in table 2). Borehole locations shown in figure 1. Boreholes identified with suffix "-0" or "-1" drilled through lower Kittanning coal horizon and "-2" drilled to less than 11 m depth.

the land surface to 13.7 m depth (fig. 3) and were generally underlain by a minimum of 6 m of low-S (<0.2 wt %) material. High-S materials in the northern area, including a pyritic pod that was penetrated by boreholes N2-0 and N2-2 (fig. 3), were placed more than 6 m above the pit floor. In the southern area, where a dragline was used, high-S materials also were placed near the surface, but underlying materials had intermediate S (0.2 to 0.5 wt %) concentrations. In the middle area, pyritic, high-S materials were randomly distributed from the surface to the pit floor.

Summaries of the acid-base account (ABA) for premining bedrock and postmining spoil data are reported as mass-weighted averages for each area (table 2). Two values of MPA were computed by multiplying total S concentra-

tion, in weight percent, by factors of 31.25 (MPA.1; Sobek et al. 1978) and 62.5 (MPA.2; Cravotta et al. 1990). On the basis of bedrock data for the northern and middle areas, average MPA computed by a factor of 31.25 was less than average NP and resulted in positive values of average NNP. Premining bedrock data were not available for the southern area. On the basis of spoil data, MPA computed by either factor resulted in negative values for average NNP for all areas, which could indicate a relative deficiency of alkaline-producing materials (Cravotta et al. 1990). Average NNP for spoil generally decreased northward across the mine (fig. 2, table 2).

Differences between average NNP for premining bedrock and postmining spoil (table 2) in the northern and middle areas are a result of lower average NP for spoil, roughly one-third of that for bedrock in each area. In contrast, average MPA for spoil is similar to that of bedrock. Differences in chemical compositions and minerals in bedrock and spoil probably are an artifact of sampling, reflecting effects of topographic positions of boreholes and premining weathering profiles. Boreholes in bedrock generally were at locations about 10 m higher elevation than comparable boreholes downslope in spoil. A stratum would be expected to be less weathered at greater depths, and calcareous strata generally were situated above high-S strata. Differences between bedrock and spoil also could result from accelerated weathering of carbonates relative to sulfides during the postmining period. However, elevated concentrations of sulfate and alkalinity in ground water from the spoil were observed, which indicates that oxidation of pyrite was active and probably promoted carbonate dissolution (Cravotta et al. 1994).

Table 1. Mineral and chemical content of bedrock samples from borehole N1.
[+ major; ? possible trace; - not detected; < less than; wt %, weight percent; g/kg, grams $CaCO_3$ per kilogram]

Sample depth interval[1]	Lithology[2]	Quartz[3]	Illite	Chlorite	Calcite	Dolomite	Siterite	Mn-siderite	Pyrite	Total sulfur (wt %)	Total carbon (wt %)	Neutralization potential (g/kg)
0.0-1.5	SS+SH	+	+	+	-	-	?	-	-	<0.05	0.11	3
1.5-3.0	SH	+	+	+	-	-	?	-	-	<.05	.16	6
3.0-4.6	SH	+	+	+	-	-	-	-	-	<.05	.14	6
4.6-6.1	SH	+	+	+	-	-	-	-	-	<.05	.39	6
6.1-7.6	SS+SH	+	+	+	-	-	+	-	-	<.05	.22	4
7.6-9.1	SH	+	+	+	-	-	?	-	-	<.05	.35	5
9.1-10.4	ST+SH	+	+	+	-	?	?	-	-	.17	1.04	2
10.4-11.0	CO	+	-	+	-	-	-	-	-	1.63	68.09	-3
11.0-12.2	UC	+	+	+	-	-	+	-	-	.09	.71	5
12.2-13.7	UC	+	+	+	?	?	+	+	-	<.05	.76	11
13.7-15.2	UC	+	+	+	?	+	+	+	-	<.05	.54	7
15.2-16.8	SH+ST	+	+	+	?	+	+	+	-	<.05	2.07	17
16.8-18.3	SH+ST	+	+	+	-	?	+	+	?	<.05	1.76	11
18.3-19.8	SH+ST	+	+	+	+	+	+	+	-	.05	1.02	18
19.8-21.3	SH	+	+	+	+	+	+	+	-	<.05	.68	25
21.3-22.9	SH	+	+	+	-	-	+	+	?	<.05	.42	12
22.9-24.4	SH	+	+	+	+	+	+	+	-	.14	1.87	13
24.4-25.9	SH	+	+	+	-	-	+	-	+	1.71	2.28	3
25.9-27.4	SH	+	-	+	?	+	+	+	+	1.80	2.38	11
27.4-29.0	SH	+	+	+	?	+	+	+	+	.63	2.17	15
29.0-30.2	SH+CO	+	+	+	-	+	?	-	+	3.64	4.15	-5
30.2-30.6	CO	+	+	-	-	-	-	-	+	3.02	69.08	-2
30.6-32.0	UC	+	+	+	-	-	?	-	+	1.04	.61	3
32.0-33.5	UC	+	+	-	-	?	+	+	?	.06	.96	22
33.5-35.1	UC	+	+	+	?	?	-	-	-	<.05	.32	6

[1] Composite sample of drill cuttings from depth interval, in meters from surface, at location of borehole N1 (figs. 1-2).
[2] Lithology determined by hand-specimen analysis: SS = sandstone; ST = siltstone; SH = shale; CO = coal; UC = underclay.
[3] Minerals identified in all samples were combined under the heading, "Quartz." These include quartz, microcline, albite, muscovite, and kaolinite.

Geohydrological Characteristics

Spoil at the mine does not always have greater hydraulic conductivity than premining or underlying bedrock (table 3). Hydraulic conductivities of spoil were more than an order of magnitude greater than those of bedrock at nests N4, M1, M4, and S2; however, conductivities of spoil were slightly less than those of bedrock at nests N2, N3, and M3. Backfill produced by bulldozers and loaders would be expected to have a more uniform particle-size distribution, similar or greater compaction, and lesser hydraulic conductivity than that produced by the dragline (Phelps and Saperstein 1982; Phelps 1983). Air circulation commonly was lost in shallow spoil during drilling in the southern area; however, no air losses occurred in the northern area, indicating greater compaction from bulldozers and loaders than from a dragline. Nevertheless, hydraulic conductivities for saturated mine spoil were similar among the three areas (table 3). For saturated spoil, hydraulic conductivities were from $10^{-8.2}$ to $10^{-3.0}$ m/s, with medians of $10^{-3.8}$ to

$10^{-3.6}$ m/s in each area. The similarity in median hydraulic conductivities of spoil could result from similar lithologies and piping and settling processes (Pionke and Rogowski 1982), by which fines are transported downward and large voids fill or collapse. Mine spoil in the southern area is several years older than that in the northern area, so a longer time has elapsed for these processes to occur.

To avoid contact between acid-forming materials and ground water, the mining plan for the northern area required placement of pyritic materials at least 3 m above the pit floor, so that they would be above the postmining water table. During January-December 1992, saturated thickness of spoil in the northern area ranged from 0.2 to 3.0 m, and across the mine ranged from 0.2 to 6.9 m (table 3). Borehole data for the northern area indicated that pyritic materials were always above the water table (fig. 3). In the southern area, borehole data generally indicated that high-S material was buried above the water table. In the middle area, high-S materials were buried both in the unsaturated zone and on the pit floor (fig. 3). High-S material on the pit floor in the middle area generally is more than 1.5-m thick and lies within the zone of water-table fluctuation.

Table 2. Acid-base-account summaries of area-weighted overburden chemical data.
[Values in g/kg as $CaCO_3$; --, no data; values in parentheses include 56 Mg/ha limestone as alkaline addition.]

Sample type[1]	Neutralization potential (NP)	Maximum potential acidity 31.25[2] (MPA.1)	Net neutralization potential[3] (NNP.1)	Maximum potential acidity 62.5[2] (MPA.2)	Net neutralization potential[3] (NNP.2)
		Northern area			
Bedrock	21.43 (21.59)	18.67	2.76 (2.92)	37.34	-15.91 (-15.75)
Spoil	7.83	15.06	-7.23	30.12	-22.29
		Middle area			
Bedrock	26.95	14.28	12.67	28.56	-1.61
Spoil	8.55	17.05	-8.50	34.10	-25.55
		Southern area			
Bedrock	--	--	--	--	--
Spoil	10.58	12.99	-2.41	25.97	-15.39

[1]Bedrock samples from boreholes 18-1, 23-6, 23-7, and N-1 (fig. 1). Spoil samples from boreholes N2, N3, N4, M1, M2, M3, S1, S2, and S4 (fig. 1). Northern area: 23-6, 23-7, N1, N2, N3, and N4. Middle area: 18-1, 23-6, M1, M2, and M3. Southern area: S1, S2, and S4.

[2]Maximum potential acidity computed by multiplying mass-weighted total sulfur concentration by a factor of 31.25 (MPA.1) or 62.5 (MPA.2) according to methods of Cravotta et al. (1990).

[3]Net neutralization potential computed by subtracting maximum potential acidity from mass-weighted neutralization potential, i.e., NNP.1 = NP - MPA.1 and NNP.2 = NP - MPA.2, according to methods of Smith and Brady (1990).

Table 3. Well construction and hydraulic-conductivity data
[Values in meters except where noted; --, no data]

Well name[1]	Latitude, north	Longitude, west	Lithology of screened interval[2]	Depth of screened interval	Ground surface elevation	Base of LK-coal elevation[3]	Ground-water head elevation		Values during June 1992[4]		
							Minimum	Maximum	Ground-water head	Saturated thickness	Hydraulic conductivity (m/s)
				Wells screened in spoil							
CK1-1	41°04'23"	79°26'39"	SH+CO?	7.6-14.1	449.75	435.65	--	--	--	--	
CK2-1	41°04'31"	79°26'41"	SH+CO?	7.6-13.5	446.53	433.06	434.10	434.49	434.10	0.98	9.27E-04
N2-1	41°04'23"	79°26'40"	SH+UC	15.8-19.2	453.78	436.10	436.28	436.47	436.28	.18	6.55E-09
N3-1	41°04'21"	79°26'42"	SH+UC	18.3-21.6	455.15	435.03	435.87	436.20	435.87	.84	2.97E-04
N4-1	41°04'31"	79°26'41"	SH+UC	10.7-14.3	446.83	433.11	434.00	436.15	434.00	.88	1.61E-05
M1-1	41°04'12"	79°26'50"	CO+UC	16.5-19.7	450.32	432.34	433.00	434.45	433.64	1.30	2.79E-05
M2-1	41°04'13"	79°26'51"	CO+UC	17.1-20.4	451.07	431.87	433.19	434.45	433.62	1.75	6.37E-04
M3-1	41°04'12"	79°26'48"	SH+UC	12.5-15.8	446.93	432.29	433.03	434.31	433.47	1.17	1.84E-06
M4-1	41°04'14"	79°26'50"	SH+UC	23.5-26.5	457.60	432.30	433.21	435.07	433.53	1.23	4.27E-04
S1-1	41°04'07"	79°27'03"	SH+UC?	29.3-32.6	460.39	428.38	430.71	432.01	430.93	2.55	3.11E-04
S2-1	41°04'06"	79°26'57"	SH+UC?	18.9-22.3	451.40	430.06	433.11	434.52	433.70	3.64	8.17E-04
S3-1	41°04'00"	79°27'01"	CO+SH	26.5-30.2	461.60	432.65	433.29	434.58	434.41	1.76	1.17E-08
S4-1	41°04'04"	79°26'59"	SH+UC	22.6-26.8	455.69	430.09	434.86	436.96	435.02	4.93	1.00E-05

Table 3. Well construction and hydraulic-conductivity data--Continued.
[Values in meters except where noted; --, no data]

Well name[1]	Latitude, north	Longitude, west	Lithology of screened interval[2]	Depth of screened interval	Ground surface elevation	Base of LK-coal elevation[3]	Ground-water head elevation		Values during June 1992[4]		
							Minimum	Maximum	Ground-water head	Saturated thickness	Hydraulic conductivity (m/s)
Wells screened in bedrock											
CK1-0	41°04'23"	79°26'39"	ST+CO	18.0-21.3	449.44	435.27	432.81	435.18	433.59	5.49	4.30E-08
CK2-0	41°04'31"	79°26'41"	SH+CO	17.4-21.3	446.53	433.06	432.34	432.60	432.34	7.15	8.32E-06
CK3-0	41°04'27"	79°26'43"	SH+CO	33.5-39.6	463.57	434.04	432.57	433.91	432.75	8.81	--
CK3-1	41°04'27"	79°26'43"	SH+CO	15.2-29.6	463.60	434.04	--	--	--	--	--
CK4-0	41°04'23"	79°26'43"	SH+CO	27.4-33.7	461.40	434.82	432.64	434.13	433.82	6.10	--
CK4-1	41°04'23"	79°26'43"	SH+CO	14.0-26.6	461.34	434.82	445.90	446.93	445.90	11.14	--
N1-0	41°04'26"	79°26'43"	UC	32.0-35.4	463.75	433.12	432.45	433.48	432.64	4.24	6.86E-06
N1-1	41°04'26"	79°26'43"	SH+UC	28.7-32.0	463.76	433.13	433.04	433.36	433.04	1.28	3.84E-08
N2-0	41°04'23"	79°26'40"	UC	20.1-23.3	453.88	436.20	433.47	434.63	433.63	3.06	1.90E-07
N3-0	41°04'21"	79°26'42"	UC	22.6-26.2	455.09	434.97	432.46	433.66	432.65	3.78	7.74E-04
N4-0	41°04'31"	79°26'41"	UC	14.6-19.8	446.77	433.05	432.39	433.47	432.41	5.46	9.39E-07
M1-0	41°04'12"	79°26'50"	UC	21.3-24.5	450.29	432.31	432.99	436.97	433.39	7.64	4.24E-09
M2-0	41°04'13"	79°26'51"	UC	22.6-25.9	451.10	431.90	433.45	434.42	433.45	8.26	--
M3-0	41°04'12"	79°26'48"	UC	18.3-21.3	446.90	432.27	432.89	434.57	433.64	8.07	1.09E-05
M4-0	41°04'14"	79°26'50"	UC	28.7-32.0	457.47	432.17	432.60	434.12	432.84	7.38	2.58E-06
S1-0	41°04'07"	79°27'03"	UC?	33.5-38.4	460.40	428.39	--	--	--	--	--
S2-0	41°04'06"	79°26'57"	UC?	24.1-27.4	451.48	430.15	424.83	427.78	426.17	2.12	2.36E-07
S3-0	41°04'00"	79°27'01"	UC+ST	32.0-35.4	461.88	432.93	427.44	433.01	432.36	5.83	--

[1]Well number indicates location (fig. 1): Prefix "CK" or "N," northern area; "M," middle area; "S," southern area. Suffix "-1," screened within horizon of mined coal; "-0," screened below horizon of mined coal.
[2]Lithology: CO = coal, UC = underclay, SH = shale, ST = siltstone. Queried where lithology uncertain because of incomplete return of drill cuttings or incomplete drill log.
[3]Base of lower Kittanning (LK) coal; in north area, base of the upper split. This elevation corresponds with the elevation of surface-mine floor where mine spoil is present.
[4]Saturated thickness corresponds with zone from ground-water surface down to the base of spoil or screen, if bedrock. Hydraulic conductivity reported using exponential notation, where 9.27E-04 = 0.000927 m/s.

Conclusions

Different methods of mining caused subtle differences in geochemical and geohydrological characteristics of spoil at a reclaimed surface coal mine in western Pennsylvania.

(1) In premining bedrock, a 1.2-m-thick stratum of pyritic shale above the lower Kittanning coal was laterally continuous across the mine. Overlying calcareous strata thinned or were absent in the northern area. Pyrite was the predominant S-bearing mineral; siderite, manganosiderite, and calcareous minerals including calcite and dolomite were the predominant carbonate minerals.

(2) Where bulldozer and loader (northern area) or dragline (southern area) methods were used to emplace backfill, pyritic, high-S materials generally were inverted relative to their stratigraphic sequence in bedrock and were placed above the post-mining water table. However, where mining methods are uncertain (middle area), high-S materials were randomly distributed from the surface to the pit floor, in the zone of water-table fluctuation.

(3) Placement of pyritic materials below a permanent water table would not have been practical at the mine because the saturated zone in spoil was locally <1 m thick. Also, because the saturated thickness of spoil exceeded 6 m in some areas, placement of pyritic materials on 3-m thick benches on the pit floor, as required by the mining plan, would not have been adequate to maintain unsaturated conditions within pyritic pods in some areas.

(4) Mass-weighted average concentration of maximum potential acidity (total S) in spoil was comparable to that in premining bedrock; however, average neutralization potential was about one-third that of bedrock. Differences in the composition of bedrock and spoil probably were an artifact of sampling and also could have resulted from accelerated weathering of carbonates relative to pyrite in spoil. Averages of net-neutralization potential for spoil in each area of the mine were negative and generally decreased northward, indicating a relative deficiency of calcareous minerals and potential for development of acidic ground-water quality, particularly in the northern area.

(5) Hydraulic conductivities of saturated spoil were not always greater than those of underlying bedrock. Hydraulic conductivities of spoil throughout the mine ranged from $10^{-8.2}$ to $10^{-3.0}$ m/s; median values were $10^{-3.8}$ to $10^{-3.6}$ m/s in each of the three areas. Similarity probably results from similar spoil lithologies, aging of the spoil, and effects of piping and settling in each area.

Acknowledgments

This study would not have been possible without cooperation of the property owners, Allan and Mary Jane Yingling and Grace Bashline (deceased), who provided access. The authors wish to thank James Fagley and James Kindell of C&K Coal Company for providing information on mining activities, Jay W. Hawkins of the U.S. Bureau of Mines for conducting aquifer tests, Roger Bowman of PaDER for surveying, and Joseph H. Schueck of PaDER for geophysical mapping.

Literature Cited

Bouwer, H. 1989. The Bouwer and Rice slug test--an update. Ground Water 27:304-309.

Cravotta, C. A., III, K. B. C. Brady, M. W. Smith and R. L. Beam. 1990. Effectiveness of the addition of alkaline materials at surface coal mines in preventing or abating acid mine drainage--Part 1. Geochemical considerations. p. 221-225. *In* Proceedings of the 1990 Mining and Reclamation Conference and Exhibition, v. 1. (Charleston, WV, April 23-26, 1990).

Cravotta, C. A. III, D. L. Dugas, K. B. C. Brady and T. E. Kovalchuk. 1994, Effects of selective handling of pyritic, acid-forming materials on the quality of ground water at a reclaimed surface coal mine, Clarion County, PA, USA. Bur. Mines IC (this Proceedings).

Glover, A. D. 1987. Coal resources of Clarion County, Pennsylvania--Part 1. Coal crop lines, mined out areas, and structure contours. PA Geol. Surv. Miner. Resour. Rep. 92.

Hawkins, J. W. and W. W. Aljoe. 1991. Hydrologic characteristics of a surface mine spoil aquifer. p. 47-58. *In* Proceedings 2nd International Conference on the Abatement of Acidic Drainage. (Montreal, PQ, September 16-18, 1991).

Phelps, L. B. 1983. Characterization of mine spoil properties as a tool for premining planning. p. 47-51. *In* 1983 Symposium on Surface Mining Hydrology, Sedimentology and Reclamation. (Univ. KY, Lexington, KY).

Phelps, L. B. and L. W. Saperstein. 1982. Spoil modification to minimize the mobilization of formed toxic fluids. p. 593-599. *In* 1982 Symposium on Surface Mining Hydrology, Sedimentology and Reclamation. (Univ. KY, Lexington, KY).

Pionke, H. B. and A. S. Rogowski. 1982. Placement of acid spoil materials. Reclam. Reveg. Res. 1:3-11.

Rosenlund, G. C., M. C. Sumner, W. M. Alam and J. E. Haacke. 1993. StratiFact, version 4.0. GRC Corporation, Wheatridge, CO.

Smith, M. W. and K. B. C. Brady. 1990. Evaluation of acid base accounting data using computer spreadsheets. p. 213-219. *In* Proceedings of the 1990 Mining and Reclamation Conference and Exhibition, v. 1. (Charleston, WV, April 23-26, 1990).

Sobek, A. A., W. A. Schuller, J. R. Freeman and R. M. Smith. 1978. Field and laboratory methods applicable to overburdens and minesoils. U.S. Environmental Protection Agency, EPA-600/2-78-054. 203 p.

Whittig, L. D. and W. R. Allardice. 1986. X-ray diffraction techniques. p. 331-362. *In* A. Klute (ed.), Methods of soil analysis, Part 1, 2d ed. American Society of Agronomy, Madison, WI.

TREATMENT OF ACID MINE DRAINAGE BY PASSIVE TREATMENT SYSTEMS[1]

Ben B. Faulkner and Jeff G. Skousen[2]

Abstract: Passive acid mine drainage treatment systems constructed on sites in West Virginia treat flows ranging from 4 to 98 L/min (1 to 26 gpm) and acidity concentrations from 170 to 2,400 mg/L. Five wetland systems reduce acidity by 3% to 76%, and iron concentrations by 62% to 80%. These wetlands are generally much smaller in area than that recommended by earlier formulas based on iron loads, but they still show good amelioration of acid and iron loads. In two of the five wetlands, limestone was not incorporated in the substrate. Iron and acid reductions were similar between wetlands with and without limestone revealing that limestone may not be important for metal removal in wetlands. Anoxic limestone drains (ALDs) reduce acidity by 11% to 100%. Based on our successes and failures in building and monitoring ALDs, the following conclusions have been reached: (1) organic matter should **not** be placed in drains owing to microorganism growth on the limestone thereby reducing limestone dissolution, (2) amount of limestone (metric tons of limestone per metric tons of acid load per year) shows little correlation to effectiveness and acidity reductions, (3) larger limestone particle size (8 to 25 cm) should be included to maintain water flow through the drain especially when some aluminum, iron, and grit accumulate in the drain, (4) oxygen intrusion into the drain must be prevented, and (5) pipes installed in drains must be large in diameter with large perforations to reduce the chance for plugging.

Additional Key Words: acidity, alkalinity, aluminum, anoxic limestone drains, iron, manganese, wetlands

Introduction

Wetlands and anoxic limestone drains (ALDs) are passive treatment systems for acid mine drainage (AMD), and do not require continual addition of chemicals as active treatment systems do. Wetlands have been used for decades in the treatment of municipal wastewater (Water Pollution Control Federation 1990), but only within the last 10 yrs have they received serious attention in the treatment of AMD. Researchers at Wright State University and West Virginia University independently noted that AMD from abandoned mined lands was improved after passing through natural Sphagnum wetlands in Ohio and West Virginia (Huntsman et al. 1978, Wieder and Lang 1982). Since then, investigators have documented many other sites where the same phenomenon was observed (Brooks et al. 1985, Burris 1984, Samuel et al. 1988). Artificial wetlands have since been constructed by operators and researchers, and results have generally been positive.

The criteria for constructing AMD wetlands is variable since the mechanisms of alkalinity generation and metal removal are not entirely understood (Hedin and Nairn 1992). Generally, sizing is dependent on acidity and flows (acid load), with considerations for iron, manganese, and aluminum removal, and pH. Oxidation, hydrolysis, and precipitation reactions produce additional acidity which must be counteracted by alkalinity. Increasing buffering capacity (alkalinity) in wetlands is accomplished by installing an ALD and/or by encouraging sulfate reduction within the wetland. Sulfate reduction can generate up to 200 mg/L of sulfides, which are available for metal complexation (Rabenhorst et al. 1992). A low redox potential is required for this process. Factors such as climate, season, organic matter inputs, and nutrient availability can dramatically affect the amount of sulfide generation and subsequent metal decrease.

---

[1]Paper presented at the International Land Reclamation and Mine Drainage Conference and the Third International Conference on the Abatement of Acidic Drainage, Pittsburgh, PA, April 24-29, 1994.

[2]Ben B. Faulkner, President, Bratton Farms, Princeton, WV, USA; Jeff Skousen, Associate Professor and Extension Reclamation Specialist, West Virginia University, Morgantown, WV, USA.

ALDs have received much attention since their discovery recently (Brodie et al. 1990, Turner and McCoy 1990) because they have the potential to add alkalinity to mine water without biological or seasonal limitations. An ALD consists of limestone buried in a trench, underdrain, or cell that is protected from the influence of atmospheric or dissolved oxygen. Acid water is intercepted underground and directed through the drain, causing limestone dissolution and the generation of alkalinity without armoring the limestone. The conditioned water is then brought to the surface and, when exposed to oxygen, the metals in the water then precipitate more rapidly than when untreated by the ALD. ALDs require AMD that is free of dissolved oxygen and are more likely to produce long-term effectiveness when iron is largely in the ferrous state and aluminum concentrations are less than 50 mg/L (Nairn et al. 1990, Skousen 1991). The objective of this paper is to evaluate the use of several wetlands and ALDs in West Virginia for treating AMD. The evaluation will be based on acidity and metal removal of the treated versus the untreated water.

Materials and Methods

The passive systems reported in this paper were constructed during 1990 to 1992 by the West Virginia Division of Environmental Protection (WVDEP) Bond Forfeiture Program (table 1). The wetlands, Keister, S.Kelly, Pierce, and Z & F, were constructed in 1990. All ALDs were constructed in 1991 or 1992.

Each wetland system was designed specifically for the site resulting in variable total metal inputs per unit area of wetland. Average flows into each wetland vary from 98 L/m (26 gpm) at Pierce to 17 L/m (4 gpm) at Keister 1. Specific construction criteria for each wetland are discussed in the Results section. In general, 0.6 to 1 m (2 to 3 ft) of organic material composed of peat and hay overlie about 15 to 30 cm (6 in to 1 ft) of limestone in each of the wetlands. Hay bales were usually used as barriers to slow and direct the water through the wetland.

The majority of the ALDs were constructed with 10- to 20-mil plastic on the bottom, filter fabric placed inside the plastic surrounding #57 (gravel-sized) limestone, and hay bales placed on top of the limestone separated by the filter fabric. The plastic was then wrapped around the limestone and hay (specific drawings and construction criteria are available from the authors). A few ALDs were constructed differently. These different designs are detailed in the Results section.

Results

Inflow and outflow water quality are presented in table 2 and represent averages over approximately 3 yrs for the wetlands and 2 yrs for the ALDs. Acidity, alkalinity, iron, manganese, aluminum, and sulfate were the parameters chosen to indicate the effectiveness of the system in treating AMD.

Wetlands

Keister The Keister 1 wetland has a relatively low metal-load-to-area ratio (14.7 g per day per m^2 (gdm^2)) (table 3). It reduced the acidity of an average 17-L/m (4-gpm) flow from 252 to 59 mg/L (76% reduction) and increased pH from 3.1 to 5.4 (table 2). Iron was reduced from 23 to 9 mg/L (62%) (tables 2 and 4), while manganese was minimally reduced from 23 to 20 mg/L (11%). Aluminum was decreased on the average from 27 to 13 mg/L (52%).

The Keister 3/2 wetland has the smallest metal-load-to-area ratio (3.1 gdm^2). It reduced the acidity of a 19-L/m (5-gpm) flow from 106 to 56 mg/L (48%) and iron from 11 to 3 mg/L (73%), but did little to reduce manganese and aluminum concentrations (table 2). This site exhibits a low acid load into the wetland compared with the other wetland sites (table 3) but doesn't show any improved capacity of decreasing acid or iron concentrations due to the larger wetland area. The large capital cost ($225,000) of installing the Keister wetlands suggests that chemical treatment might have been cheaper (caustic soda cost of $8,500 per year or ammonia cost of $9,700 per year). The site is very remote, however, with poor access, and the intermittent flows make chemical treatment inefficient. Further, the receiving stream has not had to bear the wide fluctuations in pH that are common to chemical treatment systems with intermittent flows.

S.Kelly The S.Kelly wetland site differs from the earlier design by attempting to encourage subsurface flow under and through the organic strata. The flow was directed downward into the substrate by the use of a geotextile fabric placed under and on the upstream side of the hay bale barriers. The attempt to direct the flow was unsuccessful. Most of the flow appears to pass through and over the hay bale dikes, rather than under them.

This wetland system provided limited surface area for the amount of acid load (133.5 gdm^2) and iron load (10.1 gdm^2) (tables 3 and 4). Significant reductions in iron were found throughout the sampling period, with a 31-month average of 68% reduction (from 105 to 33 mg/L). Acidity generally increased through the system for the first fall and winter after construction, but has since continued to show improvements. Apparently, AMD seeps into the wetland from the bottom, as flows increase an average of 43% from influent to effluent. Due to this condition, it is more meaningful to compare preconstruction acid loads to postconstruction loads. In the 24-month period prior to construction of the system, an average of 56 L/m (14.8 gpm) with acidity of 2,432 mg/L left the site (196,116 g acid per day or 71 mt/yr). Since the system has been constructed, the average effluent flow has been 95 L/m (25.1 gpm) with acidity of 1366 mg/L (186,867 g acid per day or 68 mt/yr). The total acid load of this site has been reduced by only 5%, but the iron load has been reduced by over 69% (14,364 to 4,514 g per day). These reductions were accomplished without any vegetation in the wetland.

Pierce This wetland employs the "classic" approach to wetland construction. It uses surface flow over a limestone-enriched, organic substrate. It also provides a moderate acid-load-to-area ratio (20 gdm^2). The system has averaged about 52% removal of the acidity and about 80% of the iron with substantial seasonal variation. It has consistently removed a small percentage of aluminum (25%) and manganese (11%) except during large flow events.

Z & F Construction of this wetland employed organic substrates similar to those previously described, but encouraged subsurface flow by means of 6-in plastic pipes under earthen barriers. This wetland provided the highest iron-load-per-area ratio (19.2 gdm^2) but has reduced metals consistently since its construction over 36 months ago. Only a mild pH enhancement has been seen despite removal of 67% of the acidity. Much of the acidity reduction is associated with the removal of iron (77%) and perhaps aluminum (63%), while manganese has sometimes been decreased and sometimes increased through the system.

Removal of an average of 67% of the acid load could be viewed as removing a total of over 25.5 mt (28 st) of acid per year. To have accomplished this chemically, about $22,000 per year in caustic soda would have been necessary. Attendant labor and sludge handling costs associated with a caustic treatment system would have likely doubled this cost. The $110,000 construction cost appears to have been well worth the investment.

All the wetland systems exhibited seasonal variability with respect to acidity and metal removal efficiency. Generally, removal efficiencies increased during summer/fall and decreased during winter/spring. All but the Keister wetlands had about 23 cm of limestone at the base of the wetland. In all cases, the limestone was coated and covered by metal precipitates, and it appeared that acid water was not flowing through the limestone because of the metal covering. Therefore when the Keister wetlands were constructed, no limestone was incorporated in the substrate. Results show that the Keister wetlands without limestone are similar in acid and iron removal as wetlands with limestone. In future wetland designs in the WVDEP AMD treatment program, a layer of limestone will not be incorporated underneath the organic material.

Anoxic Limestone Drains

Greendale Most ALDs under this project were constructed at the Greendale site in 1991 (table 1). All ALDs generated substantial alkalinity for a few months, but some were overcome as acidity returned and alkalinity diminished. Fifteen of the 19 ALDs shown in table 1 reduced the total acid load by 50% or more. Generally, aluminum was retained in the drains. Iron and manganese left the drains in various amounts, but most postdrain concentrations were slightly lower than predrain concentrations (table 2). For example, the Greendale 11 postALD water showed a pH increase from 3.1 to 6.0, an increase of alkalinity, and slight iron, manganese, and aluminum

reductions (table 2). This drain appears to be functioning with limestone dissolution and low metal retention in the drain. On the other hand, the 51 ALD raised pH from 2.8 to 3.4, reduced acidity by 41% (due to some metal retention in the drain), and slightly reduced iron, manganese, and aluminum. The drain does not generate much alkalinity and it may already be coated by metals from the water.

Kodiak An ALD and wetland were installed at this site, and acidity is reduced by 99%. However, iron, manganese, and aluminum are also retained in the drain which will cause the limestone drain to plug eventually. The use of an ALD at this site will be evaluated when water begins leaking out of the top of the drain.

Lillybrook A relatively high-pH (net alkaline), high-iron seep is being treated on this site. The water from the site joins other seepage and enters the existing sediment pond, which is completely full of sediment and supports a lush volunteer cattail population. A concrete septic tank was filled with limestone and installed at the site in November 1992. Alkalinity in the water has been increased substantially (23 to 259 mg/L) which should improve the metal removal efficiency of the existing wetland.

Preston An ALD and wetland treat a small flow of 13 L/m (3.5 gpm) with acidity of 775 mg/L and iron of 570 mg/L. Effluent water from the limestone cell has a pH of 6.0, acidity of 413 mg/L (47% reduction) and iron of 350 mg/L (40% reduction). Some iron and all aluminum are retained in the drain. The ALD-treated water then enters an aerobic wetland. At the exit of the wetland, the pH drops to 3.3, and acidity is reduced to 190 mg/L (76% reduction), and iron is further decreased to 20 mg/L (96% reduction).

Lobo Capital Two ALDs and small wetlands were installed at this site, but the landowner's activities have disrupted the function of the ALDs. The ALDs and wetlands caused a change from 470 mg/L acidity to 223 mg/L alkalinity, resulting in remarkable improvement in the quality of Glade Run, the receiving stream, for a few months (table 1). However, the drain was likely undersized hydraulically for the large flows. This problem was compounded by the presence of bacterial growth on the limestone in proximity to the hay.

Benham WVDEP has installed modified septic tanks at four locations at this site in an attempt to study ALD conditions without the difficulty of reexcavating earthen drains. In these systems, the limestone can be viewed by taking off the lid of the tank. Problems have arisen with differential settling and limestone plugging by ferric iron and grit. No data are presented in table 2 for this site.

Discussion

The most surprising finding in analyzing wetland water quality data is that limestone in wetland substrates did not appear to improve the wetlands metal removal efficiency. As more systems are constructed with and without limestone in the substrate, this finding may be substantiated and reasons may be clarified. In the wetland systems with limestone, the limestone became encrusted with metal precipitates. In fact, the metal crust was so hard that crowbars were needed to break the crust. This crust restricted the flow of water through the limestone, and eliminated the possibility of adding alkalinity to the water.

"Autopsies" of failed or poorly functioning ALDs in 1992 have been accomplished as additional trenches and wetlands were installed. It can now be said with certainty that hay should not be buried in proximity to the limestone in an ALD because it encourages the growth of organisms on the limestone, thereby reducing pore space and dissolution of the limestone. Where hay was not placed in the ALD, the limestone was clean. New ALDs were constructed without hay (originally hay was thought to serve as an oxygen sink and to promote CO_2 production through organic matter decomposition, and thereby to increase limestone dissolution), and also included larger stone (8 to 25 cm) placed at the bottom of the drain and collection zones. Substantial "grit" and metal precipitates were generated upon excavation, so measures must be taken to allow these to settle before contact with the finer limestone.

Monitoring of passive systems has led to the following general observations on ALD construction.
Organic Matter. Addition of hay (even separated from limestone by geotextile fabric) leads to problems of limestone dissolution because of growth of microorganisms. Some builders have enjoyed undocumented success using chicken litter, however, ALDs constructed under the WVDEP program are not including organic matter in the drain.

Amounts and Grade of Limestone. High limestone-to-acid-load ratios are not an important factor in ALD success. While many of the WVDEP ALDs have been inhibited by metal and microorganism coatings of the limestone, large drains (those with greater than 20 mt of limestone per metric ton of acid load per year) have not shown improved success over those with a lower ratio (table 1). The reduction in acid load per metric ton of limestone is quite variable and does not correlate with this ratio. The grade of limestone (which varied between 70 to 90% calcium carbonate equivalent in our ALDs) did not appear to be critical to limestone dissolution rates and alkalinity generation, supporting the work of Watzlaf and Hedin (1993). More acidic water seems to increase limestone dissolution.

Stone Size and Configuration. Larger limestone particle size (8 to 25 cm) increases hydraulic conductivity and may reduce the potential of plugging with iron or aluminum hydroxides. Larger stone also provides settling space for grit and other settleable matter generated during construction. However, large limestone particle size has less surface area for water contact and alkalinity generation. Contact between limestone and water can also be regulated by residence time. From our experience, about 15 to 20 hrs residence time is required for maximum alkalinity generation under a specific AMD and limestone condition. There is increasing evidence that cells or beds of limestone totally inundated with water provide better water contact and alkalinity generation.

Protection from Oxygen. Where inadequate measures were taken to prevent oxygen intrusion, iron precipitation and limestone armoring were observed. Drains must be lined and secured so that oxygen is restricted and water entering the drain is low in oxygen content. If surface water is allowed to "leak" into the drain, the system will fail.

Pipes. Observations of precipitate deposition on pipe walls and at perforations suggest that larger pipes (15 to 25 cm) with larger perforations (2.5 cm or greater) promote longevity. The use of pipes in ALDs is being reduced because of the problems of plugging.

Acknowledgements

The authors acknowledge the West Virginia Division of Environmental Protection, which constructed these passive treatment systems under the Bond Forfeiture Program, and which provided funding for sampling and analyses.

Literature Cited

Brodie, G.A., C.R. Britt, H. Taylor, T. Tomaszewski, and D. Turner. 1990. Passive anoxic limestone drains to increase effectiveness of wetlands acid drainage treatment systems. In: Proceedings, 12th National Association of Abandoned Mined Land Conference, Breckinridge, CO.

Brooks, R., D. Samuel, and J. Hill. 1985. Proceedings of the conference on wetlands and water management on mined lands. The Pennsylvania State University, University Park, PA.

Burris, J. 1984. Treatment of mine drainage by wetlands. Cont. 264, Dept. of Biology, The Pennsylvania State University, University Park, PA.

Hedin, R., and R. Nairn. 1992. Designing and sizing passive mine drainage treatment systems. In: Proceedings of the 13th West Virginia Surface Mine Drainage Task Force Symposium, Morgantown, WV.

Huntsman, B., J. Solch, and M. Porter. 1978. Utilization of a Sphagnum species dominated bog for coal acid mine drainage abatement. Abstracts, 91st Annual Meeting Geologic Society of America, Ottawa, Canada.

Nairn, R., R. Hedin, and G. Watzlaf. 1990. A preliminary review of the use of anoxic limestone drains in the passive treatment of acid mine drainage. In: Proceedings, 12th West Virginia Surface Mine Drainage Task Force Symposium, Morgantown, WV.

Rabenhorst, M., B. James, and J. Shaw. 1992. Evaluation of potential wetland substrates for optimizing sulfate reduction. p. 90-97. In: Proceedings, 1992 American Society for Surface Mining and Reclam., Duluth, MN.

Samuel, D., J. Sencindiver, and H. Rauch. 1988. Water and soil parameters affecting growth of cattails. p. 367-374. In: Mine Drainage and Surface Mine Reclamation, U.S. Bureau of Mines IC 9183, Pittsburgh, PA.

Skousen, J. 1991 Anoxic limestone drains for acid mine drainage treatment. Green Lands 21(4):30-35.

Turner, D., and D. McCoy. 1990. Anoxic alkaline drain treatment system, a low cost acid mine drainage treatment alternative. In: 1990 National Symposium on Mining. Univ. of KY, Lexington, KY.

Water Pollution Control Federation. 1990. Natural systems for wastewater treatment. WPCF, Washington, D.C.

Watzlaf, G., and R. Hedin. 1993. A method for predicting the alkalinity generated by anoxic limestone drains. In: Proceedings, 14th West Virginia Surface Mine Drainage Task Force Symposium, Morgantown, WV.

Wieder, R., and G. Lang. 1982. Modification of acid mine drainage in a fresh water wetland. p. 43-53. In: Symposium on Wetlands of the Unglaciated Appalachian Region. WV Univ., Morgantown, WV.

Table 1. Flows and acid concentrations of passive treatment systems for treating AMD. System specifications include mt of limestone, mt of limestone per mt of acid, and materials used.

Site	Limestone mt	Flow L/m	Pre-Acid mg/L	Post-Acid mg/L	% Reduction	mt Limestone / mt Acid Load	Materials
Wetlands							
Keister 1	0	17	252	59	76	----	compost
Keister 3/2	0	19	106	56	47	----	compost
S.Kelly	780	95	1,383	1,366	3	----	LS,compost,no plts
Pierce	450	98	118	57	52	----	LS, compost
Z & F	476	30	2,388	801	67	----	LS, compost
ALDs							
Greendale							
11	51	45	195	90	54	2.0	hay, #57
21	66	6	700	0	100	10.6	hay, #57
41	18	6	280	140	50	6.6	#57
42	21	19	290	100	66	6.4	hay, #57
43	43	68	600	70	88	1.8	hay, #57
44	36	19	280	220	11	10.0	#57
51	8	4	1,020	600	41	3.7	hay, #57
52	14	7	700	350	50	5.8	hay, #57
61	22	19	2,000	1,000	50	1.0	15-25 cm, #57
101	9	11	1,200	600	50	1.1	#57
102	14	19	600	310	49	3.1	15-25 cm
103	61	15	266	145	45	27.3	hay, #57
108	34	23	370	80	78	7.1	hay, #57
121	19	7	800	0	100	8.5	15-25 cm
131	15	4	750	30	96	45.0	hay, #57
Kodiak	128	15	2,210	30	99	6.6	8-12 cm, #4
Lillybrook	7	60	170	-259	100	12.5	#57
Preston	90	13	775	105	86	12.8	#57
Lobo Cap	250	87	470	-123	100	10.4	hay, #57

Table 2. Characteristics of AMD before and after passing through passive systems in WV.

Site	Flow L/m	pH		Acid mg/L		Alkal mg/L		Fe mg/L		Mn mg/L		Al mg/L		SO_4 mg/L	
		In	Out	In	Out	In	Out	In	Out	In	Out	In	Out	In	Out
Wetlands															
Keistr 1	17	3.1	5.4	252	59	--	---	23	9	23	20	27	13	673	466
Keistr 3/2	19	4.0	4.8	106	56	--	---	11	3	11	11	10	8	356	347
S.Kelly	95	2.9	3.1	1,383	1,366	--	---	105	33	51	50	157	163	2,558	2,660
Pierce	98	3.3	4.4	118	57	--	---	10	2	8	7	9	7	217	227
Z & F	30	2.5	3.5	2,388	801	--	---	376	86	51	40	206	76	2,821	1,662
ALDs															
Greendale															
11	45	3.1	6.0	195	90	0	30	130	110	24	19	3	0	300	500
21	6	2.9	5.7	700	0	0	160	190	160	160	80	28	0	1,900	1,400
41	6	2.6	6.1	280	140	0	30	160	140	40	50	4	0	1,000	1,000
42	19	3.1	6.4	290	100	0	100	22	70	95	90	24	0	1,000	1,400
43	68	2.9	6.2	600	70	0	75	120	110	90	50	80	0	1,800	900
44	19	3.1	5.6	280	220	0	25	210	150	95	50	24	0	1,100	1,100
51	4	2.8	3.4	1,020	600	0	0	140	130	200	160	100	70	2,400	2,000
52	7	2.8	4.7	700	350	0	1	130	100	170	130	55	30	1,600	1,600
61	19	2.8	4.3	2,000	1,000	0	0	300	360	140	140	140	100	3,000	2,000
101	11	2.6	4.8	1,200	600	0	6	150	300	140	120	70	10	2,300	2,000
102	19	2.8	3.7	600	310	0	0	300	100	120	90	94	17	2,060	1,500
103	15	2.8	6.1	266	145	0	80	300	210	120	90	94	0	2,100	1,500
108	23	2.9	6.0	370	80	0	50	80	80	105	96	9	1	1,300	1,300
121	7	3.0	6.8	800	0	0	340	30	30	45	12	50	0	1,100	600
131	4	3.1	6.1	750	30	0	80	41	10	160	140	88	2	2,660	2,000
Kodiak	15	2.8	4.3	2,210	30	0	0	124	1	45	2	287	3	2,900	140
Lillybrook	60	5.7	6.4	170	0	23	259	60	43	21	21	0	0	101	45
Preston	13	3.5	6.1	775	413	0	308	570	350	12	12	50	1	1,330	1,330
Lobo Cap	87	2.9	6.2	470	9	0	131	96	58	3	4	18	0	780	575

Table 3. Reduction of acidity and efficiency of five wetlands for treating acid mine drainage. Flows and chemistry from table 2 were used to calculate acid loads.

Site	Area m^2	Recommend[1] m^2	Load in[2] g/day	Load out g/day	Removal %	Load/Area gdm^2
Keister 1	408	859	6,015	1,413	76%	14.7
Keister 3/2	929	371	2,885	1,524	47%	3.1
S.Kelly	1,417	27,027	189,187	186,629	3%	133.5
Pierce	813	2,343	16,378	7,912	52%	20.1
Z & F	863	15,060	105,287	35,316	67%	122.0

[1]Recommended m^2 by U.S. Bureau of Mines for net acid mine drainage. m^2 = acid load (g/d)/7.

[2]Loads were calculated by L/m x mg/L x 1.44 = g/day.

Table 4. Removal of iron and efficiency of five wetlands in treating acid mine drainage. Loads were calculated from data in table 2.

Site	Area m^2	Load in g/day	Load out g/day	Removal %	Load/Area gdm^2
Keister 1	408	549	215	62%	1.3
Keister 3/2	929	299	82	73%	0.3
S.Kelly	1,417	14,345	4,509	68%	10.1
Pierce	813	1,388	278	80%	1.7
Z & F	863	16,578	3,792	77%	19.2

THE RELEVANCE OF THE INTRINSIC OXIDATION RATE TO THE EVOLUTION OF POLLUTED DRAINAGE FROM A PYRITIC WASTE ROCK DUMP[1]

D. K. Gibson, G. Pantelis and A. I. M. Ritchie[2]

Abstract: We have developed a simple model of the oxidation of pyrite in a waste rock dump, in which the oxidation proceeds through the dump in a series of steps. The model is used to examine the sensitivity of the overall oxidation rate to the intrinsic oxidation rate (IOR) of the pyrite. For values of IOR below a critical value, the overall oxidation rate proceeds at a constant rate until all the pyrite is consumed. The rate is proportional to the IOR and the total time to oxidize the dump is inversely proportional to it. At the other end of the scale, for an infinitely high IOR, the overall oxidation rate decreases smoothly in time from a high value. The time for complete oxidation is the same as for the critical IOR value. There remains a range of intermediate IOR values, for which the overall oxidation rate decreases in a stepwise manner. This range provides the transition from the critical IOR value (effectively one step) to the infinite IOR case (effectively an infinite number of steps). With this model the time dependence of the overall oxidation rate approaches the rate calculated for infinite IOR at quite modest values of IOR. The simple model is supported by a finite-difference calculation which gives the evolution of sulfate in the dump drainage, as well as the overall oxidation rate.

Additional Key Words: pyrite oxidation, acid mine drainage, mathematical model.

Introduction

Mathematical modeling of the progress of oxidation in waste rock dumps containing pyritic material is a powerful aid to understanding and predicting the overall behavior of the process. A basic parameter required for a model is the rate of oxygen consumption at each point in the dump. We have called this rate the intrinsic oxidation rate or IOR. This is the rate at which the reaction will proceed in that particular waste rock, under the physical, chemical, and microbiological conditions that apply. It might be expected that the IOR would be a critical factor in the overall dump oxidation rate. Our aim is to examine this expectation. We need a suitable mathematical model to achieve this aim, and therefore identification of such a model becomes a secondary aim of this paper.

There have been two main approaches in treating the IOR in dump oxidation models. Ritchie (1977) based a simple one dimensional model on the assumption that the oxidation rate is very fast compared with the rates of oxygen diffusion (the Simple Heap Model). Oxidation therefore occurs in an infinitely thin reaction front, which proceeds downwards through the dump as the pyrite is consumed. Using methods developed by Crank (1956), Ritchie derived a useful set of formulae describing the gross features of dump oxidation. However, clearly this model cannot be used for the present work as the parameter we wish to vary, the IOR, is assumed to be infinitely fast.

In the other class of model the aim is to treat the IOR more realistically by various means (Cathles and Schlitt, 1980, Davis and Ritchie, 1986 and 1987, Jaynes et al. 1984, Pantelis and Ritchie, 1992). The IOR has been described both by the shrinking core model and by various empirical expressions; both approaches require numerical solution. This class of model of oxidation in dumps has proved very successful. The fact that numerical methods are required for their solution permits two dimensional treatment and allows the inclusion of features such as gas convection and dump inhomogeneity. This degree of complexity is not appropriate to our present aim. We will neglect convection,

---

[1]Paper presented at the International Land Reclamation and Acid Mine Drainage Conference and the Third International Conference on the Abatement of Acidic Drainage, Pittsburgh, PA, April 24-29, 1994.

[2]David Gibson, Principal Research Scientist, Garry Pantelis, Senior Research Scientist, and Ian Ritchie, Senior Principal Research Scientist, Australian Nuclear Science and Technology Organisation, Lucas Heights, Australia.

which is limited to the edges of waste dumps, since in typical waste rock dumps the edges are a small fraction of the total dump volume (Harries and Ritchie, 1990). A one dimensional model is therefore adequate, and the insight gained from an analytical model is attractive.

In this paper we develop a model similar to Ritchie's Simple Heap Model, but which is not limited to an infinitely high IOR. In this model it is assumed that the IOR has a finite value wherever both oxygen and pyrite have concentrations greater than zero. Simple formulae are derived that give insight into the basic features of dump oxidation. We apply these formulae to explore the significance of the IOR to overall dump oxidation rates. Finally a simple one dimensional numerical model is used to support the results of the analytical model. The numerical model includes the rate of water infiltration and is used to find the behavior of pollutant load in the dump drainage.

Constant Intrinsic Oxidation Rate Model

A simple assumption for the basis of a dump oxidation model is that the IOR is independent of oxygen and sulfur concentrations, provided that neither is zero. This assumption has some experimental support, as it has been shown in laboratory measurements (Liu et al. 1987) that the rate is constant for oxygen concentrations from 20% (atmospheric) to 1% to 2%. Only below about 1% or so does the rate begin to drop significantly. Similar results, under certain circumstances, have been reported by Hammack and Watzlaf (1990).

Assuming the dump is homogeneous, with diffusion coefficient D, it can be shown that oxygen will initially penetrate a distance x_1, given by

$$\Delta x_1 = \sqrt{\frac{2DC_o}{S'}} \tag{1}$$

where C_o is the atmospheric oxygen concentration and S' is the IOR.

In accordance with the constant IOR model, this zone will oxidize uniformly throughout until all the sulfur is used. Thereupon the zone becomes inert and the oxygen diffuses through it to form a new oxidation zone below. It is easy to show that, for the range of IOR of interest here, the time taken for the oxygen to attain this new pseudo-steady state is short compared with the time taken to oxidize a zone; the transition time is therefore ignored in this model, and the oxidation proceeds in a series of steps. This approximation is backed up by the results of the numerical modeling that appear below.

The thickness of the subsequent steps progressively reduces owing to the increasing thickness of inert material above. The following general expression can be derived for the thickness of the nth zone:

$$\Delta x_n = \sqrt{\frac{2C_oD}{S'}}\left[\sqrt{n}-\sqrt{n-1}\right] . \tag{2}$$

The time, t_s, for the pyrite in a zone to oxidize fully is given by the ratio of the density of sulfur, ρ_{rs}, to the IOR, with a stoichiometric factor, ε, which relates the consumption of sulfur to the consumption of oxygen. The time for each step to oxidize is the same for all steps and is given by

$$t_s = \frac{\varepsilon\rho_{rs}}{S'} \tag{3}$$

The overall oxidation rate is given by

$$R = S'\Delta x_n = \sqrt{2S'C_oD}\left[\sqrt{n}-\sqrt{n-1}\right] \tag{4}$$

and the position of the nth step by

$$x_n = \sqrt{n}\sqrt{2C_0D/S'} \,. \tag{5}$$

The dump height is denoted by L; then if $x_n < L$ and $x_{n+1} > L$ the oxidation within the dump takes n+1 steps; the time to oxidize the dump, t_d, is

$$t_d = (n+1)\,t_s = (n+1)\frac{\varepsilon\rho_{rs}}{S'} \,. \tag{6}$$

Relationship between IOR and overall dump oxidation rate

We now use these formulae to look at how the IOR affects the overall oxidation rate of the dump.

Low IOR

For a sufficiently low value of IOR the thickness of the first zone will be limited by the dump height, L. In this case the dump will oxidize in one step and the overall oxidation rate will be proportional to the IOR. The critical value of IOR for this behavior is easy to establish by putting $x_1=L$ into equation 1. In terms of a nondimensional IOR (S), the criterion for the dump oxidation rate to be proportional to the value of the IOR is

$$S = \frac{S'L^2}{C_oD} < 2 \,. \tag{7}$$

The time for complete oxidation will obviously be inversely proportional to the IOR. For the critical value S=2 the time to oxidize all the pyrite in the dump is

$$t_d^0 = \frac{\varepsilon\rho_{rs}L^2}{2C_oD} \,. \tag{8}$$

High IOR

The thickness of the steps is small for large IOR (equation 2) and the time to oxidize each step is small (equation 3). Therefore after a relatively short time, with a small fraction of the dump oxidized, the value of n will be large. In equation 4 we therefore approximate $\sqrt{n}-\sqrt{n-1} = 1/2\sqrt{n}$ and use the relationship implied in equation 6 that $n = S't/\varepsilon\rho_{rs}$ to give the overall oxidation rate for high IOR as

$$R = \sqrt{\frac{C_oD\varepsilon\rho_{rs}}{2t}} \tag{9}$$

Thus, for high values of IOR, the overall oxidation rate is independent of IOR. This formula is the same as derived by Ritchie's Simple Heap Model referred to above. The time to oxidize all the material in the dump is the same as for the critical value S=2, given in equation 8.

Intermediate IOR

The strength of the Step Model is that it can be used to examine the cases between the high and low IOR limit. In particular it can be used to quantify the value of 'high IOR'. The intermediate IOR case is of practical interest, as for many dumps the values of D and the IOR are such that the thickness of the oxidation zone is 5m or so, and the number of oxidation steps is around 3 or 4. The time duration of all steps is the same, given by equation 3 and the overall oxidation rate remains constant for the duration of a step. The time to oxidize all the material in the dump oscillates between two limits with varying IOR, the lower limit being the critical value t_d^0 (from equation 8) and the upper limit being twice the lower; this oscillatory behavior arises because a step whose thickness is limited by dump bottom takes as long to oxidize as a full step. The time to totally oxidize the pyrite in the dump returns to the value given in equation 8 for all cases where the number of full length steps is a integer.

The behavior of the overall oxidation rate with time is shown in figure 1 for three values of IOR. The magnitude of the overall oxidation rate is given by equation 4 and the time metric by equation 3. The parameters used for the calculation are shown in table 1. It can be seen that over the long term the general behavior for the three cases is similar. For practical purposes, for the dump parameters used here, it is clear that if the value of the IOR is 5×10^{-8} $kg(O_2)/m^3/s$ or greater it is not necessary to know its value to describe the evolution of overall dump oxidation rates, and as shown below, pollution load. With an IOR of 10^{-8} $kg(O_2)/m^3/s$, however, the different step sizes do make a very significant difference to the overall oxidation rate over the first 80 years. The figure also illustrates the variation in the time for oxidation of all the pyrite with different IOR values, due to the interaction of the step size with the dump height.

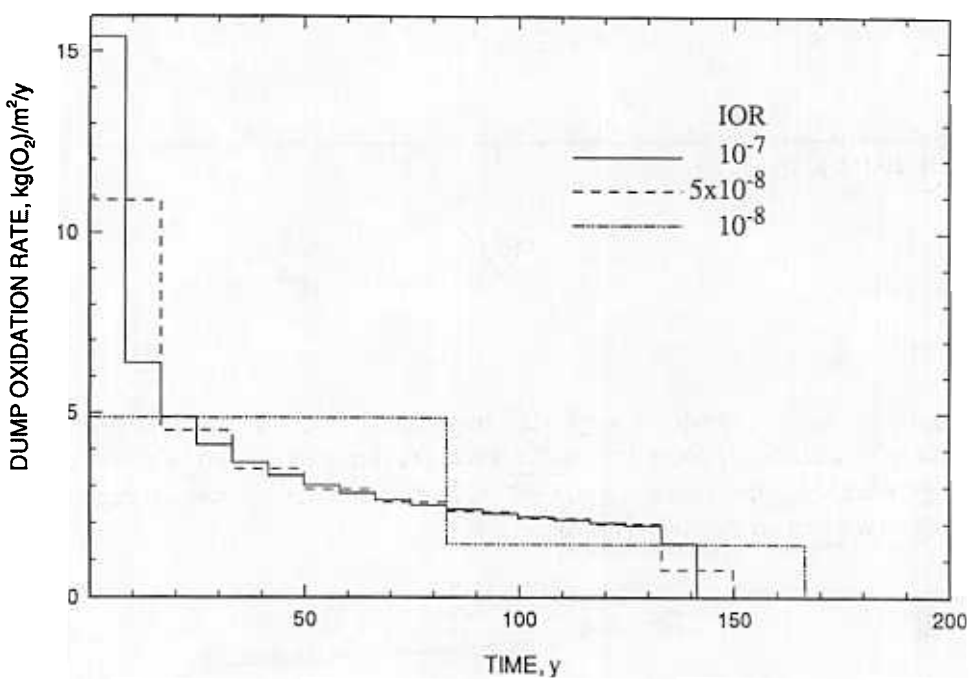

Figure 1. Overall dump oxidation rate as a function of time calculated by step model for three values of IOR.

The timescales for the oxidation of single steps can be appreciated from figure 1, namely in the range from 10 to 80 years. The time for oxidation of all the pyrite in the dump is about 150 years.

Table 1. Parameters used for dump model

Dump height L (m).....	20
Stoichiometric factor ε (mass O_2/mass S).....	1.75
Stoichiometric factor (mass SO_4/mass O_2).....	1.14
Bulk density of oxidizable sulfur ρ_{rs}(kg/m^3).....	15
Oxygen concentration in atmosphere C_0 (kg /m^3)....	0.265
Oxygen diffusion coefficient in dump D (m^2/s).....	4.5×10^{-6}
Water infiltration rate (m/y).....	0.5
Volumetric water content of dump material.....	0.1
Intrinsic oxidation rate S′ (kg(O_2)/m^3/s).....	10^{-8} - 10^{-7}

Time Evolution of Pollutants in Drainage

With pyrite oxidation we now include the transport of sulfate, the principal pollutant formed by oxidation, by water infiltrating the dump. We use a finite difference code to solve the time dependent gas diffusion equation and the pollutant transport equations. The water is assumed to move at a uniform rate vertically carrying sulfate from the point of production to the base. Two examples are shown in figure 2.

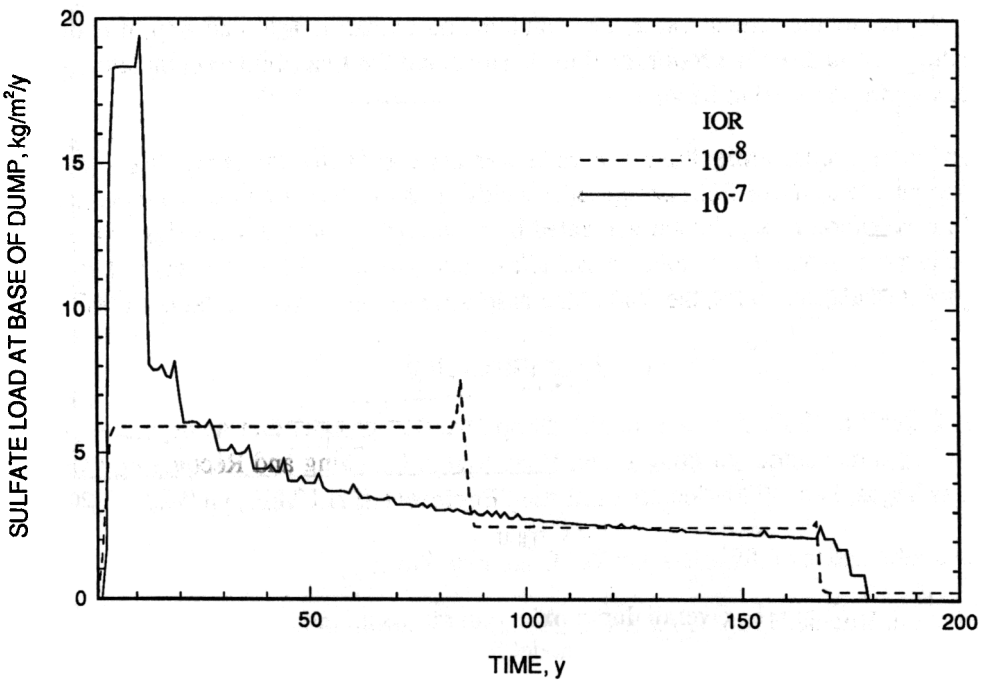

Figure 2. Time dependence of sulfate load at the base of the dump, calculated for two values of IOR

The parameters used are the same as for the analytical model and are shown in table 1. The time evolution of the pollution load at the dump base follows the oxidation rates calculated in the previous section quite closely, allowing for the time delays caused by the relatively slow water velocity.

Small spikes appear on the load curves at the end of each step. These occur because at the completion of oxidation of a step the oxygen quickly penetrates the material below and sulfate generation commences there. This sulfate is added to that in the water which is still proceeding downwards from the previous zone. This result is a consequence of the simplifying assumptions built into the model, namely the step function behavior of the IOR with both oxygen and sulfur concentration and the homogeneity in the dump composition that a one dimensional model entails. Clearly in practice, where these idealizations would not apply, one would not expect to see these spikes.

Conclusions

A simple analytical model for the oxidation of pyrite in waste rock dumps has been developed, which allows the question of the effect of the intrinsic oxidation rate on overall oxidation within the dump to be examined. The oxidation takes place in zones that become progressively deeper as the material above becomes inert after complete oxidation. The thickness of the zones is the crucial parameter. For low values of IOR the zones are thick and the overall oxidation rate and the pollutant load are comparatively low and remain constant for long periods of time. As the IOR increases, the thickness of the zones decrease and the overall oxidation rate is initially high, but decreases rapidly over the period of 10 - 20 years. Once the IOR is high enough to cause oxidation to take place in say 10 steps its value ceases to be very significant, as the difference between oxidizing the dump in 10 steps and an infinite number is not great.

The paper relates to waste rock dumps that are commonly encountered in mining operations, namely about 20m high, with lateral dimensions at least 10 times greater than this. The material has a diffusion coefficient for oxygen of the order of 5×10^{-6} m^2/s. If the IOR is greater than about 5×10^{-8} for this range of dump parameters, its value becomes unimportant to the time progression of the overall dump oxidation rate or the pollution load in the drainage. The simple oxidation model used here shows that it is only at low values of IOR that its value has practical importance. For values below the critical value, for which the dump oxidizes in one step, it is of crucial importance, as the overall oxidation rate is directly proportional to its value and the total time to completely oxidize all the pyrite in the dump is inversely proportional to its value.

A simple one dimensional finite difference code was used to justify the approximation that the time for the oxygen concentration profile to move from one pseudo-steady state to another could be ignored. This model was also used to show the time evolution of a pollutant generated by pyrite oxidation and appearing at the base of the dump as a result of water transport. Apart from some time delays and spikes in the load caused by the overlapping of pollutants from adjacent oxidation zones, the load at the base follows the overall oxidation rate closely.

Literature Cited

Cathles, L. and W. J. Schlitt. 1980. A model of the dump leaching process that incorporates oxygen balance, heat balance, and two-dimensional air convection. Proc. Symp. Leaching and Recovering Copper from As-Mined Materials. Las Vegas, Feb. 1980. Society of Mining Engineers of A.I.M.E., pp 9-27

Crank, J. 1956. The mathematics of diffusion. Oxford Clarendon Press

Davis, G. B. and A. I. M. Ritchie. 1986. A model of oxidation in pyritic mine wastes - I. Equations and approximate solutions. Appl. Math. Model. 10:314-322.

Davis, G. B. and A. I. M. Ritchie. 1987. A model of oxidation in pyritic mine wastes - II. Import of particle size distribution. Appl. Math. Model. 11:417-422.

Hammack, R. W. and G. R. Watzlaf. 1990. The effect of oxygen on pyrite oxidation. p. 257-264. In Proceedings of the Mining and Reclamation Conference. (Charleston, WV, April 23-26, 1990).

Harries J. R. and A. I. M. Ritchie. 1990. Australian experience in controlling acid generation in mine waste rock dumps. GAC-MAC Conference, Acid Mine Drainage - Designing for Closure, Vancouver. May 16-18.

Jaynes, D. B., A. S. Rogowski and H. B. Pionke. 1984 Acid mine drainage from reclaimed strip mines. 1. Model description. Water resources Research 20:233-242

Liu, M.S., R.M.R. Branion and D.W. Duncan, 1987. Oxygen transfer to Thiobacillus cultures. In Biohydrometallurgy. Proc. Int. Symp. Warwick. (eds.), P.R.Norris and D.P.Kelly.

Pantelis, G. and A. I. M. Ritchie.1992. Rate-limiting factors in dump leaching of pyritic ores. Appl.Math.Model. 16:553-559.

Ritchie, A.I.M. 1977. Heap leaching; a gas diffusion rate-limited model. AAEC/E429

MODELING OF A RECLAIMED SURFACE COAL MINE SPOIL AQUIFER USING MODFLOW[1]

Jay W. Hawkins[2]

Abstract: Improved prediction of the postmining water levels in mine spoil can be useful in preventing future acid mine drainage production. Using a computer model (MODFLOW), a reclaimed surface mine aquifer under steady-state conditions was simulated. To calibrate the hydrologic model, the hydraulic conductivity of the spoil had to be increased by as much as 200 times above values empirically determined by field tests. These modifications were justified by the presence of large open voids and conduits in the spoil. Simulated recharge to the spoil was primarily from fracture zones in adjacent unmined areas. Recharge from precipitation was established at a low level (10% of the mean precipitation), because of mining-induced changes to the soil structure. The steady-state calibrated model exhibited head levels 8.7% above and a discharge rate that was within 5.7% of measured field conditions. These results indicate that MODFLOW can be successfully used to simulate the ground water table and discharge rates of mine spoil after reclamation. Using the calibrated model, a constant-discharge test was applied to the aquifer. The model did not accurately simulate the results of an aquifer test performed in the field. The heterogeneous nature of the mine spoil is believed to facilitate unquantified anisotropic ground water flow, which was not accounted for in the simulations. However, the steady-state simulation with MODFLOW proved to be useful in modeling spoil under variable site conditions.

Additional Key Words: mine spoil aquifer, ground water modeling

Introduction

The unconsolidated nature of mine spoil has lead many hydrologists to assume that it behaves similarly to a conventional porous medium flow system. Under this assumption, ground water flow is intergranular, laminar, and subject to the limitations of Darcy's law. Caruccio and others (1984) suggested that ground water flows primarily in a pseudokarst manner, through large voids or conduits within the mine spoil. Groenewold and Bailey (1979) described the formation of such voids within mine spoil by piping and differential settling. Void formation is further facilitated by backfilling and other reclamation processes. Large spoil blocks tend to roll to the base of spoil ridges, while smaller particles tend to remain on the ridge top and sides (Rehm et al. 1980). This sorting action creates extreme aquifer heterogeneities in the form of linear high-permeability zones, parallel to spoil ridges, laterally bounded by lower permeability material. The orientation and magnitude of the void areas are dependent on overburden lithology, mining equipment used, surface mining method, direction of mining, and age of reclamation (Hawkins and Aljoe 1991; Aljoe and Hawkins 1992).

Aquifer testing performed by Hawkins and Aljoe (1991) confirmed the existence of large voids in mine spoil. They observed that pseudokarstic characteristics predominate when the aquifer is stressed, during aquifer testing or extreme recharge events. However, aquifer tests (slug, constant-discharge, and tracer tests) indicate that although the voids are common in spoil, ground water flow between voids and flow from the voids to surface discharge points is primarily laminar and diffuse, typical of a porous medium. Under steady-state conditions, the lower permeability of the porous-media material between voids is the primary controller of the volume and velocity of ground water moving through the spoil aquifer. Therefore, under steady-state conditions the aquifer as a whole behaves primarily as a porous medium.

Aquifer testing in mine spoil can be problematic in the sense that most aquifer tests are a hydrologic stress on the spoil aquifer. The methodology and formulae used in the calculation of aquifer parameters

---

[1]Paper presented at the International Land Reclamation and Mine Drainage Conference and the Third International Conference on the Abatement of Acidic Drainage, Pittsburgh, PA, April 24-29, 1994.

[2]Jay W. Hawkins, Hydrologist, U.S. Department of the Interior, Bureau of Mines, Pittsburgh, PA, USA

assume that flow is laminar, which meets the constraints of Darcy's law (Aljoe and Hawkins 1992). However, stresses caused by testing can create rapid, turbulent, nondarcian ground water flow. These possible inconsistencies should be considered when using field-generated aquifer data for modeling ground water flow in mine spoil. The primary goals of this study are to acquaint the ground water modelers with the problems in simulating mine spoil, and to give ground water professionals who work with surface mines an introduction to the problems of modeling surface mine spoil aquifers.

Site Background

The modeled site is a 3.2 ha (8 acre) parcel of a surface coal mine in central West Virginia (fig. 1). The lower and middle Kittanning coals were mined on this site between 1976 and 1977. The site was backfilled to final grade by December 1977. The modeled portion of the site was terrace backfilled with a steep grade existing at the final highwall. The central portion of the site slopes gently westward to the final highwall. A drainage ditch was installed on the site to eliminate surface water impoundment. Spoil was placed downslope below the original coal outcrop, covering unmined areas (outslope area). At the base of the spoil outslope, a "toe-of-spoil" discharge developed, which is the main outflow point for the study area.

Drill hole logs from adjacent unmined areas and existing highwall exposures illustrate that the strata are laterally continuous throughout the study area. The lower Kittanning coal is 1.2 m thick and underlain by a hard-gray claystone. The interburden between the middle and lower Kittanning coals is 4.3 m of a carbonaceous gray shale. The middle Kittanning coal is 1.4 m thick. The strata overlying the middle Kittanning coal are a 0.6 m thick carbonaceous shale and a gray sandstone averaging 11.6 m thick.

The strata at the site dip gently (less than 2%) toward the northwest. Rock exposures around the site illustrate that joint and fracture zones are common in this area. There are two principal orientations of these fractures, between N22E and N45E and between N10W and N38W. The fractures are vertical or nearly vertical and are open up to 3 cm. A prominent fracture zone (1-2 m wide) on the northern edge of the site was identified in the field. This fracture zone was shown to be a major recharge source for the site (Hawkins and Aljoe 1990). In the Appalachian region, ground water flows primarily through fractures in undisturbed strata. The fractures are created from structural stresses and from stress release caused by the removal of the overlying materials by erosion (Wyrick and Borchers 1981). During the computer simulations, other fractured areas in the buried highwall inferred from field data (e.g., water levels and tracer tests) were introduced into the model.

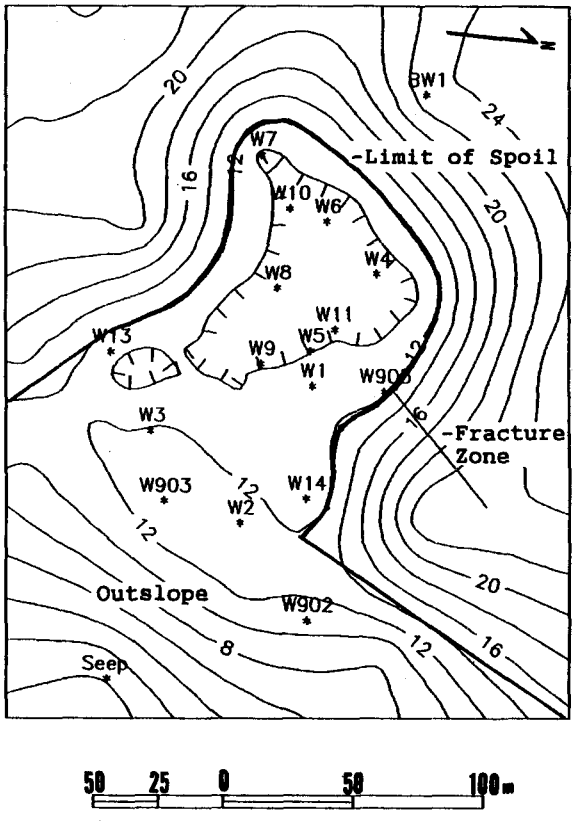

Figure 1. Topographic map of the study site. Contour interval equals 2 m.

Initially, 15 monitoring wells were installed at the site (fig. 1). One of the wells (BW-1) was drilled through undisturbed strata above the final highwall, and the remaining wells were drilled into the backfill. However, well W12 was too shallow to be of use. In 1990, three additional spoil wells (W902, W903, and W905) were installed. Water levels in the wells were monitored for several years. Hydraulic testing of the spoil (slug injection and/or withdrawal) originally was conducted to characterize geohydrology of the site.

Water level monitoring and aquifer testing were used to set up and calibrate the model. Monitoring of the site indicated that the hydrologic conditions, outflow and head levels, on July 26, 1989, were representative of steady-state conditions. No precipitation had occurred for several weeks prior to this date. Steady-state head levels for the spoil are exhibited by figure 2.

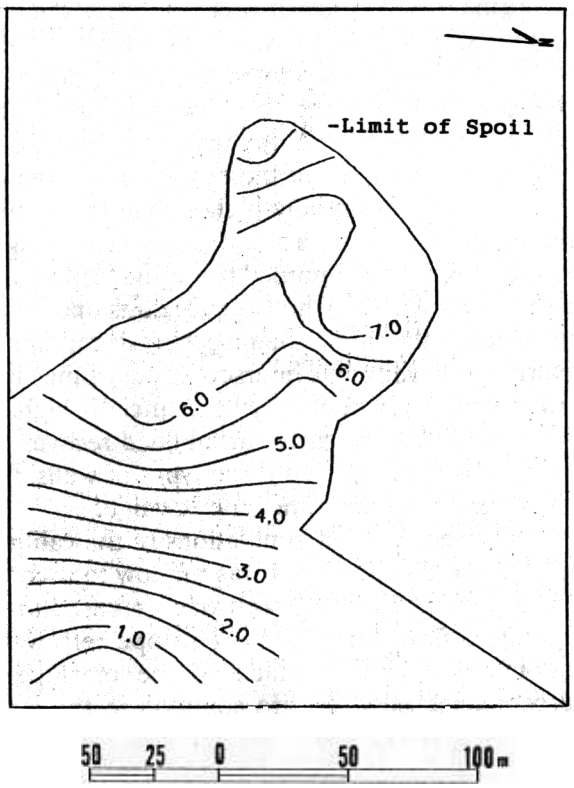

Figure 2. Water table contour map of the spoil for steady-state conditions (July 26, 1989). Contour interval equals 0.5 m.

Model Setup and Calibration

The ground water model selected for this work was MODFLOW, which was developed by the U.S. Geological Survey (McDonald and Harbaugh 1988). MODFLOW is a three-dimensional finite-difference computer model that is composed of a main program and a series of subroutine modules. Modules are created to handle specific tasks of the hydrologic system, such as setting boundary conditions, initial heads, surficial recharge and discharge, and locating pumping or injection wells. MODFLOW permits the modeler to select only the modules required for each trial run and allows new modules to be created and added independently, without altering the existing modules.

At the start of modeling, it was determined that the model set up and data input had to be simplified from the conceptual characterization. A number of simplifying assumptions were made concerning the ground water flow characteristics: (1) The overall flow system was assumed to be a porous-medium type under steady-state conditions; (2) the hydraulic conductivity was assumed to be relatively consistent throughout the spoil; (3) all the outflow was assumed to exit through the known discharge point; and (4) most recharge was assumed to be from adjacent unmined areas. Analysis of field data collected indicates that these assumptions are valid. The objective of the model calibration was to simulate the heads and outflow within 10% of field conditions. Considering the known problems in characterizing spoil, this level of closure was assumed to be an adequate site approximation.

The spoil was simulated as an unconfined aquifer; therefore, the upper bound was unspecified and the cell thickness was variable, corresponding to changes in head. A confining layer (aquitard) simulated the stratum underlying the spoil. Any leakage through this layer was assumed to be insignificant. The elevation of the underlying layer cells was based on drill hole data. The model was set up as a 180 x 240 m horizontal grid divided into cells of 15 m^2 in two layers. The cells representing spoil were designated as variable-head cells. The cells located in unmined areas, where the highwall borders the spoil, were designated as constant-head cells, because of the limited fluctuation observed there. Cells in unmined areas above the highwall were designated as no-flow cells, because limited data exist for this area, the cells are outside the area of interest, and it is thought that they will not affect the modeling of the spoil. The discharge point (seep) was initially designated a constant-head cell.

The initial head levels for the spoil wells were set at 6.56 m above the discharge (datum), which is the estimated mean for the wells in the backfilled area under steady-state conditions (July 26, 1989). The head for the highwall cells (8.2 m) was determined by extrapolation from well BW-1 (in the unmined area) to the two nearest spoil wells (wells 6 and 7), because BW-1 was too far from the highwall-spoil interface to represent the water level at that point. The initial head for the seep (datum) was 0.01 (fig. 1).

The initial spoil hydraulic conductivity (K) value (0.22733 m/d) was the geometric average, assuming a lognormal distribution of K (Freeze and Cherry 1979), for the estimated values determined from the aquifer (slug) tests. The initial K value (0.03855 m/d) that was used for highwall cells was obtained from testing well BW-1. These values had to be modified (increased) several times during the calibration phase of the modeling to be able to match the known heads and outflow for steady-state conditions. Hawkins and Aljoe (1990) observed that the bulk K for spoil may be at least an order of magnitude higher than the geometric average for the wells. Because of the existence of large voids and conduits in the spoil, the effective K for the aquifer as a whole is substantially higher than the values determined by individual slug tests. Slug tests, by design, estimate the K for only a small area surrounding the well, not necessarily reflecting an average for the aquifer. Therefore, K values obtained from slug testing of wells that do not intersect voids may not necessarily represent the spoil as a whole. The K of conduits and large voids normally cannot be tested using conventional aquifer tests because the large openings permit rapid, turbulent nondarcian flow. Therefore, the results of slug tests performed on wells that intersect conduits may be in error. Given the darcian flow equation used to determine K, the calculated values may be artificially high, if the rapid displacement recovery can be recorded (Hawkins 1993). However, the early partial head recovery is often too rapid to be measured, but is followed by a slower darcian-type recovery. In these types of wells, the K is estimated from the later darcian-type recovery, which tends to underestimate the true K value.

For the first few simulations of the calibration phase, ground water tended to impound in the backfill. The K at the discharge cell was too low to accommodate the volume of water that was known to flow through it. The K of the discharge cell was increased to 1,000 m/d to allow higher flow through that cell. To increase the total outflow, the K of the outslope cells was raised by a factor of 10 to 2.272 m/d. No wells exist in this area, therefore the K value of the outslope is conjecture. However, field observations indicate that interconnected conduits are common in the outslope and that these conduits strongly influence the ground water flow (Hawkins and Aljoe 1990).

For the initial model-calibration runs, a surface recharge package was used. Based on experience, the recharge rate was established at 10% of the mean annual precipitation rate. After several runs, it was determined that the package was complicating the model and may not be required. During early runs using the recharge package, the output head levels and outflow were higher than measured values. The model results were improved when the majority of the aquifer recharge occurred laterally from unmined areas. Razem (1983) observed that following reclamation, surface recharge is significantly lower for spoil than for adjacent unmined areas, because of the lack of soil structure, high soil compaction, and low vegetative growth for mine cover material.

The relative importance of lateral recharge from unmined areas of this site was empirically determined during monitoring and testing (Hawkins and Aljoe 1990, 1991). Ground water enters the spoil primarily through fractures exposed in the buried highwall. Once the model simulations closed in on field conditions, the recharge package was reintroduced. It is not assumed that surface recharge does not occur, just that the rate is 10% of what occurs at unmined sites.

After the first few model calibration runs, the discharge cell was changed from a constant-head to a variable-head cell to accommodate changes in the discharge elevation with higher flow rates. With the increased k, the head remained consistently low (0.001 m) and the heads and the flow neared field conditions. However, this change caused some of the cells in the center of the backfill to dry up. To alleviate this problem, the K of these cells was increased by a factor of 10 and the K of the discharge cell was decreased to 100 m/d.

An injection well (module) was added at the northern fracture zone cell (fig. 1) to simulate the inflow from this recharge source. The injection rate (17.4 m^3/d) was set at one fifth the average discharge rate, based on experience with the site. At this rate, the injection well cell tended to dry up. The K value for the center spoil cells was again increased by 10. The well cell continued to dry up.

Rather than force water into the system via an injection well, it was decided that the model would work better if the outflow was better defined and controlled. Therefore, the well package was eliminated and a general-head boundary was created for the discharge cell. The general-head boundary package for the discharge was assigned a head of 0.01 m and a conductance of 5,000. A high conductivity value was used to

ensure an adequate discharge rate. Conductance was not changed for the remainder of the model calibration. The initial head was later increased to 0.1 m to accommodate higher outflows.

These changes greatly improved the head simulation. However, the outflow was still too low. Therefore, the outslope K of the outslope wells was increased again by a factor of 10 to 22.73 m/d, based on the assumption that the outslope contained numerous highly conductive conduits. This change caused several spoil cells to dry up. The K of the outslope cells was reduced to 5 and then finally to 3 m/d. This brought the heads in the backfill to near actual levels, but the flow was almost a factor of 18 too low. At this point during the modeling, the recharge package was temporarily eliminated from the model. To account for the removal of the recharge, the K values for the highwall cells were increased to 0.3855 m/d. Because of unaccounted discrete fractures in the highwall, it is reasonable to assume that the overall K of the highwall rock is, in fact, significantly higher than the K of BW-1, which is not representative of fractured rock. The K for the northern fracture zone cell was also increased by two orders of magnitude, to 3.855 m/day.

Higher K values all along the length of the highwall yielded heads substantially above field conditions and outflow nearer the actual rate. Therefore, the K values for portions of the highwall where no fractures were known or could be inferred from the field observations and data were greatly reduced, by a factor of 2,000. This K value was based on the upper range of values for sandstone (Freeze and Cherry 1979). Where fracture zones were known to exist or were inferred from field data, the K was maintained at a higher level. For example, the K values were set at 3.855 m/d for an inferred fracture zone along the western edge of the highwall to augment the recharge from the northern fracture zone.

These model refinements brought the head levels and the discharge rate to near measured levels. Heads in the central spoil zone wells averaged 16.7% above the steady-state field values for 1989. The discharge flow was approximately 68% below the measured rate. The heads for the individual wells for the preliminary model are exhibited in table 1. Only wells that were screened in spoil to the pit floor and intersected the saturated zone were included. Wells W902, W903, and W905 were excluded because they were not installed until after 1989.

At this point, preliminary modeled heads were nearing field conditions. However, to improve simulated head values and increase the outflow, additional adjustments were made to the model input data. At this point, the recharge package was reintroduced to the model. Based on experience and trial and error, the recharge rate was set at 10% of the annual average precipitation, although this was below the anticipated recharge rate for unmined conditions.

Hawkins and Aljoe (1990) observed extreme differences in the K values for the wells in the interior spoil zone. A zone of high K was located in the center of the interior spoil zone, surrounding wells W3, W8, W9, and W13 (fig. 1). For this series of model runs, the K for this center area was based on the geometric average of these wells. A second area of elevated K values represents the spoil cells adjacent to the outslope area based on the geometric average of wells W2, W902, and W903. The K values for these two areas were at first established at the geometric average for each group of wells. Later, to

Table 1.–Summary of actual and modeled hydrologic data for steady-state conditions. Heads are in meters above datum (seep level), and flow is in liters per minute.

Well	Heads		
	July 26 1989	Preliminary model	Final model
1	5.35	7.93	7.22
3	6.10	7.37	6.62
4	7.46	8.13	7.52
5	5.80	7.99	6.83
6	6.59	8.13	7.59
7	8.21	8.17	8.28
8	6.37	8.00	6.86
9	6.13	7.83	6.87
10	6.96	8.12	7.33
11	7.44	8.05	7.39
13	6.41	7.81	6.66
Seep flow	62.10	20.10	58.50

lower the modeled heads and increase the flow, the values were increased by a factor of 10, and then 100 times the geometric average. The flow at this stage was about 2.5 times below the known outflow.

The K for the outslope was doubled, and the K of the discharge cell was increased by a factor of 20 in a continued effort to increase outflow. With these changes, the outflow was approximately one-half the measured flow rate, and the heads were similar to steady-state levels. To increase the outflow further, while not overly lowering the water level, the K for the entire site was multiplied by a factor of 2. This resulted in the final calibrated model.

The final steady-state model configuration is illustrated by figure 3. The actual steady-state head levels in the wells averaged 8.7% above the modeled head values with a range from 0.7% (well W11) to 34.9% (well W1). The root-mean-square error (standard error) for the calibrated model was 0.79 m. During the modeling, well W1 was consistently the most difficult well to match to the actual level. This may be related to the proximity of the fracture zone, which may impact the spoil ground water levels by rapid and high-volume recharge. Extreme water level differences are not unexpected in a pseudokarst system. The discharge rate of the final model was within 6% (5.7%) of the actual discharge rate (table 1). The head-contour map of the calibrated model (fig. 3) is very similar to actual site conditions (fig. 2). Additional calibration and refinement of the model may reduce the observed differences, but the possible improvement is not worth the required effort.

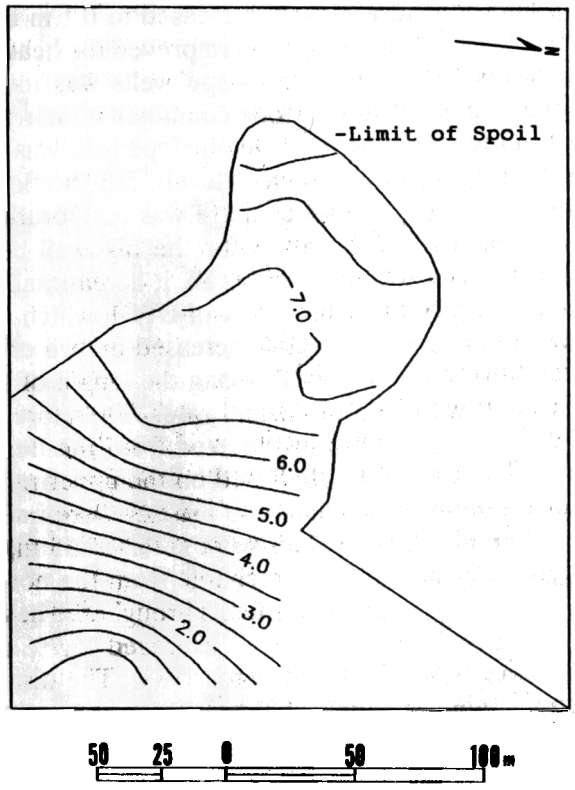

Figure 3. Final steady-state model configuration. Contour interval equals 0.5 m.

Stress Simulation

Once the steady-state model was satisfactorily calibrated, a simulated constant-discharge test was performed. This test was a simulation of an actual field test performed on June 28, 1990, when the head levels and hydrologic conditions were very similar to 1989 steady-state conditions. Well W6 was pumped at a rate of 6 l/min for 2 hours. The pumping rate was established based on the K determined from the slug test and the saturated thickness of the aquifer at well W6. Wells W8 and W10 were used as monitoring wells. At the end of the constant-discharge test performed in the field, drawdown for these wells was 0.05 and 0.04 m, respectively.

For the pumping test simulations, the initial heads were reset to the levels of the final heads from the steady-state simulation, and a well module was introduced. A pumping well was simulated at the cell containing well 6 and was pumped at the same rate and for the same length of time as in the field test. Several stress model runs were performed with the storage coefficient (storativity) value being varied. None of a series of model results satisfactorily simulated the drawdowns observed under field conditions. Initially, the storativity for the spoil was established at 0.2, which was based on calculations of effective porosity determined from tracer tests performed at this site. No drawdowns were observed at wells 8 and 10 using this value. The storativity was subsequently lowered to 0.05. However, no drawdown was produced at the monitoring wells with this simulation. The storativity was then lowered to 0.01, which is the lowest value of the range for storativity (specific yield) for unconfined aquifers suggested by Freeze and Cherry (1979). At this level, well 8 exhibited no drawdown, while well 10 exhibited a decline of 0.02 m.

The differences between the field-observed drawdowns and those from the simulated constant-discharge tests appear to be caused by the highly heterogeneous nature of spoil and the associated anisotropic ground water flow. Estimation of drawdown from a constant-discharge test is based on assumptions that the aquifer is a homogeneous material, that there is isotropic ground water flow, and that the cone-of-depression created during a constant-discharge test is relatively symmetrical. If preferred flow paths of relatively high conductivity exist in the spoil, the cone-of-depression will elongate in those directions. Monitoring wells not located along these elongation directions may exhibit lower drawdowns than predicted. However, monitoring wells located along these high conductivity zones may exhibit more drawdown than predicted.

The head differences may also be related to the potential incompatibility of the model and the ground water flow characteristics. Hawkins and Aljoe (1990) observed that under transient conditions or when a stress is applied, a spoil aquifer tends to exhibit pseudokarstic (nondarcian) characteristics. Pseudokarstic ground water flow is characterized by turbulent flow through voids or conduits. However, MODFLOW assumes ground water flow is laminar (darcian). The stress to the aquifer created by the constant-discharge test may have induced pseudokarstic ground water flow conditions in the area surrounding the pumping well, so that MODFLOW becomes incompatible to the site.

The lack of the model to simulate the constant-discharge test could also be related to the mean-root-error masking the drawdown. The mean-root-error is greater than the drawdowns observed during the field test. Therefore, some of the drawdown could be lost or hidden by lack of a closer fit during the calibration of the model.

Summary and Conclusions

Based on the modeling results, a mine spoil aquifer can be simulated for steady-state conditions using MODFLOW. The initial model setup was greatly simplified from known field conditions. For modeling steady-state conditions, the pseudokarst characteristics of mine spoil must be subordinate to the porous media characteristics. This is supported by aquifer testing and water table monitoring data. For calibration of the model, the spoil was divided into zones of equal hydraulic conductivity based on the geometric average of the wells within that portion of the site. To obtain a sufficient head and outflow match, the hydraulic conductivity determined from aquifer tests had to be increased by one to two orders of magnitude for spoil areas, a majority of the recharge was modeled flowing laterally from adjacent areas, and the recharge from precipitation was established at a rate well below conditions for unmined areas (10% of the annual precipitation rate). The K of the outslope area cells, although unknown, was set at a rate higher than that of the interior spoil cells. This increase in K was based on field observations of a network of interconnected voids and conduits in the outslope.

The steady-state model did not adequately simulate transient conditions of a constant-discharge test. Under conditions of stress, pseudokarst characteristics become more prominent and spoil heterogeneities are accentuated. The simulation, which was calibrated for steady-state conditions, did not simulate the anisotropic and nondarcian ground water flow through the spoil. MODFLOW can model anisotropic conditions. However, the magnitude and orientation of the anisotropies must be accurately known, which was not the case for this site. Because of difficulties in quantifying void hydraulic characteristics, it may not be possible to simulate a mine spoil aquifer under transient conditions using a steady-state model.

The results of the modeling effort indicate that many of the characteristics observed during field testing may not accurately represent the site. The modeling exercise also caused some rethinking and refinement of the original conceptual site characterization in terms of ground water flow and storage. To determine the widespread applicability of computer simulation of surface mine spoil aquifers, additional modeling and conceptual characterization are required. With improvements in spoil modeling, prediction of the postmining water table, ground water flow paths, and other hydrologic parameters prior to mining can be used to improve special handling of alkaline or acidic spoil and hydrologic engineering techniques, which may diminish or halt the production of AMD.

Literature Cited

Aljoe, W.W. and J.W. Hawkins. 1992. Application of aquifer testing in surface and underground coal mines. p. 541-555. In Proceedings, Focus Conference on Eastern Regional Ground Water Issues. Natl. Ground Water Assoc. Dublin, OH.

Caruccio, F.T., G. Geidel and R. Williams. 1984. Induced alkaline recharge zones to mitigate acidic seeps. p. 27-36. In 1984 Symposium of Surface Mining Hydrology, Sedimentology and Reclamation. Univ. KY.

Freeze, R.A. and J.A. Cherry. 1979. Groundwater. Prentice-Hall, Englewood Cliffs, NJ. 604 p.

Groenewold, G.H. and M.J. Bailey, 1979. Instability of contoured strip mine spoils--western North Dakota. p. 685-692 in M.K. Wali (ed.), Ecology and coal resource development.

Hawkins, J.W. 1993. Typical and atypical slug test responses observed in mine spoil. Society for Mining, Metallurgy, and Exploration, Transactions/Annual Bound Volume 1993, Littleton, CO. In press.

Hawkins, J.W. and W.W. Aljoe. 1990. Hydrologic characterization and modeling of a heterogeneous acid-producing surface coal mine spoil, Upshur County, West Virginia. p. 43-52. In Proceedings, 1990 National Symposium on Mining. Knoxville, TN, Univ. Ky.

Hawkins, J.W. and W.W. Aljoe. 1991. Hydrologic characteristics of a surface mine spoil aquifer. p. 47-68. In Proceedings, Second International Conference on the Abatement of Acidic Drainage. (Montreal, Canada, September 16-18, 1991).

McDonald, M.G. and A.W. Harbaugh. 1988. A modular three-dimensional finite-difference ground water flow model. U.S. Geol. Surv. Techniques of Water Resources Investigations TWI 6-A1.

Razem, A.C. 1983. Ground water hydrology and quality before and after strip mining of a small watershed in Jefferson County, Ohio. U.S. Geol. Surv. Water-Resources Inv. Rep. 83-4215. 39 p.

Rehm, B.W., G.H. Groenewold, and K.A. Morin. 1980. Hydraulic properties of coal and related materials, northern Great Plains. Groundwater. 18(6):551-561.

Wyrick, G.G. and J.W. Borchers. 1981. Hydrologic effects of stress-relief fracturing in an Appalachian valley. U.S. Geol. Surv. Water-Supply Paper 2177. 51 p.

NEW FUNCTIONAL POLYMERS AS SORBENTS FOR THE SELECTIVE RECOVERY OF TOXIC HEAVY METALS FROM ACID MINE DRAINAGE[1]

K. Lise Hubbard, Graham D. Darling, S. Ram Rao and James A. Finch[2]

Abstract: By a new synthetic technique, macroporous crosslinked polystyrene resin was functionalized with ligands containing sulfur, nitrogen, and/or oxygen atoms. Preliminary studies indicate that when added to a synthetic acid mine drainage (AMD) solution, some of these functional polymers were capable of selectively binding zinc without becoming "fouled" by iron. Elution of the loaded resins with acid to recover the zinc was also possible. The greatest selectivity for zinc was obtained with functional groups that contained only electronically "soft" nucleophilic centers such as sulfur and nitrogen, and not oxygen atoms, which are electronically "hard" (and prefer such "hard" electrophiles as magnesium, aluminum, or iron cations). The performance of some of these new materials exceeded that of the commercial ion-exchange resins tested with respect to capacity and selectivity.

Additional Key Words: ion-exchange resins, chelating resins, zinc, iron.

Introduction

Acid mine drainage poses a serious environmental problem (Ritcey 1989). The standard treatment, liming to neutralize the AMD and precipitate the metals, followed by disposal of the resultant sludge (MacDonald et al. 1989), does not enable metal recovery. Metal values are lost as metal hydroxides in the sludge, which is considered hazardous waste. A method enabling metal recovery would have the benefit of providing some revenue to offset the costs of treatment and disposal as well as decreasing the sludge volume and toxicity.

If toxic heavy metals could be selectively removed, the solution of remaining Fe^{+2}, Fe^{+3}, Al^{+3}, Mg^{+2} etc. could then be used as a source of ferric chloride and alum, which could then be used in municipal wastewater treatment. Untreated AMD has been used successfully as a coagulating agent in laboratory experiments (Rao et al. 1992).

It is possible to selectively extract metals of choice using ion-exchange or chelating resins. The present work is directed toward exploring the potential use of new polystyrene-based chelating resins for the selective and economical recovery of zinc from AMD. This preliminary work studied the uptakes of zinc, iron and magnesium, with the primary concern being selectivity for zinc over iron.

An ion-exchange resin consists of a chemically-inert polymer matrix, such as polystyrene ("Ps"), with a functional group attached to the polymer backbone. The functional group may be anionic, such as sulfonate, with a cationic counter-ion (e.g., $Ps—SO_3^{-}{}^{+}Na$), or cationic, such as a quaternary amine, with an anionic counter-ion (e.g., $Ps—CH_2NMe_3^{+}\ {}^{-}Cl$). It is the counter-ion that can be exchanged for ions of like charge in solution. Being quite unselective, the application of ion-exchange resins has been limited to the bulk removal of all dissolved metals. A spent resin would be regenerated by eluting off the accumulated metals, using solutions of acids (e.g., hydrochloric or sulfuric), salts (e.g., brine), or soluble complexing agents (e.g., EDTA (ethylenediaminetetraacetic acid), and DTPA (diethylenetriaminepentaacetic acid)), to recover the desired metals in concentrated solution. The resin could then be reused in the treatment process.

This project uses chelating resins, which can also be referred to as a type of ion-exchange resin. The functional group on the polymer is a chelant. Chelation (Greek chelae = "claw") takes place when the lone-pair electrons of several electron-donating heteroatoms (O, N, S: "Lewis bases") in the chelant, are able to coordinate (bond)

---

[1] Paper presented at the International Land Reclamation and Mine Drainage Conference and the Third International Conference on the Abatement of Acidic Drainage, Pittsburgh, PA, April 24-29, 1994.

[2] K. Lise Hubbard, Ph.D. student, Department of Chemistry, Graham D. Darling, Assistant Professor of Chemistry, S. Ram Rao, Research Associate, Department of Mining and Metallurgical Engineering, James A. Finch, INCO-NSERC Chair of Mineral Processing, Department of Mining and Metallurgical Engineering, McGill University, Montreal, Quebec, Canada.

simultaneously to an electron-acceptor (metal cation: a "Lewis acid"), forming a stable complex, a chelate. Chelants are multidentate ligands; monodentate ligands have only one place of attachment to the metal. Chelants can be very selective for specific ions, according to the identities, numbers, and positions of the coordinating heteroatoms in the chelant, and the overall structure of the chelant. Though relatively inert towards such non-targeted ions as Ca^{+2}, Mg^{+2} or Na^{+1}, current commercial chelating resins are less able to discriminate between transition metals, such as zinc and iron ions.

The principle determining selectivity of the chelating groups that is used in the present work is hard/soft formalism (Mackay and Mackay 1989). Metal ions are classified as hard or soft "Lewis acids" and the electron-donating heteroatom(s) of the ligand (functional group) as hard or soft "Lewis bases". A heteroatom is a soft (Lewis) base if it is polarizable and is a hard base if it is nonpolarizable . Sulfur and phosphorus are polarizable and therefore soft, nitrogen is slightly soft, and oxygen is harder. A metal ion is a soft (Lewis) acid if it has easily polarizable electrons, or has a low charge, while a hard metal ion has high charge or valence electrons which are not polarizable. The "HSAB" (Hard-Soft-Acid-Base) rule states that soft bases tend to form complexes with soft acids, and hard bases tend to form complexes with hard acids.

Fe^{+3} is hard and not readily complexed with a soft ligand, while Zn^{+2} is relatively soft and can be complexed with a soft ligand. Resins containing soft ligands are potentially selective for the removal of zinc, leaving ferric ions in solution. The chelating groups of interest will have sulfur and possibly nitrogen in them. Since oxygen-containing chelants have a tendency to complex iron, these should be avoided. Although harder than Zn^{+2}, Fe^{+2} is slightly soft, so interference may occur. Ligands that prefer to bind zinc over iron are also likelier to bind other soft cations, such as cadmium, lead, mercury, silver, copper, gold, etc. Table 1 lists some common hard and soft acids and bases.

Table 1. Common Lewis acids and bases.

Hard bases	Soft bases	Hard acids	Soft acids
O, F	N, P, S	Na^{+1}, Fe^{+3}, Ca^{+2}, Al^{+3}, Mg^{+2}	Fe^{+2}, Zn^{+2}, Ni^{+2}, Cd^{+2}, Pb^{+2}, Cu^{+2}, Hg^{+2}, Pt^{+2}, Au^{+1}, Ag^{+1}

Ion-exchange and chelating resins are easy to handle, nontoxic, safely transportable, and can be regenerated repeatedly for multiple reuse. The ideal resin should be easy and inexpensive to manufacture; have a high affinity, capacity, and selectivity for the target cation(s); be easy to recover, regenerate, and recycle; and be mechanically and chemically stable to the conditions of its use and regeneration. Crosslinked polystyrene is a proven inert and stable matrix for ion-exchange resins and other functional polymers for many applications. The design for a zinc-versus-iron-selective sorbent thus depends on the choice of an appropriate chelating functional group. As well as being selective for the metal(s) of choice, it is important to have chelating functional groups that are nonhydrolyzable (stable to acid) and that are strongly bonded to the polymer backbone, so that they are not removed during usage.

Experimental Work

Synthetic Techniques

Radical Suspension Polymerization of Divinylbenzene. Using standard methodologies (Gao et al. 1993), macroporous beads of poly(divinylbenzene), also called (vinyl)polystyrene, were prepared. The resins were characterized using Fourier transform infrared (FTIR) spectrometry to determine the degree of functionalization (C_f, the number of residual double bonds (vinyl groups) in mmol per gram of resin) (Bartholin et al. 1981). The chemical structure of poly(divinylbenzene) (polyDVB) follows:

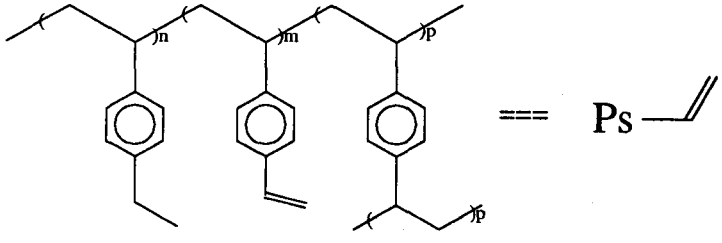

Functionalization of Poly(Divinylbenzene). It is possible to attach different functional groups to the vinyl group of the poly(divinylbenzene) using different methodologies. The method used in this study is radical-catalyzed

anti-Markovnikov addition of thiols (Gao et al. 1993). It creates a stable connection of the functional group to the polystyrene backbone through a two-carbon-unit bond. It is through the sulfide-functionality that the functional group is chemically attached to the polyDVB. The functional capacity of the resin (C_f, the number of functional groups in mmol per gram of resin) was found using elemental sulfur analysis. The following scheme shows the functionalization of poly(divinylbenzene) using thiol-containing compounds. (AIBN is 2,2'-azobis-(isobutyronitrile), a radical initiator).

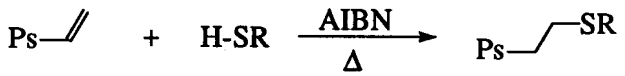

Simulated Acid Mine Drainage

The study used a synthetic AMD solution of composition like that of "les Mines Gallen" AMD (table 2). It was prepared by dissolving calculated amounts of metal sulfates, and sodium arsenite (for arsenic), in 1L of water, and adjusting the pH to 2.1. The AMD was flushed twice a week with nitrogen to minimize the oxidation of Fe^{+2} to Fe^{+3}.

Table 2. Composition of "synthetic" AMD.

Metal ion concentration	Fe^{+2}	Fe^{+3}	Cu^{+2}	Zn^{+2}	Al^{+3}	Mn^{+2}	Mg^{+2}	Cd^{+2}	As^{+3}
g/L.....	2.70	3.52	0.04	3.06	0.70	0.03	0.64	0.01	0.01
mmol/L.....	48.3	63.0	0.63	46.8	25.9	0.55	26.0	0.09	0.13

Treatment Procedure and Analysis

A weighed quantity of resin was put into a 10 mL polyethylene bottle, 5 mL of AMD was added, and the contents were mixed at room temperature using a platform shaker. After the required time of shaking, the contents were allowed to settle; centrifuging when necessary. 5 µL of solution was withdrawn, diluted to 10 mL (dilution factor of 2000), and analyzed for Fe, Zn, and Mg by atomic absorption spectrometry. The amount of resin to be tested, corresponding to 0.25 mmol of functional groups (fg), was calculated from a knowledge of the functional capacity (C_f) of that resin, using formula 1. Due to limited quantities of resin, some resins tested had less than 0.25 mmol of functional (chelating) groups.

$$\text{Mass of the resin (g)} = (0.25 \text{ mmol})/(C_f \text{ mmol fg/g}) \quad (1)$$

In the first set of experiments, 5 mL of AMD was treated using this method, and analyses for the metals were conducted after 1, 2, 4, 6, and 22 h to establish the time required to reach equilibrium. This would then be used as the treatment time in the remaining experiments. In the second set of experiments, 5 mL of unoxidized AMD (containing both ferrous (+2) and ferric (+3) ions) was used to measure the metal uptake by the resins. A third set of experiments was conducted, identical to the second, but in which the ferrous ion was oxidized to the ferric state by treatment with a stoichiometric amount of hydrogen peroxide before the AMD's treatment with the resin. The fourth set of experiments involved attempting to extract the adsorbed zinc from selected resins. Currently, only sulfuric acid has been used, though other eluents are planned. The resin, previously treated with 5 mL of AMD, was rinsed with distilled water to remove any residual AMD, then soaked in 20 mL of 4 M sulfuric acid for a few minutes. The amount of metal that was released by the resin was then measured.

The resins were evaluated using the following criteria. The **weight capacity, C**, or loading, which is the amount of metal ion (mg or mmol) adsorbed by 1 g of dry resin, was calculated. The adsorption of metal ions was indirectly measured using the difference of the initial and final concentrations of the metals in solution (measured using atomic adsorption spectrometry). The **distribution coefficient, D**, measures the partitioning of the metal between the resin and the solution. A solution-dependent value, **D** was found by dividing the capacity (mmol/g resin) by the equilibrium concentration (mmol/mL) (equation 2). The selectivity of the resins for zinc over iron was determined by calculating the **separation factor**, $S_{Zn/Fe}$ (equation 3). Also solution-dependent, it is the ratio of the distribution coefficient for zinc to that of iron. When it is high, the resin is selective for zinc; when it is low, the resin is selective for iron. The goal of this project is to develop resins with a high selectivity for zinc over iron.

$$\mathbf{D}\ (\text{mL/g}) = \mathbf{C}\ (\text{mmol } M_1\text{/g resin})/[M_1\ (\text{aq})\ (\text{mmol/mL})] \quad (2)$$

$$S_{Zn/Fe} = D_{Zn}/D_{Fe} = \frac{\mathbf{C}\ (\text{mmol Zn/g resin})\ \text{X}\ [\text{Fe (aq)}]}{\mathbf{C}\ (\text{mmol Fe/g resin})\ \text{X}\ [\text{Zn (aq)}]} \quad (3)$$

Results

Equilibrium Time

The metal uptake from unoxidized AMD by some resins over time was measured (table 3). There was no significant increase in metal uptake after 2 h. Consequently, all later tests used a treatment time between 4 and 6 h.

Table 3. Metal uptake over time from 5 mL unoxidized AMD by two resins.

Resin	Quantity, g	Time, h	Fe uptake, C, mmol/g	Zn uptake, C, mmol/g	Mg uptake, C, mmol/g
1	0.625	1	0.01	0.07	0.03
		2	0.02	0.10	0.04
		4	0.02	0.10	0.04
		6	0.02	0.10	0.04
		22	0.02	0.10	0.04
2	0.250	1	0.13	0.19	0.05
		2	0.16	0.26	0.07
		4	0.18	0.27	0.07
		6	0.18	0.27	0.07
		22	0.18	0.27	0.07

Recovery of Zinc

Two resins were treated with 20 mL of 4 M sulfuric acid in order to recover the adsorbed zinc (table 4).

Table 4. Zinc recovery from two spent resins.

Resin	Amount of resin, dry weight, g	Amount of Zn adsorbed, mg	Amount of Zn released, mg	Recovery, %
19[1]	0.22	5.90	5.00	84.7
19[2]	0.22	5.88	5.00	85.0
20[1]	0.20	6.47	5.20	80.4
20[2]	0.20	5.88	5.00	85.0

[1] AMD with Fe^{+2} and Fe^{+3}.
[2] AMD with Fe^{+3}.

Selectivity of Resins for Zinc over Iron

The distribution coefficients, ratios of zinc to iron capacity, and separation factors (Zn-Fe) for each resin tested was calculated ($S_{Zn/Fe} = D_{Zn}/D_{Fe}$) (table 5). A large $S_{Zn/Fe}$ means that the resin is selective for zinc over iron. The asterisks (*) indicate an extremely high $S_{Zn/Fe}$, whose exact value is somewhat uncertain.

Discussion

Equilibrium Time

As can be seen in table 3, the time for zinc uptake to reach its maximum was between 2 and 4 hours, depending on the resin. As a result, all tests had between 4 and 6 hour treatment times, which is estimated to have allowed all systems sufficient time to reach equilibrium.

Zinc Recovery From Resins

Two resins, **19** and **20**, previously treated with AMD were regenerated by soaking for a few minutes in 20 mL of 4 M sulfuric acid (table 4). More than 80% recovery of the zinc from the loaded resins was possible. Further tests will include determining the removal of other adsorbed metal ions, as well as determining any changes to the resin. Other eluents will be tested, such as distilled water, solutions of chelating agents such as EDTA or DTPA, hydrochloric

acid, and brine. It may not be necessary to use concentrated acid. Another method of metal recovery from the resins could be electroelution (Martins, 1993).

Table 5. Distribution coefficients, capacity ratios and Zn-Fe separation factors ($S_{Zn/Fe}$).

Resin	D_{Zn}, mL/g mixed Fe^{+2}–Fe^{+3}	D_{Zn}, mL/g Fe^{+3} only	D_{Fe}, mL/g mixed Fe^{+2}–Fe^{+3}	D_{Fe}, mL/g Fe^{+3} only	C_{Zn}/C_{Fe} mixed Fe^{+2}–Fe^{+3}	C_{Zn}/C_{Fe} Fe^{+3} only	$S_{Zn/Fe}$ mixed Fe^{+2}–Fe^{+3}	$S_{Zn/Fe}$ Fe^{+3} only
1	2.3	NA	0.2	NA	4.2	NA	10.0	NA
2	6.3	6.1	1.7	0.5	1.6	5.3	3.7	12.6
3	7.7	NA	3.1	NA	1.0	NA	2.5	NA
4	8.9	NA	2.2	NA	1.7	NA	4.2	NA
5	5.0	5.7	3.2	1.4	0.7	1.8	1.6	4.2
6	3.9	NA	1.8	NA	0.9	NA	2.1	NA
7	6.8	NA	4.5	NA	0.6	NA	1.5	NA
8	3.9	2.8	1.9	0.4	0.9	3.0	2.1	7.1
9	4.4	4.7	4.1	6.2	0.5	0.3	1.1	0.8
10	7.5	7.8	2.1	1.7	1.5	2.0	3.6	4.7
11	5.0	5.3	0.7	1.4	3.1	1.6	7.4	3.7
12	13.6	10.8	10.1	2.7	0.6	1.7	1.4	4.0
13	9.4	NA	5.9	NA	0.7	NA	1.6	NA
14	7.7	14.1	10.4	8.9	0.3	0.7	0.7	1.6
15	9.1	NA	6.7	NA	0.6	NA	1.4	NA
16	15.3	16.9	5.4	6.1	1.2	1.2	2.8	2.8
17	8.5	7.6	2.4	0.5	1.5	6.8	3.6	16
18	15.6	16.1	6.2	1.9	1.1	3.5	2.5	8.4
19	9.6	10.3	0.8	4.6	5.0	0.9	11.9	2.2
20	10.5	10.1	0.1	0.2	36	21	87*	50*
21	4.4	3.7	4.1	2.9	0.4	0.5	1.1	1.3
22	0.8	3.3	1.5	5.6	0.2	0.2	0.5	0.6
23	8.7	9.4	2.6	4.0	1.4	1.0	3.3	2.3
24	2.6	2.2	4.2	4.2	0.3	0.2	0.6	0.5
25	3.0	2.3	0.1	0.1	15	12	37*	29*
26	5.5	5.9	0.1	0.1	18	19	42*	45*
27	NA	11.4	NA	14.8	NA	0.3	NA	0.8

* Notably large values with potentially large associated error; see text. NA--not available

Uptake of Metals and Selectivity

The resins were evaluated using the calculated separation factor, $S_{Zn/Fe}$ (table 5). Table 6 ranks some resins tested with regard to their separation factor. These results are for resins tested using the oxidized AMD. The symbol C_f is the functional capacity in mmol fg/g. As some of the final (equilibrium) iron concentrations were close and possibly equal to the initial concentration, within the detection limits of the atomic absorption method used to measure them, error on the large $S_{Zn/Fe}$ values marked with an asterisk (*) is itself quite large; more accurate values will be obtained in future experiments by measuring bound metals directly, following digestion of the polymer, instead of by difference as was done here. The structure of the functional group is given, with the point of attachment to the polymer through the sulfur. A comparison between the most selective resin, **20**, and some commercial resins tested is given in table 7.

The predominant trend in comparing the selectivities of each resin when treated with AMD containing the slightly soft ferrous ion (unoxidized AMD) and when treated with the oxidized AMD (no ferrous ion, all iron existed as the harder ferric ion) was that the selectivity ($S_{Zn/Fe}$ value) tended to increase (table 5). The increase of selectivity ($S_{Zn/Fe}$) when the AMD was oxidized was significant for the following resins, with as much as a five-fold increase, **17**, **18**, **8**, **2**, **12**, and **5**. Resin **19**, on the other hand, had a much better zinc selectivity using unoxidized AMD.

As a control, polyDVB, the "non-chelating" precursor to the chelating resins, was also tested. Resin **16** consisted of "inert" vinyl groups; these may have hydrolyzed to alcohol groups under aqueous acid conditions. The $S_{Zn/Fe}$ for resin **16** was not changed when oxidized AMD was used ($S_{Zn/Fe}$ 2.8).

Table 6. Ranking of resins based on separation factor ($S_{Zn/Fe}$).
(5 mL oxidized AMD used, 6 h equilibrium time)

Resin	Structure of functional group (Ps–SR)	C_f, mmol/g	$S_{Zn/Fe}$	C_{Zn}, mg/g	C_{Fe}, mg/g
20	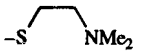	0.11	50*	31	1
26	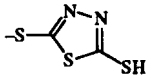	0.81	45*	18	<1
25	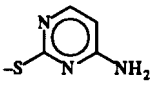	0.28	29*	7	<1
17	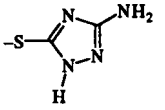	0.56	16	23	3
18	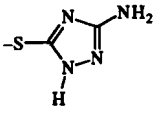	1.93	8.4	49	12
16		2.29	2.8	52	38
23	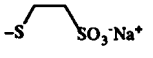	0.12	2.3	29	25
19	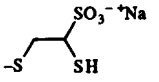	1.15	2.2	32	29
21	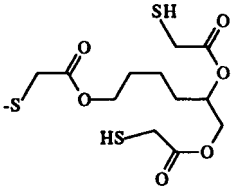	0.38	1.3	11	18
9	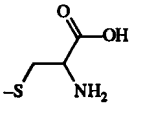	0.70	0.8	14	39
22	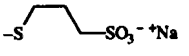	0.32	0.6	10	35
24	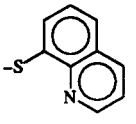	0.01	0.5	7	26

* Notably large values with potentially large associated error; see text.

As indicated by the "top three" resins (**20**, **26** and **25**, whose $S_{Zn/Fe}$'s were respectably high, table 5), it may be unnecessary to oxidize the AMD before treatment with the resins.

Since the selectivity of resin **20** was so good, future resins could be based on the aminoethanethiol functionality and derivatives thereof. The syntheses of these ligands, such as by an established method (Luhowy and Meneghini 1973), will be advantageous in this work.

The presence of a sulfonate group ($-SO_3^-$), as in resins **19**, **22**, **23**, and the commercially-available **12** and **13**, will make the resin more water-swellable, which can increase the efficiency of the resin.

Some resins (e.g., **19**, **20**, and **26**) were derived from known chelating agents. They all had excellent selectivity for zinc over iron; other heavy metals not analyzed in this study may have been adsorbed as well. These resins outperformed the commercial resins studied in terms of selectivity for zinc. Resins **21** and **24**, also based on known chelating groups, did not perform as well as hoped.

Analogs of the ligands of some of the more successful resins, such as **17**, **19**, **20**, **25**, and **26**, will be studied. They may be closely related, varying by substitution of a group or atom, for example, an amine for a thiol, or other nitrogen- or sulfur-containing entities. One possibility is to study the effect of the substitution of the sulfur by a nitrogen in the ring of the group from **26**; another possibility is to study the effect of replacing the amine by a thiol in **25**. The effects of ligands containing mostly sulfur, some sulfur and some nitrogen, or mostly nitrogen will be contrasted. The effect of ring-containing ligands will be studied. Ligands that are multidentate, ringed structures will also be studied; examples are sulfur- or nitrogen-containing analogs of crown ethers.

The commercial resins, **12**, **13**, **14**, **15** and **27** had low selectivities (table 5). The selectivity of **27**, as well as the capacity, strongly favored iron uptake from oxidized AMD, as would be expected for a carboxylate-containing chelating group. In comparison to the commercial resins, resins **17**, **18**, **20**, **25**, and **26** had better selectivities (oxidized AMD). Resin **20** had the best selectivity for zinc, and comparable capacity (31 mg Zn/g), despite the low amount of functional groups per gram of polymer (C_f = 0.11). Increasing the functionality would increase the capacity, probably surpassing those of commercial resins.

Table 7. Comparison of best experimental resin (**20**) with commercial resins.
(5 mL oxidized AMD used, 6 hour equilibrium time)

Resin	Structure of functional group	C_f, mmol/g	$S_{Zn/Fe}$	C_{Zn}, mg/g	C_{Fe}, mg/g
20	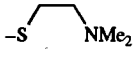	0.11	50*	31	1
12	$Ps—SO_3^-{}^+Na$ (commercial Dowex 50X8-100)	.7	4.0	33	17
14	$Ps—CH_2NMe_3^+{}^-Cl$ (commercial Amberlyst)	NA	1.6	43	55
27	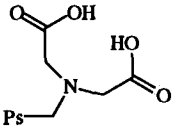 (commercial Chelex-100)	0.7	0.8	35	92

* Notably large values with potentially large associated error; see text. NA--not available

Application

A treatment process using chelating resins could consist of three stages: production of the resin by a commercial chemical manufacturer, application of the resin at the AMD site, and regeneration of the resin with metals recovery, done either on- or off- site. Resin particles could be loaded into inert plastic (polypropylene) mesh bags, which would be lowered into the AMD pond or waste stream and allowed to become saturated with metal ions, then pulled out and regenerated. The bag of regenerated resin could then be dumped back into the AMD pond for reuse. Removal of metals from an AMD solution could make it easier to recover sulfuric acid through electro-osmosis. It may be possible to make the polymer into other forms such as hollow fibers or membranes.

Conclusions

These exploratory investigations using synthetic chelating resins have shown that certain polymer-supported functional groups can serve to selectively recover zinc from synthetic AMD. Further investigations should enable the development of resins with high zinc capacities and affinities for the maximum selective recovery of zinc, leaving iron in solution. The detoxification of AMD, along with the recovery of zinc and related metals, could then be possible.

Future Work

Further work will be done in the following areas: design and synthesis of resins, testing of resins, and possible costs and application. Testing methods will use larger quantities of resins, preconditioned with sulfuric acid (pH 2), exposed to a large excess of AMD or acidic metal-containing solutions. Atomic absorption spectrometry and elemental analysis will be used to measure the metal uptakes of all metals in AMD. Methods of regeneration will be examined.

Acknowledgments

Sources of funding for this project were the Natural Sciences and Engineering Research Council of Canada (NSERC), Fonds pour la formation de Chercheurs et l'Aide à la Recherche (FCAR), and the Centre de Recherches minérales (CRM). Many thanks to Dr. P.A. Riveros (CANMET), Ken Wheeland (MEND), Brent R. Stranix for providing the cysteine-based polystyrene resins, and Dr. R. Gehr, Department of Civil Engineering and Applied Mechanics, McGill University.

References

Bartholin, M., G. Boissier, and J. Dubois. 1981. Styrene-divinylbenzene copolymers, revisited IR analysis. Makromol. Chem. 182: 2075.

Gao, J. P., F. G. Morin, and G. D. Darling. 1993. Functional polymers containing dimethylene spacers. Characterization by solid-phase ^{13}C-NMR. Macromolecules 26: 1196.

Luhowy, R. and F. Meneghini. 1973. An improved synthesis of aminoethanethiols. J. Org. Chem. 38 (13): 2405.

MacDonald, R. J. C., P. D. Kondos, S. Krevier, P. Rulinsky, and N. Wassalouf. 1989. Generation of and disposal options for Canadian mineral industry effluent sludges. p. 139-197. In Tailings and Effluent Management. M.E. Chalkley, B.R. Conard, V.I. Lakshmanan, and G. Wheeland (eds.). Pergamon, New York.

Mackay, K. M. and R. A. Mackay. 1989. Introduction to modern inorganic chemistry. Prentice Hall, Englewood Cliffs. p. 200-201.

Martins, A. H. 1993. The extraction of gold and silver by electroelution of strong-base polymeric resins. Can. Metallurgical Quarterly, 32 (1): 85.

Rao, S. R., R. Gehr, M. Riendeau, D. Lu, and J. A. Finch. 1992. Acid mine drainage as a coagulant. Minerals Eng. 5 (9): 1011.

Ritcey, G. M. 1989. Tailings management, Elsevier, Amsterdam. p. 19-20.

HYDROLOGIC ASSESSMENT OF WELLHEAD PROTECTION IN THE VICINITY OF A ROOM-AND-PILLAR COAL MINE[1]

Perry M. Jones[2] and John L. Ellenberger[3]

Abstract: The U.S. Bureau of Mines is identifying and assessing various hydrogeologic and mining variables important in delineating wellhead protection zones around public supply wells in mining regions. As part of this study, researchers are monitoring hydrologic conditions between the Solar No. 7 Mine, an active underground coal mine, and three municipal wells in the borough of Stoystown, PA. Key variables important in determining the hydrologic interaction between mining activities and municipal water use have been monitored at the Stoystown field site. These variables include pumping rates and water levels in the three municipal wells, ground-water inflow rates into the mine, and water levels and water quality in three aquifer systems. The borough of Stoystown extracts on the average a total of 125,000 L (33,000 gal) per day from the three municipal wells. An average of 567,750 L (150,000 gal) per day of ground water is pumped from the Solar No. 7 Mine. Except in one monitoring well set which was undermined, no changes in water yield or quality in the municipal wells or the monitoring wells have been seen, thus far, that can be attributed to mining activity. Results from future model simulations will be used to demonstrate how the impact of mining on water quantity and quality can be taken into account in the delineation of wellhead protection zones, and how future mine planning can be incorporated into local wellhead protection programs.

Additional Key Words: wellhead protection, room-and-pillar coal mine, municipal pumping rates, ground-water inflow to mine workings.

Introduction

1986 Amendments to the Safe Drinking Water Act established the Wellhead Protection Program, a program designed to protect ground waters that contribute drinking water to public supply wells and wellfields (U.S. Environmental Protection Agency 1990). Under this program, State and local governments are required to establish wellhead protection areas (WHPA) around public well water supplies in their State based on reasonably available hydrogeologic information on ground-water flow, recharge, and discharge, and other information deemed necessary to adequately determine the WHPA. Within these protection zones, communities will develop management approaches and contingency plans, including the implementation of land use control measures, to prevent and limit the impact of any contamination of the water supply. Aquifers which serve as significant sources of public water supply systems are protected against diminution under regulations established through the Surface Mining Control and Reclamation Act (U.S. Code of Federal Regulations 1993).

The U.S. Environmental Protection Agency has outlined six possible methods for the delineation of WHPA's around public supply wells (U.S. Environmental Protection Agency 1987). These methods vary in complexity and cost. In principle, the method chosen for delineation should depend on the complexity of the hydrologic setting. However, owing to the limited availability of hydrologic information and the relatively high costs of collecting and analyzing detailed information, most communities and permitting agencies are forced to apply simple, less precise methods for delineating WHPA's. These simple methods usually do not take into account the various hydrological complexities found in mining areas, such as abandoned and active, surface and underground mine workings, longwall mining excavations, and mine dewatering, on the size and shape of capture zones of public supply wells used for delineating wellhead protection areas. When overly-simplified methods are applied in hydrologically complex settings, there is no assurance that delineated wellhead protection zones will adequately protect the water supply from mining-induced ground-water contamination, especially following mine abandonment and partial flooding. Protection zones need to be delineated accurately enough to effectively protect the water supply while minimizing control measures placed on local land users.

---

[1] Paper presented at the International Land Reclamation and Mine Drainage Conference and the Third International Conference on the Abatement of Acidic Drainage, Pittsburgh, PA, April 24-29, 1994.

[2] Perry M. Jones, Hydrogeologist, U.S. Department of the Interior, Bureau of Mines, Twin Cities, MN, USA.

[3] John L. Ellenberger, Geologist, U.S. Department of the Interior, Bureau of Mines, Twin Cities, MN, USA.

Many well water supplies in the United States have been contaminated as a result of local and/or regional land use activities involving mining. Water from four municipal wells of the Milltown, MT, water system were found to have arsenic concentrations of more than four times the EPA maximum contaminant level for arsenic (0.05 mg/L) (Lambing 1991). These high arsenic levels were a result of the dissolution of mine tailings in the Milltown Reservoir, which were transported downstream in the Clark Fork River and its tributaries from the mining areas of Butte and Anaconda, MT. Several public water supplies in the Appalachian coal mining regions of Pennsylvania and West Virginia have either been contaminated by acid mine drainage or suffered significant decreases in well yields or total water loss owing to mine subsidence (American Water Works Association, 1992). The potential impact of nearby mining on drinking water supplies is currently a very strong concern in many mining communities throughout the United States (Shesky 1993, Thurston County (WA) Public Health and Social Services Department 1993).

To address this concern, the U.S. Bureau of Mines is identifying and assessing various hydrogeologic and mining variables important in delineating wellhead protection zones around public supply wells in mining regions. As part of this study, researchers are monitoring hydrologic conditions between an active underground coal mine and the three municipal wells of the Borough of Stoystown, PA. In this study, researchers will demonstrate how the hydrologic impact of mining can be taken into account in the delineation of wellhead protection zones and how future mine planning can be incorporated into local wellhead protection programs.

Research Site

General Description

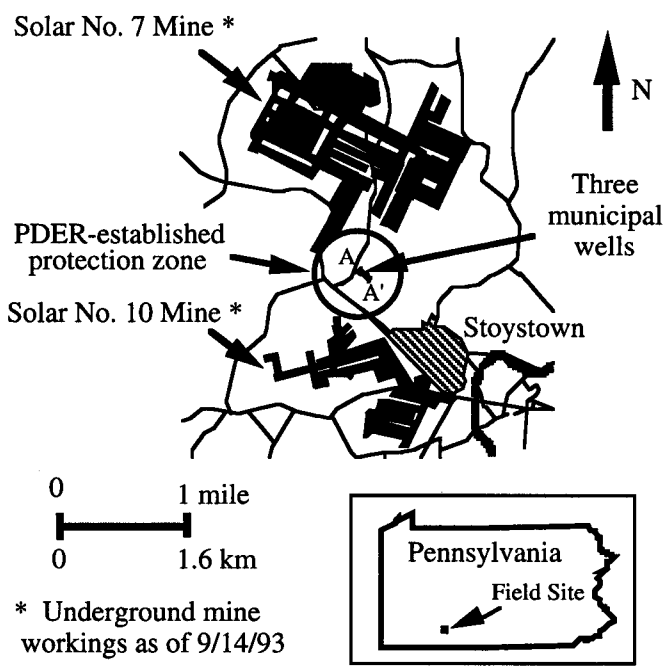

Figure 1. Plan view of field site.

The research site is located in Quemahoning Township of Somerset County, PA, just northwest of the borough of Stoystown, PA (fig. 1). The terrain is hilly with steep to moderate slopes, with a dominantly dendritic drainage pattern over the area. Topographic relief is approximately 167.6 m (550 ft). Land use consists mainly of rural dwellings and small agricultural croplands and grazing lands separated by small woodlots. Average precipitation for the Stoystown Area is roughly 104 cm (41 in) per year (National Oceanic and Atmospheric Administration, 1956-93).

Half of the 432 residents of Stoystown obtain their drinking water from three municipal wells located roughly 1.2 km (0.75 mile) northwest of the center of the borough (fig. 1). The three wells, denoted 6, 8, and 9, lie within a small stream valley less than 36.5 m (120 ft) apart (fig. 2). Wells 6, 8, and 9 are 79.25 m (260 ft), 92 m (302 ft), and 121 m (397 ft) in depth, respectively. The wells are open holes except for surface casings ranging in length from 12.2 to 12.8 m (40 to 42 ft) (fig. 2). The Pennsylvania Department of Environmental Resources (PDER) has established an 548.6-m (1,800-ft) radial protection zone around the three municipal wells to protect the water supply from any potential hydrologic impacts of mining (fig. 1).

Two active room-and-pillar underground coal mines, the Solar No. 7 and 10 Mines, are operating in the Upper Kittanning coal seam outside of the PDER-established protection zone (fig. 1). Average daily extraction rates for the Solar No. 7 and 10 Mines are 2,500 and 1,000 st, respectively (Lick 1991). At the location of the municipal wells, the Upper Kittanning coal seam lies 78 m (256 ft) below the land surface, 22.6 m (74 ft) above the Lower Worthington Sandstone.

The Upper Kittanning coal seam is present in each of the open holes of the three municipal wells (fig. 2). Local concern exists that the mining of the coal seam may impact the water quality and quantity in the three municipal wells.

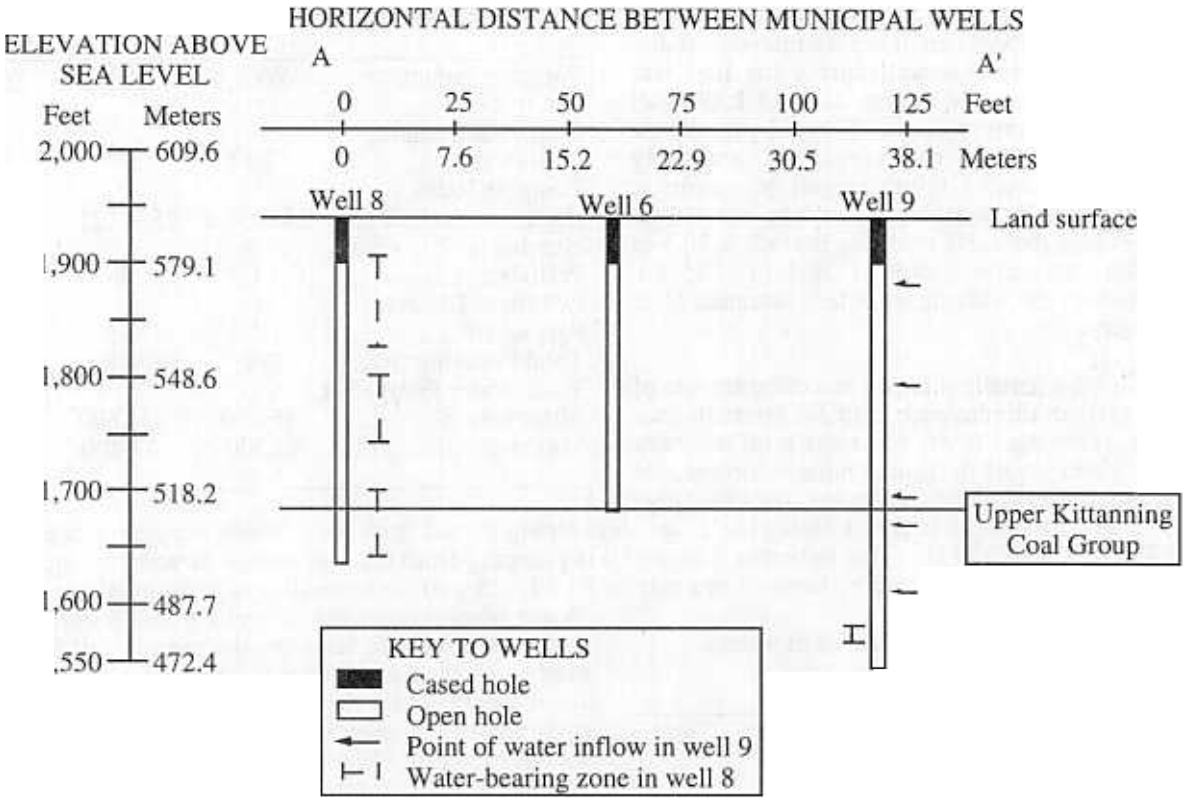

Figure 2. Vertical cross section of Stoystown municipal wells.

Active mining in the Solar No. 7 Mine is proceeding along the 1,800-ft radial protection zone surrounding the municipal wells, while active mining in the Solar No. 10 Mine is more than 1.6 km (1.0 mile) from the municipal wells, heading in a southwesterly direction away from the municipal wells. Therefore, initial hydrologic assessment has focused on the hydrologic impacts of the Solar No. 7 mine. The hydrologic impacts of the Solar No. 10 Mine are being assessed in a separate study.

Key variables important in assessing the hydrologic interaction between mining activities and municipal water are the pumping rates, water levels, and water quality in the three municipal wells, ground-water inflow and pumping rates at the Solar No. 7 Mine, and water levels and water quality in local ground-water flow systems. Each of these variables is currently being monitored and assessed at the site.

Municipal Water Quantity and Quality

Daily pumping rate and number of pumping hours vary among the three municipal wells. Daily pumping schedules for these wells varies seasonally. In general, only two of the wells are pumping at any time. A pressure/flow data-logging system was installed on each well to monitor average hourly water levels and pumping rates in the municipal wells.

The borough of Stoystown extracts on the average a total of 125,000 L (33,000 gal) per day from the three municipal wells. Under the highest water demands of 1993, the three wells pumped 257,400 L (68,000 gal) per day in July. Well 6 is pumped continuously at flow rates varying from 24.6 to 30.3 L (6.5 to 8 gal) per minute, while water levels in the well vary little from 9.75 to 12.2 m (32 to 40 ft) below the top of the well casing (table 1). This pumping scenario changes little on a seasonal and annual basis. Any water level fluctuations in well 6

appear to be due to seasonal changes in ground-water recharge rates from seasonally variable precipitation rather than to changes in pumping conditions in the two other municipal wells.

Well 8 is normally pumped over 1- to 2-h intervals four times a day, allowing water levels to recover for 4 to 5 h between pumping intervals (table 1). Pumping rates in this well during the first few minutes of pumping can be as high as 121.1 L (32 gal) per minute, decreasing to 75.7 L (20 gal) per minute after the first hour of pumping, and gradually decreasing to 53 to 60.6 L (14 to 16 gal) per minute at the end of the 2-h pumping intervals. Average drawdown during these 2-h pumping periods is 30.5 m (100 ft), but can be as much as 38.1 m (125 ft), returning back to the water level before pumping after 2 h of recovery.

Table 1 - Common Daily Pumping Schedules For Stoystown Municipal Wells *

Pumping parameter	Well 6	Well 8	Well 9
Length of Pumping Periods (h)	24	1-2	2-3
Pumping Rates (Lpm)	24.6-30.1	75.7-121.1	94.6
Number of Pumping Periods	1	4	4
Length of Recovery Periods (h)	0	4-5	3-4
Total Pumping (h)	24	4-8	8-12
Total Water Pumped (L)			
Minimum	35,400	23,600	45,400
Maximum	43,300	47,200	68,100

Well 9 is normally pumped at a constant rate of 94.6 L (25 gal) per minute over 2- to 3-h intervals four times a day, allowing 3 to 4 h for water level recovery (table 1). Water levels decline at a much slower rate in well 9 than in well 8 during pumping, only dropping between 12.2 to 15.2 m (40 to 50 ft) during the 2- to 3-h pumping period, with water levels varying between 85.3 and 106.7 m (280 and 350 ft). This indicates that well 9 is pumping from a better source of water quantity than well 8. Unlike well 8, well 9 can be pumped at a rate of 94.6 L (25 gal) for several days without becoming dry. Water level monitoring of wells 6 and 8 during 48-h constant discharge tests conducted in well 9 in this study and by Casselberry (1990) indicated no water level declines in the two shallower wells during pumping of the deeper well. No changes in the water levels of wells 6 and 9 were seen during constant discharge tests conducted in well 8, indicating no interaction between the wells. However, the tests conducted in well 8 lasted only 2 to 3 h, possibly not long enough to see the impact of pumping on local water levels.

Table 2 - Average ionic concentrations in waters from Stoystown municipal wells. *

Chemical parameter	Well 6	Well 8	Well 9
Calcium	36.2	35.4	7.1
Iron, total	0.37	0.04	< 0.01
Magnesium	10.7	10.5	2.0
Sodium	18.7	22.7	85.5
Hardness (Ca, Mg) (mg/l as $CaCO_3$)	134	132	26
pH	8.2	8.1	8.6
Alkalinity to pH 4.5 (mg/l as $CaCO_3$)	142	138	200
Sulfate	20	16	< 5

* Measurements are in mg/L unless otherwise specified.

Dissolved ion concentrations in waters from the three wells indicate that the two shallower wells obtain their water from a common source, relatively shallow bedrock aquifers, while water from well 9 is a much softer water, with lower concentrations of sulfate and iron (table 2).

Solar No. 7 Mine - Water Inflow and Pumping

Active mining in the Solar No. 7 Mine is occurring in two different sections of the mine near the 1,800-ft protection zone: sections north-to-northeast of the municipal wells and sections northwest of the wells (fig. 3). During the first 9 months of 1993, an average total of 34,200 mt/month (37,600 st/month) of coal was extracted by these two sections. In both sections of the mine, pillars are currently not being extracted, minimizing any immediate subsidence impact on the local hydrology. No future plans for mining these pillars exist.

An average of 567,750 L (150,000 gal) of ground water is pumped from the Solar No. 7 Mine on a daily basis. This average value is more than four times the average daily pumping of ground water from the Stoystown three municipal wells (125,000 L). Pumping rates from the mine vary seasonally between 473,125 L (125,000 gal) to 1,514,000 L (400,000 gal) per day. Higher pumping rates occur in spring as snowmelt occurs, while the lower pumping rates occur in the summer and winter. Water pumped from the mine is discharged to a treatment pond, where lime is added to reduce the water's acidity. Once treated, the water is discharged to a local stream.

A large amount of the ground water entering the mine is produced from abandoned sections of the mine located below local stream valleys. Roughly 50% of the workings in the mine have been secondary-mined and abandoned, with 10% of these abandoned workings lying below stream valleys. Total water inflow into abandoned sections lying below stream valleys varies seasonally from 151,000 to 492,000 L/d (40,000 to 130,000 gal/d), with an average inflow of 306,000 L (80,800 gal) per day. Although only accounting for 5% of the spatial extent of the mine, these abandoned sections account for roughly 54% of the ground-water inflow into the mine. Water flowing into these abandoned sections of the mine is thought to be produced from fractured bedrock systems located above the mined coal seam.

The rate of water inflow along active and abandoned sections of the mine is low compared to the abandoned sections of the mine below stream valleys. The roof and walls of the accessible sections of the mine are very dry, indicating that the water is being produced from aquifer systems lying below the mined coal seam.

Local Hydrogeology

Constant discharge flow tests conducted during and after well construction indicated that water from the two shallowest municipal wells, Nos. 6 and 8, is obtained mostly from shallow bedrock aquifers lying above the Upper Kittanning coal seam, while well 9 obtains most of its water from the deeper Worthington Sandstone aquifer located below the Upper Kittanning coal seam (Casselberry 1990). Using drawdown analyses developed by Theis (1935) and Jacob (1950), transmissivity values obtained from these flow tests ranged from 57 to 125 L/d/m (49 to 108 gal/d/ft) for bedrock aquifers lying above the mined coal seam, while transmissivity values for the Lower Worthington Sandstone lying below the mined coal seam varied from 798 to 2725 L/d/m (692 to 2,362 gal/d/ft).

In order to monitor flow conditions in these two different ground-water flow systems, four sets of monitoring wells were installed between the Solar No. 7 Mine and the three municipal wells. These well sets are labeled A, B, C, and D on figure 3. Three of these well sets were positioned within the established protection zone, while the fourth set was located half the distance between the municipal wells and the protection zone within a stream valley. Each set contains three wells constructed to monitor three different aquifer systems: upper fractured bedrock aquifers above the Upper Kittanning coal seam, the Upper Kittanning coal seam, and the lower Worthington Sandstone Aquifer. The wells in each set are less than 15 m (50 ft) from one another and are only opened to one of the three different aquifer systems. Water levels and water quality are being monitored in each well set on a weekly and bimonthly (every two months) basis, respectively.

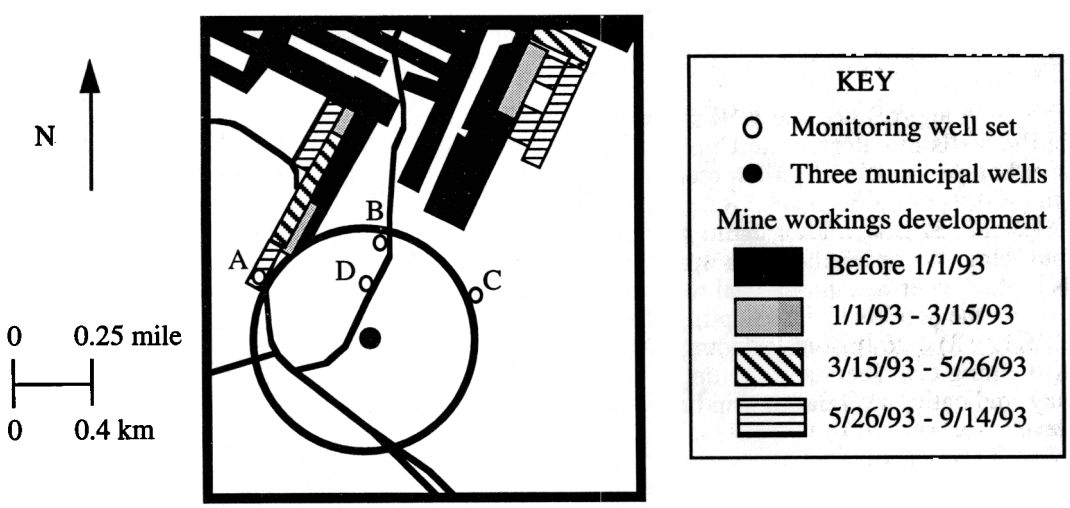

Figure 3. Locations of monitoring well sets and Solar No. 7 Mine workings development in 1993.

Water levels in three of the four monitoring well sets indicated that hydraulic head conditions in the Upper Kittanning Coal unit are lower than in the Lower Worthington Sandstone, suggesting a possible upward flow of ground water from the sandstone to the coal unit. This conclusion is supported by the observation that

most of the water entering the active sections of the Solar No. 7 Mine not beneath valley settings is produced from aquifer systems lying below the coal seam. Vertical pressure gradients in these three well sets vary among the sets and over time, ranging from 0.05 to 2.04 m (2 to 80 in) of water pressure per meter of elevation difference between the coal seam and the sandstone unit.

Average water levels in fractured aquifers above the coal seam in all of the well sets are higher than water levels in the Upper Kittanning coal seam and the Lower Worthington Sandstone, indicating flow downward in aquifers lying above the coal seam. Water quality analyses of the monitoring wells opened to aquifers above the coal seam are quite similar to chemical analyses of water from municipal wells 6 and 8, indicating common sources of water.

When pumped, wells opened to the Lower Worthington Sandstone (one well in each set) are very slow to recover, some taking weeks to months to fully recover. Slow water levels recoveries are seen in the Lower Worthington Sandstone monitoring wells of well sets located in both hillside and valley settings. These slow recoveries suggest that the sandstone at these locations is less permeable than at the location of municipal well 9. Well 9 could be intercepting a highly permeable fracture system located within the sandstone unit, with recharge potentially coming from shallow fractured units. Since water levels in the monitoring wells are much slower to recover than water levels in the municipal wells, the monitoring wells opened to the Lower Worthington Sandstone do not appear to intercept this fracture system. Future hydrologic and geochemical testing, such as isotopic dating of waters, may provide further insight into the difference between the permeability encountered in the monitoring wells as contrasted to the municipal supply wells.

Impact of Mining on the Local Hydrogeology

On June 10, 1993, 336 days after the wells were drilled, monitoring well set A was undermined. This well set is located northwest of the municipal wells along the established protection zone (fig. 3). As it undermined the well set, the mine cutting through the well opened to the Upper Kittanning Coal seam. A 30.5-m (100-ft) pillar was established around the other two wells in the set to protect their integrity. Following undermining, water entered the mine from the floor, indicating that the source of this inflowing water was below the coal seam.

Wells in monitoring well set A were pumped for water sampling purposes several times prior to the workings intercepting the well set on June 10 (336 days after drilling) (fig. 4). Significant decreases in water levels associated with this pumping were seen in all three of the wells between 230 and 245 days after well drilling (fig. 4). Because of these pumping events, water levels in these wells had not fully recovered prior to undermining.

As the mine approached the well set, water level decreases associated with the approaching workings were seen in the wells monitoring the Upper Kittanning coal seam and the upper bedrock aquifers on May 11, 1993, 30 days before the workings intercepted the well (fig. 4). On that date, the workings had approached within 122 m (400 ft) of the well set. Water levels in the upper bedrock aquifer well declined 1.5 m (5 ft) from May 11 to May 27 (322 days after drilling). This well was pumped for water sampling on May 27 (fig. 4). Following pumping, water levels in the upper bedrock aquifer well recovered to levels seen prior to May 11. Water levels in the Upper Kittanning coal well continued to decline after May 11, dropping 8.5 m (28 ft) over the 30 days prior to the workings intercepting the well (fig. 4). Before the well was actually cut by mining equipment, 8 m (26 ft) of water was standing in the Upper Kittanning coal well. Water levels in wells monitoring the Upper Kittanning coal seam and the upper bedrock aquifers in other well sets remained constant during the month of May, indicating no relationship between the recorded water declines and seasonal fluctuations in the local water levels.

Water levels in both the upper bedrock aquifers lying above the coal seam and the Lower Worthington Sandstone continued to rise during recovery from pumping as the mine passed through the well set (336 days after drilling) (fig. 4). Also the rate of water level recovery from pumping in both wells did not change following undermining, indicating that the workings did not have a long-term impact on the upper fracture bedrock aquifers and any impact on the Lower Worthington Sandstone at the time of well interception. Inflow rates and water levels in the monitoring wells will continue to be monitored and assessed over time to see if water levels in the wells return to pre-pumping levels.

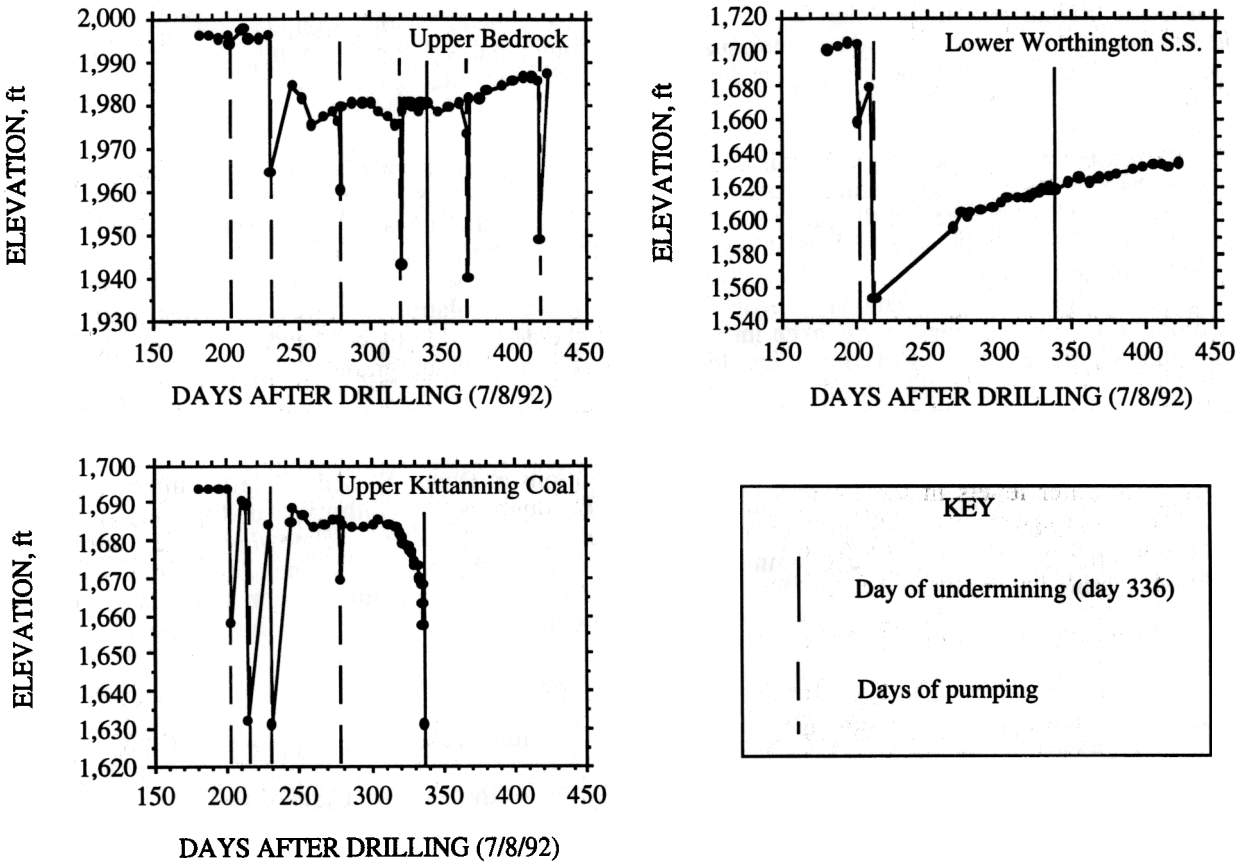

Figure 4. Water levels in monitoring well set mined through by Solar No. 7 Mine.

Water Quantity and Quality Implications of Mining on Wellhead Protection

As defined in the Safe Drinking Water Act, wellhead protection areas are "the surface and subsurface area surrounding a water well or wellfield, supplying a public water system, through which contaminants are reasonably likely to move toward and reach such water well or wellfield" (U. S. Environmental Protection Agency 1987). This definition addresses wellhead protection as a method of protecting public well water supplies from potential water quality problems. In mining regions, wellhead protection has to address both potential water quantity and quality problems that may occur as mine workings are developed and eventually abandoned.

Thus far, wellhead protection at the Stoystown field site has focused on water quantity issues as the size and shape of the capture zone for the mine changes with the advancement of workings. Water quality will become a more important issue as workings are abandoned and allowed to flood. As flooding occurs, the amount and residence time of ground water in the mine will increase, increasing the amount of water/mineral contact. Pyrite and other iron sulfide minerals present in the coal seam will be dissolved at a higher rate, increasing the acidity of the water present in the mine. Although the abandonment of the Solar No. 7 Mine is not planned for the near future, the potential hydrologic impact of future abandonment, as well as the current impacts of mining, needs to be accounted for in the current analysis of wellhead protection zone delineation.

At the Stoystown research site, average daily water inflow rates in the Solar No. 7 Mine are more than four times the average daily water extraction from Stoystown's three municipal wells. Inflow rates are expected to increase as the mine workings advance under local stream valleys north of the municipal wells. Water level and water quality will continue to be monitored in the well sets as the workings advance around the 1,800-foot protection zone. In particular, collected water quality data will be used to assess the impact of flooded mine workings on ground-water quality. Water level and quality data from the municipal wells and monitoring well

sets indicate that mining in the Solar No. 7 Mine has had no immediate impact on the Stoystown water supply. Thus far, no changes in water yield or water quality in the municipal wells or the monitoring wells, except for the undermined well set A, have been seen that can be attributed to advancing mine activity or water pumping from the mine.

Collected hydrologic information is currently being used in the Bureau's hydrologic model, Mineflow, to simulate the capture zones of the mine workings and the municipal wells and particle transport from abandoned, flooded workings. Changes in the size and shape of these capture zones will be assessed as mine workings continue to be developed in the area and new municipal pumping scenarios are implemented. The potential impact of future flooding of the Solar No. 7 Mine on the municipal water supply quality will also be addressed through a series of model simulations. Results from these model simulations will be used to demonstrate how the hydrologic impact of mining can be taken into account in the delineation of wellhead protection zones and how future mine planning can be incorporated into local wellhead protection programs.

Acknowledgment

The authors would like to acknowledge the contributions of Daniel R. Seibert, Jeff Zimmerman, Thomas M. Zimmerman, and other members of the Stoystown Borough Water Authority for their assistance in the collection of water level and water quality data. The authors would also like to acknowledge the contributions of Solar Fuel Company, Inc., particularly Kenneth Fenush, Edwin Smith, and Tom Turner, for their assistance in the collection of mine water inflow data and for providing additional hydrologic information and updated mine maps for the Solar No. 7 Mine. This study would have been impossible without their continuing support.

Literature Cited

American Water Works Association. 1992. Bad water brings criminal sentence. Waterweek 1(1):8

Casselberry, J. R. 1990. Report to Stoystown Borough Water Authority - Analysis of well No. 3 pumping test results. May 2, 1990.

Jacob, C. E. 1950. Flow in ground-water. In Engineering Hydraulics, John Wiley and Sons, New York. p. 321 386.

Lambing, J. H. 1991. Water-quality and transport characteristics of suspended sediment and trace elements in streamflow of the Upper Clark Fork Basin from Galen to Missoula, Montana, 1985-90. U. S. Geol. Surv., Water-Resources Investigations Report 91-4139. p. 73.

Lick, R. 1991. Keystone Coal Industry Manual. Maclean Hunter, Chicago. p. 856.

National Oceanic and Atmospheric Administration (NOAA). 1956-1993 Monthly Climatologic data Pennsylvania. Environmental Data and Information Service, Asheville, N.C.

Shesky, R. (Operations Consultant). 1993. Ohio Environmental Protection Agency, Division of Drinking and Ground Waters, Engineering and Operations Section. Personal Communication. June 18, 1993.

Theis, C. V. 1935. The relation between the lowering of the piezometric surface and the rate and duration of discharge of a well using ground-water storage. Transactions, American Geophysical Union 16:519-524.

Thurston County (WA) Public Health and Social Services Department. 1993. The direct and cumulative effects of gravel mining on ground water within Thurston County, Washington - Public Review Draft. Environmental Health Division, Ground Water Management Program.

U. S. Code of Federal Regulations. 1993. Title 30, 817.121(d).

U.S. Environmental Protection Agency. 1987. Guidelines for delineation of wellhead protection areas. Office of Ground-Water Protection. EPA 440/6-87-010. June 1987.

U.S. Environmental Protection Agency. 1990. Guide to ground-water supply contingency planning for local and state governments. Office of Water/Ground-Water Protection. EPA 440/6-90-003. May 1990.

THE ROLE OF SULFATE AND IONIC STRENGTH ON THE SHIFT FROM ACID TO ALKALINE MINE DRAINAGE IN SOUTHWEST PENNSYLVANIA[1]

Peter M. Jones, Shawn M. Mulvay, and Daryle Fish[2]

Abstract: Four Mile Run, Latrobe, PA, receives discharges from abandoned deep mines. In 1971, the effluent was characterized as having low pH, high acidity, and high concentrations of iron, manganese, and sulfate. After 22 yr of neglect, the water flow rate, pH, and alkalinity all increased, while the acidity, iron, manganese, and sulfate concentrations decreased. The overall loading of iron and sulfate to the stream has not changed significantly. This change from acid to alkaline drainage is fairly typical for mine effluent in the surrounding area. However, the mechanism for change is not well understood. Laboratory studies have shown that the neutralization rate of marble chips ($CaCO_3$) is depressed by high ionic strength or elevated levels of sulfate. The decrease in the rate of neutralization can be explained in terms of a static water film model. The decline in sulfate levels may be an important factor contributing to the change in water quality discharged into Four Mile Run. A similar kinetic phenomenon may occur with mine spoils and anoxic drains.

Introduction

Four Mile Run is located adjacent to the Saint Vincent College Campus in the town of Latrobe about 40 miles east-south-east of Pittsburgh, PA. The stream receives mine drainage from a series of abandoned deep mines that were used to remove coal from the Pittsburgh Seam. The run has been studied because it is the first major input of mine drainage in the Loyalhanna, a prominent area trout stream.

A comprehensive postmining study of water quality and mine drainage in the Loyalhanna Watershed was conducted in 1971 as part of Operation Scarlift (Schutz 1972). Four Mile Run received acid mine drainage (AMD) from six sources. The effluent from these sources contained elevated levels of iron, sulfate, acidity, and manganese and had a low pH. The water quality of the stream had degenerated to a point where the following parameters were reported: pH, 3.7; sulfate, 760 mg/L; acidity level, 210 mg/L.

After 22 yr, Four Mile Run still receives mine drainage with elevated levels of sulfate, iron, and manganese. However, the alkalinity and pH of the water have drastically increased to a point where the mine drainage possess a net alkalinity. The shift from acid to alkaline mine drainage is not uncommon in this region (Hedin 1993), although the factors that contribute to this change are not well understood.

Laboratory studies have shown that the rate of acid neutralization by marble chips is depressed by high ionic strength and the presence of anions such as sulfate and oxalate. These anions form relatively insoluble calcium salts. The decrease in the rate of acid neutralization is explained in terms of a static water film model.

This model has important implications beyond alkaline mine drainage. Limestone is used to neutralize effluent from mine spoils (Brady 1990) and AMD in anoxic drains (US Bureau of Mines 1992). Both of these processes are expected to have slower neutralization rates for waters with high ionic strength and elevated sulfate levels.

---

[1]Paper presented at the International Land Reclamation and Mine Drainage Conference and the Third International Conference on Abatement of Acidic Drainage, Pittsburgh, PA, April 24-29, 1994.

[2]Peter M. Jones, Student, Shawn M. Mulvay, Student, and Daryle Fish, Assistant Professor of Chemistry, Saint Vincent College, Latrobe, PA, USA.

Experimental Work

Quadruplet water samples were taken from each of the nine sampling sites on a biweekly basis during June through August 1993. Two samples from each site were acidified with HCl (pH ≤2) and refrigerated. The other two replicates were immediately analyzed for pH, conductivity, acidity, and alkalinity. Weirs were installed at sites 2-8 to determine the flow rates. The weir flow rates at sites 3-5 and 7 were checked by measuring the flows with a bucket and stopwatch. The two methods were found to differ by no more than 10%.

The pH was determined with a pH meter equipped with a combination electrode and calibrated using buffers of pH 4.00 and 7.00. Conductivities were recorded at 25°C with a conductivity meter calibrated with a 0.0100M KCl solution. Acidity and alkalinity measurements were performed as outlined in Standard Methods (Clesceri 1989).

Sulfate concentrations were determined by a turbidimetric method (Schutz 1972). Five milliliters each of sample and a conditioning reagent were added to a 100 mL volumetric flask and diluted with de-ionized water. A few crystals of $BaCl_2$ were added to the solution, and the contents were mixed for 1 min. The absorbance of the solution was measured at 420 nm and compared against known standards. The conditioning reagent was composed of 50 mL glycerol, 30 mL concentrated HCl, 100 mL ethanol, 75 g NaCl, and 300 mL of de-ionized water.

The concentrations of iron, manganese, calcium, magnesium, and sodium were determined with a flame atomic absorption spectrophotometer using the conditions shown in table 1. The metal concentrations of samples were determined from the calibration curves.

Table 1. Wavelengths and oxidant gases used in metals analysis.

Metal	Oxidant gas	Wavelength, nm
Iron	Air	386.0
Manganese	Air	403.1
Calcium	Nitrous oxide	239.9
Magnesium	Air	202.6
Sodium	Air	330.2

Neutralization studies were performed in a 1-L beaker. To the beaker were added 700 mL of de-ionized water, the appropriate quantity of salt, and a magnetic stirbar. The pH of the solution was adjusted to approximately 3 with 1/10 molar HCl. Sixty grams of marble chips were added to the stirring solution, and the pH was recorded as a function of time.

Results and Discussions

In the past 22 yr the location and flow rates of the mine drainage sites have changed. None of the drainage sites identified in the Scarlift study are known to be active along Four Mile Run (fig 1 sampling sites 52, 59, 60, 61), although the current sampling locations are in the same general area. Sampling sites 1 and 9 are the run itself, downstream and upstream, respectively, of the drainage area. Site 2 is a bore-hole drilled in 1973 as part of an exploratory study. Site 3 is the output of a wetland which is passively treating the mine drainage. Sites 4, 5, 6, and 7 are outputs from wetlands along the stream. Site 6 is fed by a number of artesian discharges 20 to 75 yd from the sampling location. Site 8 is a large artesian discharge.

The Scarlift study reported that the flow of AMD entering the stream from the original six sources averaged 213 gpm. During the summer of 1993, an average of 821 gpm of mine drainage entered the run. Recent mine subsidence upstream of the sampling area may be contributing to the higher influx of surface and ground water into the mines.

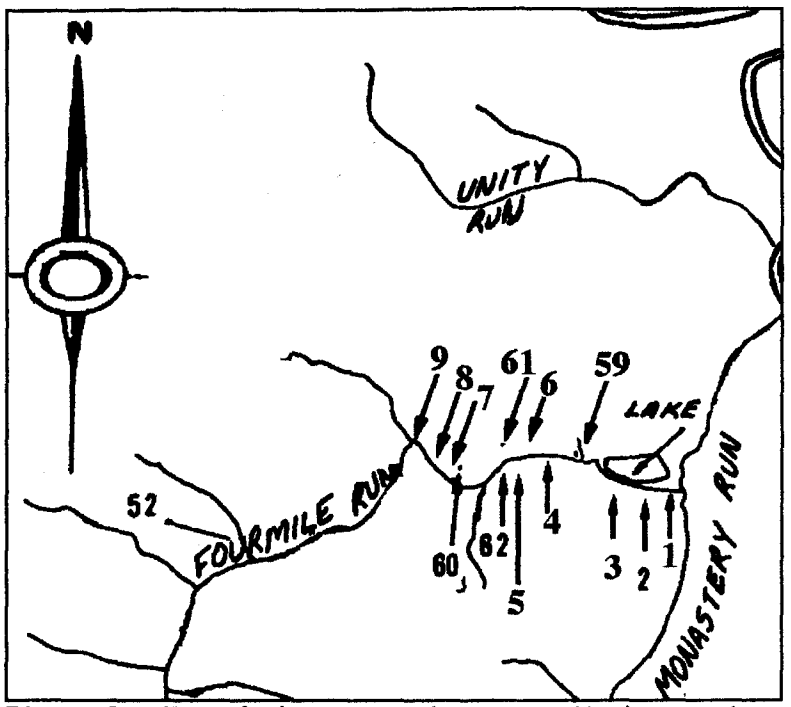

Figure 1. Map of the past and present discharge sites along Four Mile Run.

Operation Scarlift's 1971 water quality data for mine discharge sites along Four Mile Run are displayed in table 2. Except for site 53, not shown on the map, a small pond, all the effluent is quite acidic. It is plausible that the water in the pond was either neutralized by the sediments in the bottom or contained a significant quantity of uncontaminated surface water. The chemistries of the other sites are typical of AMD. The artesian like flows of these sites suggest that the mine was flooded. From the limited amount of data in the Scarlift study, it is difficult to draw many conclusions concerning the water chemistry.

Table 2. 1970 mine drainage discharges into Four Mile Run (Schutz 1972). All concentrations are expressed in mg/L.

Site	pH		Acidity		Sulfate		Iron		Manganese	
	High	Low	High	Low	High	Low	High	Low	High	Low
52	2.7	2.5	6350	1410	13600	10600	980	752	600	432
53	7.9	7.5	25	5	500	110	10	1	1	0
59	6.5	2.7	2010	825	5000	2700	574	30	60	28
60	3.1	2.5	1150	685	4400	2500	450	296	75	27
61	3.3	2.6	1225	770	6000	3750	514	164	76	44
62	3.2	2.7	1070	520	5400	3225	325	108	100	44

An overview of the current water chemistry is give in table 3. The concentrations of iron, manganese, sulfate, and acidity have declined significantly, while the pH and alkalinity have risen dramatically with respect to the Scarlift data. The mine drainage inputs from all the sources are quite hard (high concentration of Ca and Mg) and possess a large net alkalinity. The mean sulfate concentrations are 2 to 10 times larger than that predicted from the oxidation of iron pyrite, FeS_2, suggesting that the overburden is composed of sulfate containing minerals such as gypsum. The concentrations of magnesium, manganese, and sodium are fairly homogeneous from source to source, implying that they have a common origin.

Table 3. Water quality data and flow rates for mine drainage effluent entering Four Mile Run during the summer of 1993. (The data expressed as the mean ± 95% confidence limit.) All concentrations are expressed in mg/L, and flow rates are in GPM.

Site	1	2	3	4	5	6	7	8	9
pH	6.3 5±.11	6.03 ±.19	6.58 ±.13	6.35 ±.20	6.18 ±.19	5.51 ±1.7	6.06 ±.21	5.69 ±.49	7.45 ±.37
acidity	3.90 ±4.6	8.42 ±.89	0.38 ±.69	3.64 ±2.3	7.84 ±1.1	21.6 ±23	45.2 ±12	37.3 ±7.7	ND[1]
Alk.	206 ±102	381 ±112	305 ±68	262 ±79	368 ±111	247 ±247	191 ±83	286 ±94	245 ±104
SO_4	540 ±76	915 ±65	770 ±47	680 ±82	722 ±82	679 ±90	520 ±111	613 ±124	37.7 ±13
Fe	35.0 ±3.5	70.8 ±2.6	7.6 ±1.7	47.6 ±6.3	71.5 ±3.7	55.6 ±21	52.5 ±7.2	59.4 ±3.6	0.14 ±.06
Ca	184 ±13	282 ±10	263 ±7.5	262 ±8.0	258 ±8.2	234 ±23	168 ±11	188 ±12	79.5 ±6.6
Mg	64.0 ±4.3	73.0 ±3.1	77.0 ±4.8	83.7 ±2.8	83.4 ±3.4	79.4 ±5.4	67.1 ±1.3	73.6 ±3.2	27.4 ±1.7
Mn	2.93 ±.30	4.43 ±.15	2.56 ±.26	4.46 ±.15	4.08 ±.10	4.06 ±.16	3.84 ±.12	3.98 ±.11	0.10 ±.00
Na	63.1 ±4.9	95.4 ±6.5	89.0± 6.0	88.6 ±4.7	88.7 ±4.8	82.6 ±7.3	60.2 ±1.8	71.2 ±3.3	21.6 ±1.2
Flow	ND	350 ±43	26.5 ±17	25.5 ±8.4	25.5 ±8.4	140 ±57	6.5 ±5.4	235 ±256	ND

[1]ND indicates not determined.

Much of the water that currently enters the mine is most likely surface runoff entering through a large area of mine subsidence just upstream from site 8. At one spot, a culvert from the road discharges runoff directly into a subsidence pit. This would explain the large variability in discharge flow rates measured at site 8 and the lower concentration metals and sulfate in the current mine drainage.

Operation Scarlift reported that loadings of contaminates to Four Mile Run in 1970 were as follows: Mn, 38 to 77 kg/d; Fe, 120 to 400 kg/d; and sulfate 3,000 to 5,100 kg/d. The current average loadings of Mn (18.3 kg/d), Fe (273 kg/d), and sulfate (6280 kg/d) are remarkably similar. Twenty years of mineral dissolution in the mine appears to have had little impact on the current loadings. The larger volume of water currently flowing through the mine appears to be diluting the contaminants and is the main factor contributing to the lower concentrations of iron, manganese, and sulfate. The higher flow rate may also be a factor contributing to the shift from acid to alkaline mine drainage.

The capacity to neutralize the acid may have always existed, but the rate of neutralization may have been slow. To test this hypothesis, the rate of acid neutralization was studied in the laboratory. The change in pH of de-ionized water acidified with HCl and stirred over a bed of marble chips was followed with respect to time. Neutralization plots of $\ln[H^+]$ versus time were found to be linear over a pH range of 3.10 to 5.29 (fig 2). From the slope of the lines, an apparent first-order rate constant was calculated according to the following equation:

$$d[H^+]/dt = R_n\,[H^+], \qquad (1)$$

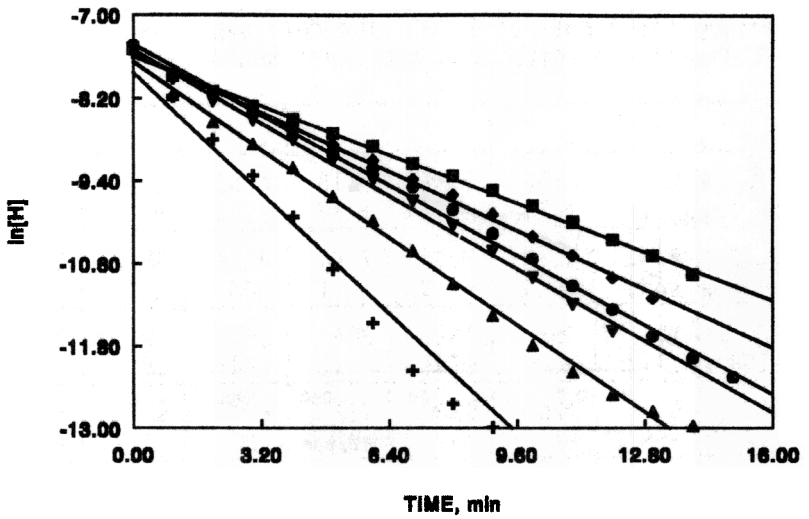

Figure 3. Plot of $\ln[H^+]$ versus time for solutions containing sulfate concentrations of (+) 0, (▲) 1600, (●) 2600 (▼) 3600, (♦) 4600, and (■) 5600 ppm.

where $[H^+]$ is the hydrogen ion concentration, t is the time, and R_n is the rate constant. pR_n, -log of R_n was found to increase linearly with increasing ionic strength (fig. 3).

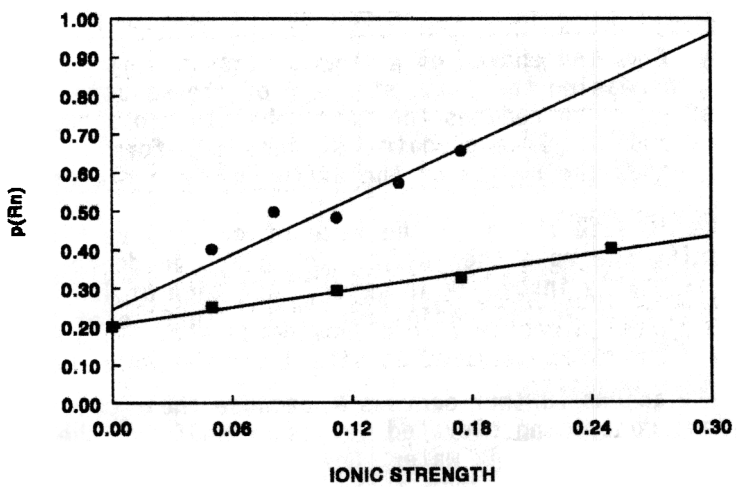

Figure 4. Plot of pR_n versus ionic strength of (●) sodium sulfate and (■) sodium chloride.

Addition of sodium sulfate depresses R_n to a greater extent than sodium chloride. In addition, pR_n was found to be a linear function of sulfate concentration with a correlation coefficient of 0.967 (fig. 4), and can be described by the following empirical equation:

$$pR_n = K\ C + pR_n o, \qquad (2)$$

where the constant K equals 7.46×10^{-5}, C is the sulfate concentration in ppm, and $pR_n o$ is -log of R_n for pure water. Addition of 6,000 ppm sulfate (Na_2SO_4) reduces R_n by about 65%. The rate of neutralization can be further depressed by elevated levels of other ions, which increase the ionic strength.

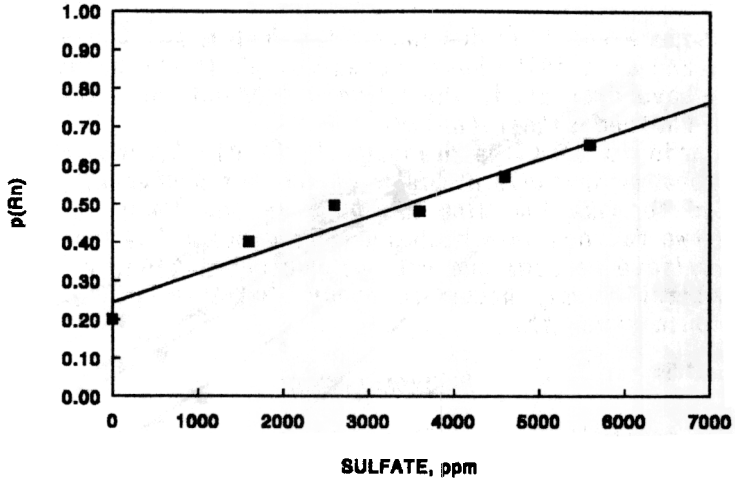

Figure 3. Plot of pR_n versus sulfate concentration for solutions of sodium sulfate.

The above changes in R_n can be explained in terms of a stationary film model. Water films are known to form at the interface between a liquid and a surface (Perry 1973). Neutralization is accomplished by the diffusion of ions through the film, and their motion can be described by the following equation (Castellan 1971):

$$l = Z e / 6 \Pi \acute{\eta} r (300), \qquad (3)$$

where l is the mobility, Z is the charge of the ion, $\acute{\eta}$ is the viscosity of the solution, and r is the ionic radius. Increasing the ionic strength of the solution increases the viscosity of the medium (Weast 1978), which reduces the ions mobility and slows the rate of diffusion. Additionally, ion pairs and larger aggregates of ions may form at higher ionic strengths (Fuoss 1959), which increases the radius of the diffusing particle and reduces its mobility.

The effect of the oxalate anion on the rate of calcium carbonate neutralization was studied to further clarify the role the sulfate ion plays in depressing the neutralization rate. Calcium oxalate is nearly insoluble in water. Addition of low levels of sodium oxalate resulted in the formation of a white precipitate on the surface of the marble chips, which completely stopped the reaction.

Sulfate and oxalate anions further depress R_n because their calcium salts are relatively insoluble. For solutions containing elevated levels of sulfate, the concentration in water film is nearly equal to that in the bulk water. However, the concentration of calcium ions in the water film should be much higher than that in the bulk water. Their concentration is governed by the K_{sp} of calcium sulfate, $K_{sp} = 2.45 \times 10^{-5}$ (Weast 1978), and the concentration of sulfate ions. With elevated levels of sulfate, the solubility of calcium ions in solution is depressed, as is the rate solubilization of limestone and R_n. Addition of oxalate anions to solution completely stops the neutralization process. The much lower $K_{sp} = 2.57 \times 10^{-9}$ (Weast 1978) of calcium oxalate severely limits the equilibrium solubility of calcium ions. The ions that dissolve quickly reprecipitate onto the chips' surface as calcium oxalate. This process is similar to armoring, which occurs when mine drainage containing elevated levels of Fe^{+3} and Al^{+3} contacts limestone (Hedin 1992). Fortunately, mine drainage does not contain significant levels of oxalate.

The depression in the neutralization rate has broader implication beyond Four Mile Run. A similar process occurs in waters flowing through anoxic drains (Brodie 1990) and mine spoils containing limestone (Brady 1990). Although elevated levels of sulfate may not severely reduce the rate of neutralization, the results of this paper suggest that the neutralization capacity of systems should be overdesigned whenever possible.

Conclusion

Four Mile Run has received mine drainage from deep mines for over two decades. In that time the flow rate, pH, and alkalinity have increased, while the acidity, iron, manganese, and sulfate concentrations have decreased. The overall loadings of iron, manganese, and sulfate to the stream have not changed significantly.

The change from acid to alkaline drainage is fairly typical for mine effluent in the surrounding area and probably involves a number of complex processes. One factor contributing to the switch from acid to alkaline mine drainage is the lower ionic strength and sulfate concentrations. These two factors have been shown to depress the rate of acid neutralization. Addition of 6,000 ppm sulfate reduces the rate of neutralization by 65%. A similar reduction in the rate of neutralization may occur in other abatement processes containing elevated levels of sulfate or ionic strength.

Acknowledgment

The authors gratefully acknowledge the financial support of this research by the U. S. Environmental Protection Agency and Saint Vincent College. Also, we would like to thank Wesley M. Gordon of the U.S. Soil Conservation Service and Gregory Phillips of the Westmoreland Conservation District for their help in identifying sampling sites and their many valuable discussions.

References

Brady, K. B. C., M. W. Smith, R. L. Beam, and C. A. Cravotta. 1990. Effectiveness of the addition of alkaline materials at surface coal mines in preventing or abating acid mine drainage: Part 2. Mine site case studies. p. 227. In Mining and Reclamation Conference and Exhibition, Charleston, WV.

Brodie, G. A., C. R. Britt, H. N. Taylor, T. M. Tomaszewski, and D. Turner. 1990. Passive anoxic limestone drains to increase effectiveness of wetlands acid drainage treatment systems. p.89. In Proceedings of the 12th Annual Conference Of The National Association of Abandoned Mine Land Programs, Breckenridge, CO.

Castellan, G. W. 1971. Physical chemistry. 2d ed. Addison-Wesley Reading, MA. p. 716

Clesceri, L.S., A. E. Greenberg, and R. R. Trussell. 1989. Standard methods for the examination of water and wastewater. 17th ed. APHA-AWWA-WPCF. p. 2-30.

Fuoss, R. M. and F. Accascina. 1959. Electrolytic conductance.Interscience. NY. p. 191

Hedin, R. S. 1993. Personal Communication

Hedin, R. S. and R. W. Nairn. 1992. Designing and sizing passive mine drainage treatment systems In Thirteenth Annual West Virginia Surface Mine Drainage Task Force Symposium.

Perry, R. H. and C. H. Chilton. 1973. Chemical engineers' handbook. 5th ed. McGraw-Hill. NY. p. 5-57.

Schutz, F. R. 1972. Operation Scarlift: mine drainage pollution abatement measures for the loyalhanna watershed study. Project SL-122, Commonwealth of Pennsylvania.

US Bureau of Mines. 1992. Abandoned mine lands program TN#12: Passive mine drainage treatment systems. Technol. News No.407.

Weast, R. C. and M. J. Astle. 1978. CRC handbook of chemistry and physics. 59th ed. CRC Press. Boca Raton, FL. p. D-266.

THE APPLICATION OF ECOLOGICAL ENGINEERING TO ACID COAL SEEPAGES IN EASTERN CANADA[1]

Margarete Kalin[2], Martin P. Smith[2] and Greg Landry[3]

Abstract: Seepages from a coal waste dump in Cape Breton, NS contain a considerable amount of iron (up to 300 mg/L) and acidity (200 to 1250 mg/L equiv. $CaCO_3$). Upon exposure to air, ferrous iron oxidizes, hydrolyzes, and precipitates, reducing the pH to 2.7. An experimental passive treatment system was developed to remove iron and acidity from the seepage water. A trench system, providing sufficient retention time for iron removal through precipitation of ferric hydroxides, was constructed. Laboratory experiments established that a phosphate-rich rock could effectively enhance iron removal from the seepage water. Consequently, two berms of phosphate rock were constructed to intercept the seepage water. Early results show some reduction in acidity and iron concentration. Water leaving the trench system enters a chemical reducing zone where, through microbial activity, alkalinity is generated and the pH is increased. Laboratory experiments established that potato waste (0.5 g/L) with sediment from the proposed reducing zone could effectively remove acidity from the seepage water. An experimental enclosure, amended with potato waste and covered with floating cattails, was set up. The results were encouraging, until retention time in the enclosure decreased below that required for the reduction process. Overall, the results show that an oxidation/reduction passive system has promise for treatment of coal-waste AMD, provided that sufficient retention time is achieved both for the iron oxidation process and its precipitation and for the alkalinity-generating process, which requires the maintenance of reducing conditions.

Additional Key Words: acid mine drainage, sulfate reducing bacteria, passive treatment.

Introduction

The Selminco Summit is a 50 ha abandoned coal waste dump near Sydney, N.S. which received waste rock from several coal mining operations from 1911 to 1973. From 1981 to 1987, a coal recovery project was undertaken on the site. Following this project, the site was graded (contoured), amended with peat and hydroseeded with a mixture of grasses. As with many mineral waste dumps, acid drainage has occurred at the Selminco Summit. The Selminco Summit has been the test site for development of a passive treatment system for acid mine drainage (AMD). The existing technology to deal with acid discharges involves chemical treatment to neutralize the water, precipitation of the metals, and discharge of an acceptable effluent to the environment. Treatment is required in perpetuity; hence passive systems are of interest, as they would offer a low-cost, low-maintenance method of AMD treatment.

Site Description

The elevation of Selminco Summit is lowest at the southeast section of the site, an area bounded by a rail line and a ditch, along which acidic seeps occur. The drainage from the site was characterized by elevated metals (particularly Fe and Al), high acidity, and low pH.

---

[1]Poster presented at the International Land Reclamation and Mine Drainage Conference and the Third International Conference on the Abatement of Acidic Drainage, Pittsburgh, PA, April 24-29, 1994.

[2]Margarete Kalin, Ecologist and Martin P. Smith, Ecologist, Boojum Research Limited, Toronto, Ontario, Canada.

[3]Greg Landry, Environmental Engineer, Cape Breton Development Corporation, Sydney, Nova Scotia, Canada.

The development of a passive system started with construction of a drainage collection system (fig. 1), a series of three precipitation cells, and two cells for establishment of chemical reducing conditions for acid reduction (Mills et al. 1989, Cairns et al. 1991, Kalin and Smith 1991, Kalin 1993). The precipitation cells have a mean depth of 1.3 m, a total volume of 2,910 m^3 and a retention time of 10.7 to 53 days, depending on flow rate. The two reduction cells have areas of 4,000 and 1,600 m^2, depths of 0.3 to 1.0 m, and estimated retention times of 0.6 to 6.8 and 0.5 to 18.4 days, respectively, depending on flow rate.

Problems were encountered due to highly variable runoff flows. For example, rain and snow melt caused excessive flows, which caused damage to berms. A freshwater runoff diversion system was installed to reduce peak flow rates. However, seepage was still entering the precipitation cells from the bottom, and natural precipitation rates were insufficient to remove most of the iron. In 1992, phosphate rock was added to the second and third precipitation cells to help precipitate iron and aluminum. A batch reducing enclosure was constructed to demonstrate the feasibility of scaling up the microbial alkalinity process to the entire reducing cell area. Potato waste was added to the enclosure to enhance the bacterial activity, and floating cattail mats were installed as a cover. The configuration of the system is shown in fig. 1.

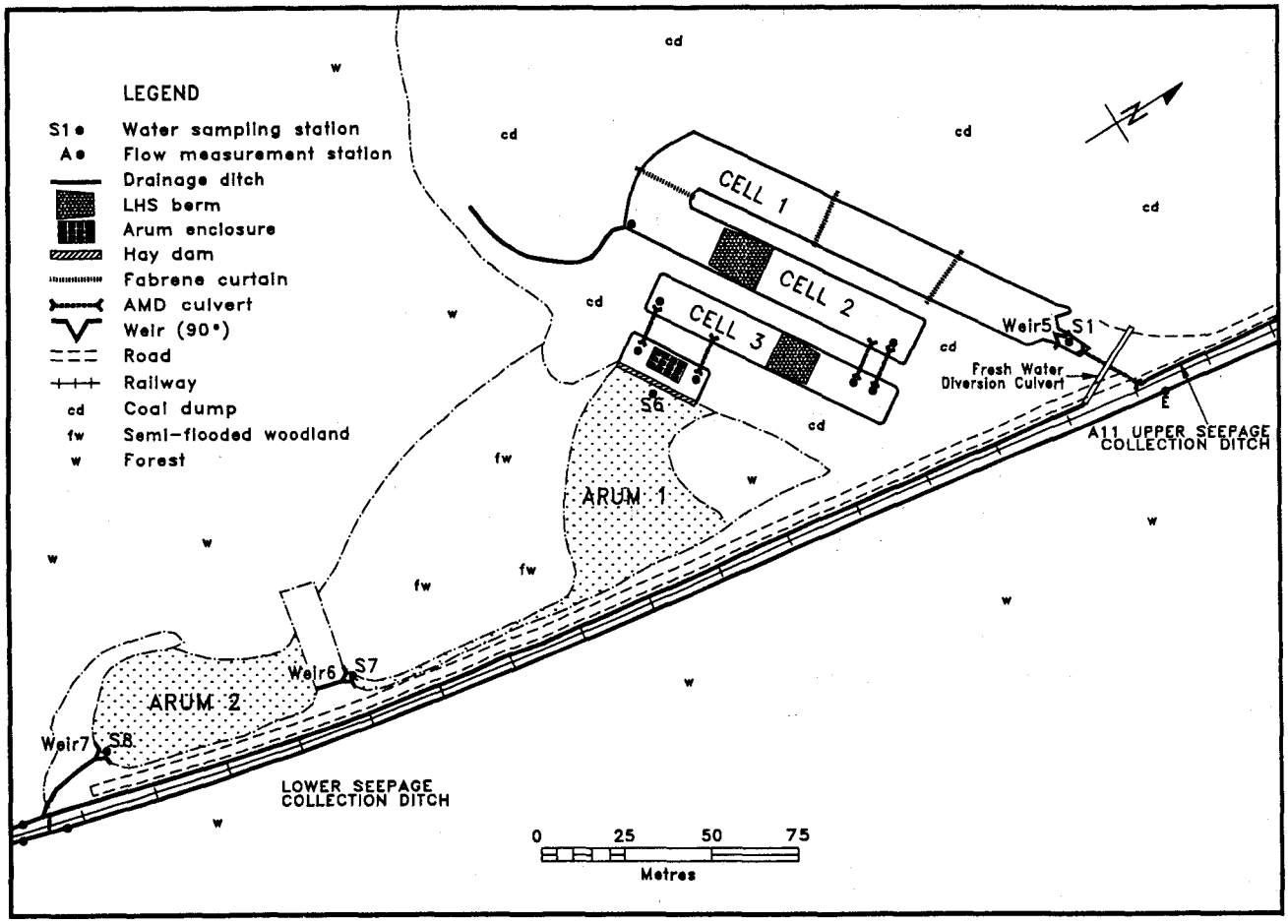

Figure 1. Layout of the Selminco Summit test cell system. Station S-1 is the inlet to the system. Cells 1, 2 and 3 are the precipitation cells. Station S-6 is the inlet to the reducing cells. Station S-8 is at the discharge from the system.

Methods and Materials

Field and Laboratory Methods

Standard methods were used for determination of redox potential (reported as E_m) and pH. Acidity and alkalinity were determined by manual titration with NaOH and H_2SO_4 or with a Metrohm 702 SM Titrino autotitrator to end points of 8.3 and 4.5 respectively. Iron was determined by inductively coupled plasma spectrophotometry (ICP), U.S. EPA method 200.7 at certified laboratories. The presence of sulfate reducing bacteria was determined in the field using an immunological assay (Rapidchek II, Conoco Ltd) that determines the presence of adenosine phosphosulfate reductase, an enzyme specific to this group of bacteria.

Laboratory Phosphate Rock Experiment

A laboratory experiment was carried out to study the chemical reactions between phosphate rock and the seepage water to help determine whether phosphate rock could be usefully applied in the field. The results of the laboratory experiment assisted the development of design parameters for construction of berms in the test cells. A phosphate-rich gravel (natural phosphate rock, Texasgulf) with a diameter of 3 to 5 mm was employed for the experiment. Three litres of natural phosphate rock (NPR) were packed into an acrylic column (i.d. 15 cm, height 42 cm). To prevent concretion, 1 L aliquots of NPR were separated by 1 L of polystyrene chips. Precipitates could settle into the void spaces of the polystyrene layer. The column was comprised of six 6-cm-thick layers. The column was suspended in an acrylic outer sleeve. Water level was controlled by an overflow port in the outer sleeve. The water level was maintained just above the top of the upper NPR layer. Water was pumped from a feed tank at a rate of 3 L/day. The inner column had a turnover time of 0.8 days. Water drained from the inner to the outer sleeve. The inner + outer sleeve had a total turnover time of 6.8 days. Water overflowed from the outer sleeve into a series of settling tanks.

Field Experiment

In late July 1992, two permeable berms were constructed, using railway ballast rock, across cell 2 and cell 3 of the precipitation system (fig. 1). Each berm was approximately 16 m long, rising from the bottom of the cell (1.3 m deep) to just above water level. All the water that passed through the cells had to pass through the berms. Sampling tubes were inserted into the berms at the time of construction to enable water samples to be taken from within the structures.

Unprocessed NPR was used because it was available from a nearer location than the processed Texasgulf material used in the laboratory column experiment. This material was spread over the upstream face of the berms to a depth of 8 cm. A total of 16 mt was applied to each berm.

Flow Rates

Flow rates were measured at various points through the system. There was a large seasonal variation in flows due to the contribution of runoff. Measured flows at station S-1 (inlet to system) ranged from 16 to 366 m^3/day with lower rates (< 50 m^3/day) in winter and much higher (and variable) rates (>200 m^3/day) in early winter and in spring. A runoff diversion was installed in July 1992, but there are no data at this point indicating whether the diversion system has, in fact, decreased the flow variation. Visually, the flow through the system appears to have stabilized.

Results and Discussion

Water Chemistry

Seepage water at the Selminco Summit contains iron, sulfate and aluminum, and it emerges from the waste pile at pH's between 3.6 and 4.5, with high acidity. When the seepage water flows into the system, the process of iron oxidation (from ferrous to ferric) begins, iron precipitates as ferric hydroxide, and the pH is further decreased.

$$4Fe^{+2} + 10\ H_2O + O_2 \rightarrow 4\ Fe(OH)_3 + 8H^+ \qquad (1)$$

Chemical analysis has been done on water samples collected at various points in the system. Table 1 shows the yearly average for several parameters since the construction of the system in 1989. The data indicate aluminum and iron are precipitating, and that pH decreases to about 2.9 at station S8.

Table 1. Selminco Summit water chemistry, 1989-93.

	Acidity, mg/L			Fe, mg/L			Al, mg/L			SO4, mg/L			pH		
Year	S-1	S-6	S-8	S-1	S-6	S-8	S-1	S-6	S-8	S-1	S-6	S-8	S-1	S-6	S-8
1989	610	403	342	52	38	39	40	27	30	1,150	993	913	3.19	3.14	3.02
1990	637	490	404	141	83	63	61	51	42	1,725	1,398	1,113	3.68	3.42	3.27
1991	798	635	531	197	87	49	56	44	37	2,091	1,557	1,400	3.61	3.23	3.20
1992[1]	705	266	247	114	35	25	40	14	12	1,927	785	751	4.12	3.60	3.17
1992[2]	754	499	384	93	35	20	35	29	25	1,690	1,395	1,114	3.30	2.76	2.72
1993	815	555	484	169	64	38	29	21	19	1,737	1,660	1,344	3.56	3.17	2.95
Average	720	475	399	128	57	38	44	31	28	1,720	1,296	1,106	3.58	3.22	3.06

[1] Before placement of phosphate berms.

[2] After placement of phosphate berms.

Phosphate Rock Tests

Phosphate rock was tested as a means of precipitating iron and aluminum and raising pH. This is achieved through the following reactions:

$$PO_4^{-3} + Fe^{+3} = Fe\ PO_4 \qquad (2)$$

$$PO_4^{-3} + Al^{+3} = AlPO_4 \qquad (3)$$

$$PO_4^{+3} + H^+ = HPO_4^{-2} \qquad (4)$$

$$HPO_4^{-2} + H^+ = H_2PO_4^- \qquad (5)$$

$$H_2PO_4^- + H^+ = H_3PO_4 \qquad (6)$$

Reactions 2 to 6 proceed in sequence. Once the iron and aluminum precipitation reactions have taken place, the pH will rise owing to the formation of phosphoric acid. This phosphate is then consumed by biological processes. The results of the column experiment are presented in fig. 2 and fig. 3. The bench-scale system was very effective and demonstrated that phosphate rock has the potential to treat Selminco seepage water.

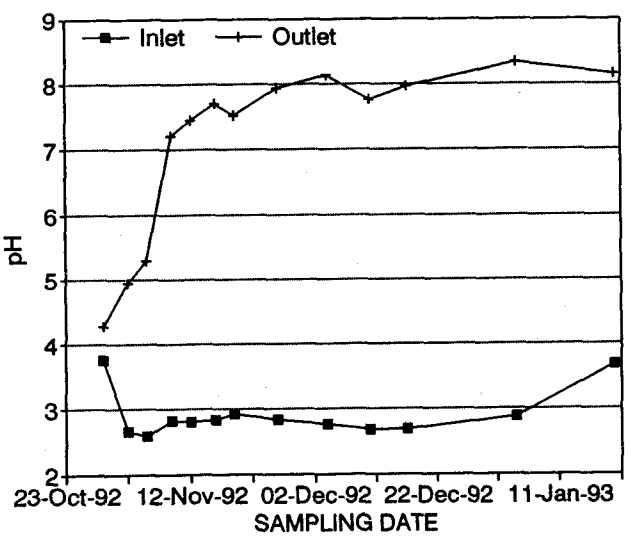

Figure 2. Solution pH at inlet and outlet of phosphate rock laboratory column experiment.

The field berms were installed in July 1992. An initial short-term impact was noted, but the effect was short-lived, as is evident in fig. 4. The reasons for the poor initial performance may have been low contact time between the rock and water and/or low permeability of the material. Since the installation of the berms, a high percentage of the iron is being removed within the system, but this removal cannot be solely attributed to the phosphate rock, owing to other changes in the flow regime, including the installation of a fresh water diversion system.

The Reducing Cells

Laboratory jar experiments demonstrated that when 0.5 g/L potato waste was added to sediment from the reducing cells, the pH increased from 2.7 to nearly 5 (fig. 5). When 10 g/L potato waste was added, pH increased to 7. Addition of potato waste also caused the E_m to drop dramatically (fig. 6) and reduced the water's acidity (fig. 7). This sediment from the reducing cell had received, in previous years, an organic amendment (hay bales) to cover the accumulated iron precipitate. The decomposition of potato waste led to a drop in E_m and provided energy sources for bacteria whose activity mediated the pH increase and removal of acidity.

The results of these tests led to the construction of an enclosure in the first reducing cell in September 1992. This enclosure contained a water volume of 40 m^3. Potato waste was added (3.75 g/L) and the water surface was covered with 12 floating cattail rafts which had been established in 1991. After about 6 weeks, the acidity within the enclosure was substantially lower than the acidity outside (fig. 8). This pattern continued until mid-December, when the differences in water quality between the inside and outside of the enclosure were no longer apparent. It is not clear why the enclosure failed, as other enclosures have remained active for 1,200 days (Kalin 1992).

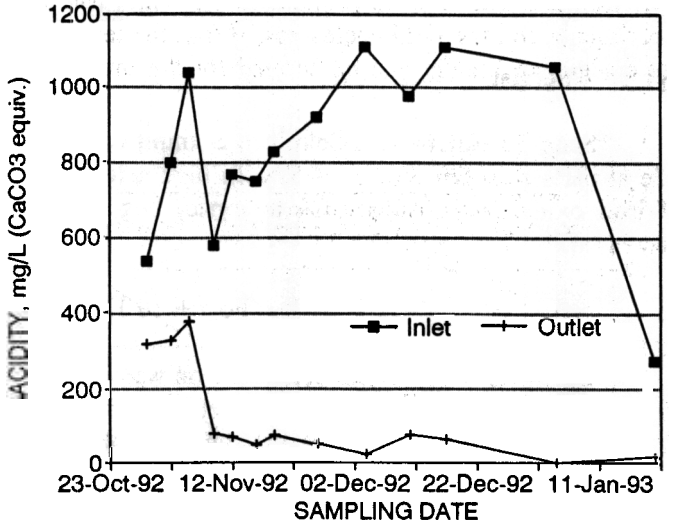

Figure 3. Solution acidity at inlet and outlet of phosphate rock laboratory column experiment.

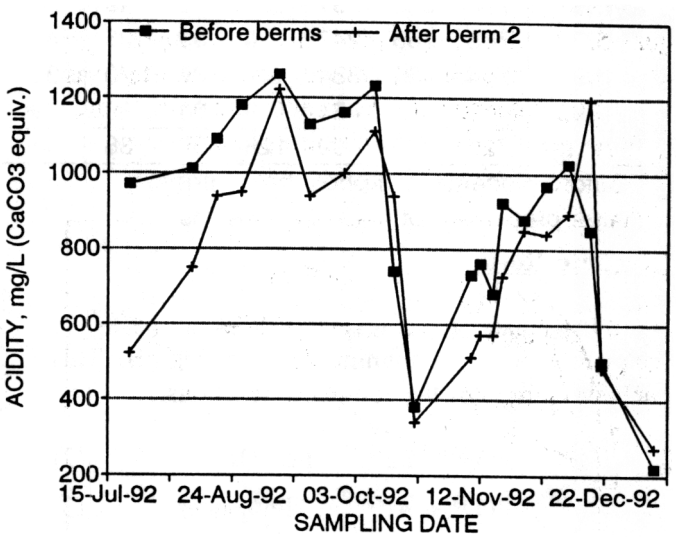

Figure 4. Acidity of water before berms and after berm 2 in Selminco Summit test cell system.

Conclusions

Through the development of a passive treatment option for the coal seepage over the 4 yr period, it became evident that flow control is essential in order to design the iron oxidation-precipitation ponds with adequate retention time. Although natural phosphate rock might be effective in assisting in removal of iron and aluminum, this field test indicates that placement methods and grain size must be more rigorously controlled for a successful application.

After iron and aluminum precipitation, alkalinity can be generated microbially, as demonstrated by the laboratory experiments and the field enclosures. From the test work carried out on-site and in the laboratory, it is anticipated that design parameters can be derived for the implementation of a passive treatment system.

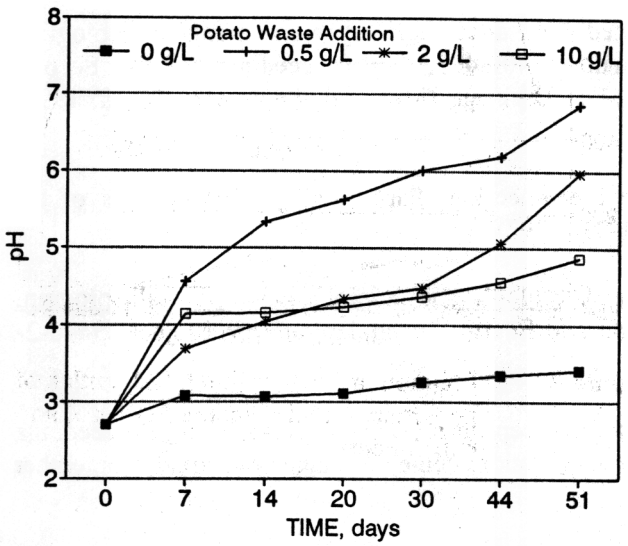

Figure 5. Solution pH in laboratory jar experiment where potato waste was added to Selminco Summit water overlying reducing cell sediment.

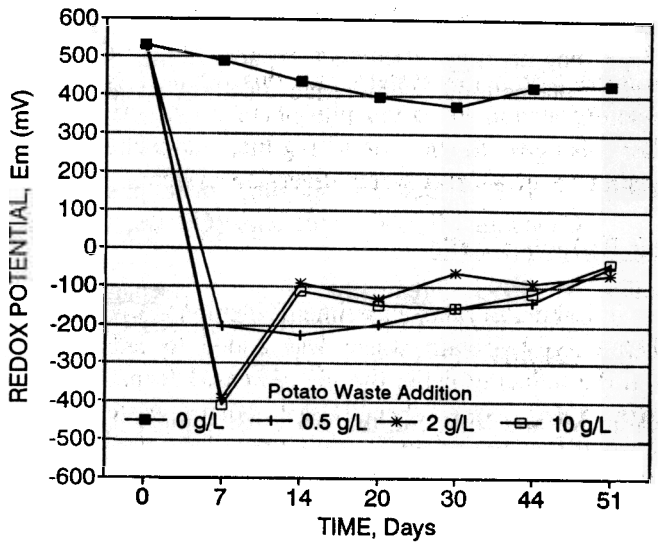

Figure 6. Solution redox in laboratory jar experiment where potato waste was added to Selminco Summit water overlying reducing cell sediment.

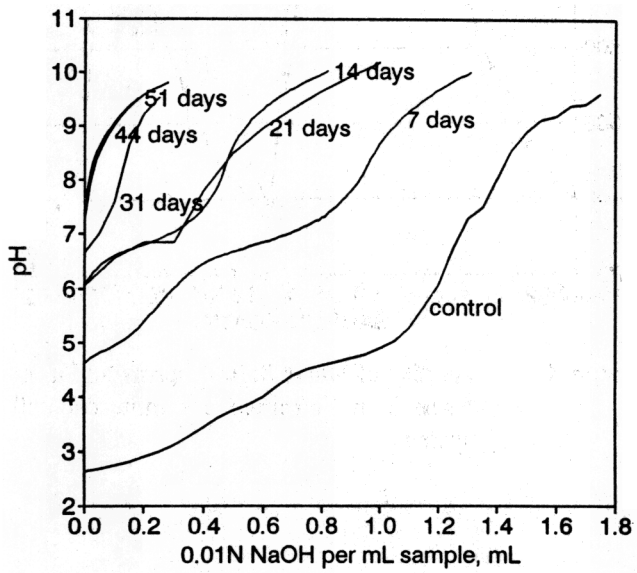

Figure 7. Acidity titration curves for solutions sampled from the laboratory jar experiment where potato waste was added to Selminco Summit water overlying reducing cell sediment.

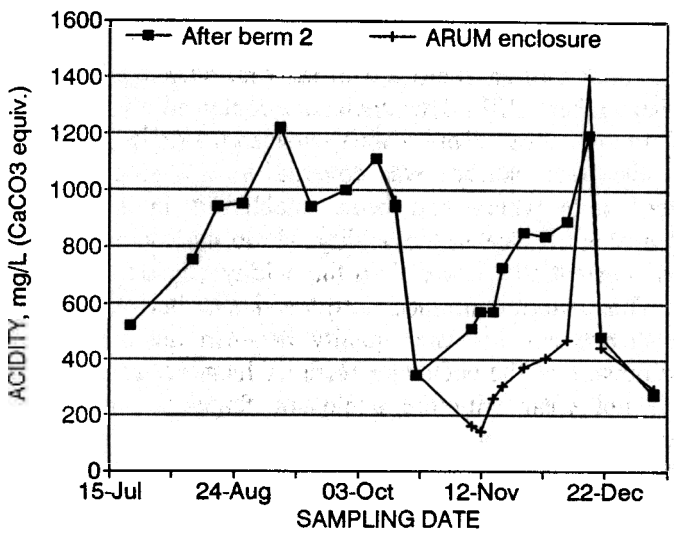

Figure 8. Solution acidity in enclosure constructed in the Selminco Summit test cell system.

Acknowledgment

The support of this project by the Cape Breton Development Corporation is greatly appreciated.

References

Cairns, J. E., R.G.I. McCready and M. Kalin. 1991. Integrated field and laboratory experiments in ecological engineering methods for acid mine drainage treatment. p 409-425. In Proceedings of the Second International Conference on the Abatement of Acidic Mine Drainage (Montreal, September 16-18, 1991) v.2.

Kalin, M. 1992. Decommissioning open pits with ecological engineering. Paper 27. In Proceedings of the Canadian Mineral Processors (Ottawa, Ontario, Jan 21-23, 1992).

Kalin, M. 1993. Treatment of acidic seepages using wetland ecology and microbiology: Overall program assessment. Final Report for Canada Centre for Mineral and Energy Technology, EMR Project 23440-2-9217/01-SQ, Ottawa. 57 pg.

Kalin, M. and M.P. Smith. 1991. Biological amelioration of acidic seepage streams. p 355-368. In Proceedings of the Second International Conference on the Abatement of Acidic Mine Drainage (Montreal, September 16-18, 1991) v.1.

Mills, A. L., P.E. Bell and A.T. Herlihy. 1989. Microbes, sediments and acidified water: The importance of biological buffering. p 1-19. In Acid stress and aquatic microbial interactions. S.S. Rao (ed.) CRC Press, Boca Raton, FL.

IN SITU TREATMENT OF ACID MINE DRAINAGE BY SULPHATE REDUCING BACTERIA IN OPEN PITS: SCALE-UP EXPERIENCES[1]

Nural Kuyucak[2] and Pascale St-Germain[2]

Abstract: Over the past three years, Noranda Technology Centre (NTC) has evaluated the feasibility of using sulphate-reducing bacteria (SRB) to treat acid mine drainage (AMD), in a pit or an underground mine. Following an initial study conducted in batch flasks that determined major process parameters (residence time, temperature effect, nutrients and substrate requirements), a conceptual flow sheet was developed. In order to confirm the concept for full-scale application, the present study included screening and selection of inexpensive nutrients and larger scale tests in a 280-L drum, a 160-L tall column and 5-L continuous reactors. The start-up conditions examined with drum tests included sediment formation (reactor inoculation methods and nutrient preconditioning), influent location and final effluent quality (e.g. metals, pH, BOD, COD, odor, etc.). The tall-column test (5 m) was conducted to define the reaction zone and the extension of H_2S dispersion in the pit. Nutrient utilization and S balance were estimated by monitoring off gases in 5-L continuous reactors as well as effluent quality. Due to the low SO_4 conversion rate found at low temperatures (e.g. 4 to 10°C), which is found in the bottom of the pit, the amount of nutrients required to treat moderate strength AMD with a high flow rate was determined to be very high, causing technical and economical difficulties in full-scale application of the process. The process was recommended for low loading situations.

Introduction

In general, sulphide precipitation offers some advantages over conventional hydroxide precipitation which is more commonly used for treating acid mine drainage (Bhattacharryya *et al.* 1981; Kuyucak *et al.* 1991) . These advantages include a high degree of metal removal (e.g. Cu, Cd, Zn, Pb, As, Hg, Ni and Fe) at low pH (pH 3 to 6) and improved sludge characteristics, i.e. chemically more stable, denser and less voluminous sludges (Peters and Ferg 1987). However, the high cost of sulphides discourages their use in treating AMD. Several researchers have proposed the use of sulphate reducing bacteria to obtain inexpensive sulphide reagents, due to their ability to convert sulphate contained in AMD to H_2S (Hammack and Edenborn 1992). During the process, SRB utilize a carbon source and generate alkalinity (Kuyucak et al. 1991). The hydrogen sulphide generated reacts with metals to form insoluble metal complexes. The organic carbon is converted to carbonates. The reactions are shown below:

$$2\,H^+ + SO_4^{2-} + 2CH_2O \xrightarrow{SRB} H_2S + 2\,HCO_3^- \qquad (1)$$

$$H_2S + M^{2+} \text{-----}> MS\downarrow + 2\,H^+ \qquad (2)$$

CH_2O represents the organic compounds used as nutrients and M represents metal ions.

---

[1]Paper presented at the International Land Reclamation and Mine Drainage Conference and the Third International Conference on the Abatement of Acidic Drainage, Pittsburgh, PA, April 24-29, 1994

[2] Noranda Technology Centre, 240 Hymus Blvd., Pointe Claire, Quebec, H9R 1G5

Several investigators have been exploring SRB processes as a possible basis for the development of cost-effective treatment for wastewaters, which have high acidity and contain sulphate and metal ions. Possibilities include passive systems for treating mine effluents (e.g. constructed wetlands, biotrenches and open pits) and reactor applications for treating metallurgical process effluents (Hedin and Nairn 1992; Kalin 1992; Wildeman 1992; Barnes *et al.* 1991; Béchard *et al.* 1991; Maree and Strydom 1987).

The results of earlier work (Phase I) at NTC, in which pure chemicals were used as nutrients, indicated that open pit application of the process would be technically feasible if the open pit could be well manipulated to be used as a large reactor (Kuyucak et al. 1991). The process economics would be basically dependent on the cost of nutrients and the degree of achieved treatment. Further research (Phase II) has, therefore, been undertaken to investigate alternative/inexpensive nutrient sources for SRB, and the parameters required for a successful process start-up and scale-up for field demonstration of the process. In addition, the technical and economical feasibility of the process were assessed and the key questions to be addressed were defined. The results of Phase II studies are discussed below.

Materials & Methods

Nutrients and Water. Selection of alternative nutrient sources was performed on two main groups of waste materials: cellulosic wastes and organic wastes. The cellulosic wastes consisted of: wood pulp, sawdust, bark, maple leaves, oat straw, fuel peat and horticultural peat. The organic wastes included: cow manure, distillers' dried grains, brewers' dried grains, dehydrated whey, molasses and starch. Combination of wood pulp, manure and brewers' dried grains was retained for all other tests. In control tests to assess the ability of the nutrient types to support SRB activity, chemical nutrients such as lactic acid (15 g/L), $(NH_4)_2SO_4$ (1.8 g/L) and K_2HPO_4 (0.35 g/L) were used. Moderate strength AMD (F-Group) was used for the tests (Kuyucak & St-Germain, 1994).

Substrate. In nutrient selection experiments, the substrate consisted of limestone and sand, in a mixture of 1:1. In scale-up parameters tests, the substrate was simply limestone. Materials examined as substrate alternatives in 2-L batch tests were: limestone, phosphate, limestone and sulphidic rocks in a ratio of 1:1, sulphidic rocks and wood chips. In another batch test, the position of nutrients vs substrate and its effect on the treatment efficiency was addressed. Mainly, three distributions were evaluated: nutrients on top of substrate, mixed and nutrients sandwiched between 2 layers of substrate.

SRB Inoculum. SRB enriched from mine sediments, as described earlier (Kuyucak *et al.* 1991), were used in all studies. The inoculum was 1% of the working water volume. In one batch test, which studied the effect of inoculum size on treatment efficiency, different inoculum proportions were added: 0.1, 1, 3, 5 and 10%. In parallel, two different inoculation techniques, i.e. pouring vs injection, were looked at. In this experiment only 0.1, 1 and 10% inoculum were studied.

Temperature. Effect of temperature on the process was addressed in two tests: at start-up, in 2-L batch tests where reactors were kept at either 20, 10 or 4^{0}C, and 5-L continuous kinetic tests where reactors were kept at room temperature and 10^{0}C.

Procedures

Different types of reactors and experimental modes were used in each study. All batch studies, including nutrient experiments and start-up parameters (solid substrate, inoculation technique and start-up temperature), were performed in 2-L reactors, usually for a 35-day period. Larger size reactors (e.g. 5-L, 280-L drum and a 5-m high, 160-L tall column) were used in continuous mode to investigate process kinetics and major parameters for process scale-up. All tests were run in duplicates. The pH was adjusted to 4.5-5, using $Ca(OH)_2$. In general, reactors consisted in a gravel (limestone) sediment inoculated with SRB (1%

v/v) on which the nutrient was layered at the bottom of each reactor. The reactor, after filled with AMD, was left until the onset of SRB activities was confirmed by an increase in pH, decrease in ORP, dark color and distinct odor of hydrogen sulphide. Once the system was established, fresh AMD was added in a semi-continuous or continuous mode as required. Details of procedures and analytical methods are described elsewhere (Kuyucak and St-Germain, 1993).

Results

Nutrient Selection

Initial experiments involved investigations of cellulosic wastes as sole nutrients for SRB. Results indicated that cellulosic wastes alone would not sustain SRB growth. Therefore, use of a mixture of wood and organic wastes was considered. Subsequently, organic and cellulosic wastes were analyzed for their C, N, and P content and were mixed with each other in order to obtain optimum C:N:P ratio of 110:7:1, which would support high SRB activity (Gerhardt 1981). Several combinations of cellulosic and organic waste materials were examined.

The mixture of wood pulp, manure and brewers' dried grain exhibited the closest results to those obtained from the control tests containing lactic acid, ammonium sulphate, and potassium biphosphate salts as nutrients (Figure 1).

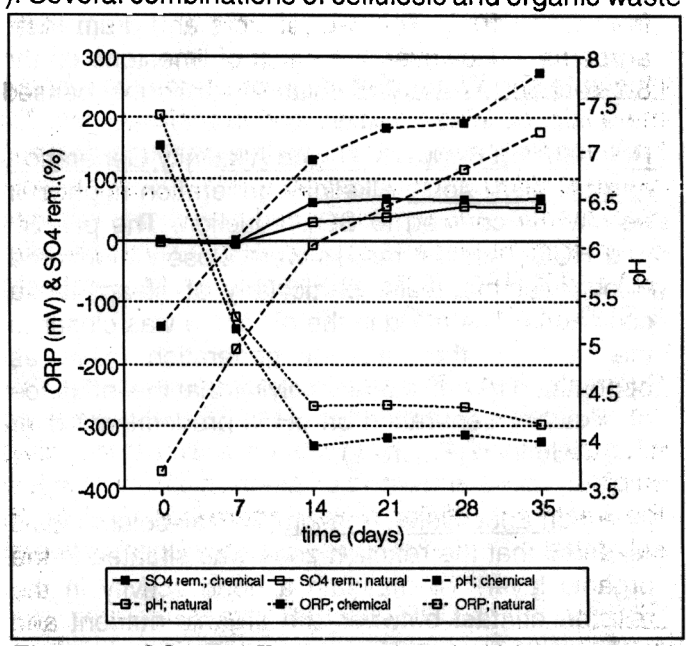

Figure 1 SO_4 and Zn removal and pH increase with the use of the mixture of woodpulp, brewers' dried grain and manure vs. lactic acid, ammonium sulphate and potassium biphosphate.

Process Parameters Investigated for Start-up

The optimal conditions required for a successful process start-up in the pit were investigated in conjunction with the use of natural nutrients (wood pulp, manure and brewers' dried grains). The parameters examined were: type of materials to be used and ways of preparing the sediment layer; need for SRB inoculum and the manner of addition; and effect of temperature and the possibility of acclimatization, as described by Ahonen and Tuovinen (1989).

Type of Sediment and Sediment Layer Preparation. Phosphate rocks and limestone gravel proved to be preferable to wood chips or sulphidic rocks, but the latter can be used. When limestone was mixed with sulphidic rocks, the process was significantly improved. When wood chips and sulphidic rocks were used alone, the increase in pH was delayed by 16-18 days, However, as time went by, indicating that a wide range of materials, particularly with a large surface area, proper permeability, and buffering capacity can be used to form the sediment layer; the process is not limited by the type of material.

Effect of Inoculum Proportions and Inoculation Method. SRB inoculation would be essential to obtain positive measurable differences in process parameters in a reasonable time frame. Based on SO_4 removal and ORP results, the optimum SRB inoculum is 1% and injection of the SRB inoculum is better than pouring it.

Effect of Start-up Temperature. Only the tests initiated and performed at room temperature showed SRB activity after 42 days, as observed by relatively high SO_4 removal, as well as significant metal removal, as

compared with results from 10 and 4°C incubation. Experimental results showed that start-up temperature was very important, as well as the incubation temperature of the inoculum, in facilitating the process start-up.

Investigations of Parameters for Process Scale-up (5-L Reactors, Drum and Tall Column Tests)

Rate of Sulfate Reduction and Effect of Temperature. The results showed that there is a relationship between rates of sulphate reduction, metal removal and dissolved organic carbon present in the system. Alkalinity generation could not be directly coupled to SO_4-reduction, since in some cases no increase in pH was observed with the increase in net SO_4 removal. At steady state, SO_4 removal rates reached about 300 mmol/m^3/d for a retention time of 280 days in the drum or 61 days in the nutrient bed. Only under reduced conditions were all metals, except Mn, removed to very low levels indicating S^{2-} precipitation. The total amount (mol) of SO_4 reduced was in excess of total amount (mol) of metals removed.

There was a decrease in SO_4 reduction rate of 43% reduction when the temperature decreased from 20 to 10°C. The total organic carbon (TOC) concentration was reduced by half by a decrease in temperature from 20 to 10°C. The 5-L reactors and drum test results with regard to sulphate reduction rates were in agreement. However, the effect of limestone on the overall process performance was more pronounced in 5-L reactors since AMD relatively uniformly passed through the gravel layer in those reactors.

Relationship Between S^{2-} and Alkalinity Generation and pH Behaviour. Alkalinity generation might not be directly coupled to SO_4 reduction. The pH, S^{2-} and HCO_3^- concentrations were closely monitored throughout the tests, particularly at steady state conditions. The trend in the pH curve was closer to the trend in the alkalinity generation curve as opposed to the S^{2-} curve, implying that the influence of alkalinity generation on pH is predominant over SO_4 reduction (Figure 2).

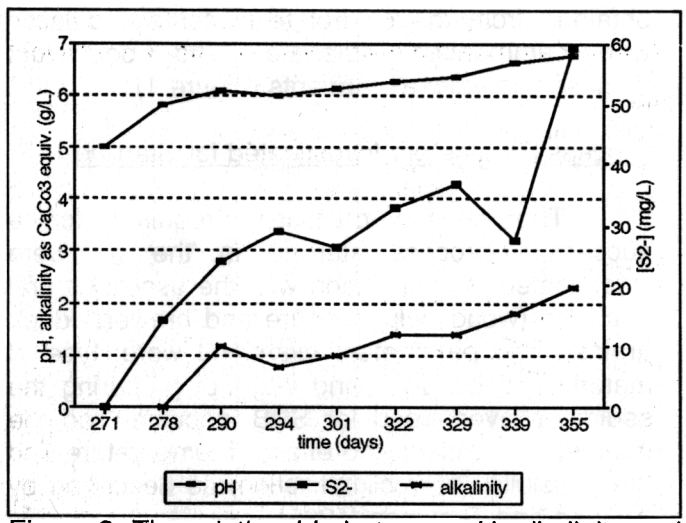

Figure 2 The relationship between pH, alkalinity and S^{2-} generation

Reaction Zone Determination. The tall-column tests revealed that the reaction zone was situated in the organic layer. To maintain a good activity in the reactor, contact between the organic nutrient and water to be treated was required. Resuspension of the nutrient bed (Kuyucak & St-Germain, 1993), which also simulates turnover in pits, resulted in improved metal removal and homogeneous distribution of bacteria in the nutrient bed.

Importance of Surface Area to Volume Ratio. The results showed that to get a true representation of the SO_4 reduction rate, retention time in the bed volume must be taken into consideration. However, when comparing drum with tall column tests, the maximal use of the nutrients can only be ensured by the presence of a large surface area (provides better contact for nutrients bacteria and AMD). In a small area and high depth case, uniform flow distribution within the nutrient bed cannot be maintained and the process efficiency declines.

Effect of Treatment on Water Quality. The effluent quality obtained from the SRB process for 14 months is summarized in Table 1. The concentration of Al, Fe and Zn fluctuated between non-detectable by ICP to 10-20 mg/L, depending on the conditions. Under oxidized conditions, the system would release Zn, Fe and Al. In particular, the Zn concentration follows the SO_4 reducing activity very closely. Mn removal was always poor. As, Cd and Cu were reduced to undetectable levels under all circumstances.

Table 1: Metal and sulphate concentrations in the effluent taken from the drum (operated for 14 months)

Parameter (mg/L)	Initial AMD (average)	Quality of effluent at different time intervals (days)										
		35	66	96	125	159	226	245	259	308	370	431
pH	2.5	6.8	6.6	6.6	6.4	6.2	5.2	4.8	5.4	6.3	6.8	6.4
Al	173	0.44	0.18	0.3	0.36	0.37	1.1	1.8	nd	nd	0.45	0.51
As	1.0	nd	0.09	nd	nd	nd	nd	nd	nd	nd	nd	nd
Cd	1.5	nd	nd	nd	nd	nd	0.05	0.04	0.04	0.04	nd	nd
Cu	47	nd	nd	nd	0.04	0.04	0.17	0.072	0.05	nd	nd	nd
Fe	160	0.74	0.19	0.69	0.76	4.77	2.66	8.99	1.12	0.19	0.54	0.13
SO_4	4000	1682	1721	2837	3720	3360	3450	2989	2989	2490	2524	2460
Mn	38	1.11	6.99	13.5	21.5	23.6	21.1	25.3	26.0	24.3	21.8	19.5
Zn	350	0.38	nd	11.4	1.44	1.33	12.8	0.01	18	nd	0.27	nd

Organic indices such as TSS, VSS, BOD, COD, TOC, TKN and TP were also analyzed as described in Standard Methods (APHA, AWWA, WPCF. 1989) for the final effluent (Table 2). The comparison of results of the filtered vs, unfiltered samples for a few heavy metal ions showed that for all metals except Fe, the difference was not significant implying that metals are not in the colloidal form in the effluent and that additional filtration will not be required in full-scale applications.

Table 2: Effluent Quality in Terms of Organic Parameters

Time of sampling (days)	Organic Parameter as Concentration (mg/L)						
	TSS	VSS	BOD	COD	TOC	TKN	TP
257[1]	156	35	30	79	27.2	28.1	< 0.05
319[2]	80	47	84	260	123	26	0.12

[1] quality of water before the addition of fresh nutrients
[2] quality of water after the addition of fresh nutrients

Effect of Influent Addition Method. The use of a baffle to introduce AMD over the sediment resulted in constant fluctuations in pH, with the general trend decreasing in the long-term. However, the baffle concept can be used, particularly on a pulsed flow. Adding influent through a tube (subsurface flow) in the sediment seemed to favor a more constant trend from day to day implying that better contact was provided between the influent, the nutrients and SRB.

Nutrient Consumption Rate. The C (available in the nutrient) utilized for the amount of sulphate reduced was computed per day using eq. 1. The theoretical nutrient consumption rate for the first 215 days at 20°C was 0.07%/d. Later, it decreased and stabilized around 0.05%/d. However, the actual value may be higher.

Composition of Off-Gases. The qualitative analysis of gases produced at 20°C showed that the gas was composed of 1.5% CO_2 and 98.5% N_2/O_2 on average. Minor amount of CH_4 (e.g. 0.023%) and no H_2S was detected. When the reactor was transferred at 10°C, CH_4 stopped being generated, indicating that activity

of methanogens was disturbed. The switch from batch to continuous mode resulted in an increasing trend in CO_2 and CH_4 concentrations and an inversely decreasing trend for N_2/O_2 content.

Discussion

General Concept. The increase in alkalinity and removal of metals from AMD with the SRB process are the result of several chemical and biological reactions. Synergism between three groups of microorganisms (acidogens, methanogens and sulphate reducers) and anaerobic conditions are essential for biochemically converting organic materials to organic acids (Tuttle *et al.* 1969; Westrich and Berner 1984; Holder *et al.* 1984; Maree and Strydom 1987; Kuhl and Jorgensen 1992; Scheeren *et al.* 1992). In addition to anaerobic and reduced conditions, oxygen may also be required to break down complex organics and oxidize CH_4 formed in the system (Morel 1983). The incorporation of additional limestone (even gypsum) into the reactors was suggested to boost the rate of alkalinity generation by buffering influent acidity, thereby allowing sulphate reduction to occur uninhibited at higher influent acidity loads (Hedin *et al.* 1991; Dvorak et al., 1991). At low temperatures, the rates of chemical and biochemical reactions are reduced, resulting in less alkalinity and H_2S generation. The cellulose decomposers (methanogens) are mainly mesophillic microorganisms and, consequently, are more sensitive to low temperatures than SRB.

Critical Parameters at Process Start-up and During Operation. At process start-up, it is necessary to establish a correct start-up procedure (Scheeren *et al.* 1992; Wildeman 1992; Dvorak *et al.* 1991). The parameters considered to be important at start-up are: pH and reducing conditions; flow rate and composition of the influent, sufficient nutrients (e.g. C, N, P and SO_4), good contact of AMD with substrate and temperature. Scheeren et al., (1992) stated that high pH (>6) and sufficient nutrients have to be maintained at start-up; however, as soon as methanogenic activity is detected (via methane gas production), the pH and dosage of phosphorous can be reduced. The concentration of an active microcosm is another critical factor. Since the sulphate reduction, $CaCO_3$ dissolution and sulphide movement processes are mainly diffusion controlled, the design should allow overcome of mass transfer limitations. Optimum amount of substrate and surface area, suitable substrate thickness and permeability and, even, gentle mixing should be considered (Morel 1983; Kuhl and Jorgensen 1992). Loading rates of acidity and metals are also critical. The actual temperature of the reservoir should be taken into account while designing the process.

Metals Removal. According to the literature (Hammack and Edenborn, 1992; Tarutis, *et al.*, 1992; Wildeman, 1992), copper, zinc, cadmium, iron, nickel and lead are retained within the reactors or wetlands as insoluble monosulphides, following their reaction with bacterially generated H_2S. Aluminum and manganese are hydrolyzed within the reactors and are retained as insoluble hydroxides or carbonates. Zinc may be retained in both carbonate and sulphide phases depending on pH and availability of S^{2-} species. Removal of some metals (e.g. Cu, Cd, As) to low levels under all circumstances was attributed to binding with organic matter and/or other oxide minerals (e.g. biocomplexation, bio-adsorption and precipitation).

Economics, Longevity. The economics of the process, which depend on the amount of nutrients required for the pit, have been calculated for a test case site and compared to the cost of conventional lime neutralization. The SO_4 reduction rate found (e.g. 0.3 $molm^{-3}d^{-1}$ H_2S at 20°C or 0.15 $molm^{-3}d^{-1}$ H_2S at 10°C) is in good agreement with the rates reported in the literature (Bolis *et al.*, 1991; Dvorak, *et al.*,1992; CD&M, 1991). Assuming that AMD contains 20 mol/d metals, that a ton of substrate material costs $40, and a **conservative rate** of H_2S generation (0.15 $molm^{-3}d^{-1}$), the amount of substrate required and the total initial cost of the process have been estimated to be 40,000 tonnes and $ 1.6 million (Canadian), respectively. For a pit with a surface area of 5000 m^2, the substrate layer would be 8 m deep. Although the theoretical life expectancy of such a substrate layer is expected to be 120 y, the efficiency would be uncertain due to its thickness. In addition to the mass transfer limitations expected, temperature at the bottom of such a pit in Canada is <10°C all year round. **In conclusion,** loadings associated with open pits such as F-Group (Kuyucak and St-Germain, 1994) is too high for passive biological systems, but the concept is viable for

treating low load situations. Researchers need to search for easily degradable, yet inexpensive, nutrients and to overcome low temperature and mass transfer drawbacks.

Acknowledgements

The authors thank Mr. K. G. Wheeland for his support of this project and for his intensive review and comments provided during the course of the study.

Literature Cited

Ahonen, L. and O. H. Tuovinen. 1989. Microbiological oxidation of ferrous iron at low temperature. *Environ. Microbiology*, 55(2): 312-316.

Barnes, L. J., Janssen, P. J. H. Scheeren, J. H. Versteegh and R. O. Koch. Simultaneous microbial removal of sulphate and heavy metals from waste water. p. 391-403. In Proceedings of EMC'91 Conference: Non-Ferrous Metallurgy-Present and Future. (Brussels, Belgium, September, 1991).

Béchard, G., S. Rajan and R. G. L. McCready. 1990. Microbiological treatment of AMD; Laboratory and field study uptake, p. 130-151. In Biominet Proceedings. (CANMET, Ottawa, Ontario Nov'90).

Bhattacharryya, D., A. B. Jumawan, G. Sun, C. Sund-Hagelberg and K. Schwitzgebel. 1981. Precipitation of heavy metals with sodium sulphide. *A.I.Chem.Eng. Symposium Series* 77:31-38.

Bolis, J. L., T. R. Wildeman and R. R. Cohen. 1991. The use of bench scale permeameters for preliminary metal removal from AMD by wetlands. National Meeting of American Society for Surface Mining and Reclamation, Durango, CO. May 14-17, 1991.

Camp Dresser and McKee, Inc. Denver, Colorado. 1991. Passive Treatment System, Plant Interim, 2nd progress report, submitted to Noranda Grey Eagle Mine.

Dvorak, D. H., R. S. Hedin, H. M. Edenborn and P. E. McIntire. 1992. Treatment of metal contaminated water using bacterial sulphate reduction: Results from Pilot Scale Reactors. *Biotechnol. Bioengineering.* 40:609-616.

Gerhardt, P. 1981. Manual of Methods for General Microbiology, Washington D.C.: ASM Publication.

Hammack, R. W. and H. M. Edenborn. 1992. The Removal of Nickel from Mine Waters Using Bacterial Sulfate Reduction. *Appl. Microbiol. Biotechnol.* 37:674-678.

Hedin, R. S., D. H. Dvorak, S. L. Gustafson, D. M. Hyman, P. E. McIntire, R. W. Nairn, R. C. Neupert, A. C. Woods and H. M. Edenborn. 1991. Use of constructed wetland for the treatment of acid mine drainage at the Friendship Hill National Historic Site, Fayette County, PA. Final Report by USBM, Pittsburgh, PA.

Hedin, R. S. and R. W. Nairn. 1992. Designing and sizing passive mine drainage treatment systems. In Proceedings of the 13th Annual West Virginia Surface Mine Drainage Task Force Symposium. (Morgantown, WV, April, 1992).

Holder, G. A., G. Vaughan and W. Drew. 1984. Kinetic studies of the microbiological conversion of sulphate to hydrogen sulphide. *Water Science Technology.* 17:183-196.

Kalin, M. 1992. Decommissioning pits with ecological engineering. In Proceedings of 24th CMP Conference. (Ottawa, Ontario, January and February, 1992). Paper no 27. and Chap. 32.

Kuhl, M. and B. B. Jorgensen. 1992. Sulphate reduction and sulphide oxidation in compact microbial communities of aerobic Films. *Applied Environmental Microbiology.* 58(4): 1164-1174.

Kuyucak, N. and P. St-Germain. 1994. Possible options for *in situ* treatment of acid mine drainage seepages. In Proceedings of the Int'l Land Reclamation and Mine Drainage Conference and the 3rd Int'l Conference on the Abatement of Acidic Drainage. (Pittsburgh, 25-29 Apr'94).

Kuyucak, N. and P. St-Germain. 1993. *In situ* bacterial treatment of AMD in open pits. Phase II Detailed laboratory evaluation of nutrients, start-up conditions and scale-up parameters. Research Report, Noranda Technology Centre, V4-1341-01. Pointe-Claire, Canada.

Kuyucak, N., D. Lyew, P. St-Germain, and K. G. Wheeland. 1991. *In situ* bacterial treatment of AMD in open pits. In Proceedings of 2nd International Conference on the Abatement of Acidic Drainage. p. 336-353, vol. 1. (Montreal, Quebec, September, 1991).

Maree, J. P. and W. F. Strydom. 1987. Biological sulphate removal from industrial effluent in an upflow packed bed reactor. *Water Research.* 21(2): 141-146.

Morel, F. M. M. 1983. Principles of Aquatic Chemistry. NY: John Wiley & Sons Publ., p. 336-338.

Nairn, R. W. and R. S. Hedin. 1992. Designing wetlands for the treatment of polluted coal mine drainage. Proceedings of the 13th Annual West Virginia Surface Mine Drainage Task Force Symposium. (Morgantown, WV, April, 1992).

Peters, R. W. and J. Ferg. 1987. Dissolution/Leaching Behavior of metal hydroxide/metal sulphide sludges from plating wastewaters. *Hazardous Waste and Hazardous Materials.* 4(4): 325-331.

Scheeren, P. J. H., R. O. Koch, C. J. N. Buisman, L. J. Barnes and J. H. Versteegh. 1992. New biological treatment plant for heavy-metal contaminated groundwater. *Trans. Institute of Mining & Metallurgy.* 101: C190-C199.

Tuttle, J. H., P. R. Dugan, and C. I. Randles. 1969. Microbial sulphate reduction and its potential utility as an acid mine water pollution abatement procedure. *Applied Microbiology.*, Feb., p. 297-302.

Westrich, J. T. and R. A. Berner. 1984. The role of sedimentary organic matter in bacterial sulphate reduction. *Limnology & Oceanography.* 29(2):236-249.

Wildeman, T. R. 1992. Constructed wetlands that emphasize sulphate. In Proceedings of 24th CMP Conference. (Ottawa, Ontario, January and February, 1992). Paper no. 32.

POSSIBLE OPTIONS FOR *IN SITU* TREATMENT OF ACID MINE DRAINAGE SEEPAGES[1]

N. Kuyucak[2] and P. St-Germain[2]

Abstract: Noranda Technology Centre conducted bench-scale evaluations of various passive techniques developed by other institutions and potential processes for *in situ* treatment of base metal acid mine drainage (AMD) seepages. The passive methods assessed included: anoxic lime drains (ALD), where limestone is kept under anoxic conditions; a limestone-organic mixture (LOM), in which the function of the process is based on the activity of sulphate reducing bacteria; a biosorbent (BIOS) approach where metals are taken up by wood wastes; and a biotrench (BT), which differs from LOM in that different nutrient types are used. Prior work suggested that the best process could be obtained by using combinations of the first three methods and that the performance of the microbiological processes was substantially affected by low temperatures. With further laboratory tests, the best combination(s) and operation parameters were determined to provide a basis for the design of field tests. The results obtained from the test of combined systems indicated that a LOM connected to a smaller size ALD bed in series would be the best combination for treating AMD. With this system, the pH can be raised from 2.5 to 7.2 and concentrations of Al, As, Cd, Cu and Fe are lowered to less than 1 mg/L. Zn and Mn concentrations are reduced from 482 and 49 mg/L to 8 and 14.7 in the final effluent. TSS, BOD and COD levels in the final effluent are 9, 1.5 and 40 mg/L, respectively. In addition, it was found that a BIOS/ALD combination can selectively remove Cu and Cd to < 0.01 mg/L and increase pH to 6.5 and its performance is not affected by low temperature. Pilot tests for the LOM/ALD system were recommended to demonstrate the efficiency of the method for removing metals and increasing pH under field conditions.

Additional Key Words: metals, removal, passive treatment, anoxic limestone, sulphate reducing bacteria, biosorbent, biosorption, biological treatment, woodwastes

Introduction

Passive methods (e.g. wetlands, use of sulphate reducing bacteria (SRB) and anoxic lime drains) have been proposed as alternatives to conventional chemical treatment (Hammer 1989; Machemer *et al.* 1990; Kuyucak *et al.* 1991; Brodie *et al.* 1992). Particularly, these processes would be useful for low flow streams or seepages of acid mine drainage, of which collection and routing to a treatment plant is unaffordable. Current passive processes being developed by other institutions include: anoxic limestone drains (ALD), lime-organic mixture (LOM), biotrenches (BT) and biosorption (BIOS). An ALD system, first developed by the Tennessee Division of Water Pollution Control (TDWPC) and the Tennessee Valley Authority (TVA) (Brodie *et al.* 1990), consists of an excavated seepage interception trench backfilled with crushed limestone and covered with plastic and clay to keep air out. The main function of such a system is to pretreat AMD by increasing alkalinity prior to a wetland.

In the LOM method, investigated by the Colorado School of Mines (Wildeman 1992; Machemer *et al.* 1990), a bed which is made up of a mixture of limestone and manure (with some soil to increase permeability) is used to remove metals and increase alkalinity. The process is mainly based on the activity of SRB and is enhanced by the presence of limestone and organic material. The BT process has been investigated by CANMET, Canada (Béchard *et al.* 1990). A pilot-scale test has been conducted for treating pyritic slates at the Halifax Airport. In this process, removal of metals and generation of alkalinity from AMD

---

[1]Paper presented at the International Land Reclamation and Mine Drainage Conference and the Third International Conference on the Abatement of Acidic Drainage, Pittsburgh, PA, April 24-29, 1994

[2]Noranda Technology Centre, 240 Hymus Blvd., Pointe Claire, Quebec, H9R 1G5

is also based on SRB activity, using slow-release carbon-based nutrients such as straw, sawdust or wood shavings.

The BIOS process involves use of biological materials such as sphagnum moss, or algae as adsorbents (or biosorbents), and has been investigated by several institutions and Noranda Technology Centre (NTC) for removing metal ions from mine effluents (Jeffers et al. 1993; Kuyucak *et al.* 1989). In another NTC study, woodwastes (e.g. sawdust, wood chips) were found to be potential biosorbents. Therefore, woodwastes as biosorbents were futher examined as a passive treatment option. A bed of biosorbents can be used as a passive treatment process by placing it where the seepage occurs. When the bed is saturated by metals, the proponents suggest it can either be disposed of (with tailings or recycled to a smelter), or washed with an appropriate eluant for recovery of metals and/or reuse of the bed.

Experience has demonstrated that the influent flow rate, contaminant concentrations, pH, alkalinity (or acidity), the capacity of the treatment system to resist changes in pH and other variables are all extremely important to system performance. In addition, most investigations to date have been limited to drainage from coal mines and pyritic slates, which are quite different from the AMD associated with sulphide metal mines. Therefore, NTC and New Brunswick Mineral Development Agreement decided to assess the capabilities of several passive processes, with the objective of developing effective methods for treating small volumes of AMD.

Phase I work showed that better treatment efficiency could be achieved with the use of combined systems (Kuyucak and St-Germain 1993a). Phase II work was designed to confirm operational paramaters for the combined systems and to provide a basis for the design of the field evaluation. In addition to design and operating requirements, economical feasibility was assessed.

Materials & Methods

The Combinations Evaluated

Each combination consisted of a main reactor connected in series to one or two other small reactors. Based on materials used, three types of reactors were employed: LOM, BIOS and ALD. The combinations tested were: LOM/BIOS/ALD, BIOS/ALD and LOM/ALD. In two combinations, LOM was used as the main reactor and, in one combination, the biosorbent bed was the main reactor (Figure 1).

The efficiency of each combination in treating moderate strength AMD at 10°C and with a retention time of 14 days, which was the optimum retention time obtained at 20°C for LOM alone, was assessed. The flow rate was set to maintain 14 days of retention time based on the void volume of the main reactor in each combination. The flow rate, therefore, varied for each combination.

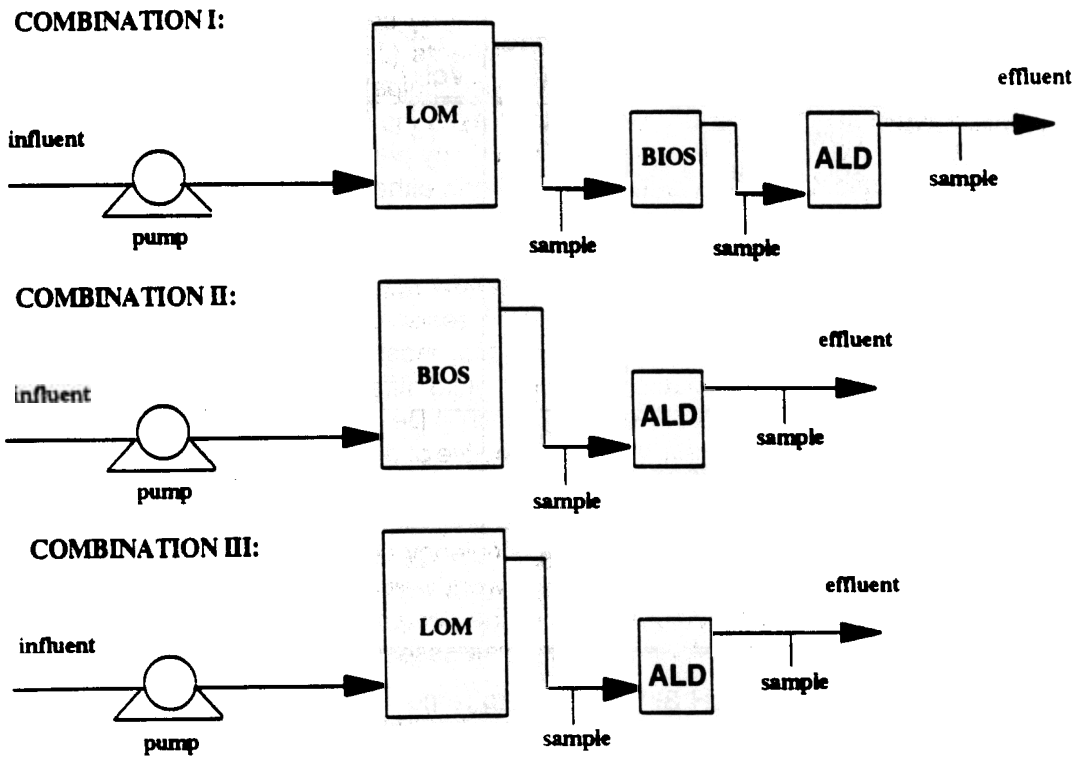

Figure 1 Reactor Configurations

Reactor Specifications

All reactors were made of plexiglass cylinders. The main reactors, with 28.8 cm I.D. X 100 cm height, had a total working volume of either 20 or 30 L, depending on the combination. Small reactors were 10 cm I.D. x 30 cm high columns with a working volume of 4 L. Influent and effluent ports (1.25 cm dia. for main reactors and 0.63 cm for the small reactors) were located on opposite sides of the reactor. The influent port was 5 cm above the base of each reactor. The effluent level in the reactors was controlled by the height of the effluent port. A drain was provided at the bottom of the reactors over which two layers of geofabric material were placed to prevent clogging of the drain. All reactors were operated in upflow mode where the influent AMD was added to the main reactor via a peristaltic pump and the overflow passively flowed through the other small reactors. Effluent out of the last reactor was collected and analyzed.

Materials Used in Each Reactor

Materials and procedures used to conduct tests with each reactor have been described elsewhere (Kuyucak and St-Germain 1993a). Specifications are also given in Table 1.

Table 1: Reactor specifications for phase II studies.

Combination	Main Reactor			Small Reactor		
	Materials Used	Working Vol.(L)	Void Vol.(L)	Materials Used	Working Vol.(L)	Void Vol(L)
LOM/BIOS/ALD	Cow manure, soil, limestone	30	14	BIOS:[1] sawdust, bark, paper sludge	4	2.5
				ALD: limestone (>93% $CaCO_3$)	4	2.1
BIOS/ALD	Bark, Woodpulp,Wood chips	30	7	limestone (>93% $CaCO_3$)	4	2.1
LOM/ALD[2]	Cow[3] manure, soil, limestone	20	4.5	limestone (>93% $CaCO_3$)	4	2

[1] Soaked with acidified tap water (pH 3) for 7 days to remove excess buffering and absorbing capacity.
[2] Constructed for the Phase II studies.
[3] 0.63 cm grade limestone used instead of 2.5 cm grade as was used in the first LOM reactor (i.e. in LOM/BIOS/ALD combination).

Composition of AMD

Moderate strength mine water (e.g. F-Group AMD from Mattabi Mines) was used throughout the experiments; its composition is given in Table 2.

Table 2: Composition of F-group mine water used in the tests.

Parameter	pH	Al	Cu	Fe	Zn	SO_4
Average Conc. (mg/L)	2.5	220	60	325	460	6300

Sampling Strategy and Analytical Procedures

Samples of the final effluent from each combination were collected every week. After approximately one month of operation, effluent samples (1 L volume) were collected weekly from each stage. The pH, redox and DO were measured using appropriate electrodes. SO_4 and metal concentrations were analyzed with an inductively coupled plasma (ICP) after samples were filtered and acidified with 3% HCl. Once a month, the same samples were also analyzed for volatile suspended solids (indicating amount of bacteria; VSS), total suspended solids (TSS), total organic carbon (TOC), biological oxygen demand (BOD), chemical oxygen demand (COD), total Kjeldhal nitrogen (TKN) and total phosphorous (TP). Except for total organic carbon (TOC), which was preserved by acidification to pH 2, VSS, TSS, BOD, COD analyses were

performed on unfiltered 500 mL samples, preserved at 4^0C. They were analyzed as respectively described in methods 5310B, 2540E, 2540D, 5210B and 5220C (Standard Methods 1989).

Results and Discussion

LOM/BIOS/ALD

Effluent Quality. The pH in the final effluent averaged 6.3. As, Cd and Cu concentrations were below the detectable limits of 0.25 mg/L while Al was at 0.7 mg/L. Fe and Zn concentrations were lowered from 305 and 449 to 21 and 181 mg/L, respectively. SO_4 was reduced by approximately 50%, the final concentration being 2887 mg/L. Mn was not removed. BOD and COD concentrations were low after each stage of the treatment. Total organic nitrogen (TKN) and total phosphorous (TP) concentrations were 5.1 and 0.05 mg/L, respectively. The ALD reactor contributed to increase the pH to 6.3 and reduce Al and Fe concentrations to those observed after the LOM stage as well as reestablishing post-LOM treatment levels offset by the BIOS stage.

SO_4 and Metal Removal Rate. The overall SO_4 removal rate, for the LOM/BIOS/ALD combination, was 0.968 mol/m^3/d, most of which occurred in the LOM reactor. The corresponding metal removal rate was 0.481 mol/m^3/d and the volumetric flow rate was 27 L/m^3/d. In spite of the fact that the total moles of SO_4 removed was greater than those of metals removed, all metals were not completely extracted from the water. The SO_4 removal rate obtained from the LOM alone at 10°C was much higher than what was expected according to the literature (i.e. 0.15 mol/m^3/d, Kuyucak and St-Germain 1993b; Kuyucak and St-Germain 1994), implying a significant contribution from the limestone present in the LOM system.

BIOS/ALD

Effluent Quality. In the BIOS/ALD process, the pH was increased from 2.4 to 6.3. The Al concentration decreased from 218 mg/L to below 0.7 mg/L and As, Cd, and Cu concentrations were lowered from 1.5, 1.8 and 61 mg/L, respectively, to below detectable limits. Fe and Zn concentrations were 3.8 and 276 mg/L in the effluent. As BIOS removed Cu and Cd, the ALD increased pH and reduced concentrations of Al, As and Fe in the final effluent. BOD and COD concentrations were negligible. The BIOS/ALD performance was also not affected by the low temperature when compared to the other systems.

SO_4 and Metal Removal Rate. For a volumetric flow rate of 14.7 L/d/m^3 at 10°C, 0.27 mol/m^3/d of metals and 0.509 mol/m^3/d of SO_4 would be removed by the BIOS/ALD system, essentially due to the ALD reactor. In the BIOS alone, the SO_4 removal rate was lower than that of the metal removal rate, indicating that the metal removal (e.g. Cd and Cu) was probably due mainly to adsorption onto the wood waste, since there was no limestone in the system.

LOM/ALD

Effluent Quality. The overall treatment results are shown in Table 3. The pH increased from 2.4 to 7.2 and the concentrations of Al, As, Cd, Cu and Fe decreased to less than 0.7 mg/L. As, Cd and Cu concentrations were under detectable limits while the Zn concentration was lowered from 482 to 8 mg/L and Mn was reduced from 48 to 15 mg/L, which was not observed before with the other tests.

The LOM reactor increased the pH to 6.0 and removed Al, As, Cd, Cu and Fe to less than 0.8 mg/L. In LOM alone, Zn and Mn concentrations decreased to 100 mg/L (i.e. 79% of total Zn) and 24.4 mg/L, respectively. The ALS system subsequently reduced the remaining Zn to 8 mg/L and Mn to 14.7 mg/L. BOD and COD levels were both negligible. The ALD reactor seemed to act as a filter by lowering VSS, TSS

and TOC levels coming from LOM. TP was low in the effluent, indicating a deficiency of phosphorous in the system. In process optimization, the use of phosphorous supplements (e.g. phosphate rocks, fertilizer) might improve the process efficiency.

Table 3: Final effluent quality achieved by the LOM/ALD combination

STREAM	pH	Concentration (mg/L)									
		BOD	TSS	TKN	NO_3	Al	As	Cd	Cu	Fe	Zn
INFLUENT	2.45	n/av	n/av	n/av	1.30	222	0.87	0.98	56	307	472
EFFLUENT	7.17	2	9	9.2	0.96	0.69	0.13	0.01	0.01	0.10	7.68

SO_4 and Metal Removal Rate. Table 4 shows that at 10°C, for a volumetric flow rate of 14.6 L/d/m^3, 0.58 mol/m^3/d of SO_4 and 0.334 mol/m^3/d of metals were removed in the LOM/ALD system. The majority of the treatment was performed by the LOM reactor while the ALD reactor only served as a polishing treatment. In spite of high SO_4 removal, metals removal (e.g. Zn) was not complete. This may imply that the limestone present in the system is making a major contribution, similar to what was observed in the LOM/BIOS/ALD system. When the data were compared to those obtained in Phase I at 20°C, better performance (particularly in Zn removal) could be expected with a longer residence time (e.g. >20 days).

Table 4: SO_4 and metal[1] removal rates in the LOM/ALD combination

Reactor type	Flow rate (L/d)	Vol.[2] flow rate (L/m^3/d)	Bed volume (m^3)	Net SO_4 removal (mmol/L)	SO_4 removal rate (mol/m^3/d)	Net metal removal (mmol/L)	Metal conc. in influent (mmol/L)	Metal removal rate (mol/m^3/d)
LOM	0.321	18.9	0.017	38.4	0.726	21.5	23.0	0.405
ALD	0.321	64.2	0.005	1.56	0.100	1.43	1.57	0.0916
L/A	0.321	14.6	0.022	40.0	0.584	22.9	23.0	0.334

[1] Includes Al, Cd, Cu, Fe and Zn
[2] Volumetric

Conclusions and Recommendations for Field Design

The LOM/ALD system would be a suitable option for treating low to moderate strength AMD; however, its capability for treating AMD should be demonstrated under field conditions where the effect of low temperature and fluctuating flow rates would be evaluated. In addition, the biosorbent bed at 10°C and 14-day retention time can efficiently remove Cd and Cu. The BIOS/ALD combination can be considered for selectively removing Cu and/or Cd and increasing pH. The field system for the LOM/ALD process should be designed for a longer retention time (e.g. 30 to 40 days) to ensure a good performance of the system. Addition of $Ca_3(PO_4)_2$ or slow-release fertilizers into the LOM cell may eliminate nutrient deficiency (i.e. P) and improve the bacterial activity. The inclusion of an ALD reactor is beneficial for maintaining the pH above 6.0 in all cases. It also acts as a filter; however its long-term performance should be monitored. Under

steady-state conditions, K, Mg and Na were unchanged from influent concentrations; only the release of Ca from the limestone was observed.

The design should also provide good flow distribution, as well as conditions to prevent the system from freezing and to keep the beds (particularly LOM) flooded at all times. Introduction of AMD to the system as down flow rather than upflow, and covering the system (e.g. with a plastic membrane and/or some bails of hay) may help to maintain anaerobic conditions and reduce heat loss. The effluent exiting the LOM/ALD system should be aerated for further polishing (particularly for removal of excess Fe, Mn, BOD and TSS).

The systems studied are more effective against low strength AMD. Seeps with SO_4 levels below 2200 mg/L and low concentrations of Fe and Al could effectively be treated with such a system for a long period of time since no armouring of limestone would occur. The cost of such a system (LOM/ALD) for treating 12 L/min of AMD is estimated to be in the range of $80 thousands (Canadian). Although life expectancy of such a system, when calculated based on theoretical requirements and available C moles in the organic materials, might be as long as 40 years (Kuyucak and St-Germain, 1993b), the life span under actual conditions should be expected to be much shorter due to physical, biological and chemical effects. Therefore, the longevity of the system should be determined for actual conditions. The form of metal precipitates in the substrate and possible options for disposal of metal-laden substrate, once it is used up, should also be investigated.

Acknowledgements

The project was funded by Noranda Minerals with contributions from CANMET and the Province of New Brunswick via the New Brunswick Mineral Development Agreement. The comments and suggestions of Dr. T. Wildeman (Colorado School of Mines), Dr. G. Béchard (CANMET), and Dr. R. Kleinmann (USBM - Pittsburgh) have been helpful in defining and interpreting this work.

Literature Cited

Béchard, G., S. Rajan, and R. G. L. McCready. 1990. Microbiological treatment of acid mine drainage; laboratory and field study update. p. 130-151. In Biominet Proceedings, CANMET Publication, Canada.

Brodie, G. A., C. R. Britt, T. M. Tomaszewski, and H. N. Taylor. 1992. Anoxic limestone drains to enhance performance of aerobic acid drainage treatment wetlands. In Proceedings of the West Virginia Surface Mine Drainage Task Force Symposium. (Morgantown, WV, April, 1992).

Brodie, G. A., C. R. Britt, H. N. Taylor, and D. Turner. 1990. Passive anoxic limestone drains to increase effectiveness of wetlands acid drainage treatment systems. p. 89-101. In Proceedings of the 12th Annual Conference of the National Association of Abandoned Mine Land Programs. (Breckenridge, CO, 1990).

Hammer, D. A. 1989. Constructed wetlands for wastewater treatment. Lewis Publishers, Chelsea, Michigan, 800 pp.

Jeffers, T. and R. .R. Corwin. 1993. Waste water remediation using immobilized biological technology. In proceedings of the International Biohydrometallurgy Symposium, August 22-25, 1993 (Jackson Hole, Wyoming).

Kuyucak, N., D. Lyew, and K. G. Wheeland. 1989. Biotechnology for mining effluent treatment. In Proceedings of the 11th Canadian Waste Management Conference. (Montreal, Quebec, 1989).

Kuyucak, N., P. St-Germain, and K. G. Wheeland. 1991. Treatment of AMD by SRB. p. 15-27, vol. 2. In Proceedings of the 2nd International Conference on Abatement of Acidic Drainages. (Montreal, Quebec, September, 1992).

Kuyucak, N., P. St-Germain, and K. G. Wheeland. 1992. Passive treatment project at Heath Steele Mines. NTC Research Report. DSS 23440-1-9203/01-SQ.

Kuyucak, N. and P. St-Germain. 1993a. Passive treatment methods for acid mine drainage. p. 319-331. In Proceedings of EPD Congress. (Denver, CO, February, 1993).

Kuyucak, N. and P. St-Germain. 1993b. *In situ* bacterial treatment of AMD in open pits, phase II: detailed laboratory evaluation of nutrients, start-up conditions and scale-up parameters. NTC Research Report, V4-1341-01.

Machemer, S. D., P. R. Lemke, T. R. Wildeman, and E. R. Bates. 1990. Passive treatment of metal mine drainage through use of a constructed wetland. p. 104-114. In Proceedings of the 16th Annual RREL Hazardous Waste Research Symp. EPA Doc. No: EPA/9-90037.

Wildeman, T. R. 1992. Constructed wetlands that emphasize sulfate reduction: a staged design process and operation in cold climates. p. 32. In Proceedings of the 24th Annual Meetings of the Canadian Mineral Processors. (Ottawa, Ontario, January, 1992).

USE OF BACTERICIDES TO CONTROL ACID MINE DRAINAGE FROM SURFACE OPERATIONS[1]

Dan Parisi[2], Jeffrey Horneman[3], and Vijay Rastogi[4]

Abstract: Anionic surfactants such as sodium dodecylbenzene sulfonate, sodium laurel sulfate, and others are effective in controlling acid production from sulfidic materials such as overburden, coal, coal refuse, ores, waste rock, and tailings. Their use in practical mining and reclamation applications, however, is only being recently documented since longer term field data are only now becoming available. This paper describes three applications of bacterial inhibitors. The first is at a surface coal mine where special handling and bacterial inhibition have prevented acid drainage from highly pyritic (more than 0.5% pyrite, neutralization potential less than 30 st per 1,000 st of $CaCO_3$ equivalent, and net deficiency of neutralizers of 15 st per 1,000 st of $CaCO_3$ equivalent) dark shale overburden for over 2 yr. The second application is at an active refuse disposal area where alkaline addition at more than three times that indicated by acid-base accounting failed to control acid production in refuse with 13% pyritic sulfur and neutralization deficiency of 444 st per 1,000 st of $CaCO_3$ equivalent. Bacterial inhibitors were successful in reducing acidity and metals in site underdrain effluent by 88% to 90%. The third application was at a silver mine where waste rock containing up to 0.37% pyrite was treated with surfactant bactericides to reduce leachate acidity by 93% and sulfates by 70%.

Additional Key Words: acid mine drainage, bactericides, coal refuse, pyritic overburden, silver waste rock, surface operations, selective handling.

Introduction

Acid is generated in soils and minerals containing pyrite or other sulfidic materials when they are exposed to the elements. The *Thiobacillus ferrooxidans* bacteria catalyze the oxidation of pyrite to acid and increase the rate of acid formation by over 1 million times (Kleinmann et al 1981). Once acid forms, it solubilizes metals, most predominant of which are iron, manganese, and aluminum. As metal content in the effluent increases, the cost of water treatment and neutralization increases exponentially. Presence of manganese is of special significance since it is so difficult to precipitate out, requiring pH above 11 or aeration or both.

Bactericides effectively control acid production (Watzlaf 1986) since the kinetics of inorganic oxidation of pyrite are extremely slow. When bacterial inhibitors reduce acid production by 80% to 95%, the effluent is unable to solubilize metals. A reduction of iron, therefore, by over 80% can produce correspondingly high savings in water treatment and in sludge removal and disposal. Similar improvements in manganese concentration lead to much greater water treatment cost reductions, often by an order of magnitude.

Application to Pyritic Overburden at a Surface Mine

This application is being made at Action Mining, Inc., of Meyersdale, PA, to mine on top of the Cover Hill summit approximately 3 miles northwest of Berlin, PA. The permit area consists of 108 acres with 56 acres

---

[1]Paper presented at the International Land Reclamation and Mine Drainage Conference and the Third International Conference on the Abatement of Acidic Drainage, Pittsburgh, PA, April 24-29, 1994.

[2]Dan Parisi, Chief Engineer, Action Mining, Inc., Meyersdale, PA, USA.

[3]Jeffrey Horneman, Project Engineer, Adobe Mining Company, Kittanning, PA, USA.

[4]Vijay Rastogi, President, MVTechnologies, Inc., Akron, OH, USA.

of Lower Bakerstown coal to be mined. Overburden analysis was requested by the Pennsylvania Department of Environmental Resources because an acid mine water discharge exists as a result of previous mining in the 1960's. Overburden analysis at the site identified two chemically and lithologically distinct and separate areas. The first area is the gray shale above the coal (fig. 1A), which the analysis showed to contain sulfur above 0.6% and neutralization potential generally well below 30. To the Pennsylvania Department of Environmental Resources, this is a potentially dangerous acid-producing zone (Smith and Brady 1990) and was of critical concern.

Table 1 shows the overburden analysis data. The second area is the brown sandstone, shale, and clay that comprise the remainder of the overburden from the top of the gray shale to the surface. This layer is mostly void of sulfur with all units less than 0.3% and all but one less than 0.01% and with positive net alkalinity.

The only significant alkaline unit on the site is the pit floor, which is a limestone as shown in table 1 and figure 1A. The mining and backfilling plan is designed to place some brown sandstone, shale, and clay spoil on the bottom. The gray shale is stripped by the drag and cast on top of the brown shale. Bacterial inhibitors are used to treat the gray shale to keep it from acidification. The concept is to keep pods of gray shale far enough above the pit floor so that it is not flushed by ground water which may flow over the pit floor after reclamation. Any rain water percolation will not acidify because the bactericide treatment will not let acid develop in the shale while it is exposed. The pods of gray shale are covered by clay and overburden well below the surface to prevent future contact with air. The operating plan is as follows:

1. The first cut is stripped utilizing a dozer and a dragline. The dozer pushes the top brown shale layer off and below the outcrop. The dragline casts the remaining spoil to the lowwall side. The last spoil removed from the pit is the dark gray shale (fig. 1B). As the spoil lies on the lowwall spoil pile, it is treated with surfactant bactericide applied as a water-based spray to keep it from producing acid while it is exposed to the elements.

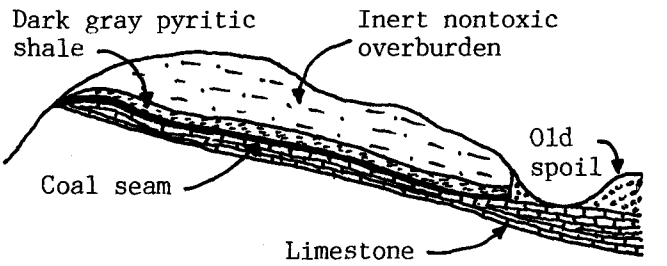

A, Premining cross section

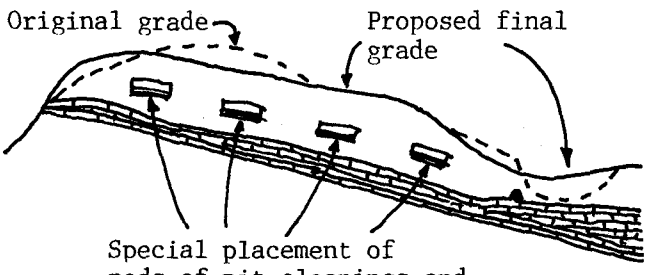

B, Postmining cross section

Figure 1. A, premining cross section of Cover Hill showing locations of coal seam, dark gray pyritic shale, and limestone; B, Postmining cross section showing selective placement of pods containing pit cleanings and pyritic shale after treatment with bactericide.

2. The coal is removed from the pit, and the pit floor is scrupulously cleaned of all coal waste. The impermeable limestone is left in place but is scarified with a dozer ripper blade to increase surface area and alkaline reactivity with any groundwater. All coal waste is special-handled by hauling it with a loader to disposal pods, which are constructed at least 10 ft above the pit floor. The pods are treated with bactericide surfactant spray.

Table 1. Overburden analysis data for Cover Hill.

Depth, ft	Thickness, ft	Graphic log	Lithologic description	Total sulfur,%	Fizz	$CaCO_3$ equivalent, st per 1,000 st of material	
						Neutralization Potential	Net Alkalinity
3	3		Topsoil, clay	0.007	0	0.96	0.74
6	3		Brown clay	0.008	0	2.60	2.35
15	9		Brown clay	0.002	0	3.05	2.99
			with	0.002	0	2.75	2.69
			sandstone	0.002	0	2.29	2.23
18	3		SS, shale stk	0.003	0	2.57	2.48
21	3		SS, clay	0.001	0	4.41	4.37
24	3		Hard clay	0.001	0	2.42	2.39
48	24		Soft brown	0.002	0	2.93	2.86
			sandstone	0.003	0	3.31	3.22
			and	0.009	0	3.95	3.67
			clay	0.004	0	4.87	4.74
				0.002	0	5.22	5.16
				0.002	0	4.66	4.60
				0.008	0	6.09	5.84
				0.226	0	9.20	2.14
51	3		Soft gray ss	0.667	0	10.07	-10.78
60	9		Dark gray	0.647	0	12.18	-8.04
			shale	0.687	0	10.91	-10.56
				1.180	0	22.28	-14.59
64	4		Dark gray	0.805	0	24.50	-0.66
			shale	0.747	1	27.13	3.78
66	2		L. Bakerstown	3.670	0	1.37	-113.32
69	3		Limestone	1.070	3	192.19	158.75

3. The next pit is started by the dozer pushing brown shale into the previous pit. The spoil from the previous cut is partly backfilled into the previous pit. The remaining spoil from the next cut is cast into the previous pit. The dark gray shale is the last spoil removed from the pit. After it is cast on the spoil pile, it is treated with surfactant bacterial inhibitors in the form of spray. After removal of the coal, the pit is cleaned and any coal waste is handled as described previously.

4. As the pits progress, the regrading of the spoil is done concurrent with the removal of overburden from the pit being mined. The dark gray shale is always treated with bacterial inhibitor spray shortly after it is exposed. After the spoil is regraded, an application of bactericide controlled-release pellets is made. Subsoil and topsoil are applied to the surface, and the area is revegetated at the first available planting date.

The bacterial inhibitor spray solution used 280 lb of 88% active surfactant in 1,000 gal of water per acre of material to be treated, or the equivalent of 0.3 lb of active ingredient per ton of material treated. The controlled-release pellets are applied at the rate of 700 lb per surface acre and contain an average of 28% surfactant. Mining at this site commenced in February 1991. In more than 2 yr no acid seeps have developed at the site.

Application at an Active Refuse Disposal Area

In September 1991, a review of the Branchton Refuse Disposal Area, located in Butler County and operated by Adobe Mining Company, Kittanning, PA, showed that the alkaline addition plan for this site was not neutralizing all the acid generated. Discharge from the underdrain due to the refuse moisture content in the active disposal area was acidic and had high levels of manganese that the treatment ponds were inadequate for handling further neutralization without additional additives and maintenance. The entire proposed refuse

disposal area is 39 acres in size. It was started in the summer of 1991, and thus far an estimated 900,000 st of refuse had been deposited over a 13.5-acre area.

The pyritic sulfur content of the combined coarse and fine refuse is as high as 14.2% with a neutralization deficiency in excess of 444 st per 1,000 st of $CaCO_3$ equivalent. Table 2 shows the sulfur forms analysis and the acid base account (Sobek et al 1978) for the refuse. The permit called for a 4-ft lift of combined coarse and fine refuse followed by a 1-ft layer of lime reject (approximately 3,000 st/acre), which has a $CaCO_3$ equivalence of 40% to 60%. The lime reject application was followed by a 2-ft layer of alkaline overburden. Additional measures to control the discharge quality included treating the refuse at the cleaning plant with caustic soda.

A new treatment plan consisting of spraying surfactant bacterial inhibitors was developed. The plan called for spray applications to be made four times a year, followed by controlled-release pellet applications prior to overburden cover. The spray used was 200 lb of 88% active sodium dodecylbenzene sulfonate per acre in 800 gal of water. Water used was taken from a nearby stream with a pH above 5 and iron content less than 7 ppm. The controlled-release pellets were applied at the rate of 600 lb per acre and had surfactant active ingredient ranging from 16.4% to 27.9%.

Bactericide spray applications were made the weeks of December 9, 1991, January 13, 1992, March 16, 1992, and August 10, 1992. The effect on underdrain water quality is shown in figure 2. Acidity (fig. 2A) dropped 88% from highs of 2,600 ppm to average around 300 ppm. Iron (fig. 2B) dropped 82% from highs of 1,000 ppm to average about 180 ppm. Most importantly, manganese (fig. 2C) dropped 90% from 50 ppm to 5 ppm. Without bactericides, manganese was extremely difficult to purge and was primarily responsible for the difficulties this site was experiencing in meeting permit requirements.

The Branchton site has since been able to meet water discharge criteria with the present treatment ponds.

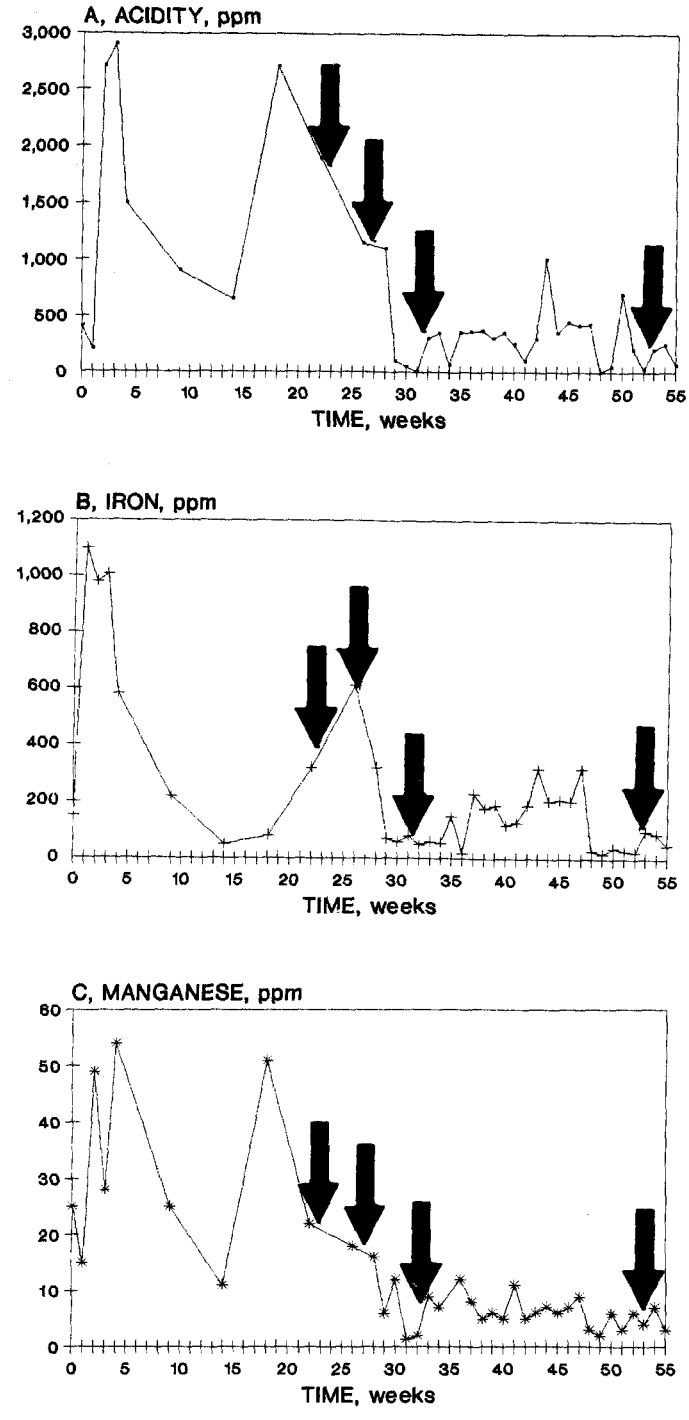

Figure 2. Underdrain water quality at the Branchton refuse disposal area before and after bactericide treatments. Black arrows indicate dates of bactericide applications.

Table 2. Analysis of refuse from the Branchton refuse disposal area.

Sulfur forms, percent				Paste pH	Acid-base account		
					$CaCO_3$ equivalent, st per 1,000 st of material		
Pyritic	Sulfate	Organic	Total		Acid potential from % sulfur	Neutralization potential	Net alkalinity
13.1	0.26	0.81	14.17	3.2	443.75	-0.65	-444.4

Application to Silver Mine Waste Rock

At a silver mine in Idaho, waste rock is placed into previously mined pits as backfil. In order to make an informed decision to use bacterial inhibitors at the site, laboratory column leaching tests were run to compare effectiveness of bactericide treatment with lime addition. These tests were run as described by Shellhorn and Rastogi (1984). Results of waste rock sulfur forms and acid-base account are given in table 3.

Table 3. Analysis of silver waste rock from Idaho mine site.

Sulfur forms, percent				Paste pH	Acid-base account		
					$CaCO_3$ equivalent, st per 1,000 st of material		
Pyritic	Sulfate	Organic	Total		Acid potential from % sulfur	Neutralization potential	Net alkalinity
0.365	0.119	0.002	0.486	4.8	15.19	0.19	-14.28

The control columns received no treatment, the bactericide columns received the equivalent of 0.1 lb of active surfactant to 1 st of material, and the lime-treated column received the equivalent of 14.28 st per 1,000 st of material as determined by the acid-base account. Results of the column tests, which were run for a period of 9 weeks, are shown in figure 3 for pH, acidity, sulfates, and T. ferrooxidans population control. In all cases, the bactericide treatment showed the best results, which are summarized in table 4.

As a result of the laboratory success, bactericide applications were made on site at a rate of 180 lb of active surfactant per surface acre applied with 800 gal of water. Each 60-ft lift was treated. Figure 4 shows results from lysimeters installed in the treated area and in an adjacent untreated area. The average improvement in water quality was 92.7% in acidity and 70.3% in sulfates. The water from the treated area averaged a pH of 5.6 over a 15-month period.

Table 4. Summary of column leach tests in 9 weeks.

Parameter	Control (no treatment)	Lime treated	Bactericide treated	% improvement bactericide over-	
				Lime	Control
pH	3.33	3.7	4.3	16.2	30.3
Acidity, ppm	503	265	78	70.6	84.5
Sulfates, ppm	708	467	193	58.7	72.7
Bacteria, log MPN[1]	5	4.3	0	100.0	100.0
Iron, ppm	32.7	8.9	1.8	79.8	94.5
Manganese, ppm	2.05	2.49	1.57	36.9	23.4
Aluminum, ppm	59.9	33.8	1.8	79.8	94.5
Copper, ppm	2.61	1.96	0.48	75.5	81.6
Zinc, ppm	5.74	4.14	1.84	55.6	67.9

[1]Most probable number.

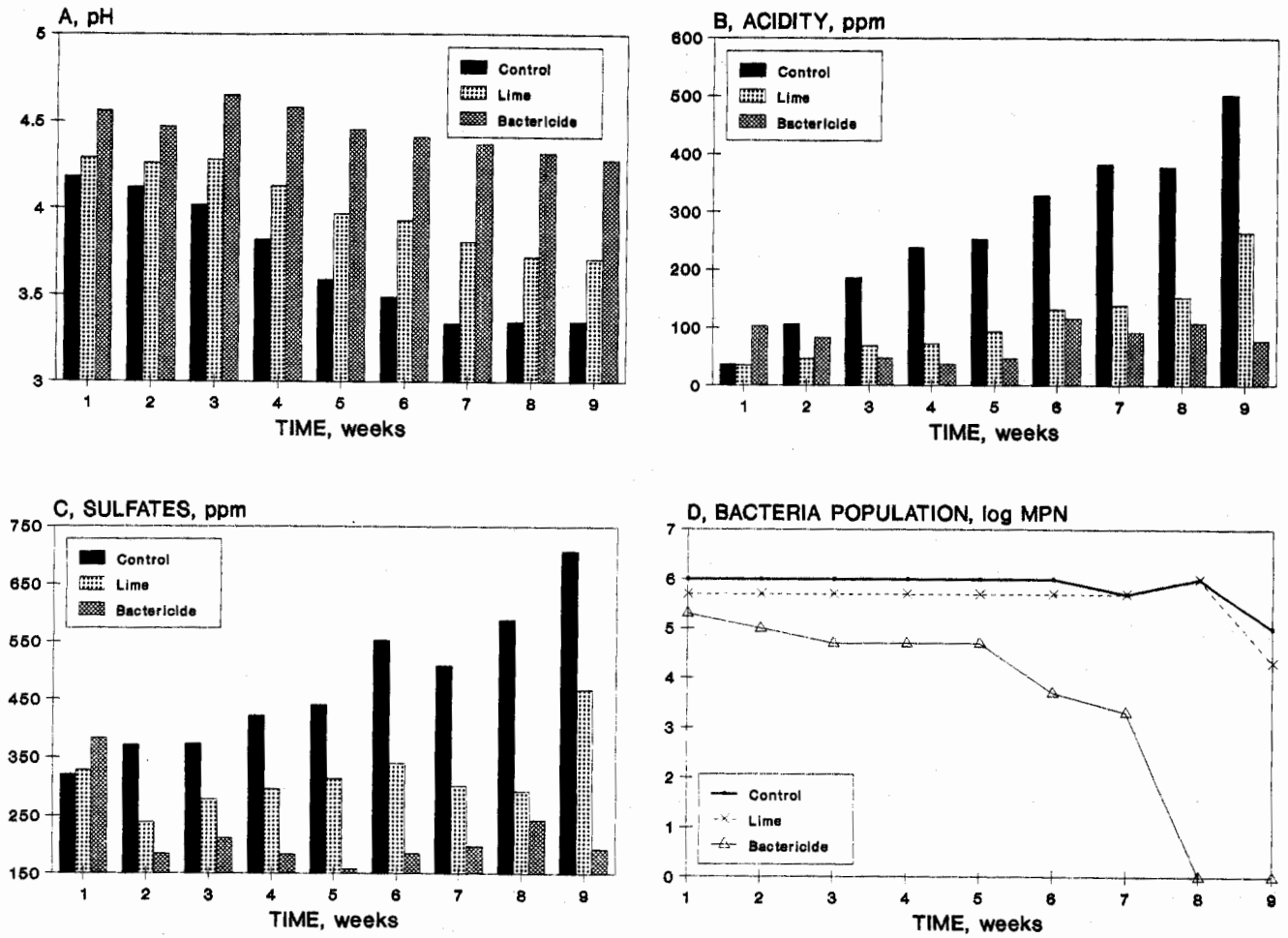

Figure 3. Results from column leaching tests on silver mine waste rock samples showing comparison between no treatment (control), lime treatment, and bactericide treatment in controlling (A) pH, (B) acidity, (C) sulfates, and (D) bacteria populations.

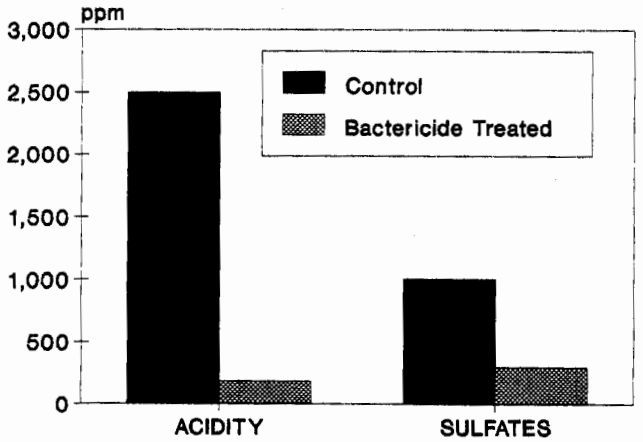

Figure 4. Actual water quality from lysimeters at mine site waste rock dump with and without (control) bactericide treatment.

Conclusions

The following conclusions can be drawn from these cases:

1. Bacterial inhibitors control acid generation and the subsequent solubilization of metals from diverse materials such as overburden, coal refuse, and metal mine waste rock.

2. Through proper planning, and utilizing a combination of technologies such as special handling, a systems approach to solving acid mine drainage can be successfully applied to resolve different problems.

3. Bactericide treatments achieve long term control through the use of controlled release systems and disciplined operations.

Literature Cited

Kleinmann, R. L. P., D. A. Crerar, and R. R. Pacilli. 1981. Biogeochemistry of acid mine drainage and a method to control acid formation. Min. Eng., 33:300-304.

Shellhorn, M. A., and V. Rastogi. 1984. Laboratory methods for determining the effects of bactericides on acid mine drainage. p. 77-82. In Proceedings of the 1984 Symposium on Surface Mining, Hydrology, Sedimentology, and Reclamation.

Smith, M. W., and K. B. C. Brady. 1990. Evaluation of acid base accounting data using computer spreadsheets. p. 213-219. In Proceedings of the Mining and Reclamation Conference and Exhibition. (Charleston, WV, April 1990).

Sobek, A. A., W. A. Schuller, J. R. Freeman, and R. M. Smith. 1978. Field and laboratory methods applicable to overburdens and mine soils. EPA 600/2-78-054, U. S. Environmental Protection Agency, Cincinnati, OH.

Watzlaf, G. R. 1986. Control of acid drainage from mine wastes using bacterial inhibitors. p. 123-130. In Proceedings of the American Society for Surface Mining and Reclamation, 1986 Annual Meeting.

EVALUATION OF HUMIDITY CELL PARAMETERS THEIR EFFECT ON PRECISION AND REPEATABILITY [1]

D. L. Pool and R. M. Balderrama[2]

Abstract: The prediction of acid rock drainage (ARD) from mineral processing tailings is an inexact procedure, and variations in results are common. The U.S. Bureau of Mines has evaluated the major parameters associated with humidity cell tests to determine their effect on the test's precision and repeatability. A set of 44-week tests on 50-yr-old tailings was performed with temperature control and changes in effluent volume and airflow. The temperature was maintained at 30° ±1° C. The airflow across the sample surface during the dry and wet air portions of the cycle was set at either 250 or 500 mL/min. The leach solution volume was varied to recover an effluent equivalent to up to 50% of the sample mass. The responses monitored were moisture removed during air addition, effluent volume, and acid in effluent (the amount of base required to titrate to pH 6), and total soluble sulfur. Changes in airflow and effluent volume affected the amounts of sulfate and acid reporting to effluent. Increased airflow resulted in more moisture removal and increased acid generation. As the effluent volume was varied, a maximum for acid generation was observed at 100 mL/325 g of sample. The data indicate that consistency in airflow and ratio of effluent volume to sample mass may improve the precision of the humidity cell test data. In addition, titration of the effluent provided a better measure of the acid content of the effluent than did pH monitoring. Precise and repeatable data should make the comparison of humidity cell data and ARD prediction between samples and testing facilities more reliable.

Additional Key Words: Humidity cell tests, acid mine drainage, AMD, acid rock drainage, ARD, tailings, fines.

Introduction

The U.S. Bureau of Mines is charged with ensuring the availability of metals to the economy with an acceptable impact on the environment. Research is underway at Reno Research Center to minimize the impact on the environment of mineral processing tailings from metal sulfide operations through source control for the prevention of acidic rock drainage (ARD). Samples of impounded tailings were collected and evaluated by static and kinetic leaching tests to determine their potential to generate ARD. Four replicate tests, to determine repeatability of modified humidity cell test results, were conducted using portions split from a well-blended head sample. During the performance of the kinetic humidity cell tests, parameters whose variation during testing could affect the consistency and magnitude of the results were identified. The parameters considered were airflow, leachant volume, air humidity, effluent volume, temperature, and percentage of water removed from a leached sample by aeration. The effects of two of these parameters, airflow rate and effluent volume, are presented in this paper.

Procedures for static ARD prediction tests are well defined, and the data from these tests are usually repeatable and comparable between laboratories. The static tests are used to make preliminary assessments of ARD generation potential and are based on acid-base accounting techniques (U.S. EPA 1978). Kinetic or accelerated weathering tests, however, are less well defined and are usually not conducted under closely controlled conditions. The authors look at these kinetic tests as a means of exposing the sample to conditions that are most likely to promote acid generation.

---

[1]Paper presented at the International Land Reclamation and Mine Drainage Conference and the Third International Conference on the Abatement of Acidic Drainage, Pittsburgh, PA, April 24-29, 1994.

[2]Danny L. Pool, Senior Researcher, Robert M. Balderrama, Senior Researcher, U.S. Bureau of Mines, Reno Research Center, Reno, NV, USA.

Kinetic tests are usually conducted in modified humidity cells and consist of wet-dry cycles to speed up acid-generating chemical or biological reactions. The general procedure for humidity cell tests was established by Carruccio (1967) and is listed by the Environmental Protection Agency (U.S. EPA 1978) as an acceptable method for ARD prediction. The configuration of the cells has been modified by others (Lawrence 1990), but the 7-day cycle of 1 day leach, 3 days dry air, and 3 days wet air is still used. The duration of the test is usually 22 to 30 weeks (Nevada Department of Conservation & Natural Resources 1993). The responses commonly monitored are volume, concentration of sulfate (mg/L), pH, and conductivity of the effluent along with the cumulative amount of sulfate (g SO_4^{2-}/kg sample) leached.

Some of the conditions that may vary during kinetic testing include temperature, airflow, and leach solution volume and composition. Tests are usually conducted at "room" temperature, which may vary as much as 10° C owing to seasonal and locality changes. Changes in application rate and quality of air and water introduced to the cells are also conditions which are loosely regulated under common methodologies. These variations have potential to impact results of the predictive tests for ARD. Data reported and analyzed in this paper are the results of screening experiments to determine the effects of variations in procedure and technique on acid generation as measured in humidity cells.

Apparatus and Materials

The apparatus used in this research consisted of an enclosed cabinet which was kept at 30°±1° C using a thermostat, with a proportional controller which regulated power to two heat tapes. Air was circulated within the chamber by a 4-in caged fan. The cells used (fig. 1) in this testing program have been accepted by the Nevada Department of Conservation & Natural Resources, Division of Environmental Protection (1993), for use on either tailings or crushed rock and are similar to those recommended by MEND and CANMET (Lawrence 1990) which are acceptable to the EPA. The cells made of acrylic plastic had an 88-mm ID with a 160-mm-high sample compartment. An air inlet port was placed at 84 mm from the bottom. The depth of the sample bed was 40 mm. The leachant was added from the top through a gas dispersion tube, which was placed 0.5 cm from the sample surface to minimize erosion and produce turbulence in the airflow. The sample was supported by a perforated plate covered with a filter cloth and sealed to the side 30 mm from the bottom of the cell. The lid was sealed with silicon tape to prevent air loss from the system. Ambient air was pumped from the room into the system using a diaphragm pump. The air picked up heat as it passed through the tubing and apparatus inside the chamber, and was then dried or humidified and distributed through the appropriate manifold. Airflow to each cell was controlled by a needle valve-flowmeter assembly. The air exiting the cells was collected in a third manifold and guided to the exterior of the cabinet. Air was dried by passing ambient air through columns of calcium sulfate (Drierite). The relative humidity (RH) was decreased to less than 0.2%. The air was humidified by passing warmed ambient

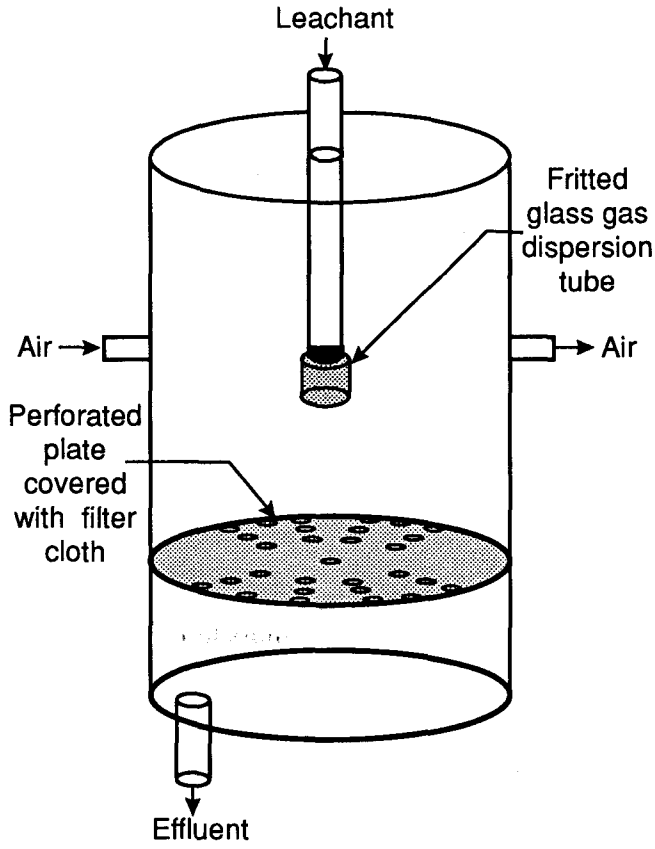

Figure 1. Schematic drawing of humidity cell used for the tests reported.

Table 1. Analyses of sample before and after 44-week humidity cell tests, percent.

Sample	Sulfur, total	Sulfur as sulfate	Sulfur as sulfide	Iron	Copper	Zinc	Lead
Head	[1] 2.40	0.28	[2] 2.12±0.05	4.0	0.080	0.080	0.01
Cell 1 tails	[1] 2.28	.14	[2] 2.14±.02	4.0	.027	.055	<.005
Cell 2 tails	[1] 2.25	.14	[2] 2.11±.01	3.8	.030	.039	.008
Cell 3 tails	[1] 2.26	.15	[2] 2.11±.07	3.8	.026	.050	.020
Cell 4 tails	[1] 2.29	.14	[2] 2.15±.11	3.8	.027	.046	<.005
Average tails	2.27	.14	2.13	3.8	.028	.048	.009

[1] Average of 2 assays. [2] Average of 2 assays with indicated variation.

air through two gas dispersion tubes submerged 250 mm in 35° C water which had been purified by a reverse osmosis (RO) process. The RH of the wet air was maintained above 90% and condensate was always present in the distribution system. The RH of the air streams was monitored to ±0.1% using a portable in-line relative humidity probe (Visala model HMI31). The RH was measured frequently during the first 20 weeks of the tests, then often enough to ensure consistency.

Water purified by RO was used to leach the samples. The water was characterized by measuring three parameters: the conductance, which ranged from 0.005 to 0.06 mS; the pH, which ranged from 4.17 to 4.87; and the oxidation reduction potential versus Ag-AgCl reference, which ranged from 273 to 391 mV. A container filled with this "characterized" leachant was placed inside the controlled temperature chamber at least 24 h before it was to be used.

The titration was conducted using a Mettler model DL25, which was capable of printing out volume added and the pH of a solution after each 0.1 mL of titrant was added. Using these data, the volume of titrant required to raise the pH to each selected pH was determined. The procedure was to place a 5- or 10-mL sample in the titrator cup and dilute to 40 mL using RO water, measure pH, and procede with the titration. A sample of RO water was titrated and a "blank" adjustment was made.

Solutions were analyzed for sulfur, copper, lead, calcium, and other metals by inductively coupled plasma (ICP), and for sulfate using ion chromatography (IC). Solids were analyzed for metals using ICP, and for total sulfur by combustion. Sulfate sulfur was determined by acid digestion in an inert atmosphere, followed by sulfur determination by ICP. Particle size distribution of the head sample was determined using a laser and white-light-based, computer-controlled particle size analyzer.

The material studied was a 30-lb sample collected from the 0-5 ft depth of a 50-yr-old copper-lead-zinc tailings impoundment. The particles in the head sample were 100% minus 150 μm, 75% minus 100 μm, and 50% minus 65 μm. The chemical analysis of this sample is listed on the first line in table 1. The main sulfidic mineral was pyrite, with minor quantities of galena, sphalerite, and chalcopyrite. The yellowish color of the tailings indicated that the tailings had been partially oxidized, and the presence of sulfate indicated that not all of the oxidized sulfur had been washed away during weathering.

Experimental Procedure

Four 325-g splits of the tailings were placed into 4 cells. The sample size was chosen to obtain a bed depth of 40 mm in each cell, which allowed the sample to be flooded during leaching without overflowing into the air lines. The cell plus sample was weighed at the start of the test, at the end of each leach step, after the dry air portion of each cycle, and again after the wet air portion of each cycle. The first cycle consisted of 1 day of leach followed by 3 days of dry air and was used to remove part of the soluble sulfate load from the samples.

All subsequent cycles were 7 days in length using the normal 1 day of leach, 3 days of dry air, and 3 days of wet air. The leach was conducted by weighing the required quantity of "characterized" leachant for each cell into individual wash bottles that could be emptied by squeezing. The leachant was introduced into each cell through the gas dispersion tube. The surface of the sample was flooded, and leachant was allowed to percolate through the sample bed. The remaining leachant was added during the next 4 to 6 h. The effluent was collected in a wide-mouth Erlenmeyer flask, which was vented to the cabinet. The volume, conductivity, oxidation potential, and metal content of each effluent was determined and recorded. Airflow was started late in the afternoon of the day of the leach.

The acid generated during the tests was monitored using three separate techniques:

1. pH Measurement: The pH of the effluent was considered to be the effect of sulfuric acid only. The concentration of acid was calculated from pH by using the definition that pH is the negative log of the H^+ activity. If it is assumed that activity and concentration are the same under the test conditions, then a solution with pH 3.2 has a H^+ concentration of $10^{-3.2}$ or 0.000631 g/L H^+. This is equivalent to (0.000631 x 49) = 0.031 g sulfuric acid per L.

2. Titration: A 5- or 10-mL aliquot of each effluent was transferred to a titration vessel, diluted to 40 mL, and then titrated using 0.01N or 0.1N sodium hydroxide in the automatic titrator. The amount of base required to adjust the pH of a sample of effluent to five different pH values was determined. The pH values selected, 3.5, 4.0, 6.0, 7.0, and 8.3, were considered as endpoints in different static tests (Lawrence 1990). During this test no attempt was made to remove the soluble CO_2 as recommended by Carruccio (1967). This simplified the procedure and accounted for all of the acidity in the solution, not just the sulfate acidity.

3. Sulfate Concentration: The sulfate content of the effluent was determined by analyzing for total sulfur in solution and assuming it was all sulfate. This assumption was confirmed on random samples by analyzing for sulfate. The acidity was calculated by assuming that all of the sulfate was from sulfuric acid.

Results and Discussion

Effect of Airflow

The percentage weight loss plotted in fig. 2 is the total for both dry and wet air portions of each cycle. The percentage was calculated based on the weight of the water contained in the sample after leaching and the weight loss during airflow. When the airflow was 250 mL/min, the wet air continued to remove moisture in spite of the condensation which occured in the system. The RH was measured in and out of the cell and usually increased about 2%, from 95% to 97%. Small changes in the pressure as the air flowed through the manifold and distribution system altered the moisture-carrying capacity of the air. After the airflow was increased to 500 mL/min, the weight loss during the wet air portion of the cycle was less than 10% of the total weight loss. The data in fig. 2 show that the average weight loss from the four replicate tests was dependent on the airflow into the cells, which affected the velocity of the air across the surface of the sample. An airflow rate of 250 mL/min over an 88-mm-diameter sample surface evaporated 36% to 58% of the water in the 40-mm-deep bed of tailings. An airflow of 500 mL/min evaporated 68% to 82% of the water.

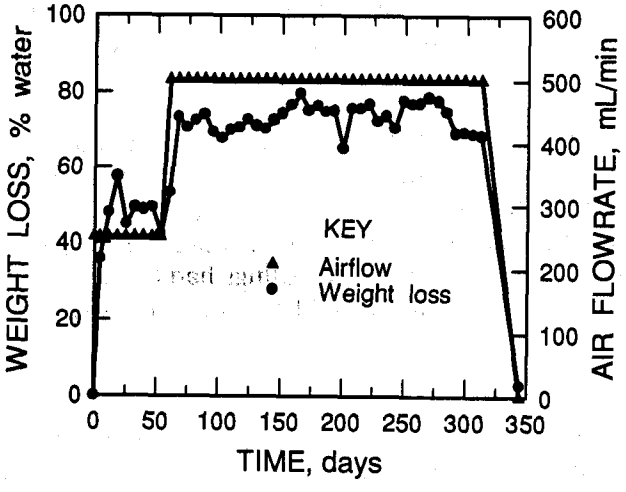

Figure 2. Effect of airflow across cell on weight loss of contained water over time.

During the last 32 days of the test, no air was pumped through the cells and the samples remained wet between leachings. In the absence of airflow, evaporation was nearly zero.

Effects of the Leachant Volume

The volume of the effluent is the difference between the amount of leachant added and the amount of liquid retained by the sample to replace evaporation. Thus, to recover a consistent volume of effluent, the airflow and the leachant volume must both be constant. The leachant removes the soluble salts and acid, thus changing the chemical and biological environment in which oxidation may occur. The data in table 2 and fig. 3 show these relationships for cell 1. Table 2 contains a description of the changes in the controlled variable and the accompanying measured responses. The values for effluent volumes and acid in solution, by titration, are averages for the days stated. The acid generation response from day 313 to day 342 shows that it is necessary to aerate the sample to generate acid. Part of the decrease in acid generation might be attributed to a depletion of sulfides in the tailings, but this is not supported by the data here and in fig. 3 since the acid generation rate increased with a decrease in leachant volume from day 208 to day 263. These data indicate that the degree of drying and the amount of effluent recovered from these tailings affected the amount of acid generated. The most acid was generated in this cell when 186 mL of leachant was added and 100 mL of effluent was recovered.

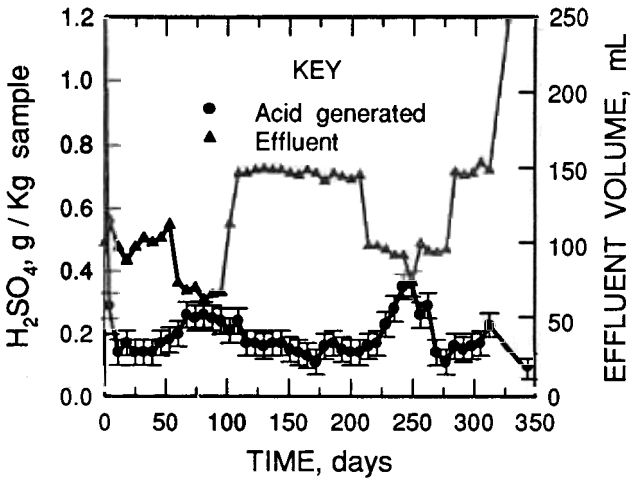

Figure 3. Effect of effluent volume on acid production, as determined by titration, over time--Cell 1.

Table 2. Data for cell 1--Timing of changes in controlled variables and the changes in two responses (effluent volume and acid generation).

Cycle No.	Segment, days		Controlled variable		Response measured		Variable changed	Cum. H_2SO_4, g/kg sample
	Start	Stop	Airflow rate, mL/min	Leachant vol, mL (ave/cycle)	Effluent vol, mL (ave/cycle)	[1]Ave H_2SO_4, g/kg sample per cycle		
0	0	4	250	150	100	0.92	Start	0.92
1-7	5	53	250	150	100	.15	None	1.97
8-13	54	95	500	150	75	.24	Air	3.41
14-15	96	109	500	190	115	.22	Leachant	3.85
16-29	110	207	500	230	150	.15	Leachant	5.95
30-38	208	263	500	186	100	.32	Leachant	8.83
39-45	264	312	500	230	150	.16	Leachant	9.95
46	313	342	0	300	340	.08	Air and leachant	[2]10.03

[1] By titration to pH 6.

[2] This value is equivalent to 0.33% S in the starting sample, which is 13.6% of the starting concentration of 2.40% total S. An extrapolation shows that if this reaction rate holds constant, a 6.8 year-long test may remove all of the sulfur. In practice it would take much longer because the rate would decrease as the amount of sulfur remaining in the sample became the controlling factor.

The optimum amount of leachant, to generate the most acid, is dependent on the amount required to replace evaporation and control the chemical and biological environment. For these tailings to produce the most acid, approximately half the weight of the sample was added as leachant with a subsequent recovery of only a third of the sample weight as effluent. The amount of water retained by the tailings at the start of the tests was 105 mL. If this is considered a "bed volume", then the data can be interpreted to show that the maximum acid was generated by almost complete drying of the sample, with an application of 1.8 bed volumes of leachant and a recovery of almost 1.0 bed volume as effluent.

Acid generation was the main response of interest. The endpoint of pH 6.0 was selected after titrating effluent samples for the first 20 weeks to pH 3.5, 4.0, 6.0, 7.0, and 8.3. The acid generation values for 6, 7, and 8.3 were almost identical while, as expected, the values for 3.5 and 4.0 were both lower than the upper group. According to the Code of Federal Regulations (1986), drainage with pH value of 6 or below is termed "acidic." A value of pH 6.0 was chosen as the endpoint for subsequent titrations because, it is the upper limit in the definition of acid drainage, and represents the value at which most of the acidity had been neutralized.

To determine if there was any difference in the values obtained by the three techniques used to measure acid generation, and to establish which values represented real or significant changes, the average data from all four cells were compared in figs. 4 to 6. The average acid generated by the four replicates between day 110 and day 207 was considered as baseline data because this was the longest period of time in which the controlled variables were held constant. The average acid generation during the baseline period was 0.15, 0.28 and 0.13 g H_2SO_4 per kilogram sample per cycle, for titration, pH, and soluble sulfate, respectively. Twice the standard deviation was calculated and added to and subtracted from the average. This estimated the random error in the system; therefore, any data outside these limits are considered to be significant, or probably the result of a change in a controlled variable. The standard deviations for the respective calculation methods were 0.02, 0.05, and 0.03 g H_2SO_4 per kilogram sample per cycle. These data show that titration and soluble sulfate have similar averages, and titration has the best precision

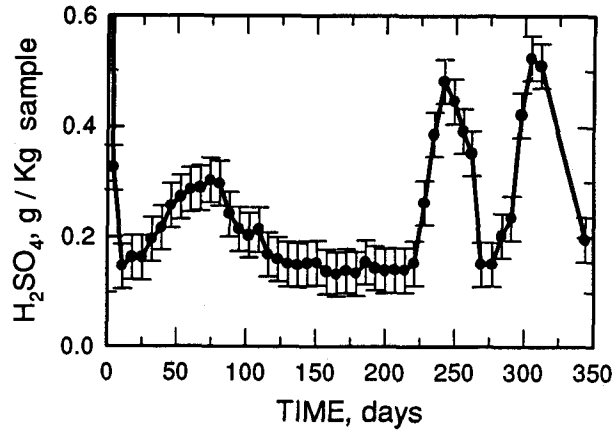

Figure 4. Acid generation, average of four cells, as determined by titration to pH 6.

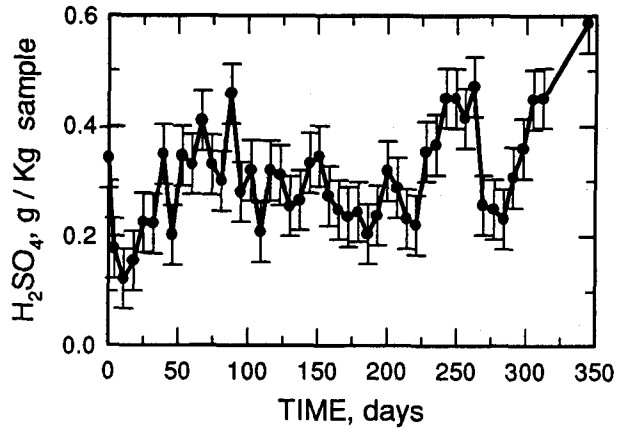

Figure 5. Acid generation, average of four cells, as determined by pH measurement.

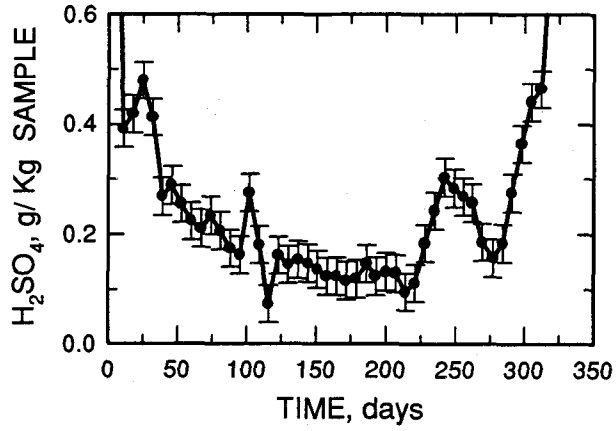

Figure 6. Acid generation, average of four cells, as determined by soluble sulfate in effluent.

during the baseline period, while pH may give a false high acid generation value because of random errors. The random errors were manifested in variations in pH meter measurements in tests conducted under the same conditions. The pH of the effluents ranged from 2.3 to 3.1 during the term of the tests, but only from 2.59 to 2.95 during the baseline period. The precision of the data from the titration method is better than that for the other methods, and any real changes in the response are more detectable if the samples are titrated to determine acidity.

Analyses for the solid material before and after the humidity tests are shown in table 1. These data show the reproducibility of the analysis of these rather high-sulfur tailings. Sulfur standards obtained from CANMET were also assayed and the results obtained were within the established limits ($\pm$0.15%) of variation (Smith and Bowman 1990). The same procedures were followed when assaying the tailing samples. The data in table 1 show that the total sulfur decreased an averaged of 0.13%, which is only 5.4 pct of the total sulfur, as determined by head and tails sulfur analysis, during more than 44 weeks of testing. These data indicate that most if not all of the sulfur collected in the effluent was from the sulfate, and that the sulfide sulfur did not change during this kinetic test. The data in tables 1 and 2 indicate that more sulfur was recovered in solution than was removed from the tailings; this is attributed to sampling and analytical variations.

Summary

Data presented in this paper are from observed trends in humidity cell tests that were conducted to measure acid rock drainage potential from a mineral processing tailings sample. The tests were conducted in a set of four in order to establish the repeatability of humidity cell tests using tailings. These data were not compared with the results in other laboratories using the same or standard samples. However, the authors feel that the responses noted should lead to further investigation on the degree of control required for each variable while conducting humidity cell tests. How to handle samples with a high sulfate load, and how this loading may affect any measurement of acid generation should be addressed in detail.

The important parameters that affect the acid production in the constant temperature humidity cell apparatus were the percent water removed and the amount of effluent recovered. The percent water removed was controlled by airflow through the cell and across the sample surface, and the amount of effluent recovered was dependent on the amount of leachant used and the airflow. The conditions at which the most acid was generated were as follows: When more than 75% of the contained moisture was removed during the 3 days of dry air and the moisture was maintained at that level for 3 days with wet air, the acid and dissolved salts were recovered by leaching with enough water to make up for the evaporative loss and recover one-third of the sample weight, which in this case was 1 bed volume. The measurement of the acid generated is best done by titrating an aliquot of the effluent as originally recommended by Carruccio (1967).

The authors' recommendation for humidity cell tests on tailings is to conduct the tests under the most consistent conditions possible and document them so others can perform comparable tests. This will make the results of these expensive long-term tests more usable in predictions of possible ARD.

Literature Cited

Carruccio, Frank T. 1967. An evaluation of factors influencing acid mine drainage production from various strata of the Allegheny group and the ground water interactions in selected areas of western Pennsylvania. Ph.D. Thesis, The Pennsylvania State Univ., University Park, PA, 213 p.

Code of Federal Regulations. 1986. 413 p. In U.S. Bureau of Mines Information Circular 9183, Mine drainage and surface mining reclamation and enforcement.

Lawrence, R. W. 1990. Acid rock drainage prediction manual, a manual of chemical evaluation procedures for the prediction of acid generation from mine wastes. Prepared for CANMET - MSL Division, Department of Energy, Mines and Resources, Ottawa, Ontario, Canada, November 30, 1990, 140 p.

Nevada Department of Conservation & Natural Resources, Division of Environmental Protection. 1993. Reno, NV, personal communication with D. Zimmerman.

Sobeck, A. A., and W. Schuller. 1978. Field and laboratory methods applicable to overburdens and minesoils. U.S. Environmental Protection Agency, EPA-600/2-78-054 (PB-280 495), 203 p.

Smith, C. W., and W. S. Bowman. 1990. RTS-1, RTS-2, RTS-3, RTS-4: Sulfide ore mill tailings reference materials. CANMET, Energy, Mines and Resources, 555 Booth St., Ottawa, Ontario, Canada, 91 p.

SIMULATED WEATHERING OF PYRITIC SHALE WITH ADDED LIMESTONE AND LIME[1]

Arthur W. Rose and Gary A. Daub[2]

Abstract: The addition of alkaline material to pyritic coal mine spoil in order to inhibit or neutralize acid mine drainage (AMD) has shown mixed success. We have conducted simulated weathering experiments with a pyritic shale containing 7% S amended by limestone and limekiln flue dust to evaluate the method. The alkaline material was added in a molar ratio of 2 $CaCO_3$:1 FeS_2 (31.25 st per 1,000 st of 1% S spoil), reacted in a container designed by Hornberger (1985).

Unamended samples produced severe AMD, leveling off after about 4 weeks at about pH 1.5, 17,000 mg/L SO_4, 19,000 mg/L $CaCO_3$ acidity, 7,000 mg/L Fe and 15 mg/L Mn. The limestone-amended samples were less acid at pH 3.4 to 4.2, 1,600 mg/L SO_4, 30 to 40 mg/L acidity, usually <1 mg/L Fe and 5 mg/L Mn. Limestone particles near the surface were coated by Fe-oxides by the fifth week; this feature extended deeper as the experiment continued. The lime-amended samples were not acid, having pH of 11.3 to 12.3, 1,500 to 2,000 mg/L alkalinity, <5 mg/L SO_4, and nondetectable Fe and Mn.

The significant levels of AMD in the limestone-amended sample probably resulted because the pore solution was not alkaline enough to prevent acidic microenvironments in which bacteria can catalyze the acid-forming reaction; the coarser grain size of 2 to 5 mm for the limestone may also be a factor. In contrast, the lime treatment appears to have completely prevented AMD, even preventing Mn mobility, which is evident in the calcite-amended experiments.

Additional Key Words: acid mine drainage, coal spoil, coal mine wastes, neutralization potential.

Introduction

The addition of supplemental limestone and other alkaline material from offsite is increasingly being used in an attempt to prevent or ameliorate the production of acid mine drainage from pyritic spoils of surface coal mining. In general, limestone or lime is added to the spoil in amounts calculated to neutralize the amount of acidity that might be generated by complete oxidation of pyritic sulfur in the overburden. Most workers in the past had considered that a ratio of 2 mols of $CaCO_3$ to 1 mol of FeS_2 (31.25 st $CaCO_3$ per 1,000 st of 1% pyritic S) was adequate to prevent or neutralize AMD (Brady et al. 1990). The success of alkaline additions was evaluated by Brady et al. (1990), who found mixed results. At most of the sites studied by Brady et al. (1990), the alkaline addition did not result in alkaline drainage, though at some sites the addition was at a ratio considerably less than 2:1. They suggested, based on the concurrent work of Cravotta et al. (1990), that the 2:1 ratio was inadequate and needed to be doubled to 4:1 (62.5 st $CaCO_3$ per 1,000 st of 1% S).

The purpose of this paper is to examine the effectiveness of two types of material for alkaline addition, limestone and limekiln flue dust, in controlled laboratory experiments. The investigation is described in more detail by Daub (1992).

Chemical Theory

It is generally accepted that pyrite oxidation by oxygen to produce AMD can be expressed as a series of reactions (Singer and Stumm 1970):

$$FeS_2(s) + 7/2O_2(g) + H_2O = Fe^{2+} + 2SO_4^{2-} + 2H^+, \quad 1)$$

$$Fe^{2+} + 1/4O_2 + H^+ = Fe^{3+} + 1/2H_2O, \quad (2)$$

---

[1]Paper presented at the International Land Reclamation and Mine Drainage Conference and the Third International Conference on the Abatement of Acidic Drainage, Pittsburgh, PA, April 24-29, 1994.
[2]Arthur W. Rose, Professor of Geochemistry, Gary A. Daub, Student (Present address, Colorado State Univ.), Pennsylvania State University, University Park, PA, USA

$$\text{and } Fe^{3+} + 3H_2O = Fe(OH)_3(s) + 3H^+. \quad (3)$$

In addition, once Fe^{3+} is present, it acts as a direct oxidant of FeS_2:

$$FeS_2 + 14Fe^{3+} + 8H_2O = 15Fe^{2+} + 2SO_4^{2-} + 16H^+. \quad (4)$$

Reaction 2 is catalyzed by bacteria of the species Thiobacillus ferrooxidans, which are most active between about pH 1.5 and 5.0. These bacteria markedly accelerate Fe^{2+} oxidation compared with inorganic rates (Singer and Stumm 1970), and since reaction 2 is commonly the rate-controlling step, they accelerate AMD production accordingly. In severe AMD, it appears that reactions 2 and 4 are the important reactions, with reaction 3 occurring where acid is neutralized.

The overall reaction for oxidation of pyrite to its products is the sum of reactions 1, 2, and 3:

$$FeS_2 + 3.75O_2 + 3.5H_2O = Fe(OH)_3 + 2SO_4^{2-} + 4H^+. \quad (5)$$

As indicated by this series of reactions, the SO_4 is released in an early step (reaction 1 or 4) and is an indication of the amount of pyrite that has been decomposed; the amounts of H^+ and Fe^{2+} in solution depend on the extent to which reactions 2, 3, and 4 have proceeded.

In the presence of acid, calcite initially neutralizes acid by the reaction

$$CaCO_3(s) + 2H^+ = Ca^{2+} + CO_2(g) + H_2O. \quad (6)$$

However, if pH is increased above about 6.5, the carbonate product will be HCO_3^- rather than CO_2:

$$CaCO_3(s) + H^+ = Ca^{2+} + HCO_3^-. \quad (7)$$

In effect, twice as much $CaCO_3$ would then be required to neutralize a given amount of acidity because the CO_2 (or H_2CO_3) requires additional neutralization to convert it to HCO_3^-. If reaction 6 is representative, the overall reaction with pyrite is

$$FeS_2(s) + 2CaCO_3(s) + 3.75O_2(g) + 1.5H_2O = Fe(OH)_3(s) + 2SO_4^{2-} + 2Ca^{2+} + 2CO_2(g). \quad (8)$$

However, this solution might still be acid, as pointed out by Cravotta et al. (1990).

If CO_2 does not escape from solution during neutralization (eq. 7), twice as much $CaCO_3$ is necessary to neutralize the AMD ($4CaCO_3$:$1FeS_2$). It appears likely that some CO_2 loss occurs during early stages of neutralization in natural environments, but in order to complete neutralization, HCO_3^- must be a product for at least some of the carbonate. A molar ratio of $CaCO_3$:FeS_2 between 2 and 4 seems likely for complete neutralization by calcite (or dolomite) in nature.

In the case of lime as a neutralizing material, the active ingredients may be CaO or $Ca(OH)_2$. These compounds undergo similar reactions:

$$CaO + 2H^+ = Ca^{2+} + H_2O, \quad (9)$$

$$Ca(OH)_2 + 2H^+ = Ca^{2+} + 2H_2O. \quad (10)$$

If the neutralizing compound is $Ca(OH)_2$, the reaction is

$$FeS_2 + 3.75O_2 + 2Ca(OH)_2 = Fe(OH)_3 + 2SO_4^{2-} + 2Ca^{2+} + 0.5H_2O. \quad (11)$$

The difference in reaction stoichiometry for $CaCO_3$ versus lime, in combination with the method commonly used to determine neutralizing potential (NP) of alkaline materials, leads to some ambiguities in current methods for alkaline addition. The NP method (Sobek et al. 1978) measures NP by reaction 6, in which all carbonate is released as $CO_2(g)$, yet reaction 7 implies that a need for twice as much $CaCO_3$ may be appropriate. In contrast, the NP technique measures CaO and $Ca(OH)_2$ by reactions 9 or 10, but commonly expresses the results in terms of $CaCO_3$ determined by reaction 6; i.e., an impure lime sample

may produce a result of 800 st $CaCO_3$ per 1,000 st of sample. In actuality, most lime materials are mixtures of CaO, $Ca(OH)_2$, $CaCO_3$, and probably other materials, and conversion from CaO to $Ca(OH)_2$ to $CaCO_3$ with exposure to water and air is likely.

Methods

The sample of pyritic shale used in the experiments was collected at the Emigh-1 Mine approximately 3 km north of Phillipsburg, PA, in a group of strip mines operated by Al Hamilton Contracting Co. and known as the Penn South group. Approximately 25 kg of pyritic shale from a 20 cm-thick zone immediately overlying the Middle Kittanning Coalbed (C coal) was collected from an active part of the mine. The sample was crushed to pass 1 cm, and a 0.5-kg split was pulverized and analyzed to contain 7.0% S and 0.17% carbonate carbon. Other materials used were the Valentine Limestone from Centre Lime and Stone, Pleasant Gap, PA, and limekiln flue dust from the same source. Chemical analyses of these materials are listed in table 1.

The simulated weathering procedure of this study is modified from the method of Hornberger (1985), as also used by Williams et al. (1982) and Morrison et al. (1990). In this method, 1 kg of the crushed sample is placed in a 2-L plastic leaching vessel above a layer of 6-mm-diameter glass beads. A measured amount of de-ionized water is then poured into the vessel, wetting the sample and draining gradually into the beads in the bottom of the container. This configuration allows the wet sample to oxidize in the presence of air. After a specified period of time, the water is drained from a plug at the bottom of the vessel, and an additional aliquot of water is added to the top, flushing residual AMD from the sample. The volume of effluent is measured and analyzed chemically. The columns were placed in an air-tight enclosure through which water-saturated air was circulated to minimize evaporation during the experiment; however, 5% to 10% of the water was still lost in some form.

The sample of Valentine Limestone was crushed and sieved. The 2- to 5-mm sieve fraction was used in the experiments. Duplicate columns were prepared with 220 g of limestone thoroughly mixed with 1 kg of shale. This ratio was calculated from the 2:1 molar ratio of $CaCO_3$ to FeS_2. In a similar

Table 1. Analyses of materials.
(Data in weight percent unless otherwise indicated)

	Valentine Limestone[1]	Limekiln flue dust[2]	Shale
SiO_2.....	0.64%	7.80%	NA
Al_2O_3.....	0.22	3.88	NA
Fe_2O_3.....	0.96	3.79	NA
CaO.....	54.5	56.0	NA
MgO.....	0.36	0.75	NA
MnO.....	0.005	0.75	NA
K_2O.....	NA	0.44	NA
LOI[3].....	43.7	18.6	NA
S.....	0.01	NA	7.0
Carbonate C...	NA	NA	0.17
CO_2.....	NA	17.2	NA
Neutralization Potential[4]..	NA	957.	NA
Insoluble Residue.....	NA	22.	NA

1 Valentine Limestone from Centre Lime and Stone Co. Pleasant Gap, PA, analyzed by the company.
2 Baghouse lime, Centre Lime and Stone Co., Pleasant Gap, PA, analyzed by Scott Atkinson, Materials Research Laboratory, PA State Univ., plus CO2 and neutralization potential by Joel Morrison, PA State Univ. For the limekiln flue dust, an x-ray diffraction pattern indicates calcite and unidentified poorly crystalline mineral(s). Calculated to contain 39% calcite, 22% insoluble residue, and remainder soluble and mostly "lime."
3 Loss on ignition.
4 st $CaCO_3$-equivalent per 1,000 st

manner, 231 g of limekiln flue dust were mixed with a 1-kg sample. The flue dust was in particles from dust to 1 mm in size, and was used without sieving, again at a 2:1 ratio of $CaCO_3$ neutralizing equivalent based on a neutralization potential of 950 st $CaCO_3$ per 1000 st. A pair of vessels were also prepared with no alkaline addition, asa control. The three pairs of vessels were tested on a flushing interval of 1 week and a water volume of 200 mL, which have been standard conditions for most previous studies using the method.

Immediately after the effluent was drained from the vessels, the water was tested for pH, Eh, specific conductance, temperature, and alkalinity. The effluent was then filtered through Whatman #41 filter paper, and hot acidity and sulfate were determined. The remaining filtered effluent was acidified with 2 mL of concentrated HNO_3 and later analyzed by plasma spectometry for Fe, Mn, and Ca. Methods are summarized in table 2. Effluent temperatures, which represent laboratory temperature, ranged from 20.5° to 28° C during the experiments. The weekly draining, refilling and analysis were continued regularly for 12 weeks, after which some effluents were discarded while others were analyzed up to the 20th week, when the experiment was discontinued.

Table 2. Analytical methods

Method	Procedure
pH	Combination electrode with pH 4, 7 and 10 buffers
Specific conductance	Method 120.1 of E.P.A. (1979) using Beckman Model RC-16C conductivity bridge.
Alkalinity	Bausch and Lomb alkalinity test kit.
Acidity	Method 305.1 of E.P.A (1979), using heated solution with added H_2O_2 to oxidize Fe.
Sulfate	Turbidimetric, using method 375.4 of E.P.A. (1979).
Fe, Mn, Ca	Plasma spectromety (ICP), with dilution for samples >800 mg/l.

Results

In general, the duplicate columns reproduced within about 20% of their mean. Although this difference is appreciable, it does not significantly affect any of the conclusions, so the duplicate columns have been averaged.

The results are illustrated in figure 1. Compared to the pH values of 1.5 in the untreated vessels, the limestone-amended vessel started at pH 7.6 for week 1 and leveled off at pH values of 3.4 to 4.2. Thus, the limestone treatment clearly produced a higher pH, but the solutions were nevertheless distinctly acid. Sulfate values averaged about 1,600 mg/L compared to 17,000 mg/L in the untreated samples, and acidity was about 30 to 40 mg/L $CaCO_3$, compared with 19,000 mg/L in the controls. Iron was generally undetectable (<0.2 mg/L) in the calcite-amended samples compared with about 7,000 mg/L in the controls. However, Mn averaged about 5 mg/L compared with 10 to 20 mg/L in the controls.

The lime-amended samples had pH values of 11.3 to 12.3 and consistently contained large amounts of alkalinity (approximately 1,500 mg/L $CaCO_3$). Sulfate was mostly less than 5 mg/L, and both Fe and Mn were undetectable.

Examination of the limestone-amended sample showed that after about 5 weeks, limestone fragments near the surface of the column were coated with reddish-brown iron oxide. By the end of the experiment, the limestone in the top centimeter was 90% to 100% coated, and in the zone 2 to 5 cm below the surface, 40% to 60% of the limestone was coated. Coating was generally lacking at the bottom of the vessel. Iron oxide also stained the walls of the container above the water level. The iron oxides seemed to form in areas of increased aeration and lower moisture. Crystals of gypsum were also noted on the surface of the column, indicating that measured sulfate in the effluent does not represent all the sulfate that was formed.

Iron oxide and gypsum were not observed on the lime-amended column, but the material did

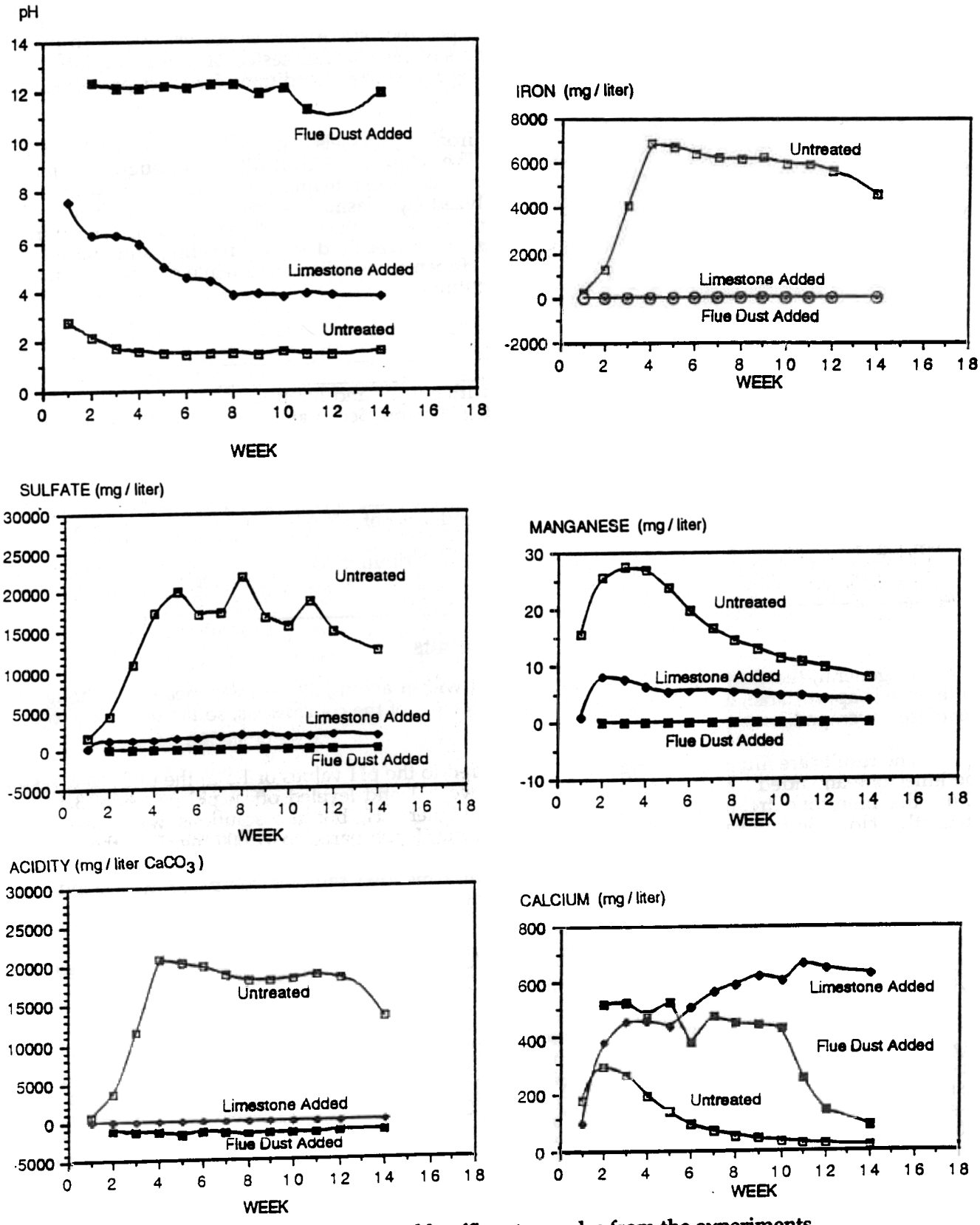

Figure 1. Concentration of solutes in weekly effluent samples from the experiments.

consolidate to a hard but porous block within a few weeks, indicating some sort of cementation. One column of the pair was broken up at week 7 by inserting a glass stirring rod through the material, allowing better infiltration of water but not significantly affecting the effluent.

Discussion

The limestone treatment markedly decreased the amount of acid produced and improved the leachate quality, but did not prevent formation of AMD. The pH values for one column were about 3.5 for weeks 8 to 14, and low but appreciable values of acidity were generated. The presence of 1,500 to 2,000 mg/L SO_4 indicates that acid was being formed in these columns but was in part being neutralized. Concentrations of Mn exceeded the allowable limit for effluents.

In contrast, the lime-amended samples produced essentially no SO_4 and no detectable Fe or Mn. The effluents contained considerable alkalinity and had a high pH, actually higher than that allowed for mine discharges. In view of the fact that gypsum was undersaturated by a factor of about 10^{-2}, the lack of SO_4 in the effluent indicates that essentially no pyrite was being oxidized in these samples; the acid-forming reaction was prevented.

Two possible reasons are suggested for the difference between the effects of limestone and lime. The limestone was coarser than the lime (2 to 5 mm vs. powdery to 1 mm), leading to higher reactivity for the lime particles. Secondly, the lime produces a more strongly alkaline environment. As a result of these differences, we suggest that some small volumes (micro-environments) in the limestone-amended sample lacked significant alkalinity, and bacteria were able to metabolize to create acidity and dissolved SO_4^{2+}, Fe^{2+}, and Mn^{2+}. This acidity was later largely neutralized, but if the neutralization occurred where this packet of solution encountered a limestone particle, the resulting precipitation of Fe oxides coated the limestone. After a few weeks, increasing proportions of the near-surface limestone particles were coated, drastically reducing their effectiveness in maintaining a neutral environment.

In contrast, the lime treatments appear to have completely prevented acid formation. It is hypothesized that the pore water in the lime-amended vessel was everywhere so alkaline that no micro-environments favorable for pyrite oxidation were present. The pH is so alkaline that normal Fe-oxidizing bacteria cannot metabolize, and inorganic oxidation is evidently slow.

Based on these data, the use of lime for alkaline addition appears to be preferable to use of limestone. In addition to its efficacy in preventing AMD, the limekiln flue dust used in this study is a waste product available at little cost except haulage. The addition of lime at a 2:1 ratio of NP ($CaCO_3$ equiv.) to FeS_2 is more effective than a 2:1 ratio of $CaCO_3$.

A complication to the above statements is that a CO_2 analysis of our sample of limekiln flue dust indicated about 40% $CaCO_3$, either as unreacted limestone or from CO_2 absorption from the air. Although this calcite "impurity" is less desirable because of the stoichiometric considerations previously discussed, it may also be an advantage. The $Ca(OH)_2$ and similar compounds are relatively soluble, so that they may be significantly leached from the spoil in a few years. However, $CaCO_3$ has relatively low solubility at near-neutral conditions, so a mixture of the two may preserve a near-neutral environment over a longer term than pure lime.

Conclusions

Laboratory experiments on a highly pyritic shale from a surface coal mine show that amendment with limekiln flue dust at a 2:1 molar ratio of NP ($CaCO_3$:FeS_2) is completely effective in preventing formation of acid effluent. In contrast, addition of limestone at the same ratio allows the formation of a slightly acid effluent, though it is markedly less concentrated than the untreated sample. In the limestone-amended sample, particles of limestone in the aerated zone are coated with Fe oxides and thereby inhibited from acting as effective sources of alkalinity. This process may explain some of the poor results from alkaline addition in the past. Fine grain size and thorough mixing may improve the results of limestone addition. Lime products probably prevent formation of acid because of their much more extreme pH effects as well as their fine grain size, and deserve careful trial as alkaline amendments. A mine-scale trial and several large test cells with varying amounts of lime are currently being evaluated at the Kauffman Mine of Al Hamilton Contracting in Boggs Township, Clearfield County, PA, with support by the Pennsylvania Energy Development Authority.

Acknowledgements: We are grateful to the Pennsylvania Energy Development Authority and the Al

Hamilton Contracting Co. for supporting this research, and to Ken Maney and others of Hamilton for assistance and discussion. Reviews of the manuscript by Keith Brady, Charles Cravotta and two unidentified reviewers were very helpful.

Literature Cited

Brady, K.B.C, M.W. Smith, R.L. Beam, and C.A. Cravotta III. 1990. An evaluation of the effectiveness of alkaline addition at surface coal mines in preventing or abating acid mine drainage. 2. Mine site case studies. p. 227-241. In J. Skousen, J. Sencindiver and D. Samuel, (eds.), Proceedings of the 1990 Mining and Reclamation Conference and Exhibition, WV Univ. Publ. Ser. (Charleston, WV, April 23-26, 1990).

Cravotta, C.A. III, K.B.C.Brady, M.W.Smith, and R. L. Beam. 1990. An evaluation of the effectiveness of alkaline addition at surface coal mines in preventing or abating acid mine drainage. 1. Geochemical Considerations. p. 221-225. In J. Skousen, J. Sencindiver and D. Samuel (eds.), Proceedings of the 1990 Mining and Reclamation Conference and Exhibition, WV Univ. Publ. Ser.(Charleston, WV, April 23-26, 1990).

Daub, G.A. 1992. A simulated weathering experiment investigating the factors controlling the generation and neutralization of acid mine drainage. B.S. Thesis, Department of Geosciences, PA State University, 67 p.

Hornberger, R.J. 1985. Delineation of acid mine drainage potential of coal-bearing strata of the Pottsville and Allegheny Groups in western Pennsylvania. M.S. thesis, PA State University, 558 p.

Morrison, J., B.E. Scheetz, D.W. Strickler, E.G. Williams, A.W. Rose, A. Davis, and R.R.Parizek. 1990. Predicting the occurrence of acid mine drainage in the Alleghenian coal-bearing strata of western Pennsylvania; An assessment by simulated weathering (leaching) experiments and overburden characterization. Geol. Soc. America Spec. Paper 248, p. 87-99.

Singer, P.C. and W. Stumm. 1970. Acid mine drainage: the rate determining step. Science 167:1121-1123.

Sobek, A.A., W.A. Schuller, J.A. Freeman, and R.M. Smith. 1978. Field and laboratory methods applicable to overburden and minerals. U.S. Environmental Protection Agency Rep. EPA-600/2-78-054, 204 p.

U. S. Environmental Protection Agency. 1979. Methods for chemical analysis of water and wastes. Cincinnati, OH.

Williams, E.G., A.W. Rose, R. R. Parizek and S.A.Waters. 1982. Factors controlling the generation of acid mine drainage. PA Min. and Min. Resour. Res. Inst., Final report to U.S. Bureau of Mines, 265 p.

AMD CLEANUP USING NATURAL ZEOLITES[1]

Larry E. Schultze, Monica J. Zamzow, and Paul R. Bremner[2]

Abstract: The U.S. Bureau of Mines is investigating the use of natural zeolites to remove metals from acid mine drainage (AMD). The loading characteristics of Al^{3+}, Ca^{2+}, Cu^{2+}, Fe^{2+}, H^{+}, Mg^{2+}, and Zn^{2+} were studied for samples of clinoptilolite from Barstow, CA, Buckhorn, NM, and Hector, CA. The relative order of cation selectivity was $Zn^{2+} > Ca^{2+}, Cu^{2+} > Fe^{2+} > H^{+} > Mg^{2+} > Al^{3+}$. The order of exchange capacity for the three zeolites was Hector > Barstow > Buckhorn, which corresponds to the Na content of the three zeolite samples. An acid mine drainage sample from the Rio Tinto Mine, an abandoned copper mine in northeastern Nevada, was used to measure the zeolites' cleanup potential. This water contained, in mg/L, 152 Al^{3+}, 502 Ca^{2+}, 101 Cu^{2+}, 595 $Fe^{2+/3+}$, 80 Mn^{2+}, and 61 Zn^{2+}. At an approximate flow rate of 4 mL/min (5 bed vol/h), 75% as much zeolite was required to clean the water to drinking water standards when the Hector material was used as compared with the zeolites from Buckhorn or Barstow. Zeolites were regenerated using 25% sodium chloride solutions. Loading and regeneration studies show no detectible degradation in the loading ability of the zeolites through 18 cycles.

Introduction

The U.S. Bureau of Mines is investigating alternate methods of treating water from mines producing acidic drainage (AMD). The water is characterized by metal sulfates that exceed State or Federal discharge limits (Bureau of Mines, 1975; Beszedits and Netzer, 1986). The acidity of the water originates from oxidation of iron sulfide minerals through a complex combination of chemical and bacterial action, primarily with pyrite, to form sulfuric acid. The acidic water leaches metal cations from the contacted minerals. AMD is a problem with both some modern mining operations and some abandoned mines. The most common approach to treating AMD is lime addition to precipitate metals and neutralize acidity (Patterson, 1985). Although this method is relatively simple and inexpensive, it does have the following disadvantages: (1) It generates a large volume of sludge which is costly to dispose of and in some cases is classified as hazardous, (2) at around 4° C, the precipitation layer in settling ponds undergoes an inversion that results in mixing of the solids and liquids, (3) it may not produce an effluent sufficiently low in metal content, and (4) the metal values are lost (Pahlman and Khalafalla, 1988).

To help meet present and possibly more stringent future Environmental Protection Agency (EPA) and State requirements, naturally occurring zeolites are being explored as ion exchangers to exchange the metal ions with sodium ions. More than 30 distinct species of zeolite occur in nature, of which mordenite, clinoptilolite, ferrierite, chabazite, erionite, phillipsite, and analcime occur in sufficient quantity to be considered as viable mineral resources (Vaughan, 1978).

The objectives of this investigation are to define the cation exchange characteristics of natural zeolites and to determine their efficiency in cleaning up AMD waste streams. Since the goal is to reduce impurities to below drinking water standards, the EPA standards are included for reference in table 1.

Table 1. EPA drinking water standards.

Metal ion	Drinking water concentration, mg/L
Cd.	0.01
Cr.	.05
Cu.	1
Fe.	.3
Mn.	.05
Ni.	.015
Pb.	.05
Zn.	5

Source: The Water Encyclopedia, 1970.

[1]Paper presented at the International Land Reclamation and Mine Drainage Conference and the Third International Conference on the Abatement of Acidic Drainage, Pittsburgh, PA, April 24-29, 1994.

[2]Larry E. Schultze, Research Chemist, Monica J. Zamzow, Chemical Engineer, and Paul R. Bremner, Chemical Engineer, Reno Research Center, U.S. Bureau of Mines, Reno, NV, USA.

Test Materials and Solutions

Zeolites

Tests were conducted on three natural zeolites[3] from two States in the Western United States:

Clinoptilolite, Hector, CA
Clinoptilolite, Barstow, CA
Clinoptilolite, Buckhorn, NM.

These zeolites were selected for further study from a field of 30 zeolites on which several preliminary tests were done (Zamzow and Murphy, 1992). They exhibited superior physical integrity and loading ability. The three zeolites were used as received at minus 20 plus 60 mesh.

Single-Ion Solutions

Test solutions were prepared from reagent grade chemicals using water purified by reverse osmosis. Solution concentrations were verified by inductively coupled plasma (ICP) spectrographic analysis.

Mine Wastewater

Wastewater was obtained from an abandoned copper mine (Rio Tinto) tailings pond in northeastern Nevada. This wastewater had a pH of 2.2. Table 2 shows its analysis.

Table 2.--Wastewater analysis, mg/L

Metal	Concentration
Al.	152
Ca.	502
Cd.	.19
Co.	4.8
Cu.	101
Fe.	595
K	24
Mg.	382
Mn.	80
Na.	95
Ni.	1.9
Zn.	61

Experimental Procedures

Composition and Mechanical Properties

Table 3 contains the results of X-ray diffraction and ICP analyses for the three zeolites. Exchangeable cation concentrations were converted to milliequivalents per gram (meq/g) for ease in making comparisons of loading capacities.

Attrition tests were done by placing 25 g of dry zeolite (minus 20-, plus 60-mesh) in a 250-mL volumetric flask with 75 mL of deionized water. The flask was shaken at 150 rpm for 1 h by a Fisher Versa-Bath[4]. The zeolite was then thoroughly dried and screened through a 100 mesh screen. The weight of the minus 100- mesh fraction was used to calculate the percent attrition.

---

[3]Zeolites were purchased from a commercial supplier.

[4]References to specific brand products do not imply endorsement by the Bureau of Mines.

Table 3.--Zeolite X-ray diffraction and ICP analyses

Location	Mineralogy (X-ray diffraction)
Barstow, CA.	Clinoptilolite > > quartz > mordenite.
Buckhorn, NM	Clinoptilolite.
Hector, CA	Clinoptilolite > quartz > mordenite.

	Chemical analysis, meq/g			
	Na	K	C	Mg
Barstow, CA	1.17	0.31	0.65	0.34
Buckhorn, NM	.52	.25	1.20	.91
Hector, CA	1.52	.23	.34	.16

Breakthrough Profiles

Studies were performed using 30- by 1.0-cm glass columns at ambient temperature. Each column was loosely packed with approximately 35 g of zeolite. The columns were operated under flooded conditions using a reservoir containing 1 L of loading solution at the top of each column. The bottom outlets of the columns were fitted with control valves to regulate the flow rates of the effluent to 1 mL/min ($\approx$1.4 bed vol/h). Each column was loaded with a 0.02N sulfate solution of the test cation. A 0.02N solution of H_2SO_4 was used in the H^+ studies. These concentrations were chosen to represent some of the higher concentrations known to exist in AMD. For example, 0.02N H_2SO_4 is pH 1.8 and 0.02N Ca is 401 mg/L.

The column effluents were periodically measured for volume and pH and analyzed for Na^+ and test cation concentrations. As the test progressed, the test cation concentration in the effluent abruptly increased and approached that of the loading solution with a simultaneous drop in Na^+ concentration. The point where the test cation began to increase in concentration in the effluent was considered the breakthrough point. The effluent prior to breakthrough typically contained <1 mg/L of the test cation and 0.022N Na^+. The loading, in milliequivalents (meq), was determined from the volume of the effluent and the change in concentration from the 0.02N loading solution. The cation exchange capacity (meq/g) was then calculated based on grams of zeolite in the column.

Rio Tinto Wastewater

A 1.5- by 30-cm column containing zeolite from Hector, CA, was used to treat 1 L of Rio Tinto wastewater. The zeolite was discarded and fresh zeolite placed in the column. The effluent from the first pass was treated with the fresh zeolite. The zeolite was again discarded, and replaced with fresh, and the effluent from the second pass was treated. This sequence was repeated 10 more times for a total of 12 treatments of 1 L of Rio Tinto wastewater. The total weight of zeolite used in the 12 columns was recorded. This test was repeated using each of the clinoptilolites. Treatment was continued until the effluent exceeded or matched that obtained in the first test. The flow rate throughout all the tests was about 5 bed vol/h.

Recycle

Multiple cycle tests were done by loading a 35-g sample of Hector clinoptilolite with metals from a 250-mL sample of Rio Tinto in a 1.5- by 30-cm column at a flow rate of 5 bed vol/h. The zeolite was regenerated using 34 mL of 25% NaCl solution. This was accomplished by flooding the column and allowing it to stand for 1/2 h before draining and reflooding. The final portion (approximately 7 mL) of eluate was allowed to stand overnight to increase the contact time. The zeolite was subjected to 18 loading and stripping cycles.

Results and Discussion

In single cation-solutions containing no competing cations, the breakthrough point is a measure of the affinity of the zeolite for that particular cation. The greater the loading prior to breakthrough, the greater the affinity. Table 4 summarizes the data for the breakthrough studies.

Table 4. Breakthrough values for three clinoptilolite zeolites, meq/g.

Ionic specie	Origin of zeolite		
	Barstow, CA	Buckhorn, NM	Hector, CA
Al^{3+}.....	0.15	0.05	0.25
Ca^{2+}.....	.65	.10	1.05
Cu^{2+}.....	.45	.28	.95
Fe^{2+}.....	.13	.18	.50
H^{+}	.28	.30	.36
Mg^{2+}.....	0	0	.35
Zn^{2+}.....	.45	.20	1.20

Data from table 4 was used to predict the following orders of cation selectivity for a 0.02N single-cation solution:

Barstow: $Ca^{2+} > Cu^{2+}, Zn^{2+} > H^{+} > Al^{3+} > Fe^{2+} > Mg^{2+}$
Buckhorn: $H^{+} > Cu^{2+} > Zn^{2+} > Fe^{2+} > Al^{3+} > Ca^{2+} > Mg^{2+}$
Hector: $Zn^{2+} > Ca^{2+} > Cu^{2+} > Fe^{2+} > H^{+} > Mg^{2+} > Al^{3+}$

For the Barstow and Hector samples, the orders of selectivity indicate that, given equinormal concentrations, Ca^{2+} is preferred over most of the other tested cations. This means that, when dealing with AMD for which the concentration of Ca^{2+} is frequently greater than that of any other cation, enough exchange capacity will be needed to remove most of the Ca^{2+} before other cations will be able to successfully compete for exchange sites. The sequence for the Hector sample more accurately represents general selectivity since that sample contains few exchangeable cations other than Na^{+} (table 3). Previously published data, containing breakthrough profiles for each of the tests summarized in table 4, demonstrate that Na^{+} is the exchanged cation in these tests (Bremner and Schultze, 1993). The sequence for the Buckhorn sample, for example, includes competition of cations for sites already occupied by Ca^{2+}, a cation that is not readily displaced.

The order of zeolite capacity from table 4 is Hector > Barstow > Buckhorn. This is considered a general order because it holds for most of the cations: Al^{3+}, Ca^{2+}, Cu^{2+}, Mg^{2+}, and Zn^{2+}. For Fe^{2+} and H^{+} the order is Hector > Buckhorn > Barstow, where the values for Barstow and Buckhorn zeolites are very similar and may be indistinguishable. The order Hector > Barstow > Buckhorn corresponds to the Na^{+} content in table 3 and is consistent with Na^{+} being the principal exchangeable cation.

Table 5 shows the percent loss for the zeolites due to attrition (Zamzow and Schultze, 1993). The rate of attrition is important because a high rate requires more zeolite makeup, which increases cost. Also, the fines produced through attrition will plug the column, thereby reducing the efficiency of the operation.

Table 5.--Attrition loss of clinoptilolite zeolites

Origin of zeolite	Percent loss
Barstow, CA	5.1
Buckhorn, NM	9.2
Hector, CA	2.1

Results from tests to clean up the Rio Tinto wastewater demonstrate that the concentration of most cations can be decreased at least to drinking water standards (table 6). The clinoptilolite from Hector, CA, required 370 g to achieve the same effluent levels achieved using 490 g or 493 g of the clinoptilolites from Buckhorn or Barstow, respectively. More of the clinoptilolites from Barstow or Buckhorn is needed because many of the exchange sites are already occupied by Ca (table 3), which is not easily displaced by the cations present in the wastewater. The tests were designed to obtain pure water rather than to optimize zeolite usage. Similar discharge compositions should be feasible using smaller quantities of zeolite if a countercurrent contact method is employed.

Data from the recycle tests (fig. 1) demonstrate good recycle characteristics for zeolites. There is no measurable decrease in cation exchange through multiple loading and stripping cycles beyond some stabilization during the first few cycles. As predicted from single-cation studies, the majority of the exchange capacity is utilized by Ca^{2+}.

Table 6.--Metals removed from copper mine wastewater

Metal	Head, mg/L	Effluent, mg/L
Al	152	<3.2
Ca	502	24
Cd	.19	<.03
Co	4.8	<.31
Cu	101	<.05
Fe	595	<.1
K	24	<14
Mg	382	144
Mn	80	<.03
Na	95	1900
Ni	1.9	.83
Zn	61	<.96

Conclusions

The above results demonstrate that clinoptilolites can remove metal cations commonly found in acid drainage wastewaters. Most cations can be reduced to meet drinking water standards. The extent of loading and the preference for one cation over another varies according to the ratios of Ca and Na present in the zeolite, with Na being more easily exchanged. Loaded zeolites can being regenerated using a NaCl solution, and multiple cycles of loading and stripping exhibit no deterioration of exchange capacity. Based on the research results, some site criteria have been established where zeolites would have a high probability of success in the field. Field tests are planned for the near future.

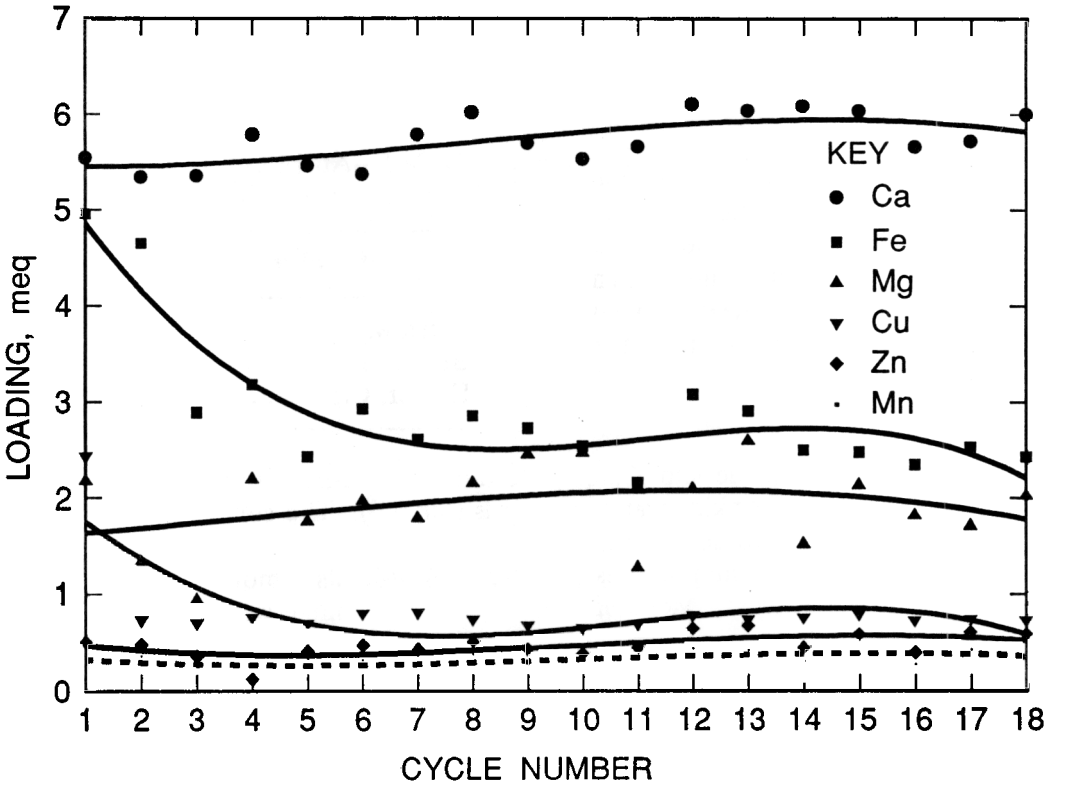

Figure 1. Effect of recycling on metals loading.

References

Beszedits, S. and A. Netzer. 1986. Removal of heavy metals from wastewaters. B & L Information Services, P.O. Box 458, Station L, Toronto, ON, Canada M6E 2W4, p. 120-184.

Bremner, P. R. and L. E. Schultze. 1993. Exchange characteristics of metal cations commonly found in acidic drainage: presented at Zeolite '93, 4th International Conference on the Occurrence, Properties, and Utilization of Natural Zeolites, Boise, Idaho, June 20-28, 1993. Available from Bureau of Mines, Reno, NV.

Bureau of Mines Interdisciplinary Research Task Force Committee. 1975. Implications of the Water Pollution Control Act of 1972 for the Mineral Resource Industry. BuMines IC 8681, 61 p.

Patterson, J. W. 1985. Industrial wastewater treatment technology, second edition. Butterworth, 467 p.

Pahlman, J., and S. Khalafalla. 1988. Use of lignochemicals and humic acids to remove heavy metals from process waste streams. BuMines RI 9200, p. 2.

Vaughan, D. E. W. 1978. Properties of natural zeolites. In Natural zeolites: occurrence, properties, use. L. B. Sand and F. A. Mumpton, eds. Pergamon, p. 353-355.

Zamzow, M. J. and J. E. Murphy. 1992. Removal of metal cations from water using zeolites. Separation Sci and Technol. 27(14):1969-1984.

Zamzow, M. J. and L. E. Schultze. 1993. Treatment of acid mine drainage using natural zeolites: presented at Zeolite '93, 4th International Conference on the Occurrence, Properties, and Utilization of Natural Zeolites, Boise, Idaho, June 20-28, 1993. Available from Bureau of Mines, Reno, NV.

A DEMONSTRATION OF THE FEASIBILITY OF TREATING ACID MINE DRAINAGE BY AN IN SITU ELECTROCHEMICAL METHOD[1]

Gene Shelp, Ward Chesworth, Graeme Spiers,and Liangxue Liu[2]

Abstract: A series of laboratory experiments were conducted to evaluate the effectiveness of an electrochemical approach to ameliorate AMD. An electrochemical cell was constructed using a block of massive sulfide-graphite rock from the Sherman Iron Ore Mine of Temagami, Ont., Canada as the cathode, scrap iron as the sacrificial anode, and acidic leachate collected from the mine site as the electrolyte. The cell raised the pH of ~41.0 L of leachate from 3.0 to a maintenance value of ~5.5. This result was accompanied by a significant decrease in redox potential from >550 to <300 mv. Furthermore, iron sulphate precipitate formed, with a concomitant lowering of Al, Ca, and Mg solution concentrations. The study clearly demonstrated the electrochemical approach to be a technically feasible and practical method of ameliorating AMD.

Additional Key Words: acid mine drainage, electrochemistry, cathode, anode, EMF, redox potential, amelioration.

Introduction

Acid mine drainage (AMD) results from bacterially catalyzed oxidation of sulfide-rich mining wastes. AMD is considered the single greatest environmental problem facing the Canadian mining industry because of the potential threat contaminated acid waters pose to aquatic ecosystems occurring within the vicinity of both operating and abandoned mining operations.

At its simplest, the production of AMD can be described by the following stoichiometric equation

$$2FeS_2 + 7.5O_2 + 7H_2O \xleftrightarrow{\text{(bacteria)}} 2Fe(OH)_3 + 4H_2SO4 \qquad (1)$$

This equation shows iron sulfide (pyrite) weathering to iron hydroxide and sulphuric acid. Methods of dealing with AMD can readily be related to this reaction. One set of methods, such as liming, organic-biological filtration systems (Dvorak 1991, Kuyucak 1991) and wetlands (Kalin 1984, 1987, 1990, 1991, Hammer 1990, Karathanasis and Thompson 1991, Stark 1991) treats the products of the reaction. A more fundamental approach is to attack the problem at the source by preventing the reactants on the left-hand side of the reaction from coming together. This approach includes bactericides (Sobek 1987), mineral coatings on the surface of sulfide grains (Nicholson 1990, Ahmed 1991), engineered covers (Collin 1990, Broman 1991, Nicholson 1991, Yanful 1991), submergence (McCready 1987, Ritcey 1991), sphagnum bogs (Brown 1991), iron-pan (Blenkinsop 1991, Ahmed 1991), and biofilm (Blenkinsop 1991).

In 1991 Dofasco Inc. and the University of Guelph began research to develop technology to ameliorate acid mine drainage problems associated with the recently decommissioned (1990) Sherman open pit iron mine, Temagami, Ont., Canada. The deposit occurs within an Algoma-type banded-iron formation (BIF). During mining a residual band of sulfide-rich graphitic bedrock, described as sulfide-facies iron formation, was exposed for approximately 2 km along the

---

[1]Paper presented at the International Land Reclamation and The Drainage Conference and the Third International Conference on the Abatement of Acidic Drainage, Pittsburg,PA, April 24-29, 1994.

[2]Gene Shelp, Ph.D. Candidate, Ward Chesworth, Professor, Graeme Spiers, Research Scientist, Liangxue Liu, Research Assistant, Land Resource Science, University of Guelph, Guelph, Ontario, Canada, N1G 2W1.

north side of the South Pit, one of five open pits occurring on the property. The sulfide-rich zone contains blebs, nodules, stringers, and massive lenses of pyrite up to 1.5 m wide and tens of meters long. The South Pit acidic waters were generated by the interaction of oxygenated surface water and groundwater with the sulfide-rich formation. The pH 3.0 - 3.1 waters contain high concentrations of iron, manganese, aluminum, and other metals.

Options including perpetual treatment with lime were considered to reduce the rate of oxidation of sulfide minerals. The most practical option, although expensive and possibly ultimately ineffective, involved filling the pit with the sulphidic material and then installing an impermeable material cover.

The main objective of our research is to evaluate an alternative treatment, namely, an in situ electrochemical technology designed to change AMD to within environmentally acceptable chemical levels. In equation 1, a redox reaction, electrons are produced by the forward half-reaction and consumed by the backward half-reaction. The forward reaction rate can therefore be slowed, or even prevented, by supplying electrons. This may be achieved by making the sulfide-rich rocks the cathode of an electrochemical cell and a material of greater electroactivity than pyrite the sacrificial anode. The fundamental electrochemical reaction is a transfer of electrons from the anode to the cathode. Theoretically, this transfer should inhibit acid-generating reactions by both creating a reducing environment on the surface of the sulfide mineral and also reducing the activity of Thiobacillus ferrooxidans by increasing the pH of the microsites through the conversion of hydrogen ions (H^+) to elemental hydrogen (H_2).

The desired effect may be illustrated (fig. 1) using Eh and pH as master variables. Acid mine drainage would plot to the upper left of the normal field of natural surface and near-surface waters. The electrochemical treatment is expected to bring the AMD to within the normal region by inhibiting the oxidation of the primary sulfide minerals while minimizing the long-term costs of amelioration. The final pH of the system should be controlled by the hydrolysis reaction for some form of iron oxyhydoxide or basic iron sulfate.

This paper presents the results of a series of laboratory experiments that demonstrate the effectiveness of the proposed electrochemical approach to ameliorate AMD.

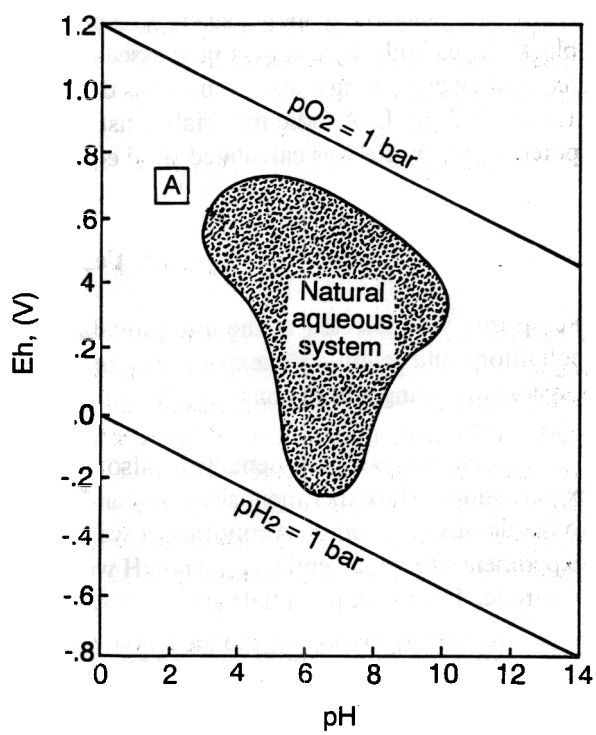

Figure 1. Eh-pH diagram showing where Sherman Mine leachate (A) plots relative to the field of natural aqueous systems (after Baas Becking et al., 1960).

The Experimental Setup

Figure 2 shows the experimental cell. The sulfide block shown with approximate dimensions of 45 cm L by 30 cm W by 30 cm H, was sawn from a sample of the sulfide facies iron formation, weighing approximately 1 mt, collected at the Sherman Mine site. The block had between 10% and 15% pyrite and was of fissile character with minor fractures extending through the thickness of the block. The initial step was to saturate the blocks with South Pit leachate collected at the mine in order to establish the electrical continuity required for an operating cell. The 2 L of water absorbed by the block corresponds to a porosity of approximately 4%. Subsequently, the block was placed into a Nalgene tank (fig. 2) with silicone used to establish a water tight seal along the bottom and sides of the block. A 3-cm head of water was maintained upstream to ensure that acidic leachate generated during the experiment collected in the downstream pond. The head differential was maintained by an electronic level controller and peristaltic pump system. The upstream and downstream ponds contained 27.5 and 41.3 L, respectively.

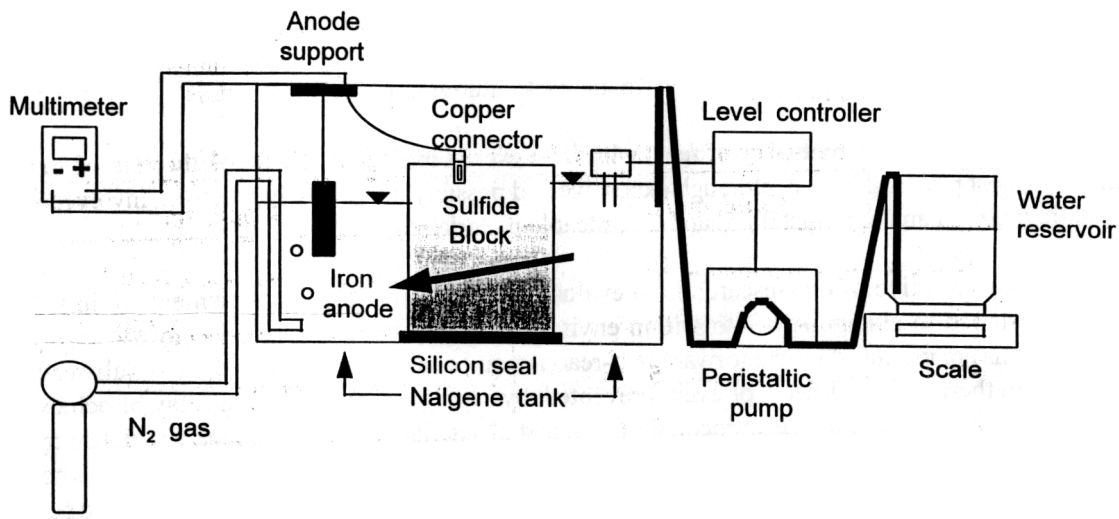

Figure 2. Electrochemical cell setup

The sacrificial anode, suspended in the downstream pond, was attached to the semiconductive sulfide-graphite block, the cathode, by a copper plug assembly. The possibility of oxide coatings forming on the surface of the anode was reduced by generating anoxic conditions through purging the pond with nitrogen. Dissolved O_2 was maintained between 1.0 and 1.2 mg/L. Anodic materials must have standard oxidation potentials greater than that of pyrite. The oxidation potential for pyrite was calculated from equation 2, to be -376 mv .

$$\mathbf{FeS_2 + 8H_2O \xleftrightarrow{\text{(bacteria)}} Fe^{3+} + 2HSO_4^- + 14H^+ + 15e^-} \qquad \mathbf{(2)}$$

Scrap iron was selected as the most suitable anode because it is considered both environmentally safe under natural conditions and relatively inexpensive. For iron or any other anodic material to function effectively, the cell must be capable of raising and maintaining the leachate pH above 5.5, close to the theoretical pH of rain water.

Laboratory experiments were also designed to test the ability of the cell to respond to simulated natural system perturbations. The experiment simulated an influx of acidity into the South Pit by a one time addition of ~3.5 L of AMD to the downstream pond. A multimeter was used to record EMF and current on a daily to weekly basis throughout the experiment. Redox potential (Eh) and pH were measured using an Accumet 1000 series meter with a Ag-AgCl reference electrode. The redox potentials are standardized to the hydrogen scale.

Water samples were taken periodically and analyzed for various aqueous species by inductively coupled plasma atomic emission spectroscopy (ICP-AES). Precipitate samples were collected periodically for x-ray diffraction, scanning electron microscopy and elemental analysis. X-ray diffraction analysis was conducted using a RIGAKU D/Max-A powder diffraction system, with the specimen being analyzed from 3° to 90°2θ, at 0.02°2θ increments with a 4 s integration time. Precipitate samples were coated with 20 nm Au and examined with a Cambridge 250 scanning electron microscope equipped with a Noran thin-window energy-dispersive detector and a Tracor 5500 analyzer (SEM-EDS). Precipitate subsamples were analyzed for total metal content by ICP-AES following dissolution with 2M HCl-HNO_3.

Results and Discussion

AMD is a problem in the environment not only because of acidity but also because the solutions are rich in species inimical to the biosphere, as illustrated by the chemical analysis (table 1) of South Pit water. However, a rise in pH is

directly related to the formation of precipitates of iron phases with an accompanying diminution of toxic species by simultaneous precipitation or adsorption. We can demonstrate this by monitoring pH, Eh,and Al content in the aqueous phase. Al^{3+} is the principal ionic form of aluminum considered toxic to plant and animal species in acidic-leachate-contaminated aquatic environments.

Table 1. Chemistry of AMD from South Pit, Sherman Mine (pH=3.0)

Conc, mg/L		Conc, mg/L	
Fe	10	Ni	0.1
Al	10	SO_4^{-2}	1,500
Mn	5	Cl^-	7
Zn	0.16	F^-	1.4
Cu	0.1		

Source: Data courtesy of Syd Bartle, Dofasco Inc.

EMF and Current

The cell generated voltages exceeding 800 mV. This value can be predicted from the difference between the calculated oxidation potential of pyrite (FeS_2), -376 mV, and that of the oxidation of elemental iron to ferrous iron, +440 mV. During the latter stages of the experiment, the EMF decreased to a steady state value of ~350 mV. The current also decreased from an initial value of 25 mA to a level at ~7 mA.

pH and Redox

The pH increased increased linearly to between 5.4 and 5.5 after forty days (fig. 3). The redox potential of the system decreased from an initial value exceeding 550 mV to ~300 mV (fig. 3). These Eh-pH conditions approach those of reduced forms of iron and sulfur. Consequently, oxidixing reactions occurring on the sulfide mineral surface microsites will be significantly inhibited.

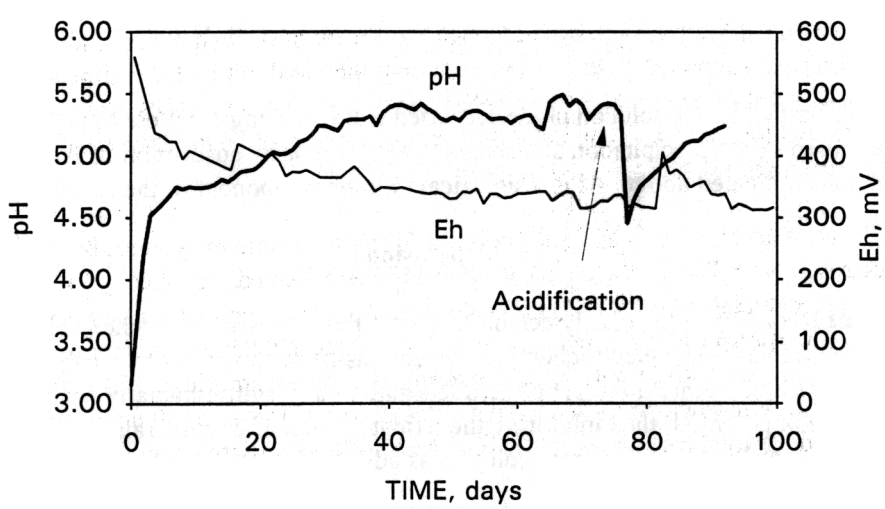

Figure 3. Changes in Eh and pH with time.

The ability of the system to respond to additional acidity following neutralization of the existing leachate was evaluated by a one-time addition, on day 77, of ~3.5 L of pH 3 leachate. The pH decreased from 5.30 to 4.45 (fig. 3) with a concomitant Eh increase from 314 to 418 mV. The pH and Eh recovered to values prior to the pH pulse within 16 days.

Precipitate Formation

When pH reached a steady-state value, a reddish-brown secondary solid phase was observed precipitating on the bottom of the experimental tank. SEM examination revealed a precipitate composed of a network of acicular crystals (fig. 4) with apparent trigonal symmetry. X-ray diffraction of specimens collected at various times throughout the experiment

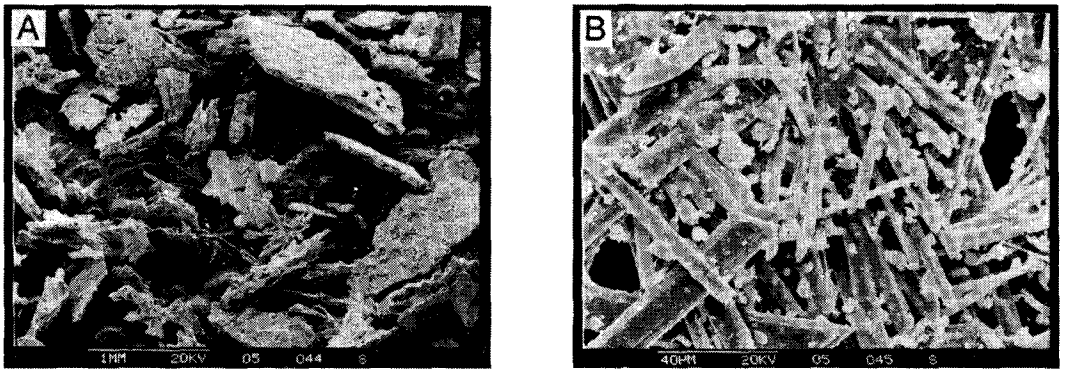

Figure 4. Scanning electron micrographs of precipitate: A) low magnification micrograph, B) higher magnification of acicular crystals within the aggregates.

revealed two predominant d-spacings at 4.75 $\pm$ 0.01 and 8.27 $\pm$ 0.01 nm. Although these two d-spacings are common to the iron sulfate hydrate mineral coquimbite ($Fe_2(SO_4)_3 \cdot 9H_2O$), the crystallinity of the precipitate is insufficient to enable positive identification by X-ray diffraction. Chemical analyses indicate a modal composition of approximately 43% Fe, 18% S, 21% Ca, and 15% Mg , 0.7% Al (fig. 5).

Aluminum Chemistry

Aluminum concentration in the solution phase decreased from 10.5 mg/L to less than 0.01 mg/L within 30 days. This decrease may be caused by the precipitation of a separate Al phase or by adsorption of Al by, or incorporation into, the Fe rich precipitate. As indicated above, Al is a significant minor component of the solid phase.

Conclusion

The results of this laboratory study clearly demonstrate that the proposed electrochemical approach is an effective treatment for acid mine drainage. The electrochemical system has been shown to be capable of generating sufficient voltage and current to raise and maintain the pH of acid leachate to an environmentally acceptable level of 5.5 and to significantly reduce the redox potential, thus inhibiting the oxidation of sulfide minerals. Furthermore potentially toxic elements such as aluminum may be scavenged from solution as adsorbed or structural components during the formation of a relatively stable iron sulfate precipitate.

Future research will focus on an examination of both leachate chemistry and on the nature of solid precipitates, especially as potential scavengers for contaminant metals. Other possible anodic materials will also be examined.

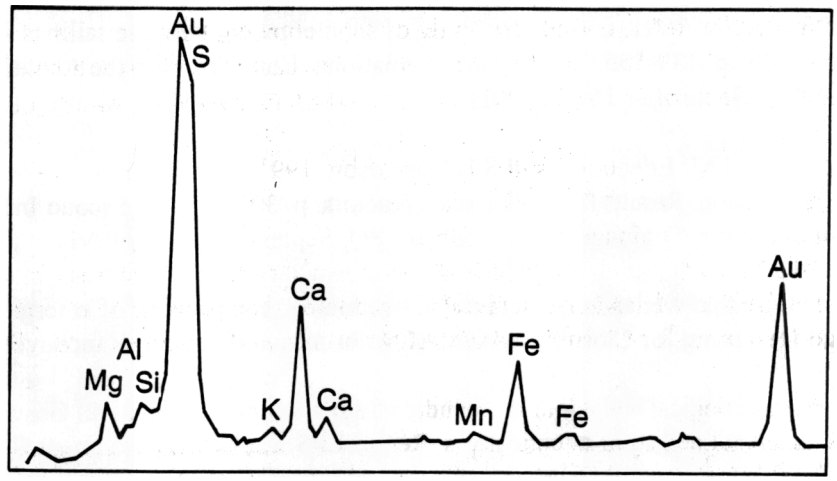

Figure 5. Energy dispersive spectrum of the iron sulfate precipitate.

Acknowlegements

The authors acknowledge the financial support of Dofasco Inc. in the early stages and of NSERC (Natural Sciences and Engineering Research Council) and URIF (University Research Incentive Fund) of the Ontario Ministry of Education and Universities for supporting the ongoing program. Special thanks to Syd Bartle, Raw Materials Manager, Dofasco Inc., for his enthusiasm and logistical support.

References

Ahmed, S.M. 1991. Electrochemical and surface chemical methods for the prevention of the atmospheric oxidation of sulfide tailings. p. 305-319. In Proceedings, Second International Conference on the Abatement of Acidic Drainage, v.2. (Montreal, PQ, September 16-18, 1991).

Baas Becking, L.G.M., I.R.Kaplan, and D. Moore. 1960. Limits of the natural environment in terms of pH and oxidation potentials. J. of Geology 68:243.

Blenkinsopp, S.A., 1991. The use of biofilm bacteria to exclude oxygen from acidogenic mine tailings. p. 369-377. In Proceedings, Second International Conference on the Abatement of Acidic Drainage, v.1. (Montreal, PQ, September 16-18, 1991).

Broman, G., P. Haglund, and E. Mattsson. 1991. Use of sludge for sealing purposes in dry covers - Development and field experiences. p. 515-527. In Second International Conference on the Abatement of Acidic Drainage, v.1. (Montreal, PQ, September 16-18,1991).

Brown, A., 1991. Proposal for the mitigation of acid leaching from tailings using a cover of muskeg peat. p. 517-527. In Second International Conference on the Abatement of Acidic Drainage, v.2. (Montreal, PQ, September 16-18, 1991).

Collin, M. and A. Rasmuson. 1990. Mathematical modelling of water and oxygen transport in layered soil covers for deposits of pyritic mine Tailings. p. 311-334. In Acid Mine Drainage-Designing for Closure; GAC/MAC Joint Annual Meeting, Vancouver, BC.

Doepker, R.D. and P.L. Drake. 1991. Laboratory study of submerged metal-mine tailings 3: Factors influencing the dissolution of metals. p. 139-155. In Second International Conference on the Abatement of Acidic Drainage, v.1. (Montreal, PQ, September 16-18, 1991).

Dvorak, D.H., R.S. Hedin, H.M. Edenborn, and S.L. Gustafson. 1991. Treatment of metal contaminated water using bacterial sulfate reduction: Results from pilot-scale reactors. p. 301-314. In Second International Conference on the Abatement of Acidic Drainage, v.1. (Montreal, PQ, September 16-18, 1991).

Hammer, D.A. 1990. Constructed wetlands for acid water treatment - An overview of emerging technology. p. In Acid Mine Drainage-Designing for Closure; GAC/MAC Joint Annual Meeting, Vancouver, BC.

Kalin, M. 1984. Long-term ecological behaviour of abandoned uranium mill tailings - 2. Growth patterns of indigenous vegetation on terrestrial and semi-aquatic areas, Report EPS 3/HA/2, Environment Canada.

Kalin, M. and R.O. Everdingen. 1987. Ecological engineering: biological and geochemical aspects - phase1 experiments. p. 565-590. In Proceedings - Acid Mine Drainage (Halifax, NS, Canada, March 23-26, 1987).

Kalin, M. 1990. Ecological engineering applied to base metal mining waste. p. 407-414. In Acid Mine Drainage: Designing For Closure; GAC/MAC Joint Annual Meeting, Vancouver, BC.

Kalin, M. and M.P. Smith. 1991. Biological amelioration of acidic seepage streams. p. 355-368. In Second International Conference on the Abatement of Acidic Drainage, v.1. (Montreal, PQ, September 16-18, 1991).

Karathanasis, A. and Y.L Thompson. 1991. Metal speciation and retention patterns in a high metal load acid mine constructed wetland of southeastern Kentucky. p. 485-496. In Second International Conference on the Abatement of Acidic Drainage, v.2. (Montreal, PQ, September 16-18, 1991).

Kuyucak, N., D. Lyew, P. St.-Germain, and K.G. Wheeland. 1991. In situ bacterial treatment of AMD in open pits. p. 335-353. In Second International Conference on the Abatement of Acidic Drainage, v.1. (Montreal, PQ, September 16-18, 1991).

McCready, R.G. 1987. A review of the physical, chemical, and biological measures to prevent acid mine drainage: an application to the pyritic Halifax Shales. In: Proceedings - Acid Mine Drainage (Halifax, NS, Canada, March 23-26, 1987).

Nicholson, R.V., R.W. Gillham, and E.J. Reardon. 1990. "Pyrite oxidation in carbonate-buffered solution: 2: Rate control by oxide coatings", Geochimi. et Cosmochimi. Acta 54 (395-402).

Nicholson, R.V., F.F. Akindunni, R.C. Sydor, and R.W. Gillam. 1991. Saturated tailings covers above the water table: the physics and criteria for design. p. 443-460. In Second International Conference on the Abatement of Acidic Drainage, v.1. (Montreal, PQ, September 16-18, 1991).

Ritcey, G.M. 1991. Deep water disposal of pyritic tailings - a simulation for acid prediction. p. 421-442. In Second International Conference on the Abatement of Acidic Drainage, v.1. (Montreal, PQ, September 16-18, 1991).

Sobek, A.A. 1987. The use of surfactants to prevent AMD in coal refuse and base metal tailings. In Acid Mine Drainage Seminar (Halifax, NS, March 23-26, 1987).

Stark, L.R., W.R. Wenerick, P.J. Wuest, and F.M. Williams. 1991. Adding a carbon supplement to simulate treatment wetlands improves mine water quality. p. 465-483. In Second International Conference on the Abatement of Acidic Drainage, v.2. (Montreal, PQ, September 16-18, 1991).

Yanful, E.K. and R. Nicholson. 1991. Engineered soil covers for reactive tailings management: theoretical concepts and laboratory development. p.461-485. In Second International Conference on the Abatement of Acidic Drainage, v.1. (Montreal, PQ, September 16-18, 1991).

AN EVALUATION OF A PEAT-WOOD CHIP-MICROFLORA ADMIXTURE TO ACT AS AN AMELIORANT FOR ACID MINE DRAINAGE[1]

Gene Shelp[2], Gord Southam[3], Graeme Spiers[2], Liangxue Liu[2], and Ward Chesworth[2]

Abstract: Peat was investigated as a potential source of indigenous microflora capable of: (1) providing a suitable carbon source for sulfate-reducing bacteria (SRB) through the anaerobic degradation of black spruce (*Picea mariana*) and trembling aspen (*Populus tremuloides*) wood chips, (2) complexing metals to form relatively insoluble sulphide minerals through the reduction of sulfate to sulphide, and (3) surviving exposures to extremely acidic conditions. Enumeration studies, combined with measurements of dissolved organic carbon, indicated sufficient available carbon was generated by anaerobic degradation of cellulose to support a viable population of SRB. The bacterial systems showed signs of recovery within 2 to 3 weeks following acidification to pH 3.0. The reestablishment of active microbial systems was indicated by the formation of a black iron sulphide precipitate.

Additional Key Words: acid mine drainage, sulphate reducing bacteria, cellulolytic bacteria, peat, wood waste.

Introduction

Acid mine drainage (AMD), associated with the weathering of sulfide-rich tailings and waste rock, is the single greatest environmental problem facing the Canadian mining industry. The acidic waters, containing high levels of potentially toxic trace elements, pose a substantial threat to aquatic ecosystems located within the immediate vicinity of sulphur-rich coal, base metal (Cu, Ni, Pb, Zn) and precious metal (Ag, Au) mining activities.

One of the most promising areas of AMD amelioration research is the study of organic-biological-inorganic interactions. In laboratory studies, Tuttle et al. (1969a) demonstrated that significant decreases in the concentrations of sulfate and iron in AMD could be achieved by treatment with wood dust inoculated with both cellulose-degrading bacteria and SRB. These results were visually manifested by the formation of a black iron sulfide precipitate through the reduction of sulfate to sulfide. In addition, during a 10-day culture period the pH increased from 3.6 to 7.0. The ability of the SRB to significantly reduce concentrations of sulfate and subsequently form complexes with iron and other heavy metals depends upon the availability of a soluble organic carbon source, and a suitable pH-Eh environment. According to Postgate (1984), the activity of SRB is inhibited at a pH<4.5 and at redox potentials exceeding -100 mV (SHE).

Field examination of an acid leachate stream seeping through a wood dust dam (Tuttle et al., 1969b) showed significant increases both in pH, from 2.84 to 3.38, and in the activity of heterotrophic bacteria. These increases were associated with significant decreases in both sulfate, from 8.765 to 6.1 μmol/mL, and iron, from 1.067 to 0.313 μmol/mL, in water downstream from the dam relative to that in the upstream pond. These changes were attributed to an active population of heterotrophic microflora, including dissimilatory SRB, occurring within and below the sawdust dam. Furthermore, with sawdust as the sole nutrient source, Tuttle (1969b) noted that mixed cultures containing cellulose-degrading bacteria and SRB were capable of reducing sulfate at pH 3.0, whereas pure cultures of SRB did not reduce sulfate below pH 5.5. Such studies demonstrate the potential benefits of biotreatment and suggest that indigenous microflora could be utilized when developing biologically mediated amelioration techniques.

---

[1]Paper presented at the International Land Reclamation and Mine Drainage Conference and the Third International Conference on the Abatement of Acidic Drainage, Pittsburg, PA, April 24-29, 1994.

[2]Gene Shelp, Ph.D Candidate, Graeme Spiers, Research Scientist, Liangxue Liu, Research Assistant, Ward Chesworth, Professor of Geochemistry, Department of Land Resource Science, University of Guelph, Guelph, Ontario, N1G 2W1.

[3]Gord Southam, Research Associate, Department of Microbiology, University of Guelph, Guelph, Ontario, N1G 2W1

In northern Canada, where metal mining is prevalent, the success of biological approaches may largely depend on the ability of the microorganisms to remain metabolically active under near-freezing conditions. Organic deposits native to the northern regions, such as peat, may provide a potential source of indigenous microflora capable of degrading cellulosic material, reducing sulfate to sulfide, and also surviving unfavorable thermal conditions. Locally-available wood products, such as chips and process waste, may provide a suitable appropriate carbon source capable of supporting a viable microbial culture.

Peat is composed of organic materials such as fulvic acids, humic acids, cellulose, hemicellulose, lignin, and bitumen as well as mineral material, water, and dissolved gases such as carbon dioxide, oxygen, and methane. In addition to peat providing a consortium of microorganisms, the reactive organic component is capable of adsorbing and complexing cationic forms of metals (Stevenson 1982; Henrot and Weider 1990) and reducing anionic forms of certain metals to cationic forms (Szalay and Szilagyi 1967, Goodman and Cheshire 1982) which may then be adsorbed. Furthermore, Gambrell et al. (1977) found that the stability of the metal complexes, especially of copper, lead, and cadmium, decreased as reduced materials were subjected to oxidizing conditions. Consequently, anaerobic conditions are required to fully utilize the adsorption capacity of peat materials as an important sink for metals. This adsorption capacity for metals may be especially critical during periods of low pH and relatively low bacterial activity encountered during spring thaw.

This paper presents results from a series of experiments conducted to examine the following: the ability of peat material to provide a suitable consortium of microflora; the ability of indigenous cellulolytic microflora to degrade black spruce (*Picea mariana*) and trembling aspen (*Populus tremuloides*) wood chips under optimum ionic and ambient thermal conditions and, subsequently, provide an adequate supply of available carbon to support a viable population of SRB; and the ability of the microflora to withstand chronic and acute exposures to acidity levels characteristic of AMD.

Materials and Methods

Spruce and poplar wood chips were shredded and sieved to less than 4-mm. The peat, collected from a minerotrophic organic deposit, is characterized by a pH of 5.66 and a high base saturation (10,000 to 15,000 ppm Ca, 1,500-6,500 ppm Mg).

The degradation experiments were conducted at 25 ± 2 °C. For each experiment 20 g each of wood chips and peat were placed in nine 500-mL Erlenmeyer flasks with 200 mL of a balanced salt solution (pH 7) and stoppered with aluminum foil. The balanced salt solution consisted of 1.0 g $(NH_4)_2SO_4$, 1.0 g K_2HPO_4, 0.2 g $MgSO_4$, 0.1 g $CaCl_2$, and 10.0 g $FeCl_3$ made up to 1L with deionized water adjusted to pH 7.0 with 5M H_2SO_4, and then sterilized at 121°C for 15 min.

The pH and Eh of the supernatant were recorded weekly. The redox potentials presented in this paper were standardized to the hydrogen scale. Five-milliliter solution samples were pipetted, filtered through Whatman No. 44 filter paper, and analyzed colorimetrically for dissolved organic carbon. Following each extraction, 5 mL of the balanced salt solution were added to maintain the initial volume.

The first stage of each experiment was allowed to proceed for 11 weeks to allow development of viable microfloral populations. The degradation of a piece of filter paper (Whatman No. 44) placed in each flask provided visible evidence of an active population of cellulose-degrading microflora. The second stage involved exposing the mixed bacterial cultures to acid, followed by an evaluation of their ability to survive and rebound to the activity levels that would be required to ameliorate AMD. Of the nine replicates, three were given an acute exposure to acid, and three were given a chronic exposure; the remaining three were not exposed to acid.

Acute exposure consisted of acidification by the addition of 5M H_2SO_4 until the system stabilized at pH 3.0 twice within a 4-day period. This treatment was considered a worst-case scenario, with recovery of the system demonstrating

the ability of indigenous mixed cultures to survive harsh conditions not normally associated with laboratory cultures. However, for both wood species, difficulty was experienced during the attempt to acidify the systems to pH 3. Although the samples were vigorously mixed during the acidification process, the pH rebounded to values exceeding 3.0 within 3 to 7 days suggesting that some pockets of alkalinity may have survived the mixing process. Chronic exposure involved the lowering of the pH using 5M H_2SO_4 by one pH unit per week until pH 3 was reached. Following acidification, the same monitoring procedures were used with no additional nutrient solution being added to the flask after the solution phase was sampled.

For microbiological analyses, the bacteria were enumerated 1 day prior to the initial acidification at week 11 and 12 for poplar and spruce, respectively, and 1 and 3 weeks after acidification. Flasks were agitated weekly and aliquots of the fluid phase were removed from within the peat-wood chip material. A modified Hungate technique (Hungate, 1969) was used to enumerate the cellulolytic bacteria, whereas the SRB were enumerated with the standard five-tube most probable number (MPN) method (Mara and Williams, 1970). All cultures were incubated at 25° C. An additional control, consisting of peat and the balanced salt solution, was set up to determine whether a viable population of SRB could be established with peat as the sole carbon source.

Results and Discussion

The effects of anaerobic degradation of spruce and poplar wood chips are shown on figures 1 and 2. The initial pH of the solution produced from poplar wood chips (pH 6.0) is typically higher than that for spruce (pH 5.0), and represents the equilibrium pH for the simple hydrolysis of different wood species. Physicochemical data obtained from the solution phase are presented below and discussed by wood species.

Prior to Acidification

Immediately prior to acidification both spruce and poplar showed a final solution pH of approximately 7.0 (fig. 1 and 2). A similar trend was noted for the peat control, which also had an initial equilibrium pH of less than 6.0. In both the treatments and the peat control, the rise in pH was accompanied by a significant decrease in redox potential, from an initial value of ~+300 mV to -150 mV. Even after several weeks of purging with N_2, the Eh remained relatively constant. Such data suggest that active microbial cultures exist that are capable of altering their environment to establish favourable Eh/pH conditions.

The existence of active microbial populations is further supported by the presence of significant concentrations of relatively low molecular weight organic compounds in solution (DOC). In the case of spruce, the DOC content, which was ~300 μg/mL C after 1 week, levelled off at ~400 μg/mL C after 3 weeks. The poplar DOC level, on the other hand, remained relatively constant at 200 μg/mL C throughout the preacidification period. The observed trends may be the result of predominantly hydrolysis reactions and not due to bacterial degradation of cellulose.

Period Following Acidification

Distinctly different trends in pH, Eh, and DOC are evident for the treatments following acidification (fig. 1 and 2). For spruce, the unacidified samples showed no significant deviations from the apparent equilibrium values for all measured parameters. In contrast, acidification resulted in immediate decreases in DOC, with the rate of change being proportional to the rate of acidification. Once pH 3 conditions were established, the DOC content of the solution remained relatively constant at 200 μg/mL C for both treatments. The redox potentials for acidified samples increased significantly, from -100 to +100 mV, possibly due to the strong oxidizing effect of sulphuric acid at low redox potentials and, to a lesser degree, the decrease in bacterial activity. However, by the 19th week both acid treatments showed signs of recovery towards the earlier equilibrium conditions. Redox potentials decreased with a concomitant slow increase in pH. These results indicate that the spruce systems appear to recover, with the rate of recovery being independent of the method of acidification.

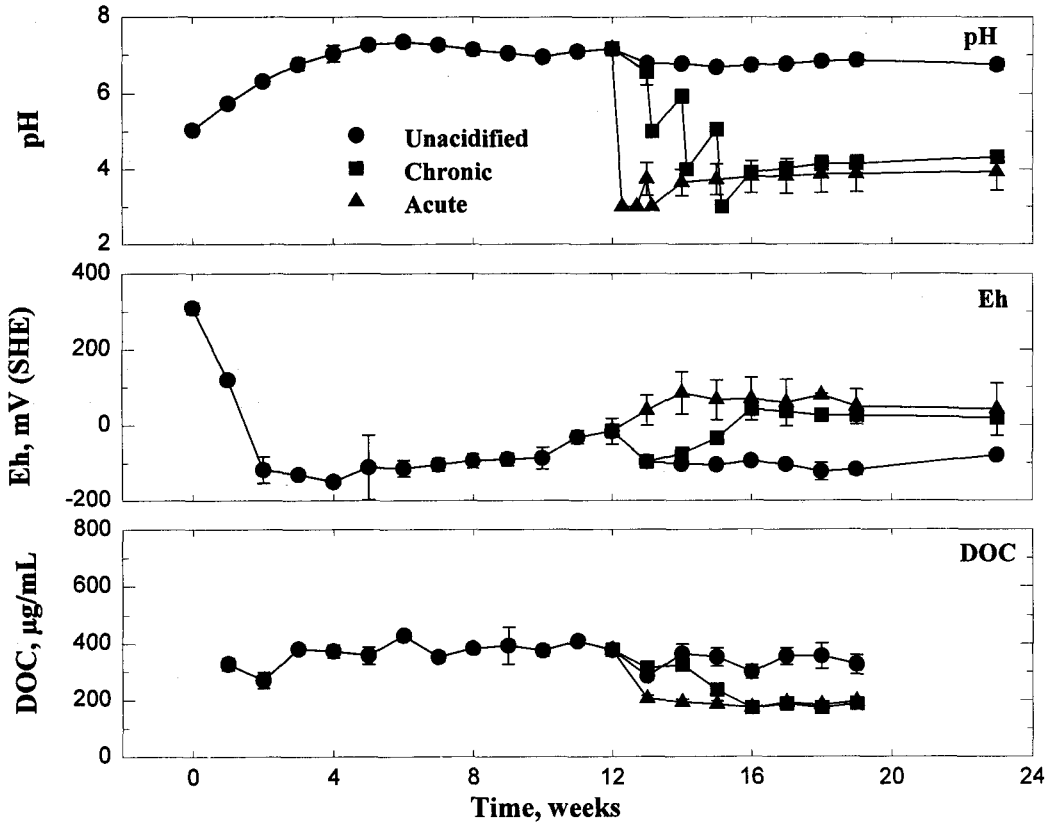

Figure 1. Temporal changes in pH, Eh, and DOC for the solution phase of spruce wood chips under anaerobic decomposition with various acidification treatments.

In contrast to spruce, the pH of the poplar unacidified samples decreased from 7.0 to stabilize at approximately 6.0. The redox potentials remained relatively constant at ~-100 mV. Following week 11, DOC increased linearly, with a twofold to threefold increase by week 17. On acidification, the redox potentials in both the acute and chronic systems increased initially, from -100 to approximately +150 mV. Again, these changes are a result of the strong oxidizing effect of H_2SO_4. The redox potentials slowly decreased to approximately +50 mV (acute) and 0 mV (chronic) by week 22. This decrease is attributed to the activity of the bacteria. The DOC content for the acute treatment remained relatively constant, whereas that for the chronic treatment initially increased and then declined to the pre-acidification level of ~200 ug/mL by week 17.

Thus, although differences apparently exist in the individual microcosm dynamics, the apparent pH and Eh trends for the acute and chronic acidification treatments of spruce and poplar suggest that both systems are capable of recovering from exposures to high levels of acidity.

Bacterial Studies

Cellulolytic Bacteria. The existence of active cellulolytic bacterial populations is indicated by complete breakdown of filter paper in all flasks by Week 22. Although the numbers are relatively low, the initial enumeration results show that cellulolytic bacteria appear to have been more successful at colonizing poplar than spruce (table 1). Lower DOC values were observed for poplar, at 200 µg/mL C, than for spruce, at 350 µg/mL C. Since dissolved organic carbon measurements represent the residual net soluble carbon resulting from both cellulose degradation and microbial

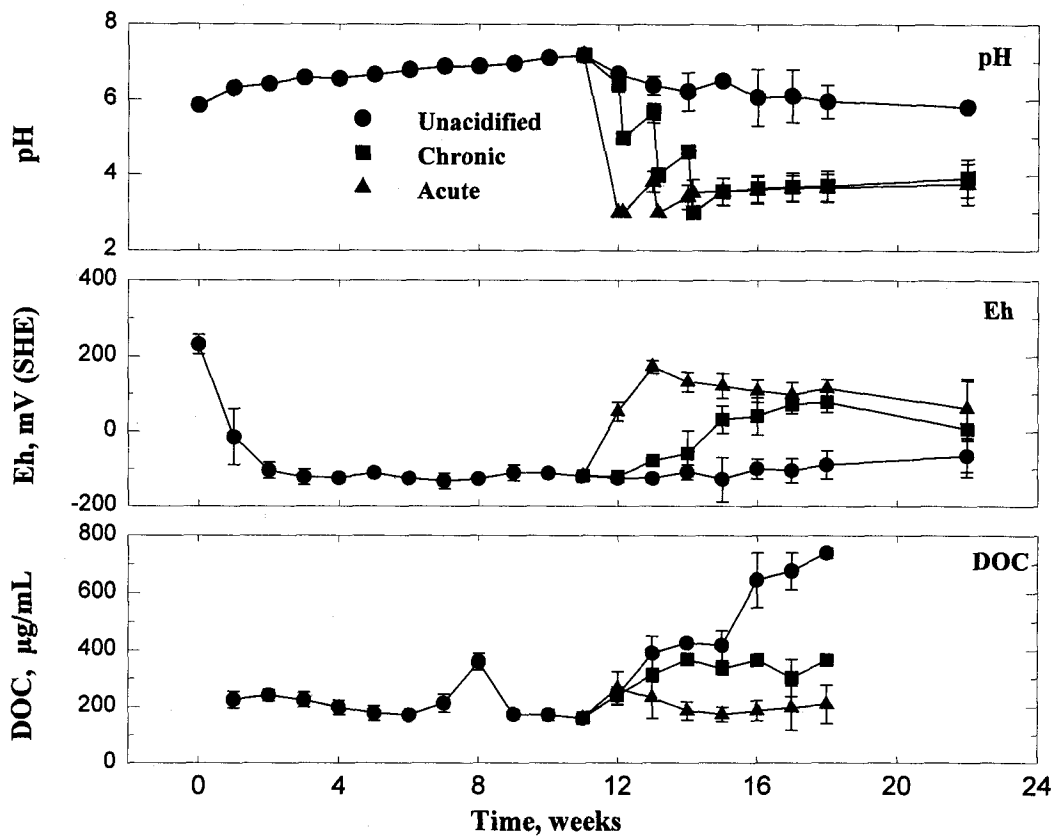

Figure 2. Temporal changes in pH, Eh, and DOC for the solution phase of poplar wood chips under anaerobic decomposition with various acidification treatments.

Table 1. Plate counts in colony forming units per mL for cellulolytic bacteria

Wood species	Treatment	Enumeration date		
		1 day prior to acidification	Time following acidification	
			Week 1	Week 3
Spruce	Acute	10	7,800	1,300
	Chronic	120	1,650	900
	Unacidified	130	250	600
Poplar	Acute	1,200	3,300	160
	Chronic	2,550	5,000	15
	Unacidified	1,500	>31,000	700

metabolism, the DOC results support the preference for poplar. The apparent preference of the cellulolytic bacteria for poplar may be due to the lower lignin content relative to spruce.

Following acidification, the populations of cellulolytic bacteria for both spruce and poplar showed significant increases. Although solution samples were collected from within the wood chip-peat layer, the enumeration results are most likely representative of planktonic and not sessile forms of cellulolytic bacteria. Consequently, the higher counts likely resulted from the liberation of sessile forms, including spores, from cellulosic material on the addition of sulphuric acid. The general decrease in bacterial counts from week 1 to week 3 is due to a return to a predominantly sessile population.

Sulfate-Reducing Bacteria. The changes in the SRB populations for spruce and poplar are shown in table 2. Prior to acidification, the populations in the solution of all flasks with spruce were very low, 79 to 920 MPN/mL. The results are

Table 2. Most Probable Number per mL for sulfate reducing bacteria

Wood species	Treatment	Enumeration date		
		1 day prior to acidification	Time following acidification	
			Week 1	Week 3
Spruce	Acute	79	13000	1300
	Chronic	49	280	1700
	Unacidified	920	33	33
Poplar	Acute	11000	35000	1300
	Chronic	28000	160000	12000
	Unacidified	3300	23	180

similar to those for cellulolytic bacteria, in that significantly higher bacterial counts were obtained for the acute treatment, at 13,000 MPN/mL, immediately following acidification. Again, the higher counts may have resulted from the liberation of sessile forms from both suspended and accumulated precipitate material on the addition of sulphuric acid. After 3 weeks the bacterial counts for both treatments, acute (3,300 MPN/mL) and chronic (1,700 MPN/mL), suggest that mixed SRB populations are capable of surviving extremely acidic conditions. The unacidified spruce and poplar samples showed a decrease in the population of planktonic SRB during the same period. Sessile SRB were not enumerated because this would have disturbed pH-Eh microenvironments, and thus deleteriously affected the ability of the SRB's to withstand these acid conditions (Schindler and Turner, 1982).

The poplar treatments showed substantially higher counts (acute, 11,000 MPN/mL and chronic, 28,000 MPN/mL) than spruce prior to acidification, even though the pH and Eh data of the two systems were similar at approximately 7.0 and -100 mV. These data indicate that poplar may be a preferred cellulose substrate. The flasks were examined visually throughout the experiments. The formation of a black amorphous FeS precipitate was used as an indicator of an active SRB population (Postgate, 1984). All unacidified replicates for both spruce and poplar blackened to a point where the solution phase was opaque. For the poplar, one of three replicates for each treatment turned black. The remaining replicates, for both poplar and spruce, showed visual evidence suggesting active SRB populations. Furthermore, these observations suggest that anaerobic degradation of wood chips can provide sufficient available carbon to support an active microbial population capable of ameliorating AMD.

Since the concentration of iron in the balanced salt solution exceeded 34,000 mg/L, sulfide concentrations are assumed to have remained well below levels considered toxic to SRB. Consequently, sulphide toxicity is not considered responsible for the changes in the population size of SRB with time for the different treatments.

Conclusion

The results of this study clearly show that peat is an excellent source of indigenous anaerobic microflora capable of generating significant levels of dissolved organic carbon through biodegradation of wood chip cellulose. The DOC levels are sufficient to support a thriving population of SRB to reduce sulfate to sulfide, with the subsequent formation of relatively insoluble iron sulfide precipitates. The microfloral populations have demonstrated an ability to survive the very high levels of acidity characteristic of acid mine drainage.

Acknowlegements

The authors acknowledge the financial support of Natural Sciences and Engineering Research Council (NSERC), and University Research Incentive Fund (URIF) of the Ontario Ministry of Education and Universities and the Environmental Youth Corps program of the Ministry of Northern Development and Mines. We also thank Karim Jaber and Will Gower-Levinson for excellent technical support.

References

Gambrell R. P., R. A. Khakid, M. G. Verloo and W. H. Patrick, Jr. 1977. Transformations of heavy metals and plant nutrients in dredged sediments as affected by oxidation-reduction potential and pH. Part II. Materials and methods, results and discussion. Contract Report #DACW-39-74-C-0076, Office of Dredged Material Research, U.S. Army Engineer Waterways Experiment Station, Vicksburg, MS.

Goodman, B. A. and M. V. Cheshire. 1982. Reduction of molybdate by soil organic matter: EPR evidence for formation of both Mo(v) and Mo(iii). Nature 299: 618-620.

Henrot, J., and R. K. Weider. 1990. Processes of iron and manganese retention in laboratory peat microcosms subjected to acid mine drainage. J. of Environ. Quality 19(2), 312-320.

Hungate R. E. 1969. A roll-tube method for the cultivation of strict anaerobes. p. 117-132. In Methods in microbiology Academeic Press, Inc., Ltd., London.

Mara D. D. and D. J. A. Williams. 1970. The evaluation of media used to enumerate sulfate reducing bacteria. J. Appl. Bacteriology 33: 543-552.

Postgate, J. R., 1984. The Sulfate-reducing Bacteria. 2nd Edition, Cambridge University Press, New York

Schindler, D.W. and M. A. Turner. 1982. Biological, chemical and physical responses of lakes to experimental acidification. Water, Air, and Soil Pollution 18: 259-271.

Stevenson, F. J., 1982. Humus geochemistry, composition, reactions. Wiley-Interscience, New York

Szalay, A. and M. Szilagyi. 1967. The association of vanadium with humic acids. Geochim. et Cosmochim. Acta 31:1-6.

Tuttle, Jon H, P. R. Dugan, and C. I. Randles. 1969(a). Microbial sulfate reduction and its potential utility as an acid mine water pollution abatement procedure. Appl. Microbiol. 17 (2): 297-302.

Tuttle, Jon H., P. R. Dugan, C. R. MacMillan, and C. I. Randles. 1969(b). Microbial dissimilatory sulfur cycle in acid mine water. J. of Bact. 97: 297-302.

MASS BALANCE ASSESSMENT OF INITIAL WEATHERING PROCESSES DERIVED FROM OXYGEN CONSUMPTION RATES IN WASTE SULFIDE ORE[1]

Bo Strömberg[2], Steven Banwart[2], John W. Bennett[3] and A. I. M. Ritchie[3]

Abstract: A stoichiometric model for initial weathering processes in fresh waste rock has been developed for Aitik ore. Based on element mass balances, solubility equilibrium, mineralogy of unreacted waste rock, and literature data, we identified the dominant geochemical processes and determined geochemical reaction rates for weathering of pyrite, chalcopyrite, calcite, plagioclase and biotite using fluxes derived from large experimental columns filled with waste rock. The oxidation rate of reduced Fe and S was based on O_2-consumption rates that were previously determined in the columns. In the fresh waste rock, acidity production from pyrite weathering and rapid consumption of acidity by calcite dissolution dominate the proton balance. At an acidity production rate of 7.8 meq. kg^{-1} $year^{-1}$ of waste rock and a calcite alkalinity reservoir of 0-60 meq. kg^{-1}, we expect the waste rock leachate to remain near-neutral pH for 0-8 years. When calcite is consumed and pH drops, dissolution of previously precipitated copper on the the order of 0-1.8 mmole copper kg^{-1} of waste rock may temporarily increase the pollution load at the site.

Introduction

The release of heavy metals, sulfate, and acidity from mining waste exposed to the atmosphere is a potentially serious and long lasting environmental problem. Metal release rates depend critically on geochemical and transport processes that controls pH and redox buffer systems. Published data on chemistry of waste leachates (Wai et al. 1980, Sullivan and Yelton 1988) illustrate the correlation between trace metal concentrations and pH. At neutral pH, precipitation of (hydr)oxide metal precipitates or adsorption of free metal species on mineral surfaces can limit concentrations of trace metals. Acid leachates, however, often exhibit trace metal concentrations orders of magnitude higher (Karlsson et al. 1988) because of the higher solubility of secondary phases and the lack of adsorption at low pH. To predict pollution loads and implement efficient remediation strategies, processes controlling the pH buffer system need to be understood and predicted.

We have previously studied geochemical processes at the Aitik mining waste rock site in northern Sweden (Strömberg and Banwart 1994), using field data. Due to the low pH (3.5-4) of drainage waters from the waste rock heaps, thermodynamic solubility constraints suggest that copper released from sulfide weathering is essentially conserved in the aqueous phase. The low pH conditions are caused by the relatively rapid acidity

---

[1]Paper presented at the International Land Reclamation and Mine Drainage Conference and the Third International Conference on the Abatement of Acidic Drainage, Pittsburgh, PA, April 24-29, 1994.

[2]Bo Strömberg, M Sc, Steven Banwart, Ph D, Royal Institute of Technology, Stockholm, Sweden.

[3]John W. Bennett, Senior Research Scientist (D Sc, Ph D), A. I. M. Ritchie, Senior Principal Research Scientist (D Sc, Ph D), Australian Nuclear Science and Technology Organisation, Lucas Heights, NSW, Australia.

generation from pyrite oxidation in comparison with the rate of alkalinity production from silicate mineral weathering. Contributions to the total alkalinity mass balance for the heaps indicated calcite dissolution was small. Trace amounts of calcite are found in the fresh waste rock, however, and are assumed to react rapidly to completion soon after dumping of the waste rock. The average age of these heaps is approximately 8 years old.

In this paper, we investigate geochemical processes in fresh waste rock from the same site, using large experimental columns (0.8 m diameter x 2 m) filled with waste rock. Here we propose that the dominating geochemical reactions are simultaneous dissolution of sulfide minerals and calcite. We follow these reactions using water chemistry analysis of leachate from the columns. Based on element mass balances, solubility equilibrium considerations, results from mineralogical investigations of unreacted waste rock, and literature data, we construct a stoichiometric model for leachate genesis in the columns.

Column Experiments

The column experiments are part of an environmental assessment program for the Aitik waste rock site, which has been in progress for 2 years. Six columns are in operation, each filled with approximately 1,500 kg of waste rock. Bennett et al. (1993) determined O_2-consumption within the columns as a measure of sulfide mineral dissolution rates. The columns are unsaturated with water and are operated under oxic conditions, open to the atmosphere both from the top and the bottom. Irrigation rate and temperature within the columns are maintained close to that at the site (irrigation rate: 0.7 m year^{-1}; temperature: 5 °C). These large-scale column experiments approach the complexity of the field scale such as a range of particle sizes, a complex mineralogy, and possibly heterogeneous flowpaths. In contrast to field studies, however, the column experiments retain the capacity to determine precise element mass balances and the possibility to manipulate hydrologic and chemical inputs.

A total of 12 water samples were taken from the columns during experimental weeks 7 - 15. The samples were autoclaved (200 kPa for 30 min.) and acidified (10 ml concentrated HNO_3 to 40 ml sample) at the time of sampling and analysed within one week. Analyses on filtered (0.2 µm pore-diameter cellulose acetate membranefilteres) and unfiltered samples showed no measurable difference in composition. Total concentrations of dissolved metals were measured using inductively coupled plasma - atomic emission spectroscopy (ICP-AES, ARL-3580) and flame atomic adsorption spectroscopy (Perkin-Elmer 100B). Silicon was determined spectrophotometrically using molybdenum blue as chromogen. Anions were analysed using a Tecator 6200 ion chromatograph. Alkalinity was determined by volumetric titration of an unacidified aliquot of each sample by strong acid to the H_2O-CO_2 endpoint, and is reported as bicarbonate ion concentration. Proton activity was measured within one hour after sampling using a combined glass electrode - Ag/AgCl(s) and reference electrode system (Metroohm 691) calibrated with standard buffer solutions at pH 4 and 7, respectively.

Results and Discussion

Calculation of Aqueous Speciation

Table 1 gives the composition of column effluents. Speciation calculations for effluent composition from waste rock columns were carried out using the geochemical code PHREEQE (Parkhurst et al. 1980) with the original WATEQ thermodynamic data base (Truesdell and Jones 1974) revised by Nordstrom et al. (1991). Because the columns are maintained at oxic conditions with unsaturated water flow, we fixed pe by assuming equilibrium with the atmospheric reservoir of $O_2(g)$. Table 2 summarizes the degree of saturation with respect to selected minerals. Calcite, previously identified in rock samples (Bergström 1981), is near saturation. The effluents are also near saturation with respect to gypsum, chalcedony, and amorphous aluminum hydroxide, as possible alteration products of the rock matrix.The apparent partial pressure of $CO_2(g)$ as calculated from aqueous speciation is $pCO_2 = 10^{-2.4}$ atm. Effluents are at or near saturation with respect to several possible secondary copper-bearing minerals (tenorite, azurite, brochantite). These copper minerals have been identified in natural bedrock where supergene enrichment occurred (Cook 1978).

Table 1. Composition of column effluents, Mean concentrations ± 1 S.D.

$[SO_4^{2-}]$	19 ± 2.0	mM	$[Ca^{2+}]$	16 ± 2.7	mM	$[Al^{3+}]$	19 ± 0.9	μM
$[HCO_3^-]$	1.6 ±0.5	"	$[Mg^{2+}]$	2.5 ± 0.7	"	[Fe]total	1.5 ± 0.4	"
$[Cl^-]$	1.7 ± 0.9	"	$[K^+]$	0.87 ± 0.4	"	[Cu]total	5.5 ± 3.2	"
$[H_4SiO_4]$	0.28 ± 0.1	"	$[Na^+]$	3.6 ± 1.9	"	$[Zn^{2+}]$	29 ± 33	"
pH	7.2 ± 0.2	"	[Mn]total	0.11 ±0.02	"			

Table 2. Saturation index (S.I. ± 1 S.D.) with respect to selected minerals[1].

Calcite ($CaCO_3$)	-0.26 ± 0.4	$Cu(OH)_2(am)$	-1.4 ± 0.22[2]
Gypsum ($CaSO_4$*2H2O)	0.10 ± 0.1	Antlerite ($Cu_3SO_4(OH)_4$)	-1.2 ± 0.72[2]
Chalcedony (SiO_2)	0.23 ± 0.1	Brochantite ($Cu_4SO_4(OH)_6$)	0.40 ± 0.92[2]
$Al(OH)_3(am)$	0.66 ± 0.1	Malachite ($Cu_2CO_3(OH)_2$)	-0.57 ± 0.42[2]
Kaolinite ($Al_2Si_2O_5(OH)_4$)	9.3 ± 0.4	Azurite ($Cu_3(CO_3)_2(OH)_2$)	-0.09 ± 0.72[2]
$Fe(OH)_3(am)$	2.9 ± 0.3	Tenorite (CuO)	-0.35 ± 0.22[2]
Manganite (MnOOH)	6.0 ± 0.3	Cupric ferrite ($CuFe_2O_4$)	16 ± 0.52[2]
Alunite ($KAl_3(SO_4)_2(OH)_6$)	8.2 ± 1.0	Smithsonite ($ZnCO_3$)	-1.6 ± 0.33[3]
Jarosite ($KFe_3(SO_4)_2(OH)_6$)	1.8 ± 0.4	Franklinite ($ZnFe_2O_4$)	15 ± 0.83[3]

[1]Saturation index = log (IAP/ Kg'), where IAP is the ion activity product and Kg' is the conditional solubility product at experimental temperature, pressure and ionic strength.

[2]thermodyn. data Vieillard (1988).

[3]thermodyn. data Lindsay (1979).

Stoichiometric Model

Sulfide minerals are far from equilibrium in oxic environments, and weathering is constrained only by reaction kinetics or transport of molecular oxygen. Sulfide content in the Aitik waste rock is dominated by pyrite with smaller quantities of chalcopyrite, pyrrhotite, and sphalerite, as shown by examination of thin sections (table 3). Elemental analysis determined total sulfur and metal content of the rock, although pyrite and pyrrhotite cannot be distinguished from each other by this method.

Table 3. Mineral Composition of unreacted waste rock[1]

Plagioclase (oligoclase, Ab. 70%, An. 30%)		10-30 vol.%
Albite	$NaAlSi_3O_8$	
Anorthite	$CaAl_2Si_2O_8$	
K-feldspar	$KAlSi_3O_8$	10-30 vol.%
Biotite	$K(Fe_{1.5}Mg_{1.5})AlSi_3O_{10}(OH)_2$	10-20 vol.%
Muscovite	$KAl_2(AlSi_3O_{10})(OH)_2$	1-34 vol.%
Quartz	SiO_2	20-30 vol.%
Pyrite and pyrrhotite	FeS_2 and FeS	0.4-1.7 vol.%
Chalcopyrite	$CuFeS_2$	0.1-0.4 vol.%
Sphalerite	ZnS	0.01-0.06 vol.%
Calcite	$CaCO_3$	0-0.3 vol.%

[1]Sulfide content is estimated from elemental analysis of sulfur (Leco) and metals (powder XRF; Philips 1600). Distribution of rock forming minerals was estimated by examination of 50 thin sections (Bergström, 1981).

We consider oxidative weathering of pyrite by equation 1 and chalcopyrite by equation 2, as dominating sulfide phases. In defining the stoichiometry of equations 1 and 2, iron and copper are assumed to be conserved in solid phases. We reach this conclusion by noting that the fluxes of Fe(total) and copper from the columns are at least three orders of magnitude less than sulfate fluxes and oxygen consumption rates. The R and subscript denotes net forward reaction rate.

$$FeS_2(s) + 15/4O_2(aq) + 7/2H_2O \xrightarrow{R_{py}} 4H^+ + 2SO_4^{2-} + Fe(OH)_3(s) \quad (1)$$

$$CuFeS_2(s) + 17/4O_2(aq) + 7/2H_2O \xrightarrow{R_{ch}} 4H^+ + 2SO_4^{2-} + Fe(OH)_3(s) + CuO(s) \quad (2)$$

Calcite dissolution is an important source of alkalinity over the time scale of these experiments. Calcite content is low, however, even in fresh samples of unreacted rock (0-0.3 vol.%, Bergström 1981). The dissolution rate can be characterized as fast (e.g., Plummer et al. 1978) compared to the rate of acidity input and water flow rates in natural systems (Langmuir 1971). We calculate degassing of CO_2 by evaluating the mass balance for inorganic carbon.

$$CaCO_3(s) + H^+ \xrightarrow{R_{ca}} Ca^{2+} + HCO_3^- \quad (3)$$

$$HCO_3^- + H^+ \xrightarrow{R_{dg}} H_2O + CO_2(g) \quad (4)$$

An additional source of alkalinity is irreversible dissolution of primary minerals such as feldspars and micas. Table 3 lists dominant rock-forming minerals identified in samples from the site. We consider weathering of biotite by equation 5 and plagioclase by equations 6 and 7. Using mass balance considerations similar to those for iron and copper, we assume aluminum and silicon to be conserved in solid phases as weathering products. We neglect the weathering of K-feldspar and muscovite as sources of K^+ because fluxes of Mg^{2+} and K^+ as tracers for biotite weathering alone agree within a factor of two.

$$KMg_{1.5}Fe_{1.5}AlSi_3O_{10}(OH)_2(s) + 4H^+ + 3/8O_2(aq) + 3/4H_2O \xrightarrow{R_{bi}} K^+ + 3/2Mg^{2+} + 3/2Fe(OH)_3(s) + Al(OH)_3(s) + 3SiO_2(s) \quad (5)$$

$$NaAlSi_3O_8(s) + H^+ + H_2O \xrightarrow{R_{al}} Na^+ + 3SiO_2(s) + Al(OH)_3(s) \quad (6)$$

$$CaAl_2Si_2O_8(s) + 2H^+ + 2H_2O \xrightarrow{R_{an}} Ca^{2+} + 2Al(OH)_3(s) + 2SiO_2(s) \quad (7)$$

We also consider possible immobilization of calcium and sulfate as gypsum (equation 8).

$$Ca^{2+} + SO_4^{2-} + 2H_2O \xrightarrow{R_{gy}} CaSO_4{*}2H_2O(s) \quad (8)$$

Element Mass Balances for Waste Rock Columns

To estimate the reaction rates for the geochemical processes described in the previous section, we carry out a mass balance calculation for the waste rock columns. The mass balance for molecular oxygen includes a measured rate of oxygen consumption, J_{O_2} (mole O_2 kg^{-1} s^{-1}), and rates of the oxygen-consuming reactions R_{py}, R_{ch}, and R_{bi} (mole kg^{-1} s^{-1}). The consumption of molecular oxygen was previously determined for these columns to be on average $(2.4\pm0.8) * 10^{-10}$ moles kg^{-1} s^{-1} for the waste rock matrix (Bennett et al. 1993).

$$J_{O2} = 15/4R_{py} + 17/4R_{ch} + 3/8R_{bi} \quad (9)$$

A relationship between pyrite and chalcopyrite weathering is required, we therefore introduce a linear dependence between mineral reaction rate, R, mineral volume abundance, V, and relative reactivity. The dependence on mineral abundance can be expected for a reaction where accessibility to surface area is critical (surface controlled kinetic reaction). Steger and Desjardins (1978) showed with weathering experiments that the relative reactivity of chalcopyrite is approximately one-half that of pyrite.

$$R_{ch} = 1/2 \frac{V_{ch}}{V_{py}} R_{py} \quad (10)$$

The dissolution rates for biotite (R_{bi}, equation 5) and albite (R_{al}, equation 6) are given by using effluent concentrations, C (mole dm^{-3}), of Mg^{2+} and Na^+ as tracers for the respective reactions. The flow rate through the columns, Q, was $9.3 * 10^{-6}$ dm^3 s^{-1} and M, total mass of waste rock within the columns, is approximately 1,500 kg.

$$R_{bi} = 2/3\ C_{Mg}\ Q/M \quad (12)$$

$$R_{al} = C_{Na}\ Q/M \tag{13}$$

Dissolution of anorthite, R_{an} (equation 7), is given by assuming a stoichiometric dissolution with respect to the end member composition of plagioclase (table 3). In any case, we expect the contribution of calcium from anorthite dissolution to be small in comparison with that from calcite dissolution. Laboratory studies at neutral pH show dissolution rates of anorthite and albite to be within one order of magnitude (Amrhein and Suarez 1988, Knauss and Wolery 1986). Calcite dissolution rate at neutral pH and atmospheric pCO_2, however, is at least 5 orders of magnitude faster (Plummer et al. 1978).

$$R_{an} = 3/7\ R_{al} \tag{13}$$

A mass balance for sulfate (equation 14) gives the rate of gypsum precipitation, R_{gy} (equation 8).

$$R_{gy} + C_{SO4}\ Q/M = 2R_{py} + 2R_{ch} \tag{14}$$

A mass balance for Ca (equation 15) gives the rate of calcite dissolution, R_{ca} (equation 3). Comparing the rate of calcite dissolution with the total proton balance (equation 16) gives a mass balance for inorganic carbon and thus CO2 degassing, Rdg (equation 4).

$$R_{ca} + R_{an} = R_{gy} + C_{Ca}\ Q/M \tag{15}$$

$$4R_{py} + 4R_{ch} = R_{ca} + 4R_{bi} + R_{al} + 2R_{an} + R_{dg} \tag{16}$$

Geochemical Reaction Rates

Table 4 lists reaction rates for processes 1 - 8, obtained by solving equations 9 through 16. Acidity input from pyrite weathering and rapid acidity consumption by calcite dissolution dominate the proton balance.

Because speciation calculations indicate equilibrium with respect to calcite, the net rate of dissolution is apparently controlled by relatively slow acidity input from sulfide weathering with rapid reaction kinetics for calcite dissolution. The slightly elevated partial pressure of CO_2 as calculated from aqueous speciation indicates slow mass transfer for CO_2 between aqueous and gaseous phases. Because the carbonate system is open to the atmosphere, most of the inorganic carbon dissolved from calcite is released as carbon dioxide gas.

As opposed to rapid calcite dissolution, primary silicate mineral weathering is kinetically controlled and dissolution rates are not directly coupled with acidity input from sulfide weathering. Silicate weathering also contributes slightly to oxygen consumption due to the release of ferrous iron. Biotite and plagioclase weathering have previously been identified as dominant alkalinity sources in large-scale natural systems (Giovanoli et al. 1988). In the initial weathering of waste rock studied here, the relatively small reservoir of calcite dominates alkalinity generation due to fast dissolution kinetics.

We estimate the capacity of the calcite alkalinity reservoir to be 0 - 60 meq. kg^{-1} of waste rock based on the calcite content (table 3). The acidity production rate is 7.8 meq. kg^{-1} $year^{-1}$ of waste rock (table 4, equations 1

and 2). We therefore expect the waste rock leachate to remain pH neutral for 0-8 years. When calcite is depleted, the remaining slow silicate weathering will be insufficient to consume all acidity inputs from sulfide weathering, and leachate pH will consequently drop. This is in agreement with pH measurements of drainage water from older waste rock at the Aitik site. The reaction rates from these calculations are therefore only valid during the relatively short period of calcite buffering when waste rock is initially deposited at the Aitik site. Weathering rates on geologic timescales, or on the lifetime of the Aitik waste deposit, may depend on hydrologic and climatic conditions, formation of inhibiting secondary phases, and depletion of the sulfide minerals (Strömberg and Banwart, 1994).

The effluent data and the calculations show an accumulation of copper in secondary phases during calcite pH buffering. At an accumulation rate of 0.22 mmole kg^{-1} $year^{-1}$ (equation 2), we can expect to have a reservoir of precipitated copper on the order 0-1.8 mmole kg^{-1} of waste rock when all calcite has been consumed. Subsequent dissolution of this reservoir due to decrease in pH after calcite is consumed may temporarily increase the pollution load at the site.

Table 4. Geochemical reaction rates.in mole kg^{-1} s^{-1} of waste rock.

Equation 1	Rpy	(Pyrite diss.)	$5.5 * 10^{-11}$	Equation 5	Rbi	(Biotite diss.)	$1.0 * 10^{-11}$
Equation 2	Rch	(Chalcopyrite diss.)	$6.9 * 10^{-12}$	Equation 6	Ral	(Albite diss.)	$2.2 * 10^{-11}$
Equation 3	Rca	(Calcite dis.)	$9.6 * 10^{-11}$	Equation 7	Ran	(Anorthite diss.)	$9.6 * 10^{-12}$
Equation 4	Rdg	(CO2 deg.)	$7.1 * 10^{-11}$	Equation 8	Rgy	(Gypsum precip.)	$6.4 * 10^{-12}$

Acknowledgments

We thank Hans Jönsson, Boliden Mineral AB, for making water chemistry and mineralogical data available to us. Funding was received from the vonKantzow foundation (Sweden) and the Swedish Waste Research Council.

References

Amrhein, C. and D. L. Suarez. 1988. The use of a surface complexation model to describe the kinetics of ligand-promoted dissolution of anorthite. Geochim. Cosmochim. Acta 52, pp. 2785-2793.

Bennett J. W., M. J. Comarmond, and A. I. M. Ritchie 1993. A report to Boliden Mineral AB on oxidation rates of Aitik dump material - column studies, ANSTO/C337.

Bergström, U. 1981. Mineralogisk undersökning av generalprov från Aitik, Boliden Mineral AB, GCM/AIM/26/81 (in Swedish).

Cook, R. B. 1978. Famous Mineral Localities: Chuquicamata, Chile. The Mineralogical Record, Sept. -Oct., pp. 321-333.

Giovanoli, R., J. L. Schnoor, L. Sigg, W. Stumm, and J. Zobrist. 1988. Chemical weathering of crystalline

rocks in the catchment area of acidic Ticino Lakes, Switzerland. Clays and Clay Minerals 36, pp. 521-529.

Karlsson, S., B. Allard, and K. Håkansson. 1988. Characterization of suspended solids in a stream receiving acid mine effluents, Bersbo, Sweden. Appl. Geochem. 3, pp. 345-356.

Knauss, K. G., and T. J.Wolery. 1986. Dependence of albite dissolution kinetics on pH and time at 25 °C and 70 °C. Geochim. Cosmochim. Acta 50, pp. 2481-2497.

Langmuir, D. 1971. The geochemistry of some carbonate groundwaters in central Pennsylvania. Geochim. Cosmochim. Acta 35, pp. 1023-1046.

Lindsay, W. L. 1979. Chemical Equilibria in Soils. Wiley Interscience, N.Y.

Nordstrom, D. K., L. N. Plummer, D. Langmuir, E. Busenberg, H. M. May, B. F. Jones, and D. L. Parkhurst. 1991. Revised chemical equilibrium data for major water-mineral reactions and their limitations. In Chemical Modeling of Aqueous Systems II (eds D. C. Melchoir and R. L. Bassett), Chap 31, pp. 398-413, ACS Symposium Series 416.

Parkhurst, D. L., D. C. Thorstenson, and L. N. Plummer. 1980. PHREEQE - A computerized program for geochemical calculations. U.S. Geol. Survey, Water- Resources Invest 80 - 96.

Plummer, L. N., T. M. L. Wigley, and D. L. Parkhurst. 1978. The kinetics of calcite dissolution in CO2 water systems at 5 °C to 60 °C and 0.0 to 1.0 atm CO2. The Amer. J. of Sci. 278, pp. 179-216.

Steger, H. F., and L. E. Desjardins. 1978. Oxidation of sulfide minerals, 4. Pyrite, Chalcopyrite and Pyrrhotite. Chem. Geol. 23, pp. 225-237.

Strömberg, B., and S. Banwart. 1994. Kinetic modelling of geochemical processes at the Aitik mining waste rock site in northern Sweden. Appl. Geochem. (accepted for publication).

Sullivan, P. J., and J. L. Yelton. 1988. An evaluation of trace element release associated with acid mine drainage. Environ. Geol. Water Sci. 12, pp. 181-186.

Truesdell, A. H., and B. F. Jones. 1974. WATEQ, a computer program for calculating chemical equilibria of natural waters. J. Res. U.S. Geol. Surv. 2, pp. 233-248.

Vieillard, P. 1988. Propriétés thermochimiques des composés du cuivre Atlas de données thermodynamiques. Sci. Geol. Bull. 41, pp. 289-308.

Wai, C. M., D. E. Reece, B. D. Trexler, D. R. Ralston, and R. E. Williams. 1980. Production of acid water in a lead-zinc mine, Coeur d'Alene, Idaho. Environ. Geol. 3, pp. 159-162.

IRON AND MANGANESE DYNAMICS IN LABORATORY WETLAND MESOCOSMS: IMPLICATIONS FOR COAL MINE DRAINAGE TREATMENT[1]

William J. Tarutis, Jr.[2] and Richard F. Unz[3]

Abstract: The interstitial water dynamics of iron, manganese, and sulfide in wetland mesocosms exposed to different synthetic acidic mine waters were characterized to determine if the presence of iron, manganese, or sulfate influenced the anoxic removal of these metals. Twelve wetland mesocosms (PVC columns) were constructed in the laboratory employing spent mushroom compost as the organic substrate. Control columns received semiweekly additions of NaCl or Na_2SO_4 solutions (adjusted to pH 3 with HCl) for a period of 13 weeks. Treatment columns consisted of semiweekly additions of pH 3 solutions of (1) Fe(III) + Mn(II), (2) Fe(III) + SO_4, (3) Mn(II) + SO_4, or (4) Fe(III) + Mn(II) + SO_4 (added as metal chlorides or Na_2SO_4). After 8 and 13 weeks of exposure, interstitial water samples were collected and analyzed for pH, redox potential, sulfide, and metals, using standard procedures. Substantial acidification had occurred between 8 and 13 weeks of exposure. Iron and manganese acted synergistically with respect to metal removal, although iron had no influence (p=0.7) on manganese removal after 13 weeks. The inclusion of sulfate in synthetic mine water caused a slightly greater, but statistically significant (p<0.05), iron removal in mesocosms relative to mesocosms not receiving sulfate. Sulfate had no effect (p=0.5) on manganese removal. The results of this study suggest that the generation of sulfide by bacterial sulfate reduction can effectively retain iron, but not manganese, within anoxic soils. However, long-term removal of iron by this mechanism may be limited by an eventual decline in sulfate reduction owing to insufficient decomposable organic substrates or soil acidification.

Additional Key Words: coal mine drainage, wetlands, anoxic treatment, acidification.

Introduction

The mechanisms responsible for the removal and retention of iron, manganese, and sulfate in constructed wetlands receiving acidic mine drainage (AMD) include the formation of metal oxides (Wieder et al. 1990) and metal sulfides (Machemer and Wildeman 1992). The diagenetic remobilization of iron and manganese during suboxic diagenesis results in the diffusion of soluble metals from the subsurface into the overlying water, where they may ultimately arrive at the wetland effluent and be discharged. It has been suggested (Tarutis et al. 1992) that long-term metal retention in AMD wetlands would be enhanced by active sulfate reduction and the subsequent formation of metal sulfides. The purpose of this paper is to characterize the interstitial water dynamics of iron, manganese, and sulfide in wetland

---

[1]Paper presented at the International Land Reclamation and Mine Drainage Conference and the Third International Conference on the Abatement of Acidic Drainage, Pittsburgh, PA, April 24-29, 1994.

[2]William J. Tarutis, Jr., Assistant Professor of Ecology, Wilkes University, Wilkes-Barre, PA, USA.

[3]Richard F. Unz, Professor of Environmental Microbiology, The Pennsylvania State University, University Park, PA, USA.

mesocosms exposed to synthetic mine drainages and to test whether or not the presence of iron, manganese, or sulfate in the synthetic mine waters influenced the anoxic removal of these metals.

Materials and Methods

Twelve simulated wetlands were constructed in the laboratory using PVC columns (75 cm x 15 cm i.d.) with PVC caps cemented to their base. Each column was completely filled with air-dried spent mushroom compost (SMC) obtained from the Mushroom Research Center, The Pennsylvania State University, University Park, PA. The dried SMC was used as received from the facility. Distilled water was added, and each column was covered with a loose-fitting PVC cap to prevent evaporation during a 6-month stabilization period. The columns were maintained in a temperature-controlled room at 22° C. At semiweekly intervals, 1 L of solution was aspirated from the water surface and replaced with distilled water. The stabilization period allowed the SMC to settle and create ambient conditions conducive to sulfate reduction. After the stabilization period, 1 L of different synthetic mine waters was added twice per week over a 13-week period in the same fashion as described above. The experiments, performed using duplicate columns, consisted of four treatments and two controls as described in table 1.

Table 1. Chemical composition of synthetic mine waters[1] to which the wetland mesocosms were exposed.

	Concentration, mg/L					
Treatment	Fe	Mn	SO_4	Na	Cl	pH[2]
Control . .	0	0	0	200	310	3.0
SO_4 only .	0	0	500	240	0	3.0
Fe(III) + Mn(II) .	200	100	0	0	510	3.0
Fe(III) + SO_4 . . .	200	0	500	240	380	3.0
Mn(II) + SO_4 . . .	0	100	500	240	130	3.0
Fe(III) + Mn(II) + SO_4 . . .	200	100	500	240	510	3.0

[1] Fe and Mn were added as chlorides and SO_4 was added as sodium salt.
[2] pH adjusted with HCl.

Differences among treatment means were analyzed by Student's *t*-test for paired data. After 8 and 13 weeks of exposure to the synthetic mine waters, interstitial water samples (10 mL) were obtained by hypodermic syringe at 5-cm depth intervals through prefitted septa cemented along the PVC column wall. Samples were immediately analyzed for redox potential (epoxy-body platinum electrode calibrated with ZoBell's solution [ZoBell 1946]), pH (plastic-body pH combination electrode), and sulfide (specific-ion electrode). Samples were then acidified to pH<2 with HNO_3, and organic matter was removed by the addition of 0.08M $AlCl_3$, followed by centrifugation (Robbins 1989), and analyzed for iron and manganese by flame atomic absorption spectrophotometry (AAS).

Results

Concentration-depth profiles of redox potential, pH, iron, manganese, and sulfide measured in the columns after 8 and 13 weeks of exposure to the synthetic mine waters are shown in figures 1-5. All mesocosms were entirely anoxic with redox potentials ranging from -250 to -350 mV during the initial weeks of the experiment (figs. 1-5); a pungent sulfide odor characteristic of active sulfate reduction was noticeable throughout the entire 13-week study period. There was essentially no difference in the concentration of dissolved constituents between the two control columns (with and without sulfate in the absence of

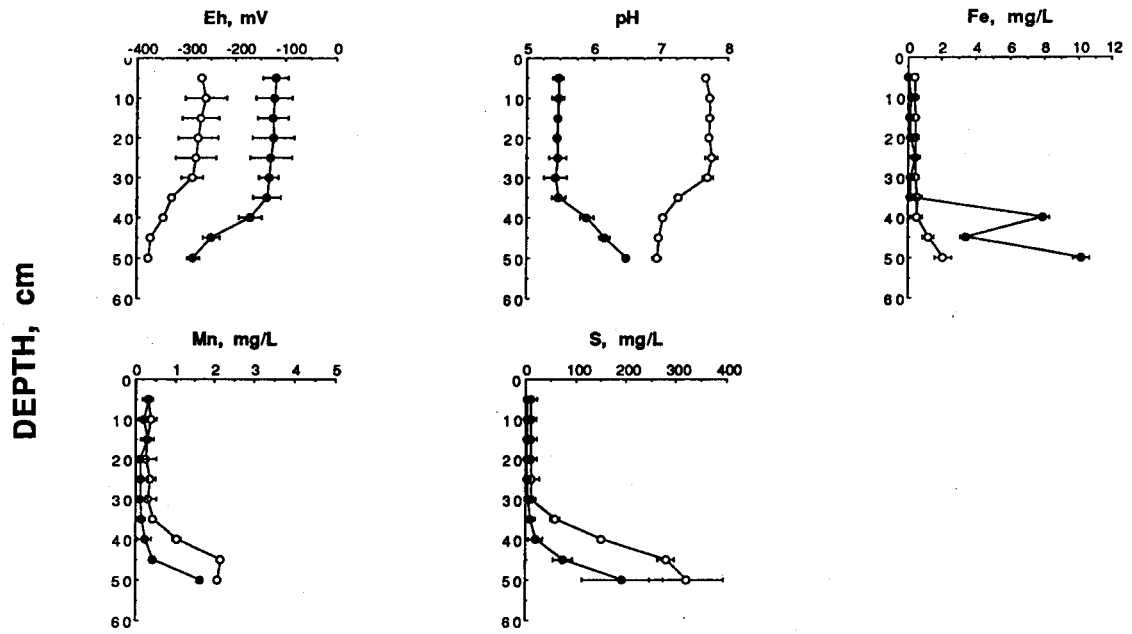

Figure 1. Interstitial water depth profiles of control (SO_4 only) columns after 8 (○) and 13 (●) weeks of exposure. Points are means of duplicate samples, and error bars equal one standard deviation.

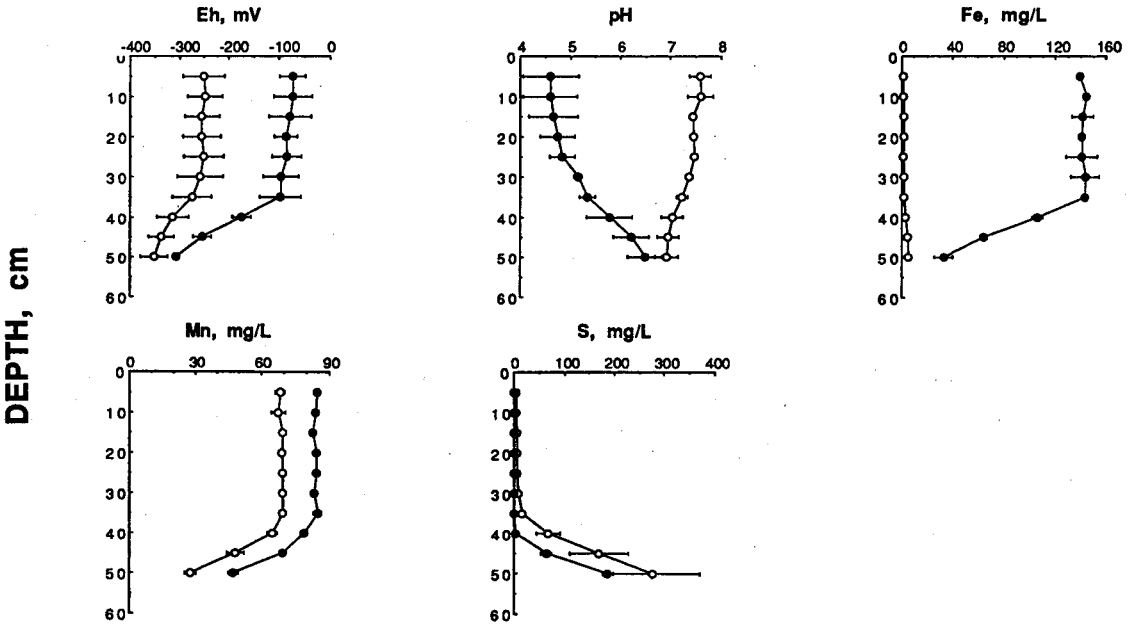

Figure 2. Interstitial water depth profiles of [Fe(III) + Mn(II)] treatment columns after 8 (○) and 13 (●) weeks of exposure. Points are means of duplicate samples, and error bars equal one standard deviation.

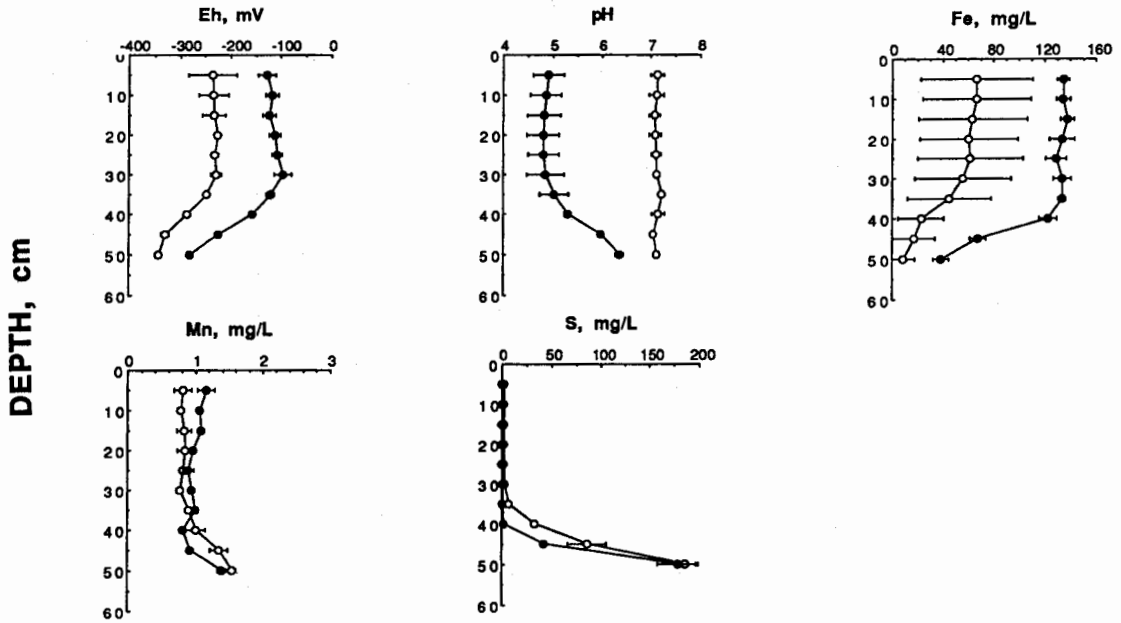

Figure 3. Interstitial water depth profiles of [Fe(III) + SO_4] treatment columns after 8 (○) and 13 (●) weeks of exposure. Points are means of duplicate samples, and error bars equal one standard deviation.

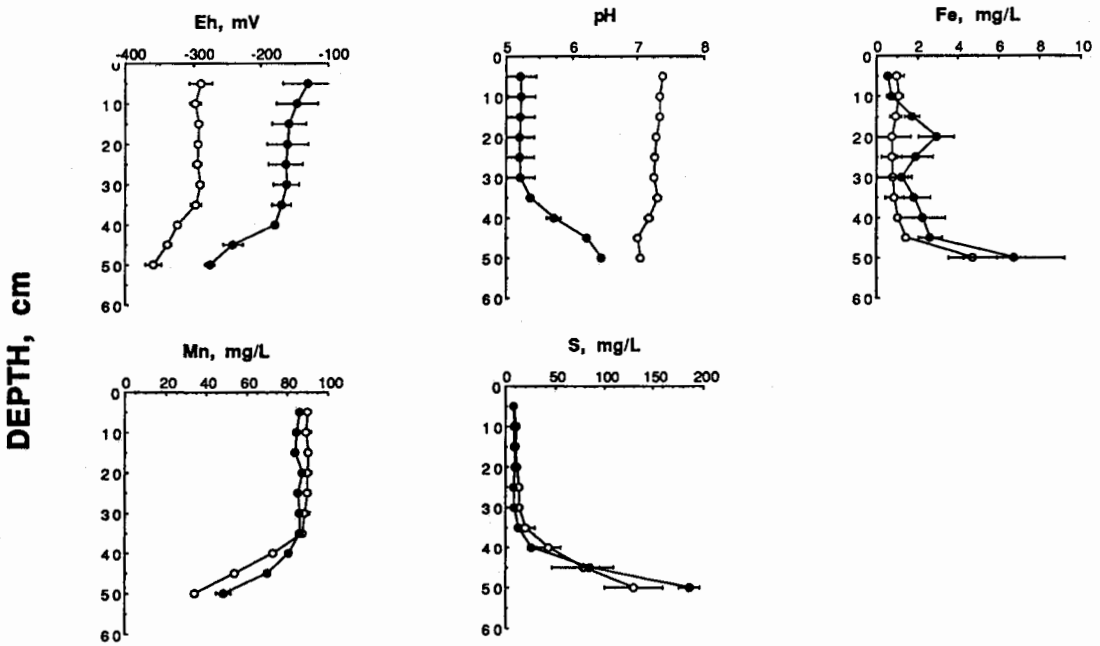

Figure 4. Interstitial water depth profiles of [Mn(II) + SO_4] treatment columns after 8 (○) and 13 (●) weeks of exposure. Points are means of duplicate samples, and error bars equal one standard deviation.

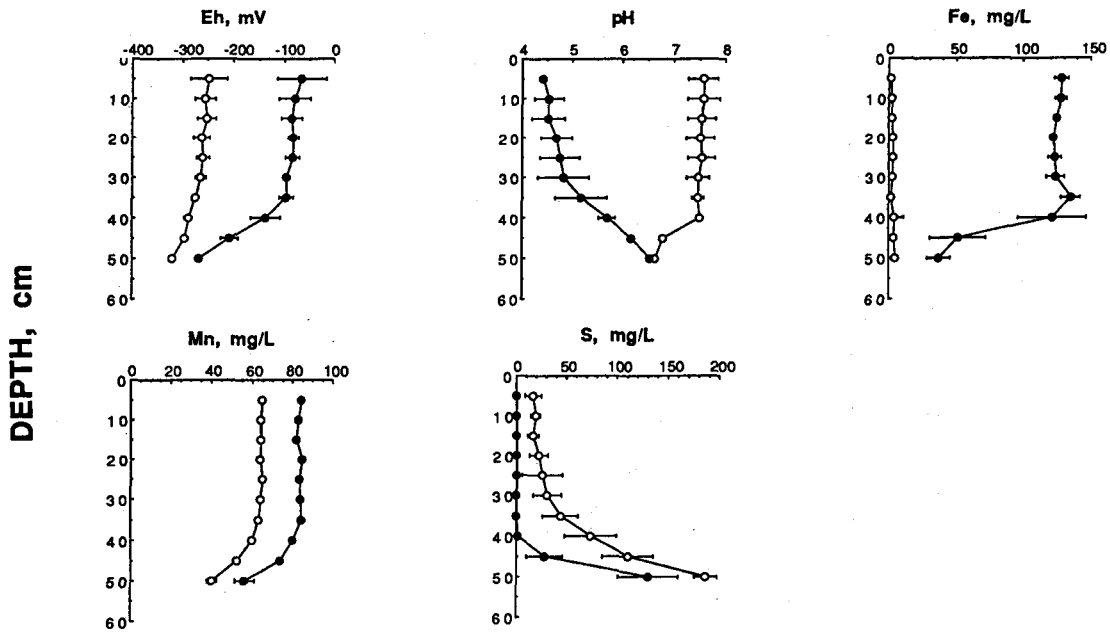

Figure 5. Interstitial water depth profiles of [Fe(III) + Mn(II) + SO_4] treatment columns after 8 (○) and 13 (●) weeks of exposure. Points are means of duplicate samples, and error bars equal one standard deviation.

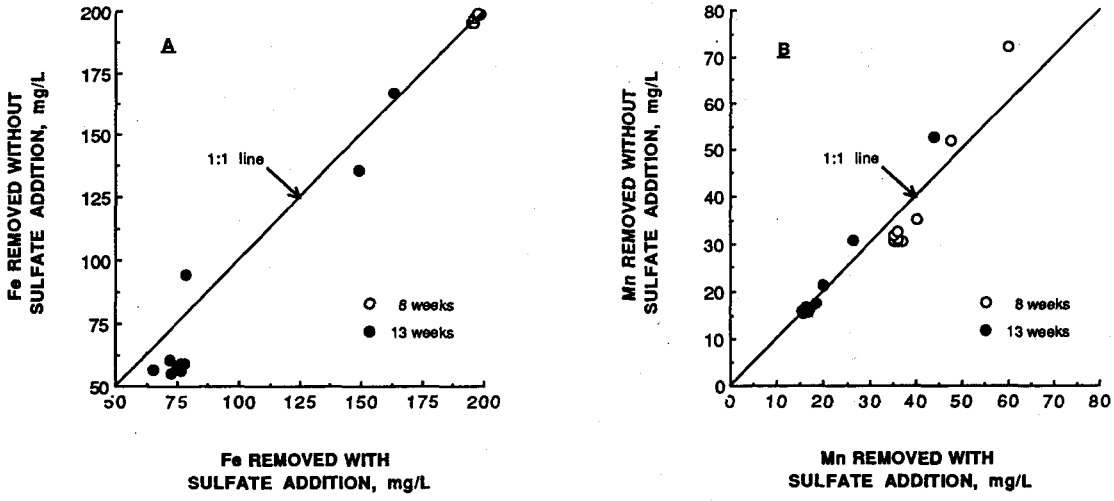

Figure 6. Comparison of removal of (A) iron and (B) manganese with and without sulfate addition for samples taken at various depths.

metals) after either 8 or 13 weeks of exposure (fig. 1). Without exception, the addition of acidic water caused a marked decrease in the pH of interstitial water in the upper portion of the columns, from circumneutrality to about 4.5 to 5.5 between the two sampling periods, which corresponded with a 100- to 200-mV increase in redox potential. In addition, after each sampling period the pH of interstitial water tended toward neutrality with increasing depth. Dissolved iron and manganese concentrations were low in the control columns, and dissolved sulfide increased dramatically in the lower 15 cm of all columns (figs. 1-5).

During the 13-week treatment period, the interior of all columns exposed to iron turned black almost immediately upon addition of synthetic mine water, but this seemed to decline throughout the course of the experiment. This was most pronounced in columns receiving both iron and manganese compared with columns receiving iron only. Columns not receiving iron showed no evidence of black color. The effect of iron and manganese on metal removal was statistically determined by comparison (paired *t*-test) of samples obtained from equal depths for selected treatments (table 2). The addition of manganese greatly enhanced iron removal during the first 8 weeks of exposure ($p<0.0005$); however, after 13 weeks of exposure manganese had little effect on iron removal, although it was statistically significant ($p=0.002$). Similarly, the addition of iron significantly enhanced manganese removal after 8 weeks ($p<0.0005$), but after 13 weeks no enhancement was observed ($p=0.686$). The addition of sulfate had a slight, but statistically significant, effect on the removal of iron after both 8 and 13 weeks ($p=0.019$; fig. 6A); sulfate had no effect on manganese removal over the same period ($p=0.472$; fig. 6B).

Discussion

The lack of an oxic zone in the wetland mesocosms afforded the opportunity to study the removal of iron and manganese from the synthetic mine waters in a totally anoxic environment. Such environments are common in the sediments of natural wetlands rich in organic carbon (Mitsch and Gosselink 1986). This was not a problem in the wetland mesocosms since carbon-rich SMC was used as the organic substrate.

The anoxic circumneutral conditions in the simulated wetlands are typical of waterlogged soils and sediments (Lindsay 1979). The addition of acidic solutions during the first 8 weeks did not appreciably affect the pH of the interstitial waters, but substantial acidification did occur during the following 5 weeks. Alkalinity generation by the decomposition of organic matter effectively buffers the pH of anoxic sediments exposed to acidified waters (Herlihy and Mills 1986). Herlihy et al. (1987) have shown alkalinity generation by sulfate reduction to be an important pH-buffering mechanism in lakes receiving AMD. In addition, the release of calcium from anoxic sediments provides another pH-buffering mechanism (Davison and Woof 1990). Gypsum ($CaSO_4 \cdot 2H_2O$) is a major component of SMC (Lohr et al. 1984) and is a potential source of calcium. Both sulfate reduction and calcium release probably contributed to the maintenance of circumneutral pH in the wetland mesocosms in this study, but these processes cannot go on indefinitely. For example, Carignan and Tessier (1988) found that acidic lake sediments eventually lose their capacity to generate alkalinity by sulfate reduction after prolonged exposure to acid rain.

A consequence of acidification is the potential for the rapid oxidation of iron sulfides by ferric iron (Moses et al. 1987). Acidification is brought about initially by the addition of acidic mine water to the columns. As the pH drops below 5, the rate of iron sulfide oxidation by free ferric iron increases dramatically, generating ferrous iron, sulfate, and hydrogen ions (Moses et al. 1987). This contributed to the observed decrease in pH and the increase in dissolved iron concentrations between the two sampling periods (figs. 1-5).

Examination of concentration-depth profiles revealed that iron was removed from solution far more easily and to a much greater extent than manganese. Dissolved sulfide preferentially complexes iron, forming the black iron monosulfide mineral mackinawite

(FeS; Morse et al. 1987). Iron was removed from solution more effectively in the presence of manganese (compare fig. 2 and fig. 5 with fig. 3; table 2). Manganese commonly forms mixed Ca-Mn-Mg carbonates or mixed Fe-Mn sulfides by coprecipitation (Middelburg et al. 1987). Columns in which both metals were added were much more black relative to columns receiving iron only. This suggests the formation of a mixed Fe-Mn sulfide mineral of lower solubility than "pure" iron monosulfide. Conversely, Arakaki and Morse (1993) found that adsorption of manganese to mackinawite to be quantitatively much more important (generally >90%) than coprecipitation; therefore, the rapid formation of black FeS likely enhanced manganese removal by adsorption (table 2).

The removal of iron and manganese was not affected to any appreciable extent by the addition of sulfate to the columns (figs. 6A and 6B; table 2). It was hypothesized that sulfate addition would stimulate bacterial sulfate reduction and provide additional sulfide to precipitate metals. Limited analysis of interstitial water sulfate revealed uniformly high sulfate levels (>500 mg/L) in all columns. It appears that gypsum in SMC provided sufficient sulfate for bacterial reduction, at least over the time frame of these experiments.

Higher metal removals were observed near the bottom of all columns treated with synthetic mine water, which corresponded spatially with increased dissolved sulfide concentrations (figs. 2-5). This was most likely due to a higher detention time near the column bottom. The mean detention time in the columns was about 40 days; however, the addition and removal of solutions from the top of the columns likely caused a decrease in detention time near the surface and an increase near the bottom. Thus, spatial

Table 2. Comparison (paired *t*-test) of iron and manganese removal for various treatment combinations.

Treatment[1]	*t*-statistic	d.f.[2]	*p*-value
Pooled data:			
Fe: SO_4 vs Mn+SO_4	5.285[3]	39	<.0005
Mn: SO_4 vs Fe+SO_4	4.791[3]	39	<.0005
Fe: Mn vs Mn+SO_4	2.450[3]	39	.019
Mn: Fe vs Fe+SO_4	0.726	39	.472
8 weeks:			
Fe: SO_4 vs Mn+SO_4	5.772[3]	19	<.0005
Mn: SO_4 vs Fe+SO_4	7.256[3]	19	<.0005
Fe: Mn vs Mn+SO_4	2.188[3]	19	.041
Mn: Fe vs Fe+SO_4	1.713	19	.103
13 weeks:			
Fe: SO_4 vs Mn+SO_4	3.549[3]	19	.002
Mn: SO_4 vs Fe+SO_4	0.410	19	.686
Fe: Mn vs Mn+SO_4	3.181[3]	19	.005
Mn: Fe vs Fe+SO_4	1.330	19	.199

1 The variable appearing before the colon is the object of the treatment. The parameter immediately following the colon was tested for its effect on the variable relative to the additional treatment, indicated by "vs."
2 d.f.=degrees of freedom.
3 Significant at the 0.05 level.

The biogeochemical interactions of carbon and sulfur were found to influence the removal and release of iron and manganese under reducing conditions characteristic of AMD wetland soils. Iron and manganese appeared to act synergistically with respect to the net removal of these metals under anoxic conditions, probably due to manganese adsorption and coprecipitation reactions with iron sulfides. The results of this study suggest that the generation of sulfide by bacterial sulfate reduction can effectively retain iron, but not

manganese, within the anoxic soil. However, long-term removal of iron by this mechanism may be limited by an eventual decline in sulfate reduction due potentially to insufficient decomposable organic substrates or soil acidification.

Literature Cited

Arakaki, T. and J.W. Morse. 1993. Coprecipitation and adsorption of Mn(II) with mackinawite (FeS) under conditions similar to those found in anoxic sediments. Geochim. Cosmochim. Acta 57:9-14.

Carignan, R. and A. Tessier. 1988. The co-diagenesis of sulfur and iron in acid lake sediments of southwestern Québec. Geochim. Cosmochim. Acta 52:1179-1188.

Davison, W. and C. Woof. 1990. The dynamics of alkalinity generation by an anoxic sediment exposed to acid water. Water Res. 24:1537-1543.

Herlihy, A.T. and A.L. Mills. 1986. The pH regime of sediments underlying acidified waters. Biogeochem. 2:377-381.

Herlihy, A.T., A.L. Mills, G.M. Hornberger, and A.E. Bruckner. 1987. The importance of sediment sulfate reduction to the sulfate budget of an impoundment receiving acid mine drainage. Water Resour. Res. 23:287-292.

Lindsay, W.L. 1979. Chemical equilibria in soils. Wiley-Interscience, New York.

Lohr, V.I., S.H. Wang, and J.D. Wolt. 1984. Physical and chemical characteristics of fresh and aged spent mushroom compost. HortSci. 19:681-683.

Machemer, S.D. and T.R. Wildeman. 1992. Adsorption compared with sulfide precipitation as metal removal processes from acid mine drainage in a constructed wetland. J. Contam. Hydrol. 9:115-131.

Middelburg, J.J., G.J. De Lange, and C.H. van der Weijden. 1987. Manganese solubility control in marine pore waters. Geochim. Cosmochim. Acta 51:759-763.

Mitsch, W.J. and J.G. Gosselink. 1986. Wetlands. Van Nostrand Reinhold, New York.

Morse, J.W., F.J. Millero, J.C. Cornwell, and D. Rickard. 1987. The chemistry of the hydrogen sulfide and iron sulfide systems in natural waters. Earth-Sci. Rev. 24:1-42.

Moses, C.O., D.K. Nordstrom, J.S. Herman, and A.L. Mills. 1987. Aqueous pyrite oxidation by dissolved oxygen and by ferric iron. Geochim. Cosmochim. Acta 51:1561-1571.

Robbins, C.W. 1989. Sample preparation for determining ions in dark colored sodic soil extracts. Soil Sci. Soc. Am. J. 53:721-725.

Tarutis, W.J., R.F. Unz, and R.P. Brooks. 1992. Behavior of sedimentary Fe and Mn in a natural wetland receiving acidic mine drainage, Pennsylvania, U.S.A. Appl. Geochem. 7:77-85.

Wieder, R.K., M.N. Linton, and K.P. Heston. 1990. Laboratory mesocosm studies of Fe, Al, Mn, Ca, and Mg dynamics in wetlands exposed to synthetic acid coal mine drainage. Water, Air, and Soil Pollut. 51:181-196.

ZoBell, C.E. 1946. Studies on redox potential of marine sediments. Bull. Am. Assoc. Petrol. Geol. 30:477-513.

LABORATORY AND PILOT-SCALE STUDIES ON THE TREATMENT OF ACID ROCK DRAINAGE AT A CLOSED GOLD-MINING OPERATION IN CALIFORNIA[1]

Thomas Wildeman[2,3] John Cevaal[4], Kent Whiting[4], James Gusek[3], and Joseph Scheuering[5]

Abstract: Acid rock drainage from a closed gold-mining operation in northern California was studied first in the laboratory and then on the pilot scale to determine the technical feasibility of passive treatment. The drainage has a pH of 3.8, and concentrations of Cu, Fe, Mn, Ni, and Zn of 140, 190, 28, 0.93, and 40 mg/L respectively. The laboratory studies concentrated on the question of whether local organic and soil materials could be used to support sulfate reduction in a passive treatment system. Samples were incubated at laboratory temperatures for a period of 4 weeks. Soil and wood processing wastes from the immediate vicinity proved to be too acidic to maintain a large population of sulfate reducers. The most reasonable material for sulfate reduction was a mixture of equal amounts by weight of cow manure, planter mix soil, and limestone chips. The final solutions had pH's of 6.5 to 6.9, and average Cu, Fe, Mn, Ni, and Zn concentrations of 0.02, 1, 5, 0.05, and 0.1 mg/L, respectively. Based on the laboratory results, a pilot system was constructed that consisted of a lined steel container filled with a substrate volume that measured 2 by 3 by 12 m. The substrate mixture was the same as used in the laboratory tests. Raw manure from a dairy farm was mixed into the substrate for the sulfate-reducing bacterial (SRB) inoculum. Loading of the system was based on the estimate that 0.3 mol sulfide per cubic meter of substrate per day would be generated, and the inflow of heavy metals should not exceed the sulfide generated. Using these principles, the flow was set at approximately 800 mL/min. Over the course of 9 months, the pilot system achieved removal of Cu and Ni below the effluent standards of 1.0 and 0.7 mg/L. Dissolved Zn concentrations in the effluent averaged approximately 0.1 mg/L, compared with an effluent standard of 0.02 mg/L. Dissolved Fe concentrations in the effluent varied with the seasons, reaching a minimum of 1 mg/L in the summer and rising to a maximum of 120 mg/L in the winter. There is a significant increase in concentrations of Fe in unfiltered waters. This implies that, in a full-scale system, a settling-polishing pond will be needed.

Additional Key Words: Constructed wetland, heavy metals treatment, sulfate reduction, pilot scale reactors

Introduction

In 1989, the use of anaerobic, subsurface wetlands that emphasize sulfate-reduction was in the developmental stage. In eastern United States, systems using mushroom compost that treated coal mine drainage were being studied by scientists at the U. S. Bureau of Mines (Hedin et al. 1988 and 1989, McIntire and Edenborn 1990). In the West, research at the Colorado School of Mines (CSM) was concentrating on the removal of contaminants from metal-mine drainages by sulfate reduction, also using mushroom compost as the substrate (Machemer and Wildeman 1992, Machemer et al. 1993, Wildeman et al. 1993). In 1990, two breakthroughs on wetlands treatment significantly advanced research at CSM: (1) The determination that the primary anaerobic removal process is sulfate reduction and sulfide precipitation mediated by microbes (Reynolds et al. 1991). (2) The loading of a sulfate-reducing system can be determined by the rule of thumb that the level of microbial sulfate reduction should always exceed the amount of sulfide precipitation (Machemer et al. 1993, Wildeman et al. 1993).

These two findings allowed development of anaerobic wetland systems by a staged design process similar to other mineral processing schemes. In particular, because microbial processes dominated, laboratory studies to determine suitable substrates and sulfate-reducing inocula can be conducted with a reasonable degree of certainty. Also, these laboratory studies could be conducted to determine if "in principle" a treatment technique can be effective. Then, because effective treatment relies upon a balance between sulfate reduction and metal sulfide precipitation, bench- and pilot-scale experiments can determine the proper loading factors and how a treatment system can be adapted to on-site conditions.

---

[1]Paper Presented at the International Land Reclamation and Mine Drainage Conference and the Third International Conference on the Abatement of Acidic Drainage, Pittsburgh, PA, April 24 - 29, 1994.

[2]Chemistry and Geochemistry, Colorado School of Mines, Golden, CO 80401, (303) 273-3642, Geochemistry Program Paper No. 004.
[3]Knight Piesold & Co., 1600 Stout Street, Suite 800, Denver, CO 80202, (303) 629-8788
[4]Camp Dresser & McKee, 1331 17th Street, Suite 1200, Denver, CO 80202, (303) 298-1311
[5]Noranda Minerals Corp., 2501 Catlin, Suite 201, Missoula, MT 59801, (406) 721-9704

This paper reports on the first pilot-scale passive treatment system that was constructed using these concepts. The site was the Grey Eagle gold mine in northern California, where it is necessary to treat a continuous flow of seepage from a tailings impoundment. The seepage also contains acid rock drainage from historic mining. The composition of the commingled waste water stream is given in table 3. The mine site is owned by Noranda Grey Eagle Mines Inc. which funded the development project.

Laboratory Study

The laboratory study concentrated on microbiology and had the following objectives: (1) To identify a suitable substrate of soil and organic material that would be readily available at the mine site. (2) To measure the removal of the contaminants from the discharge water by analyzing the changes in the substrate-water system with time. (3) To determine a local source of SRB that can be used as the inoculum for the pilot cell.

Local soils and wood wastes were collected from the vicinity of the mine, and were mixed with water in a 1:1 by volume ratio. These paste samples were analyzed for pH, Eh, and electrical conductivity. These general tests indicated that the most easily available materials were unsuitable, primarily because the paste pH's were less than 5. At this low pH, sulfate reduction is severely inhibited (Postgate 1979). To meet objective 2 and determine what types of materials could be considered for objective 1, a protocol for microbiological tests was devised as shown in table 1. It was assumed that limestone, cow manure, and organic soil could be found close to the mine site, so this was established as the base substrate. Other substrates used at the Big Five pilot system in Idaho Springs, CO (Wildeman et al. 1993) were used to give a more complete test of objective 2. To test objective 3, various materials were used without a sulfate-reducing bacterial inoculum being added.

Two features of this type of laboratory study help with the success of the final treatment design. First, qualitative observations and indicative measurements are just as important as analytical measurements. Consequently, during the 4-week study, pH, Eh, color, and odor within the bottles were measured. Second, because the analytical tests are simple, a large number of combinations of organic material, soil, and other amendments can be investigated. At the end of the experiment, selected bottles were sent for analysis in which filtered samples of the supernatant water were analyzed for a suite of metals.

Table 1. Experimental protocol for the laboratory tests on the mine drainage.

Base substrate: 1/3 planter soil mix, 1/3 manure, 1/3 limestone chips.
Base mix: 30 g of substrate, 90 g of mine drainage. For the anaerobic cultures, add a minor amount of distilled and sterilized water to fill to the top of the bottle. For the aerobic cultures, no extra water is added and the bottle is left 3/4 full. Record the extra water added.

Bottle No.	Culture Bottle Composition
1 - 6	Base substrate with base drainage-substrate mix.
7 - 9	Big Five Cell E substrate with base drainage -substrate mix.
10	Base substrate with mix of 10 g substrate to 100 mL drainage.
11	Base substrate with mix of 25 g substrate to 100 mL drainage.
12	Base substrate with mix of 60 g substrate to 60 mL drainage.
13	Cow manure with base drainage-substrate mix.
14	Sheep manure with base drainage-substrate mix.
15	Planter mix with base drainage-substrate mix.
16	Limestone chips with base drainage-substrate mix.
17	1/4 planter mix, 3/4 manure with base drainage-substrate mix.
18	1/2 limestone chips, 1/2 manure with base drainage-substrate mix.
19	1/2 planter mix, 1/2 manure with base drainage-substrate mix.
20	1/3 limestone, 1/3 sawdust, 1/3 manure with base drainage-substrate mix.
21	1/3 limestone, 1/3 sawdust, 1/3 planter mix with base drainage-substrate mix.
22	1/3 planter mix, 1/3 sawdust, 1/3 manure mix with base drainage - substrate mix.
23	Original Big Five mushroom compost with base drainage-substrate mix.
24-35	Bottles 1 - 5, 8, 17, 19, 20, 21, 22 and 23 run under aerobic conditions.
36	Base drainage-substrate mix with 10 g of Big Five Cell E substrate added.

Table 2. For the test bottles in table 1, visual observations, pH, electrochemical measurements of hydrogen sulfide, and colorimetric measurements of dissolved copper.

Bottle	Color[1]	pH	H_2S[2]	Copper[2]
1	B	6.5	+	±
2	B	6.7	+	±
3	B	6.7	+	0
4	B	6,7	+	0
5	B	6.7	+	0
6	S	6.8	+	0
7	SS	5,8	+	+
8	SS	5.7	+	NA
9	SS	5.6	0	NA
10	A	6.2	0	NA
11	B	6.7	+	NA
12	B	6.9	+	NA
13	B	6.8	+	NA
14	S	7.1	0	NA
15	A	6.5	0	NA
16	A	6.1	0	0
17	B	7.0	+	NA
18	B	6.9	+	NA
19	B	6.9	+	NA
20	A	6.1	0	NA
21	A	4.7	0	NA
22	S	5.9	0	NA
23	S	6.3	0	NA
24	SS	7.0	0	NA
25	SS	6.9	0	NA
26	SS	6.9	0	NA
27	SS	6.9	0	NA
28	SS	6.8	0	NA
29	SS	4.0	0	NA
30	B	7.0	0	NA
31	B	7.8	0	NA
32	S	7.4	0	NA
33	A	3.9	0	NA
34	A	6.8	0	NA
35	A	6.2	0	NA
36	B	6.9	+	NA

[1]B = Bottle black throughout; SS = all of sediment blackened; S = part of sediment blackened; A = no blackening, water is clear or pale brown.
[2]For the hydrogen sulfide and copper tests, qualitative estimates were made and ++ = strongly positive, + = positive, ± = uncertain, and 0 = not detected, and NA = not analyzed.

Table 2 gives the 2-week results of indicative observations on the bottles. Already strong indications of what substrates would successfully promote the growth of sulfate-reducing bacteria are seen. For example, in bottles 17 and 19, which had appreciable manure in the substrate, the bottles had blackened and H_2S was present. Bottles 30 and 31 had the same substrate mixes as bottles 17 and 19, but the caps had been loosened in an attempt to keep the bottles aerobic. However, sulfate reducing bacterial activity was so strong that these bottles had also turned black. Bottle 21 with no manure had a low pH and no blackening.

The results of analyses on selected bottles are shown in table 3. Although this is a static experiment, the concentrations of contaminants give some indication of what to expect in a flowing system. First, concentrations of sulfate show that vigorous sulfate reduction occurred in bottles (1, 9, 10, 11, 12, 36) that contained organic material other than mushroom compost. Next, in the bottles that contained varying amounts of the base substrate of 1/3

Table 3.Contaminant concentrations in mg/L in the original drainage water (OW), the final supernatant waters in the test bottles, and the regulatory effluent limit (EF).

Bottle or Sample	Cd	Cu	Fe	Mn	Ni	Zn	SO_4=
OW	0.088	140	290	28	0.95	40	1,500
1	<0.005	0.025	0.31	0.63	0.05	0.021	173
9	<0.005	<0.005	54	12	0.02	0.077	997
10	<0.005	0.94	40	7.6	0.10	2.3	1,630
11	<0.005	2.7	25	6.4	0.07	0.83	744
12	<0.005	0.13	2.5	0.99	0.04	0.17	274
21	0.006	0.77	39	7.4	0.12	4.3	591
36	<0.005	0.027	0.09	2.1	0.02	0.10	250
EF	0.01	1.0	0.3	None	0.7	0.02	None

planter mix, 1/3 manure, and 1/3 limestone (1, 10, 11, 12), it appears that a ratio of 10 g of substrate to 100 mL of mine drainage lacks sufficient organic material to effect vigorous sulfate reduction. Finally, it appeared that reaching the effluent limits for Cd, Cu, and Ni would be possible, but achieving the regulatory limits for Fe and Zn would be more problematic.

Treatment Decisions

The results of the laboratory study were encouraging enough that it was decided to forego bench-scale experiments and immediately design and construct a small pilot cell. However, there were still some questions to be answered on the selection of the substrate materials. In particular, the first set of local materials were not suitable for an anaerobic treatment system, and it was necessary to make another search for materials that gave good results in laboratory studies. In addition, the inocula of SRB came from Colorado sources and sources from northern California had to be located. Consequently, while the physical design of the pilot-scale reactor was being developed, another round of laboratory tests were performed to find suitable organic materials and sulfate-reducing inocula. Because the base substrate mix of manure, limestone, and planter's soil mix was effective in promoting the activity of SRB and removing contaminants, the search for local materials centered upon these materials. They were found, but had to be transported extensive distances.

The manure came from a dairy farm and appeared to be processed so that it contained primarily hay with very little soil. It tested positive as an inoculum for sulfate reducing bacteria; however, the growth of bacteria was slow. In the final designation of the substrate for the pilot reactor, it was decided to use the processed manure for the substrate formulation, but to include 10% of raw, unprocessed manure as the bacterial inoculum.

Pilot-Plant Study

Design of the Treatment Module

The passive treatment system module (PTSM) consisted of influent piping, substrate, and effluent piping installed in a welded steel tank. The rectangular tank was 10.9 m long, 2.7 m wide, and 2.7 m high and open at the top. The interior of the tank was covered with a bituminous polymer coating to protect the steel. The bottom of the tank was covered with a 15-cm layer of 1-cm diameter clean gravel. A network of 5-cm diameter perforated PVC pipe was constructed on the gravel layer. An additional 7 cm of gravel was placed on the exposed gravel and pipes. The top of the gravel was covered with needle-punched polyester geotextile fabric.

The substrate consisted of equal masses of processed manure, 1-cm diameter limestone, and dark fine-grained soil. The three components were blended and added to the PTSM in such a way that the substrate was not allowed to fall more than 1 m to minimize compaction. For inoculum, a portion of the substrate was blended with the raw manure and placed in the PTSM at the 1/3 and 2/3 level. A distribution network of perforated 5-cm-diameter PVC similar in configuration to the effluent piping was installed on top of the substrate. Water passes downward through the 2-m-thick substrate and is collected in the effluent piping located at the base of the tank. Flow through the system is controlled hydraulically by the elevation of the effluent pipe relative to the level of water within the module.

Table 4 Sulfide generation in mol/L for the passive treatment system module based on sulfate reduction. For comparison, the metals removal in mol/L is also shown.

Date	Sulfate (mg/L) In	Sulfate (mg/L) Out	Sulfide (Molar) Produced	Metals (Mn+Fe+Ni+Cu+Zn+Cd), (Molar) In	Metals (Mn+Fe+Ni+Cu+Zn+Cd), (Molar) Out	Metals (Mn+Fe+Ni+Cu+Zn+Cd), (Molar) Removed
9/24/91	2,900	1,100	0.0188	0.0083	0.0002	0.0081
10/8/91	2,600	2,600	0.0000	0.0091	0.0001	0.0090
10/21/91	3,000	2,200	0.0083	0.0083	0.0005	0.0079
11/5/91	2,700	2,300	0.0042	0.0087	0.0006	0.0081
12/3/91	2,600	2,200	0.0042	0.0087	0.0008	0.0070
1/8/92	2,600	2,100	0.0052	0.0084	0.0015	0.0069
2/25/92	2,700	2,100	0.0063	0.0090	0.0019	0.0071
3/24/92	3,200	2,600	0.0063	0.0137	0.0027	0.0109
4/28/92	3,000	2,300	0.0073	0.0109	0.0015	0.0093
5/26/92	3,000	2,200	0.0083	0.0106	0.0005	0.0101
6/30/92	2,900	2,400	0.0052	0.0102	0.0004	0.0098

Operation

The loading of the PTSM was based on the limiting reactant concept for loading of a sulfate-reducing reactor (Machemer et al. 1993, Wildeman et al. 1993). The premise is that the rate of generation of sulfide by the bacteria must meet or exceed the rate of flow of heavy metals (Mn + Fe + Cu + Zn) into the reactor. Based on previous studies (Reynolds et al. 1991, Wildeman, et al. 1993), the rate of sulfide generation was estimated to be 0.3 mol of S^{2-} per m^3 per day. The metals concentration in the influent totals ~ 800 mg/L. Therefore, using an average molecular weight of 55 g/mol for the metals in the drainage, this results in a metals influent concentration of 0.014 mol/L. Given the volume of the PTSM as 55 m^3, the total sulfide produced per day is 16.5 mol. Therefore, the flow was set so at 800 mL/min that the metals input would not exceed 16.5 moles/d.

To start the test, impoundment seepage was added until the substrate was thoroughly soaked and water breached the surface. Then, the system was left to incubate for 2 weeks. The sulfate in the seepage and the easily extracted organic compounds from the manure serve as excellent nutrients for the SRB. After 2 weeks, it was assumed that the system was an active bioreactor. The initial flow was set at 800 mL/min, and the PTSM was continuously operated for 22 months from October 1991 through July 1993. During this time the physical operation of the PTSM was free of problems.

For the first 10 month period, the analytical results on total constituents in the effluent are given in figure 1. In figure 2, the total concentrations of Fe in the influent and effluent as well as the dissolved Fe concentration in the effluent are shown. For the other constituents, except for excursions in Cu at the beginning of the study and Zn at the end of the period, the concentrations of dissolved constituents were only slightly less than the concentrations of total constituents. During this time, the composition of the influent water was essentially the same as that given in table 3, except in March when annual recharge of the aquifer increased concentrations of contaminants in the drainage by 10% to 70%. This increase can be seen for Fe in figure 2. In table 4, the analytical results of sulfate concentrations in the influent and effluent are presented. The molarity of heavy metals in the influent and effluent are also shown so that the balance between sulfide produced and metals removed can be compared.

At the mine site, Eh, pH, and temperature measurements were performed twice a week as part of the on-site maintenance program. The PTSM tank was built of steel and was above ground. In addition, the tank was not insulated . As a consequence, it responded quite well to changes in temperature as the seasons changed. Figure 3 gives the on-site values of Eh and temperature over the course of the 10 month study. Twice during the study, the temperature of the substrate at various depths and locations was determined. In both instances, the temperature range in the PTSM was less than 3° C with respect to both depth and lateral position.

Analysis of Operation

For the first 6 weeks of operation, removal results were excellent and followed the results achieved in the laboratory study. However, beginning in November, iron removal began to decrease in two respects. In the effluent,

a large difference between total and dissolved iron was observed, and the concentration of Fe increased in both the dissolved and total fractions. This increase could not be attributed to a change in the concentration of Fe in the mine drainage, which was approximately constant until March.

At least two properties of the PTSM operation can account for the change in dissolved Fe concentration. First, as has been shown in Colorado studies of sulfate-reducing reactors (Machemer and Wildeman 1992), in the first 6 weeks, two factors operate to promote metals removal. First, metals are readily removed by adsorption onto sites in the organic substrate. However, after 6 weeks, most of the sites are filled and this method of removal is no longer available; therefore, metal removal decreases. Also during the first 6 weeks, small molecular weight organic compounds are readily available to the SRB. This availability of nutrients causes large bacterial activities in the initial stages of operation. As seen in table 4, other than the anomalous value on October 8, the largest sulfate reduction values occur in the first 4 weeks of operation.

Startup in September, just as temperatures in the tank started falling, can also account for the increase in Fe concentration. SRB activity is known to decrease with temperature decreases, and Kuyucak et al. (1991) found the most drastic decrease when the temperature fell below 10° C. In the PTSM, the temperature fell below 10° C on about November 15 and did not rise above 10° C until about April 15. Fe concentrations would be most affected by a reduction in SRB activity because FeS is the form of iron sulfide formed and it is the most soluble of the acid-volatile sulfides (Machemer et al. 1993, Wildeman et al. 1993).

The reason for the increase in total Fe concentration is not known because material suspended in the effluent was not analyzed. If the increase was from geochemical conditions in the effluent, two reasons could best explain the increase. First, there was a high concentration of suspended organic material in the effluent, especially at the beginning of operation. Cu is strongly adsorbed onto organic material (Machemer and Wildeman 1992), and the large discrepancy between total and dissolved copper in the beginning of operation could be accounted for by suspended organic material. However, during the first month of operation, there is little difference between total and dissolved iron. Thus it appears that adsorption onto suspended organic material may not be the only reason for the increase in total Fe.

The other strong possibility for this difference is the presence of suspended ferric hydroxide in the water. Between pH 6 and 7, which are the operating pH's of the PTSM, ferric hydroxide would be stable at Eh's above 200 mV (Wildeman et al. 1993). The values of Eh in the effluent in figure 3 show that 200 mV was exceeded on about December 15. Consequently, this might account for the large difference between dissolved and total iron during the winter. However, when the Eh of the effluent falls below 200 mV on about May 1, there is still a difference between total and dissolved iron. This behavior suggests that the difference between total and dissolved iron is due to one or a combination of the following causes: (1) The difference is not caused by just one chemical constituent in the effluent water, (2) the difference may be caused by some physical condition in the PTSM that allows suspended Fe to remain in the effluent, or (3) the difference is caused by Fe precipitates still forming after the water has left the PTSM.

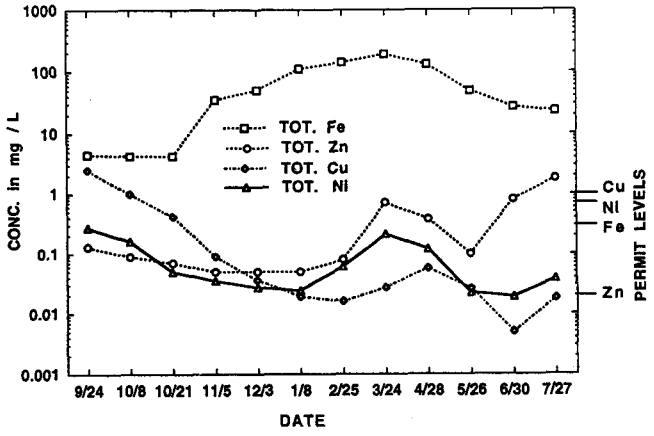

Figure 1. Unfiltered effluent metal concentrations in mg/ L.

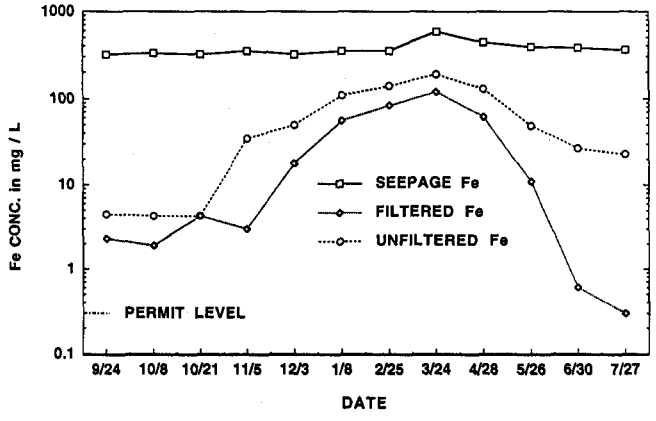

Figure 2. Influent (seepage) and filtered and unfiltered Fe concentrations in mg/L in the PTSM.

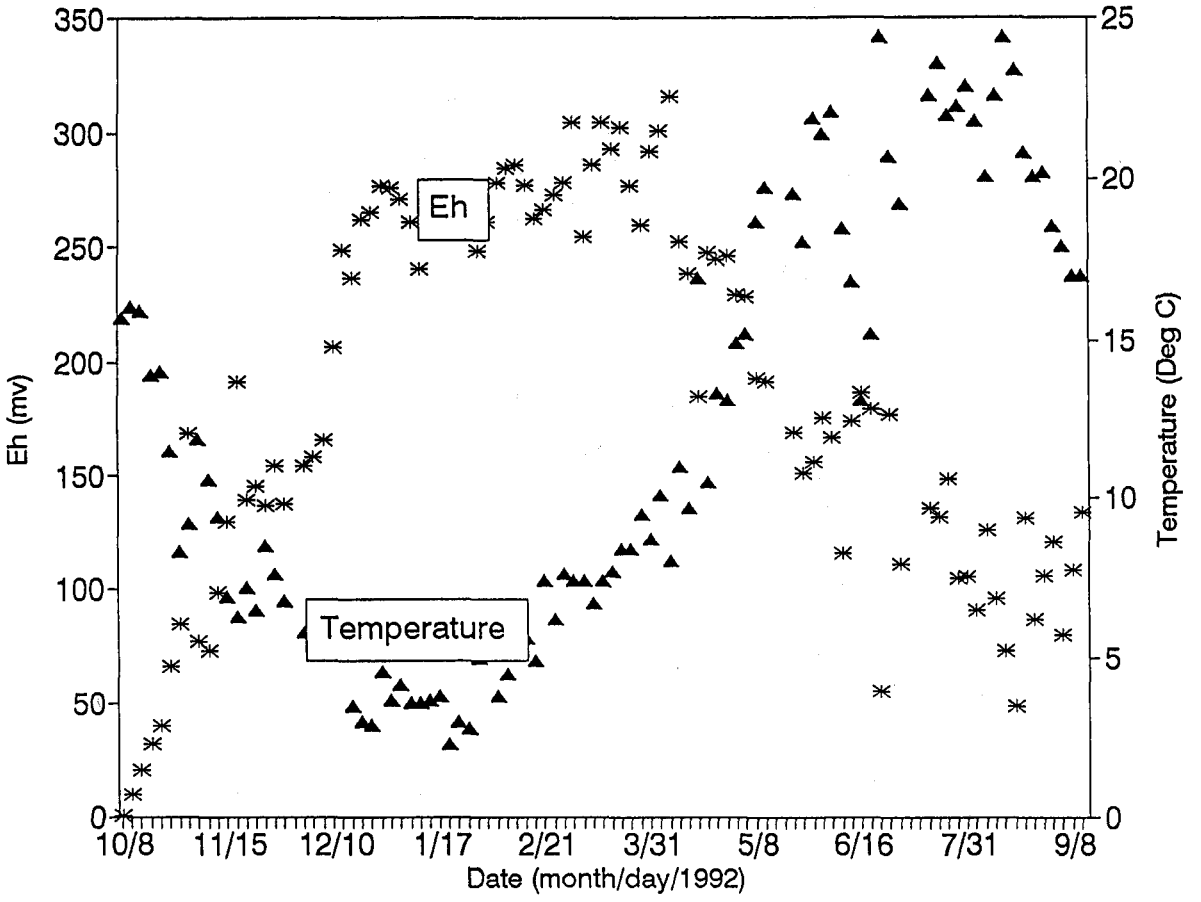

Figure 3. Variation of oxidation-reduction potential (Eh) with PTSM temperature in 1991 and 1992.

The frequent monitoring of the temperature and Eh along with the Fe and sulfate concentration values gives some insight into the activity changes of SRB with temperature. For the PTSM, Eh increased as temperature decreased with little time lag during the fall. The highest Eh occurred in mid December at the lowest temperature. However, the Eh remained high until the end of March, whereas the temperature started rising at about the end of January. In table 4, examination of the sulfide produced implies that the decrease in the rate of sulfate reduction correlates well with decrease in temperature and increase in Eh. However, the peak in the Fe concentration was at about the time when the system is impacted by the increase in metals in the influent. During the time of reduced SRB activity, Ni, Cu, and Zn were consistently removed, quite likely because they form less soluble sulfides. Apparently, the capacity to remove metals continued even though sulfate reduction is diminished.

Conclusions

From this study, a number of conclusions can be made concerning the theoretical and practical development of anaerobic wetlands and reactors to treat mine drainage. The limiting reactant concept of balancing sulfide production with metal inflow appears to control the operation of the PTSM. In addition, when there is not enough sulfide generated, the concentration changes in the effluent can be predicted. Also, there appears to be some excess capacity in the reactor, so that if SRB activity is diminished or Eh increases, removal of Ni, Cu, and Zn will continue, but Fe removal may decrease. From the point of view of substrate development, other organic materials will work as well as mushroom compost as long as they contain a good source of SRB, contain a good supply of organic nutrients, and provide a near-neutral pH environment for bacterial growth. Finally, the expected relation between temperature, SRB activity, Eh, and contaminant removal has been established in the field.

On a practical basis, this study has shown that for anaerobic systems, a well-designed laboratory program will give an excellent indication of how effective removal will be. Also, laboratory experiments will provide the information needed to select the proper substrate materials and inocula. The information provided by these laboratory studies is adequate; thus for typical acid mine drainages, bench-scale studies are not necessary. From an operational viewpoint, nothing unusual occurred during the operation of the PTSM, and typical mine personnel were able to monitor and operate the system.

Acknowledgments

L. Destrampe of Noranda, David Updegraff of the Colorado School of Mines, and Roger Olsen and Susan Morea of Camp Dresser and McKee contributed significantly to the project.

Literature Cited

Hedin, R. S., R. Hammack, and D. Hyman. 1989. Potential importance of sulfate reduction processes in wetlands constructed to treat coal mine drainage. p. 508-514. In D. A. Hammer (ed.), Proceedings of the International Conference on Constructed Wetlands. Lewis Publishing, Ann Arbor, MI.

Hedin, R. S., D. M. Hyman, and R. W. Hammack. 1988. Implications of sulfate-reduction and pyrite formation processes for water quality in a constructed wetland: preliminary observation. p. 382—388. In Mine Drainage and Surface Mine Reclamation, U. S. Bu. Mines IC 9183.

Kuyucak, N., O, St-Germain, and K. G. Wheeland. 1991. In-situ bacterial treatment of AMD in open pits. p. 335-254. In Proceedings of the Second International Conference on the Abatement of Acidic Drainage. (Montreal, PQ, September 16-18, 1991).

Machemer, S. D. and T. R. Wildeman. 1992. Organic complexation compared with sulfide precipitation as metal removal processes from acid mine drainage in a constructed wetland. J. Contaminant Hydrology 9:115-131.

Machemer, S. D., J. S. Reynolds, L. S. Laudon, and T. R. Wildeman. 1993. Balance of S in a constructed wetland built to treat acid mine drainage, Idaho Springs, Colorado, USA. Appl. Geochem. 8: 587-603.

McIntire, P. E., and H. M. Edenborn. 1990. The use of bacterial sulfate reduction in the treatment of drainage from coal nines. p. 409-415. In J. Skousen, J. Sencindiver, and D. Samuel (eds.), Proceedings of the 1990 Mining and Reclamation Conference, WV Univ. Publications, Morgantown, WV,

Postgate, J. R. 1979. The Sulphur-Reducing Bacteria. Cambridge Univ. Press, New York. 151 p.

Reynolds, J. S. et al. 1991. Determination of the rate of sulfide production in a constructed wetland receiving acid mine drainage. p. 175 - 182. In Proceedings of the 1991 National Meeting of the American Society of Surface Mining and Reclamation. Am. Soc. Surf. Min. and Reclam. Princeton, WV.

Wildeman, T. R. 1991. Drainage from coal mines: chemistry and environmental problems. p. 499-511. In, D. C. Peters (ed.), Geology in Coal Resource Utilization, Tech Books, Fairfax, VA.

Wildeman, T.R., G.A. Brodie, and J.J. Gusek. 1993. Wetland Design for Mining Operations. BiTech Publishing Co., Vancouver, BC, Canada 300 pp.

PROOF-OF-PRINCIPLE STUDIES FOR PASSIVE TREATMENT OF ACID ROCK DRAINAGE AND MILL TAILING SOLUTIONS FROM A GOLD OPERATION IN NEVADA[1]

Thomas R. Wildeman[2,3], Lorraine H. Filipek[2,4], and James Gusek[4]

Abstract: Laboratory investigations were conducted to determine "in principle" whether passive treatment is a reasonable option for two water types produced by a surface gold operation in Nevada. One water was acid rock drainage (ARD) containing elevated arsenic and selenium. Arsenic was reduced first by allowing $Fe(OH)_3$ to form and then adsorbing anionic arsenic onto the positively charged precipitate. Then, all heavy metals, arsenic, and selenium were removed to within drinking water standards in bottle studies that promoted sulfate reduction at room temperature for 5 weeks. The second water type was underdrainage and seepage from a mill tailing pond containing elevated cyanide, nitrate, ammonia, copper, mercury, and selenium. The pH of the solutions was about 8, and the tailing underdrain solution contained greater concentrations of contaminants than the seepage. Both anaerobic and aerobic static tests were conducted at room temperature for 5 weeks. The aerobic tests were successful in reducing cyanide, ammonia, nitrate, copper, mercury, and selenium. Arsenic was reduced if soil as well as algae was present. In the anaerobic tests, cyanide, nitrate, copper, mercury, and selenium were reduced, whereas ammonia and arsenic were either unaffected or increased. The results of the laboratory tests were used to design a settling pond-anaerobic-aerobic passive system for the acid rock drainage and an aerobic passive system for the underdrainage and seepage. The pilot-scale ARD system and the aerobic algal pond for the tailing water were recently constructed to confirm the laboratory results.

Additional Key Words: Heavy metals, arsenic, selenium, cyanide, nitrate, ammonia, passive treatment, constructed wetlands

Introduction

Passive treatment methods that rely on aerobic reactions have been used to treat acid rock drainages (ARD) from coal mines. When the water has an initial pH greater than 5.5 and also has net alkalinity, aerobic constructed wetlands that precipitate iron hydroxides can be effective (Wildeman, Brodie, and Gusek 1993). Some ARD, especially that associated with metal mines, has a lower pH and higher concentrations of iron and other heavy metals. This type of water requires anaerobic passive treatment (Hedin and Nairn 1990). The anaerobic systems rely on bacterially mediated precipitation of metal sulfides.

Currently, little information exists on the ability of passive systems to treat (1) ARD that contains arsenic and/or selenium in concentrations above the Federal drinking water standards or (2) alkaline pH drainage containing low levels of cyanide. Both of these water types have been associated with gold mining operations in the arid regions of the Western United States. High arsenic and selenium concentrations in water are common in arid regions because these elements are more soluble in the natural alkaline and saline waters associated with this type of environment (Jacobs 1989). Additionally, alteration of rocks associated with gold mineralization often produces elevated concentrations of arsenic in ground water. Cyanide and alkaline waters are the products of mineral processing methods that are used to extract gold from ore (van Zyl 1984).

This study presents the results of two laboratory investigations conducted to determine "in principle" whether passive treatment is a reasonable option for these two water types. Both water types were collected from a surface gold mine operation in Nevada where closure is being considered within the decade. The laboratory investigations were the first stage in the investigation of passive systems suitable for closure.

---

[1]Paper Presented at the International Land Reclamation and Mine Drainage Conference and the Third International Conference on the Abatement of Acidic Drainage, Pittsburgh, PA, April 24 - 29, 1994.

[2]Knight Piesold and Co., 1600 Stout St. Suite 800, Denver CO 80202, (303) 629-8788.
[3]Department of Chemistry and Geochemistry, Colorado School of Mines, Golden, CO 80401, (303) 273-3642 FAX (303) 273-3629, Geochemistry Program Paper No. 003.
[4]Now at the U. S. Geological Survey, M.S. 972, Box 25046, Denver, CO 80225, (303) 236-7726.

Table 1. Substrates and waters used for the laboratory study.

Substrates used for waste rock drainage		Substrates used for tailings drainage	
Code	**Composition**	**Code**	**Composition**
MLI-B	3/4 M, 1/4 L, 10 g I-B	SI-T	1/2 S, 1/2 I-T
SMLI-B	1/2 S, 1/3 M, 1/6 L	SMI-T	1/2 S, 5/12 M, 1/12 I-T
L	100% L	I-T	100% I-T
H-M	100% H-M	A	100% A
H-J	100% H-J		C-M
100%	C-M	AS	1/3 A, 2/3 S

SUBSTRATE KEY

Substrate Code	Inoculum Code
M = Manure	I-B = Inoculum from Big Five Wetland
l = Limestone	H-M = Horse Manure
S = Mine site soil	H-J = Horse juice
A = Algal solution from seepage pond	C-M = Cow manure
	I-T = Anaerobic slime from seepage pond

WATER KEY

Waste Rock-Drainage		Tailings Water	
Code	Description	Code	Description
#1	Drainage from old waste rock dump issuing from Pipe 1, pH = 2.7	CP	Water from seepage pond taken from the pump outlet to insure a mixture of all sources
#2	Drainage from toe of waste rock pile issuing from Pipe 2, pH = 4.1	U	Water from tailings underdrain collected at the inlet pump into the storage pond
#3	Drainage from new waste rock pile issuing from Pipe 3, pH = 4.7	MX	A mix of 100 volumes of underdrain water to 15 volumes of seepage pond water to simulate water stored in the lined pond
1-2-3	A mix of waters from pipes 1, 2 and 3 in a ratio of 3-1: 3-2: 1-1 to simulate fresh pond water		

In the first case, water tested is ARD from a waste rock pile that contains water with concentrations of iron, arsenic, and selenium as high as 600, 10, and 1 mg/L, respectively. This drainage is presently being collected in a lined settling pond and is subsequently pumped to an alkaline milling process circuit. The drainage is intercepted and transported to the settling pond in three pipes, in volume ratios of three parts pipe 1, three parts pipe 2, and one part pipe 3. The ARD from pipe 1 had the lowest pH and a distinctive red color that was suspended $Fe(OH)_3$ that settled out upon aging for approximately 16 h.

The other water type is underdrainage and seepage from a drained mill tailing facility receiving cyanide effluents. The underdrainage contains concentrations of cyanide, nitrate, ammonia, mercury, arsenic, and selenium in excess of Federal drinking water standards. The seepage has lower concentrations of cyanide, associated nitrogen compounds, and metals than the underdrainage, which suggests that it has undergone some treatment by natural processes. The underdrainage and seepage are currently collected in ponds and reused in the gold extraction process.

The primary goals of the "proof-of-principle" experiments were (1) to determine the best types of microbial ecosystems to remove As and Se in both acidic and alkaline waters and (2) to determine whether aerobic, anaerobic, or a combination of processes is the most effective passive treatment method for the tailing drainages. Secondary objectives were to (1) determine local sources of sulfate-reducing bacteria (SRB) and bacteria and/or algae capable of

Table 2. Waste rock drainage test bottles - all bottles are anaerobic.

Bottle[1]	Substrate code	Substrate amount, g	Water Code	Water amount, mL	Inoculum	Inoculum amount, g
1	MLI-B	60	#1	60	I-B	10
2(1)	MLI-B	60	#1	60	I-B	10
3	MLI-B	40	#1	80	I-B	10
4	SMLI-B	60	#1	60	I-B	10
5	SMLI-B	40	#1	80	I-B	10
6	H-M	50	#1	60	H-M	50
7	H-J	60	#1	60	H-J	60
8	C-M	60	#1	60	C-M	60
9	L	30	#1	100	None used	NAP[2]
10	None used	NAP[2]	#1	100	None used	NAP
11	MLI-B	40	#3	80	I-B	10
12	SMLI-B	60	#3	60	I-B	10
13	SMLI-B	40	#3	80	I-B	10
14(13)	SMLI-B	40	#3	80	I-B	10
15	None used	NAP	#3	100	None used	NAP
16	L	30	#3	100	None used	NAP
17	MLI-B	40	1-2-3	80	I-B	10
18(17)	MLI-B	40	1-2-3	80	I-B	10
19	SMLI-B	60	1-2-3	60	I-B	10
20	SMLI-B	40	1-2-3	80	I-B	10
21	H-M	50	1-2-3	60	H-M	50
22	H-J	60	1-2-3	60	H-J	60
23	C-M	60	1-2-3	60	C-M	60
24	None used	NAP	1-2-3	100	None used	NAP

[1]Bottle Numbers in parentheses designate duplicates. [2]NAP means not applicable

degrading cyanide and associated nitrogen species and (2) develop a mix of organic and inorganic materials (labeled "substrates") that would promote the appropriate microbial activity. The anaerobic tests were patterned after those performed by Reynolds et al. (1991), and the aerobic tests were patterned after those of Duggan et al. (1992).

Collection of Materials

Waste rock ARD and tailing drainages, materials for substrates, and inoculum candidates were collected in May 1992. Individual samples of ARD were collected from each of the three pipes draining into the settling pond. Because any future passive treatment system would treat the settling pond water, a 3-3-1 by volume composite of the ARD waters from the three pipes was made (labeled "1-2-3") and used in some of the bottle tests. Tailing underdrain water and seepage from the tailing dam were also sampled individually. Currently, the ratio of tailing underdrain water to seepage is about 100 to 15. One closure option is to treat this mixed water. Accordingly, a mix of 100 volumes of underdrain water to 15 volumes of seepage water was made (MX) and used in some of the bottle tests.

Table 1 provides a key to the various substrate and inoculum materials that were gathered. Inocula for SRB were collected at a cattle feedlot. Typically, the best sources for SRB bacteria are fresh, wet manure and the mucky places in a feedlot or farm. On this feedlot, all the manure was quite dry. The only mucky place was the area around the watering trough for the horses. In table 1, this muck is labeled "horse juice."

The tailing seepage pond contained abundant floating algae and a blackish anaerobic slime in the sediments. These materials were collected to serve as aerobic and anaerobic inocula, respectively, for the tailing drainage tests because they were expected to contain microbes already acclimated to cyanide and metals (Duggan, et al. 1992, Wildeman, et al. 1993). For most of the other bottles in the anaerobic study, SRB inoculum from the Big Five Pilot Wetlands (Wildeman, Brodie, and Gusek 1993) was used.

Table 3. Tailing water test bottles.

Bottle[1]	Substrate code	Substrate amount	Water code	Water amount, mL	Inoculum	Inoculum amount	Aerobic
25	SI-T	60 g	CP	60	I-T	30 g	No
26	SMI-T	50 g	CP	80	I-T	5 g	No
27(26)	SMI-T	50 g	CP	80	I-T	5 g	No
28	None used	NAP[2]	CP	100	None used	NAP	No
29	I-T	30 g	CP	100	I-T	30 g	No
30	SI-T	60 g	U	60	I-T	30 g	No
31(30)	SI-T	60 g	U	60	I-T	30 g	No
32	SMI-T	50 g	U	80	I-T	5 g	No
33	None used	NAP	U	100	None used	NAP	NAP
34	I-T	30 g	U	100	I-T	30 g	No
35	SI-T	60 g	MX	60	I-T	30 g	No
36	SMI-T	50 g	MX	80	I-T	5 g	No
37	None used	NAP	MX	100	None used	NAP	NAP
38	A	30 mL	CP	100	A	30 mL	Yes
39	AS	30 g	CP	100	A	15 mL	Yes
40	None used	NAP	CP	100	None used	NAP	NAP
41	A	30 mL	U	100	A	30 mL	Yes
42(41)	A	30 mL	U	100	A	30 mL	Yes
43	AS	30 g	U	100	A	15 mL	Yes
44	None used	NAP	U	100	None used	NAP	NAP
45	A	30 mL	MX	100	A	30 mL	Yes
46	AS	30 g	MX	100	A	15 mL	Yes
47	AS	30 g	MX	100	A	15 mL	Yes
48	None used	NAP	MX	100	None used	NAP	NAP

[1]Bottle numbers in parentheses designate duplicates. [2]NAP means not applicable

In both anaerobic and aerobic laboratory studies, a source of neutral to alkaline soil or limestone is needed to help raise pH, control hydraulic permeability, and serve as adsorption sites for bacteria and contaminants (Bolis et al. 1992, Duggan et al. 1992). Alkaline soil from the mine site and limestone from the nearest quarry were collected to serve these functions.

Experimental Design

The collected waters and materials were shipped overnight to the Colorado School of Mines, and the experiments were set up the following day. Splits of the water samples were sent to Core Laboratories for chemical analysis. Materials larger than 10 mesh were removed from the substrate candidates, and mixes of the material were made in the combinations given in table 1. The codes for the substrates and waters are given in table 1.

The anaerobic tests were conducted in 150 mL screwcap culture bottles. A small amount of head space was left in the bottles to accommodate gases evolved during the experiment because this minimizes solution loss. The bottles were incubated for 5 weeks in boxes at ambient temperatures in the laboratory. The aerobic tests were conducted in 500-mL wide-mouthed erlenmeyer flasks that are covered with 250-mL beakers to allow gas exchange. The bottles were incubated for 5 weeks on a sunny window ledge at ambient temperatures in the laboratory. The protocol for the ARD experiments is given in table 2. The protocol for the tailing drainage experiments is given in table 3.

All bottles except 9 and 16 were unsealed to allow access to the solutions during the test period. Color, odor, pH, and Eh were recorded for each bottle once per week. Bottles 9 and 16 were sealed to ensure that atmospheric oxygen did not invade the systems and cause armoring of the limestone. Spot colorimetric tests on a few drops of solution were conducted using HACH kit reagents. The spot tests were conducted once during the course of the experiment for Fe and Cu on both water types, and twice during the experiment for cyanide on the tailing drainages. At the end of the experiments, quantitative determinations were made on representative bottles.

Table 4. Chemistry of waste rock drainages and test bottles after 5 weeks of incubation. All concentrations are in mg/L for unfiltered (total) water.

Bottle	Original	1	2	3	10	Original	20	24	Water Stds
Water	Pipe 1	Pipe 1	Pipe 1	Pipe 1	Pipe 1	1+2+3	1+2+3	1+2+3	NAP[1]
Substrate	NAP	MLI-B	MLI-B	MLI-B	None	NAP	SMLI-B	None	NAP
Sulfate	3370	5360	5130	4350	3850	2160	2350	2070	NAP
Arsenic	12	0.4	0.4	0.4	3	2.7	0.3	0.3	0.05
Cadmium	0.17	0.003	<0.003	<0.003	0.06	0.066	<0.003	0.04	0.01
Chromium	0.50	<0.05	<0.05	<0.05	0.5	0.20	<0.05	0.20	0.05
Copper	18	0.7	1.1	0.55	32	7.4	0.3	15	1.0
Iron	620	4.8	3.6	4.3	422	200	2.8	131	0.3
Manganese	12	1.7	1.4	1.8	11	6.7	5.2	6.4	0.05
Selenium	1.0	<0.01	<0.01	<0.01	<0.01	0.3	<0.01	0.01	0.01
Zinc	2.9	0.2	0.15	0.05	5.4	1.8	<0.05	3.0	5.0
pH	2.5	7.6	7.5	7.4	2.1	2.4	7.1	1.9	6-9

[1]NAP means not applicable

Results and Discussion

Anaerobic ARD Experiments

All bottles that tested whether the local cow manure, horse manure, or "horse juice" materials (not shown) were suitable SRB inocula, had Eh values below -100 mV, black solids, and strong hydrogen sulfide odors, indicating that all three materials were good sources of SRB inoculum. The final pH of ARD test bottles that used soil from the site was somewhat lower than that of bottles with undiluted manure, but still above pH 7. In addition, the Eh in bottles with soil tended to decrease over time in a manner that was similar to that in bottles that did not contain soil. These results indicate that the soil can be used to provide hydraulic control within the substrate in the anaerobic passive treatment system.

Initial values for pipe 1 and the expected holding pond water and results for regulated constituents after 5 weeks of incubation are given in table 4 for selected tests. In all cases the analyses were performed on whole, unfiltered waters. Bottles 1 and 2 are duplicates and provide intra-experimental variability. Bottles 10 and 24, which are controls of pipe 1 and 1-2-3 water, respectively, were analyzed to determine whether 5 weeks of iron hydroxide settling causes significant decreases in the concentration of other metals. Bottle 20 simulates the expected holding pond (1-2-3) water to be treated with a mixture of sand, manure, and limestone, the probable substrate of choice.

The results indicated that the pH is raised from around 2 to above 7 and concentrations of cadmium, chromium, selenium, and zinc are reduced to within drinking water standards in all analyzed bottles. Iron and arsenic were reduced by over 95 %, but were not brought to within drinking water standards. Manganese was reduced by 50 to 80 %. Typically, manganese is the most difficult element to remove from ARD (Duggan et al. 1992). These results suggest that the anaerobic system will produce significant reduction of contaminants. However, to meet water quality standards, an aerobic polishing stage may be necessary after the anaerobic treatment.

Analysis of the aged water from pipe 1 (bottle 10) and the 1-2-3 mix (bottle 24), when compared with the original waters, shows that the concentration of Fe is reduced by 30 %. Also, the pH of these waters dropped upon storage, suggesting that Fe(III) hydrolyzed and precipitated from solution. Concomitantly, arsenic in aged pipe 1 water was reduced from 12 to 3 mg/L and in the simulated holding pond water from 2.7 to 0.2 mg/L. In addition, selenium was reduced to less that 0.01 mg/L in both waters. These elements occur in the water as the oxyanions arsenate and selenate. At the low pH of the ARD, the ferric hydroxide precipitate has a high positive surface charge and readily adsorbs the arsenate and selenate anions. Removal of selenium to below drinking water standards and the significant reduction in arsenic makes containment of the ARD in a holding pond a reasonable first step in passive water treatment.

Table 5. Chemistry of tailing waters and test bottles after five weeks of incubation. All concentrations are in mg/L for unfiltered (total) water.

Bottle	Original	30	31	32	41	43	Original	26	39	46	Water Stds.
Water	Underdrain	Underdrain	Underdrain	Underdrain	Underdrain	Underdrain	Seep	Seep	Seep	MX	NAP[1]
Aerobic	NAP	No	No	No	Yes	Yes	NAP	No	Yes	Yes	NAP
Substrate	NAP	SI-T	SI-T	SMI-T	A	AS	NAP	SMI-T	AS	AS	NAP
Cyanide-Total	<4.0	<0.2	<0.2	<0.2	<0.2	<0.2	0.10	<0.2	<0.2	<0.2	0.2
Cyanide, WAD	4	<0.2	<0.2	<0.2	<0.2	<0.2	0.06	<0.2	<0.2	<0.2	0.2
Ammonia (as N)	14	16	11	0.44	0.27	0.08	2.1	8.6	0.19	0.20	-
Nitrate and Nitrite (as N)	19	1.0	1.1	1.9	0.31	0.73	8.3	2.2	0.31	0.60	-
Sulfate	400	15	16	66	478	430	390	210	391	450	250
Thiocyanate	14	<2.5	<2.5	4.9	0.4	<0.25	<0.1	4.4	<0.25	<0.25	-
Arsenic	0.09	0.17	0.15	0.17	0.11	<0.05	<0.05	-	-	<0.05	0.05
Copper	3.3	<0.05	<0.05	0.30	<0.05	<0.05	0.06	-	-	<0.05	1.0
Iron	0.05	1.8	2.5	1.2	<0.1	<0.1	<0.03	-	-	<0.1	0.3
Mercury	0.27	<0.002	<0.002	<0.002	<0.002	<0.002	0.004	<0.002	<0.002	<0.002	0.002
Manganese	0.47	7.6	2.0	2.2	2.15	0.15	1.6	1.35	0.45	0.75	0.05
Selenium	0.2	<0.01	<0.01	<0.01	<0.01	<0.01	<0.1	<0.01	<0.01	<0.01	0.01
pH	8.0	6.6	6.5	6.5	7.5	7.0	7.3	7.1	7.5	7.5	6-9

[1]NAP means not applicable.

Tailing Drainage Experiments

Cyanide, related nitrogen species, and other regulated constituents are present in the underdrain in higher concentrations than in the seepage. Thus, the tailing drainage experiments concentrated on this water and the MX water. The results showed that cyanide was destroyed to below 0.2 mg/L in all bottles within 4 weeks. These results indicate that either an anaerobic or aerobic system will destroy cyanide and confirm previous results on anaerobic tests reported by Filas and Wildeman (1992).

Bottles 30, 31, and 32 tested the various anaerobic substrates, and bottles 41 and 43 tested aerobic substrates with underdrainage water. Bottles 26 and 39 tested anaerobic and aerobic substrates, respectively, with the tailing seepage (CP). Bottles 43 and 46 tested the same substrates with the underdrainage water and the mix of seepage pond and underdrainage water (MX). The results for constituents of interest are presented in table 5. For comparison, the analytical results for the original waters and solution mixes are given. In all cases the analyses were performed on whole, unfiltered waters.

Anaerobic Experiments. The black sludge sampled from the seepage pond proved to be an excellent source of SRB for anaerobic passive treatment of tailing drainages. After 1 week, some of the anaerobic bottles that contained the tailing sludge inoculum had negative Eh's and smelled of hydrogen sulfide. The concentration of sulfate was also reduced, confirming that bacterial sulfate reduction was operating. At the cyanide concentrations in these waters, the SRB were not killed. From the results of experiments that studied a tailings solution containing much higher concentrations of total cyanide, Filas and Wildeman (1992) suggested that, below a cyanide concentration of about 10 mg/L, sulfate reduction was possible. Only a small supply of this black, pond sludge exists. If a large anaerobic system were built using this inoculum, the material would have to be mixed with other sources and incubated for a period of time to produce an adequate supply.

The results for nitrogen species were mixed. As discussed previously, cyanide was removed. Thiocyanate was also removed. The ammonia concentration remained high, which was expected in an anaerobic treatment system. The nitrate plus nitrite concentrations were significantly reduced. They were probably converted to nitrogen gas because the concentration of ammonia was not appreciably changed.

Copper, mercury, and selenium were reduced to below drinking water standards. Iron, manganese, and arsenic, which had not been completely removed in the anaerobic ARD tests, were also not reduced to below drinking water standards in the tailing drainages. In fact, these elements were at higher concentrations in the final solutions than in the original underdrain water. It appears that the anaerobic conditions caused dissolution of these elements from the soil, manure, and/or inoculum that were used in the substrate mixes. Apparently, an equilibrium between solid phases and the solutions has been established in these bottles.

These anaerobic test results indicate that an anaerobic passive system will not remove all the contaminants to Federal water quality standards.

Aerobic Experiments. Both the algae alone and the soil-algae mix reduced ammonia, nitrate plus nitrite, and thiocyanate to concentrations that were below the results for the anaerobic experiments. The qualitative tests conducted during the experiment indicated that the concentration of cyanide decreased faster in the bottles with soil and algae (AS) than in the bottles with algae alone (A). At the end of the experiment, the Eh's in those bottles containing only algae (41, 42, 45) had fallen significantly below those of the other aerobic bottles. This decrease in Eh may be the result of death and decay of the algae and suggests that, if an algal pond were not designed properly, the water in the pond could turn anoxic. This phenomenon exists in the current seepage pond at the site, where buried dead algae provided the anaerobic inoculum.

The results of the qualitative tests suggested that the soil-algae mixture functioned better than the algae alone. As reported in table 5, the concentrations of constituents confirm this result. The soil-algae mixture reduced all contaminants except manganese in the underdrain water and in the underdrain-seepage mixture to below drinking water standard concentrations. As seen from bottle 41, algae alone did not reduce arsenic concentrations. Based on the laboratory studies, an algal system containing soil would be the best passive system for removal of all the constituents in the tailing water.

Design Conclusions

For ARD waters containing high concentrations of arsenic and/or selenium, anaerobic passive treatment is possible "in-principle". A holding pond prior to the anaerobic cell would remove substantial quantities of both anions before the water entered the sulfate-reducing treatment system. The anaerobic cell may not remove all constituents to drinking water quality standards. If necessary, an aerobic polishing system can be installed after the sulfate-reducing system to remove these contaminants.

For tailing waters that contain moderate concentrations of cyanide and other metals, the laboratory studies suggest that the best passive system would be an algal pond containing sandy soil. This system removes iron, manganese, and arsenic, as well as all cyanide and its degradation products. Also, such an aerobic system would appear to be a good candidate for the polishing of iron, manganese, and arsenic from the waters exiting the sulfate-reducing anaerobic cell. A possible design for such a system is given by Wildeman et al. (1993).

Literature Cited

Bolis, J. L., T. R. Wildeman, and H.E. Dawson. 1992. Hydraulic conductivity of substrates used for passive acid mine drainage treatment. p. 79-89. In Proceedings of the 1992 National Meeting of the Am. Society of Surface Min. and Reclamation. Am. Soc. Surf. Min. and Reclam., Princeton, WV.

Duggan, L.A., T. R. Wildeman, and D. M. Updegraff. 1992. The aerobic removal of manganese from mine drainage by an algal mixture containing *Cladophora*. p. 241-248. In Proceedings of the 1992 National Meeting of the American Society of Surface Mining and Reclamation. Am. Soc. Surf. Min. and Reclam., Princeton, WV.

Filas, B. A., and T. R. Wildeman. 1992. The use of wetlands for improving water quality to meet established standards. p. 157-176. In Proceedings From Successful Mine Reclamation Conference, Nevada Mining Association, Reno, NV.

Hedin, R.S. and R.W. Nairn. 1990. Sizing and performance of constructed wetlands: case studies p. 385-392. In Proceedings of the 1990 Mining and Reclamation Conference and Exhibition, v.2. Charleston, WV.

Jacobs L. W., (ed.) 1989. Selenium in Agriculture and the Environment. American Society of Agronomy, Madison, WI. 233 pp.

Reynolds, J. S. et al. 1991. Determination of the rate of sulfide production in a constructed wetland receiving acid mine drainage. pp 175 - 182. In Proceedings of the 1991 National Meeting of the American Society of Surface Mining and Reclamation. Am. Soc. Surf. Min. and Reclam. Princeton, WV.

van Zyl, D. (ed.) 1984. Conference on Cyanide and the Environment. Colorado State Univ. Fort Collins, CO. 400 pp.

Wildeman, T.R., G.A. Brodie, and J.J. Gusek. 1993. Wetland Design for Mining Operations. BiTech Publishing Co., Vancouver, BC, Canada 300 pp.

Wildeman, T. R., D. M. Updegraff, J. S. Reynolds, and J. L. Bolis. 1994. Passive bioremediation of metals from water using reactors or constructed wetlands. p. 13-25. In Emerging Technology for Bioremediation of Metals. Lewis Publishers, Boca Raton, FL.

Wildeman, T. R. et al. 1993. Passive treatment methods for manganese: preliminary results from two pilot sties. p. 665-677. In Proceedings of the 1993 National Meeting of the American Society of Surface Mining and Reclamation. Am. Soc. Surf. Min. and Reclam. , Princeton, WV.

AMD-TIME: A SIMPLE SPREADSHEET FOR PREDICTING ACID MINE DRAINAGE[1]

Paul F.Ziemkiewicz[2]

Abstract: Regulatory agencies and industry need a method for predicting the duration and extent of acid mine drainage (AMD) from specific rock masses. The most widely accepted method for predicting AMD is acid base accounting (ABA). ABA only estimates whether there will or will not be a problem. It does not estimate ultimate acid loading, treatment costs nor duration of liability. Nonetheless, the principle behind acid base accounting is reasonable: that there is a relationship between the acid generation and neutralization potentials of a given rock mass. This paper presents a spreadsheet which uses ABA data in a dynamic fashion to predict acid generation, loading, concentration and duration. The spreadsheet uses conventional variables plus three new ones: percent sulfur flux (%Sf), net deliverable neutralization (NDN) and net deliverable acidity (NDA).

The spreadsheet and preliminary validation are presented though it is recognized that a great deal of work is needed before this becomes a reliable prediction tool.

Introduction

Acid Base Accounting.

Acid Base Accounting (ABA) was developed in the early 1970's by researchers at West Virginia University to identify and classify geologic strata encountered during mining (West Virginia University, 1971). A history of Acid Base Accounting is provided by Skousen et al. (1990).

Since its development, ABA has been used extensively in the United States and other countries for premining overburden analysis. Its popularity largely stems from its simplicity. It uses two key parameters: Maximum potential acidity (MPA) and neutralization potential (NP). MPA is estimated by multiplying per cent pyrite sulfur by 3.125 yielding the total acid produced. NP is the acid consumed by the rock in a titration procedure. Both MPA and NP age given in calcium carbonate equivalents.

Acid neutralization in spoil dumps-a paradigm. ABA operates on the assumption that acid producing and acid neutralizing rocks are thoroughly mixed. Violation of this assumption can remove large portions of the alkaline rock mass from the equation.

Most coal spoils consist of mixtures of acid producing and acid neutralizing rocks. AMD can form despite a dominance of alkaline rock in the spoil. AMD may form in localized pockets within the backfill. And, while finding the path of least resistance to the downstream side of the dump, its acidity is influenced only the alkalinity directly in its path. Once this is overcome, AMD flows freely to the nearest stream while the remaining alkalinity persists as a spectator to the process. Dissolution of calcite is controlled by pH and the partial pressure of carbon dioxide. Where pore water gas is confined, and exposed to mineral acidity, its pH will remain around 6.2 the-buffering point of bicarbonate and carbonic acid. In the absence of mineral acidity, its pH will reflect bicarbonate saturation ~ 8.3. In either case, additional calcite will dissolve only upon addition of acidity and outgassing of carbon dioxide. So, unless contacted directly by acidity, most of the spoil calcite will simply remain in solid form. So, the presence of alkalinity in the dump does not ensure that it will be a factor in neutralizing acidity. To be an efficient process, the acid-forming and alkaline rock must be thoroughly mixed.

---

[1] Paper presented at the International Land Reclamation and Mine Drainage Conference and the Third International Conference on the Abatement of Acidic Drainage, Pitttsburgh, PA, April 24-29, 1994.

[2] Director, National Mine Land Reclamation Center, West Virginia University, Morgantown, WV, USA.

This largely becomes a materials handling issue. Where there is insufficient alkalinity available it would be necessary to add it to the rock. Otherwise, if one relies on random spoil dumping the system would need an overwhelming supply of alkaline rock.

The AMD-TIME Spreadsheet

The preceeding cautionary remarks are meant as background for anyone using an AMD prediction process based on ABA, including this spreadsheet. The estimates generated by either ABA or AMD-TIME are only as good as the estimates of MPA, Np and the operator's materials handling practices.

In developing AMD-TIME the following assumptions were made:

1. Within fairly narrow limits pyrite oxidizes at a nearly fixed rate. It is about 7% per year.
2. The pyrite oxidation rate is the rate limiting step.
3. Rock geometry and porosity are simple multipliers. For example the following factors might be multiplied against 7%.

sandstone	100%
shale	50%
refuse with fines	20%

4. The resulting value is called sulfur flux.

AMD-TIME uses conventional variables plus the following:

%Sf/yr	Percentage of remaining pyritic sulfur oxidized and leached per year.
FLOW	Annual rainfall X surface area X net infiltration.
NDN	Net deliverable neutralization potential. This is the proportion of NP that is exposed to acid water and is able to react with it.
NDA	Net deliverable acidity. This is the proportion of MPA that oxidizes.

AMD-TIME operates on the Quatro Pro spreadsheet developed by Borland International, Inc. Quatro Pro is similar to Lotus 1,2,3 and, except for the graphics would probably work equally well. The spreadsheet only uses several hundred KRAM so it will work on nearly all IBM compatible desktop computers. Naturally, machine power and higher order Intel chips will make it work more quickly.

AMD-TIME was developed for simplicity, not elegance. It uses empirical rather than deterministic variables. Table 1 shows the working end of AMD-TIME. The user only needs to enter the following data:

target NP/MPA ratio
years of mining
acid rock production (tons of rock produced in mining)
surface area (acres)
%Sf/yr
%S pyritic (from ABA)
%NP natural (from ABA)
%NP added
%NDN
%NDA
cost of alkaline amendment ($)
amendment NP (%)

cost of water treatment chemical ($/t)
life of mine coal production (t)

AMD-TIME will then estimate acid loads, concentrations and alkalinity for the next several hundred years. AMD-TIME automatically estimates the chemical cost of water treatment for the life of AMD production. It also automatically estimates the required amount of alkaline amendment needed to reach a target NP/MPA ratio. If you enter that amount at the "%NP added" block the spreadsheet will estimate the cumulative cost of amendment. Costs in current dollars are given in absolute amounts and in dollars per raw tonne of coal.

Comparison of Estimates to Small Scale Field Data:

As configured AMD-TIME is an acidity model. It can also be run as a sulfate model. This was used to compare various variable combinations to data from 11 year old 400 ton test piles at Island Creek's Upshur Complex (Table 2. Two net infiltration values and three Sf and NDA rates were tested in a factorial arrangement. Sf was calculated for each sampling interval (for a discussion of this experiment see Ziemkiewicz and Meek, 1994). For each pile, Sf was slow during the first six months, then accelerated to a maximum within about 10 months. Three estimates of Sf were evaluated in this study: 1) low-Sf integrated over one year, 2) medium-Sf integrated over the last 7 months and 3) high-Sf integrated over the last 5 months.

The column on the left of the table indicates observed sulfate concentrations at the end of year one and at the end of year 11. The best fit for each pile and variable combination was chosen and is indicated by the shading.

The best fits occurred with either of the two variable combinations:

PILES:	1,3	2,4,5,10
NET INFILTRATION %	50	75
Sf	low	high
NDA(%)	100	50

It was surprising that only two scenarios captured the best fits for all of the test piles. Piles 1 and 3 were primarily sandstone while the other piles were mainly shale. It is logical that high NDA fits better with the sandstones given its greater porosity. Why net infiltration appeared higher on the shale than on the sandstone is a mystery unless this actually estimates residence time of water. These analyses are only the early stages of what will be a rigorous

AMD-TIME was run on the SH and LS1 piles using three sulfur flux rates (high, medium and low). The results were compared observed sulfate concentrations from the same piles. Results indicated that the mid range Sf gave the best fits to observed values when NDA was held at 100% (figures 1 and 2).

Conclusions

Like all predictive tools, AMD-TIME is only as good as the variables which make it run. Values for its controlling variables are generated independently of AMD-TIME. AMD-TIME is not a crystal ball. It simply translates acid base accounting data into acid loads and treatment costs per time. Since it uses empirical variables it is useful to compare predictions within set boundary conditions to field observations. Users will be able to fine tune the imput variables such as sulfur flux, net infiltration, NDN and NDA for their local conditions. As experience with these variables improves so will the quality of the estimates. The Spreadsheet is non-proprietary and copies can be obtained by sending a clean diskette to the author with a self-addressed, stamped mailer.

Literature Cited

Skousen, J., R.M. Smith, and J. Sencindiver. 1990. Development of the Acid-Base Account. Green Lands 20(1):

32-37.

West Virginia University. 1971. Mine spoil potentials for water quality and controlled erosion. 14010 EJE 12/71. Contract with West Virginia University by the U.S. Environmental Protection Agency, Washington, D.C.

Ziemkiewicz, P.F. and Meek, F.A. 1994. Long term behavior of acid forming rock: results of 11-year field studies. Paper presented at the International Land Reclamation and Mine Drainage Conference and the Third International Conference on the Abatement of Acidic Drainage, Pittsburgh, PA. April 24-29, 1994.

TABLE 1. AMD-TIME SPREADSHEET. ESTIMATED LONG-TERM ACID GENERATION AND COST OF TREATMENT

SITE:	ABC MINING
TARGET NP/MPA:	1
YEARS OF MINING:	2

VARIABLE BLOCK

ACID ROCK PRODUCTION ARP (T)	3672108
SURFACE AREA (ACRES)	60
RATE OF S LOSS (%Sf/YR)	2.00
FLOW (L/YR)	138766500
%S	0.338
%NP NATURAL	0.019
%NP ADDED	2.090
%NP TOTAL	2.109
% NET DEL. NEUTRALIZATION (NDN)	25
%NET DELIVERABLE ACIDITY (NDA)	50
REQUIRED NP (%)	2.09
REQ'D ALKALINE AMENDMENT (%)	2.20
COST ALK. AMENDMENT ($/TON)	12.00
AMENDMENT NP (%)	95
COST OF WATER TRT CHEMICAL ($/T)	60
ACID CAPITAL (T)	19393
ALKALINE CAPITAL (T)	19361

RESULTS BLOCK

LIFE OF MINE PRODUCTION	(TONS)	648000
COST OF WATER TREATMENT	($)	517
COST OF ALKALINE AMENDMENT	($)	969437
COST OF WATER TREATMENT	($/RAW T	0.00
COST OF ALKALINE AMENDMENT	($/RAW T	1.50
TOTAL COST-WATER TREATMENT + AMENDMENT	($/RAW T	1.50

Figure 1. Observed and predicted [SO4] shale control pile (SH).

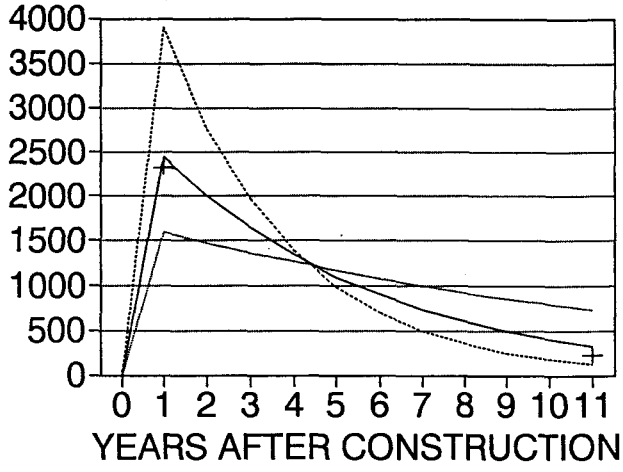

Figure 2. Observed and predicted [S04] 1% limestone amended pile.

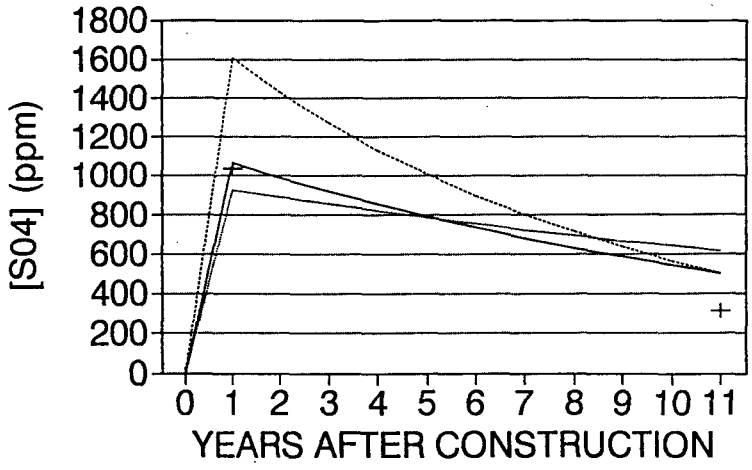

+ OBS. [SO4] —— high Sf —— medium Sf ------ low Sf

TABLE 2. Use of AMD-TIME spreadsheet to evaluate net deliverable acidity and sulfur flux rates. Sulfur flux rates are derived from observed rates in the field:

Low rate= rate integrated over full first year.

Medium rate= rate integrated over last 6 months.

High rate= rate integrated over the last 3 months.

100% SHALE CONTROL (SH)

ROCK MASS (KG)	365920
AREA (AC.)	0.05
FLOW (L/YR)	200250
%S	0.310
PYRITE S (KG)	1134
NET INF. (%)	75

%Sf/day	0.0204	0.0204	0.0500	0.0500	0.0800	0.0800
NDA (%)	100	50	100	50	100	50

Year	Observed [SO4]	Predicted [SO4]					*
0	0	0	0	0	0	0	0
1	2323	1219	610	2835	1417	4303	2152
2		1132	566	2362	1181	3214	1607
3		1051	525	1968	984	2400	1200
4		975	488	1640	820	1792	896
5		905	453	1366	683	1338	669
6		840	420	1138	569	999	500
7		780	390	948	474	746	373
8		724	362	790	395	557	279
9		672	336	658	329	416	208
10		624	312	549	274	311	155
11	220	579	290	457	229	232	116

SANDSTONE/SHALE LAYERED WITH 1% LIMESTONE AMENDMENT (LS2)

ROCK MASS (KG)	376000
AREA (AC.)	0.05
FLOW (L/YR)	200250
%S	0.330
PYRITE S (KG)	1241
NET INF. (%)	75

%Sf/day	0.0110	0.0110	0.0200	0.0200	0.0300	0.0300
NDA (%)	100	50	100	50	100	50

Year	Observed [SO4]	Predicted [SO4]					*
0	0	0	0	0	0	0	0
1	1038	732	366	1309	654	1928	964
2		703	351	1217	608	1728	864
3		675	338	1131	565	1549	774
4		649	324	1051	526	1388	694
5		623	312	977	489	1244	622
6		598	299	908	454	1115	558
7		575	287	844	422	999	500
8		552	276	785	393	896	448
9		531	265	730	365	803	401
10		510	255	678	339	720	360
11	312	490	245	631	315	645	322

* = Best prediction curves.

IMPROVED INTERPRETATIONS OF GROUNDWATER CHEMISTRY IN SHALLOW PERCHED FLOW SYSTEMS ON THE ALLEGHENY PLATEAU

Christopher Abate (1), Keith Brady (2), and Arthur W. Rose (3). ((1) Franklin & Marshall College, Lancaster, PA, (2) PADER, Harrisburg, PA, (3) Pennsylvania State University, University Park, PA).

In evaluation of surface mine impact, chemical analyses of groundwater from wells and springs are used for evaluation of pre-existing water quality and estimates of bedrock alkalinity. However, analyses from seeps and springs are typically quite different from that of wells (Brady et al, 1992). Where bedrock alkalinity is known to exist it is reflected in the groundwater quality but much less clearly in the spring water quality. Further, groundwater quality and bedrock chemistry are non-uniform in shallow rocks due to weathering processes and variation in residence times.

A conceptual geologic model and two-dimensional finite element simulation of vertical groundwater flow have been developed for shallow coal-bearing rocks of the Allegheny Plateau (Abate, 1993). Steady-state simulations were calibrated using annual water budget and piezometric data. Data were collected at sites characterized by shallow groundwater associated with major coal-underclay pairs "perched" well above regional groundwater flow systems. The shallowest saturated zones recharge only through surface infiltration and discharge through a combination of vertical leakage and cropline seepage. As a result, considerable spatial variability in groundwater velocity is defined and simulated flowpath lengths in saturated zones range from tens to thousands of meters.

Though recharging groundwater is undersaturated with respect to the primary sources of alkalinity within the aquifer, it must have sufficient contact time to develop an alkaline signature. Therefore, the range of residence times for groundwaters parcels suggested by simulated flow patterns supports the observation of dilute discharge from cropline seeps. Wells completed in the cores of the hills sample slower moving water while flowpaths of all lengths converge at cropline seeps.

APPLICATION OF THE NOVEL MILL TAILINGS AGGLOMERATION TECHNOLOGY FOR PREVENTION OF ACID MINE DRAINAGE

Laxman M. Amaratunga. (School of Engineering, Laurentian University, Sudbury, Ontario Canada P3E 2C6).

It is well known that environmental hazards, in particular the acid generation and subsequent liberation of heavy metals results from the surface disposal of sulphide mineral bearing mill tailings. Most Canadian base metals such as nickel, copper, zinc and lead, as well as uranium and precious metal milling operations are producers of reactive mill tailings containing the major sulphide gangue minerals such as pyrite, pyrrhotite and arsenopyrites.

A novel and environmentally safe mill disposal technology by cold-bond tailings agglomeration process (CBTA) is currently being developed at Laurentian University. This process has been adapted to prevent acid mine drainage from reactive mill tailings.

A preliminary study was undertaken to evaluate the application of the concept of agglomeration of reactive mill tailings using various alkaline binders and incorporating suitable chemical additives. The binders and additives are selected for their effectiveness in the prevention or retardation of the initial chemical and biochemical oxidation reactions of sulphide mineral leading to acid generation. Following a cold-bond, cold curing tailings agglomeration process, various types and dosages of chemical binders and their additives were employed. The additives under investigation were lime, sodium lauryl sulphate, potassium phosphate dibasic, sodium chloride and sodium benzoate. Some of these chemicals are well known acid neutralizers and others are inexpensive anionic surfactants, detergents and fertilizers acting as bactericides. Most of these additives have been reported in the literature as effective chemical agents used in the prevention and control of acid mine drainage from sulphide minerals.

The paper also presents a leachate study to investigate the acid generation potential from each batch of reactive tailings agglomerates containing various binders and non-toxic additives.

PROBABILISTIC ASSESSMENT OF THE LONG-TERM PERFORMANCE OF THE PANEL MINE TAILINGS AREA

Juris K. Balins (1), John B. Davis (1), and Roger A. Payne (2). ((1) Golder Associates Ltd., Toronto, ON, Canada, (2) Rio Algom Limited, Elliot Lake, ON, Canada).

Rio Algom's Panel Uranium Mine, located about 16 km northeast of Elliot Lake, Ontario, originally operated between 1958 and 1961. It was reactivated in 1979 and operated continuously until 1990. In all, the mine produced about 14 million tonnes of potentially acid generating, low level radioactive uranium tailings; about 5% pyrite (by weight) with less than 0.1% U_3O_8. The tailings area consists of two rock rimmed basins; the Main Basin into which tailings were deposited and the South Basin which served as a clarification pond. Topographic lows around the perimeter are closed by a total of six containment dams (zoned earthfill embankments).

To minimize the acid generating potential within the tailings, a decommissioning plan to flood the impounded tailings is being implemented. The anticipated performance of engineered structures (dams, spillways, channels, etc.) and the flooded tailings concept, over time periods in the order of thousands of years, have been addressed using probabilistic methods, based on subjective probability distributions consistent with available site specific information. The probable costs associated with long-term inspection and maintenance of the facility, as well as the probable costs and environmental consequences (e.g. tailings releases) associated with potential dam failures due to disruptive events such as floods, droughts and earthquakes were determined using a probabilistic model which consists of five, essentially independent, sub-models: a Maintenance Model, an Earthquake Response Model, a Flood Response Model, a Drought Model and an Integration Model. The principal conclusion derived from this assessment is that, for a well designed, constructed and maintained facility, there is very little likelihood that water and/or tailings solids will be released as a result of a containment dam failure; annual probability of the order of 10^{-6}. Failure to maintain the facility over the long-term significantly increases the likelihood of dam failure with resultant release of water and suspended tailings solids.

MICROCOSM MODEL TO STUDY MICROBIAL GROUPS INVOLVED IN AMD TREATMENT

Geneviève Béchard, Soundaram Rajan and W. Doug Gould. (CANMET, Department of Natural Resources Canada, Ottawa, Ont., Canada)

Acid mine drainage (AMD) is an important inorganic pollutant generated at mining locations throughout the world. CANMET has developed a microbial treatment system which effectively treated simulated acidic drainage using cellulosic substrates. Alfalfa was found to be an excellent substrate in continuous mode reactors. To optimize the microbial activities implicated in the treatment process, a better understanding of the complex microbial interactions involved in AMD amelioration was required. We hypothesized that at least three metabolic groups were involved in the treatment process: facultative anaerobic fermenters, cellulose degraders and sulfate-reducing bacteria (SRB). In the present study, a microcosm model was developed to study the initiation of microbial AMD treatment. The microcosms, referred to as treated microcosms, were prepared as follows: 300 mL erlenmeyer flasks were filled with fresh alfalfa, sterilized by autoclaving and rinsed. The microcosms were filled with simulated AMD and inoculated. A first experiment compared the performance of the treated microcosms to flasks containing fresh alfalfa in order to verify that the treated alfalfa could sustain AMD treatment as well as fresh alfalfa. In batch cultures treated alfalfa was a better substrate for acidic drainage treatment than fresh alfalfa. In a second experiment, microcosms with an initial pH value greater than 4 were shown to treat AMD more rapidly than microcosms with an initial pH lower than 4. In a third experiment, vitamin-amended microcosms did not treat AMD more rapidly and more effectively than non-amended microcosms. Representative strains of targeted metabolic groups were isolated from the pilot-scale laboratory model: a *Penicillium*-like fungus; *Sporocytophaga* sp.; *Lactococcus lactis* ss *lactis; Clostridium bifermentans; Clostridium glycolicum*; and *Desulfovibrio* sp. The isolated microorganisms were used in a fourth microcosm experiment to determine whether all groups essential for AMD treatment initiation had been identified. Results of this study will be presented and implications for treatment optimization will be discussed.

DEVELOPMENT OF A REACTION PATH APPROACH TO MODELING POST-MINING PIT WATER GEOCHEMISTRY

David A. Bird, W. Berry Lyons (1), and Glenn C. Miller (2). ((1) Hydrology/Hydrogeology Program, University of Nevada, Reno; (2) Department of Environmental Resource Sciences, University of Nevada, Reno).

The impacts of mining on water quality in the U.S. have become the focus of increased environmental concern in recent years. An assessment of potential mining impacts on water quality is necessary because of possible adverse effects that include acid mine drainage and high trace metal concentrations. Open pit mines that require dewatering will likely see the eventual development of pit lakes after mine closure. The water quality that evolves in pit lakes will be a function of many variables including: ore and host lithology/mineralogy, acid generating and acid neutralizing potential, local ground-water chemistry, trace metal adsorption, oxidation/reduction reactions, limnological mixing, water temperature, reaction kinetics, biological activity, and others. This study evaluates hydrogeochemical modeling software that might be appropriate for modeling post-mining, pit water geochemistry, and applies them to an actual mining environment. Data from the Cortez Mine, a carbonate-hosted, open pit, precious metal mine in Nevada, is used in an inverse model (BALANCE, USGS) to determine geochemical mass transfer that has occurred between the mine wall rock and the pit lake. These results guide the development of a forward reaction path model that may be used for future mine sites. After modification to include over 200 minerals and aqueous species of arsenic, cadmium, copper, lead, mercury, silver, thallium, and zinc, PHREEQE (USGS) was used in reaction path modeling. MINTEQA2 (EPA) was used to model mineral precipitation and trace metal adsorption onto hydrous ferric oxide. The study demonstrates that pit lake chemical evolution can be modeled with available software packages, using existing mine environments to guide model development. This method represents a reasonably valid approach, with substantial cost savings over long-term modeling studies that utilize laboratory test and complicated ground-water flow models.

EVALUATION OF ORGANIC ADDITIVES USED TO ENHANCE BACTERIAL SULFATE REDUCTION IN MINE WATER TREATMENT SYSTEMS

S.L. Borek, D.H. Dvorak, R.W. Hammack, and H.M. Edenborn. (U.S. Bureau of Mines, Pittsburgh, PA, USA).

Several organic additives, including dairy whey, brewers' yeast, beet molasses, peach peelings, sodium lactate, and polylactic acid, were examined for their relative ability to support bacterial sulfate reduction. In one series of tests, flasks of sulfate-reducing bacteria were amended with the different organic additives, and the H_2S generated from each treated flask was monitored over time. In a second series of tests, the dissolved sulfate concentration was monitored over time for anaerobic mixtures containing synthetic mine drainage, organic sediment from a constructed wetland, and fermented or unfermented organic additives. As expected, the type and concentration of organic additive used influenced the extent to which the sulfate reduction rate increased, and the duration of this increase. Dairy whey was found to sustain a higher and longer-term sulfate reduction increase than the other additives, so it was evaluated further in the field by adding it to the organic substrate of a constructed wetland used for treating acid mine drainage. Sulfate concentrations in amended and unamended sections of the wetland were compared over time to determine the effect of the whey addition on the sulfate reduction rate. Preliminary results showed an increased pH and decreased sulfate concentrations for the amended section, indicating a greater rate of bacterial sulfate reduction than in unamended sections.

THE EFFECTS OF TEMPERATURE, HUMIDITY, PARTICLE SIZE, AND LEACHING INTERVAL ON LEACHATE QUALITY USING WEATHERING CELLS AND SOXHLETS

William S. Bradham and Frank T. Caruccio. (University of South Carolina, Columbia, SC, USA)

Mine overburden analytical techniques employ static tests such as acid/base accounting, and empirical tests such as weathering cells and soxhlets to predict post-mining drainage quality. The overburden weathering conditions created by the two empirical techniques are quite different, the weathering cell employing ambient storage and leaching temperatures, and the soxhlet technique using high temperature storage and boiling water leaching. Due to these disparities, the two techniques produce distinct and often contradictory results. To address these concerns, this study was designed to use Multifactored Analysis of Variance (ANOVA) and linear regression models to identify the significant factors controlling leachate quality in weathering cells and soxhlets and demonstrate how each of those factors influences leachate quality. The factors of storage temperature and humidity were evaluated as a single variable called "storage". Other factors tested were overburden chemistry, particle size, leachant temperature, and leaching interval. The overburden analytical techniques were found to be most sensitive to variations in storage condition with the lowest pyrite oxidation and calcium carbonate dissolution rates resulting from abiotic, low temperature storage. High temperature storage (105°C) resulted in increased pyrite oxidation rates, dependent on overburden chemistry, accompanied by a concurrent increase in calcium carbonate dissolution in high NP samples. Mineral equilibrium calculations indicated that the secondary formation of calcium sulfate minerals from high temperature storage of pyrite rich, high NP samples, provides a highly soluble source of Ca^+ and SO_4^{-2} during subsequent leaching events. Longer periods of storage at high temperatures resulted in higher total sulfates, indicating that pyrite oxidation may occur in the apparent absence of water. In the case of samples for which 2 and 4 day oven storage produced alkaline leachates, but 7 day storage produced acidic leachates, high temperature pyrite oxidation at longer intervals of storage does not seem to be balanced with an increase of calcium carbonate dissolution. Applications of this research include methods of normalizing and comparing the results of disparate overburden analytical techniques. The study also provides greater insight into pyrite oxidation and acid mine drainage remediation.

BACTERIAL METABOLISM IN ACID MINE DRAINAGE

Elaine K. Brenner (1), Fred J. Brenner (2), and Scott Bovard (2). ((1) New Jersey Institute of Technology, Newark, New Jersey, USA; (2)Grove City College, Grove City, PA, USA.).

Constructed wetlands have been used for over a decade as passive treatment systems for acid mine drainage (AMD). In theory, these systems reduce heavy metal concentrations by increasing retention time, vegetative uptake, and bacterial metabolism. A seven year study of four wetland systems in northwest Pennsylvania compared the mean growth rate of metal oxidizing and aerobic and anaerobic sulfate reducing bacteria.

Throughout the seven year study, discharges from the wetland systems at mine Site 1 continually had pH values below 6.0 while iron and manganese concentrations exceeded 7 and 4 mg/l, respectively. Moreover, the efficiency of these systems apparently declines since there was a trend toward increased metal concentrations over the seven years following an initial decline. While at Site 2, pH values were generally greater than 6.0 and the iron concentrations were less than 7 mg/l in the discharges from both systems, but manganese concentrations exceeded 4.0 mg/l. At both sites, substrate iron and manganese concentrations increased throughout the seven years.

In the more acidic environment that existed in the wetland systems at Site 1, the rate of increase in iron and manganese bacteria in response to increasing metal concentrations in the water and substrate was significantly greater than it was in the more alkaline systems at Site 2.

THE ROLE OF BACTERIA IN THE RETENTION OF FE AND MN IN A CONSTRUCTED WETLAND RECEIVING COAL MINE DRAINAGE

L.A. Brickett and H.M. Edenborn. (U.S. Bureau of Mines, Pittsburgh, PA, USA)

Constructed wetlands have been built throughout the Appalachian coal mining region to passively treat acid mine drainage. Bacteria in the wetlands promote the precipitation and dissolution of Fe and Mn compounds directly via their metabolic activity and by influencing environmental Eh and pH. Continuous gradient gels (CGG's) containing various Fe and Mn compounds were used previously to qualitatively assess the stability of these redox-sensitive compounds at depth in wetland sediments. In this study, indigenous bacteria involved in the transformation of Fe and Mn were incorporated into the gel matrix of CGG's and were incubated for varying lengths of time in the sediment of a constructed wetland in northwestern PA. CGG's containing Fe and Mn compounds were placed in the sediment adjacent to the bacteria-containing gels. After incubation, the distribution and fate of incorporated bacteria were determined and compared to zones of Fe and Mn compound stability and dissolution. The direct and indirect role of bacteria in the retention of Fe and Mn compounds in the study wetland is discussed.

ACID MINE DRAINAGE AMELIORATION BY WETLANDS - STUDY OF A NATURAL ECOSYSTEM

Melanie M. Brown (1), Keith Atkinson (1), and Carolyn Wilkins (2). ((1) University of Exeter, Camborne School of Mines, Cornwall, U.K.,(2) CSM Associates, Cornwall, U.K.

The county of Cornwall, UK, has been extensively mined for the mineral deposits. Part of the legacy of this activity, which had its peak at the end of the 19th century, is the numerous and persistent discharges of acid mine drainage from old mine workings, waste rock dumps and tailings dams. Passive treatment systems to improve the quality of these discharges are required. The potential of wetlands as treatment systems for these discharges has been investigated by examining, in detail, part of a 41 Ha long-established natural wetland which improves water quality in an abandoned mining district. This area receives mine drainage, with high levels of metals and metalloids, principally copper and zinc and arsenic. The mining in this area flourished in the 17th and 18th centuries; consequently the study of the substrate and the change in metal concentrations and associations with depth provides valuable information on the long term functioning of wetlands as sinks for heavy metals. The results are based on chemical analysis, sequential extractions, metal speciations and SEM analysis. This work provides insight into the long term functioning and longevity of acid mine drainage amelioration by wetlands which are in equilibrium with the surrounding environment. This is an aspect of wetland treatment which cannot yet be examined in artificially constructed ecosystems and it provides information which can be applied to the design and implementation of constructed wetland systems.

LONG-TERM STUDY OF CONSTRUCTED MODEL WETLANDS FOR TREATMENT OF ACID MINE DRAINAGE

Joseph P. Calabrese, Alan J. Sexstone, Devinder K. Bhumbla, Jeffrey G. Skousen, Gary K. Bissonnette, and John C. Sencindiver. (West Virginia University, Morgantown, WV, USA).

Although bioremediation of acid mine drainage (AMD) with constructed wetlands provides an alternative technology to chemical treatment methods, little is known about the sustainability of these systems in treating this long-term environmental problem. Studies were conducted to investigate treatment of AMD with constructed cattail (*Typha*) wetlands in greenhouse model systems. The wetlands (480 x 60 x 60 cm), which employ a peat/soil substrate, received a natural source AMD (430 mg/L iron, 2,900 mg/L sulfate, pH 2.75) at a rate of 60 L/day with a retention time of 3 to 4 days. During the first years of the study, greater than 60% of the total iron applied was retained in sediments, with ~15% of this total as reduced iron sulfides (80% acid volatile sulfides / 20% pyrites) and the remainder constituting pools as exchangeable > oxides > organically complexed. Subsurface anoxic sediments ($\geq$ 10 cm) continue to exhibit highly reduced conditions (-100 to -300 mV) and near neutral pH (6.0 $\geq$ 30 cm). These conditions support an active microbial sulfate-reducing populations as indicated by MPN quantification (10^6 to 10^8 cells/g [wwt]) and significant $^{35}S\text{-}SO4^{2-}$ reduction rates (100 to 600 n moles gwm^{-1} day^{-1}). Overall, active sulfate-reducers may account for the 80% decrease in SO_4^{2-} concentrations in lower sediments. Currently, iron removal predominates under acidic pH in surficial water by complexation and oxide formation as a result of both chemical and microbiological processes. Subsurface sediments contain higher concentrations of dissolved iron and may be attributed to active bacterial iron reduction. However, excess alkalinity buffers interstitial water near pH 6.0 due to limestone dissolution and active bacterial sulfate reduction. Remobilization of metals was not exhibited in Wetland #1 where AMD-loading was replaced with freshwater after a 2-year period, suggesting that retention in the wetland matrix can remain stable even after a 12 month period. Wetland #4 continues to produce a neutral effluent high in soluble iron after 3 years of AMD addition, suggesting that this system functions similarly to an anoxic limestone drain.

EFFECTS OF OVERBURDEN ANALYSIS ARTIFACTS ON LEACHATE QUALITY

Frank T. Caruccio, William S. Bradham, and Gwendelyn Geidel. (University of SC, Columbia, SC, USA).

Overburden analyses can be grouped into two broad categories; static or dynamic techniques. The static or whole rock analyses measure and balance the acid and neutralization potentials. The various procedures are clearly outlined and the precision of the test is satisfactory. The dynamic tests determine leachate quality by subjecting the overburden samples to a variety of simulated weathering conditions (humidity cells, columns, and soxhlet reactors) and as found in this study, the leachate quality may be more controlled by the physical configurations of the testing method than the chemistry of the sample. The physical variables affecting leachate quality and the precision of the tests, other than the sample chemistry, include 1) ambient temperature (both in the laboratory and storage conditions), 2) humidity of the pore space, 3) degree of saturation and specific yield, 4) particle size, and 5) temperature of the leachant. These artifacts are associated with specific tests and further affect the degree to which the natural conditions are simulated by the testing procedure. Extending the application of these laboratory affects to field conditions has broad implications with regard to 1) undersaturated conditions of humidity, 2) air-locking within samples, 3) variations due to electro-chemical oxidation of pyrite, 4) the release of manganese, and 5) efficacy of submergence. Dynamic tests, coupled with field measurements, indicate that the backfill geochemistry is generally under reduced conditions, enhancing the dissolution and solubility of metals. For example, when evaluated through radioisotopic studies, we found the manganese associated with acidic drainages to be of recent age, suggesting a source to be charred hardwoods that are commonly buried at the base of backfills (white oak ash may have up to 15,000 ppm Mn). Further, evaluation of stoichiometric relationships of leaching test data, indicate that electro-chemical oxidation of pyrite occurs rarely, if at all, in the coal associated geohydrologic regimes and consequently submergence of acid producing materials, due to the limited oxygen transfer, is an effective mechanism to arrest oxidation reactions.

MINERALOGICAL CHARACTERIZATION OF A WASTE ROCK DUMP PRODUCING ACID MINE DRAINAGE, LA MINE DOYON (QUÉBEC)

Marc Choquette (1), Pierre J. Gélinas (1), Denis Isabel (1), and René Lefebvre (2).((1) Université Laval, GREGI, Département de géologie et de génie géologique, Québec, QC, Canada, G1K 7P4. (2) INRS Géoressources, Sainte-Foy, Qc, Canada, G1X 4N8.)

A research program is on-going since 1991 on the hydrological, geochemical and physical processes operating in a waste rock dump producing acid mine drainage (AMD) at La Mine Doyon in Northwestern Québec. We present here the results of the mineralogical characterization done to identify the geochemical processes related to AMD production. The dump is 500 m x 900 m, and is more than 30 m high. It is the site of pyrite oxidation producing a leachate with a pH around 2,2 and an acidity between 40 000 and 80 000 g/l. Heat released by pyrite oxidation has increased temperature up to 65ºC within the dump. Waste rock samples for mineralogical and geochemical characterization were obtained from drill cuttings and trenches. Mineralogy was determined by X-ray diffraction and SEM. The acid generating rock type is a sericite schist containing 4% to 7% pyrite, sericite (muscovite and paragonite), quartz, Mg-chlorite and minor amounts of calcite. Jarosite, indicative of acidic conditions, was observed in the interlayer space of sericite, where the potassium necessary for its formation is present. This phenomenon is believed to contribute to the high acid production observed in these rocks by opening the rock structure and allowing more pyrite to be exposed to oxidizing solutions. At the surface of the dump, calcite is still present and accessible, thus preventing jarosite formation by maintaining a higher pH. The sericite alteration sequence observed is first the formation of a smectite-type clay which is later altered to amorphous silica pseudomorphic of the clay. The smectite-type clay is poorer in aluminium than sericite and incorporates magnesium. The source of magnesium is most probably chlorite. Mineralogical characterization of these samples is still on-going but the indications so far are that phyllosilicates contribute to partial leachate neutralization.

AMD PREDICTION AND CONTROL METHODS - AN UPDATE FROM AUSTRALIAN CASE STUDIES

William P. Clarke, Peter A. Ryan, and Chris J. Joyce (AGC Woodward-Clyde Pty Ltd, Brisbane, Australia)

Testwork and advanced modelling methods used to predict the generation and impact of AMD for the purpose of designing AMD mitigation works are presented. The performance of specific models is evaluated by examining a number of AMD case studies at Australian coal and metalliferous mines. The case studies include preventative works (eg. proactive measures such as waste scheduling, wetland construction) and remediation works (eg. liming and compaction of surface wastes, introduction of external capping materials). Predicted seepage rates and water quality are compared with field data collected before and after the implementation of AMD control measures. The parameters used in the prediction models are reviewed in light of the comparisons between actual and predicted data.

In association with ABA, geochemical and kinetic testing, three principal models, LEACH, PITQUAL, and ENTEC are used for predicting AMD and designing control measures. The leachate quality model (LEACH) simulates the movement of solutes through mine wastes subject to infiltration, dispersion, adsorption, ion exchange, precipitation dissolution and complexation reactions. Infiltration rates are assessed using the unsaturated flow model HELP. Any waste type and layering configuration can be accommodated by modifying the geochemical database read by the program. Parameters such as leachable salt content, sulphide content, voidage (which affects oxygen permeability), hydraulic conductivity, and particle sizes are specific to each case and must be supplied by the user.

The pit water quality model (PITQUAL) assesses the quality of water in decommissioned mine pits and wetland retention basins. Unlike LEACH, PITQUAL considers a batch system (eg. a water body in a mine void). Sources of acid and salt are introduced to the water body as the simulation progresses according to the frequency of flushing events, dissolution rates, and groundwater infiltration. ENTEC, a mine planning and environmental package, is used to design the earthworks associated with wetland basins, waste dumps, etc.

USE OF A BROMIDE TRACER TO DETERMINE RETENTION TIME OF MINE DRAINAGE IN ANOXIC LIMESTONE DRAINS

A.R. Cooper, L.A. Brickett, and S.L. Borek. (U.S. Bureau of Mines, Pittsburgh, PA, USA).

A tracer test using sodium bromide (NaBr) was performed on two anoxic limestone drains (ALD's) to determine the retention time (RT) of mine drainage in the ALD's. The Howe Bridge ALD, located in Jefferson County, PA, is the larger of the two drains with the capacity to hold 133,280 L of water. It has a mean flow rate of 87 L/min and has an estimated RT of 25.5 h. The Morrison ALD, located in Clarion County, PA, has the capacity to hold 20,090 L of water, a mean flow rate of 8.0 L/min and an estimated RT of 41.9 h. Estimated RT's were determined by dividing the estimated capacity of the drain by the flow rate, then expressing the result in hours. The tracer test consisted of pouring a concentrated solution of NaBr into an access area near the beginning of the drain and then measuring the concentration of bromide in the effluent water. Mean RT's were calculated from the change in the concentration of bromide over the duration of the test. The Howe Bridge ALD had a mean RT of 42 h, while the Morrison ALD had a mean RT of 87 h.

CONSTRUCTED WETLANDS HANDBOOK

Luise K. Davis. (Soil Conservation Service, Philadelphia, PA, USA)

Constructed wetlands can be an effective and low-cost means of treating mine drainage. However, the successful use of wetland treatment depends on proper sizing, design, operation, and maintenance. The effective application of constructed wetland treatment to mine drainage has been hampered because much of the useful information on constructed wetlands is scattered throughout the literature. There has thus been a need for a concise, easy to use handbook specific to the use of constructed wetlands on mined lands.

The U.S. Environmental Protection Agency, the Soil Conservation Service, and the Pennsylvania Department of Environmental Resources are cooperating in the development of a Handbook to assist the mining industry in the appropriate and effective use of constructed wetlands on mined lands in the northeastern United States.

The Handbook will discuss the basis for wetland treatment, its advantages and disadvantages, the components of constructed wetlands (hydrology, soils, vegetation, microbiology), and the concepts of ecological engineering. The Handbook will discuss the siting, design, construction, operation, maintenance, and monitoring of wetlands. Additional values, such as landscape enhancement, and potential problems, such as mosquitoes and muskrats, will also be covered. The Handbook will consider aerobic wetland systems (free water surface wetlands), compost wetlands, and anoxic limestone drains.

The Handbook is part of a series that includes the use of constructed wetlands to treat agricultural wastewater and runoff, domestic wastewater, and stormwater runoff. The Handbook is scheduled for publication in the fall of 1994.

CONSTRUCTED VERTICAL FLOW AERATED WETLANDS DESIGNED FOR THE REMOVAL OF MANGANESE FROM ACIDIC MINE DRAINAGE

M. DeLeo, T. McMillen, P. Colberg, N. Swoboda-Colberg, and J. Smith. (University of Wyoming, Laramie, WY, USA).

Constructed wetlands are used to mitigate water quality problems related to both wastewaters and mine drainage. Wetlands are most often constructed with inconsistent design recommendations and function with varying degrees of success. Typically, wetlands are classified as either free water surface (FWS) or vegetated submerged bed (VSB). FWS wetlands are considered to be aerobic, while the VSB type are usually anaerobic; however, both redox conditions probably exist in both designs.

Wetland is described in which the main reactive bed consists of a layer of limestone gravel overlain by a fine gravel filter and soil. Ponded water on the soil infiltrates through the soil layer, through the filter and then through the larger volume of limestone media. Since the soil has the lowest hydraulic conductivity of the three layers and the limestone is vented to the atmosphere, water flows through the lime stone in an unsaturated condition.

Laboratory results obtained from studies in 36 large-scale model wetland columns suggest that the vertical wetland design employed in this investigation very effective in both neutralizing acid mine drainage (pH 4.3 $\rightarrow$ pH 8.5) and precipitating heavy metals -- especially manganese (mn). Variations in the nominal water flow velocity, which averaged 2.1×10^{-6}m/s, and forced ventilation of wetlands had no apparent influence ont he efficiency of acid neutralization or metals removal.

Studies undertaken to determine the mechanisms responsible for Mn removal suggest that although the columns support active populations of manganese-oxidizing bacteria, their role in overall removal in Mn was minimal in comparison with the chemical precipitation reactions mediated by the limestone. One interesting observation was the existence of sulfate-reducing bacteria in all the active, Mn-removing columns. These organisms are strict anaerobes which suggests the existence of redox microzones in the model wetlands although the potential role of sulfidogens, if any, in Mn removal is uncertain.

LABORATORY MODELLING OF SUBAQUEOUS DISPOSAL ENVIRONMENTS

Serena J. Domvile (1), Michael G. Li (1), Diana D. Sollner (1), and Hugh R. Wilson. ((1) Klohn-Crippen Consultants Ltd., Richmond, BC, Canada; (2) Metall Mining Corp., Edmonton, AB, Canada).

Subaqueous disposal of sulphidic mine wastes and mine workings has shown promise in controlling or preventing acid generation in many case studies. The relative reactivities of sulphides, status of oxidation and acidification processes prior to submersion and site-specific conditions are expected to influence the depth of water cover required to meet long term water quality objectives.

The Izok Project in Canada's Northwest Territories, currently in feasibility studies, is incorporating subaqueous deposition into its waste management and acid rock drainage (ARD) control strategies. Although tailings would be submerged from the onset of mining operations, waste rock would be exposed to weathering for several years prior to flooding and maintenance of a permanent water cover.

Phase I investigations were conducted at the laboratory scale using column leaching tests for modelling disposal conditions. Representative samples of waste rock and tailings were obtained from drill core and metallurgical testing programs, respectively. Waste rock was weathered under laboratory conditions prior to implementing continuous water cover conditions. Tailings were covered with a 1.0 m water cover. Simulation of lake mixing and downward water infiltration was conducted in the laboratory. Dissolved oxygen profiles were measured across the water cover. Water quality of the water cover at different depths and over time was monitored to decipher the diffusion of oxidation products.

THE ALTERATION OF ARSENIC-BEARING TAILINGS, AND THE RELEASE OF CONTAMINANTS TO SURFACE WATERS IN COBALT, ONTARIO

C.G. Dumaresq and F.A. Michel, Carleton University, Ottawa, Ontario, Canada
K.S. Subramanian, Health Canada, Ottawa, Ontario, Canada

Silver was mined in Cobalt, Ontario, from 1904 until the 1980's. Silver occurs in veins close to or at the surface, in association with nickel and cobalt arsenide and sulfarsenide minerals in a calcite, dolomite, quartz matrix. Previous workers identified supergene alteration reactions which occur in the surface veins. Arsenide and sulfarsenide minerals are oxidized, producing arsenic and sulfuric acids. These acids react with the carbonates, raising the pH. As the pH increases, secondary arsenate minerals such as scorodite ($(Fe,Al)AsO_4 \cdot 2H_2O$) and erythrite ($Co_3(AsO_4)_2 \cdot 8H_2O$) are precipitated. Upon further oxidation these minerals break down, releasing arsenate and metals to the environment. There are numerous tailings deposits in the Cobalt area, with reddish orange to greenish alteration zones in the top 50 cm. During the summer, water soluble, white to orange-brown crusts form on the tailings surface. X-ray analyses indicate that these crusts are composed primarily of gypsum ($CaSO_4 \cdot 2H_2O$) and thenardite (Na_2SO_4), but chemical analyses show that the crusts contain up to 19000 ppm arsenic. The presence of these arsenic-rich crusts provides evidence that the supergene alteration reactions identified as occurring in the surface veins are also occurring in the tailings alteration zones. The oxidation of arsenide and sulfarsenide minerals in tailings, and the dissolution of secondary minerals and crusts, results in the release of large quantities of arsenic and heavy metals to surface waters in the Cobalt area. Contaminants also originate from natural sources such as soil, glacial till, and groundwater. Except for one lake, As concentrations in local water bodies range from 0.040 to 6.510 ppm. The stream which drains the Cobalt area is estimated to carry an annual average of 18000 kg of arsenic to Lake Temiskaming, part of the Ottawa River system.

TREATMENT OF ACID MINE WATER WITH A SEQUENTIAL CELL CONSTRUCTED WETLAND

David P. Eddy. (Graduate Program in Ecology, Penn State University, University Park, PA 16802 USA).

A pilot scale wetland experiment was designed to examine the effects of sequential substrates on pH, Fe, and Mn treatment. Combinations of two substrates, spent mushroom substrate (SMS) and crushed limestone ($CaCO_3$) arranged in series, were tested under controlled conditions in a greenhouse. Sixteen constructed wetlands, containing two cells each, measured 1.0 m long, 0.15 m deep and 0.26 m wide. Each combination was replicated four times. Synthetic acid mine water containing 50 mg/L Fe and 25 mg/L Mn at a pH of 3.5-4.0 was delivered to each of the 16 wetlands at a flow of 10 mL/min. Metal loadings per cell were 2.77 g Fe m^{-2} d^{-1} and 1.38 g Mn m^{-2} d^{-1}. All four substrate sequence treatments (SMS→SMS, SMS→$CaCO_3$, $CaCO_3$→SMS, $CaCO_3$→$CaCO_3$) retained 100% of the iron and elevated pH to above neutrality, with no signs of saturation after 271 days. However, only the crushed limestone substrate retained Mn on a sustained basis, except when preceded by mushroom compost. Results (1) confirm reports of effective Fe and pH treatment using constructed wetlands, (2) cast doubt on the effectiveness of a wetland design that follows a compost wetland with a bed of limestone for Mn treatment, and (3) demonstrate the positive aspects of treating mine water with crushed limestone alone.

BIOACCUMULATION OF METALS IN CONSTRUCTED WETLANDS USED TO TREAT ACID DRAINAGE

G.S. Edwards and P.A. Mays. (TVA, Norris, TN. USA).

Constructed wetlands are being used extensively as a potential mitigation for acid drainage. However, removal of metals to meet compliance requirements has varied among wetlands, ranging from partial to total success. In addition, wetlands are sinks for contaminants found in acid drainage, and bioaccumulation of these contaminants to levels that would adversely affect the food web is of growing concern. The primary objective of this project was to determine whether bioaccumulation of metals occurs in wetlands constructed for treatment of acid drainage. Water, sediment, plant and benthos samples were collected from two wetlands constructed by the Tennessee Valley Authority and a natural wetland in the spring and fall of 1992, and metal concentrations were determined. One of the constructed wetlands, Impoundment 1, has generally been in compliance for NPDES; the other, Widow's Creek, has never been in compliance. Preliminary results indicate similarities in sediment and plant metal concentrations between Impoundment 1 and the natural wetland and greater metal concentrations in the sediment and plants at Widow's Creek. Data also indicate that Mn, Zn, Cu, Ni, and Cr are being accumulated in the plants at each wetland. However, accumulation of metals by these plants probably accounts for only a small percentage of the removal of the annual metal load supplied to each wetland. Bioaccumulation of metals in the benthic organisms at each wetland is currently being investigated.

THE USE OF SULFATE REDUCTION TO REMOVE METAL FROM ACID MINE DRAINAGE

A. Paul Eger. (Minnesota Department of Natural Resources, St. Paul, MN, USA).

Seven combinations of organic substrate and limestone have been studied for their ability to support sulfate reduction and remove metals from acid mine drainage. The substrates include 45 and 180-day old municipal compost, composted yard waste, horse manure, wood shavings, and peat. Nine rows of 55-gallon barrels connected in series received drainage from two different mine waste stockpiles. The input drainages had average pH of 4.2 and 5.1, with average sulfate concentrations of 900 and 2200 mg/L and average trace metal concentrations of 13 and 81 mg/l copper, 1.7 and 4.6 mg/L cobalt, 40 and 90 mg/L nickel, and 1.2 and 3.1 mg/L zinc. All the substrates except peat were successful in neutralizing the drainage. The pH in the peat system decreased from 5.1 to 4.3. All substrates did reduce metal concentrations by over 90%. Samples collected from between the series of barrels have demonstrated that some of the substrates which have been in operation for three years have begun to lose treatment efficiency. The metal removal in the first third of the system dropped from about 90% for the first two years to 40 -60% during the third year of operation. Although the drainage has been neutralized and metals removed , the effluent from the system contained elevated levels of dissolved organics and nutrients. BOD values generally exceeded 60 mg/l with a maximum total concentration of 780 mg/L. Total phosphorus concentrations routinely exceeded 2 mg/L , while the maximum concentration was 22.7 mg/L.

GEOLOGICAL AND GEOCHEMICAL CONTROLS ON THE COMPOSITION OF WATERS DRAINING FROM DIVERSE MINERAL DEPOSITS

Walter H. Ficklin, Kathleen S. Smith, and Geoffrey S. Plumlee. (U. S. Geological Survey, Denver, CO, USA)

The Colorado Mineral Belt hosts a broad spectrum of mineral deposits, each having characteristic structural features, host rocks, wallrock alteration, gangue minerals, and trace metals. Mine-drainage waters that we have sampled and analyzed from a variety of mineral deposit types in the Mineral Belt show extreme variations in pH and dissolved metal content: the pH varies from 1.7 to 7.8, iron concentrations range from less than 1 to as high as 8000 mg/L, zinc concentrations range from 20 to 700000 µg/L, and copper concentrations range from less than 1 to as high as 500000 µg/L. The concentrations of arsenic and metals such as rare earth elements, uranium, thorium, lead, nickel, cobalt, and chromium range from less than 1 µg/L to as high as tens of mg/L. In general, most metals show trends of decreasing concentration with increasing pH; however, some near-neutral waters can have dissolved zinc concentrations as high as 170 mg/L. Along with geochemical processes (such as sorption, mineral precipitation/dissolution, and evaporation) and biologically mediated processes (such as bacterial iron oxidation), mineral deposit geology is a fundamental control on the compositions of the mine-drainage waters. Important geologic controls include: (1) the types and abundances of pyrite and other metal-sulfide minerals in the deposits; (2) the acid buffering capacity of the mineral deposit host rocks, and gangue material; and (3) the accessibility of the sulfides for weathering. Other important controls, such as climate, topographic setting, and mining and mineral processing methods, generally modify the environmental effects mandated by mineral deposit geology and geochemical processes. For example, the mining method used influences drainage water compositions by controlling the amounts of sulfides exposed to weathering, the amount of atmospheric oxygen available during weathering, and the amount of evaporation that can occur. The study of water draining active and abandoned mines provides predictive capabilities to supplement standard static and kinetic laboratory predictive tests, which can be hampered by non-representative sample size and time scale. Thus, a realistic approach to predicting acid-forming potential of new mines may be derived from the study of existing mines in deposits having similar geologic characteristics.

POTENTIAL RECLAMATION OF THE BREWER PIT BY ADDITION OF PHOSPHATE ROCK

Lorraine H. Filipek (1)*, Barbara A. Filas (1), James M. Stonehouse (2) and Ru Wen (2). ((1) Knight Piesold and Co., Denver, CO, USA; (2) Brewer Gold Co., Jefferson, SC, USA. *Present affiliation: US Geological Survey, Denver CO, USA).

The Brewer Pit is the central feature of the Brewer Gold Mine located in Chesterfield County, South Carolina. The pit is presently inactive and closure is planned within the next year. The pit has begun to fill with ground water, which is acidic as a result of oxidation of pyrite. As an alternative to the costs of perpetual pumping and treating of the pit water, the option of allowing the pit to remain flooded and to neutralize and stabilize the water, pit floor, and wall rock by adding phosphate rock was considered. The effectiveness of phosphate rock addition was investigated by thermodynamic modeling and long-term kinetic laboratory investigations. Thermodynamic modeling confirmed that the phosphate rock addition to the flooded pit would raise the pH while maintaining low concentrations of dissolved phosphate. Two options were tested in the laboratory experiments: (1) addition of phosphate rock directly into the acid water and (2) addition of phosphate to a dry pit following one-time pumping and treatment of the existing acid water. The results indicated that the phosphate rock addition increased pH and decreased metal concentrations significantly compared to control experiments. The significant dissolved iron and aluminum in the pit water reacted with phosphate to control its concentration at low levels, suggesting that adding phosphate rock directly into the pit water is preferable to addition of phosphate to a dry, dewatered pit.

THE TOLERANCE OF WETLAND PLANT SPECIES TO ACID MINE DRAINAGE: A METHOD OF SELECTING PLANTS SPECIES FOR USE IN CONSTRUCTED WETLANDS RECEIVING MINE DRAINAGE.

K. Garbutt, D.L. Kittle and J.B. McGraw (West Virginia University Morgantown, WV, USA)

Little work exists on the appropriate selection of plant species for wetlands, yet this can have important implications for the long term success of a project. In constructed wetlands, higher plants serve several purposes substrate consolidation, stimulation of microbial processes, wildlife habitat, and aesthetics. The choice of wetland species should be based on a knowledge of local conditions, the relative ability of species to tolerate the conditions found in a particular watershed, and their ability to provide the functions listed above.

We exposed five commonly occurring wetland species to a range of AMD treatments (pH 2.5 -6.5). These treatments were created by either acidifying or neutralizing a standard AMD source (pH 2.9 - 3.1). To summarize the results. *L. oryzoides* did not grow well in any of the acid mine drainage treatments. *A. calamus* only grew well above pH 5.5. All species appeared to be adversely affected by low pH. *T. latifolia* was more tolerant of a wide range of pH than *J. effusus* and *S. cyperinus*. However, *J. effusus* and *S. cyperinus* appears to grow equally as well or better at intermediate pH. *T. latifolia* appeared least affected by low pH.

On the basis of these results we can make the following recommendations. If the pH of the AMD is 4.5 or below both *T. latifolia* is most suitable for inclusion in a constructed wetlands. Above pH 4.5 *J. effusus* and *S. cyperinus* could also be included and be expected to survive and flourish. It might also be possible to use these results as bio-indicators of wetland status. If pH is below 4.5 and *J. effusus* and *S. cyperinus* are present they will appear in poor conditions, similarly if pH is below 5.5 and *A. calamus* is present it will appear in poor condition. A thin poor quality stand of *Typha* may indicate water with pH lower than 3.0.

CHARACTERIZATION AND MONITORING OF A WASTE ROCK DUMP PRODUCING ACID MINE DRAINAGE, LA MINE DOYON (QUEBEC)

Pierre Gélinas (1), Marc Choquette, René Lefebvre (2), and Denis Isabel (1). ((1) Université Laval, Département de géologie et de génie géologique, (2) INRS Géoressources, Sainte-Foy).

A characterization, monitoring and modelling research program is on-going since 1991 on the hydrological, geochemical and physical processes related to acid mine drainage production from a waste rock dump at La Mine Doyon in Northwestern Quebec. The research program focusses on the South Dump which covers 45 hectare and is 30 m thick. The leachate produced has a pH around 2,2 and an acidity between 40 000 and 80 000 mg/L. Temperature within the dump (40 to 65°C) is measured with thermistors intalled in six wells in which gas-sampling is also done. Leachate sampling and flow measurements are made at three weir stations in leachate-collection ditches around the dump. Other hydrological data are provided by infiltration measurements by lysimeters and meteorological conditions recording at an on-site station. The wells within and around the dump allow piezometric level measurements. Mineralogical characterization revealed the presence of new minerals. The pH and relative concentration of chemical components in the pore fluids were obtained from leaching or press extractions. Water content, grain density and a gravity survey were used to derive porosity and water saturation. Grain size analysis was used to indirectly derive the capillary and relative permeability properties. Airborne and surface infrared thermographic surveys revealed evidences of temperature-driven air flow patterns within the dump. The integrated studies using those data (hydrology, hydrogeology, geochemistry, and modelling of physical processes) improve our understanding of AMD production in waste dumps.

WHEAL JANE, ITS ABANDONMENT AND TREATMENT OF THE RESULTANT DISCHARGE

Roger M. Hamilton (1), Raymond R. J. Waite (1), Nicholas A. Postlethwaite (2) and Michael Cambridge (3). ((1) National Rivers Authority, Exeter, U.K.; (2) Marcus Hodges Environment, Exeter, U.K.; (3) Knight Piésold & Partners, Ashford, U.K.)

It was recognized that the abandonment of Wheal Jane, a tin mine in South West England, would result in water level recovery and the discharge of acidic, metal-rich water. Investigations to facilitate the prediction of discharge location, time, volume and quality are described. Mine records were insufficiently detailed to allow accurate prediction of location. The slow filling of the large and complex void immediately sub-surface made it difficult to predict the time of discharge. The initial estimate of flow was unreliable and subsequently revised. First flow was about 5,000 m^3/d but later increased to a maximum of 40,000 m^3/d. Currently, average flow is 25,000 m^3/d. Quality of the rising minewater varied with time and depth, making it impossible to predict the discharge quality. Pumping and conventional treatment are keeping the problem under control, but temporary suspension of this programme led to an unexpected discharge which polluted 50 km^2 of tidal waters. Modifications to the treatment system include a novel reconstruction of a tailings dam to facilitate sludge disposal. Passive treatment methods are being tested prior to recommending a long term solution.

PERFORMANCE OF THE HOWE BRIDGE PASSIVE TREATMENT SYSTEM

Robert S. Hedin, John W. Kleinhenz, John R. Odoski, and George R. Watzlaf. (U.S. Bureau of Mines, Pittsburgh, PA, USA).

The Howe Bridge passive treatment system was built in October 1991 to treat acid mine drainage discharging from two abandoned exploration wells. The mine water has pH 5.0-5.5 and is contaminated with 225-300 mg/L Fe^{2+}, 30-40 mg/L Mn, and 1100-1400 mg/L sulfate. The total mine water flow rate averages 140 L/min. Before construction of the treatment system, the discharges flowed untreated into Mill Creek, significantly decreasing its quality. The treatment system consists of two anoxic limestone drains (ALD-1 and ALD-2), two oxidation/settling ponds, and a large wetland that is underlaid with limestone. ALD-1 contains 455 metric tons of limestone gravel. ALD-2 contains 132 metric tons of limestone. The oxidation/settling ponds have a total surface area of 314 m^2 and are constructed with a clay substrate. The wetland has a surface area of 2788 m^2 and is constructed with a limestone gravel substrate overlain by 0.3m of spent mushroom compost. Water discharges from the wetland through slotted drain pipe laid within the limestone gravel. On average, the whole treatment system decreases iron concentrations from 279 mg/L to 80 mg/L, acidity from 482 mg/L to 150 mg/L, and manganese from 41 mg/L to 35 mg/L. Most of the decrease in Mn appeared to result from dilution. The ALDs generate 150-175 mg/L of alkalinity and have no effect on concentrations of Fe or Mn. Flow through the oxidation/settling ponds decreases concentrations of Fe by an average of 94 mg/L. On average, flow through the down-flow wetland decreases Fe concentrations by 127 mg/L and acidity by 212 mg/L. Fe removal by the oxidation/settling ponds did not display any seasonality. Removal of Fe and acidity in the down-flow wetland was highly seasonal: contaminant removal was 50% lower in winter than in summer. The poster will describe the construction of the Howe Bridge passive treatment system and provide summaries and analyses of the water quality data for January 1991 through December 1993.

PERFORMANCE OF THE MORRISON PASSIVE TREATMENT SYSTEM

Robert S. Hedin, John W. Kleinhenz, John R. Odoski, and George R. Watzlaf. (U.S. Bureau of Mines, Pittsburgh, PA, USA).

The Morrison passive treatment system was built in October 1990 to treat water seeping from the outslope of a reclaimed surface mine. The mine water has a pH of 5.0-5.5 and is contaminated with 175-250 mg/L Fe^{2+}, 45-55 mg/L Mn, 375-450 mg/L acidity, and 1100-1500 mg/L sulfate. The flow rate of the mine water is 3-11 L/min. Before construction of the passive treatment system, the water was treated chemically by a mining company. The passive treatment system consists of an anoxic limestone drain (ALD), a settling pond, and two wetland cells. The ALD is 50 m long by 1 m wide by 1 m deep and contains 64 metric tons of limestone. The settling pond has a surface area of 520 m^2 and is constructed with a clay substrate. The wetlands have a total surface area of 571 m^2 and are constructed with a manure substrate. On average, the treatment system decreases Fe from 216 mg/L to <1 mg/L, acidity from 413 mg/L to 0 mg/L, and Mn from 51 mg/L to 11 mg/L. Dilution by uncontaminated water appears to decrease concentrations of all parameters by ~40%. Flow through the ALD increases concentrations of alkalinity by 250 mg/L, decreases concentrations of Fe by 15 mg/L, and has no effect on Mn or sulfate. Fe removal occurs primarily in the oxidation/settling pond, while Mn removal occurs in the wetland cells. The poster will describe the construction of the Morrison passive treatment system and provide summaries and analyses of the water quality data for November 1990 through December 1993.

THE BARK CAMP RUN DEMONSTRATION CONSTRUCTED WETLANDS

William W. Hellier. (PA Dept. of Environmental Resources, Harrisburg, PA, USA).

Six Typha wetlands were constructed at the Bark Camp Run abandoned deep mine and coal processing site in Clearfield County, PA to study in detail wetlands' performance in mitigating acid mine drainage (AMD). The dimensions are 52 m by 8 m. The substrate is 60 cm deep. Three of the wetlands are sampled at three intermediate points, and three are sampled at four intermediate points. The intermediate points each have four sampling wells that extend to different depths. The wetlands were started up in November, 1992. A full year's data have been obtained based on an influent flow of approximately 3 m^3/d to each wetland.

Median values for influent quality are: pH 3.0, net acidity 206 mg/L, [Fe] 25 mg/L, [Mn] 2 mg/L and [Al] 11 mg/L. Median values for effluent quality are pH 6.4, net alkalinity 72 mg/L, [Fe] 4 mg/L, [Mn] 6 mg/L, and [Al] 2 mg/L for one wetland, with comparable results for all six wetlands. Interstitial water quality varies with depth and distance through a given wetland. Interstitial water quality displays transient and possibly seasonal effects following start up. There is a tendency also toward steady values for some of the pollution indicators at different depths and distances through the wetlands. The performance of the wetlands may be affected by the addition of small amounts of anhydrous NH_3 to the influent.

Pollutant levels of effluent PO_4^{-3} are not evident. Almost all of the effluent N is NH_3. During the first 2 to 3 months following startup, NH_3 rose to about 10 mg/L and then steadily declined to < 1 mg/L after 6 months. Elevating influent NH_3 appears to result in elevated effluent NH_3.

Flow patterns were determined at varying depths within two of the wetlands using NaBr as a tracer. The tracer recovery is lower and the detention time is longer the greater the depth in the wetlands.

HYDROLOGICAL AND GEOCHEMICAL MASS BALANCES FOR A LARGE ACTIVE ACID PRODUCING WASTE ROCK PILE, LA MINE DOYON (QUÉBEC)

Denis Isabel (1), Marc Choquette (1), Pierre J. Gélinas (1), René Lefebvre (2), Édith Bourque (3) and Miroslav Nastev (1). ((1)GREGI, Département de Géologie et de Génie Géologique, Université Laval, Québec, QC, Canada, G1K 7P4; (2) INRS-Géoressources, Sainte-Foy, QC, Canada, G1X 4N8; (3) Département de Génie Civil, Université Laval, QC, Canada, G1K 7P4)

Monitoring and characterization work has been going on for three years at "La Mine Doyon" South waste rock pile. This large (20,7 millions metric tons) reactive rock pile is surrounded by ditches and ponds where the total effluent discharge and quality are continuously monitored and registered through 3 automated gauging stations. A dedicated weather station is also operating on the site. A set of 6 monitoring wells located within the pile allow the monitoring of water levels. Air pressure, air composition and temperature within the rock mass are also monitored. Moreover, lysimeters were installed at various depth in the upper part of the pile.

Analysis of the data is based on various techniques like rainfall-runoff events modelling, base flow separation of hydrographs, numerical modelling of groundwater flow with a four layers model, measurement of acid production through relations with the measurement of heat production and measurement of acidic material accumulated within the rock pile. This analysis brings us some original findings: Water loss through evaporation is very important, almost 1/3 of the water budget, despite the cold climate and the lack of a vegetative cover; The waste rock pile does not contribute to peak flow during rainfall-runoff events; Annual release of acidity through drainage does not match annual acidity production. This imply the annual accumulation of a large quantity of acidic compounds within the pile. Geochemical analysis of drilling and trench samples support this.

VARIATION IN COMPUTING ACID-BASE ACCOUNTING IN THE U.S.

W. L. Joseph(1) , K. B. C. Brady (2), and Eric F. Perry (3). ((1) Office of Surface Mining, Denver, CO; (2) Bureau of Mining and Reclamation, Harrisburg, PA; (3) Office of Surface Mining, Pittsburgh, PA).

Review of published and unpublished sources has revealed that there are various acid / base accounting formulas and associated terminology being used in the United States. Comparisons of the various methods indicate that quite different conclusions can be reached on the same data set depending on which formula is used. In the early 1970's researchers at West Virginia University developed acid-base accounting (ABA) to compute liming rates for revegetation of acidic mine spoils. In regions where acid mine drainage problems existed, ABA also became a tool to predict post-mining water quality. Subsequently, ABA has been adopted across the United States as both a revegetation and mine drainage prediction tool. Since the publication of Sobek, et al. in 1978, several modification have been proposed. These modifications tend to be refinements of the original methods to meet regional needs. Some have suggested that the original method of computing ABA (neutralization potential - maximum potential acidity) can underestimate acid potential and even more conservative approaches have been proposed. These approaches include modifications to the neutralization potential test procedure where siderite-rich rocks are present. Additionally, some have suggested that total sulfur is preferable to forms of sulfur because of problems with determination of pyritic sulfur. When interpreting ABA information it is important to know which formula(s) and analysis method(s) are being applied.

A LABORATORY STUDY OF EQUILIBRIUM pH-BUFFERING REACTIONS IN SULFIDE MINE TAILINGS

Jasna Jurjovec (1) , Carol J. Ptacek (2), and David W. Blowes (1). ((1)Waterloo Centre for Groundwater Research, University of Waterloo, Waterloo, ON, Canada; (2) National Water Research Institute, Burlington, ON, Canada)

Oxidation of sulfide minerals in mine tailings produces low pH water containing dissolved metals such as: Zn, Cu, Pb, Cd, Ni, and As. In order to predict the extent of mobilization of dissolved metals it is necessary to understand reactions controlling the pH of the pore water. A laboratory column experiment conducted using mine tailings from the Kidd Creek metallurgical site in Timmins, Ontario, showed a sequence of pH-buffering mineral dissolution reactions which consume H^+ generated by sulfide oxidation. The H^+-consuming reactions can be divided into two groups: a series of mineral-equilibrium reactions and a series of aluminosilicate-dissolution reactions. In the column experiment we observed a series of pH-buffering plateaus. Geochemical calculations conducted using MINTEQA2 indicate water samples discharging from the column approach equilibrium with respect to a series of pH-buffering minerals. This reaction series consists of: calcite/dolomite (pH 7.0-6.0), siderite (pH 5.5-5.0), $Al(OH)_3$ (pH 5.0 - 4.4) and $Fe(OH)_3$ (pH 4.2-3.5). Dissolution of each of these minerals maintains the pH at the given buffering plateau until the mineral has been depleted. The results of the column experiment are consistent with observations made at several inactive tailings impoundments where water affected by sulfide oxidation reactions has been displaced into deeper tailings. Simulations conducted with the combined geochemical equilibrium, solute-transport model PHREEQM, show a series of pH- buffering plateaus that are similar to those observed in the laboratory study.

NINE YARDS AND A CLOUD OF DUST

The Operation of a Fly Ash Grouting Process to Abate an Acid Mine Drainage Discharge

Michael J. Klimkos (Pa. Dept. of Env. Res., Bureau of Mining and Reclamation)

A 15 ha. site located in Clinton county is the site of an acid mine drainage abatement project using fluidized bed fly ash. The project involved three distinct phases, mapping, drilling and grouting. Fields where "hot zones" exist were selected to be drilled and grouted on ten foot centers. The hot zones were pods of pyrite rich, acid producing material buried within the backfill with common dimensions of 18 m by 18 m. The drill holes were 10 cm in diameter. The depth of the drill holes ranged from 3 m to 7 m depending on the depth to the pit floor. Perforated 6.25 cm PVC casing was placed in the drill holes to allow for dispersion of the grout material into the backfill. Because fluidized bed fly ash is the result of coal combustion in the presence of limestone the ash exhibited some of the qualities of portland cement. When the ash is mixed with water a pozzolanic reaction is created and when cured a low strength concrete is formed. The ash was mixed with water in a ratio that varied by volume from 1 part water to 1 part ash to 1 part water to 1.6 parts ash. This grout mixture was then pumped under pressure into the well until it refused to take any further grout or the grout leaked from the ground. The purpose of this mixture was to coat the acid producing material found in the backfill, coat the pit floor and seal any fractures or leaks that may exist in the pit floor. Some areas of the site, particularly those areas with a high clay content took very little grout. These areas were capped and trenched using fly ash grout to dam groundwater from moving through the hot spoil and prevent rainwater from percolating through the spoil. This project utilized a waste product to remediate a relatively small (1.9 to 2.5 l/s maximum) discharge that was affecting 11.3 km of native trout streams. A total of 2007 m^3 was pumped into 545 holes. It is estimated that an additional 765 m^3 were used in the capping operations. There were 5305 man-hours spent in the drilling, grouting and capping operations. Groundwater monitoring is planned for the next few years to determine the effectiveness of the grouting operation in AMD abatement.

REDUCTION OF PYRITE OXIDATION IN BROWN COAL OVERBURDEN IN FIELD EXPERIMENTS

Robert Kringel. (Ruhr-Universität Bochum, Bochum, FRG)

Large scale open-pit mining for brown coals of miocene age and its conversion to electrical energy near site characterizes the western regions of the federal state Northrhine-Westfalia / Germany. The acidification of a lake in the vicinity of closed and refilled open-pit workings has brought the problem of acid rock drainage (ARD) into focus. The acid-forming potential is contained in the overburden. These are unlithified fine to middle grained quartz-sands of marine origin, and may contain up to 0.26 wt.% pyrite-sulfur (av.) with little acid neutralizing capacity. Pyrite oxidation is taking place on temporary surfaces, which are constantly renewed and buried during mining operations. Approx. 14 % of the total pyrite inventory of the open-pit-mines are oxidized during normal operations. It was the task of a research project (currently ongoing) to explore methods to **a.)** minimize pyrite oxidation and **b.)** prevent the acidification of the overburden, thus reducing the quantity of oxidation products and improving the quality of leacheate, contributing to groundwater recharge. Representative overburden-material was mixed with finely ground limestone, calciumoxide, fly-ash and alkaline fertilizer-phosphates with different mass ratios of up to 1.5 wt.%. The mixture was deposited in experimental dumps in the pit-mine and exposed to weathering. In 110 days 42 % of the pyrite in a reference-dump were oxidized, while only between 8 % and 37 % were oxidized in the treated dumps. Acidification was prevented in all treated dumps. Analyses of the leacheate showed high concentrations of iron and sulfate in the reference dump, while only moderate amounts of sulfate and no iron were mobilized in the treated dumps. Investigations of the sediments showed that pyrite surfaces in the treated dumps (where little oxidation occurred) were coated with secondary minerals, presumably iron-hydroxides.

INTERPLAY OF GEOCHEMICAL, ELECTROCHEMICAL AND MICROBIAL CONTROLS IN THE OXIDATION OF COMMON SULFIDE MINERALS

Y. T. John Kwong, John R. Lawrence, and George D. W. Swerhone. (National Hydrology Research Institute, Saskatoon, SK, Canada)

Using polished thin sections of sulfide-containing rocks as starting material, parallel chemical and microbial weathering experiments were conducted to elucidate the relative importance of geochemical, electrochemical and microbial controls in the oxidation of common sulfide minerals. The sulfides examined include pyrite, pyrrhotite, chalcopyrite, galena and sphalerite. Their composition, including trace element content, was determined by electron microprobe analysis. Their rate of oxidation was assessed by chemical analysis of the leachates and image analysis of the mineral grains by laser and scanning electron microscopy. Inter- and intra-granular Eh was monitored during the course of the experiments using specially designed microelectrodes to detect the occurrence of galvanic reactions. Results obtained to date indicate that for sulfides occurring in isolation, mineral composition and morphology and selective microbial colonization largely control their relative reactivity. In a mineral assemblage with different sulfides in contact with each other, their relative weatherability is governed by their position in the electrochemical series. Under optimum pH conditions, microbial mediation greatly enhances the sulfide oxidation rate but the order of the sulfide reactivity does not change. The trace and minor element composition of individual sulfide minerals, however, can greatly affect the electrochemical property of the mineral and hence its weatherabilty. Thus, Fe-rich sphalerite is more susceptible to oxidative dissolution than Fe-poor sphalerite when in contact with pyrite. Data obtained in these experiments will facilitate more accurate prediction of the time-lag involved in the production of acid mine drainage and the evolution of its water chemistry.

NUMERICAL MODELLING OF PHYSICAL PROCESSES IN A WASTE ROCK DUMP PRODUCING ACID MINE DRAINAGE, LA MINE DOYON (QUEBEC)

René Lefebvre (1), Pierre Gélinas (2), and Denis Isabel (2). ((1) INRS Géoressources, Sainte-Foy, Québec, (2) Université Laval, Département de géologie et de génie géologique, Québec).

A characterization, monitoring and modelling program is on-going since 1991 on the hydrological, geochemical and physical processes contributing to acid mine drainage (AMD) in a waste rock dump at La Mine Doyon in Northwestern Quebec. Numerical modelling is used to study the interaction of physical processes: heat production and transfer, water infiltration, air convection and oxygen supply by diffusion and advection. The model is based on the general-purpose multiphase fluid and heat flow numerical simulator TOUGH2 (developped by Karsten Pruess at Lawrence Berkeley Laboratory). The program, called TOUGH AMD, models processes specific to AMD production with a three component system (oxygen, air less oxygen and water) and new subroutines are used to compute oxygen consumption and heat production caused by pyrite oxidation as well as pyrite mass balance and sulphate transport. Pyrite oxidation within waste rock blocks is represented by a reaction core model. Oxygen supply by diffusion and air advection is considered. Modelling is applied to a well documented field case with known physical and transfer properties. The results indicate the impact of permeability and anisotropy on the AMD production rate and show the importance of temperature-driven air convection within the dump for oxygen supply and heat transfer. The model also shows the interactions between fluid and heat flows and between infiltration and mass accumulation and release from the dump. Modelling is also used to evaluate the impact of potential AMD control methods.

STUDY OF THE FERROUS OXIDATION PROCESS IN AMD SEEPAGES

Jing-Yao Liu and Margarete Kalin. (Boojum Research Limited, Toronto, Ontario, Canada).

Iron is the dominant element in acid mine drainage (AMD); its oxidation state is the major factor controlling the pH of AMD. In this work, iron oxidation rates were measured in a field seepage and several AMD samples in the laboratory. The pH's of the test samples (including the field seepage) ranged from 1.81 to 3.66. Iron concentrations ranged from 10 mg/L to 4000 mg/L. Excluding other possible microbial and geochemical effects, the pure iron oxidation process can be expressed as a pseudo first-order reaction. The rate constants in the test samples ranged from 0.00017/min to 0.00030/min. The data are quite consistent with previous studies on buffer systems. The experimental results indicate that pure iron oxidation of AMD in the open air can be described as a first-order reaction. The oxidation rate constant can be used to determine the retention time of AMD in a field precipitation pond. However, other microbial processes also need to be considered as well.

REMEDIATION OF MINE DRAINAGE IN CONSTRUCTED WETLANDS: EFFECTS OF pH AND IRON CONCENTRATION

Mark C. Magness and Martin C. Rabenhorst. (University of Maryland, College Park, MD, USA).

The remediation of acid mine drainage (AMD) has been the focus of research for many years with few cost effective methods developed. Early observations that AMD became lower in metal concentration and higher in pH after passing through natural wetlands sparked much interest in developing constructed wetlands for low cost remediation. The two mechanisms with greatest long term potential for iron retention are the precipitation of 1) oxides and 2) sulfides. Previous studies using flow-through laboratory mesocosms and AMD with pH 3.0 and 1mM Fe have demonstrated that sulfate reduction (sulfidization) can be an important process in the removal of iron and increasing the pH of AMD in flow-through systems. Although sulfidization has been shown to be important under certain conditions, the effects of various influent parameters have not been studied. Therefore the objectives of this study were to evaluate the effects of influent pH and iron concentration on AMD remediation in flow through wetland systems. To accomplish this, a laboratory mesocosm study was initiated to evaluate the effects of five pH levels (2.0, 2.5, 3.0, 3.5, and 4.0) and four iron concentrations (1mM, 2mM, 4mM, and 8mM). Duplicate mesocosms were packed with a mixture of composted cow manure and wheat straw to a density of a straw bale (0.1 g/cm^3) and a depth of 135cm. The AMD moved through the substrate using a gravity flow system at a flow rate of 2 cm/day (approximately 4000 ft^2/gallon/min) . Porewater was extracted and analyzed biweekly at depths of 5, 10, 15, 20, 30, 40, 50, 75, 100, and 135cm for pH, pe, $S^=$, Fe, Mn, and Al. All mesocosms have a zone near the surface which is more oxidized and acid. Below this is a zone with higher pH, lower pe, and increased sulfide levels where Fe is being effectively removed through sulfidization. In mesocosms with higher Fe loading (8mM) the oxidized-acid zone is of greater thickness. A similar trend is observed with mesocosms treated with low pH influent (pH 2.0), which also possess a thicker oxidized-acid zone than mesocosms of higher pH. The increased thickness of the oxidized and acid zone may have an adverse impact on the effective life of these systems.

THE INFLUENCE OF MOLYBDENUM MINING ON THE ENVIRONMENT & PLANNING FOR CLOSURE

Susan F. Mathieu (Placer Dome Canada Limited, Endako Mines Division, Endako, BC, Canada).

Molybdenum (Mo) is an essential trace element for plants and animals, however the potential for Mo toxicity exists in organisms exposed to elevated environmental levels. To understand the influence of molybdenum mining on the surrounding ecosystem, extensive research has been conducted at the Endako Mine by mine personnel and independent consultants. Results show that the influence of the mine is confined to the streams receiving pit discharge or tailings seepage, and to the immediately adjacent soils and vegetation. Elevated Mo concentrations in streams (5-30 mg/L) were not toxic to periphytic algae or macroinvertebrates as abundance, diversity and productivity either increased or remained the same as control streams (<0.1 mg/L). Juvenile trout, stocked in a pit lake with Mo levels ranging up to 50 mg/L, developed normally and did not bioconcentrate Mo in their tissues. Metal analysis of hair samples from moose and deer indicated that elevated Mo concentrations in the vegetation did not impair Cu uptake and metabolism. All evidence indicates that remedial treatment and/or wildlife restrictions are not required for the final closure plan.

DECONTAMINATION AND RECLAMATION OF HIGHLY CONTAMINATED MINE WASTES - WITH PARTICULAR REFERENCE TO ARSENIC

Paul B Mitchell and Keith Atkinson. (Camborne School of Mines, University of Exeter, Redruth, UK).

Widespread arsenic contamination in SW England has resulted from both mining activity and natural mineralisation. In many areas background soil concentrations exceed the recommended UK guidelines. In most cases, there appears to be no significant long- or short-term risk to human health associated with these elevated concentrations. However, in extreme cases, the potential for acute poisoning through the accidental ingestion of contaminated solids may exist. Consequently, where sites containing highly contaminated materials have been identified, there is a need to take some remedial action to reduce the associated risks to acceptable levels. One possible approach is the use of mineral processing techniques (and adaptations) to physically or chemically separate the contaminant, leaving a "clean" product, suitable for vegetative growth or other end-uses. Samples of arsenic-contaminated soils, mine and mineral processing wastes, were collected from a major abandoned mine site in West Cornwall (UK), where losses of arsenic trioxide to the atmosphere during the calcining and condensation resulted in a highly contaminated area surrounding the calciner and flues. Arsenic concentrations up to 30 % have been determined. The major arsenic species is scorodite ($FeAsO_4.2H_2O$). The time and chemically mediated reactions linking arsenic trioxide and scorodite are examined, and the significance of scorodite for ground and surface water contamination and human health are considered. The estimated water contamination potential has been validated in accelerated leaching tests. A range of decontamination techniques have been assessed, including: gravity separation, size separation, and acid and alkaline leaching. Comparative results are presented, and the relative economic benefit of each approach is discussed. The resulting by-product is assessed for its capacity to support vegetation.

PREDICTION OF MINEWATER CHEMISTRY FROM AVAILABLE MONITORING DATA, NORANDA MINERALS' BELL MINE, BRITISH COLUMBIA

Kevin A. Morin (1), Nora M. Hutt (2), and Ross McArthur (3). ((1) Morwijk Enterprises Ltd., 47-115 Kamehameha Highway, Kaneohe, Hawaii, USA 96744 [address current to 3/31/94], (2) Normar Enterprises, Box 357, Wildwood, Alberta, Canada T0E 2M0, (3) Noranda Minerals Inc., Bell Mine, P.O. Box 2000, Granisle, British Columbia, Canada V0J 1W0).

Mining companies annually collect and analyze numerous water samples to ensure the local environment is protected and regulatory permit requirements are fulfilled. After several years the total number of water-chemistry analyses in a mine's database can be in the thousands. This database has a commonly unrecognized use in providing predictions of future water chemistry. The predictions are based on the basic philosophy that, if a trend can be recognized through the years of past chemistry, then the trend should point to future water chemistry. This philosophy holds unless an important factor, such as a major earthquake, occurs in the future, but did not occur during the past monitoring period.

The statistical assessment of a water-chemistry database is based on means and standard deviations, which can be calculated by most spreadsheet packages on the market. If the data display statistically normal trends, then the statistical parameters can be calculated directly from the database. Otherwise, the data must be adjusted or filtered, such as through logarithms which are also in spreadsheet packages, in order to first obtain a normal trend. The statistical relationships are then compiled into an "empirical water-chemistry model". This model is similar to hydrology models in that it predicts, for example, a peak annual concentration of one-hour duration.

A minesite's empirical water-chemistry model can then be used for various purposes, including (1) estimating future water-treatment costs, (2) refining water-retention times in ponds in order to obtain a particular range of metal concentrations, (3) determining the acceptable degree of failure in water-quality control technologies such as clay covers, and (4) negotiating closure bonds with regulatory agencies. Noranda Minerals' Bell Mine, in British Columbia, is used to demonstrate the approach and application of an empirical water-chemistry model.

THE MANAGEMENT AND TREATMENT OF ACID MINE DRAINAGE, PELTON COLLIERY, CESSNOCK, NEW SOUTH WALES, AUSTRALIA.

K. Wayne Perry (Wayne Perry & Associates Pty Ltd - Environmental Consultants Newcastle, Australia).

Pelton Colliery is an abandoned Colliery located 7 km south west of Cessnock, within the Hunter Valley of New South Wales. The site serves as a coal handling and processing facility for Ellalong Colliery, which is operated by the Newcastle Wallsend Coal Company. The coal has a high sulphur content (pyritic) and when weathered produces an acidic leachate. Runoff from the waste products - coarse washery reject and tailings are acidic (pH 2.5 - 4 range). Existing surface soils and certain rock strata are also acidic.An existing water management system was in place, but proved to be inadequate during extended periods of heavy rainfall, which occurred in 1991. Discharges of acidic runoff occurred on a number of occasions, into the main watercourse, Black Creek and resulted in a number of complaints from downstream water users. An upgraded water management system was designed and implemented during 1992, at a cost of almost $1 million. The design catered for a lag effect whereby acidic leachate would be generated some 24 to 48 hours after the storm event.

- A series of new storage dams and enlargement of existing dams to cater for the design storm (10% AEP), followed by a 1% AEP storm within 24 hours of the design storm. Each storage dam is fitted with a combination of self siphoning pipes to maintain adequate storage capacity and pumps.
- Augmentation of the existing lime treatment plant to double its throughput to 4,000m^3/day. This raises the pH of water from 2.5 to 7.6.
- A series of high capacity pumps, to supply water to the lime treatment plant and the Process Dam.
- An emergency pump is diesel-operated, in case of power blackouts during storms, and is designed to pump large quantities of water into abandoned underground workings.
- An upgraded environmental monitoring program was implemented to ensure that the system is checked regularly. At the same time, a Site Environmental Procedures Manual was prepared and implemented to ensure that the system is operated and maintained correctly.

Since finalisation of the water management system, the site has withstood a number of storm events discharge of acidic water off-site.

A COUPLED MODEL OF AIR FLOW AND HEAT TRANSPORT IN MINE WASTE

Benjamin Ross, Ning Lu, and Joel Gottlieb. (Disposal Safety Incorporated, Washington, DC, USA).

Active oxidation of pyritic materials in mine wastes can generate large amounts of heat, causing formation of gas convection cells. A coupled buoyant air flow and conductive-convective heat transfer model has been developed, which can be used to calculate the amount of oxygen available to oxidize pyritic materials in the waste.

The model is based on the assumption that the relative humidity is always 100%. Two governing equations are derived, one for the temperature and one for the air pressure. The pressure equation is derived from a volume balance, Darcy's Law, and the ideal gas law. It accounts for air expansion or contraction and water evaporation or condensation when air moves through pressure and temperature gradients. The temperature equation is derived from an energy balance that includes conduction, sensible heat convection, latent heat convection, and work done when the gas changes volume. Node-centered finite differences are employed to solve the governing equations in space and time. The temperature equation is solved explicitly by advancing in time, and at each time step the pressure equation is solved for the steady-state gas flow.

The model is used to simulate heat and air flow in a typical waste dump with flat surface and steep sides. Two cases are simulated, one with the top surface open to the atmosphere and another with the top surface covered with an impermeable layer. Both cases assume that there is a hot spot in the dump before simulations begin. Simulations show that temperature gradients and air velocities are much larger when the system is open to the atmosphere, but a convection cell is observed even if the top surface is covered.

WATAIL: A TAILINGS BASIN MODEL TO EVALUATE TRANSIENT WATER QUALITY OF ACID MINE DRAINAGE

Jeno M. Scharer (1), William K. Annable (2), and Ronald V. Nicholson (2). ((1) Dept. Chem. Eng., University of Waterloo, Waterloo, ON, Canada, (2) Waterloo Centre for Groundwater Research, Univ. Waterloo, Waterloo, ON).

A computer program (WATAIL) has been developed to assist in the management of water quality associated with the disposal of sulphide tailings. The objective of the program is to provide comparisons of mass loading rates of the major oxidation products (sulphate, iron, acidity) to surface water draining from the tailings watershed. The program focuses on rehabilitation strategies based on engineered covers, including underwater scenarios. The program applies fundamental kinetic, thermodynamic, and physical transport principles together with field data to simulate mass release to both groundwater and surface water. The tailings and the surrounding watershed are divided into regions which can be characterized as either drained unsaturated tailings of varying moisture content or ponded tailings. Pyrite (FeS_2), pyrrhotite (Fe_7S_8) or a mixture of the two can be specified. Concentrations in the outflow represent average monthly values from which mass loadings are computed. Model subroutines include: parameter allocation, initial chemical inventory, sulphide oxidation, solute transport, pH calculation and speciation, and material balance on solids. The kinetics of oxidation coupled with the transport of oxygen into the tailings are key components of the model. Solute transport includes both chemical dynamics and equilibrium processes. The dynamic reactions are sulphide oxidations and weathering while equilibrium calculations are employed to model aqueous speciation, neutralization/buffering reactions, and secondary solid phase equilibria. Both surface water and groundwater flows are calculated from water balances and applications of Darcy's Law. The transport of the dissolved constituents is distributed to simulate dispersion along the flowpaths. This methodology, together with the evolution of a sulphide depleted zone above the water table, provides a realistic, quasi-three-dimensional approach to the simulations. The concentrations and loading history predicted with the model provide a guide to planning abatement strategies.

PYRITE REDUCTION IN LARGE SIZED COAL VIA HEAP LEACHING

Frederick A. Sharp. (U.S. Bureau of Mines, Pittsburgh, PA, USA).

Conventional coal preparation removes bulk inert materials, i.e., stone and free pyrite. Additional pyrite removal requires further size reduction and cleaning at increased cost. A passive and inexpensive process to remove pyrite from coal by biologically mediated heap leaching was studied. This process has been tested by the Bureau of Mines in large scale (9 to 21 metric ton) heap leaching systems, using indigenous bacteria, and allowing natural acids and oxidants to accumulate in the recycled lixiviant. Fifty percent of the pyrite was removed by heap leaching run-of-mine stoker size, Pgh. #8 coal from Phillipi, WV. A second test using conventionally cleaned and sized (.65 cm x 1.9 cm), Pgh. #8 coal from Powhatten mine, OH, removed about 12% of additional pyrite. With this coal, 32% of the pyrite was removed in large column studies, and 97% was removed when it was ground to less than 100 microns. A third test with a relatively low sulfur, run-of-mine Pgh. #8 coal from Pershina mine, McDonald, PA realized a 7% sulfur reduction. The effectiveness of heap leaching is apparently related to the size of the coal and the dispersion of pyrite within the coal matrix.

CASE STUDY: MAKING DRINKING WATER AND TABLE SALT FROM COAL MINE DRAINAGE IN POLAND

Janusz Sikora (1), Krzysztof Szyndler (2), and Rodi Ludlum (3). ((1) Debiensko Coal Mine, Poland, (2) Energotechnika Ltd., Poland, (3) Resources Conservation Company, Bellevue, WA, USA)

Massive amounts of water are discharged from Polish mines each day: an estimated 2.5 million liters per minute, or 3.6 billion liters per day. About 60% of this drainage can be used for drinking, agriculture or industry. The rest, 1.4 billion liters per day, are saline waters that drain directly to rivers and cause substantial damage to Polish water resources. The largest amount of salty drainage is pumped from 18 mines located in southwestern Poland, in the upper courses of Poland's two main rivers, the Vistula and Odra. More than 3.6 million mt of salt was released to the Vistula in 1991. Mine drainage to these rivers is harmful to plant and animal life, causes corrosion and eliminates economical use of the rivers along their entire 400 km stretch through Poland. The drainage problem also intensifies the severe lack of drinking water. To combat this problem, a large environmental project has been built near Katowice which eliminates highly brackish wastewater discharge from two coal mines: Debiensko and Budryk. All drainage from the two mines is desalinated in a reverse osmosis plant followed by two evaporators and a salt crystallizer. The result is zero liquid discharge to the Odra river from these two mines, eliminating 280 mt per day of salt discharge. Approximately 14.4 million liters per day of mine drainage is treated in the desalination plant at Debiensko. The plant recovers about 9.8 million liters per day of drinking water and process water, 4.5 million liters per day of distilled water and 250 mt per day of pure sodium chloride for sale as table salt and other uses. The plant started up in the fall of 1993.

PREDICTION OF ELEMENT DISPERSION IN MINE-DRAINAGE SYSTEMS BASED UPON GEOCHEMICAL PRINCIPLES

Kathleen S. Smith (U.S. Geological Survey, Box 25046, Denver Federal Center, Denver, CO 80225-0046)

The degree of dispersion of a chemical element is controlled by the mobility of that element in its particular environment. The mobility of an element in the surficial environment is generally controlled by the nature of its primary mineral(s) and its transport in water. Water transport of a dissolved chemical element is dominantly controlled by the tendency of that element to form secondary minerals (solubility reactions) and the ability of that element to interact with solid phases (adsorption/desorption and coprecipitation reactions). Many solubility reactions and adsorption reactions are predictable and can be used to anticipate the degree of element dispersion. For example, some elements that are expected to be mobile under acidic (pH < 3) oxidizing conditions (such as in the area of an oxidizing, high-pyrite ore body) include Al, As, Cd, Co, Cu, Fe, Mn, Mo, Ni Pb, Se, U, and Zn. Under slightly less acidic conditions (pH 3.5-4.5), Fe is often rendered immobile by the formation of secondary hydrous-oxide precipitates. Arsenic, Cu, Mo, Pb, Se, and U in solution can be immobilized by adsorption or coprecipitation with these secondary iron-rich precipitates. Under non-acidic (near neutral pH) oxidizing conditions (such as in the area of an oxidizing sulfide ore body in a carbonate environment), Fe and Al are generally immobilized by the precipitation of secondary oxide phases. Arsenic, Cu, Mo, Pb, Se, and U are likely adsorbed or coprecipitated by secondary oxide phases; cadmium, Co, Ni, and Zn also may be adsorbed or coprecipitated depending on the amount and type of these phases formed. Reducing (anaerobic or anoxic) conditions can alter the mobility of some elements; uranium is usually rendered quite immobile under reducing conditions. These examples illustrate but a few of the geochemical principles that can be used to predict the mobility and interaction of elements, and hence element dispersion, at mined sites. Such information is essential for land-use planning, mine-drainage treatment, ground water and surface water protection, regulatory decisions, and cleanup and reclamation practices in areas impacted by mineral development.

THE EFFECTS OF FLY ASH BLENDING RATES AND ASH PROPERTIES ON LEACHATE QUALITY FROM FLY ASH/COAL REFUSE MIXTURES

B. R. Stewart, M. L. Jackson, and W. L. Daniels. (Virginia Tech, Crop and Soil Environmental Sciences, Blacksburg, VA 24061-0404).

The vast majority of Appalachian coal refuse materials produce some acid mine drainage (AMD) due to the oxidation of pyrite. Blending amendments in the coal refuse to stop pyrite oxidation or neutralize the acidity produced could largely eliminate the generation of AMD from coal refuse. A column study was initiated to examine the effects of various bulk-blended acid mine drainage treatments including fly ash, topsoil, lime, and rock phosphate. Three fly ash materials were blended with a highly pyritic coal refuse. A non-alkaline ash was blended with refuse at one rate (20% w/w), while one of the alkaline ashes was blended at two rates (20%, 33% w/w) and the other at 4 rates (5%, 10%, 20%, 33% w/w). All treatments were compared with unblended control columns containing only coal refuse. The columns have been leached under unsaturated conditions at the rate of 2.5 cm/week for over 2 years. The pH of the leachate from the unamended controls quickly dropped to < 2 with very high levels of Fe, Mn, and SO_4^{2-}. The pH of the leachate from the columns blended with 5% alkaline fly ash dropped to < 2.5 after 10 weeks of leaching. The pH of the leachate from the columns blended with 10% alkaline fly ash remained above 7.5 for 20 weeks but declined to < 2.5 after 40 weeks. The pH of the columns blended with non-alkaline fly ash (20% w/w) had an initial pH of 4.5 and gradually declined to < 3 after 60 weeks of leaching. Leachate pH from the columns blended with higher rates (20% and 33%) of alkaline fly ash remained above 7.5 for over 2 years. When the pH of a refuse/fly ash blend drops to 2.0, we see enhanced stripping of some elements, particularly Mn, from the ash. If fly ash alkalinity is inadequate to balance potential acidity, accelerated leaching of ash bound metals may occur. The co-disposal of fly ash in acid forming zones of a coal refuse pile should be discouraged unless acid/base balance concerns are met.

EFFECT OF LIME ADDITION ON THE LEACHATE CHEMISTRY OF A PENNSYLVANIA COAL MINESOIL

William J. Tarutis, Jr. and Brian F. Oram. (Wilkes University, Wilkes-Barre, PA, USA).

The effect of lime addition on the leachate chemistry of an acidic (pH 3) coal minesoil is currently being studied using batch and continuous-flow (column) reactors. Minesoil was collected from a spoil pile located in the anthracite coal region at Wilkes-Barre, Pennsylvania. The soil was sieved to obtain the <4.6-mm fraction used in all experiments. This fraction was analyzed for pH, electrical conductivity (EC), cation exchange capacity, SMP lime requirement (exchangeable acidity), organic matter content, and total sulfur content (potential acidity). Preliminary experiments using batch equilibrations of minesoil and water (1:1) to which different amounts of lime were added (1, 2, 4, and 6% calcium carbonate equivalent, dry weight basis) revealed a pH increase of 1-2 units within 5 minutes, followed by a similar increase in pH over the subsequent 2-week period. Equilibrations without minesoil (lime and water only) were employed as controls. The results indicate a good correlation between calculated lime requirements from the minesoil-lime equilibrations and from total sulfur content; SMP lime requirements were much lower. Lime requirement values based on total sulfur content were then used for column studies. Leaching experiments are currently underway and consist of duplicate 7.5-cm PVC columns filled with sieved minesoil (with or without added lime) and continuously leached with distilled water applied to each column by a peristalic pump capable of delivering up to 7 mL/min. Leachate from each column will be collected at known pore-volume intervals and analyzed for pH, EC, Fe, Mn, Ca, Mg, alkalinity, and SO_4 using standard procedures. The results obtained will contribute to an understanding of the processes controlling the leachate chemistry of minesoils in the region and will supplement current research on reclaming coal-mined land in the vicinity.

IMPACT OF SEASONAL VARIATIONS ON THE GEOCHEMISTRY OF PORE WATERS AND PORE GASES OF ACID MINE TAILINGS: A FIELD STUDY

Normand Tassé, Diane Germain, and Mario Bergeron. (INRS-Géoressources, Sainte-Foy, PQ, Canada)

Temperature and rainfall are seasonal parameters that affect the rate of sulphide oxidation in acid mine tailings. Temperature controls chemical equilibria and kinetics of reactions, whereas rainfall affects the degree of water saturation (and, in turn, oxygen diffusion), and the overall downward transportation of pore waters. It is thus important to determine to which extent these factors do alter geochemical data that can be used to modelize long term oxidation of sulphidic tailings. Pore gases and pore waters of an acid mine tailings impoundment of northwestern Quebec were sampled twice at 7 localities, through the vadose and upper saturated zones, in August and October 1991. Gases were sampled at 10 cm intervals and analyzed for O_2, CO_2, CH_4 and N_2. Water was obtained by squeezing 15 to 25 cm sections of aluminum tubes and by pumping PVC piezometers, and analyzed for Eh, pH, and major and trace elements.

Significant variations (that is, larger than 10-15 %) are observed when summer and fall data are compared. Profiles of O_2 and CO_2 proportions in pore gases are transposed to either larger or smaller values, and the tendency is related to the overall grain-size characteristics of the sampled station. For instance, for O_2, lower fall proportions in fine-grained tailings can be explained by slower gas diffusion in soils retaining more water. On the other hand, higher fall proportions in coarse-grained tailings rather reflect lower oxidation rates related to colder fall temperatures, in well-drained soils. Several factors contribute to distort pore water profiles from summer to fall, to an extent that no simple systematic variations stand out from the comparison of the seven profile pairs. Effects observed are related to one or more of the following: higher water table, larger pore water content, larger rates of downward transportation, lower rates of sulphide oxidation, lower temperatures, different solubilities, and so forth.

THE PERFORMANCE OF THE JENNINGS ENVIRONMENTAL CENTER ANOXIC LIMESTONE DRAIN

George R. Watzlaf, John W. Kleinhenz, John R. Odoski, and Robert S. Hedin. (U.S. Bureau of Mines, Pittsburgh, PA, USA).

An anoxic limestone drain (ALD) was constructed to treat acid mine drainage at the Jennings Environmental Center in Slippery Rock, PA. The mine water flows from an abandoned underground mine in the Middle Kittanning coal seam. On average, the mine water has pH 3.3 and contains 10 mg/L Fe^{3+}, 63 mg/L Fe^{2+}, 21 mg/L Al, and 9 mg/L Mn. The average flow rate is 92 L/min. The ALD, constructed during the spring of 1994, consists of six buried limestone cells connected by buried pipes. The beds are 1.0-1.3 m wide and 1.0-1.3 m high. The six cells of limestone have a total linear length of 175 m. The ALD contains 364 metric tons of limestone. The chemical and hydraulic performance of the ALD was monitored between April 1994 and December 1994. The average effluent of the ALD had a pH of 6.3 and contained 177 mg/L alkalinity, <1 mg/L Fe^{3+}, 62 mg/L Fe^{2+}, <1 mg/L Al and 9 mg/L Mn. In September 1994, a leak developed between the 2nd and 3rd ALD cell. Between September and December 1994, the percentage of mine water flowing out of the leak increased from 6% to 90% of the total flow, while the percentage of mine water flowing from the ALD effluent decreased from 94% to 10% of the total flow. Measurements of hydraulic pressures within the ALD in November and December indicated that the permeability of the second, third, and fourth cells had decreased significantly since construction of the ALD. These losses in permeability coincided with areas of maximum aluminum retention. Partial excavation of the ALD in September 1994 revealed that the limestone rocks in these cells were covered with gelatinous deposits of aluminum hydroxide. The poster will detail the chemical performance of the ALD and the hydraulic problems encountered during its 8 months of operation.

WATER QUALITY AND FLOW RATES DURING STORM EVENTS AT TWO CONSTRUCTED WETLANDS RECEIVING MINE DRAINAGE

Frederick M. Williams (1), Lloyd R. Stark (1), and Robert P. Brooks (2). ((1) Department of Biology, (2) School of Forest Resources, Pennsylvania State University, University Park, PA, USA)

Flow rates, pH, iron concentration, and manganese concentration were measured during several storm events at two constructed wetlands receiving mine water. During a substantial rain event, flow rates at wetland outlets surpassed flow rates at wetland inlets. Differences in wetland area at the two sites are thought to be partly responsible for differences in behavior. A significant positive correlation existed between local rainfall and outflow rates at the larger wetland, but not between rainfall and inflow rates. During storm events, outlet pH, relative to inlet pH, was slightly elevated at the larger wetland, but depressed at the smaller wetland. However, over the course of one year, rainfall was uncorrelated to outlet pH in the larger wetland. A substantial rain event at the smaller wetland resulted in a temporary elevation in outlet iron concentrations, with treatment efficiency reduced to near zero. However, in the larger wetland, treatment efficiency was not significantly affected by storm events. Although rainfall and outlet iron concentration were not significant correlates at the larger wetland, flow rate was positively correlated to outlet iron concentration. A normal manganese treatment efficiency of 50% at the smaller wetland was reduced to zero during a heavy rain. The similarities and differences of the storm related behavior of the two wetlands is discussed with respect to size, configuration, and other design factors.

MONTANA RECLAMATION: A PROGRESS REPORT ON THE GOLDEN SUNLIGHT MINE. WHAT'S WORKING BEST

R. David Williams. (U.S. Bureau of Land Management, Butte, MT, USA.)

Placer Dome (USA's) Golden Sunlight Mine near Whitehall, Montana proposed a major expansion in March of 1988. This expansion and the attendant permitting history and operational monitoring were the subject of a 1992 talk at the Second International Conference on Environmental Issues and Waste Management in Energy and Mineral Production in Calgary. That talk focused mainly on the permit issues and the permitting agencies' and the Golden Sunlight Mine's responses to those issues. This paper will summarize the technical progress on several of the issues which surfaced during the preparation of the Environmental Assessment. These issues included: Steep slope reclamation of the waste dump complex with potential for the development of acid rock drainage, reclamation of the two tailing impoundments and questions surrounding the amount and disposition of poor quality water projected to accumulate in the pit at the conclusion of mining operations. In order to quantify progress on these issues the permit included extensive monitoring of reclamation test plots. This monitoring will enable the mine and the permitting agencies to evaluate the reclamation measures most effective in protecting the environment. This paper will summarize progress to date on two extensive monitoring programs on the waste dump complex and a monitoring program on Tailing Impoundment I. These test plots are monitored for water infiltration and all major indicators of acid rock drainage, including, CO_2, O_2, temperature, pore water composition and water infiltration into the waste or tailing material. This information will include plots with different liming rates, steepness, aspects, and cover material in order to determine what combination is most effective at limiting acid rock drainage. Additional information will be presented on the mine's extensive waste characterization program.

PRE- AND POST- CONSTRUCTION ANALYSIS OF A WETLAND USED FOR MINE DRAINAGE CONTROL

Karen M.Wise and William J. Mitsch. (The Ohio State University, School of Natural Resources, Columbus, OH, USA).

A 0.39 ha constructed wetland in Athens County, Ohio is being evaluated for its ability to remove contaminants from acidic mine drainage. The wetland receives water flow from Lick Run stream which is contaminated by two major abandoned underground mine seeps. The wetland effluent is then directed back into Lick Run, a tributary of the Hocking River. Data were collected 1.5 years prior to construction and 11 months following completion of the passive wetland system. Preconstruction data reported average spring quarter 1991 and 1992 iron concentrations in the stream at the future wetland influent and effluents sites to be 330 and 106 mg/L, while spring quarter 1993 showed iron levels at the wetland influent and effluent to be 64 and 3 mg/L, respectively. Iron removal percentages were 68% prior to the construction of the wetland and 95% following its completion. Preconstruction data were analyzed using a dynamic computer model and preliminary comparison with the first 11 months of the wetland data show the actual iron removal rates to be 4 $g\ m^{-2}\ day^{-1}$ compared to the predicted value of 6.5 $g\ m^{-2}\ day^{-1}$ (based on data collected from April 1991-March 1992, under similar hydrologic conditions).

SAND-BENTONITE MIXTURE AS A COVER FOR MANAGING REACTIVE MINE WASTES

Ernest K. Yanful (1), and Keith S. Shikatani (2). ((1) Department of Civil Engineering, The University of Western Ontario, London, Ontario, Canada, (2) Mineral Sciences Laboratory, Noranda Technology Centre, Québec, Canada).

Engineered covers, constructed from natural clays and tills, are currently being evaluated in Canada under the MEND (Mine Environment Neutral Drainage) program as a strategy for managing reactive mine wastes. A major disadvantage of these natural materials is their non-availability at or near many mine sites, especially in some parts of Eastern Canada. In addition, these materials gain one to two orders of magnitude in hydraulic conductivity, **k**, upon freezing and thawing. Increase in **k** would result in an increase in the amount of water percolation through the cover and, ultimately, in the quantity of seepage. To address the problem, a project was initiated in 1992 at the Noranda Technology Centre to evaluate a 92% sand and 8% bentonite mixture, as an alternative to natural clays and tills. The results indicated that the sand-bentonite can retain nearly 92% of its initial saturation down to a suction of 15 m of water (pF 3.18). Residual moisture contents averaged 16% at a suction of 36 m of water (pF 3.56). Laboratory drainage column evaluation of the mixture in a three-layer capillary barrier system indicated that it can retain 90% of its initial saturated moisture content over a period of 43 days under evaporation. Subsequent re-wetting restored the original moisture content. Hydraulic conductivity of the compacted saturated mixture was of the order of 1×10^{-9} cm/s and the effective diffusion coefficient of gaseous oxygen was determined to be 2×10^{-9} m^2/s at 90% saturation. In addition to these desirable properties, it has recently been observed by other researchers that such a sand-bentonite mixture is resistant to the negative impacts of freeze-thaw. These findings suggest that sand-bentonite mixtures could be preferred alternatives to natural clays and tills in the design and construction of covers for preventing or controlling acid drainage from reactive mine wastes.

REMOVAL OF HEAVY METAL IONS AND SYNTHESIS OF FERRITE FROM ACID MINE DRAINAGE BY MODIFIED FERRITE COPRECIPITATION

K. Yang (1), M. Misra (1), R. K. Mehta (1), M. E. Kravetz (2), and T. E. McNeel (2). ((1) Mackay School of Mines, University of Nevada, Reno, Nevada, USA, (2) Buckman Laboratories, Inc., Memphis, TN, USA).

Acid Mine Drainage (AMD) containing heavy metal ions is a large environmental problem. Among many treatment approaches considered in the literature, one approach is the ferrite coprecipitation for removing heavy metal ions from waste water. However, the conventional technique is performed at an elevated temperature and, therefore, treating large quantities of AMD is not feasible. Recently, in a joint research venture involving Buckman Laboratories, Inc. and the Department of Chemical and Metallurgical Engineering at the University of Nevada-Reno, a novel proprietary 3-stage selective metal and ferrite co-precipitation process was developed to remove heavy-metal ions from a variety of mine drainage at ambient temperature. Using this process, copper and aluminum compounds were selectively recovered in the first and second stages, while the spinel mixed ferrite was produced in the third stage. Experimental results and the demonstration using Noranda Tailing water and Berkeley Pit water will be presented along with the use of possible environmental applications of the mixed ferrite product produced from such process.

CONSTRUCTION AND PERFORMANCE OF ANOXIC LIMESTONE DRAINS INSTALLED TO TREAT ACID MINE DRAINAGE ON ABANDONED MINE LANDS IN WEST VIRGINIA

Bernie Yednock. (USDA, Soil Conservation Service, Morgantown, WV, USA).

This poster describes the construction and performance of three anoxic limestone drains (ALD) on the Ridenour abandoned mine land site in Monongalia County, WV. The ALDs were constructed by the Soil Conservation Service to treat acid mine drainage flowing from abandoned Pittsburgh coal underground mines. Each ALD was constructed by excavating a trench, lining it with 20 mil polyethylene sheeting, filling the excavation with #57 limestone gravel (78% $CaCO_3$ content), and covering with 0.6 meters of clay fill. Wells placed within each ALD allow sampling of raw mine water before it contacts the limestone. Water samples have been collected monthly at the sites for 9-12 months. ALDs have produced mine water with alkalinities exceeding 250 mg/L. One ALD has consistently produced alkalinities exceeding 400 mg/L. Alkalinity concentrations as high as 722 mg/L have been measured. A positive relationship between the mineral acidity of the raw water and the effluent concentrations of alkalinity exists. The results indicate that the assumption that alkalinity generation by ALDs is limited to 300 mg/L is incorrect in cases where the raw water has a very high mineral acidity. Detailed aspects of the ALD construction and treatment will be discussed

THE RATE OF PYRITE DISSOLUTION: COMPARISON OF FIELD AND LABORATORY STUDIES

Paul F. Ziemkiewicz and Raymond J. Lovett. (National Mine Land Reclamation Center, West Virginia University, Morgantown, WV, USA)

Regulatory approval for a new mining operation often hinges on an expedient and reliable method for predicting the acid producing potential of the overburden rock. An important component of this prediction process involves the rate at which pyritic sulfur will oxidize and leach from the rock mass. It has been variously suggested that oxidation is quick and that leaching is slow; that the reverse is true and that various types of pyrite react at very different rates.

Data are presented which indicate that pyrite oxidation is relatively predictable and slow, that there is little difference between pyrites of very different sources: sandstone (cubic, low formation temperature), shale (non-cubic forms) and hydrothermal pyrite (cubic, high temperature). Biotic and abiotic rates are nearly the same and high pH oxidation occurs nearly as fast as low pH oxidation. Particle size appears to influence the rate substantially. Leaching, at least under Appalachian conditions is fast, making pyrite oxidation the rate controlling factor. For applied purposes, however, oxidation and leaching are combined as sulfur flux. Rates of sulfur flux are similar in both small scale field trials and under laboratory conditions supporting the concept of slow oxidation and efficient leaching.

Sulfur flux rates derived from several laboratory weathering processes are compared to those obtained under field conditions.

Aachib, M. 128
Abate, C. 401
Adams, R. L. 218
Ahmed, S. M. 57
Aiken, S. R. 87
Al, T. A. 208
Aljoe, W. W. 178
Amaratunga, L. M. 401
Annable, W. K. 423
Atkinson, K. 406, 421
Aubé, B. C. 87, 138
Aubertin, M. 128
Baker, R. C. 226
Balderrama, R. M. 326
Balins, J. K. 402
Banwart, S. 363
Béchard, G. 403
Bell, A. V. 113
Belzile, N. 148
Bennett, J. W. 363
Bergeron, M. 426
Bhumbla, D. K. 406
Bissonnette, G. K. 406
Bird, D. A. 403
Blowes, D. W. 208, 417
Borek, S. L. 404, 408
Bourque, E. 416
Boury, E. M. 226
Bovard, S. 405
Bowders, J. J. 168, 226
Boyle, D. R. 234
Bradham, W. S. 404, 407
Brady, K. B. C. 242, 401, 417
Bremner, P. R. 341
Brenner, E. K. 405
Brenner, F. J. 405
Brickett, L. A. 405, 408
Broman, P. G. 32
Brooks, R. P. 427
Brown, M. M. 406
Burns, G. R. 2
Calabrese, J. P. 406
Cambridge, M. 414
Caruccio, F. T. 404, 407
Cevaal, J. 379
Chambers, D. B. 67
Chapuis, R. P. 128
Chesworth, W. 348, 356
Choquette, M. 407, 414, 416
Clarke, W. P. 408
Colberg, P. 409
Cooper, A. R. 408
Cravotta III, C. A. 242
Dakers, R. G. 67
Daniels, W. L. 425
Darling, G. D. 273
Daub, G. A. 334
Davis, J. B. 402
Davis, L. K. 409
Day, S. J. 77
DeLeo, M. 409
DiMatteo, M. R. 242
Dinger, J. S. 188
Domvile, S. J. 410
Dvorak, D. H. 404
Dumaresq, C. G. 410
Eddy, D. P. 411
Edenborn, H. M. 404, 405
Edwards, G. S. 411
Eger, A. P. 412
Ellenberger, J. L. 281
Evangelou, V. P. 96
Evans, A. W. 158
Faulkner, B. B. 250
Feasby, D. G. 67
Ferguson, K. D. 12
Ficklin, W. H. 412
Filas, B. A. 413
Filion, M. P. 22
Filipek, L. H. 387, 413
Finch, J. A. 273
Firlotte, F. W. 22
Fish, D. 289
Gabr, M. A. 168, 226
Garbutt, K. 413
Geidel, G. 407
Gélinas, P. J. 407, 414, 416, 419
Germain, D. 426
Gibson, D. K. 258
Goldsworthy, M. H. 67
Göransson, T. 32
Gottlieb, J. 423
Gould, W. D. 403
Gusek, J. 379, 387
Gustafson-Minnich, L. C. 242
Hamilton, R. M. 414

Hammack, R. W. 404
Hawkins, J. W. 265
Hedin, R. S. 415, 427
Hellier, W. W. 416
Horneman, J. 319
Hubbard, K. L. 273
Hutt, N. M. 422
Isabel, D. 407, 414, 416, 419
Jackson, M. L. 425
Jambor, J. L. 208
Jones, C. E. 104
Jones, Perry M. 281
Jones, Peter M. 289
Joseph, W. L. 417
Joyce, C. J. 408
Julien, M. R. 22
Jurjovec, J. 417
Kalin, M. 296, 420
Kittle, D. L. 413
Kleinhenz, J. W. 415, 427
Klimkos, M. J. 418
Kravetz, M. E. 429
Kringel, R. 418
Kwong, Y. T. J. 419
Kuyucak, N. 303, 311
Lacombe, P. F. 22
Landry, G. 296
Lawrence, J. R. 419
Lefebvre, R. 407, 414, 416, 419
Li, M. G. 410
Liu, J. 420
Liu, L. 348, 356
Lovett, R. J. 430
Lu, N. 423
Ludlum, R. 424
Lyons, W. B. 403
Magness, M. C. 420
Markkola, K. 2
Mathieu, S. F. 421
Mays, P. A. 411
McArthur, R. 422
McGraw, J. B. 413
McMillen, T. 409
McNeel, T. E. 429
Meek, Jr., F. A. 41, 49
Mehta, R. K. 429
Michel, F. A. 410
Miller, G. C. 403
Miller, S. H. 2
Misra, M. 429
Mitchell, P. B. 421
Mitsch, W. J. 428
Morin, K. A. 422
Mulvay, S. M. 289
Nastev, M. 416
Nicholson, R. V. 423
Nikraz, H. R. 158
Ninesteel, J. J. 218
Odoski, J. R. 415, 427
Oram, B. F. 426
Pantelis, G. 258
Parisi, D. 319
Patterson, R. J. L. 12
Payne, R. A. 402
Perry, E. F. 417
Perry, K. W. 422
Pettit, C. M. 67
Pierce, W. G. 148
Plumlee, G. S. 412
Pool, D. L. 326
Postlethwaite, N. A. 414
Press, M. E. 158
Ptacek, C. J. 417
Rabenhorst, M. C. 420
Rajan, S. 403
Rao, S. R. 273
Rastogi, V. 319
Rauch, H. W. 218
Riley, M. D. 113
Ritchie, A. I. M. 258, 363
Rose, A. W. 334, 401
Ross, B. 423
Runner, M. S. 168
Ryan, P. A. 408
Scharer, J. M. 67, 423
Scheuering, J. 379
Schultze, L. E. 341
Sencindiver, J. C. 406
Sexstone, A. J. 406
Sharp, F. A. 424
Shelp, G. 348, 356
Shikatani, K. S. 429
Sikora, J. 424
Skousen, J. G. 250, 406
Smith, C. N. 234
Smith, J. 409

Smith, K. S. 412, 425
Smith, M. P. 296
Sollner, D. D. 410
Southam, G. 356
Spiers, G. 348, 356
St-Arnaud, L. C. 87, 138, 198
St-Germain, P. 303, 311
Stark, L. R. 427
Stewart, B. R. 425
Stonehouse, J. M. 413
Strömberg, B. 363
Subramanian, K. S. 410
Swerhone, G. D. W. 419
Swoboda-Colberg, N. 409
Szyndler, K. 424
Tarutis, Jr., W. J. 371, 426
Tassé, N. 426
Tremblay, R. L. 122
Unz, R. F. 371
Van Zyl, D. 2
Waite, R. R. J. 414
Watzlaf, G. R. 415, 427
Wen, R. 413
Whiting, K. 379
Wildeman, T. R. 379, 387
Wilkins, C. 406
Williams, F. M. 427
Williams, R. D. 428
Wilson, H. R. 410
Winterhalder, K. 148
Wise, K. M. 428
Wiseman, M. E. 87, 148
Wong, J. Y. 104
Woyshner, M. R. 138, 198
Wunsch, D. R. 188
Yanful, E. K. 113, 138, 429
Yang, K. 429
Yednock, B. 430
Zamzow, M. J. 341
Ziemkiewicz, P. F. 49, 395, 430

*U.S. GOVERNMENT PRINTING OFFICE:1994-509-021/05003